4–8 August 2008
Denver Marriott Tech Center Hotel
Denver, Colorado U.S.A.

Book of Abstracts

57th Annual Conference on Applications of X-ray Analysis
Denver X-ray Conference

Joint meeting with ICRS-8

The 8th International Conference on Residual Stresses

Reception Sponsors

PANalytical

Chemplex Industries, Inc.

GE Inspection Technologies

Thermo Scientific

Plenary Session: **Stress and Society**

ICRS

DENVER X-RAY CONFERENCE®

ICDD

Sponsored by
International Centre for Diffraction Data

Advances in X-ray Analysis

Proceedings of the Denver X-ray Conference

And the Proceedings of the 8th International Conference on Residual Stresses

Attention Authors!

Please submit your manuscripts for Volume 52 of Advances in X-ray Analysis (AXA) and the ICRS-8 Proceedings by 1 September 2008

See http://www.dxcicdd.com/advances/authors.htm for guidelines.

Did you know…

Several high quality DXC manuscripts are selected for advance publication in the March issue of the journal, Powder Diffraction and select ICRS-8 papers will also be invited for publication in a special issue of Journal of Engineering Materials and Technology.

Contribute to the Success of Fellow X-ray Scientists…

Publishing your manuscript in the historical series, AXA, ensures that your work is available to fellow XRD & XRF scientists for years to come.

DENVER X-RAY CONFERENCE®

ICRS

AXA

Dedicated to XRD & XRF analysts for over 50 years

ICDD®

57th Annual Denver X-ray Conference & The 8th International Conference on Residual Stresses

4–8 August 2008

Denver Marriott Tech Center Hotel • Denver, Colorado U.S.A.

2008 Denver X-ray Conference Organizing Committee

Robert L. Snyder, Chair, Georgia Institute of Technology, Atlanta, GA
W. Tim Elam, Co-chair EDAX, Inc., Mahwah, NJ & University of Washington, Redmond, WA
John A. Anzelmo, Anzelmo & Associates, Inc., Madison, WI
Thomas Blanton, Eastman Kodak Company Research Labs, Rochester, NY
Victor E. Buhrke, Past Chair, Consultant, Portola Valley, CA
Denise Flaherty, International Centre for Diffraction Data, Newtown Square, PA
John V. Gilfrich, Emeritus, SFA, Inc./NRL, Bethesda, MD
George J. Havrilla, Los Alamos National Laboratory, Los Alamos, NM
Ting C. Huang, Emeritus, IBM Almaden Research Center, San Jose, CA
James A. Kaduk, INEOS Technologies, Naperville, IL
Terry Maguire, International Centre for Diffraction Data, Newtown Square, PA
Scott T. Misture, NYS College of Ceramics at Alfred University, Alfred, NY
I. Cev Noyan, Columbia University, New York, NY
Brian Toby, APS—Argonne National Laboratory, Argonne, IL
René Van Grieken, University of Antwerp, Antwerp, Belgium
Mary Ann Zaitz, IBM, Hopewell Junction, NY

ICRS-8 Advisory Board

I. Cev Noyan, Columbia University, New York, NY
Aaron Krawitz, University of Missouri, Columbia, MO
Camden R. Hubbard, Oak Ridge National Lab, Oak Ridge, TN
Mark Bourke, Los Alamos National Lab, Los Alamos, NM
Tom Holden, Northern Stress Technologies, Deep River, Ontario, Canada

ICRS-8 Program Committee Chairs

Michael Prime, Los Alamos National Laboratory, Los Alamos, NM
Ersan Üstündag, Iowa State University, Ames, IA

Future DXC Conference Date

27–31 July 2009
Crowne Plaza Hotel
Colorado Springs, Colorado

2008 Denver X-ray Conference & ICRS-8 Program
Table of Contents

Exhibitor Booth Assignments....2
Exhibit Floor Plan....3
2008 Exhibitors....4
Information for Poster Session Authors & Chairs....12
Information for Session Speakers & Chairs....12
General Information....12
How to Find Publications....13
Evening Technical Sessions and Social Functions....14
Local Attractions....14
Monday Workshops
- Texture Analysis with Area Detectors....15
- Introduction to Rietveld....15
- Quantitative Analysis I....15
- Basic XRF....15
- Non-ambient XRD....15
- Combined Use of X-rays & Neutrons....15
- Quantitative Analysis II....16
- Energy Dispersive XRF....16

Tuesday Workshops
- Cultural Heritage & Conservation Apps I....16
- ICRS Workshop on Stress Analysis I....16
- XRF Specimen Preparation I....16
- Trace Analysis....17
- Cultural Heritage & Conservation Apps II....17
- Nanomaterials & Their Apps....17
- ICRS Workshop on Stress Analysis II....17
- High-throughput X-rays....17
- XRF Specimen Preparation II....17

DXC Monday XRD Poster Session....18
DXC Tuesday XRF Poster Session....20
DXC & ICRS Plenary Session: Stress & Society....22
DXC Wednesday Sessions
- New Developments in XRD & XRF Instrumentation....22
- Analysis of Nanomaterials....23
- Thin Films....24
- Fusion & Industrial Applications of XRF....24

DXC Thursday Sessions
- Cultural Heritage I....25
- Industrial Applications....25
- Regulatory Applications....26

2008 Denver X-ray Conference & ICRS-8 Program
Table of Contents

Cultural Heritage II 26
X-ray Microimaging 27
Microbeam X-ray Analysis I 27
High Temperature In-situ Analysis 28
Trace Analysis 28
DXC Friday Sessions
Microbeam X-ray Analysis II 29
Small Angle Scattering 29
Quantitative Analysis 30
ICRS Thursday Poster Session 31
ICRS Wednesday Sessions
Diffraction Techniques: Synchrotrons—Macrobeam & High Energy I 34
Modeling I 35
Diffraction Techniques: Laboratory Applications 36
Industrial Applications: Engineered Stresses 36
ICRS Thursday Sessions
Diffraction Techniques: Synchrotrons—Macrobeam & High Energy II 37
Diffraction Techniques: Neutron I 37
Relaxation Techniques: Hole Drilling 38
Relaxation Techniques: Slitting 38
Materials Engineering I 38
Industrial Applications: Layers & Composites 39
Industrial Applications: Thermal Processing 39
Diffraction Techniques: Neutron II 40
Diffraction Techniques: General Methods 40
Relaxation Techniques: Deep Hole & Contour 41
Other Measurement Techniques 41
Materials Engineering II 41
Industrial Applications: Miscellaneous 42
Industrial Applications: Welding 42
ICRS Friday Sessions
Diffraction Techniques: Synchrotrons—Microbeam 43
Modeling II 44
Fatigue & Fracture 44
Industrial Applications: Distortion & Machining 45
Industrial Applications: Friction Stir Welding 45
Abstracts 46
Author Index 200
Hotel Layout 208
ICRS Program-at-a-Glance ..... Inside back cover
DXC Program-at-a-Glance ..... Back Cover

Sponsor Appreciation

Special thanks to our premier sponsor:

PANalytical

Special Thanks to our evening reception sponsors:

Chemplex INDUSTRIES, INC.

GE Inspection Technologies

Thermo SCIENTIFIC

And to our coffee break sponsors:

PANalytical

GE Inspection Technologies

MDI Materials Data

And to our media sponsors

materialstoday

Exhibitor Information

Exhibit Information

Exhibits will be located in the Rocky Mountain Event Center (formerly the Columbine Ballroom) on the Ground Floor of the hotel. Please see the hotel layout on page 208 for the exact location.

Exhibit Hours:

Monday 10:00 a.m.–5:00 p.m.
Tuesday 10:00 a.m.–5:00 p.m.
Wednesday 12:00 p.m.–7:00 p.m.
Thursday 10:00 a.m.–2:00 p.m.

Don't miss the vendor-sponsored Wine and Cheese Reception Wednesday Evening 5:00–7:00 p.m.

2008 Denver X-ray Conference Booth Assignments as of July 2008

Company Name	Booth #(s)
American Stress Technologies	37
AMPTEK, Inc.	61
Analytical Services, Inc.	43
Anton Paar USA	45
Australian X-ray Tubes (AXT)	16
Blake Industries, Inc.	1
Bruker AXS, Inc.	22, 23, 24 & 25
Brushwellman Electrofusion Products	31
Chemplex Industries, Inc.	62
Corporation Scientifique Claisse Inc.	50 & 51
e2v Scientific Instruments Ltd	40
EDAX Inc.	29
GE Inspection Technologies	58 & 59
Hecus X-ray Systems GmbH	47
Herzog Automation Corp	18
HORIBA Jobin Yvon	33
Incoatec GmbH	13
Inel	32
Innov-X Systems	60
ICDD	52 & 53
Kitco Inc.	2
Materials Data, Inc. (MDI)	20 & 21
Micro Photonics	7
Mike Handley Analytical Services	17
MOXTEK, Inc.	28
PANalytical	54, 55, 56 & 57
Photonic Science Ltd.	3
PREMIER Lab Supply, Inc.	10 & 11
Princeton Instruments	9
PROTO Manufacturing Inc.	5 & 6
Rigaku	34, 35 & 36
Rocklabs	17
SCT/Euro-Industries	19
Sigma Chemicals	16
SII NanoTechnology USA, Inc.	39
Skyray Instrument	48 & 49
SPECTRO	30
SPEX Sample Prep LLC	38
TEC	46
Thermo Scientific	26 & 27
UltraVolt, Inc.	4
Wiley-Blackwell	44
Xenocs	8
XIA	12
XOS	41 & 42

Exhibit Floor Plan

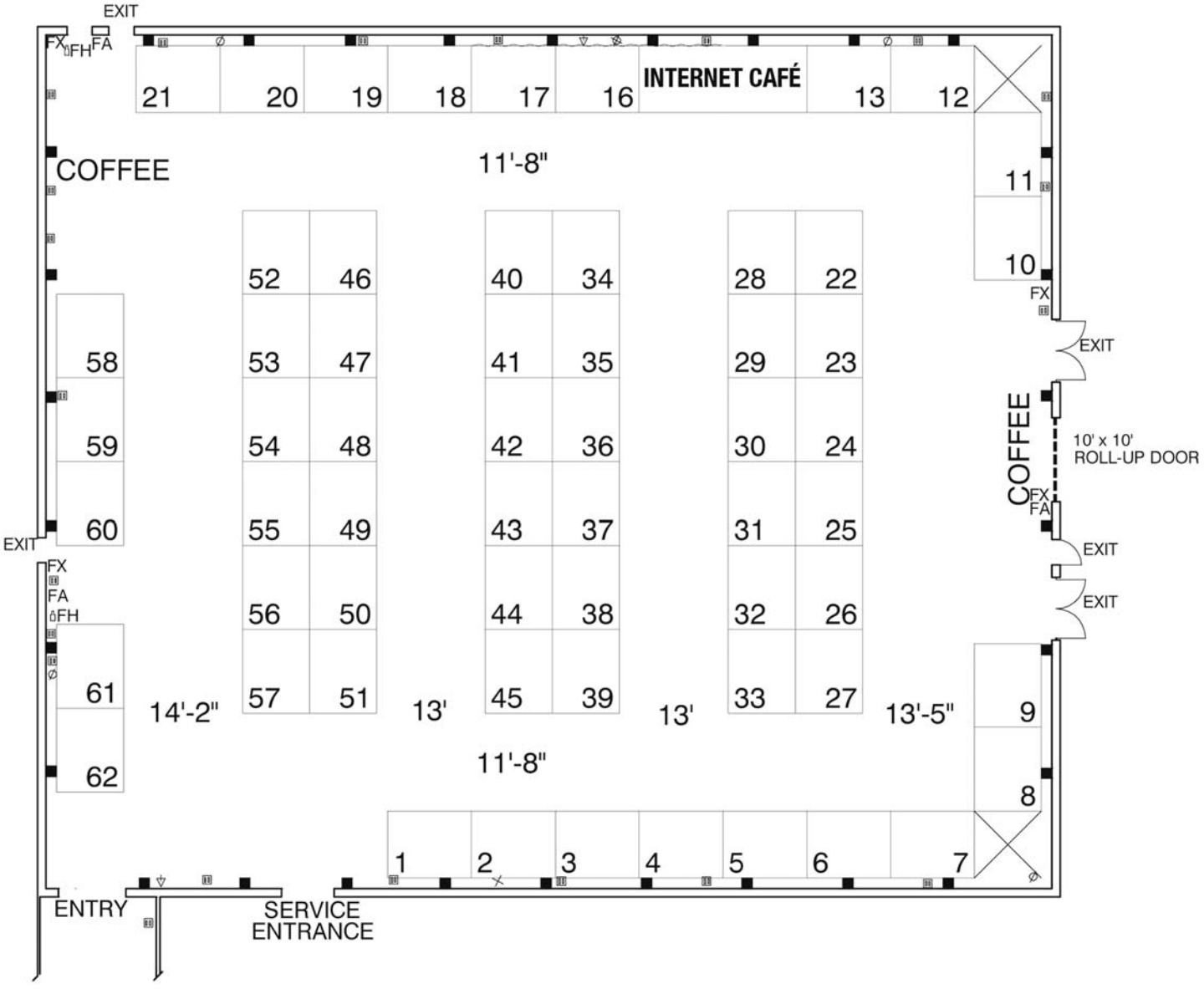

2008 Exhibitors

Company	Exhibitor Products
American Stress Technologies ***Booth: 37*** 840 Watercrest Way Cheswick, PA 15024 Phone: 724-410-1030 E-mail: info@astresstech.com Web: www.astresstech.com	Displaying our XSTRESS 3000 X-Ray diffraction system with a G3 goniometer for measuring residual stress. Also, being displayed is the PRISM Optical Imaging system for measuring residual stress. PRISM uses the stress-relaxation technique where a small hole is drilled into the material thus relaxing the stress along the hole boundaries. This deformation can be measured precisely using our electronic speckle pattern interferometry system.
AMPTEK, Inc. ***Booth: 61*** 14 DeAngelo Drive Bedford, MA 01730 Phone: 781-275-2242 E-mail: sales@amptek.com Web: www.amptek.com	Featuring thermoelectrically cooled Si-PIN, SDD and CdTe detectors, with their Preamplifiers and Digital Pulse Processors (DPP). Simple to use, low-cost systems for both laboratory and field use. The XR-100SDD detector and X-123SDD complete handheld spectrometer have 139eV resolution at 100,000 counts/ sec. See why OEMs have made Amptek their #1 choice.
Analytical Services, Inc. ***Booth: 43*** P.O. Box 7895 The Woodlands, TX 77387 Phone: 866-419-9229 E-mail: john@analyticalservicesinc.com Web: www.analyticalservicesinc.com	Analytical Services, Inc. is the manufacturer of calibration standards for the petroleum lubricants & crude oil industries. We have been in business for 15 years and strive for customer satisfaction. We also offer the standards for the WEEE/RoHS methods and Biodiesel industry. Please visit our web site at www.anlyticalservicesinc.com.
Anton Paar USA ***Booth: 45*** 10215 Timber Ridge Drive Ashland, VA 23005 Phone: 800-722-7556 E-mail: info.us@anton-paar.com Web: www.anton-paar.com	With 1000 employees worldwide, Anton Paar provides a dense customer support network. The company offers the most comprehensive range of attachments for non-ambient XRD and is a major supplier of small-angle X-ray equipment worldwide. The SAXSess system is the most versatile small-and-wide-angle X-ray scattering set-up on the market.
Australian X-ray Tubes Pty Ltd. ***Booth: 16*** U3/59 Myoora Road Terrey Hills, NSW 2084 Australia Phone: +61-2-94501359 E-mail: tubes@axt.com.au Web: www.axt.com.au	AXT supplies replacement X-ray tubes for most manufacturers with ready-to-ship inventory. Products include a new Varian ultra high performance tube for Philips/PANalytical PW2400 and similar equipment. Tubes are also available for ARL, Bruker, Siemens, Spectro, Rigaku and Shimadzu.
Blake Industries, Inc. ***Booth: 1*** 660 Jerusalem Rd Scotch Plains, NJ 07076 Phone: 908-233-7240 E-mail: blake4xray@worldnet.att.net	Blake Industries will be exhibiting X-ray diffraction equipment and accessories including goniometer heads, rotary tables, etc.

Company	Exhibitor Products
Bruker AXS, Inc. ***Booths: 22, 23, 24 & 25*** 5465 E. Cheryl Parkway Madison, WI 53711 Phone: 608-276-3000 E-mail: info@bruker-axs.com Web: www.bruker-axs.com	Bruker AXS designs and manufactures analytical X-ray systems for elemental analysis, materials research and structural investigations. Our innovative solutions enable a wide range of customers in heavy industry, chemistry, pharma, semiconductor, life science and nanotechnology to make technological advancements and to accelerate their progress.
Brushwellman Electrofusion Products ***Booth: 31*** 44036 South Grimmer Blvd. Fremont, CA 94538 Phone: 510-623-1500 E-mail: electrofusion@brushwellman.com Web: www.electrofusionproducts.com	Leader in the fabrication of Beryllium X-Ray tube and detector window assemblies for analytical, scientific, and medical industries. Thin beryllium windows (down to 8µm), protective coatings, metallic coatings for transmission windows, and a wide array of joining technologies. Other services include Electron Beam Welding, Vacuum Furnace Brazing, and Water Jet Cutting.
Chemplex Industries, Inc. ***Booth: 62*** 2820 SW 42nd Avenue Palm City, FL 34990 Phone: 772-283-2700 E-mail: sales@chemplex.com Web: www.chemplex.com	XRF Sample Preparation Equipment, Accessories, Supplies and Standards. Floor and table top sample grinders; comminution dishes, vials and ball pestles; manual and automatic briquetting presses; briquetting dies and aluminum pellet cups; grinding/briquetting powdered and tabletted additives; consumable liquid sample cups; thin-film sample support windows in rolls, precut circles and SpectroMembrane® carrier frames; automatic fusion machines; pre-fused fusion fluxes; SpectroCertified® Oil Standards.
Corporation Scientifique Claisse Inc. ***Booths: 50 & 51*** 350, rue Franquet, porte 45 Sainte-Foy, Quebec, G1P 4P3 Canada Phone: 418-656-6453 E-mail: info@claisse.com Web: www.claisse.com	World leader in sample preparation by fusion for XRF spectrometry, Claisse offers automatic fusion apparatus and platinum-ware for bead preparation. Industry leading fused fluxes feature the lowest moisture/highest purity with integrated non-wetting agents. See the new weighing/dosing machine “TheAnt” and the “rFUSION Modular System” for the latest in automated fusion capabilities.
e2v Scientific Instruments Ltd ***Booth: 40*** Sirius House, Watery Lane Wooburn Green High Wycombe, Bucks HP10 0AP UK Phone: +44 0 1628 533060 E-mail: e2vsi@e2v.com Web: www.e2vsi.com	e2v scientific instruments manufactures high performance detectors and pulse processors for x-ray spectroscopy. Both Silicon Drift Detectors (SDD) and LN-cooled Si(Li) detectors are produced for industrial and research applications ranging from Microanalysis (EDS) and X-Ray Fluorescence (XRF) to high rate synchrotron techniques like X-Ray Absorption Spectroscopy (XAS).
EDAX Inc. ***Booth: 29*** 91 McKee Drive Mahwah, NJ 07430 Phone: 201-529-4880 E-mail: info.edax@ametek.com Web: www.edax.com	Since 1962, EDAX Inc. has been a leader in technology, performance and value for energy dispersive X-ray fluorescence analytical systems. Today, the EDAX product range has expanded to include EDS/WDS X-ray microanalysis, EBSD, SEM/TEM electron diffraction and crystallographic analysis, and micro-EDXRF measurement systems.

2008 Exhibitors

Company

GE Inspection Technologies
Booths: 58 & 59
50 Industrial Park Road
Lewistown, PA 17044-9344
Phone: 866-243-2638
Web: www.geinspectiontechnologies.com

GE Inspection Technologies is a leading innovator in technology-driven non-destructive testing (NDT) inspection solutions that deliver productivity, quality and safety. The company produces radiographic, ultrasonic, remote visual inspection and eddy current solutions for applications in a wide range of industries, including aerospace, power generation, oil & gas, process and automotive.

Hecus X-ray Systems GmbH
Booth: 47
Reininghausstrasse 13 A
Graz, A-8020
Austria
Phone: +43-316-48 11 18
E-mail: office@hecus.at
Web: www.hecus.at

The new *Hecus S3-MICRO: SAXS/SWAXS/GISAXS for the routine bio-nanoanalytical laboratory*. Revolutionary X-ray point-focussing optics (exclusive from Xenocs, Grenoble) provide higher brilliance than rotating anodes and bridge the gap to synchrotron beamlines. Extremely economical through 50-Watt microfocus tube. Applications: protein solution SAXS, nanoparticle sizing, thin-film structure analysis, LC phase mapping, nanopowder porosity.

Herzog Automation Corp.
Booth: 18
16600 Sprague, Suite 400
Cleveland, OH 44130
Phone: 440-891-9777
E-mail: herzog@herzogautomation.com
Web: www.herzogautomation.com

Herzog Automation Corp. is the leading supplier of manual and fully automatic sample preparation systems for spectrographic and X-ray analysis, tube delivery systems for sample transport, and laboratory automation for the steel, aluminum, cement and mining industries. Please visit our web site at www.herzogautomation.com for our full product line.

HORIBA Jobin Yvon
Booth: 33
3880 Park Avenue
Edison, NJ 08820-3012
Phone: 732-494-8660
E-mail: john.enterline@jobinyvon.com
Web: www.jobinyvon.com

XGT: X-Ray Fluorescence Microscopes provide the highest spatial resolution (10-microns) of any EDXRF microscope available. Our unique monocapillary X-Ray guidetubes using coaxial technology ensure¬What You See Is What You Measure. 100-micron and/or 1.2mm guidetubes with fast automated switching between tubes for increased sensitivity. XGT Exclusive-SLICE Software a NEW XRF methodology library for sample identification designed to archive, query, and compare X-Ray Spectra.

Incoatec GmbH
Booth: 13
Max-Planck-Strasse 2
Geesthacht, 21502
Germany
Phone: +49 4152 889 381
E-mail: administration@incoatec.de
Web: www.incoatec.de

Incoatec offers the microfocus source IμS™ and multilayer optics used in X-ray analytic equipment. Incoatec components and subunits enable scientists to form X-ray beams according to their individual requirements in various applications such as protein crystallography and high-resolution X-ray diffractometry. Incoatec also manufactures customized optics for synchrotrons.

Inel
Booth: 32
P.O. Box 147
Stratham, NH 03885
Phone: 603-778-9161
E-mail: inelinc@aol.com
Web: www.inel.fr

Inel is pleased to introduce the Equinox series of powder diffractometers. From the Equinox 1000 to 6000, there are diffractometers for all applications and budgets. We offer new systems, upgrades to existing systems such as software and hardware upgrades for Scintag and of course our unique curved position sensitive detectors.

Company	Exhibitor Products
Innov-X Systems ***Booth: 60*** 100 Sylvan Road, Suite 100 Woburn, MA 01801 Phone: 781-938-5005 E-mail: krussell@innovxsys.com Web: www.innov-xsys.com	Home of portable XRF for on-site, in-situ analysis of Mg-U; ppm to 100%. Handhelds with weather-proof, ultra-rugged integrated PC control or our classic removable PDA. X-50 Mobile XRF for closed-beam field operation at up to 25 times the power of handhelds for solids or liquids. Customized factory on-line and high volume sorting XRF's. Applications: RoHS, Geology, Environmental, Metals & Mining, and More.
International Centre for Diffraction Data ***Booths: 52 & 53*** 12 Campus Boulevard Newtown Square, PA 19073 Phone: 610-325-9814 E-mail: info@icdd.com Web: www.icdd.com	ICDD's material identification databases are designed for rapid materials identification and interfaced with diffractometers and data analysis systems of the world's leading software developers and manufacturers of X-ray equipment. The PDF is available in PDF-2 Release 2008 (211,107 entries); PDF-4+ 2008 (285,402 entries), PDF-4/Minerals 2008 (29,607 entries); and PDF-4/Organics 2008 (341,540 entries).
Kitco Inc. ***Booth: 2*** 620 Cathcart, Suite 900 Montreal, QC, H3B 1M1 Canada Phone: 514-875-4820 Web: www.platinum.kitco.com	Internationally renowned for precious metals, Kitco supplies a full line of crucibles and platinum ware for major XRF fusion machines. Kitco's products also include platinum dishes, electrodes, etc. Our terms to credit precious metals are among the most competitive in the industry. Visit our website at platinum.kitco.com for more details.
Materials Data, Inc. (MDI) ***Booths: 20 & 21*** 1224 Concannon Blvd. Livermore, CA 94550 Phone: 925-449-1084 E-mail: MDI@materialsdata.com Web: www.materialsdata.com	MDI develops and distributes software tools for X-Ray Powder Diffraction. MDI's industry-leading software (Jade, Ruby, Shadow, Riqas, jPowd, DataScan and FilmScan) enables customers to automate older systems, acquire, analyze and simulate XRD data delivering visually rich, reliable content. MDI (http://www.materialsdata.com) is the largest independent XRD software company in the world.
Micro Photonics ***Booth: 7*** 4972 Medical Center Circle Allentown, PA 18106 Phone: 610-366-7103 E-mail: info@microphotonics.com Web: www.microphotonics.com	The sole distributor of STOE diffractometers, Xenocs' microbeam source and optics, and Photonic Science detectors. We are the USA's number one source for X-ray diffraction equipment. We have a solution for all of your diffraction needs.
Mike Handley Analytical Services ***Booth: 17*** 16502 La Avenida Drive Houston, TX 77062 Phone: 281-286-8393 E-mail: info@myxrf.com Web: www.myxrf.com	Supplies sample preparation equipment (Rocklabs, Breitlander), consumables (Pt-ware and borate flux), refurbished X-Ray equipment, service, repair, maintenance, training, and application support to users of XRF equipment.

2008 Exhibitors

Company

MOXTEK, Inc.
Booth: 28
452 West 1260 North
Orem, UT 84057
Phone: 801-225-0930
E-mail: jpeterson@moxtek.com
Web: www.moxtek.com

MOXTEK, INC. is a leading provider of components for x-ray analytical instrumentation. MOXTEK products include small, low-power x-ray tubes; ultra low-noise JFETs for x-ray and gamma ray detectors; high-performance, room-temperature PIN diode detectors; and AP3 polymer and DuraBeryllium™ EDS and WDS detector windows, including sealed proportional counter windows for light element analysis.

PANalytical
Booths: 54, 55, 56 & 57
117 Flanders Road
Westborough, MA 01581
Phone: 508-647-1100
E-mail: amcc.info@panalytical.com
Web: www.panalytical.com

PANalytical has provided innovative X-ray solutions from the first commercial diffractometer (1948) until today. XRD systems now feature hard radiation suitable for laboratory PDF experiments, a new SAXS solution and new non-ambient/humidty solutions. The Axios WDXRF systems offer SST-mAX X-ray tubes with ZETA technology for ultimate long term stability. Epsilon 5 and the Minipals cover the range of EDXRF applications.

Photonic Science Ltd.
Booth: 3
Rue Maryse Bustie
38590 St Etienne de St Geoirs
France
Phone: +33 4 7693 57 20
E-mail: info@photonic-science.com
Web: www.photonic-science.co.uk

Photonic Science manufactures X-ray CCD detectors for diffraction: powder, small molecule, proteins, thin films, as well as low flux X-ray scattering experiments (small and wide angle) and imaging applications: phase contrast, diffraction enhanced as well as very high resolution tomography. PSL will also introduce a new back scattered Laue system.

PREMIER Lab Supply, Inc.
Booths: 10 & 11
2714 SW Edgarce Street
Port St. Lucie, FL 34953
Phone: 772-873-1700
E-mail: info@premierlabsupply.com
Web: www.premierlabsupply.com

Sample Preparation Specialists by XRF for Liquids, Loose Powders, Pressed Pellets and Fusions. We manufacture and supply Liquid XRF Sample Cups, Films, Grinding & Binding Products, Glassware, PHOENIX Fusion Machines and Platinum Lab Ware items. http://www.premierlabsupply.com.

Princeton Instruments
Booth: 9
3660 Quakerbridge Road
Trenton, NJ 08619
Phone: 609-587-9797
E-mail: moreinfo@piacton.com
Web: www.piacton.com

Princeton Instruments' X-Ray Group, the manufacturer of scientific X-ray systems, has introduced new X-ray systems—PIXIS-XO, Quad-RO, NanoXF and PIXIS-XF—for direct and indirect detection of X-rays between <30 eV and >50 KeV. Stop by booth #9 to discuss your specific requirements with our product specialists.

PROTO Manufacturing, Inc.
Booth: 5 & 6
1980 E. Michigan Avenue
Ypsilanti, MI 48198
Phone: 313-965-2900
E-mail: xrdlab@protoxrd.com
Web: www.protoxrd.com

PROTO Manufacturing is a leading provider of portable and laboratory based XRD residual stress measurements systems, X-ray tubes and custom XRD systems. PROTO Manufacturing also provides residual stress measurement services through it's laboratories in the United States and Canada.

Company

Rigaku
Booths: 34, 35 & 36
9009 New Trails Drive
The Woodlands, TX 77381
Phone: 281-362-2300
E-mail: info@rigaku.com
Web: www.rigaku.com

Rigaku provides the world's most complete line of X-ray diffraction and X-ray fluorescence instruments and components, including benchtop XRD and WDXRF systems, multilayer optics, the modular and extensible Ultima IV and SmartLab® diffractometers with SAXS and in-plane capabilities, and the ZSX Primus series of high-powered WDXRF spectrometers with mapping capabilities, in either tube-above or tube-below configurations.

Rocklabs Ltd
Booth: 17
161 Neilson Street
Auckland
New Zealand
Phone: +64 9 634 7696
E-mail: sales@rocklabs.com
Web: www.rocklabs.com

Rocklabs are World Leaders in the manufacture of sample preparation equipment for analytical chemistry. Products include ring and puck mills (shatterbox), with agate, chrome steel/carbon steel, tungsten carbide and zirconia heads/pots. The range includes crushers, rotating sample dividers, Mechanized and Automated Sample Preparation Systems capable of processing more than 1000 samples per day. Plus Certificated Reference Material for gold assaying.

SCT/Euro-Industries
Booth: 19
3578 Hartsel Drive, Unit #E356
Colorado Springs, CO 80920
Phone: 719-264-6111
E-mail: sct@euro-industries.net
Web: www.sct-ceramics.com

SCT is an ISO certified producer of ceramics-to-metal and sapphire-to-metal seals and assemblies. In particular, SCT is the word's largest provider of brazed ceramics/metal assemblies to a worldwide base of X-ray tube manufacturers for medical and industrial applications. The entire process, including design, rapid prototyping, small to high volume production, brazing, welding, testing, etc. is located on a single integrated site.

Sigma Chemicals
Booth: 16
228 Balcatta Road
Balcatta, 6021
Western Australia
Phone: +61 89 345 2233
E-mail: keith.tyler@sigma-chem.com.au
Web: www.sigma-chem.com.au

Sigma Chemicals is a leading manufacturer of Ultra Pure Borate Fluxes and supplies to every part of the World. We are able to manufacture customised products to meet every chemist's requirements. Our flux customers also take advantage of our custom designed Platinum labware manufactured by our subsidiary Sigma Precious Metals.

SII NanoTechnology USA, Inc.
Booth: 39
19865 Nordhoff Street
Northridge, CA 91324
Phone: 818-280-0745
E-mail: info@siintusa.com
Web: www.siintusa.com

SII NanoTechnology USA Inc, features the world's largest reliable LN2 free, excellent resolution, Silicon Drift, X-Ray Detector. Despite extremely high-throughput, there is virtually zero peak shift or loss in resolution. Optimized for XRF, the Vortex® cycles without degradation in performance featuring cool down times of < 3 minutes. Visit us in booth # 39.

Skyray Instrument Co. Ltd.
Booths: 48 & 49
Skyray Building, Tsing Hua Science Park
1666 South Weicheng Road
Kunshan, 215347
People's Republic of China
Phone: +86 755 8145 9353
E-mail: sales@gold-tester.com
Web: www.gold-tester.com

Plating Thickness Analysis Expert: it is tailor-made for rapid and non-destructive detection of plating thickness and elemental content in large-size devices. It adopts the top lightening structure,3-D movable sample platform and laser positioning system, which enables the possibility of the point-by point detection of plating thickness and elemental content on large-size parts.

Exhibitor Products

2008 Exhibitors

Company	Exhibitor Products
SPECTRO ***Booth: 30*** 91 McKee Drive Mahwah, NJ 07430 Phone: 201-642-3000 Web: www.spectro.com	SPECTRO Analytical Instruments, Inc., is a recognized global leader in ED-XRF, ICP and Arc/Spark spectroscopy. SPECTRO offers a complete line of ED-XRF instrumentation including the SPECTRO iQ II, the SPECTRO XEPOS that can be delivered with pre-installed application packages, the SPECTRO MIDEX M and the compact SPECTRO PHOENIX II system.
SPEX Sample Prep LLC ***Booth: 38*** 203 Norcross Avenue Metuchen, NJ 08840 Phone: 800-LAB-SPEX x 465 E-mail: sampleprep@spexcsp.com Web: www.spexcsp.com	SPEX SamplePrep provides products for grinding, pressing and pelletizing for XRF and other analytical methods, this includes Freezer/Mills, the world's only true cryogenic mills. In addition to this SPEX SamplePrep offers Katanax one and 5 place Electric Fluxers for inorganic sampling by fusion for XRF, AA, ICP and wet chemistry analysis.
TEC ***Booth: 46*** 10737 Lexington Drive Knoxville, TN 37932 Phone: 865-966-5856 E-mail: info@tecstress.com Web: www.tecstress.com	TEC will be displaying the TEC 4000 X-Ray Diffraction System. TEC provides portable residual stress and retained austenite measurement equipment and laboratory services. Any size part can be measured in house or in the field without the need for destructive sectioning. TEC's Materials Testing Services are A2LA accredited and ISO 9001 registered.
Thermo Scientific ***Booths: 26 & 27*** 5225 Verona Road Madison, WI 53711 Phone: 608-276-6100 E-mail: analyze@thermofisher.com Web: www.thermo.com/elemental	Thermo Scientific will highlight our solutions for materials analysis and characterization from portable to fully automated operation. We will display product enhancements to our Niton portable, hand-held X-Ray probes, the ARL QUANT'X ED-XRF spectrometer, the ARL Advant'X XRF with IntelliPower and ARL 9900 X-Ray Workstation with integrated XRF-XRD capability.
UltraVolt, Inc. ***Booth: 4*** 1800 Ocean Avenue Ronkonkoma, NY 11779 Phone: 631-471-4444 E-mail: csd@ultravolt.com Web: www.ultravolt.com	UltraVolt manufactures over 450 models of standard product high efficiency high-voltage DC/DC converters. Output voltages range from 0 to 62V through 0 to 40kV with output power from 4W to 250W. Units feature output over-current protection with self-recovery. Ultra-low ripple is available down to <3mV. Modular and rack-mount units available.
Wiley-Blackwell ***Booth: 44*** 111 River Street 4-02 Hoboken, NJ 07030 Phone: 201-748-6000 Web: www.wiley.com	Wiley is a global publisher of professional, consumer, scientific and technical books, journals, textbooks and education materials. Among it's many imprints are the world renowned "For Dummies" line as well as Webster's New World, CliffNotes, Frommers, Betty Crocker books, and Jossey-Bass. To see more about these and our other imprints, visit Wiley at www.wiley.com.

Company	Exhibitor Products
Xenocs ***Booth: 8*** 19, rue Blumet Sassenage, F-38360 France Phone: +33 4 76 26 9540 E-mail: info@xenocs.com Web: www.xenocs.com	Xenocs, distributed in the USA by MicroPhotonics, supplies X-ray optics and sources for XRD, XRR, SAXS/WAXS, WD-XRF, EPMA. The newly introduced single reflection Fox3D optics deliver unprecedented flux in a high quality beam, leading to significant improvements in data quality. Combined with GeniX source, the result is equivalent to a traditional RAG, but in an economical, low-maintenance, and user-friendly package.
XIA LLC (formerly X-ray Instrumentation Associates) ***Booth: 12*** 31057 Genstar Road Hayward, CA 94544 Phone: 510-401-5760 E-mail: sales@xia.com Web: www.xia.com	X-ray Instrumentation Associates (XIA) produces advanced X-ray detector electronics and related instruments for applications in research and industry. Our core technology is high-performance digital pulse processors, available in both flexible stand-alone and dedicated embedded configurations. From low-power, handheld spectrometry to integrated multielement systems, XIA provides state of the art solutions at an affordable price.
X-ray Optical Systems, Inc. ***Booths: 41 & 42*** 15 Tech Valley Drive East Greenbush, NY 12061 Phone: 518-880-1500 E-mail: info@xos.com Web: www.xos.com	XOS manufactures X-ray optics and beam systems. The company's design, manufacture, and characterization capabilities of polycapillary, monocapillary and doubly curved crystal optics, enables a range of focusing and collimating lens options. The product line of polychromatic and monochromatic X-Beam's provides an optimized integration of X-ray optics and sources. Applications include texture, stress, and phase ID, as well as film thickness and composition measurements.

Information for: Poster Session Authors & Chairs, Session Speakers & Chairs & General Information

Poster Presentation Authors

Poster papers are to be posted 15 minutes prior to the start of the session. Authors should be present during the hours of 6:00 p.m.–8:00 p.m. Four-foot-high by eight-foot-wide poster boards will be provided. YOU SHOULD BRING YOUR OWN THUMBTACKS OR VELCRO. Posters should have the name and local phone number of the presenting author displayed should someone wish to contact the author while at the conference. The three best papers in each session will be selected and will receive certificates by mail. The names of the winners will be posted the following morning on an announcement board near the conference registration desk. PLEASE REMOVE YOUR POSTER IMMEDIATELY AFTER THE POSTER SESSION. ICDD is not responsible for any poster(s) left in the room.

Oral Presentation Authors

All speakers are asked to meet with their Session Organizer 15 minutes before the start of their session in the room in which the session will be held. These meetings assure the organizer that you are present, and also give you time to prepare your presentation materials.

Speaker Ready Room

A preparation room will be available for speakers' use during the conference. Please check at the conference registration desk for the exact location.

Manuscripts

Manuscripts for publication in *Advances in X-ray Analysis*, Volume 52, can be deposited at the conference registration desk throughout the week. The CD-ROM will also include the proceedings for the 8th International Conference on Residual Stresses. If you have not yet prepared your manuscript, remember the deadline for submission is 1 September 2008. Please mail two hard copies of the manuscript to:

Denise Flaherty, ICDD
12 Campus Boulevard
Newtown Square, PA 19073-3273 U.S.A.

General Information

Poster Boards

The poster boards used during the evening poster sessions will be 4' high x 8' wide boards. Authors must bring their own thumbtacks or Velcro.

Employment Clearinghouse

We will have a separate bulletin board to announce employment opportunities. Prospective employers and employees should bring announcements with them for posting.

How to Find Publications and Presentations of the Denver X-ray Conference

The Denver X-ray Conference has been held annually for 57 years. In recent history, approximately 200 presentations have been given at each conference and between 50 and 100 papers are annually published in the proceedings of the Denver X-ray Conference, *Advances in X-ray Analysis* (AXA). In 1996, *Advances in X-ray Analysis* transitioned from a book format, published by Plenum Press, to a CD format, published by the ICDD. In an agreement with Plenum, Volumes 1 through 39 (1957-1996) were published in a single CD. Since 1996, there has been an annual CD release corresponding to each year's conference. The series, *Advances in X-ray Analysis,* is now contained in 51 Volumes and represents approximately 2900 articles from experts in the field.

Since AXA is published as an electronic proceedings, it is not indexed by all electronic search engines. Internet searches can find both publications and proceedings of the Denver X-ray Conference, but users need to be directed to use the appropriate web portals. Fortunately, major web portals such as Google, Google Scholar, Scitation and SciFinder can be used.

Publications by Direct Search

The easiest way to find publications in AXA is to use the cumulative author and title index that is contained in the AXA CD. A CD has been sent to each registered attendee of the Denver X-ray Conference since 1996. For those that do not attend the conference, the CDs, both past and present, are available for sale from the ICDD.

Chemical Abstract Services indexes all Volumes of AXA. Web portals relating to Chemical Abstract Service, such as SciFinder and Dialog, are able to search AXA and find title and abstract content. These are paid services, often available through libraries or employers.

Past Publications by Free Web Access 1996-2003

The ICDD, in collaboration with the Denver Organizing Committee, have made available past volumes of AXA proceedings starting from 1996. Access to past volumes is provided free of charge, though the webpage http://www.icdd.com/resources/axasearch/AXA_login.php.

Volumes are posted approximately 12 months after publication of the CD which is typically one year after the conference. Today, publications from 1996 to 2003 are available with search capability and full publication content from the webpage.

Presentation Searches through Scitation and Powder Diffraction

In 2003, the ICDD and Denver Organizing Committee announced a collaboration between AXA and *Powder Diffraction*. Starting in 2003, the entire program of the Denver X-ray Conference has been annually published in *Powder Diffraction*, this includes all presentations and authors. In addition, an annual edition of *Powder Diffraction* containing select (15–20) publications from each annual meeting is published. Institutional and library subscribers of *Powder Diffraction* are sent a copy of the AXA CD. *Powder Diffraction* is published by the American Institute of Physics (AIP) and can be searched through AIP's web portal Scitation. Scitation provides authors and titles for presentations, as well as abstracts for published papers in *Powder Diffraction*, free of charge. Full publications can be downloaded by subscription or individual per article payment.

Googling

Google searches by author name will typically find content from the ICDD web site as well as the Scitation web site. Please remember that Scitation references are through *Powder Diffraction*, not AXA, which is why an author name search is more effective than a journal search. Google has the advantage of finding presentation titles, as well as author titles. Google Scholar has a more narrowly defined search engine that finds publication content. An author search on Google Scholar will identify publications in *Powder Diffraction*, but not presentation or proceedings content.

Overall, the most comprehensive search is to use Google with author names. This finds presentations and publications cross-referencing content on multiple web sites. If the results are too broad, try to narrow the range by adding typical keywords (e.g., X-ray, fluorescence, diffraction, Rietveld, etc).

Evening Technical Sessions & Social Functions & Local Attractions

Spouses are welcome to attend all social functions. Wine & Cheese Receptions and Poster Sessions will be held in the Evergreen Ballroom, unless noted otherwise.

Sunday
3 August *6:00–8:00 pm* Welcoming Reception
Sponsored by Thermo Scientific & ICDD

Monday
4 August *6:00–8:00 pm* XRD Poster Session and Wine & Cheese Reception
Sponsored by PANalytical

Tuesday
5 August *6:00–8:00 pm* XRF Poster Session and Wine & Cheese Reception
Sponsored by Chemplex Industries, Inc. & GE Inspection Technologies

Wednesday
6 August *5:00–7:00 pm* Vendor-sponsored Wine & Cheese Reception to be held in the exhibit hall—Rocky Mountain Event Center

Spouses' Coffee Hour
All spouses are invited to attend a complimentary coffee hour, sponsored by the Denver X-ray Conference. Coffee, tea and pastries will be served in the Conifer 2 room from 9:30 to 10:30 a.m. on Monday and Tuesday. Information on local attractions and activities of interest will be provided.

Local Attractions*

Museums

Denver Art Museum, (303) 640-2793

Museum of Western Art, (303) 296-1880

Denver Museum of Natural History, (303) 322-7009

IMAX Theater, (303) 370-6300

Gates Planetarium, (303) 370-6351

Molly Brown House Museum, (303) 832-4092

Performing Arts

Denver Center for the Performing Arts, (303) 893-3272

Center Attractions, (303) 893-4100

Denver Center Theater Company, (303) 893-4000

Symphony Orchestra (Boettcher Concert Hall), (303) 592-7777

Temple Buell Theater, (303) 640-2862

Opera Colorado, (303) 778-6464

Paramount Theater, (303) 534-8336

Other Area Attractions

Denver Botanic Gardens, (303) 331-4000

Hudson Gardens, (303) 797-8565

The Denver Zoo, (303) 331-4100

Elitch Gardens, (303) 455-4771

Coors Field, (303) 762-5437

Mile High Stadium, (303) 649-9000

Red Rocks Outdoor Amphitheater, (303) 572-4700

Fiddler's Green Outdoor Amphitheater, (303) 220-7000

South Metro Denver Movie Theaters

AMC Theaters, Highlands Ranch 24
C-470 & Broadway, (303) 790-4262

Mann Theaters, Tamarac Square
7777 E. Hampden, (303) 755-5100

United Artists, Continental
Hampden & I-25, (303) 758-2345

United Artists, Greenwood Plaza
8141 E. Arapahoe Road, (303) 741-1200

*Reprinted with permission from Denver Marriott Tech Center, Denver CO.

Monday morning 9:00 a.m.–12:00 p.m.

XRD

Texture Analysis with Area Detectors

Evergreen "A"

Organizers & Instructors:

B. B. He, Bruker AXS, Inc., Madison, WI
T. N. Blanton, Eastman Kodak Company, Rochester, NY
R. Tissot, Sandia National Labs, Albuquerque, NM
U. Preckwinkel, Bruker AXS, Inc., Madison, WI

Advantages of area detectors for texture analysis have been well recognized by many users. Compared to point or line detectors, texture can be measured using area detectors with high sensitivity, high speed and high accuracy. Area detectors can reveal the microstructure and texture information simultaneously. Texture measurement is extremely fast since diffraction intensities and backgrounds for multiple poles and multiple directions can be measured simultaneously. The orientation relationship between different layers of films or coating and substrate can be accurately measured since all diffraction patterns of all layers and substrate are collected with the same sample orientations. This workshop will cover the recent progress in theory, instrumentation, data collection and analysis strategy with area detectors for texture analysis.

Introduction to Rietveld

Evergreen "B"

Organizer & Instructor:

J.A. Kaduk, INEOS Technologies, Naperville, IL

The first half of this Workshop will be aimed at beginners to the Rietveld method. We will cover some basic theory, but the main emphasis will be on the actual process of refinement, which parameters to refine, and what the parameters mean. In the second half, the emphasis will be on quantitative phase analysis, the use of chemical information in the refinement and its interpretation, and other topics of interest.

XRF

Quantitative Analysis I

Evergreen "C"

Organizer & Instructors:

M. Mantler, Vienna University of Technology, Vienna, Austria
B. Vrebos, PANalytical, Almelo, The Netherlands
W.T. Elam, EDAX/University of Washington, Redmond, WA

Part 1 (Morning):

1. Classical fundamental parameter models and mathematical foundation.
2. Fundamental parameter models for thin films (introduction).
3. Coherent and incoherent scattering (introduction).
4. Compensation Methods.
5. Obtaining net intensities (includes background subtraction, line overlaps).

Basic XRF

Evergreen "D"

Organizers & Instructors:

W.T. Elam, EDAX/University of Washington, Redmond, WA
G.J. Havrilla, Los Alamos National Laboratory, Los Alamos, NM

This workshop provides a basic introduction to the principles of XRF, and is specifically aimed at those new to the field. It will consist of a general overview of the technique, followed by more specific details of the basic principles with emphasis on understanding how to use XRF and what its capabilities are. A few particular applications will be presented to provide an understanding of how the basic principles affect actual practice.

Monday afternoon 2:00 p.m.–5:00 p.m.

XRD

Non-ambient XRD

Evergreen "A"

Organizer & Instructors:

S.T. Misture, NYS College of Ceramics at Alfred University, Alfred, NY
E.A. Payzant, Oak Ridge National Laboratory, Oak Ridge, TN
S. Skinner, Imperial College London, London, England
C. Resch, Anton Paar GmbH, Graz, Austria

Use of high temperature instrumentation for laboratory X-ray, synchrotron, and neutron diffraction systems will be covered in detail. The workshop will focus on high temperature studies under controlled atmosphere, and will include details of instrumentation and calibration, with special emphasis on pitfalls and problems. Finally, some examples of applications and advanced data analysis will be included.

Combined Use of X-rays and Neutrons

Evergreen "B"

Organizer & Instructors:

A. Huq, **J. Hodges, L. Coates**, Spallation Neutron Source, Oak Ridge, TN

X-rays and Neutrons are complementary scattering techniques for characterizing structures and dynamics of materials of interest that range from solid state oxides to proteins. Neutron scattering lengths are independent of the atomic number of elements as a result of which neutrons can distinguish between isotopes of the same element and are good at detecting light elements in the presence of heavier elements in families of compounds such as metal oxide, hydrides, etc. In biological samples, one can make use of the substitution of hydrogen with deuterium to locate their position. This half-day workshop will be dedicated to understanding the fundamentals

of using both X-rays and Neutrons along with specific examples of how to analyze combined sets of X-ray and Neutron data from the same sample.

XRF

Quantitative Analysis II — Evergreen "C"

Organizer & Instructors:

M. Mantler, Vienna University of Technology, Vienna, Austria
B. Vrebos, PANalytical, Almelo, The Netherlands
W.T. Elam, EDAX/University of Washington, Redmond, WA

Part 2 (Afternoon):
1. Analysis of thin films.
2. Modeling (computing) of inc+coh scattering, polarization.
3. EDS: Detector response function.
4. EDS: Background subtraction.
5. EDS: Artifacts in spectra.

Energy Dispersive XRF — Evergreen "D"

Organizer & Instructors:

B. Scruggs, EDAX, Inc., Mahwah, NJ
J. Heckel, Spectro Analytical, Kleve, Germany
C. Streli, P. Wobrauschek, Atominstitut—Vienna University of Technology, Vienna, Austria

The Energy Dispersive X-ray Fluorescence (ED-XRF) workshop provides a comprehensive review of XRF spectroscopy for both the beginner and experienced X-ray spectroscopist. Topics to be covered are instrumentation including sources and detectors, and qualitative and quantitative analysis. Applications will be discussed including mobile, online, bulk and micro ED-XRF analyses.

Tuesday morning 9:00 a.m.–12:00 p.m.

XRD & XRF

Cultural Heritage and Conservation Applications I — Evergreen "A"

Organizer & Instructors:

K. Trentelman, Getty Conservation Institute, Los Angeles, CA
L. Glinsman, National Gallery of Art, Washington, D.C.
A. Drews, Ford Research & Advanced Engineering, Dearborn, MI
C. McGlinchey, The Museum of Modern Art, New York, NY
C. Namowicz, Getty Conservation Institute, Los Angeles, CA

This workshop will explore the application of XRF and XRD to the study of cultural heritage materials. Lectures will describe the types of questions about works of art these techniques are used to help answer; the limitations of analyzing works of art, where sampling or even touching the object may not be allowed; the types of instrumentation that have been utilized in this field over the past several decades; and the optimization of portable XRF instruments. In addition, a panel discussion and hands-on session will explore further the issues and challenges involved in the analysis of works of art.

XRD

ICRS-8 Workshop on Stress Analysis I — Evergreen "D"

Organizers & Instructors:

I.C. Noyan, Columbia University, New York, NY
M. Prime, Los Alamos National Laboratory, Los Alamos, NM
C.E. Murray, IBM – T.J. Watson Research Center, Yorktown Heights, NY
T.R. Watkins, Oak Ridge National Laboratory, Oak Ridge, TN
A. Ulyanenkov, Bruker AXS GmbH, Karlsruhe, Germany
M. Hill, University of California, Davis, CA
D. Goudar, University of Bristol, Bristol, UK
D. Brown, Los Alamos National Laboratory, Los Alamos, NM

This workshop will cover stress determination techniques using mechanical and diffraction methods as well as briefly reviewing basics of stress/strain and residual stress. It will be a basic tutorial aimed at engineers starting out to make such measurements, select measurement techniques, or just understand and interpret results. We will cover hole drilling, slitting, contour, layer removal and eigenstress analysis, as well as neutron and X-ray diffraction techniques.

XRF

XRF Specimen Preparation I — Evergreen "C"

Organizer & Instructors:

J.A. Anzelmo, Anzelmo & Associates, Inc., Madison, WI
D. Broton, CTL Group, Skokie, IL
L. Arias, Bruker AXS, Madison, WI
J. Metz, Sharp and Howells Pty Ltd, Bulleen, Australia

The workshop will begin in the morning with a review of simple ratio method techniques and continue through more advanced internal ratio preparation methods of analysis involving the fusion process (Metz). A discussion of sample preparation physics and a detailed discussion of the fusion method of sample preparation will follow (Anzelmo). The afternoon session will begin with an overview of the sampling process including equipment and techniques starting from the bulk sample through specimen preparation (Broton). This will be followed by a detailed description of liquid analysis techniques and equipment (Arias).

Trace Analysis — Evergreen "B"

Organizer & Instructors:

P. Wobrauschek, Atominstitut—TU Wien, Vienna, Austria
R. Van Grieken, University of Antwerp, Antwerp, Belgium
G. Havrilla, Los Alamos National Laboratory, Los Alamos, NM

Motivation to analyze sample on their trace element contents are many fold, mostly driven by possible health hazards of some chemical elements, but also while observing changing material characteristics.Trace analysis requires physical and technical efforts to improve detection limits in XRF. A variety of approaches are available as modern excitation sources and X-ray optics to improve the beam quality, excitation geometries can be varied from conventional 45 degree incidence to gracing incidence leading to TXRF. Sample preparation techniques like micro spots using nanoliter to picoliter droplets open new interesting fields of applications. Impact and importance on a wide range of materials including environmental and biological systems will be given.

Tuesday afternoon 2:00 p.m.–5:00 p.m.

XRD & XRF

Cultural Heritage and Conservation Applications II — Evergreen "A"

Organizer & Instructors:

K. Trentelman, Getty Conservation Institute, Los Angeles, CA
L. Glinsman, National Gallery of Art, Washington, D.C.
A. Drews, Ford Research & Advanced Engineering, Dearborn, MI
C. McGlinchey, The Museum of Modern Art, New York, NY
C. Namowicz, Getty Conservation Institute, Los Angeles, CA

Instrument Representatives:

B.Kaiser, Bruker-AXS, Kennewick, WA
J. Feuer, Innov-X System, Woburn, MA
S. Piorek, Thermo Fisher Scientific, Billerica, MA

For description, please see Cultural Heritage and Conservation Applications I on page 16.

Nanomaterials and Their Applications — Evergreen "E&F"

Organizers & Instructors:

R.L. Snyder, Georgia Institute of Technology, Atlanta, GA
V. Petkov, Central Michigan University, Mt. Pleasant, MI
Z.L. Wang, Georgia Institute of Technology, Atlanta, GA
B. Bunker, University of Notre Dame, Notre Dame, IN

This workshop will focus on the synthesis, applications and characterization of nanomaterials. We will begin with a broad survey of their synthesis and unusual properties with a wide survey of their applications. We will then move on to focus on the ways we can characterize these atomic and molecular structured materials.

XRD

ICRS-8 Workshop on Stress Analysis II — Evergreen "D"

Organizers & Instuctors:

I.C. Noyan, Columbia University, New York, NY
M. Prime, Los Alamos National Laboratory, Los Alamos, NM
C.E. Murray, IBM – T.J. Watson Research Center, Yorktown Heights, NY
T.R. Watkins, Oak Ridge National Laboratory, Oak Ridge, TN
A. Ulyanenkov, Bruker AXS GmbH, Karlsruhe, Germany
M. Hill, University of California, Davis, CA
D. Goudar, University of Bristol, Bristol, UK
D. Brown, Los Alamos National Laboratory, Los Alamos, NM

For description, please see Stress Analysis I on page 16

High-throughput X-rays — Evergreen "B"

Organizer & Instructors:

B. Toby, Argonne National Laboratory–APS, Argonne, IL
K. Chapman, APS—Argonne National Laboratory, Argonne, IL
B. He, Bruker AXS, Inc., Madison, WI

New powder diffraction methods and instrumentation, particularly at synchrotron X-ray sources, have greatly expanded experimental capabilities. Complete high quality diffraction measurements, with a data range suitable for pair distribution analysis, can be collected in a fraction of a second. The new 11-BM instrument at the APS offers high resolution diffraction patterns, optimal for indexing, structure solution and refinement, which can be collected in less than an hour. This 11-BM instrument will be available to the public for mail-in use—a first for US powder diffraction. The goals of this half-day workshop are to provide an overview to the instrumentation utilized for high-throughput diffraction capabilities and some background on the support infrastructure needed to support high-throughput work. In the case of the 11-BM diffractometer, attendees will learn about how to use this instrument for their own research.

XRF

XRF Specimen Preparation II — Evergreen "C"

Organizer & Instructors:

J.A. Anzelmo, Anzelmo & Associates, Inc., Madison, WI
D. Broton, CTL Group, Skokie, IL
L. Arias, Bruker AXS, Madison, WI
J. Metz, Sharp and Howells Pty Ltd, Bulleen, Australia

For description, please see XRF Specimen Preparation I on page 16.

Monday, 4 August, XRD Poster Session
Evergreen Ballroom, 6:00 p.m.–8:00 p.m.

Reception Sponsor

PANalytical

The Monday evening Poster session will be held in conjunction with a Wine and Cheese Reception, sponsored by PANalytical.

Chairs: **T.N. Blanton**, Eastman Kodak Company Research Labs, Rochester, NY
J.A. Kaduk, INEOS Technologies, Naperville, IL

Session chairs will select the three best posters for awards.

D-3 X-ray Probe Analyses of Complicated Precipitates Formed in Copper-Base Alloys
S. Sato, Y. Takahashi, T. Sanada, NISSAN ARC, LTD., Kanagawa, Japan
K. Shinoda, K. Wagatsuma, S. Suzuki, Tohoku University, Miyagi, Japan 46

D-7 State-of-the-Art Multilayer Optics for Diffractometry
B. Hasse, C. Michaelsen, A. Oehr, F. Hertlein, S. Kroth, Incoatec GmbH, Geesthacht, Germany 46

D-10 Synthesis, Structural and Chemical Characterization of $Ca(HO_3PCH_2)_2$-N(H)-$(CH_2)_6$-N(H)-$(CH_2PO_3H)_2 \cdot 2H_2O$
L. León-Reina, A. Cabeza, R.M.P. Colodrero, M.A.G. Aranda, University of Málaga, Málaga, Spain
E. Barouda, K.D. Demadis, University of Crete, Crete, Greece 46

D-12 Particle Size Analysis of Sub Micron Materials Using Ultra Small Angle X-ray Scattering
K. Nagao, T. Konya, R. Matsuo, Y. Iwasaki, Rigaku Corporation, Tokyo, Japan 47

D-13 A Study on The Total Evaluation of Pharmaceutical Products Using General Purpose XRD Equipment
M. Sasaki, T. Kubo, A. Kishi, Rigaku Corporation, Tokyo, Japan 47

D-14 X-ray Diffractometric Determination of Chrysotile Asbestos in Building Materials with Rietveld Refinement
T. Asahi, S. Kobayashi, T. Matsudaira, K. Nakayama, M. Kitano, T. Nakamura, Meiji University, Kanagawa, Japan 47

D-15 Investigation of Co-Crystallized Pharmaceutical Ingredients Using Synchrotron Radiation
M. Herrmann, U. Förter-Barth, H. Kröber, P.B. Kempa, M. Juez-Lorenzo, Fraunhofer ICT, Pfinztal, Germany
S. Doyle, ISS ANKA FZK, Karlsruhe, Germany 48

D-21 Usage of Probability Scoring to Sort XRPD Scans of Dying Protein on Similarity
T. Degen, PANalytical B.V., Almelo, The Netherlands
I. Margiolaki, J.P. Wright, European Synchrotron Radiation Facility (ESRF), Grenoble, France 48

D-23 Zirconium Oxide: Rietveld and Reverse Monte Carlo Analyses
F. Zhang, S. Lun, A. Lui, S.-W. Chan, Columbia University, New York, NY
P.J. Chupas, P.L. Lee, Argonne National Laboratory, Argonne, IL
J.C. Hanson, W.A. Caliebe, Brookhaven National Laboratory, Upton, NY 48

D-26 Quantitative Determination of Asbestos in Bulk Insulation by XRD
D.S. Kendall, R.A. Martinez, US EPA, Denver, Colorado 49

D-29 High-Temperature Characterization of Three-Dimensional Distribution of Residual Stresses in CrN Coatings on Steel
K.J. Martinschitz, Ch. Kirchlechner, J. Keckes, R. Daniel, Ch. Mitterer, University of Leoben, Leoben, Austria 49

D-31 Mechanical Properties of Thin Films Characterized by a Combination of $\sin^2\psi$; and X-ray Diffraction Substrate Techniques
K.J. Martinschitz, J. Keckes, University of Leoben, Leoben, Austria 50

D-32 X-ray Diffraction Study of Anisotropic State of Residual Stress After Down-Cut and Up-Cut Face Grinding
Z. Pala, N. Ganev, Czech Technical University in Prague, Prague, Czech Republic
J. Drahokoupil, ASCR, Prague, Czech Republic 50

D-38 Probing the Micro-Mechanical Behavior of Bone Via High-Energy X-rays
J. Almer, Argonne National Laboratory, Argonne, IL
S. Stock, Northwestern University, Chicago, IL 50

D-39 The X-ray Diffraction Characteristics of Different Materials
Y. Zhang, J. Liu, X. Xu, Beijing University of Technology, Beijing, P.R.China 51

D-43 New Analytical Expression of the Threshold Limit of the Mixing Parameter of Pseudo-Voigt Function
F. Hadj Larbi, A. Khereddine, D. Bradai, USTHB, Algiers, Algeria 51

D-52 Residual Stresses After CMP on Thin Films
W.-E. Fu, Industrial Technology Research Institute, Hsinchu, Taiwan
M.-K. Chen, C.-C.A. Chen, National Taiwan University of Science and Technology, Taipei, Taiwan 51

Monday, 4 August, XRD Poster Session
Evergreen Ballroom, 6:00 p.m.–8:00 p.m.

WITHDRAWN

D-59 The Rietveld Refi...
A. Yilmaz, S. Seyyi..., Ankara, Turkey 52

D-61 Automated SAXS Measurements of Protein Solutions with a Laboratory Based SAXS System
M. Kriechbaum, P. Laggner, P. Herrnegger, Austrian Academy of Sciences (IBN), Graz, Austria and Hecus X-ray Systems GmbH, Graz, Austria....52

D-63 Quantification of Retained Austenite in ASTM A743 Grade CA6NM Cast Martensitic Stainless Steel Through X-ray Diffraction
J.V. Rojas Marín, A. Toro Betancur, National University of Colombia, Antioquia, Columbia 52

D-65 A New High-Throughput SAXS Screening Tool
P. Kotnik, H. Schnablegger, Anton Paar GmbH, Graz, Austria
G. Langenbucher, Anton Paar USA, Ashland, VA....53

D-68 X-ray Diffraction and High Pressure Studies on Organic Thermal Energy Storage Materials—TRIS(Hydroxymethyl) Aminomethane (TRIS)
W.-M. Chien, V.K. Kamisetti, J.C. Fallas, E.D. Emmons, D. Chandra, A.M. Covington, University of Nevada–Reno, Reno, NV
R.S. Chellappa, Carnegie Institution of Washington, Washington, DC
M. Kunz, S. Clark, Lawrence Berkeley National Laboratory, Berkeley, CA....53

D-70 Grazing-Incidence Diffraction Applied as a Crosscutting Tool in the Nanobio Regime
B.D. Pate, X. Han, The Dow Chemical Company, Midland, MI
D.T. Keane, Northwestern University, Chicago, IL
S.P. Wargacki, R.A. Vaia, M.F. Durstock, Air Force Research Laboratory
H-S. Kim, S.-M. Choi, Korea Advanced Institute of Science and Technology 53

D-71 X-ray Diffraction Characterization of MOVPE ZnSe Films Deposited on (100) GaAs Using Conventional and High-Resolution Diffractometers
T.N. Blanton, C.L. Barnes, M. Holland, K.B. Kahen, Eastman Kodak Company, Rochester, NY
V. Gupta, F. Bai, Rochester Institute of Technology, Rochester, NY 54

Post Deadline Posters:

D-73 Measurement Conditions for Quantitative Analysis Using the Rietveld Method
E. Kagami, A. Takase, Rigaku Corporation, Tokyo, Japan 54

D-74 Phase Transformation and Structural Behavior Studies of Li-Based Hydrides After Pressure Hydriding/De-Hydriding Cycling
W.-M. Chien, J.H. Lamb, D. Chandra, University of Nevada–Reno, Reno, NV....54

D-76 Chemometric Applications in Quantitative X-Ray Powder Diffraction of Intact Consolidated Samples
M.D. Moore, C. Hair, P.L.D. Wildfong, Duquesne University, Pittsburgh, PA 55

D-77 The Use of Net Analyte Signal Orthogonalization in the Separation of Multi-Component Diffraction Patterns Obtained from X-Ray Powder Diffraction of Intact Compacts
M.D. Moore, R.P. Cogdill, S.M. Short, C. Hair, P.L.D. Wildfong, Duquesne University, Pittsburgh, PA....55

D-78 Analysis of Focused Beam Powder X-ray Diffraction Using Curved Crystal Optics
A. Bingölbali, C.A. MacDonald, University at Albany, SUNY, Albany, NY 56

Tuesday, 5 August, XRF Poster Session
Evergreen Ballroom, 6:00 p.m.–8:00 p.m.

Reception Sponsors

GE Inspection Technologies

Chemplex INDUSTRIES, INC.

The Tuesday evening Poster session will be held in conjunction with a Wine and Cheese Reception, sponsored by Chemplex Industries, Inc. and GE Inspection Technologies.

Chairs: **P. Palmer**, San Francisco State University, San Francisco, CA
J. Kawai, Kyoto University, Kyoto, Japan

Session chairs will select the three best posters for awards.

F-45 High-Resolution XRF in 35-60 KEV:-Lanthanides' K-Spectra
M. Mizusawa, K. Sakurai, National Institute For Materials Science, Ibaraki, Japan
Y. Terada, Japan Synchrotron Radiation Research Institute, Spring-8, Hyogo Japan 57

C-6 Thin Film Technology for Preparation of X-ray Waveguide-Resonators
E.V. Egorov, V.K. Egorov, IMT RAS, Chernogolovka, Moscow District, Russia
R.E. Ayala-Jiménez, Fisichem Incorporated, Miami, FL
M.S. Afanas'ev, MIREA, Moscow, Russia 57

C-4 Radioisotope Rh-101 as X-ray Source for Instruments on Space Missions
Ch. Stenzel, Astrium Gmbh, Friedrichshafen, Germany
Ch. Schroer, Tu Dresden, Dresden, Germany
B. Lengeler, RWTH Aachen, Germany
R. Vianden, Univ. of Bonn, Germany 58

F-16 Radioactive Sample Effects on EDXRF Spectra
C.G. Worley, Los Alamos National Laboratory, Los Alamos, NM 58

F-57 Tabletop Spectrometer for Grazing Incidence XRF
N. Zoeger, D. Ingerle, C. Streli, F. Meirer, P. Wobrauschek, Atominstitut, Tu Wien, Vienna, Austria
G. Pepponi, Fondazione Bruno Kessler-irst, Povo, Italy 58

F-56 Micro X-ray Fluorescence Spectrometer for Light Element Analysis with Low Power Tube Excitation
S. Smolek, C. Streli, N. Zoeger, P. Wobrauschek, F. Meirer, Atominstitut, Tu Wien, Vienna, Austria 59

F-55 Grazing-Exit-XRF Experiments at Hasylab Beamline L
F. Meirer, C. Streli, P. Wobrauschek, N. Zoeger, Atominstitut, Tu Wien, Vienna, Austria
G. Pepponi, Fondazione Bruno Kessler-irst, Povo, Italy 59

F-54 Sample Morphology: Influence on Total Reflection X-ray Fluorescence Analysis
C. Horntrich, F. Meirer, C. Streli, P. Kregsamer, N. Zoeger, P. Wobrauschek, Atominstitut, Tu Wien, Vienna, Austria
G. Pepponi, Fondazione Bruno Kessler-irst, Povo, Italy 60

F-59 Dosage of Silica in Polymers by X-ray Fluorescence
P. Ricou, S. Kodjie, X. Shen, Arkema Inc., King of Prussia, PA 60

F-30 Development of Soil Standard Materials Containing Hazardous Metals for X-ray Fluorescence Analysis
Y. Shibata, J. Suyama, M. Kitano, T. Nakamura, Meiji University, Kawasaki, Kanagawa, Japan 60

F-19 Preparation of the Multi-Layered Plastic Reference Materials for Confocal 3D-Micro X-ray Fluorescence Analysis
K. Nakano, K. Tsuji, Osaka City University, Osaka, Japan 61

F-22 Sample Preparation for Total-Reflection X-ray Fluorescence Analysis of Blood Samples
K. Tsuji, H. Matsui, M. Hino, H. Wanibuchi, Osaka City University, Osaka, Japan
H. Kohno, K. Aranami, Y. Shimizu, T. Yamada, Rigaku Industrial Corporation, Osaka, Japan 61

F-23 Large Area Silicon Drift Detectors
A. Pahlke, T. Eggert, S. Pahlke, R. Stoetter, F. Wiest, KETEK GmbH, Munich, Germany 62

F-17 Crystalline Phase Analysis and Elemental Analysis of Alkali-Washed Fly Ash and Activated Sludge Ash
A. Ohbuchi, M. Kitano, T. Nakamura, Meiji University, Kanagawa, Japan 62

F-58 X-ray Fluorescence (XRF) Analysis of Hanford Low Activity Waste Simulants: Method Development
D.M. Missimer, A.R. Jurgensen, R.L. Rutherford, Savannah River National Laboratory, Aiken, SC 62

F-47 Analysis of Ores and Concentrates by Using Benchtop WDXRF
Y. Kataoka, H. Homma, Y. Yamada, H. Kohno, Rigaku Industrial Corporation, Osaka, Japan
H. Inoue, Rigaku Americas Corporation, The Woodlands, TX 63

Tuesday, 5 August, XRF Poster Session
Evergreen Ballroom, 6:00 p.m.–8:00 p.m.

C-10 The Synergy of XRD and XRF in a Shale and Slate Analysis
L. Fields, M. Martin, Rigaku Americas Corporation, The Woodlands, TX 63

F-33 Handheld XRF for Archaeometallurgical Studies: In-Situ Alloy and Metal Analysis of a Private Sword Collection
J. Feuer, T. Turner, K. Russell, Innov-X Systems, Inc., Woburn, MA 63

F-46 Applications of Polarized EDXRF ... amples
T. Nakamura, T. M ... poration, Osaka, Japan
H. Inoue, Rigaku ... The Woodlands, TX 64

WITHDRAWN

F-78 Tissue Elemental Mapping Using HDXRF with Doubly Curved Crystals
D. Li, Z. Chen, X-ray Optical System, Inc., East Greenbush, NY
A.H. Koeppen, S.C. Michael, V.A. Medical Center, Albany, NY 64

F-70 Healthy Pharmaceutical Drugs—Control of Impurities in Active Pharmaceutical Ingredients by EDXRF
K. Behrens, A. Scothern, H. Ress, Bruker AXS GmbH, Karlsruhe, Germany
A. Seyfarth, Bruker AXS Inc., Madison, WI 64

F-84 Evaluation of X-ray Fluorescence Spectrometers for Possible Implementation in a Manufacturing Laboratory—Metals In Alumina
L.L. Brehm, D.W. Burns, The Dow Chemical Company, Midland, MI 65

Post Deadline Posters:

C-21 Structure Analysis and Extinction Coefficient of PbSe Colloidal Nanocrystals
I. Moreels, D. De Muynck, F. Vanhaecke, Z. Hens, Ghent University, Ghent, Belgium 65

F-73 Expanding the Analytical Range of WDXRF—New XRF Analyzer Crystals
K. Behrens, Bruker AXS GmbH, Karlsruhe, Germany
A. Seyfarth, Bruker AXS Inc., Madison, WI 66

F-75 The Quantitative Link—The Way to Better Results
K. Behrens, Bruker AXS GmbH, Karlsruhe, Germany
L. Arias, A. Seyfarth, Bruker AXS Inc., Madison, WI 66

F-88 Analysis of Sapphire and Ruby by EDXRF
R.E. Phillips, Thermo Scientific, West Palm Beach, FL
C.M. Breeding, Gemological Institute of America 67

Plenary Session: Stress and Society
Wednesday a.m. Evergreen Ballroom

Chairs: **I.C. Noyan**, Columbia University, New York, NY
M. Prime, Los Alamos National Laboratory, Los Alamos, NM
E. Üstündag, Iowa State University, Ames, IA

8:30 Chairman of the Denver X-ray Conference, Welcoming Remarks
Robert L. Snyder, Georgia Institute of Technology, Atlanta, GA

8:35 Presentation of Awards

2008 Birks Award presented to Rene Van Grieken, University of Antwerp, Antwerp, Belgium
Presented by: **Tim Elam**, EDAX/University of Washington, Redmond, WA

2008 Jerome B. Cohen Student Award (winner announced at the plenary session)
Presented by **Cev Noyan**, Columbia University, New York, NY

2008 McMurdie Award presented to Jeffrey Dann, OSRAM Sylvania, Towanda, PA
Presented by: **Thomas Blanton**, Eastman Kodak Company Research Labs, Rochester, NY

8:45 Plenary Session Remarks by the Chairs

The following are the invited papers to be presented during the plenary session:

9:00 S214 Materials State Awareness: Dealing with Uncertainty in Design and Service
R.B. Thompson, Iowa State University, Ames, IA . . . 68

9:45 S191 Dental Stress, Mechanical Not Psychological, Even Some Residual Stress
M. Bagby, West Virginia University School of Dentistry, Morgantown, WV . . . 68

10:30 Break

11:00 S212 Residual Stresses in U.S. Nuclear Power Systems
A.A. Csontos, U.S. Nuclear Regulatory Commission, Washington, D.C. . . . 68

11:45 S190 More Miles for Tired Iron: The Application of Engineered Compressive Residual Stresses in Aging Aircraft
M. Shepard, US Air Force Research Laboratory, WPAFB, OH . . . 69

XRD & XRF New Developments in XRD & XRF Instrumentation
Wednesday p.m. Evergreen "A"

Chair: **V.E. Buhrke**, Consultant, Portola Valley, CA

1:30 D-19 High-Performance Silicon Strip Detector for In-House XRD System
T. Taguchi, H. Toraya, M. Kuribayashi, Rigaku Corporation, Tokyo, Japan
P. Grybos, R. Szczygiel, P. Maj, AGH University of Science and Technology, Krakow, Poland . . . 70

1:45 D-6 X-ray Diffractometry with a Microfocus Source
B. Hasse, C. Michaelsen, Incoatec GmbH, Geesthacht, Germany
U. Preckwinkel, H. Cordes, N. Yang, Bruker AXS Inc., Madison, WI . . . 70

2:00 D-34 Wavelet Analysis of X-ray Diffraction Signal From Measurements of Stress and Austenite
G. Roy, CANMET/MTL, Ottawa, Ontario, Canada . . . 70

2:15 D-51 New High-Performance Device for Parallel-Beam X-ray Diffractometer Scan
H. Toraya, Rigaku Corporation, Tokyo, Japan . . . 71

2:30 D-25 An Innovative EDXRD Probe
C.M. Dozier, N. Anibou, XStream Systems, Inc., Sebastian, FL . . . 71

2:45 D-66 Detectors for Demanding X-ray Diffraction Experiments
K. Knorr, B. Hinrichsen, G. Vanhoyland, Bruker AXS, Karlsruhe, Germany . . . 71

3:00 F-71 New S2 PICOFOX Benchtop TXRF
A. Seyfarth, M. Rider, Bruker AXS Inc., Madison, WI
H. Stosnach, A. Gross, Bruker AXS Microanalysis, Berlin, Germany . . . 72

3:15 Break

3:30 F-53 New Development for the Automation of Borate Fusion Sample Preparation for XRF
L. Bérubé, Corporation Scientifique Claisse, Sainte-Foy, Quebec, Canada 72

3:45 F-81 High Volume Scrap Material Sorting Using XRF
E. Brown, D. Carolan, X. Chen, J. Egan, B. Hubbard-Nelson, R. Nasella, I. Rosmarin, R. Russell, D. Sackett, C. Weaver, Innov-X Systems, Inc., Woburn, MA 73

4:00 F-76 Turn-Key Solutions with Integrated Flexibility From Package to Real Solution
K. Behrens, Bruker AXS GmbH, Karlsruhe, Germany
K. Roscoe, A. Seyfarth, Bruker AXS Inc., Madison, WI 73

4:15 F-7 Development of a Novel Multi-Element Silicon Drift Detector Array
L. Feng, V.D. Saveliev, C.R. Tull, S. Barkan, M. Takahashi, E.V. Damron, SII NanoTechnology USA Inc., Northridge, CA. 73

4:30 F-64 Expanding the Detector Efficiency of Silicon Drift Detectors with Optimized Radiation Entrance Window
A. Niculae, H. Soltau, G. Lutz, P. Lechner, A. Bechteler, R. Eckhardt, K. Hermenau, PNSensor GmbH, Munich, Germany
O. Jaritschin, A. Liebel, A. Simsek, PNDetector GmbH, Munich, Germany
G. Schaller, F. Schopper, L. Strüder, MPI Semiconductor Laboratory, Munich, Germany 74

4:45 F-66 Mg-Based Multilayer XRF Analyzers with Two- and Three-Layers Structure Design
Y. Platonov, J. Rodriguez, G. Fournier, Rigaku Innovative Technologies, Auburn Hills, MI
K. Shimizu, Rigaku Industrial Corporation, Osaka, Japan 74

5:00 C-3 Microfocus Liquid-Metal-Jet X-ray Tubes and Applications
O. Hemberg, M. Otendal, Excillum AB, Stockholm, Sweden
T. Tuohimaa, H.M. Hertz, Royal Institute of Technology, Stockholm, Sweden 75

XRD & XRF Analysis of Nanomaterials
Wednesday p.m. Evergreen "B"

Chairs: **R.L. Snyder**, Georgia Institute of Technology, Atlanta, GA
V. Petkov, Central Michigan University, Mt. Pleasant, MI

1:30 D-75 Possibilities and Limitations of X-Ray Diffraction Using High Energy X-rays on a Laboratory System
H. te Nijenhuis, M. Gateshki, M. Fransen, PANalytical, Almelo, The Netherlands 76

1:50 C-17 *Invited*—Formation of Novel Oxide Nanostructures
Z.L. Wang, Georgia Institute of Technology, Atlanta, GA 76

2:20 C-18 Pulsed Laser Deposition Technique for the Synthesis of Nanostructures
J.-I. Hong, M. Kirkham, J. Bae, Z.L. Wang, R.L. Snyder, Georgia Institute of Technology, Atlanta, GA 77

2:40 F-60 *Invited*—XAFS Studies of Nanosystems: How X-ray, Electron Microscopy, and Optical Techniques Each Contribute to Structural Characterization
B.A. Bunker, University of Notre Dame, Notre Dame, IN. 77

3:10 Break

3:40 C-12 *Invited*—Hard X-ray Full Field 3D Imaging with sub-50 nm Resolution
A. Tkachuk, M. Feser, F. Duewer, J. Gelb, G. Hsu, S. Wang, W. Yun, Xradia, Inc., Concord, CA 77

4:10 D-57 Alumina-Supported Palladium Catalyst Crystallite Size Determination by EXAFS, XRD, and TEM
E.J. Peterson, T.R. Conant, P. Burton, A. De La Riva, J.P. Gabaldon, L.R. Houk, H. Pham, K. Lovato, J. Paiz, A.K. Datye, University of New Mexico Center for Micro-Engineered Materials, Albuquerque, NM. 77

4:30 D-33 *Invited*—Natural Nanoparticle Shape, Structure, Properties and Reactivity from X-ray Studies
G.A. Waychunas, B. Gilbert, Y.-S. Jun, J.F. Banfield, Lawrence Berkeley National Laboratory, Berkeley, CA
H. Zhang, University of California at Berkeley, Berkeley, CA
C. Kim, Chapman University, Orange, CA 78

4:50 D-72 Analysis of the Crystalline Structure and Magnetic Properties of Fe Nanoparticles
T.C. Monson, D.L. Huber, J.M. Lavin, Sandia National Labs, Albuquerque, NM
V. Petkov, Central Michigan University, Mt. Pleasant, MI
Y. Ren, APS – Argonne National Laboratory, Argonne, IL 78

XRD Thin Films

Wednesday p.m. Evergreen "C"

Chairs: **T.N. Blanton**, Eastman Kodak Company Research Labs, Rochester, NY
T. Huang, Emeritus, IBM Almaden Research Center, San Jose, CA

2:00 D-60 *Invited*—Determination of Crystallographic Polarity of Thin Films Using High Resolution XRD
K. Inaba, Rigaku Corporation, Tokyo, Japan . . . 79

2:30 D-28 Local Residual Stresses and Thermal Fatigue in CrN Coatings on Steel Characterized by High-Temperature Synchrotron X-ray Diffraction
K.J. Martinschitz, Ch. Kirchlechner, R. Daniel, Ch. Mitterer, J. Keckes, University of Leoben, Leoben, Austria . . . 79

2:50 D-30 A Novel Diffraction Technique to Determine Mechanical Moduli of Fibre-Textured Thin Films
K.J. Martinschitz, J. Keckes, University of Leoben, Leoben, Austria . . . 80

3:10 F-32 Simultaneous Determination of Main, Minor and Trace Elements in Fertilizers by Total Reflection X-ray Fluorescence
R.E. Ayala-Jiménez, C.H. Alvarado, Fisichem Inc., Miami, FL . . . 80

3:30 Break

3:50 D-1 *Invited*—Long Range Scans and Many-Beam Effects for High-Resolution X-ray Diffraction From Multilayered Structures
T.A. Ulyanenkova, T. Baumbach, University Karlsruhe, Karlsruhe, Germany
A.I. Benediktovich, I. Feranchuk, Belarussian State University, Minsk, Belarus
A. Ulyanenkov, Bruker AXS GmbH, Karlsruhe, Germany . . . 80

4:20 D-36 Grain Growth and Texture Sharpening in Copper, Nickel and Palladium Thin Films, Investigated by Non-Ambient X-ray Diffraction Measurements
Y. Kuru, M. Wohlschlögel, U. Welzel, E. Mittemeijer, Max Planck Institute for Metals Research, Stuttgart, Germany . . . 81

4:40 D-9 Determination of Activation Energy in Textured Metal-Metal Multilayer Films Via 2D XRD
M.A. Rodriguez, D.P. Adams, R.G. Tissot, Sandia National Laboratories, Albuquerque, NM . . . 81

XRF Fusion & Industrial Applications of XRF

Wednesday p.m. Evergreen "D"

Chair: **J.A. Anzelmo**, Anzelmo & Associates, Inc., Madison, WI

1:30 F-34 *Invited*—Further Studies of the Borate Fusion Method of Sample Preparation
M. Loubser, P.H. van Rooyen, J.P.R. de Villiers, University of Pretoria, Pretoria, South Africa . . . 82

2:00 F-83 Further Studies of the Borate Fusion Method of Sample Preparation: The Applications
M. Loubser, P.H. van Rooyen, J.P.R. de Villiers, University of Pretoria, Pretoria, South Africa . . . 82

2:20 F-74 Iron Ore Analysis—A New Approach for New Requirements
K. Behrens, Bruker AXS GmbH, Karlsruhe, Germany
A. Seyfarth, Bruker AXS Inc., Madison, WI . . . 82

2:40 F-9 New Development in Lithium Borate Fusion for Ferroalloys
P. Daigle, Corporation Scientifique Claisse, Inc., Ste-Foy, Quebec, Canada . . . 83

3:00 Break

3:20 F-82 *Invited*—Applications of XRF in the Oil Industry
R.W. Morton, ConocoPhillips, Bartlesville, OK . . . 83

3:50 F-50 Optimizing the Balance of Quality and Turnaround Time for a Process Control XRF Laboratory
S.W. Bowe, Kennecott Utah Copper, Magna, UT . . . 83

4:10 F-2 Finding an Element Tracer for Use in the Early Detection of 4½ Bearing Failure In J52P408 Engines by EDXRF
G.R. Humphrey, Joint Oil Analysis Program, Pensacola, FL . . . 84

4:30 F-44 Analysis of Heavy and Light Elements by Compact X-ray Fluorescence Spectrometer
K. Muraoka, Y. Araki, T. Utaka, K. Taniguchi, Institute of X-ray Technologies Co. Ltd, Osaka, Japan . . . 84

XRD & XRF Cultural Heritage I
Thursday a.m. Evergreen "A"

Chair: **K. Trentelman**, Getty Conservation Institute, Los Angeles, CA

9:00 F-77 *Invited*—Confocal X-ray Fluorescence of Paintings: Deconstructing an Atypical 17th C. Collaboration From Antwerp, Assessing a 14th C. Catalonian Panel, and Imaging a Lost N.C. Wyeth
J. Mass, Winterthur Museum, Winterthur, DE
A. Woll, Cornell High Energy Synchrotron Source, Ithaca, NY
C. Bisulca, Istituto di Ricerca sulle Onde Elettromagnetiche, Florence, Italy
M. Cushman, Williamstown Art Conservation Center, Williamstown, MA
N. Ocon, North Carolina Museum of Art, Raleigh, NC . . . 85

9:30 F-13 *Invited*—Discovery of a Hidden Van Gogh Painting by Means of High-Energy XRF Mapping
J. Dik, Technical University of Delft, The Netherlands
K. Janssens, University of Antwerp, Belgium
G. Van der Snickt, University of Antwerp, Belgium
K. Rickers, DESY, Hamburg, Germany
L. Van der Loeff, Kroeller-Mueller Museum, Otterlo, The Netherlands . . . 85

10:00 C-2 Ancient Warriors and the Origin of Chinese Purple
Z. Liu, Lawrence Berkeley National Laboratory, Berkeley, CA . . . 86

10:20 Break

10:40 C-1 XRF and XRD Analysis of Converted Lead Pigment on a Georgia O'Keefe Pastel Drawing
L.B. Brostoff, R.J. Speakman, Museum Conservation Institute, Smithsonian Institution, Suitland, MD
C. Maynor, Smithsonian American Art Museum, Smithsonian Institution, Washington, DC . . . 86

11:00 F-48 Research in the Identification and Provenancing of 20th Century Photographs
D.C. Stulik, A. Kaplan, Getty Conservation Institute, Los Angeles, CA
D. Miller, California State University at Northridge, Northridge, CA . . . 87

11:20 F-51 Determination of Strontium Concentrations in Calcium-Based Grounds with XRF & ICP-MS
C. Namowicz, M. Walton, K. Trentelman, Getty Conservation Institute, Los Angeles, CA . . . 87

11:40 F-68 X-ray Fluorescence of a Medieval Mosan Reliquary of Saint Amandus
J. Giaccai, Walters Art Museum, Baltimore, MD . . . 88

XRD & XRF Industrial Applications
Thursday a.m. Evergreen "B"

Chairs: **R.L. Snyder**, Georgia Institute of Technology, Atlanta, GA
E.A. Payzant, Oak Ridge National Laboratory, Oak Ridge, TN

9:00 D-37 *Invited*—X-ray and Thermal Analysis of Cements and Concrete for Evaluation of Cement Additives and Concrete Admixtures
J.P. Nicolich, D.R. Brown, F.G. Serafin, U.B. Latosiewicz, J.H. Cheung, P.J. Sandberg, W. R. Grace & Co. - Conn., Cambridge, MA . . . 89

9:30 D-2 Application of 2-Dimensional XRD for the Characterization of Microstructure of Self-Leveling Compounds (SLC)
S. Seifert, J. Neubauer, F. Goetz-Neunhoeffer, University of Erlangen-Nuremberg, Erlangen, Germany
H. Motzet, Schoenox GmbH, Rosendahl, Germany . . . 89

9:50 D-4 Quantitative In-Situ X-ray Diffraction Analysis of Early Hydration of Portland Cement at Defined Temperatures
C. Hesse, F. Goetz-Neunhoeffer, J. Neubauer, University of Erlangen-Nuremberg, Erlangen, Germany
M. Braeu, BASF Construction Chemicals, Trostberg, Germany
P. Gaeberlein, BASF Construction Chemicals GmbH, Trostberg, Germany
M. Degenkolb, PCI GmbH, Augsburg, Germany . . . 89

10:10 F-1 Analysis of Platinum Group Elements (PGE) by Means of Total Reflection X-ray Fluorescence (TXRF) Spectrometry
H. Stosnach, Bruker AXS Microanalysis GmbH, Berlin, Germany . . . 90

10:30 Break

10:50 D-20 *Invited*—Probing Thin-Layered and Nano-Structured Materials—X-ray Scattering Tools
J.F. Woitok, PANalytical, Almelo, The Netherlands 90

11:20 D-41 Residual Stress Analysis of Non-Polar GaN Epi-Layers By GIXRD
Y.-i. Jang, K.-h. Park, LG Electronics Institute of Technology, Seoul, Korea
S.-r. Cho, H.-k. Kwon, LG Innoteck, Seoul, Korea 91

11:40 D-16 Study on the X-ray Diffraction Behavior of a Big Crystal Grain in Oriented 3% Silicon Steel
J.F. Fang, Zh.L. Tian, J. Huo, J.Y. Zhang, Y. Zhang, Central Iron and Steel Research Institute, Beijing, P.R.China 91

XRF Regulatory Applications
Thursday a.m. Evergreen "C"

Chair: **W.T. Elam**, EDAX/University of Washington, Redmond, WA

9:00 F-85 *Invited*—Screening Toys and Consumer Goods with Handheld XRF
S. Piorek, Thermo NITON Analyzers LLC, Billerica, MA 92

9:30 F-8 Forensics Applications of X-ray Fluorescence Microscope
S. Mamedov, J. Goldey, G. Setola, A. Whitley, Horiba Jobin Yvon Inc., Edison, NJ. 92

9:50 F-28 FDA Regulatory Applications of Field Portable EDXRF
R.M. Jacobs, U.S. FDA, Alameda, CA
P.T. Palmer, CA SFSU, San Francisco, CA. 92

10:10 F-40 Searching for Pure Tin on Electronic Components: Tin Whisker Prevention
G.J. Havrilla, M. Sweet, Los Alamos National Laboratory, Los Alamos, NM 93

10:30 Break

11:00 F-72 RoHS Compliance in Paints and Resins
A. Seyfarth, Bruker AXS Inc., Madison, WI
A. Buehler, K. Behrens, Bruker AXS GmbH, Karlsruhe, Germany
J. Sardisco, Analytical Services, The Woodlands, TX 93

11:20 F-79 Choosing XRF for RoHS Applications
J.R. Bogert, Matrix Metrologies, Holbrook, NY. 94

11:40 F-43 Analysis of Elements in Environmental Samples by Micro-XRF
Y. Araki, Institute of X-ray Technologies Co. Ltd, Osaka, Japan
S. Maeo, M. Krämer, Osaka Electro-Communication University, Osaka, Japan
T. Utaka, K. Taniguchi, Institute of X-ray Technologies Co. Ltd, Osaka, Japan and Osaka Electro-Communication University, Osaka, Japan. 94

XRD & XRF Cultural Heritage II
Thursday p.m. Evergreen "A"

Chair: **K. Trentelman**, Getty Conservation Institute, Los Angeles, CA

2:00 C-8 *Invited*—Portable XRD/XRF Instrumentation for the Study of Works of Art
G. Chiari, Getty Conservation Institute, Los Angeles, CA
P. Sarrazin, inXitu, Inc., Mountain View, CA
M. Gailhanou, Université Paul Cézanne, Marseille, France 95

2:30 F-25 *Invited*—XRF Detection of Heavy Metal Pesticides in Archaeological and Anthropological Artifacts
A.N. Shugar, Art Conservation Dept., Buffalo State College, Buffalo, NY 95

3:00 F-52 On the Use of Handheld XRF for Determination of Arsenic and Mercury in a Museum Collection
K. Cross, P.T. Palmer, San Francisco State University, San Francisco, CA. 96

3:20 Break

3:40 F-49 Issues, Transitions and Collaborations Associated with Use of Hand-Held XRF in Natural History Museums
C. Podsiki, The Field Museum, Chicago, IL 96

4:00 D-47 Cultural Heritage Studies with High-Energy X-rays at the APS 1-ID Beamline
D.R. Haeffner, J.D. Almer, Argonne National Laboratory, Argonne, IL
F. Casadio, Art Institute of Chicago, Chicago, IL
D.C. Dunand, Northwestern University, Evanston, IL
B.D. Newbury, ExxonMobil Development Company, Houston, TX
M.L. Young, Ruhr-Universität, Bochum, Germany 97

4:20 F-6 The Yin and Yan of XRF Analysis as a Tool in the Investigation of Cultural Heritage Works
B.J. Kaiser, Bruker AXS, Kennewick, WA 97

4:40 F-61 SANDRA: A Portable XRF System for Non Destructive Studies of Mexican Cultural Heritage
J.L. Ruvalcaba Sil, Universidad Nacional Autónoma de México, Mexico DF, Mexico 97

XRD & XRF X-ray Microimaging
Thursday p.m. Evergreen "B"

Chair: **Q. Shen**, Northwestern University, Chicago, IL and APS—Argonne National Laboratory, Argonne, IL

1:30 C-13 *Invited*—Time Resolved X-ray Full-Field Micro-Imaging of Transient Fluid Dynamics
K. Fezzaa, APS – Argonne National Laboratory, Argonne, IL 98

2:00 F-12 *Invited*—A High Resolution Hard X-ray Bioimaging Facility At SSRL
P. Pianetta, J. Andrews, S. Brennan, SLAC, Menlo Park, CA
E. Almeida, NASA Ames Research Center, Moffett Field, CA
M. van der Meulen, Cornell University, Ithaca, NY
A. Tkachuk, J. Gelb, J. Rudati, M. Feser, W. Yun, Xradia, Concord, CA 98

2:30 C-19 3-D Tomographic Studies of Annealed Nanoporous Gold Using Transmission X-ray Microscope (TXM) at Advanced Photon Source
Y.-c. Chen, Q. Shen, Northwestern University, Evanston, IL and Argonne National Laboratory, Argonne, IL
Y. Chu, J. Yi, Argonne National Laboratory, Argonne, IL
M. Cox, D.C. Dunand, Northwestern University, Evanston, IL 99

2:50 D-58 Nanostructure Analysis of Metallic Materials by Coherent X-ray Diffraction Micro-
Y. Takahashi, H. Furukawa, H. Kubo, K.
Y. Ni
E. M ., Japan. 99

Moved to Friday ICRS session "Diffraction Techniques: Synchrotrons—Microbeam"

XRD & XRF Microbeam X-ray Analysis I
Thursday p.m. Evergreen "B"

Chairs: **K. Tsuji**, Osaka City University, Osaka, Japan
G.J. Havrilla, Los Alamos National Laboratory, Los Alamos, NM

3:30 C-9 *Invited*—Realtime XRF and XRD Imaging—The Instrumentation and the Applications
K. Sakurai, National Institute for Materials Science, Ibaraki, Japan 100

4:00 F-39 A Top-Down Approach Using X-ray Imaging Techniques: Instrumental Developments and Applications in Life Science
B. De Samber, T. Schoonjans, G. Silversmit, B. Vekemans, L. Vincze, R. Evens, K. De Schamphelaere, C. Janssen, B. Masschaele, L. Van Hoorebeke, University of Ghent, Ghent, Belgium
S. Bohic, European Synchrotron Radiation Facility, Grenoble, France
K. Rickers, G. Falkenberg, Hamburger Synchrotronstrahlungslabor at DESY/PETRA III, Hamburg, Germany 100

4:20 F-38 Applications of Confocal Micro X-ray Fluorescence 3-Dimensional Elemental Imaging
B.M. Patterson, Los Alamos National Laboratory, Los Alamos, NM. 101

4:40 C-22 Combined Micro-Xrf/Xrpd Tomography for the Characterization of FeCrAlY-Foam-Based Catalysts
K. Janssens, W. De Nolf, University of Antwerp, Wilrijk, Belgium
F. Basile, P. Benito, S. Bugani, G. Fornasari, L. Morselli, E. Scavetta, D. Tonelli, A. Vaccari, University of Bologna, Bologna, Italy 101

XRD High Temperature In-situ Analysis

Thursday p.m. Evergreen "C"

Chair: **S.T. Misture**, NYS College of Ceramics at Alfred University, Alfred, NY

2:00 D-35 *Invited*—In-Situ Characterisation of Novel Fuel Cell Materials
S.J. Skinner, Imperial College London, London, UK 102

2:30 D-11 In-Situ XRD Analysis of the Growth of ZnO Nanowires
M. Kirkham, Z.L. Wang, R.L. Snyder, Georgia Institute of Technology, Atlanta, GA 102

2:50 D-17 Kinetics of Particle Growth for Supported Pt And Pt/Pd Determined Using HTXRD
A.R. Drews, R.J. Kudla, Ford Research and Advanced Engineering, Dearborn, MI 102

3:10 D-54 In Situ Heating Studies on the Internal Stresses of Multilayer Environmental Barrier Coatings
B.J. Harder, K.T. Faber, Northwestern University, Evanston, IL
J. Almer, Advanced Photon Source, Argonne, IL
K.N. Lee, Rolls Royce Corporation, Indianapolis, IN 102

3:30 Break

3:50 D-48 Novel Processing of Nickel Containing Cordierite Glass-Ceramics for Microporous Gas Separation Membranes
M.E. Miller, S.T. Misture, Alfred University, Alfred, NY 103

4:10 D-44 Study of Combustion Syntheses by Time-Resolved X-ray Diffraction: Comparison of Synthesis Mechanisms for Different Combustion Modes
C. Curfs, J. Wright, G.B.M. Vaughan, ESRF, Grenoble, France
H. Boutefnouchet, Badji Mokhtar University, Annaba, Algeria 103

4:30 D-55 Nanoscale Photocatalysts Derived from Layered Phases: Formation and Characterization
E.J. Nichols, S.T. Misture, Alfred University, Alfred, NY 104

XRF Trace Analysis

Thursday p.m. Evergreen "D"

Chair: **M.A. Zaitz**, IBM, Hopewell Junction, NY

2:00 F-67 *Invited*—High-Definition X-ray Fluorescence: Principles and Applications
W.M. Gibson, D. Li, H. Huang, Z. Chen, X-ray Optical Systems, Inc., East Greenbush, NY 105

2:30 F-5 MCLLS Approach to EDXRF Analysis on XOS Devices
R.P. Gardner, F. Li, NC State University, Raleigh, NC
Z. Chen, M. Cusack, X-ray Optical Systems, Inc., East Greenbush, NY 105

2:50 F-18 Preconcentration of the Environmental Water by Agar for XRF Analysis
K. Nakano, K. Okubo, K. Tsuji, Osaka City University, Osaka, Japan 105

3:10 F-31 Heavy Metal Analysis of Water Samples Down to Sub-ppb Level by Using X-ray Fluorescence Analysis Combined with the Concentration Techniques
S. Hayakawa, M. Iwaki, Y. Nishimoto, K. Yamane, T. Hirokawa, Hiroshima University, Hiroshima, Japan. 106

3:30 Break

3:50 F-35 Automated Picoliter Solution Deposition for TXRF Analysis of Semiconductor Samples
C.M. Sparks, ATDF, Austin, TX
U. Fittschen, G. Havrilla, Los Alamos National Laboratory, Los Alamos, NM 106

4:10 F-37 Picoliter Deposition for MXRF Calibration and Quantification Using Prototype Thermal Inkjet Technology
U. Fittschen, G.J. Havrilla, Los Alamos National Laboratory, Los Alamos, NM 106

4:30 F-63 Synchrotron XRF Analyses of Element Distribution in Fossilized Sauropod Dinosaur Bones
A.R. Pyzalla, M. Dumont, Max-Planck-Institut fuer Eisenforschung GmbH, Duesseldorf, Germany
N. Zoeger, C. Streli, P. Wobrauschek, Atomic Institute of the Austrian Universities, Wien, Austria
M. Sander, University of Bonn, Bonn, Germany 107

XRD & XRF Microbeam X-ray Analysis II

Friday a.m. Evergreen "A"

Chairs: **K. Tsuji**, Osaka City University, Osaka, Japan
G.J. Havrilla, Los Alamos National Laboratory, Los Alamos, NM

8:30 C-11 *Invited*—Using Focused Hard X-rays for Investigations Related to Nuclear Waste Disposal
M.A. Denecke, Institut für Nukleare Entsorgung, Karlsruhe, Germany 108

9:00 D-40 Nanodiffraction From Perfect/Weakly-Deformed Single Crystals
H. Yan, Brookhaven National Laboratory, Upton, NY
O. Kalenci, C. Noyan, Columbia University, New York, NY
C. Murray, IBM TJ Watson Research Center, Yorktown Heights, NY
J. Maser, Argonne National Laboratory, Argonne, IL 108

9:20 D-27 Bifocal Miniature Toroidal X-ray Mirrors
S. Cornaby, D. Smilgies, D. Bilderback, CHESS, Ithaca, NY 108

9:40 F-20 Applications of Polycapillary Optics to Micro and Two Dimensional XRF Analysis
K. Tsuji, A. Matsuda, Osaka City University, Osaka, Japan
K. Nakano, Osaka City University, Osaka, Japan and JST Innovation Plaza Osaka, Osaka, Japan
S. Komatani, S. Ohzawa, H. Uchihara, Horiba. Ltd., Kyoto, Japan 109

10:00 Break

10:20 C-7 *Invited*—Latest Developments of Advanced X-ray Optics and Their Applications in X-ray Microanalysis
N. Gao, Z. Chen, I. Ponomarev, Y. He, W.M. Gibson, X-ray Optical Systems, Inc., East Greenbush, NY 109

10:50 F-24 Study of Microheterogeneity Using μ XRF, INAA, and Chemometric Methods
J.L. Molloy, J.R. Sieber, R. Zeisler, National Institute of Standards and Technology, Gaithersburg, MD 109

11:10 D-5 Analysis of Shear Stress Distribution in Al (Cu) Interconnects Induced by Electromigration Based on Schmidt's Law and Studied by Synchrotron Polychromatic X-ray Microdiffraction
K. Chen, K.N. Tu, UCLA, CA
N. Tamura, B.C. Valek, Lawrence Berkeley National Laboratory, Berkeley, CA 110

11:30 F-42 Quantitative Analysis of Nano-Particle by XRF
T. Utaka, N. Kawada, K. Taniguchi, Institute of X-ray Technologies Co. Ltd., Osaka, Japan and Osaka Electro-Communication University, Osaka, Japan
S. Maeo, M. Kurakado, Osaka Electro-Communication University, Osaka, Japan
Y. Araki, K. Muraoka, T. Itoh, Institute of X-ray Technologies Co. Ltd., Osaka, Japan 110

XRD Small Angle Scattering

Friday a.m. Evergreen "B"

Chair: **J. Ilavsky**, APS – Argonne National Laboratory, Argonne, IL

8:30 C-20 *Invited*—Structure and Kinetics of Self-Assembled Nanocyrstal Systems Probed by Small Angle X-ray Scattering Techniques
X.-M. Lin, J. Wang, Argonne National Laboratory, Argonne, IL 111

9:00 D-49 *Invited*—Flexibility and High Throughput: Supporting SAXS Users at a Joint Industrial Academic Beamline
S. Weigand, B. Stillwell, D.T. Keane, Northwestern University, Evanston, IL
W.E. Guise, E.I. DuPont de Nemours & Co., Wilmington, DE
J.P.G. Quintana, Argonne National Laboratory, Argonne, IL 111

9:30 D-65 A New High-Throughput SAXS Screening Tool
P. Kotnik, H. Schnablegger, Anton Paar GmbH, Graz, Austria
G. Langenbucher, Anton Paar USA, Ashland, VA 111

9:50 D-69 Ultra-Small-Angle X-ray Scattering (USAXS) Imaging, Contrast Mechanism and Applications
F. Zhang, G.G. Long, J. Ilavsky, P.R. Jemian, APS—Argonne National Laboratory, Argonne, IL
L.E. Levine, National Institute of Standards and Technology, Gaithersburg, MD 112

10:10 Break

10:30 D-53 *Invited*—Addressing Challenges in Materials Engineering and Biotechnology Through Combined SAXS and SANS Measurements
A.J. Allen, NIST, Gaithersburg, MD . . . 112

11:00 D-56 *Invited*—Characterization of Nanomaterials for Laser Fusion Targets
T. van Buuren, T. Willey, S. Kucheyev, C. Saw, T. Baumann, A. Hamza, Lawrence Livermore National Laboratory, Livermore, CA
J. Ilavsky, APS—Argonne National Laboratory, Argonne, IL
A. Nikroo, General Atomics Co., San Diego, CA . . . 112

11:30 D-18 Quantitative Measurement of Nanoparticle Halo Formation Around Colloidal Microspheres in Binary Mixtures Using Small-Angle X-ray Scattering
J. Ilavsky, F. Zhang, G.G. Long, P.R. Jemian, APS—Argonne National Laboratory, Argonne, IL
V.T. Milam, Georgia Institute of Technology, Atlanta, GA
J.A. Lewis, University of Illinois at Urbana-Champaign, Urbana, IL . . . 113

XRF Quantitative Analysis
Friday a.m. Evergreen "C"

Chair: **W.T. Elam**, EDAX/University of Washington, Redmond, WA

8:30 F-11 *Invited*—Generating Reliable Qualitative and Quantitative XRF Results to Support FDA Lab and Field Investigations
P.T. Palmer, P. Baker, K. Cross, San Francisco State University, San Francisco, CA
R. Jacobs, San Francisco District Laboratory, FDA, Alameda, CA . . . 114

9:00 F-62 XRF by Simultaneous Use of K- and L-Lines of an Element
M. Mantler, Technische Universitaet Wien, Vienna, Austria
B. Beckhoff, Physikalisch Technische Bundesanstalt, Berlin, Germany . . . 114

9:20 F-80 Benefits of Improved Resolution for EDXRF
R. Redus, T. Pantazis, J. Pantazis, A. Huber, Amptek, Inc., Bedford, MA
B. Cross, CrossRoads Scientific, El Granada, CA . . . 115

9:40 F-41 Lα/Lβ Intensity Ratio Depends on the Spectrometer Resolution
J. Kawai, R. Shioi, N. Sasaki, K. Okada, G. Kinugawa, S. Kunimura, T. Yamamoto, Kyoto University, Kyoto, Japan . . . 115

10:00 Break

10:20 F-4 Elemental Analysis of Polyofelins by X-ray Fluorescence Using Characterized Polymer Standards
D.W. Burns, T.L. Lewis, T. Bradley, Dow Chemical, Freeport, TX
T. Hasan, W. Rigot, Dow Chemical, Midland, MI
F. Franklin, Dow Chemical, Houston, TX . . . 115

10:40 F-15 Improving Trace Element Detection in EDXRF by Reducing Pileup Artifacts
W.T. Elam, B. Scruggs, M. Solazzi, J. Nicolosi, EDAX, Inc., Mahwah, NJ . . . 116

11:00 F-26 Preconcentration, Quantitation, and Speciation of Sub-ppm Levels of Arsenic (III) and (V) in Water Via Hand-Held XRF
P.E. Baker, R. Johnson, P.T. Palmer, San Francisco State University, San Francisco, CA
R.R. Jacobs, San Francisco District Laboratory, FDA, Alameda, CA . . . 116

ICRS Workshop on Stress Analysis

Tuesday, 5 August
9:00 a.m.–5:00 p.m.
See description on page 16.

Thursday, 7 August, ICRS-8 Poster Session & Dinner
Evergreen Ballroom, 6:00 p.m.–9:00 p.m.

S5 Stress Gradients in $Ti_xCr_{1-x}N$ Coatings
A. Ulyanenkov, H. Guérault, Bruker AXS GmbH, Karlsruhe, Germany
V.V. Uglov, V.M. Anishchik, S.V. Zlotski, Belarussian State University, Minsk, Belarus
T.A. Ulyanenkova, T. Baumbach, University Karlsruhe, Karlsruhe, Germany
A. Lazar, Institute of Solid State Physics, Minsk, Belarus 117

S6 Residual Stress Analysis with Multiple HKL Rings Collected By Area Detectors
B.B. He, Bruker AXS Inc., Madison, WI 117

S9 Assessing the Quality of X-ray Optic Surfaces of Si Crystals Cut By Diamond-Wire and Rotating Blade Sawing Techniques
M. Wieczorek, X. Huang, J. Maj, R. Conley, J. Qian, A. Macrander, R. Khachatryan, Argonne National Laboratory, Argonne, IL
C. Christensen, Diamondwire Technology, Colorado Springs, CO 117

S17 Investigations of Lattice Spacing on IN718 Via Neutron Larmor Diffraction
J. Repper, M. Hofmann, W. Petry, C. Krempaszky, E. Werner, TU München, Garching, Germany
T. Keller, Max-Planck-Institute for Solid State Research, Stuttgart, Germany 118

S23 Influence of Alloy Composition on Residual Stress in Heat Treated Aluminium Alloys
J.S. Robinson, University of Limerick, Limerick, Ireland
E.C. Oliver, ISIS, Rutherford Appleton Laboratory, Oxford, UK 118

S43 Optimizing Steel Welding Procedures By Using Neutron and X-ray Diffraction
V. Luzin, Bragg Institute, ANSTO, Menai, NSW, Australia
B. Gross, Welding Technology Institute of Australia, Newington, NSW, Australia
P. Bendeich, Institute of Materials and Engineering, ANSTO, Menai, NSW, Australia
T. Gnäupel-Herold, NCNR, NIST, Gaithersburg, MD 118

S50 New Developments at Materials Science Diffractometer STRESS-SPEC at FRM II
J. Kornmeier, R. Wimpory, R. Schneider, Hahn-Meitner-Institut (HMI), Berlin, Germany
M. Hofmann, J. Repper, A. Ostermann, G.A. Seidl, W. Tekouo, TU München, Garching, Germany
U. Garbe, H.G. Brokmeier, GKSS-Forschungszentrum Geesthacht GmbH, Geesthacht, Germany
C. Randau, H.G. Brokmeier, TU Clausthal, Clausthal-Zellerfeld, Germany 119

S54 Texture Evolution During Severe Plastic Deformation and Residual Stresses at Low and High Temperature of a Copper Matrix Reinforced by Niobium Nanotubes
J.B. Dubois, V. Vidal, L. Thilly, P.O. Renault, University of Poitiers, Futuroscope, France
S. Van Petegem, U. Stuhr, H. Van Swygenhoven, Paul Scherrer Institute, Villigen-PSI, Switzerland
F. Lecouturier, Laboratoire National des Champs Magnétiques Pulsés, Toulouse, France 119

S60 Micro-Mechanical Modelling of Elastic Thin Films and Comparison with In Situ Tensile Test with X-ray Diffraction Measurement
G. Geandier, O. Castelnau, LPMTM / CNRS, Villetaneuse, France
L. Thilly, E. Le Bourhis, P.-O. Renault, Ph. Goudeau, LPM-PhyMAT, Poitiers, France 120

S67 Studies of Strontium Titanate Thin Films by X-ray Method
H. Ji, Y.R. Li, University of Electronic Science & Technology of China, Chengdu, P.R.China
X.Y. Zhou, Y. Wang, The Hong Kong Polytechnic University, Hong Kong, P.R.China 120

S68 SALSA: Residual Stress Determination Using Neutrons
D.J. Hughes, T. Pirling, J-C. Collet-Fenetrier, S. Rowe, Institut Laue Langevin, Grenoble, France 121

Thursday, 7 August, ICRS-8 Poster Session & Dinner
Evergreen Ballroom, 6:00 p.m.–9:00 p.m.

S72 Detailed Profiling of Residual Stress in a Cold Expanded Hole
D.J. Hughes, Institut Laue Langevin, Grenoble, France 121

S73 Plastic Strain Mapping by Peak Broadening Analysis in Titanium
F. Hofmann, S.Y. Zhang, T.S. Jun, A.M. Korsunsky, University of Oxford, Oxford, Oxfordshire, Great Britain 121

S76 Cyclic Variation of Residual Stress Induced by Machining
J. Outeiro, Portuguese Catholic University, Lisbon, Portugal
J. Pina, University of Coimbra, Coimbra, Portugal
J. Kornmeier, Hahn-Meitner-Institut (HMI), Berlin, Germany
M. Hofmann, TU München, Garching, Germany....122

S92 Residual Stress Analysis in Thick HVOF Inconel 718 Coatings For Future Repair Applications
A. Manescu, Universita Politecnica delle Marche, Ancona, Italy
C. Lyphout, University West, Trollhattan, Sweden....122

S93 Micro Area X-ray Residual Stress Measurement Using Multilayer Mirror Optics
K. Sasaki, Y. Hirose, R. Monzen, A. Hosokawa, T. Sasaki, Kanazawa University, Kanazawa, Japan 122

S95 Genetic Algorithms Used For Optimisation of Elastic Properties
J. Tarasiuk, K. Wierzbanowski, AGH University of Science and Technology, Kraków, Poland
A. Lodini, Université de Reims Champagne Ardenne, Reims, France 123

S97 Corrections in X-ray Grazing Incidence Technique Used For Stress Measurement
S. Wronski, K. Wierzbanowski, A. Baczmanski, AGH University of Science and Technology, Kraków, Poland
A. Lodini, LACM, Université de Reims Champagne Ardenne, Reims, France 123

S98 Relaxation of Residual Stresses in Thin Films Investigated Using Synchrotron Radiation
T. Matsue, Niihama National College of Technology, Niihama, Japan
T. Hanabusa, K. Kusaka, Tokushima University, Tokushima, Japan
O. Sakata, Japan Synchrotron Radiation Research Institute/SPring-8, Hyogo, Japan....123

S101 Residual Stress Evaluation of Railway Rails
S. Takahashi, T. Sasaki, Y. Hirose, Kanazawa University, Kanazawa, Japan
F. Aoki, East Japan Railway Company, Saitama, Japan 124

S105 Approaches to the Problem of the Inverse Laplace Transform in Residual Stress Analysis by Comparison of Experimental Results of $\sigma(\tau)$ and $\sigma(z)$
T. Manns, B. Scholtes, University of Kassel, Kassel, Germany
I.A. Denks, Ch. Genzel, Hahn-Meitner-Institute Berlin, Berlin, Germany 124

S108 Multiaxial Stress Analysis with Area Detector Type Diffraction Method
T. Sasaki, S. Takahashi, K. Sasaki, Y. Hirose, Kanazawa University, Kanazawa, Japan
Y. Kobayashi, Hitachi, Ltd., Kawasaki, Japan....125

S110 Residual Stress Evaluation of The Surface of Railway Rails with Synchrotron Radiation
T. Sasaki, Y. Miyazawa, S. Takahashi, R. Matsuyama, Y. Hirose, Kanazawa University, Kanazawa, Japan....125

S111 Non-Destructive Hardness Testing of Steel Materials Using X-ray Diffraction
S. Takago, K. Funaki, H. Yasui, K. Fujii, Industrial Research Institute of Ishikawa, Kanazawa, Japan
T. Sasaki, Y. Hirose, Kanazawa University, Kanazawa, Japan 125

S112 Effect of The Bottom-Hole Fillet Radius on The Residual Stress Analysis By The Hole Drilling Method
M. Scafidi, B. Zuccarello, Università degli Studi di Palermo, Palermo, Italia
E. Valentini, SINT Technology s.r.l. - Calenzano, Firenze, Italia 126

S115 Welding Residual Stress of Austenitic Stainless Steel and Its Measurement By Hole-Drilling Method
L. Rongfeng, Wuhan Iron and Steel Corporation, Hubei, P.R.China 126

S123 X-ray In-Situ Residual Stress Measurement of Fiber Reinforced Plastic Composite
Y. Watanabe, M. Nishida, Kobe City College of Technology, Kobe, Hyogo, Japan 127

S128 HRXRD Strain Analysis on DRIE Etched Silicon
A. Neels, IMT-UniNE / CSEM, Neuchâtel, Switzerland
A. Dommann, CSEM, Neuchâtel, Switzerland
A. Schifferle, O. Papes, E. Mazza, ETHZ, IMES, Zürich, Switzerland....127

S129 STRAINET: Stress and Texture Analysis Standardising Interfaces
R.C. Wimpory, R. Schneider, Hahn-Meitner-Institut (HMI), Berlin, Germany
A.G. Youtsos, NCSR Demokritos, Athens, Greece
O. Kirstein, Bragg Institute, ANSTO, Australia
M. Hofmann, TU München, Garching, Germany
C. Ohms, European Commission, Joint Research Centre, Petten, The Netherlands
H.G. Brokmeier, TU Clausthal, Clausthal Zellerfeld, Germany and GKSS-Forschungszentrum Geesthacht GmbH, Geesthacht, Germany 128

S135 Neutron Diffraction Stress Analysis of Near Surface Stress Gradients of Surface Treated Steel Samples
J. Gibmeier, J. Kornmeier, Hahn-Meitner-Institute, Berlin, Germany
M. Hofmann, TU München, Garching, Germany 128

S137 Evidence and Analysis of Thermal Static Strain Aging in The Deformed Surface Zone of Finish-Machined Hardened Steel
J. Gegner, L. Schlier, W. Nierlich, SKF GmbH, Schweinfurt, Germany 129

S139 In-Situ Investigation of Grain Rotations During Tensile Straining of Steel Wires
M. Moscicki, H. Pinto, A. Borbély, A.R. Pyzalla, Max-Planck-Institut fuer Eisenforschung GmbH, Duesseldorf, Germany 129

S143 Residual Stress Fields of Aeronautical Materials Caused By Mechanical Surface Treatments
Y.K. Gao, X.-R. Wu, Beijing Institute of Aeronautical Materials, Beijing, P.R.China 129

S145 Surface Residual Stresses in Dry Turning of 0.45% C Steel
T. Leppert, University of Technology and Life Sciences, Bydgoszcz, Poland
R.L. Peng, Linköping University, Linköping, Sweden 130

S147 Usability of A Standard Sample of Sinter Glass Disc
V. Novosel–Radović, F. Šafar, K. Dužić, Sisak Tube Mill Ltd, Sisak, Croatia
N. Radović, University of Zagreb, Zagreb, Croatia 130

S149 Analysis of Shear Stress Distribution in Al (Cu) Interconnects Induced By Electromigration Based on Schmidt's Law and Studied By Synchrotron Polychromatic X-ray Microdiffraction
K. Chen, K.N. Tu, UCLA, CA
N. Tamura, B.C. Valek, ALS—Lawrence Berkeley National Laboratory, Berkeley, CA 131

S150 Measuring Residual Stresses in Stainless Steel Using XRD—Recent Experiences within a Vamas Inter-Comparison Excersise
A.T. Fry, J.D. Lord, NPL, Teddington, Middlesex, UK 131

S159 Residual Stresses in Brush-Plated Gold Coating
H. Lille, J. Kõo, A. Ryabchikov, Estonian University of Life Sciences, Tartu, Estonia
R. Laaneots, Tallinn University of Technology, Tallinn, Estonia 131

S165 Phase Composition and Internal Stress Development During the Oxidation of Iron Aluminides
P. Brito, H. Pinto, A.R. Pyzalla, Max-Planck-Institut für Eisenforschung GmbH, Düsseldorf, Germany
M. Spiegel, Salzgitter Mannesmann Forschung GmbH, Düsseldorf, Germany
M. Klaus, Ch. Genzel, Hahn-Meitner Institut Berlin (c/o BESSY), Germany 132

S171 Microscopic Load-Sharing in a Duplex Stainless Steel and the Influence of Phase Properties
R. Lin Peng, S. Johansson, Linköping University, Linköping, Sweden
G.C. Chai, Sandvik Materials Technology, Sweden
A. Ellerman, T. Manns, University of Kassel, Germany 132

S178 The Basic Relationship Between Residual Stress Profile Patterns and Fatigue Life of Precision Machined Surfaces in Rolling Contact
Y.B. Guo, A.W. Warren, The University of Alabama, Tuscaloosa, AL 133

S179 Finite Element Modeling of Residual Stress Profile Patterns in Hard Turning
Y.B. Guo, The University of Alabama, Tuscaloosa, AL 133

S182 Layer Growing/Removing Method for Determination of Residual Stresses in Orthotropic Non-Homogeneous Cylinders
J. Kõo. J. Valgur, Estonian University of Life Sciences, Tartu, Estonia 133

S183 Microstructure and Residual Stresses of High-Strength Steel to Aluminium Alloy Friction Stir Welds
R.S. Coelho, A. Kostka, H. Pinto, A. Pyzalla, Max-Planck-Institut für Eisenforschung GmbH, Düsseldorf, Germany
J. dos Santos, GKSS Forschungszentrum Geesthacht GmbH, Geesthacht, Germany 134

S184 The New Engineering Neutron Diffraction Instrument at HFIR and Its Application to Studies of the Behavior of Structural Materials
C.R. Hubbard, W.B. Bailey, K. An, J. Schmidlin, Oak Ridge National Laboratory, Oak Ridge, TN 134

S193 Simulation of the Effect of Shear Stresses on the Measured Stresses Inside 50 mm ID Pipes
M. Belassel, J. Pineault, Proto Mfg. Ltd., Oldcastle, Ontario, Canada
M. Brauss, Proto Mfg. Inc., Ypsilanti, MI 134

Thursday, 7 August, ICRS-8 Poster Session & Dinner
Evergreen Ballroom, 6:00 p.m.–9:00 p.m.

S195 VULCAN—The Diffractometer at the SNS for Engineering Mechanics
K. An, X.-L. Wang, A.D. Stoica, C.R. Hubbard, Oak Ridge National Laboratory, Oak Ridge, TN
T.M. Holden, Northern Stress Technology, Deep River, Ontario, Canada
P.K. Liaw, H. Choo, The University of Tennessee, Knoxville, TN 134

S202 Thermal Modeling and Experimentation for Residual Stress Prediction in Braze-Welded Beryllium via a Surrogate $CuZn_{10}$ Alloy
P. Backlund, J. Lee, S. Shah, C. Seepersad, J. Howell, E. Taleff, University of Texas at Austin, Austin, TX
M. Prime, Los Alamos National Laboratory, Los Alamos, NM 135

S204 The Engineering Materials Diffractometer "TAKUMI" at J-PARC
S. Harjo, K. Suzuya, K. Aizawa, T. Nakatani, M. Arai, J-PARC Center, JAEA, Tokai, Ibaraki, Japan
A. Moriai, Y. Morii, QUBS, JAEA, Tokai, Ibaraki, Japan
Y. Tomota, Ibaraki Univ., Hitachi, Ibaraki, Japan
K. Akita, Musashi Inst. Tech., Tokyo, Japan
K. Shirakihara, Suzuka College of Tech., Suzuka, Mie, Japan 135

S210 Residual Stresses and Failure in a Welded Cobalt-Molybdenum HCP Alloy
P. Huson, E. Criss, B. Kad, University of California – San Diego, San Diego, CA
M. Prime, Los Alamos National Laboratory, Los Alamos, NM 136

S217 Simulation of Time-Of-Flight Neutron Diffraction Using a New Sample Kernel
S.-Y. Lee, E. Üstündag, Iowa State University, Ames, IA
L. Li, I.C. Noyan, Columbia University, New York, NY
B. Clausen, Los Alamos National Laboratory, Los Alamos, NM 136

S219 Neutron Diffraction Study of Stress Distribution in Steel Sheet Around Active NiTi Inserts
V. Davydov, M. Vrána, P. Lukás, Nuclear Physics Institute, Řež, Czech Republic
B. Malard, J. Pilch, P. Šittner, Institute of Physics, Praha, Czech Republic 137

Post Deadline Posters:

S220 Effects of Overloads and Underloads on Cold-Worked Holes in Fatigue
R. Reuter, J. Harter, AFRL/RBSM, WPAFB, OH
D. Hill, CaStLE 137

S222 Residual Stress Distribution in Sinters of Distaloyae and Distaloyhp
S.J. Skrzypek, M. Goly, AGH-University of Science and Technology, Kraków, Poland
A. Bergmark, Höganäs AB, Sweden 137

S223 Interface Residual Stresses in Dental Zirconia Using Laue Micro-Diffraction
H.A. Bale, J.C. Hanan, Oklahoma State University, Stillwater, OK
N. Tamura, M. Kunz, Advanced Light Source, Berkeley, CA
P. Coelho, V. Thompson, New York University, New York, NY 138

ICRS-8 Diffraction Techniques: Synchrotrons—Macrobeam and High Energy I
Wednesday p.m. Pikes Peak

Chairs: **J. Almer**, Argonne National Laboratory, Argonne, IL
M. Daymond, Queen's University, Kingston, Ontario, Canada

1:30 S140 *Invited*—In-Situ Synchrotron X-ray Tomography Studies of Creep Void Evolution in Brass Alloys and Steels
A.R. Pyzalla, K. Dzieciol, A. Isaac, F. Sket, A. Borbely, G. Suathoff, Max-Planck-Institut fuer Eisenforschung GmbH, Duesseldorf, Germany
T. Buslaps, M. Di Michiel, ESRF, Grenoble, France 139

2:00 S37 Study of Computerized Tomography and Strain Mapping in the Vicinity of Crack Tip in Steel Material Using Synchrotron White X-ray
J. Shibano, T. Arai, S. Miura, M. Kobayashi, Kitami Institute of Technology, Kitami, Hokkaido, Japan
K. Kajiwara, JASRI, Sayo-cho, Hyogo, Japan
K. Kiriyama, T. Shobu, JAEA, Sayo-cho, Hyogo, Japan
K. Suzuki, Niigata Univ., Niigata, Niigata, Japan 139

2:20 S109 Simultaneous Measurement of Imaging and Strain of Fatigue Crack in Steel Bars Using High-Energy Synchrotron Radiation
T. Shobu, Japan Atomic Energy Agency, Sayo-gun, Hyogo, Japan
K. Tanaka, Meijo University, Nogoya-shi, Aichi, Japan . . . 140

2:40 S39 Characterization of a New Bone Reconstructed at the Interfaces with Implants
A. Benmarouane, A. Lodini, UFR Sciences Exactes et Naturelles, LACM, Reims, France
T. Buslaps, V. Honkimaki, ESRF, Grenoble, France
T. Hansen, ILL, Grenoble, France . . . 140

3:00 break

3:30 S14 *Invited*—Measuring Strain in Amorphous Solids by High-Energy X-ray Scattering
T.C. Hufnagel, Johns Hopkins University, Baltimore, MD . . . 140

4:00 S28 Elastic-Plastic Deformation of a Polycrystalline Titanium Alloy Studied In Situ by Energy-Dispersive Synchrotron X-ray Diffraction
S.Y. Zhang, X. Song, A. Korsunsky, University of Oxford, Oxford, UK . . . 141

4:20 S80 Residual Stress Determination in Surface Treated Alumina Samples Applying Beam Limiting Masks
T. Manns, B. Scholtes, University of Kassel, Kassel, Germany
A. Rothkirch, HASYLAB at DESY, Hamburg, Germany . . . 141

4:40 S30 The Bauschinger Effect in Nanofilamentary Cu/Nb Wires Evidenced By In-Situ Tensile Tests Under Synchrotron Radiation
L. Thilly, P.O. Renault, V. Vidal, University of Poitiers, PHYMAT, Futuroscope, France
S. Van Petegem, H. Van Swygenhoven, Paul Scherrer Institute, Villigen, Switzerland
F. Lecouturier, LNCMP, Toulouse, France . . . 142

ICRS-8 Modeling I
Wednesday p.m. Longs Peak

Chairs: **C. Tome, I. Beyerlein**, Los Alamos National Laboratory, Los Alamos, NM

1:30 S66 *Invited*—Residual Stresses in Friction Stir Welding: Numerical Simulation and Experimental Verification
G. Buffa, L. Fratini, S. Pasta, University of Palermo, Italy . . . 143

2:00 S53 Influence of the Welding Sequence on Residual Stresses in Laser Welded T-Joints of Aluminium Alloys
P. Staron, F.S. Bayraktar, W. Machold, S. Riekehr, M. Koçak, A. Schreyer, GKSS Research Center, Geesthacht, Germany . . . 143

2:20 S55 The Influence of Annealing on Residual Stresses at Weld Stop/Start Positions
S.K. Bate, I. Symington, Serco Technical & Assurance Services, Warrington, UK
P. Hurrell, Rolls-Royce Plc, Derby, UK
J.A. Francis, M. Turski, University of Manchester, UK . . . 144

2:40 S56 Finite Element Analysis and Neutron Diffraction Evaluation of Residual Stress in Stellite Coating by PTA Process
A. Nady, A. Benmarouane, H. Bonnefoy, A. Lodini, UFR Sciences Exactes et Naturelles, LACM, Reims, France
V. KloseK, M.H. Mathon, Laboratoire Léon Brillouin, CEA Saclay, Gif sur Yvette, France. . . . 144

3:00 break

3:30 S185 *Invited*—Using Finite Element Analysis and Synchrotron X-ray Diffraction to Understand Stress Distributions in Deforming Polycrystals
M.P. Miller, J.-S. Park, P.R. Dawson, Cornell University, Ithaca, NY
T.-S. Han, Yonsei University, Seoul, Korea. . . . 145

4:00 S87 Modeling the Relaxation Due to Twinning in an HCP Zirconium Alloy
M.R. Daymond, R.Y. Zhang, F. Xu, R.A. Holt, Queen's University, Kingston, Ontario, Canada . . . 145

4:20 S116 Modeling and Measurement of Residual Macro and Lattice Strains During Four-Point Bending of Zircaloy-2
F. Xu, R.A. Holt, M.R. Daymond, Queen's University, Kingston, Ontario, Canada
R.B. Rogge, National Research Council, Chalk River Laboratories, Chalk River, Ontario, Canada. . . . 145

4:40 S216 Inverse Analysis of Engineering Neutron Diffraction Data
S.-Y. Lee, B. Denizer, Y. Kim, H. Ceylan, E. Üstündag, Iowa State University, Ames, IA. . . . 146

ICRS-8 Diffraction Techniques: Laboratory Applications
Wednesday p.m. Blanca Peak

Chairs: **C. Goldsmith**, IBM Corporation, Hopewell Junction, NY
T. Watkins, Oak Ridge National Laboratory, Oak Ridge, TN

1:30 S79 *Invited*—Industrial Challenges for Residual Stress XRD Applications
A. Haase, R. Stabenow, A. Schafmeister, GE Inspection Technologies, Ahrensburg, Germany 147

2:00 S16 X-ray Stress Measurement of Nickel-Base Single Crystal Superalloy Using Two-Dimensional Detector
K. Tanaka, Meijo University, Nagoya, Japan
S. Machiya, Daido Institute of Technology, Japan
Y. Akiniwa, Nagoya University, Nagoya, Japan 147

2:20 S40 Analysis of Residual Stress in Polycrystalline Coatings – From Scientific Technique to Industrial Method
A.C. Vermeulen, PANalytical, Almelo, The Netherlands 147

2:40 S41 Application of X-ray Diffraction Stress Analysis at Constant Penetration Depth for the Determination of Both Real-Space Residual-Stress and Lattice-Parameter Gradients
M. Wohlschlögel, U. Welzel, E.J. Mittemeijer, Max Planck Institute for Metals Research, Stuttgart, Germany 148

3:00 break

3:40 S96 Residual Stress Measurements by X-ray Diffraction: Critical Evaluation of Error Sources
R. Machado, A. Kuznetsov, C.A. Achete, Divisão de Metrologia de Materiais, INMETRO, RJ, Brasil
T. Hirsch, Institut fuer Werkstoffechnik, Bremen, Germany 148

4:00 S124 Residual Stress Estimation of Ti Casting Alloy by X-ray Single Crystal Measurement Method
A. Shiro, T. Hanabusa, The University of Tokushima, Tokushima, Tokushima, Japan
M. Nishida, Kobe City College of Technology, Kobe, Hyogo, Japan
T. Jing, Harbin Institute of Technology, Harbin, P.R.China 149

4:20 S168 ASTM Standards for Residual Stress Measurement
C.O. Ruud, Emeritus, The Pennsylvania State University, State College, PA 149

4:40 S105 Approaches to the Problem of the Inverse Laplace Transform in Residual Stress Analysis by Comparison of Ex
T. Manns, B. Scholte
I.A. Denks, Ch. Gen Berlin, Germany

Moved to ICRS Poster Session

ICRS-8 Industrial Applications: Engineered Stresses
Wednesday p.m. Maroon Peak

Chairs: **J. Bunch**, The Boeing Company, Seattle, WA
M. Hill, University of California, Davis, CA

2:00 S208 Experimental Investigation of Residual Stress in Laser Shock Peened Friction Stir Weld Joints
O. Hatamleh, NASA – Johnson Space Center, Houston, TX
A.T. DeWald, M.R. Hill, Hill Engineering, LLC, McClellan, CA 150

2:20 S78 Thermal Stability of Mechanical Surface Treatment Induced Residual Stress in Austenitic Stainless Steel by Neutron and Synchrotron Diffraction
A.D. Evans, European Synchrotron Research Facility (ESRF), Grenoble, France
M. Turski, S. Clitheroe, J. Kelleher, P.J. Withers, University of Manchester, Manchester, UK 150

2:40 S74 Small Creep Deformations and Residual Stress Relaxation in Welded and Shot Peened AlMgSiCu Aluminum Alloys
S. Daichendt, T. Hirsch, Institut fuer Werkstofftechnik, Bremen, Germany 150

3:00 S99 Near Surface Stress Gradients Analysis by GIXRD on Laser Shocked 6056 Aluminium Alloy Samples
H.B. Song, LIM UMR CNRS 8006, ENSAM, Paris, France
P. Peyre, LALP UPR CNRS 1578, Arcueil, France
V. Ji, ICMMO/LEMHE UMR CNRS 8182, Orsay, France
C.H. Jiang, Shanghai Jiaotong University, Shanghai, P.R.China 151

3:20 break

3:40 S188 Residual Stress Measurements Using Synchrotron X-ray on Nickel-Based Superalloy at Cryogenic Temperatures
K. Akita, D. Miyashita, S.-i. Ohya, Musashi Institute of Technology, Setagaya, Tokyo, Japan
Y. Ono, T. Yuri, T. Ogata, National Institute for Materials Science, Tsukuba, Ibaraki, Japan
T. Shobu, Japan Atomic Energy Agency, Sayo-gun, Hyogo, Japan 151

4:00 S64 Effect of Residual Stresses on Fatigue Strength of Severe Surface Deformed Steels by Shot Peening
Y. Akiniwa, H. Kimura, Nagoya University, Nagoya, Japan. 151

4:20 S117 Using XRD Elastic and Plastic Strain Data to Evaluate the Effectiveness of Different Cold-Working Techniques in Aerospace Materials
B.S. Matlock, Technology for Energy Corp., Knoxville, TN
D.J. Snoha, S.M. Grendahl, US Army Research Laboratory, Aberdeen Proving Ground, MD 152

4:40 S151 Numerical and Experimental Investigation on Shot-Peening Induced Deformation: Application to Sheet Metal Forming
F. Cochennec, E. Rouhaud, L. Roucoules, UTT ICD-LASMIS, Troyes, France
B. Flan, Sisson-Lehmann Wheelabrator Group, Charleville-Mézières, France 152

ICRS-8 Diffraction Techniques: Synchrotrons—Macrobeam and High Energy II
Thursday a.m. Pikes Peak

Chairs: **J. Almer**, Argonne National Laboratory, Argonne, IL
M. Daymond, Queen's University, Kingston, Ontario, Canada

8:30 S70 *Invited*—Advances in Near Surface Residual Stress Gradient Analysis of Polycrystalline Materials by Means of Energy Dispersive Diffraction
I.A. Denks, Hahn-Meitner-Institut Berlin, Berlin, Germany 153

9:00 S148 Fatigue Damage Evaluation of Rail[illegible]re Using High Energy Synchrotron Radiation
K. Matsumo[illegible]arch Institute, Tokyo, Japan
T. Shoubu, [illegible] 153
WITHDRAWN

9:00 S61 The New High Energy Materials Science Beamline (HEMS) at PETRA III
N. Schell, F. Beckmann, H.-U. Ruhnau, R. Kiehn, A. Schreyer, GKSS-Research Center, Geesthacht, Germany 153

9:20 S134 In-Situ Study of the Cyclic Deformation Behaviour of the Magnesium Base Wrought Alloy AZ31 By Means of High Energy Synchrotron Diffraction
J. Gibmeier, Hahn-Meitner-Institute, Berlin, Germany
M. Götting, B. Scholtes, University of Kassel, Kassel, Germany 154

ICRS-8 Diffraction Techniques: Neutron I
Thursday a.m. Pikes Peak

Chairs: **D. Brown**, Los Alamos National Laboratory, Los Alamos, NM
X.-L. Wang, Oak Ridge National Laboratory, Oak Ridge, TN

10:30 S205 *Invited*—Evaluation of Substructure Parameters by Peak Profile Analysis of High-Resolution Neutron Diffraction Spectra
P. Lukáš, P. Strunz, V. Davydov, Nuclear Physics Institute, Řež, Czech Republic
R. Kužel, Charles University, Prague, Czech Republic 155

11:00 S192 Techniques for Neutron Stress Determination with High Spatial Resolution
T. Gnäupel-Herold, NIST Center for Neutron Research, Gaithersburg, MD 155

11:20 S127 Neutron Diffraction Stress Measurement—Remarks on Calibration and Alignment
C. Ohms, European Commission, Joint Research Centre, Petten, The Netherlands 155

11:40 S172 Accurate Specimen Mounting and Alignment for Neutron Strain Mapping at ORNL
C.R. Hubbard, W.B. Bailey, J. Schmidlin, Oak Ridge National Laboratory, Oak Ridge, TN
J. James, Open University, Milton Keynes, UK. 156

12:00 Lunch break

Session will continue at 1:30. See page 40 for Diffraction Techniques: Neutron II.

ICRS-8 Relaxation Techniques: Hole Drilling
Thursday a.m. Longs Peak

Chair: **J. Robinson**, University of Limerick, Limerick, Ireland

8:30 S154 *Invited*—Improved Sensitivity From Multiple Images in Residual Stress Measurement By ESPI Hole-Drilling
G.S. Schajer, University of British Columbia, Vancouver, BC, Canada
M. Steinzig, Los Alamos National Laboratory, Los Alamos, NM 157

9:00 S104 A New Procedure for the Evaluation of Residual Stresses by the Hole Drilling Method Based on Newton-Raphson Technique
G. Petrucci, M. Scafidi, Università degli Studi di Palermo, Palermo, Italy 157

9:20 S181 The Application of Digital Image Correlation Techniques for Measuring Residual Stress By Incremental Hole Drilling
J.D. Lord, National Physical Laboratory, Middlesex, UK
P. Whitehead, Stresscraft Ltd., Leicestershire, UK. 157

9:40 S3 Combination of Different Measurement Techniques for the Determination of Residual Stress Distributions in Weldments with Mechanical Surface Treatments
T. Nitschke-Pagel, K. Dilger, Institute of Joining and Welding, University of Braunschweig, Braunschweig, Germany 158

ICRS-8 Relaxation Techniques: Slitting
Thursday a.m. Longs Peak

Chair: **M. Prime**, Los Alamos National Laboratory, Los Alamos, NM

10:30 S126 *Invited*—Residual Stress Measurements on Thin Films with a Focused Ion Beam Equipment
N. Sabaté, C. Cané, I. Gràcia, CNM-CSIC, Barcelona, Spain
D. Vogel, A. Gollhardt, B. Michel, IZM-FHG, Berlin, Germany
K.J. Kang, Chonnam National University, Kwangju, Korea. 159

11:00 S125 Microscale Residual Stress Measurement in Steel Using Focused Ion Beam Slotting and Digital Image Correlation
N. Daynes, G. Horne, P.J. Heard, D.Z.L. Hodgson, A. Shterenlikht, University of Bristol, Bristol, UK 159

11:20 S35 Characterization of Longitudinal Residual Stresses in Friction Stir Welds Using the Cut-Compliance Technique
A.P. Reynolds, C. Canaday, University of South Carolina, Columbia, SC 160

11:40 S69 Residual Stress Measurements in Steel Beams Using the Incremental Slitting Technique
D.Z.L. Hodgson, D.J. Smith, A. Shterenlikht, University of Bristol, Bristol, UK
M.B. Prime, Los Alamos National Laboratory, Los Alamos, NM 160

ICRS-8 Materials Engineering I
Thursday a.m. Blanca Peak

Chairs: **C. Murray**, IBM – T.J. Watson Research Center, Yorktown Heights, NY
T. Gnaupel-Herold, NIST Center for Neutron Research, Gaithersburg, MD

8:30 S22 *Invited*—Diffraction Analysis of Stress Gradients in Tin Thin Films: An Explanation for the Occurrence of Whisker Formation?
M. Sobiech, U. Welzel, E.J. Mittemeijer, Max Planck Institute for Metals Research, Stuttgart, Germany
W. Hügel, A. Seekamp, Robert-Bosch GmbH, Reutlingen, Germany 161

9:00 S15 Micro Stress Accumulation in Multiphase Superalloys
J. Repper, M. Hofmann, W. Petry, C. Krempaszky, E. Werner, TU München, Garching, Germany 161

9:20 S27 Residual Stresses and Load Partitioning in Novel Metal/Ceramic Composites Exhibiting Lamellar Microstructures
S. Roy, A. Wanner, Universität Karlsruhe (TH), Karlsruhe, Germany
J. Gibmeier, Hahn Meitner Institute Berlin, Berlin, Germany. 161

9:40 S31 Size Effect in the Plasticity of Multiscale Nanofilamentary Cu/Nb Composite Wires During In-Situ Tensile Tests Under Neutron Beam
V. Vidal, L. Thilly, P.O. Renault, University of Poitiers, Futuroscope, France
U. Stuhr, S. Van Petegem, H. Van Swygenhoven, Paul Scherrer Institute, Villigen, Switzerland
F. Lecouturier, LNCMP, Toulouse, France 162

10:00 break

10:40 S213 Characterization of Strained Silicon on Insulator (sSOI) Substrates Using High-Resolution X-ray Diffraction
M. Wormington, Bede Scientific Inc., Centennial, CO
T. Lafford, P. Ryan, Bede plc, Durham, UK 162

11:00 S161 High Pressure Deformation Study of Zirconium
S.C. Vogel, D.W. Brown, H. Reiche, T.A. Sisneros, H.M. Volz, J. Zhang, Y. Zhao, Los Alamos National Laboratory, Los Alamos, NM
N. Nishiyama, Y. Wang, APS – Argonne National Laboratory, Argonne, IL 163

11:20 S59 In-Situ X-ray Diffraction Study of Nanocrystalline Metals
S. Brandstetter, S. Van Petegem, J. Zimmermann, B. Schmitt, H. Van Swygenhoven, Paul Scherrer Institut, Villigen, Switzerland 163

11:40 S77 Neutron Diffraction Study of Intergranular Stress Development in Austenitic Stainless Steel Weld Metal
S. Sharma, R. Haigh, L. Edwards, M.E. Fitzpatrick, The Open University, Milton Keynes, Bucks, UK
M. Turski, University of Manchester, Manchester, UK 163

ICRS-8 Industrial Applications: Layers and Composites
Thursday a.m. Maroon Peak

Chair: **M. Hill**, University of California, Davis, CA

8:50 S201 *Invited*—A Study of Residual Stresses in Vacuum Plasma Sprayed Tungsten Coatings
T.-S. Jun, S.Y. Zhang, G. Thomas, P. Grant, A. Korsunsky, University of Oxford, Oxford, England 165

9:20 S142 Residual Stress Profiles in Alumina-Zirconia Ceramic Composites Fabricated By Tape Casting
J. Ruiz-Hervias, UPM, Madrid, Spain
A. Steuwer, T. Buslaps, ESRF, Grenoble, France
J. Gurauskis, C. Baudin, Instituto de Ceramica y Vidrio (CSIC), Madrid, Spain 165

9:40 S121 Neutron Diffraction Studies on Strain Evaluation of Rebar in Reinforced Concrete
H. Suzuki, Japan Atomic Energy Agency, Japan
M. Kanematsu, Tokyo University of Science, Japan
K. Kusunoki, Yokohama National University, Japan 166

10:00 S26 Residual Stresses of EB-PVD Thermal Barrier Coatings Exposed at High Temperature
K. Suzuki, Niigata University, Niigata, Japan
T. Shobu, Japan Atomic Energy Agency, Sayo, Hyogo, Japan
K. Tanaka, Meijo University, Nagoya, Japan 166

ICRS-8 Industrial Applications: Thermal Processing
Thursday a.m. Maroon Peak

Chair: **J. Bunch**, The Boeing Company, Seattle, WA

10:40 S156 Neutron Diffraction Measurements on a Large Size Roller Bearing Ring
R.H. Vegter, SKF Engineering & Research Center, Nieuwegein, The Netherlands
T. Pirling, Institut Laue-Langevin, Grenoble, France
M. Peel, European Synchrotron Radiation Facility, Grenoble, France 167

11:00 S175 The Effects of Casting Parameters and Heat Treatment on Residual Stress and Microstructure Variations of an Al-Si Alloy
M. Sadrossadat, S. Johansson, Linköping University, Linköping, Sweden 167

11:20 S90 Residual Stress Distribution Below Subsurface Carburized Layer in Carbon Steel Gear by Neutron Diffraction
Y. Sakaida, M. Kawauchi, Shizuoka University, Hamamatsu, Shizuoka, Japan
M. Manzanka, Yamaha Motor, Hamamatsu, Shizuoka, Japan 167

11:40 S131 Development Of Induction Surface Hardening Process For Small Diameter Carbon Steel
D. Suzuki, K. Yatsushiro, S. Shimizu, Yamanashi Industrial Technology Center, Yamanashi, Japan
Y. Sugita, YS Electronics, Yamanashi, Japan
M. Saito, Asakawa Heat Treatment, Yamanashi, Japan
K. Kubota, Marushin Heat Treatment, Yamanashi, Japan 168

ICRS-8 Diffraction Techniques: Neutron II
Thursday p.m. Pikes Peak

Chairs: **D. Brown**, Los Alamos National Laboratory, Los Alamos, NM
X.-L. Wang, Oak Ridge National Laboratory, Oak Ridge, TN

1:30 S209 *Invited*—Neutron Diffraction Measurements of Residual Stress in Welds Fabricated From Highly Anisotropic Materials
T.M. Holden, Northern Stress Technologies, Deep River, Ontario, Canada
D.W. Brown, B. Clausen, Los Alamos National Laboratory, Los Alamos, NM
D.G. Carr, Australian Nuclear Science and Technology Organisation, Lucas Heights, NSW, Australia 169

2:00 S122 Residual Stress Measurement of Coarse Crystal Grain in Titanium Casting Alloy by Neutron Diffraction
M. Nishida, Kobe City College of Technology, Hyogo, Japan
A. Shiro, Harbin Institute of Technology, Harbin, P.R.China
T. Jing, Neutron Scattering Lab, Puspiptek, Indonesia
M.R. Muslih, T. Hanabusa, Tokushima University, Tokushima, Japan 169

2:20 S107 Internal Stress Generation in Pure Titanium During Cyclic Loading
E.C. Oliver, STFC Rutherford Appleton Laboratory, Oxfordshire, UK
M.R. Daymond, Queen's University, Kingston, Ontario, Canada 169

2:40 S176 Applicability of the $\sin^2(\psi)$ Tilt Method in Neutron Strain Mapping
C.R. Hubbard, Oak Ridge National Laboratory, Oak Ridge, TN
R.A. LeMaster, J.V. Kolwyck, University of Tennessee at Martin, Martin, TN 170

ICRS-8 Diffraction Techniques: General Methods
Thursday p.m. Pikes Peak

Chair: **E. Üstündag**, Iowa State University, Ames, IA

3:20 S42 *Invited*—Grain Statistics in Neutron Stress Experiment
V. Luzin, Bragg Institute, ANSTO, Menai, NSW, Australia 171

3:50 S11 Assessment of Machining Induced Near-Surface Damage on the Basis of X-ray Elastic Constants
W. Pfeiffer, B. Blug, V. Fuhr, E. Reisacher, Fraunhofer IWM, Freibrug, Germany 171

4:10 S29 A Method for Determination of 2nd Rank Strain Tensor From Nanocrystalline Diffraction Data and Its Application to Micromechanical Deformation
A. Mehta, M. Bibee, SLAC/Stanford, Menlo Park, CA
D. Bronfenbrenner, UC Berkeley, Berkeley, CA 171

4:30 S48 X-ray Diffraction at Constant Penetration Depth – A Viable Approach for Characterizing Steep Residual Stress Gradients
T. Erbacher, E.ON Kernkraft, Hannover, Germany
A. Wanner, O. Vöhringer, Universitaet Karlsruhe, Karlsruhe, Germany
T. Beck, Forschungszentrum Jülich, Jülich, Germany 172

4:50 S65 Application of Energy-Dispersive Diffraction to the Analysis of Highly Inhomogeneous Residual Stress Fields in Thin Film Structures
M. Klaus, W. Reimers, Technische Universität Berlin, Berlin, Germany
Ch. Genzel, Hahn-Meitner-Institut Berlin, Berlin, Germany 172

5:10 S158 Diffraction Stress Measurement on Coarse Grained Materials
T. Hanabusa, K. Kusaka, The University of Tokushima, Tokushima, Japan
M. Nishida, Kobe City College of Technology, Kobe, Japan 173

ICRS-8 Relaxation Techniques: Deep Hole and Contour
Thursday p.m. Longs Peak

Chair: **M. Hill**, University of California, Davis, CA

1:30 S218 *Invited*—From Surface Profile to Residual Stress Using the Contour Method
Y.S. Xiong, J. Kelleher, P. Frankel, P. Withers, University of Manchester, Manchester, UK. 174

2:00 S113 Mapping Multiple Residual Stress Components Using the Contour Method and Superposition
P. Pagliaro, B. Zuccarello, University of Palermo, Palermo, Italy
M.B. Prime, B. Clausen, M.L. Lovato, M.L. Steinzig, H. Swenson, Los Alamos National Laboratory, Los Alamos, NM
J.S. Robinson, University of Limerick, Limerick, Ireland
G.S. Schajer, University of British Columbia, BC, Canada 174

2:20 S4 Validation of a New Deep Hole Drilling (DHD) Technique for Measuring Near Yield Residual Stresses
A.H Mahmoudi, C.E. Truman, D.J. Smith, M.J. Pavier, University of Bristol, Bristol, UK 174

2:40 S51 Influence of Cold Compression on the Residual Stresses in 7449 Forgings
J.S. Robinson, University of Limerick, Limerick, Ireland
C.E. Truman, S. Hossain, University of Bristol, Bristol, UK
E.C. Oliver, ISIS, Rutherford Appleton Laboratory, Didcot, UK
D.J. Hughes, Institut Laue Langevin, Grenoble, France
M.E. Fox, University of Manchester, Manchester, UK. 175

ICRS-8 Other Measurement Techniques
Thursday p.m. Longs Peak

Chair: **J. Robinson**, University of Limerick, Limerick, Ireland

3:30 S84 Determination of the Residual Stress Fields Around Scratches in Al Alloys
M.K. Khan, M.E. Fitzpatrick, L. Edwards, The Open University, Milton Keynes, UK
S.V. Hainsworth, University of Leicester, Leicester, UK 176

3:50 S71 Residual Stresses in a Machined and Shrink Fitted Assemblies
B. Su, F. Hossainzadeh, D. Smith, C. Truman, University of Bristol, Bristol, UK 176

4:10 S45 Procedures for Nondestructive RS-Measurements of Inner Surfaces of Ball Bearing Components
J. Epp, T. Hirsch, Institut fuer Werkstofftechnik, Bremen, Germany 176

4:30 S106 Complementarity of Experimental and Numerical Methods for Determining Residual Stress States
G. Roy, CANMET/MTL, Ottawa, Ontario, Canada 177

4:50 S120 Detection of Surface Residual Stresses in Materials by Photoacoustic Images of Microindented Areas
A.L. Glazov, K.L. Muratikov, Physical-Technical Institute of RAS, St. Petersburg, Russia 177

5:10 S57 Residual Stresses Analysis in Brush-Plated Galvanic Coatings Deposited From Nickel Sulfate Electrolyte
H. Lille, J. Kõo, A. Ryabchikov, Estonian University of Life Sciences, Tartu, Estonia 178

ICRS-8 Materials Engineering II
Thursday p.m. Blanca Peak

Chairs: **C. Murray**, IBM – T.J. Watson Research Center, Yorktown Heights, NY
T. Gnaupel-Herold, NIST Center for Neutron Research, Gaithersburg, MD

1:40 S82 Residual Stresses in Cold-Drawn Rods: Effect of an Alternative Treatment
J. Ruiz-Hervias, M. Elices, Universidad Politecnica de Madrid, Madrid, Spain
M. Hofmann, J. Rebelo-Kornmeier, TU München, Garching, Germany. 179
V. Luzin, Bragg Institute, Menai NSW, Australia

2:00 S100 Neutron Diffraction Study of Intergranular Stress Development in Zr-2.5%Nb
O. Zanellato, M.E. Fitzpatrick, L. Edwards, The Open University, Keynes, UK
M.R. Daymond, Queen's University, Kingston, Canada 179

2:20 S102 Residual Stresses in Metal Matrix Composites for Heat Sink Applications During Thermal Cycling
M. Schöbel, H.P. Degischer, TU Vienna, Vienna, Austria
T. Buslaps, M. di Michiel, ESRF, Grenoble, France
T. Poeste, R. Schneider, HMI Berlin, Berlin, Germany
S. Kleiner, EMPA, Thun, Germany
J. Hemptenmacher, DLR, Köln, Germany
A. Herrmann, IPP, Garching, Germany 180

2:40 S141 Residual Stresses and In-Situ Measurement of Phase Transformation in Low Transformation Temperature (LTT) Welding Materials
T. Kannengiesser, A. Kromm, M. Rethmeier, Federal Institute for Materials Research and Testing, Berlin, Germany
J. Gibmeier, Hahn-Meitner-Institute, Berlin, Germany 180

3:00 break

3:20 S197 *Invited*—Why Should We Give Up the $\sin^2\psi$ and All Similar Methods?
B. Ortner, University Leoben, Leoben, Austria 180

3:50 S164 Load Partitioning in a Duplex Stainless Steel with Surface Strength Gradient and Residual Stresses
R. Lin Peng, S. Johansson, Linköping University, Linköping, Sweden
J. Gibmeier, Hahn-Meitner-Institut Berlin GmbH, Berlin, Germany
G.C. Chai, Sandvik Materials Technology, Sweden 181

4:10 S189 Assessment of Load Distribution in DP 600 Dual Phase Steel By Means of In-Situ Neutron Diffraction
M. Seefeldt, S. Dillien, K.U. Leuven, Heverlee-Leuven, Belgium 181

4:30 S81 Development of Microstresses of the Hot Extruded Magnesium Alloy AZ31 Under Cyclic Testing Conditions
M. Huppmann, W. Reimers, Technische Universität Berlin, Berlin, Germany 182

4:50 S62 Combined In Situ Neutron Diffraction and Acoustic Emission Investigation of the Deformation Mechanisms in M...
WITHDRAWN
O. Murán
M.R. Barn..., Geelong, Australia
E.C. Oliver, ISIS Facility, Didcot, UK 182

ICRS-8 Industrial Applications: Miscellaneous
Thursday p.m. Maroon Peak

Chair: **J. Bunch**, The Boeing Company, Seattle, WA

1:40 S198 Experimental Determination of Residual Stresses Around Hydride Blisters in ZrNb Pressure Tubes
J.R. Santisteban, Centro Atomico Bariloche, Bariloche, Argentina
A. Steuwer, M. Peel, ESRF, Grenoble, France
G. Domizzi, Centro Atomico Constituyentes, San Martin, Argentina 183

2:00 S63 X-ray Studies of Strained Silicon on Insulator
M. Bibee, A. Mehta, S. Brennan, P. Pianetta, Stanford Synchrotron Radiation Laboratory, Menlo Park, CA 183

2:20 S2 Residual Stress Relaxation in Welded Joints Under Static and Cyclic Loading
M. Farjian-Sohi, T. Nitschke-Pagel, K. Dilger, University of Braunschweig, Braunschweig, Germany 184

2:40 S203 Neutron Diffraction Measurement of Residual Stresses in Friction Stir Processed Nanocomposite Surface Layer
H. Xu, K. An, J. Qu, C.R. Hubbard, Z. Feng, X.-L. Wang, Oak Ridge National Laboratory, Oak Ridge, TN 184

ICRS-8 Industrial Applications: Welding
Thursday p.m. Maroon Peak

Chair: **M. Hill**, University of California, Davis, CA

3:30 S152 Residual Stress Analysis of Aluminium Welds with High Energy Synchrotron Radiation at the HARWI II Beamline
T. Fischer, A. Schreyer, GKSS Research Centre, Geesthacht, Germany
R. Martins, Joint Research Centre, Petten, The Netherlands 185

3:50 S119 Residual Stress Mapping in a Pipe Weld Repair Using High Energy X-ray Diffraction
P.J. Bouchard, British Energy Generation Ltd., Gloucester, UK
M. Turski, The University of Manchester, Manchester, UK
L. Edwards, ANSTO, Sydney, NSW, Australia . . . 185

4:10 S163 The Relaxation of Residual Welding Stresses Upon Progressive Sectioning of Welds
J. Altenkirch, Manchester Materials Science Centre, Manchester, UK and ILL, Grenoble, France
A. Steuwer, ESS Scandinavia Secretariat, Lund, Sweden
M.J. Peel, ESRF, Grenoble, France
P.J. Withers, Manchester Materials Science Centre, Manchester, UK . . . 186

4:30 S94 Study on the Effect of Welding Residual Stresses on Crack-Tip Constraint
X.B. Ren, Z.L. Zhang, Norwegian University of Science and Technology (NTNU), Trondheim, Norway
B. Nyhus, SINTEF Material and Chemistry, Trondheim, Norway . . . 186

4:50 S155 Investigation of Residual Stress Distribution in Ferritic Steel Weld Measured by Neutron and Synchrotron Diffraction
A.M. Paradowska, Rutherford Appleton Laboratory, UK
J.H.W. Price, R. Ibrahim, Monash University, Australia
T.R. Finlayson, The University of Melbourne, Australia
U. Lienert, APS—Argonne National Laboratory, Argonne, IL
R. Blevins, ANSTO, Sydney, NSW, Australia . . . 186

5:10 S47 Measurement of R[illegible]DS and IFS Plates Using XRD
C.S. Kishore[illegible] University, Tamilnadu, India . . . 186

WITHDRAWN

ICRS-8 Diffraction Techniques: Synchrotrons—Microbeam
Friday a.m. Pikes Peak

Chairs: **G. Ice**, Oak Ridge National Laboratory, Oak Ridge, TN
N. Tamura, Lawrence Berkeley National Laboratory, Berkeley, CA

8:30 S186 *Invited*—X-ray Microdiffraction Techniques for Measuring Local Microstructure and Strain Distributions
J.D. Budai, B.C. Larson, G.E. Ice, J.Z. Tischler, T.Z. Ward, Oak Ridge National Laboratory, Oak Ridge, TN
W. Liu, Argonne National Laboratory, Argonne, IL
D.D. Sarma, Indian Inst. of Science, Bangalore, India . . . 187

9:00 S52 Smaller is Stronger: In-Situ Laue Diffraction
R. Maaß, J. Zimmermann, S. Van Petegem, H. Van Swygenhoven, Paul Scherrer Institut, Villigen, Switzerland . . . 187

9:20 S132 Spatially Resolved Strain Measurements on Micro Moulds
A. Kienzler, B. Okolo, V. Schulze, A. Wanner, D. Löhe, Universität Karlsruhe (TH), Karlsruhe, Germany . . . 188

9:40 S146 Determination of Stress and Texture Gradient in CdTe Thick Films Using a High Energy White Microbeam
P. Gergaud, V. Consonni, G. Feuillet, CEA-LETI, MINATEC, Grenoble, France
T. Buslaps, European Synchrotron Radiation Facility, Grenoble, France . . . 188

10:00 break

10:20 S88 *Invited*—Nanoscale Diffraction Microscopy at the CNM/APS Hard X-ray Nanoprobe Beamline
M. Holt, J. Maser, R. Winarski, V. Rose, G.B. Stephenson, Argonne National Laboratory, Argonne, IL . . . 189

10:50 S167 In-Situ Study of Electromigration Induced Strain/Stress Evolution and Distribution in Sn-Cu Lead-Free Solder Joints Using Synchrotron White Beam X-ray Microdiffraction
K. Chen, Lawrence Berkeley National Lab, Berkeley, CA and UCLA, Los Angeles, CA
N. Tamura, Lawrence Berkeley National Lab, Berkeley, CA
F.Y. OuYang, K.N. Tu, UCLA, Los Angeles, CA . . . 189

11:10 S25 The Reverse of Triaxial Strain Fields in a Multiferroic $BiFeO_3$ Thin Film As Studied Using Scanning X-ray Microdiffraction
C.W. Bark, K.C. Cho, Y.M. Koo, S. Ryu, H.M. Jang, Pohang University of Science and Technology (POSTECH), Pohang, Korea
N. Tamura, ALS—Lawrence Berkeley National Laboratory, Berkeley, CA . . . 189

11:30 D-58 Nanostructure Analysis of Metallic Materials by Coherent X-ray Diffraction Microscopy
Y. Takahashi, H. Furukawa, H. Kubo, K. Yamauchi, Osaka University, Osaka, Japan
Y. Nishino, T. Ishikawa, RIKEN Spring-8 Center, Hyogo, Japan
E. Matsubara, Kyoto University, Kyoto, Japan. . . . 190

ICRS-8 Modeling II
Friday a.m. Longs Peak

Chairs: **C. Tome, I. Beyerlein**, Los Alamos National Laboratory, Los Alamos, NM

8:40 S86 Residual Stress and Deformation Simulation of Nitrided Discs
L. Barrallier, MecaSurf Laboratory, Arts et Metiers ParisTech, Aix en Provence, France
P. Vardon, Eurocopter, Marignane, France
D. Deloison, EADS Innovation Works, Suresnes, France 191

9:00 S91 Phase Transformation Involving Residual Stresses During Gaseous Nitriding of Steel
S. Jegou, R. Kubler, L. Barrallier, Laboratoire MecaSurf, Arts et Metiers ParisTech, Aix-en-Provence, France
F. Roch, Aubert et Duval, ERAMET Group, Paris, France 191

9:20 S20 Prediction of Residual Stress Distribution in Plasma Nitrided Tool Steel
B. Podgornik, J. Vižintin, University of Ljubljana, Ljubljana, Slovenia
V. Leskovšek, Institute for Metals and Technologies, Ljubljana, Slovenia
D. Nolan, University of Wollongong, Wollongong, NSW, Australia 192

9:40 S170 On Surface Texture and Integrity in Machined Surfaces
A.K. Balaji, A.R. Paranjpe, C. Rakurty, The University of Utah, Salt Lake City, Utah 192

10:00 break

10:30 S32 Measurement of the Residual Stress Field in an Aluminium Alloy 2014A Component of Complex Geometry
S. Hossain, M. Fardi, D.J. Smith, C.E. Truman, University of Bristol, Bristol, UK
U. Stuhr, Paul Scherrer Institute, Villigen, Switzerland 192

10:50 S75 In-Situ Strain Measuring ... Neutron Diffraction
U. Wasmuth, ... Universität München, Garching, Germany 193

WITHDRAWN

10:50 S130 Finite Element Simulation of Residual Stress Profiles in Peen Forming Process
H.Y. Miao, C. Perron, National Research Council Canada, Québec, Canada
M. Lévesque, École Polytechnique de Montréal, Québec, Canada 193

11:10 S138 Study on the Residual Stress and the Distortion of the Large Gears or Axles During the Heat Treatment
Y. Wang, Y. Ling, R. Kastelein, Z.A. Xu, SIRRIS, Zwijnaarde, Belgium 193

ICRS-8 Fatigue & Fracture
Friday a.m. Blanca Peak

Chair: **D. Smith**, Bristol University, Bristol, UK

8:30 S180 *Invited*—In Situ Probing of Crack Growth Retardation During Cyclic Loading
S.Y. Lee, H. Choo, P.K. Liaw, The University of Tennessee, Knoxville, TN
K. An, C.R. Hubbard, Oak Ridge National Laboratory, Oak Ridge, TN 194

9:00 S153 Impact of Zirconium Hydride Precipitates on Fracture of a Zirconium Alloy
M. Kerr, M.R. Daymond, R.A. Holt, Queen's University, Kingston, Ontario, Canada
J.D. Almer, APS – Argonne National Laboratory, Argonne, IL 194

9:20 S18 On the Improvement of the Fatigue Behaviour of Austenitic Stainless Steel Due to Surface Residual Stresses Produced by Low Temperature Carburizing
G. Minak, Università di Bologna, Bologna, Italia 194

9:40 S136 Operational Residual Stress Formation in Vibration-Loaded Rolling Contact
J. Gegner, W. Nierlich, SKF GmbH, Schweinfurt, Germany 195

10:00 break

10:20 S34 *Invited*—Accounting for Residual Stress in Integrity Assessment of 3-D Structure
R.J. Bucci, M.A. James, Alcoa Technical Center, Alcoa Center, PA
D.L. Ball, Lockheed Martin Aeronautics Co., Fort Worth, TX 195

10:50 S206 Measurements of Residual Stress Fields in Fracture Coupons and Relation to Observed Fracture Properties
M.R. Hill, University of California, Davis, CA
J.E. VanDalen, Hill Engineering, LLC, McClellan, CA. 196

11:10 S89 Fatigue Crack Growth in Plastically Bent Beams
K.W. Jones, M.L. Dunn, University of Colorado, Boulder, CO 196

11:30 S199 Residual Stress Effects on Fatigue Life of Welded Structures Using LEFM
Z. Barsoum, I. Barsoum, Royal Institute of Technology (KTH), Stockholm, Sweden 196

ICRS-8 Industrial Applications: Distortion and Machining
Friday a.m. Maroon Peak

Chair: **J. Bunch**, The Boeing Company, Seattle, WA

8:30 S7 *Invited*—Prediction of Distortion of Airframe Components Made From Aluminum Plates
S. Nervi, ESRD Inc., Saint Louis, MO
B.A. Szabó, Washington University in St. Louis, Saint Louis, MO
K.A. Young, Boeing Co., Saint Louis, MO 197

9:00 S200 Distortion Prediction in Machined Aerospace Components
T.D. Marusich, Third Wave Systems, Minneapolis, MN. 197

9:20 S133 Residual Stresses and Surface Workhardening Induced by Micro Cutting Processes
H. Autenrieth, B. Okolo, V. Schulze, A. Wanner, D. Löhe, Universität Karlsruhe (TH), Karlsruhe, Germany 197

9:40 S177 Characteristics of Residual Stress Profiles in Hard Turned Versus Ground Surfaces With and Without a White Layer
A.W. Warren, Y.B. Guo, The University of Alabama, Tuscaloosa, AL 198

ICRS-8 Industrial Applications: Friction Stir Welding
Friday a.m. Maroon Peak

Chair: **J. Bunch**, The Boeing Company, Seattle, WA

10:30 S10 Residual Stress Determination in AZ31 Friction Stir Welds Using X-ray and Neutron Diffraction
L. Commin, J.-E. Masse, L. Barrallier, Laboratoire Mécasurf, Arts Et Métiers Paristech, Aix En Provence, France . . 199

10:50 S196 Effect of Pressure on the Residual Stress Development in the Linear Friction Welded Ti-6246
S. Zabeen, M. Attallah, M. Preuss, University of Manchester, Manchester, UK
S. Bray, Rolls-Royce plc, Derby, UK. 199

11:10 S194 Residual Stress in Friction Stir Welded Aluminum Alloys
J.A. Pineault, M. Belassel, Proto Mfg. Ltd., Oldcastle, Ontario, Canada
H.J.K. Lemmen, Delft University of Technology, Delft, The Netherlands
M. Brauss, Proto Mfg. Ltd., Ypsilanti, MI 199

D-3

X-RAY PROBE ANALYSES OF COMPLICATED PRECIPITATES FORMED IN COPPER-BASE ALLOYS

Shigeo Sato[1], Yohei Takahashi[1], Takashi Sanada[1], Kozo Shinoda[2], Kazuaki Wagatsuma[3] and Shigeru Suzuki[2]
1) NISSAN ARC, LTD.
2) Institute of Multidisciplinary Research for Advanced Materials, Tohoku University
3) Institute for Materials Research, Tohoku University

The electrical conductivity and mechanical properties of copper-base Cu-Ni-Si alloys can be improved by aging and cold rolling prior to aging. Further improvement of the properties can be achieved by addition of small amount of elements (e.g. Fe) to the alloy. In order to understand the mechanism of the improvement of the properties, the formation and growth processes of precipitates during aging were investigated by the analyses of anomalous small angle scattering (ASAXS) and X-ray absorption fine structure (XAFS). The ASAXS and XAFS results showed that the Cu-Ni-Si alloys without cold rolling exhibited growth of Ni_2Si precipitates with uniform size, whereas wide size distribution of Ni_2Si precipitates was formed in the cold rolled alloys. The wide size distribution was suppressed for the cold rolled alloy added with a small amount of Fe, resulting in formation of precipitates with homogeneous size. XRD measurements were also carried out to analyze microstructural change of Cu matrix with precipitation. The XRD results showed that the size of Cu crystallite in the cold rolled alloys without Fe addition became large at peak aging condition, while no significant size change of Cu crystallite was observed in the cold rolled alloy with Fe addition. It could be deduced that the wide size distribution of precipitates for the cold rolled alloys without Fe was related to the microstructural change in Cu matrix. On the other hand, the Fe addition is likely to result in homogeneous growth of precipitates.

D-7

STATE-OF-THE-ART MULTILAYER OPTICS FOR DIFFRACTOMETRY

B. Hasse, C. Michaelsen, A. Oehr, F. Hertlein, S. Kroth
Incoatec GmbH, Max-Planck-Strasse 2, 21502 Geesthacht, Germany

In this poster, we give an overview on the state-of-the-art beam-shaping multilayer optics for diffractometry. Nowadays a large variety of 1D and 2D optics are available with optimized properties for the customer's applications. We explain the manufacturing process of these optics, summarize the different type of optics and give some examples of typical applications which benefit from the new possibilities.

The optics consist of bent substrates with shape tolerances below 100 nm, upon which multilayers are deposited with single layer thicknesses in the nanometer range and up to several hundreds of layer pairs. Additionally these multilayers were designed with lateral thickness gradients within ± 1% deviation of the ideal shape. This means that a deposition precision in the picometer range is needed. We use sputtering methods for deposition, optical profilometry in order to characterize the shape and X-ray reflectometry to characterize the multilayers. The microstructure is investigated by transmission electron microscopy. The beam parameters like monochromaticity, flux, brilliance and divergence demonstrate for different lab applications the quality of the multilayer optics.

D-10

SYNTHESIS, STRUCTURAL AND CHEMICAL CHARACTERIZATION OF $Ca(HO_3PCH_2)_2$-N(H)-$(CH_2)_6$-N(H)-$(CH_2PO_3H)_2 \cdot 2H_2O$

L. León-Reina[a], A. Cabeza[b], R.M.P. Colodrero[b], M.A.G. Aranda[b], E. Barouda[c], K.D. Demadis[c]
[a]*Servicio Central de Apoyo a la Investigación, Universidad de Málaga, 29071-Málaga, Spain*
[b]*Department of Inorganic Chemistry, University of Málaga, 29071-Málaga, Spain*
[c]*Department of Chemistry, University of Crete, Voutes, Heraklion GR-71003, Crete, Greece*

The structural and functional chemistry of inorganic-organic hybrid materials have recently attracted considerable attention due to a plethora of potential applications such as gas storage, catalysis, and ion exchange [1]. In the area of metal phosphonates, special attention has recently been placed on the use of tetraphosphonates for the preparation of new crystalline compounds with open structures. Phosphonic acids are versatile ligands that allow synthetic access to a great number of structural motifs varying from closely packed 3-D to pillared-layered or open framework structures depending on the nature of the organic groups and the metal ion used [2].

We have focused our study on the synthesis, structural and chemical characterization of a new calcium hexamethylenediamine-*tetrakis*(methylenephosphonate) material, $Ca(HO_3PCH_2)_2$-N(H)-$(CH_2)_6$-N(H)-$(CH_2PO_3H)_2 \cdot 2H_2O$ (**I**). This compound has been prepared as polycrystalline powder at room temperature and also by hydrothermal procedure. The X-ray thermodiffractometry study in combination with thermal analysis shows the existence of an anhydrous phase at 250ºC, (**II**). The rehydration of **II** occurs spontaneously and reversibly at room temperature. Both phases crystallize in triclinic unit cells and their structures have been solved by *ab initio* methodology from strictly monochromatic laboratory X-ray powder diffraction data. The frameworks have been refined by the Rietveld method. **I** and **II** show layered frameworks with the tetraphosphonate groups bridging Ca^{2+} centers (Figure 1). The layers are held together only by H-bonding.

The water molecules are situated in the interlamellar space, interacting by H-bonds and their loss at 250ºC causes a reversible "sliding" of the layers to give the anhydrous phase. The intercalation of NH_3 in **I** led to a new crystalline phase. The relationship between the crystal structures of the different phases will be reported.

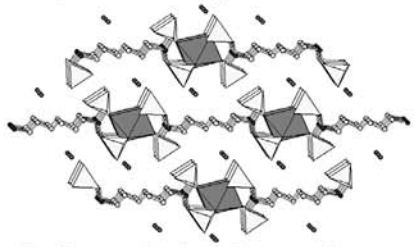

Figure 1. Structure of **I** with the water molecules as red spheres between the organo-inorganic layers.

References

[1] F. Constantino, T. Bataille, N. Audebrand, E.L. Fur, C. Sangregorio, *Cryst. Growth Des.* 7, **2007**, 1881.

[2] K.D. Demadis in: *"Progress in Solid State Chemistry Research"*, Ed. Ronald W. Buckley, 2007, 109.

D-12

PARTICLE SIZE ANALYSIS OF SUB MICRON MATERIALS USING ULTRA SMALL ANGLE X-RAY SCATTERING

Keigo Nagao, Takayuki Konya, Ryuji Matsuo and Yoshio Iwasaki

Rigaku Corporation

3 – 9 – 12 Akishima-shi Matsubara-cho, Tokyo 196-8666, Japan

Small angle X-ray scattering (SAXS) is the most useful method to evaluate the particle size and the molecular structure in nano materials. The conventional SAXS instrument (for example, three slits geometry) is limited to 100nm. Recently, the measurement of sub micron scale using SAXS is required in order to evaluate the property of various materials. In this range, it needs to collect the profile data less than $0.07nm^{-1}$ in order to analyze using SAXS for sub micron particle. Right now, we have succeeded to take a ultra small angle X-ray scattering (USAXS) data easily using the Rigaku SmartLab with pseudo Bonse-Hart geometry configuration. In other word, the SmartLab can support the range from sub nano to sub micron scale by WAXS, SAXS and USAXS. In this presentation, the small angle resolution in this geometry has been evaluated. We will report some examples of sub micron materials using the SmartLab with pseudo Bonse-Hart geometry configuration.

The SmartLab is one of conventional instruments for powder and thin film materials. But, it is possible to perform special measurement such a USAXS.

D-13

A STUDY ON TNE TOTAL EVALUATION OF PHARMACEUTICAL PRODUCTS USING GENERAL PURPOSE XRD EQUIPMENT

Miho Sasaki, Tomikatsu Kubo, Akira Kishi

Rigaku Corporation

3 – 9 – 12 Akishima-shi Matsubara-cho, Tokyo 196-8666, Japan

The study of phase transitions among the various solid states is important to the pharmaceutical products. For example, in the process of drug synthesis requires to evaluate characterization of polymorphism and qualitative and quantitative analysis of impurities. In the process of tableting, it is required to estimate the amount of pharmaceutical products in the tablet, to evaluate impurities polymorphic forms and the content uniformity in a tablet of drug and excipient. In this way, for many evaluations, it takes very long time to evaluate one new medicine, generally. In this presentation, the qualitative and quantitative analysis of impurities polymorphic forms in tablets have been evaluated through the transmission mode. The characterization of polymorphism of a drug substance has been evaluated to use simultaneously performing XRD and DSC measurements on the same sample. These measurements have been made using the Rigaku Ultima IV 2 kW theta- theta design for horizontal sample mounting goniometer configured for the total evaluation of pharmaceutical products.

D-14

X-RAY DIFFRACTOMETRIC DETERMINATION OF CHRYSOTILE ASBESTOS IN BUILDING MATERIALS WITH RIETVELD REFINEMENT

Tomoharu Asahi, Shinji Kobayashi, Takaomi Matsudaira, Kenichi Nakayama, Masaru Kitano, Toshihiro Nakamura

Department of Applied Chemistry, Meiji University, Kawasaki, 2148571, Japan

Asbestos are fibrous silicates with properties of heat resistant, chemically inert and electrical insulators. And asbestos are known to be carcinogenic materials. They have been used widely as industrial products, so it is serious problem in Japan that a great number of building materials include asbestos. Building material for the testing was sampled from ceiling of chemical laboratory. For sample preparation, the board was crushed by hammer and pulverized with ball mill. Crystalline phases of chrysotile ($Mg_3Si_2O_5(OH)_4$), calcite ($CaCO_3$), vaterite ($CaCO_3$), quartz (SiO_2), and small amounts of amorphous and impurities were

identified on the diffraction pattern. So, the test board was considered to be calcium – silicate board. Coexisting of numerous crystalline phases may cause mutual interferences of the analytical lines and neighboring lines. Therefore, quantitative analysis of chrysotile in ceiling board has been conducted with powder XRD / Rietveld refinement. Combination of Rietveld refinement and internal standard method enabled to determine the chrysotile in complex matrix. The analytical result of chrysotile content in building materials obtained from Rietveld refinement was validated by three quantitative method that is, calibration curve method, matrix flashing method, standard addition method. Analytical results derived from these methods were in good agreement with the result obtained by Rietveld refinement method.

D-15

INVESTIGATION OF CO-CRYSTALLIZED PHARMACEUTICAL INGREDIENTS USING SYNCHROTRON RADIATION

M. Herrmann, U. Foerter-Barth, H. Kröber, P.B. Kempa, M. Juez-Lorenzo
Fraunhofer ICT, Pfinztal, Germany
S. Doyle
ISS ANKA FZK, Karlsruhe, Germany

Co-crystals are widely discussed, particularly for pharmaceutical applications. The term is most commonly used in order to describe a crystal containing two or more components together. Thus, co-crystals may encompass molecular compounds, molecular complexes, solvates, inclusion compounds, channel compounds, clathrates and other types of multicomponent systems in a crystalline state. The production and especially a detection of co-crystals, however, are far from being clear, as no clear structure based definition of a co-crystal exists. At Fraunhofer ICT various processing methods for pharmaceutical co-crystals are tested, amongst them supercritical fluid technologies and mechanical processes. The microstructures of samples obtained from these tests have been investigated by means of X-ray diffraction at the ANKA Synchrotron, in order to distinguish co-crystals from pure physical blends. Cocrystallization tests have been performed with combinations of the pharmaceutical ingredients paracetamol, cholesterol, caffeine, ibuprofen and lactose.

D-21

USAGE OF PROBABILITY SCORING TO SORT XRPD SCANS OF DYING PROTEIN ON SIMILARITY

Thomas Degen[a], Irene Margiolaki[b], Jonathan P. Wright[b]
[a]PANalytical B.V., Lelyweg1,7603 EA Almelo, The Netherlands
[b]European Synchrotron Radiation Facility (ESRF), Grenoble, France

In a wide range of applications it is required to sort arbitrarily collected XRPD scans into clusters of similar scans. Additionally it is essential to sort these clusters and the scans in the clusters for similarity too.

One rather new application area is the fast measurement of protein powders in capillaries on synchrotron beam lines. The data collection is usually carried out as a series of 5 to 6 short (2 minute) measurements. Then the capillary is translated with respect to the beam exposing a fresh region of unaffected protein sample to it for the next series of scans.

The radiation induced protein decay is not only visible by fading intensities, but also by peak shifts due to varying unit cell parameters. For further analysis like e.g. Rietveld refinements hundreds or even more scans first need to be sorted into classes of similar scans.

We will demonstrate the implementation and usage of probability scoring and cluster analysis in X'Pert HighScore Plus. First clusters of similar HEWL (hen egg-white lysozyme) scans are created and then both these clusters and the scans inside each cluster are sorted on similarity. This approach creates a sorting that shows a perfectly continuous pseudo-decay axis.

D-23

ZIRCONIUM OXIDE: RIETVELD AND REVERSE MONTE CARLO ANALYSES

Feng Zhang, Siu Lun Alan Lui and Siu-Wai Chan
Department of Applied Physics & Applied Mathematics and MRSEC center, Columbia University, New York, New York 10027
Peter J. Chupas, Peter L. Lee
Argonne National Laboratory, Argonne, Illinois 60439
Jonathan C. Hanson, Wolfgang A. Caliebe
Brookhaven National Laboratory, Upton, New York 48824

The amorphous-to-cubic (a-c) crystallization of nanoZrO_2 in a reducing environment was studied by synchrotron X-ray diffraction. Rietveld analysis was performed to study the changes in crystallite size and lattice parameter as the cubic phase emerged. The pair distribution function (PDF) was obtained from the Fourier transformation of the normalized XRD patterns. A reverse Monte Carlo (RMC) simulation was applied to provide details of the local structure during the crystallization process as well as to calculate partial PDFs of Zr-Zr and Zr-O during the crystallization. The number of Zr's next-nearest neighbors of Zr remains 12, whereas the number of O's as nearest neighbors of Zr increases from 6.7 to 7.3 as the material evolves from an amorphous into a cubic structure, suggesting the persistence of a high concentration of oxygen vacancies. These simulated atomic structures show that the local structure of the amorphous phase bears resemblance to the short-range arrangement of cubic ZrO_2,

consistent with the results of X-ray absorption near edge spectroscopy (XANES) at Zr L_{II} and L_{III}. The amorphous-tocrystalline phase transformation is affected by the environment. Under an oxidizing condition, the amorphous phase crystallizes directly to tetragonal and subsequently to monoclinic zirconia.

D-26

QUANTITATIVE DETERMINATION OF ASBESTOS IN BULK INSULATION BY XRD

Douglas S. Kendall and Richard A. Martinez
National Enforcement Investigations Center, U. S. Environmental Protection Agency, Building 25, Denver Federal Center, Denver, CO 80225. Email: kendall.douglas@epa.gov

Asbestos containing insulation and other construction materials occur in many buildings in the United States. Renovating or demolishing these buildings may release asbestos to the environment and expose people. The U.S. EPA has issued regulations to control and prevent releases. For regulatory purposes the cut-off concentration is one percent. This is not a health or risk based level, but rather is an attempt to distinguish materials manufactured with asbestos from those which contain incidental amounts of asbestos. Nevertheless, the one percent limit is important in measuring the concentration of asbestos in building materials, and is critical in enforcing the regulations.

Asbestos in bulk insulation is typically measured using polarized light microscopy (PLM). This method is fast, and can reliably determine the presence or absences of asbestos in almost all building materials. However, in order to comply with EPA regulations the concentration of asbestos must also be determined. PLM is not well suited for making quantitative measurements, especially on materials close to the one percent limit. Work at NEIC has shown that XRD can successfully deal with a variety of building materials. X-ray diffraction can be used to make quantitative measurements of asbestos content that are precise and unbiased, even near the one percent limit.

For the EPA, asbestos is the fibrous minerals chrysotile, amosite, crocidolite, actinolite, tremolite and anthophyllite. The EPA long ago issued an XRD method for bulk asbestos, but the method has not been thoroughly validated. The EPA method uses silver filters to present the sample to the diffractometer as a thin layer. Correction for absorption is based on the silver diffraction lines. Modern diffractometers with array detectors are much faster at acquiring data with an acceptable signal to noise ratio than the diffractometers available when the method was first issued. The use of an array detector makes the silver filter method reasonably efficient, with sample analysis taking less than one hour. Data and techniques will be presented that show the quality of the results that may be attained. Sample preparation will be discussed. Data on the bias and precision of the method will be presented.

D-29

HIGH-TEMPERATURE CHARACTERIZATION OF THREE-DIMENSIONAL DISTRIBUTION OF RESIDUAL STRESSES IN CrN COATINGS ON STEEL

K.J. Martinschitz[a], Ch. Kirchlechner[a], R. Daniel[b], Ch. Mitterer[b], J. Keckes[a]
[a]*Erich Schmid Institute for Materials Science, Austrian Academy of Sciences and Department of Materials Physics, University of Leoben , Leoben, Austria*
[b]*Department of Physical Metallurgy and Materials Testing, and Christian-Doppler Laboratory forAdvanced Coatings, University of Leoben, Leoben, Austria*

High-temperature characterization of residual stresses in coated surfaces can be used to understand phenomena contributing to the thermal fatigue of working tools. Since the thermal fatigue is often a local phenomenon, it is necessary to develop methods which can be used to characterize degradation phenomena with a good spatial resolution.

In this contribution, results from a high-temperature characterization of residual stress depth and lateral gradients will be presented. As a model system, samples of CrN coatings on steel thermally cycled using a laser beam in the temperature range of 50-650 °C up to 100 000 times were selected. A depth gradient of stresses in the irradiated spot was characterized using high-energy synchrotron X-ray diffraction at the EDDI beamline of BESSY (Berlin, Germany). A lateral distribution of stresses was characterized at a G3 beamline of Hasylab (Hamburg, Germany). In both cases, the samples were analysed in-situ in a temperature range of 25-700 °C using a heating chamber DHS1100 (Anton Paar GmbH, Graz, Austria). In this way, it was possible to determine 3D distribution of residual stresses in the irradiated spot as a function of temperature whereby the structures exhibited complex changes in the morphology and in the residual stress state as a consequence of laser irradiation. The presented approach allows a complex three dimensional characterization of thermo-mechanical processes in coating-substrate composites and opens the possibility to understand phenomena related to the thermal fatigue of coated tools.

This work was supported by Austrian NANO Initiative within the project "StressDesign - Development of Fundamentals for Residual Stress Design in Coated Surfaces". The authors are grateful for the support from the European Union.

D-31

MECHANICAL PROPERTIES OF THIN FILMS CHARACTERIZED BY A COMBINATION OF sin2ψ AND X-RAY DIFFRACTION SUBSTRATE TECHNIQUES

K.J. Martinschitz and J. Keckes

Erich Schmid Institute for Materials Science, Austrian Academy of Sciences and Institute of Metal Physics, University of Leoben , Leoben, Austria

X-ray diffraction is routinely used to characterize elastic strains in polycrystalline thin films by applying $\sin^2\psi$ method. Those strains are however dependent on the *hkl* reflection measured. Macroscopic stresses imposed on the film can be easily determined by X-ray diffraction substrate curvature technique which is based on the measurement of rocking curves on the substrate symmetrical reflections at different sample positions. The macroscopic stress can be then calculated using Stoney's formula.

By comparing experimental macroscopic stresses (from the curvature method) and elastic strains (from $\sin^2\psi$ technique), it is possible to evaluate a variety of parameters like thin films X-ray elastic constants, mechanical elastic constants and grain-interaction models. In this contribution, the possibilities of the use of both techniques will be demonstrated. This work was supported by Austrian NANO Initiative within the project "StressDesign - Development of Fundamentals for Residual Stress Design in Coated Surfaces".

D-32

X-RAY DIFFRACTION STUDY OF ANISOTROPIC STATE OF RESIDUAL STRESS AFTER DOWN-CUT AND UP-CUT FACE GRINDING

Zdenek PALA[1], Nikolaj GANEV[1], Jan DRAHOKOUPIL[1,2]

[1]Department of Solid State Engineering, Faculty of Nuclear Sciences and Physical Engineering, Czech Technical University in Prague, Trojanova 13,
120 00 Prague, Czech Republic

[2]Department of Metals, Institute of Physics, ASCR, Na Slovance 2, 182 21 Prague, Czech Republic

Machining by face grinding is inherently an anisotropic surface treatment and, therefore, ground surfaces are palpable examples that epitomize anisotropy in residual stresses (RSs). In particular, normal RSs frequently vary significantly in value and character (i. e., tensile or compressive), appreciable shear RSs occur in the direction of grinding and gradients of RSs are present even in shallow depths of several micrometers in thickness. Moreover, during face grinding two fundamentally different processes of material removal are alternately in progress - up-cut and down-cut grinding. The contribution focuses on a detailed X-ray diffraction analysis and electron microscopy investigation of the above mentioned regimes of grinding.

Studied samples, which were manufactured from three types of steels - mild carbon steel *C45*, corrosion-resistant steel *M300* and high speed steel *M41*, underwent annealing before the actual grinding by a corundum abrasive wheel. Macroscopic residual strains were measured in six azimuths φ for both positive and negative tilts ψ and the calculation of macroscopic RSs was performed by using Dölle - Hauk and least square fitting method. Microscopic RSs and mean coherent scattering domain sizes were evaluated by single line profile-fitting method for each obtained {211} diffraction peak of ferrite in order to unveil possible direction-dependent dissimilarities. The geometry of the diffraction experiment was considered carefully with regard to the sense of rotation of abrasive wheel and to the translation of sample.

D-38

PROBING THE MICRO-MECHANICAL BEHAVIOR OF BONE VIA HIGH-ENERGY X-RAYS

Jonathan Almer[1] and Stuart Stock[2]

[1]X-ray Operations and Research, Argonne National Laboratory, Argonne, IL

[2]Department of Molecular Pharmacology and Biological Chemistry, Northwestern University, Chicago, IL

Bone is a highly-adaptive, particulate-reinforced composite which, through a complex hierarchical structure, achieves excellent mechanical performance. The composite preserves, to a large degree, the desirable properties of the individual components: high toughness of the bone matrix, collagen fibrils stabilized by water, and high stiffness of the reinforcing phase, nano-sized crystallites of carbonated apatite. The fracture propensity of bone has been linked to both bone fracture strength and loading spectra, so it is important to quantify mechanical input to bone and identify "weak-link" microstructures or changes in global parameters characterizing microarchitecture. Numerous investigators have quantified this mechanical input *in vivo* with strain gages attached to cortical bone. With attached strain gages, however, the mechanical response of volumes beneath the bone's surface can only be inferred indirectly. This limitation hinders understanding of effects such as bone remodeling, in which mechano-transduction must translate the forces applied to the whole bone to instructions at the cellular level directing adaptation of the bone.

In light of these issues, we have recently applied wide- and small-angle X-ray scattering techniques to study the micro-mechanical response of bone on different length scales. High-energy X-rays (80 keV) and a transmission geometry are used for bulk sampling through transverse cross-sections of hydrated bones under *in situ* compressive loading. The aggregate macroscopic response is determined using strain gages and a load cell. Simultaneously, wide-angle scattering is used to quantify texture, domain size and internal strains and stresses in the apatite mineral phase, while small-angle X-ray scattering is used to determine

the collagen response along the longitudinal axis. Combined, these data provide unique information about load transfer between the constituent phases of bone. In addition to *in situ* loading, effects of hydration on internal strain are presented.

D-39

THE X-RAY DIFFRACTION CHARACTERISTICS OF DIFFERENT MATERIALS

Yiliang Zhang, Jinyan Liu, Xuedong Xu
(College of Mechanical Engineering & Applied Electronics Technology, Beijing University of Technology, Beijing 100022, P.R. China)

To solve the engineering problem faced when detecting residual stress of material such as stainless steel and aluminium alloy by using X-ray method, three different materials - carbon steel (Q235), stainless steel (1Cr18Ni9Ti) and aluminium alloy (LY12) were demarcated by equal intensity girder demarcating method and detected by X-ray system and electromotive method respectively when gradual loading by using a modified residual stress detecting equipment and self-edit detecting software. Then X-ray diffraction characters of different materials were obtained by comparing with theoretical values. The results show: 1) the stainless steel appears two diffraction peaks when it is diffracted by X-ray. Although 127°K_α diffraction peak is strikingly marked, the calculated stress can't reflect the real stress according to this peak; however, although the peak back ratio of 149°K_β diffraction peak is lower, it can be the basis to calculate stress. 2) Aluminium alloy also have two diffraction peaks when it is diffracted by X-ray. But for aluminium alloy, only can the 158° peak reflect the change of the stress. The experiments prove: X-ray diffraction peaks at some angles can't reflect the real change of stress which is a common problem.

Keywords: X-ray, residual stress, electromotive method, equal intensity girder demarcating, diffraction characteristic of material.

D-43

NEW ANAYTICAL EXPRESSION OF THE THRESHOLD LIMIT OF THE MIXING PARAMETR OF PSEUDO-VOIGT FUNCTION

F. HADJ LARBI*, A. KHEREDDINE, D. BRADAI
**alarbi_fay@yahoo.fr*
Faculty of Physics, USTHB, BP 32 El-Alia, Dar El Beida, Algiers, Algeria

We revisit the theory of X-ray Diffraction Profile Analysis relative to the pseudo-Voigt function (noted *pV)*. We present a generalization of the analytical expressions of integral breadth, full width at half maximum and Fourier transform of the *pV* function. The main result is a new analytical expression of the threshold limit of the mixing parameter η which is depending of the Gaussian and Lorentzian components of full width at half maximum of the pV function. The new expression is used to develop a new algorithm for the fit procedure. The efficiency of the proposed program is tested on different experimental line profiles and seemed better than earlier available programs.

D-52

RESIDUAL STRESSES AFTER CMP ON THIN FILMS

Wei-En Fu[1], Meng-Ke Chen[2], Chao-Chang A. Chen[2]
[1]Center for Measurement Standards, Industrial Technology Research Institute, 321 Kuang Fu Rd., Sec. 2, Hsinchu, Taiwan 300
[2]Department of Mechanical Engineering, National Taiwan University of Science and Technology, 43, Sec.4, Keelung Rd., Taipei, Taiwan 106

In needs of global surface planarization in the semiconductor manufacturing industry as the feature sizes of Integrated Circuit (IC) components continue to shrink, Chemical Mechanical Polishing (CMP) has emerged as the fasted-growing operation in the past decade. The CMP processes employ both chemical and mechanical interactions to planarize chemically modified surface layers using slurries composed of chemicals and submicron-sized particles. Consequently, the success of the high quality production for IC components depends considerably on the performance of the CMP processes. Thus, it is necessary to evaluate the CMP produced surface integrity such as surface finish and surface stresses to enhance the performance of CMP.

The goal of this study was to determine the surface and subsurface residual stress after CMP processes for thin films. Two different thin films of W and TiN on silicon wafer were chemical-mechanical polished at designed parameters with different down pressures and relative velocities to generate the stress differences on surface and below surface. The stress measurements, then, were performed on the PANalytical X'Pert MRD diffractometer. In order to study the stresses of thin films below 1 μm, the diffractometer was aligned to the configuration of grazing-incidence X-ray diffraction (GIXRD) with its principles based upon the conventional sin2Ψ method to measure the changes of lattice strains. According to Hooke's law, the lattice strains were converted to residual stresses, assuming the thin films are elastically isotropic. For the subsurface residual stresses, a multi-reflection method was used to measure the stress gradients below the surface as a function of GIXRD penetration depth and film thickness. The variations of surface and subsurface residual stresses from different CMP planarization conditions were evaluated with the distribution of the stress gradient along the depth of thin films.

D-59

THE RIETVELD REFINEMENT OF THE RARE EARTH ORTHOBORATES

Ayşen Yılmaz[a*], Semih Seyyidoglu[a,b]
[a]Middle East Technical University, Chemistry Department, 06531, Ankara, Turkey
[b]Tetra Technological Systems, 34335, Balmumcu İstanbul

Borate containing compounds have long been the subject of interest over many decades, motivated by their extraordinary optical properties [1]. The structural description of some rare earth-activated orthoborates corresponding to the empirical formula $LnBO_3$ (Ln= La, Nd, Sm, and Eu) were reinvestigated using solid state wet reactions by Mahiou's group [2]. The rare-earth borates are characterized by a high structural flexibility caused in the linkage planar/non-planar BO_3- groups and BO_4-tetrahedra, which can occur as isolated or condensed fundamental building units [3].

WITHDRAWN

In the present research, we prepared $LnBO_3$ (Ln=Y, La, Nd, Sm, Eu, Gd, Dy, Ho, Er, Tm, Yb, Lu) powder samples by using with Ln_2O_3 and H_3BO_3 (ratio=1:2) at 900°C for 1 hour and 1000°C for 5 hour heatings were applied in muffle furnace. Then, their XRD patterns at 700, 900, 1000°C were investigated. For $GbBO_3$, space group was found to be $P6_3/mmc$ and the unit cell parameters were found as a=3.83302(9), and c=8.9084(3) Å. The R values were found as Rexp=2.87, Rwp=10.65, GOF=13.73. Finally, their pure lanthanide orthoborate phases and crystal structure analysis were performed by Rietveld Analysis using High Score Plus.

References:

1. L. Li, P. Lu, Y. Wang, X. Jin, G. Li, Y. Wang, L. You, j. Lin, Chem. Mater., 14, (**2002**), 4963-4968.
2. S. Lemanceau, G. Bertrand-Chadeyron, R. Mahiou, M. El-Ghozzi, J.C. Cousseins, P. Conflant, R.N. Vannier, J.Solid State Chemistry 148, (**1999**), 229-235.
3. H. Huppertz, B.V.D. Eltz, R.D. Hoffmann, H.Piotrowski, J. Solid State Chemistry 166, (**2002**), 203-212.
* Corresponding Author e-mail: ayseny@metu.edu.tr

D-61

AUTOMATED SAXS MEASUREMENTS OF PROTEIN SOLUTIONS WITH A LABORATORY BASED SAXS SYSTEM

Manfred Kriechbaum, Peter Laggner and Philipp Herrnegger
Institute of Biophysics and Nanosystems Research, Austrian Academy of Sciences, Graz, Austria and Hecus X-ray Systems GmbH., Graz, Austria

Combining the availability of a high-flux laboratory small-angle X-ray scattering (SAXS) camera employing a high-brilliance micro-beam delivery system with point-focus and automatized data evaluation software, we are developing a compact and reliable system for online and high-throughput measurements for low resolution structures of proteins in solution. During such automated SAXS measurements the radius of gyration and relative mol.wt., as well as the real-space function (distance distribution function) of the scattering curve (after buffer subtraction) are calculated in certain time-intervals and the measurements are automatically stopped if no significant changes or improvements in the real-space functions can be achieved. Additionally, a low-resolution model is calculated. First results, using the protein lysozyme as a benchmark test, will be shown.

D-63

QUANTIFICATION OF RETAINED AUSTENITE IN ASTM A743 GRADE CA6NM CAST MARTENSITIC STAINLESS STEEL THROUGH X-RAY DIFFRACTION

Rojas Marín, Jessika Viviana, Toro Betancur, Alejandro
Tribology and Surfaces Group, School of Materials Engineering, National University of Colombia

Martensitic stainless steels are widely used for manufacturing hydraulic components such as turbines, impellers and liners, due to their excellent mechanical properties, which are, to some extent, related to the amount of retained austenite in the microstructure.

Diverse methods have been used to determine the amount of retained austenite in steels, such as quantitative metallographic analysis, magnetic methods, dilatometric measurements, differential thermal analysis and Mossbauer spectroscopy. One of the most successful techniques for this purpose is, however, X-ray diffraction, mainly because the results obtained are quite reliable once the preparation of the samples is adequate. Nevertheless, a major drawback arises when retained austenite from a region close to the surface of the samples transforms to martensite during polishing, which avoids proper quantification of phases in the material.

In this work, X-ray Diffraction was used to identify and quantify retained austenite in an AISI A743 grade CA6NM martensitic stainless steel. The analyses were carried out at several temperatures, which were selected according to typical tempering treatments applied to hydraulic turbines. Also, improved surface preparation techniques were developed to allow measurement of retained austenite at room temperature. The results obtained by X-ray diffraction were compared to and validated with dilatometric measurements.

D-65

A NEW HIGH-THROUGHPUT SAXS SCREENING TOOL

P. Kotnik, H. Schnablegger
Anton Paar GmbH, A-8054 Graz, Austria
G. Langenbucher
Anton Paar USA, Ashland, VA

Small Angle X-ray Scattering (SAXS) is an established technique for nano-structure analysis in various application fields. However, the technique has not been widely used for combinatorial or, more generally, automated measurements till now. Technical limitations have prevented maintaining the desired resolution of the measurement while achieving the high through-put requirement.

A combination of several technological concepts has lead to the design of a SWAXS system for high-resolution and high-throughput measurements.

The technical aspects include requirements to simultaneously characterize materials in the small and wide angle range for documentation of nano-structure and phase behavior, a short exposure time to reduce radiation damage and other stability effects, and a control software which can coordinate the system components, acquire data, and convert the two-dimensional scattering image into the desired result.

All these requirements were met in the SAXSess system. The technical aspects and selected results are discussed.

D-68

X-RAY DIFFRACTION AND HIGH PRESSURE STUDIES ON ORGANIC THERMAL ENERGY STORAGE MATERIALS - TRIS(HYDROXYMETHYL) AMINOMETHANE (TRIS)

[1]Wen-Ming Chien, [1]Vamsi K. Kamisetti, [1]Juan C. Fallas, [1]Erik D. Emmons, [1]Dhanesh Chandra, [2]Aarron M. Covington, [3]Raja S. Chellappa, [4]Martin Kunz, and [4]Simon Clark
[1] Metallurgical and Materials Engineering /MS388, University of Nevada, Reno, Reno, NV 89557
[2] Department of Physics /MS220, University of Nevada, Reno, Reno, NV 89557
[3] Carnegie/DOE Alliance Center, Geophysical Laboratory, Carnegie Institution of Washington, Washington, DC 20015
[4] Advanced Light Source, Lawrence Berkeley National Laboratory, Berkeley, CA 94720

Organic thermal energy storage materials, or Orientationally disordered crystals (ODIC), such as polyalcohols and amines are useful for thermal energy storage due to the presence of the solid state phase transitions where the latent heat can be utilized to store energy. The effects of temperature and pressure on the X-ray diffraction patterns and Raman spectra of tris(hydroxymethyl) aminomethane ($C(CH_2OH)_3NH$, TRIS) were measured. X-ray diffraction and DSC results show that the $\alpha \rightarrow \gamma$ solid state phase transition of TRIS occurs at 133.7°C and the crystal structure change from orthorhombic (α-phase) to BCC (γ-phase) at ambient pressure (1 atm). The volume thermal expansion equations of α and γ phases were calculated as $V_\alpha = 0.01789xT(K) + 146.73$ (298-403 K) and $V\gamma = 0.07901xT(K) + 128.62$ (403-418 K). At room temperature, the high pressure synchrotron X-ray diffraction patterns and Raman spectra by using Diamond Anvil Cell (DAC) show that TRIS undergoes a phase transition ($\alpha \rightarrow \beta$) starting at ~1 GPa. A new high pressure β-phase were observed at a pressure range from ~1 GPa to 9.3 GPa. The effects of hydrogen bonding on the broad OH and sharp NH stretching modes will be discussed. Detail results of temperature dependent effects on high pressure Raman spectra and Pressure-Temperature (P-T) phase diagram of TRIS will be presented.

D-70

GRAZING-INCIDENCE DIFFRACTION APPLIED AS A CROSSCUTTING TOOL IN THE NANOBIO REGIME

Brian D. Pate[1], Xue Han,[1] Denis T. Keane,[2] Stephen P. Wargacki,[3] Richard A. Vaia,[3]
Michael F. Durstock,[3] Hyo-Sik Kim,[4] Sung-Min Choi[4]
1: The Dow Chemical Company; 2: Northwestern University; 3: Air Force Research Laboratory; 4: Korea Advanced Institute of Science and Technology

The detailed structure of thin films is a critical determinant in a broad range of useful physical processes. Both in-plane, interfacial structure and depth-dependent features can be significant depending on the process of interest. Grazing-incidence diffraction has been employed as a crosscutting technique to characterize these structural aspects of, for instance, films of (a) mono- and multilayer tobacco mosaic virus organized via convective assembly; (b) spin-coated and annealed poly-3-hexylthiophene and composites; (c) spin-coated and annealed mesogenic metallophthalocyanines and related derivatives; and (d) inorganic species deposited via a variety of processes. We will highlight our method development in this area and those aspects of the results which provide insight into important structure/property correlations.

D-71

X-RAY DIFFRACTION CHARACTERIZATION OF MOVPE ZnSe FILMS DEPOSITED ON (100) GaAs USING CONVENTIONAL AND HIGH-RESOLUTION DIFFRACTOMETERS

T.N. Blanton, C.L. Barnes, M. Holland, K.B. Kahen, Eastman Kodak Company, Rochester, New York 14650-2106
V. Gupta, F.Bai, Rochester Institute of Technology, Rochester, New York 14623-2106

ZnSe-based heterostructures grown on GaAs substrates have been investigated for use in pin-diode LED applications. ZnSe has a large band gap, 2.76 eV, as well as a near lattice match to GaAs, 5.669 Å vs. 5.654 Å, respectively. In this study a metallorganic vapor phase epitaxy (MOVPE) deposition technique is used to produce doped and undoped thin films of ZnSe on (100) GaAs.

Understanding the effect of deposition parameters on the crystallographic quality of the ZnSe films is important for optimizing the performance of these devices. X-ray diffraction is well suited for analyzing epitaxial thin films deposited on single-crystal substrates. In this study a conventional Bragg-Brentano diffractometer (BBD) has been used to screen samples for phase identification, crystallite size, presence of polycrystalline ZnSe, and initial rocking curve (RC) analysis. A limitation of the conventional diffractometer is that the smallest RC full width at half maximum that can be achieved is 500-600 arc seconds. As deposition parameters are optimized and the RC limit of the conventional diffractometer is reached, analysis is moved to a 4-bounce high-resolution diffractometer (HRD). Although more time for analysis is required, using the HRD has an RC resolution advantage, where RCs of <20 arc seconds are obtained for neat GaAs wafers.

Combining the BBD and HRD instruments for analysis of ZnSe films grown on GaAs substrates allows for an efficient means of high sample throughput combined with an accurate measurement of film alignment.

D-73

MEASUREMENT CONDITIONS FOR QUANTITATIVE ANALYSIS USING THE RIETVELD METHOD

Erina Kagami and Aya Takase
Rigaku Corporation
3 – 9 – 12 Akishima-shi Matsubara-cho, Tokyo 196-8666, JAPAN

The Rietveld method has been widely used for quantitative analysis of powder samples. However, the influence of the measurement conditions such as the geometry and silt sizes on accuracy and reliability of the analysis results is often overlooked. Those conditions need to be carefully selected to minimize the errors associated with the instrument and the pattern fitting method. This is because the measurement conditions could increase the systematic errors of diffraction angles, decrease diffraction intensities, or cause diffraction profiles that cannot be reproduced and fit well by the commonly used profile functions such as pseudo Voigt and Pearson VII. These changes of the diffraction pattern cause errors of the estimation of integrated intensities and result in inaccurate and unreliable quantitative analysis. In order to see the effects of various measurement conditions, the quantitative analysis results of diffraction patterns collected under different conditions were compared.

A randomly oriented powder sample with less than 30 μm grain size was used to eliminate the errors associated with the sample. The diffraction patterns were collected with different geometry, divergence angle of the incident beam, and resolution of the receiving optics. The Rietveld analysis results of those patterns were compared regarding the accuracy and reliability of the quantity of each phase in the sample. A horizontal sample mount diffractometer, Ultima IV, was used for data collection and powder diffraction pattern analysis software, PDXL, was used for the Rietveld analysis.

The results of comparison and effects of each measurement condition on the quantitative analysis are discussed in this presentation.

D-74

PHASE TRANSFORMATION AND STRUCTURAL BEHAVIOR STUDIES OF Li-BASED HYDRIDES AFTER PRESSURE HYDRIDING/DE-HYDRIDING CYCLING

Wen-Ming Chien, Joshua H. Lamb and Dhanesh Chandra
Metallurgical and Materials Engineering /MS388, University of Nevada, Reno, Reno, NV 89557

Li-based complex hydrides have been a promising candidate for the hydrogen storage materials because $Li_2NH \Leftrightarrow LiNH_2$ reaction possess a large amount of reversible hydrogen storage (6.5 wt.%). In this study, we investigated the effect of the pressure cycling and performed the X-ray diffraction studies to determine the phase transformation and structural behaviors of both $Li_2NH/LiNH_2$ and $LiNH_2/Li_3AlH_6$ systems. The degradation of hydrogen storage capacities of $Li_2NH/LiNH_2$ system after pressure cycling showed 2.55 (~10.25 bar) and 2.95 wt% (~0.86 bar) hydrogen storage loss after 1100 cycles at 255°C. X-ray diffraction results of the products after pressure cycling showed mainly Li_2NH and LiH phases, and the impurity Li_2O phase. The phase analysis results showed the Li_2NH phase reduced from 77% to 13%, and LiH phase increases from 18% to 57% after 1100 cycles. The results of the effect of the impurity gases in hydrogen showed that the O_2 and NH_3 have the most impact of the hydrogen storage capacities. X-ray diffraction study results of $LiNH_2/Li_3AlH_6$ system showed that there is a phase transformation between 165°C to 200°C. Li_3AlN_2 phase was formed after re-hydriding $LiNH_2/Li_3AlH_6$ at 325°C for 20 hours. Detail results of structural behaviors and pressure isothermals of different cycles will present.

D-76

CHEMOMETRIC APPLICATIONS IN QUANTITATIVE X-RAY POWDER DIFFRACTION OF INTACT CONSOLIDATED SAMPLES

Michael D. Moore, Colleen Hair, Peter L.D. Wildfong
Duquesne University, Mylan School of Pharmacy, Pharmaceutics

Purpose. Demonstrate the suitability of reflectance and transmission geometry multivariate calibrations in quantitative X-ray powder diffraction (XRPD) of intact quaternary pharmaceutical compacts.
Methods. Quaternary compacts consisting of two crystalline materials (anhydrous theophylline and lactose monohydrate), and two disordered materials (microcrystalline cellulose and starch) were prepared. Mixtures of varied composition were compressed into 13 mm cylindrical compacts at pressures ranging from 67.0 – 268.1 MPa. Compacts were analyzed by XRPD in reflectance and transmission geometries, using Cu K_α radiation (λ = 1.5406 Å, 2-60º 2 , 0.02º step, 45.0 kV, 40.0 mA). Quantitative models of composition were estimated using univariate calibrations, which were compared with multivariate methods including principle components regression (PCR), classical least squares regression (CLS), and partial least squares regression (PLS) over entire diffraction patterns (corrected for nonlinear axis shift).
Results. Quantitative univariate models for the two crystalline components resulted in R^2 = 0.895 and 0.935 respectively for reflectance and transmission geometries. Quantitative multivariate models, were generated using CLS, PCR, and PLS. Superior linearity in transmission geometry was observed for crystalline components (R^2 = 0.967, 0.969, and 0.973 respectively from CLS, PCR, and PLS models). Linearity was slightly improved for disordered components using reflectance geometry (R^2 = 0.928, 0.927, and 0.951 respectively from CLS, PCR, and PLS models). All multivariate models, which demonstrated significantly improved signal-to-noise, sensitivity, and selectivity relative to univariate models, were able to predict compositions of both disordered and crystalline phases; CLS was the most successful owing to its ability to generate regression vectors highly correlated to the pure component diffraction patterns.
Conclusions. Traditional univariate XRPD calibrations for quantitative phase determination cannot discriminate between different disordered components. Multivariate modeling improves signal-to-noise, sensitivity, and selectivity, improving the quantitative power of low-diffracting disordered constituents. The increased accuracy of transmission measurements for crystalline components is afforded by a larger irradiated sample volume, while increased accuracy of the reflectance measurements for disordered components is likely due to increased angular resolution.

D-77

THE USE OF NET ANALYTE SIGNAL ORTHOGONALIZATION IN THE SEPARATION OF MULTI-COMPONENT DIFFRACTION PATTERNS OBTAINED FROM X-RAY POWDER DIFFRACTION OF INTACT COMPACTS

Michael D. Moore, Robert P. Cogdill, Steven M. Short, Colleen Hair, Peter L.D. Wildfong
Duquesne University, Mylan School of Pharmacy, Pharmaceutics

Purpose. Demonstrate the use of net analyte signal (NAS) orthogonalization as a means to accurately separate multi-component diffraction patterns thereby permitting the calculation of multivariate figures of merit (FOM) to evaluate the suitability of transmission and reflectance modes of quantitative X-ray powder diffraction (XRPD) on intact consolidated samples.
Methods. A four-component system consisting of two crystalline materials (anhydrous theophylline and lactose monohydrate), and two disordered materials (microcrystalline cellulose (MCC) and starch) was employed. Powder mixtures of varying composition were compressed into 13 mm cylindrical compacts varying in compression. The compacts were analyzed by XRPD in both reflectance and transmission geometries, using a PANalytical X'Pert Pro MPD with Cu K_α radiation (λ = 1.5406 Å). Quantitative models of composition were estimated using partial least squares regression and classical least squares regression. FOM were used to compare geometrical modes of analysis.
Results. Quantitative models were successfully generated for each individual component using whole pattern analysis. The R^2 values for theophylline, lactose, MCC and starch were 0.97, 0.98, 0.96, and 0.97 for the transmission data, and 0.92, 0.95, 0.95, and 0.95 for reflectance data, respectively. Though the transmission geometry showed superiority in specificity and accuracy, the reflectance geometry showed increased angular resolution.
Conclusions. The use of XRPD in the analysis of intact compacts remains an important mainstay in the characterization of solid state phenomena. Accurate separation of multi-component diffraction patterns with respect to the covariance structure enables direct observation of changes to material structure without compromising the intensity of correlated angular variables. Multivariate FOM provide additional descriptors for model performance permitting a direct comparison between reflectance and transmission mode analyses. Transmission provides an enhancement in signal-to-noise, sensitivity and precision, albeit somewhat attributable to decreased effects from sample displacement. The ability of multivariate FOM to discriminate model performance from data collected via two separate modes of analysis provides impetus for the increasing use of chemometric tools in PXRD applications.

D-78

ANALYSIS OF FOCUSED BEAM POWDER X-RAY DIFFRACTION USING CURVED CRYSTAL OPTICS

Ayhan Bingölbali and C. A. MacDonald
Center for X-ray Optics, University at Albany, SUNY, Albany, NY 12222

X rays emitted isotropically from a conventional source can be focused onto a small sample area to give efficient utilization for powder diffraction with torroidal crystal optics. Measurements were made using a very low power (~30 W) microfocus source for several small inorganic standard samples. Diffracted peak width, resolution, and intensity were analyzed. The resolution determined from the uncertainty in measured peak location was much smaller than the peak width due to the focussed beam, and was limited by the pixel size of the area detector. A simulation model was developed to understand the diffraction ring shape and width, and a simple geometrical model was used to predict peak width. Good agreement was found between the simulation, the geometrical calculation and the measured peak width data.

F-45

HIGH-RESOLUTION XRF IN 35-60 KEV:-LANTHANIDES' K-SPECTRA

Mari Mizusawa and Kenji Sakurai
National Institute for Materials Science, 1-2-1, Sengen, Tsukuba, Ibaraki 305-0047 Japan
Yasuko Terada
Japan Synchrotron Radiation Research Institute, SPring-8, Sayo-gun, Hyogo 679-5198, Japan

A brilliant X-ray source in the high-energy region is extremely attractive for studying heavy elements such as Lanthanides, because it is possible to excite K shell electrons. In the present study, we developed a wavelength-dispersive XRF spectrometer for high-energy X-rays (35-60 keV). This will help us to explore both the chemical environment and electronic structure of Lanthanides, which are strongly correlated to the materials. exotic properties. The experiments were performed at BL37XU B-branch, SPring-8, Harima, Japan. The primary X-ray photons used are 10^{th} harmonics of an undulator beam, and the energy is 75.5 keV. The samples measured were cerium and gadolinium compounds. The typical energy resolution obtained was 39 eV and 58 eV, at Ce $K\beta_1$ (39.2574 keV) and Gd $K\beta_1$ (48.6964 keV), respectively. The spectra are ca. 10 times better than those obtained by means of conventional energy-dispersive measurement using a Ge detector, which can usually resolve only 2 peaks, $K\beta_1$ and $K\beta_2$. As it is now possible to separate $K\beta_1$ and $K\beta_3$ peaks, as well as $K\beta_2$ and $KO_{II,III}$, changes in the spectra due to chemical effects can be studied much better than before. Further details of instrumentation and some typical high-resolution spectra for Lanthanides' compounds will be presented.

References
[1] K. Sakurai, M. Mizusawa, and Y. Terada, Rev. Sci. Instrum **78,** 066108 (2007).
[2] M. Harada and K. Sakurai, Jpn. J. Appl. Phys., **37,** 2740 (1998).
[3] M. Harada and K. Sakurai, Spectrochimica Acta, **B54,** 29 (1999).

C-6

THIN FILM TECHNOLOGY FOR PREPARATION OF X-RAY WAVEGUIDE-RESONATORS

E.V. Egorov[1], R.E. Ayala-Jiménez[2], M.S. Afanas'ev[3], V.K. Egorov[1]
[1] IMT RAS, Chernogolovka, Moscow district, 142432 Russia
[2] Fisichem Incorporated, Miami, USA
[3] MIREA, Moscow, Russia

The invention of planar X-ray waveguide-resonator (PXWR) is the great present for nanotechnology and the direct challenge for X-ray synchrotron facilities [1]. PXWR is a very simple device but it allows to form thread X-ray beams with width 7÷200 nm characterized by an enhanced radiation density and a low flux angular divergence. These devices have beautiful perspectives for fundamental material researches and a wide practical applications. So, it is very important to pay attention to the technological peculiarities of it's preparation.

The waveguide-resonator is formed by couple planar dielectric reflectors placed opposite each other on distance, which must be smaller as the coherence length of the quasimonochromatic X-ray radiation transported by the device. The distance is defined by the thickness of strips deposited on edges of one reflector in the couple. According to our opinion, the deposit technology must supply a very high thickness uniformity on all length of the strips [2]. But for the practical purposes it is very important to know the critical value for the strips thickness nonuniformity. This work is devoted to the discussion of the technological thickness inaccuracy at the strips deposition and to the evaluation of permissible non-parallelism between reflectors forming the waveguide-resonance channel. The experimental results to be presented demonstrate that the typical standard inaccuracy of the conventional methods of long coating deposition $l \approx 100$ mm is acceptable for PXWR preparation.

[1] V.K. Egorov, E.V. Egorov. Background of X-ray nanophotonics based on the planar air waveguide-resonator // X-ray Spectrometry. V36. 2007. pp. 381-397.
[2] V.K. Egorov, E.V. Egorov. Application on an planar X-ray waveguide for structure study of thin film coating // Thin Solid Films. V398-399. 2001. pp. 405-412.

C-4

RADIOISOTOPE RH-101 AS X-RAY SOURCE FOR INSTRUMENTS ON SPACE MISSIONS

Ch. Stenzel, Astrium GmbH, Friedrichshafen, Germany; Ch. Schroer, Technical Univ. of Dresden;
B. Lengeler, RWTH Aachen; R. Vianden, Univ. of Bonn, Germany

For exploration missions to Mars or the Saturnian's moons the employment of X-ray instruments (XRD and XRF) is envisaged. Due to the harsh mass and volume restrictions only radioisotopes are suited as X-ray sources for instruments traveling on spaceships for several years. Isotopes, which have been applied so far, are not optimal for these missions in terms of half-life and X-ray energy (Fe-55) or specific activity (radioactivity/mass for Am-241).

Rh-101 represents an optimum choice concerning half-life (3.3 a) and X-ray energy (18 keV) for diffraction and fluorescence experiments of crushed samples from the planet's surface. Powder diffractometry with the much higher energy compared to Fe-55 would result in a reduced radiation background. Also a much broader excitation range for XRF is possible.

A source with an activity of several 100 MBq can be produced via a nuclear reaction in a cyclotron using light ions at a moderate consumption of beam time and by applying conventional techniques for separating and enriching the radioactive isotopes from the original Ru-target. This would yield a photon flux of about 10^6 photon/s in the detection angle.

First experimental results on the available production rates, additional gamma ray radiation, and the performance in a standard XRD/XRF laboratory set-up will be presented.

F-16

RADIOACTIVE SAMPLE EFFECTS ON EDXRF SPECTRA

Christopher G. Worley
Los Alamos National Laboratory, MS G740, Los Alamos, NM 87545

Energy dispersive X-ray fluorescence (EDXRF) is a rapid and often straightforward method to determine sample elemental composition. Spectra covering most of the periodic table can be collected in a few minutes or less, and elemental content can be easily determined if there is adequate energy resolution. Pulse pile-up, escape peaks, and sample diffraction effects can complicate spectra when using a Si(Li) detector, but these artifacts can be deciphered by an experienced analyst.

Radioactive samples, however, can introduce artifacts that further complicate spectral interpretation, particularly when using portable instruments where the detector is located in close proximity to the instrument analysis window held against the sample. Gamma rays emitted by a sample are indistinguishable to the detector from X-rays of the same energy, but radioactive sample gamma energies are normally too high to be of concern in EDXRF. However, spectra collected from alpha particle emitters can contain X-ray emission peaks. For example, plutonium-239 EDXRF spectra exhibit a prominent uranium L X-ray emission peak series. When a plutonium-239 atom alpha decays, there is some probability that the uranium-235 daughter nucleus will be left in an excited state that can then transfer its excess energy to an electron through internal conversion.[1] If the electron is then ejected upon absorption of this energy, an X-ray photon or Auger electron will be emitted. Hence, the uranium L X-ray series is emitted due to sample radioactive decay rather than source-induced X-ray fluorescence, and quantifying the uranium based on observed peak intensities can lead to erroneous results.

A portable EDXRF instrument was used to collect spectra from plutonium and other radioactive samples. Examples will be presented and compared with data collected with a WDXRF instrument to demonstrate the differences to which sample radiation-induced X-ray emission affects the detectors on these two types of instruments.

1. D. Reilly, N. Ensslin, and H. Smith, Jr. *Passive Nondestructive Assay of Nuclear Materials*, U.S. Government Printing Office: Washington, D.C., 1991.

F-57

TABLETOP SPECTROMETER FOR GRAZING INCIDENCE XRF

N. Zoeger[1], D. Ingerle[1], C.Streli[1], F. Meirer[1], P. Wobrauschek[1], G. Pepponi[2]
[1]*Vienna University of Technology, Atomic Institute of the Austrian Universities,Stadionallee 2, A-1020 Vienna, Austria*
[2]*Fondazione Bruno Kessler-irst, Via Sommarive 18, I-38050 Povo, Italy*

Secondary ion mass spectrometry (SIMS) is routinely used for determining profile shapes, junction depths, and doses of dopants in Si wafers. However, in case of ultra shallow junctions (USJ) SIMS is going towards its intrinsic limits. Whereas the depth resolution and quantification in the deeper regions are still sufficient with SIMS, the native oxide-induced matrix effects are limiting factors for the technique if dose and distribution in the first nanometres are required.

Therefore a more complete characterization of USJ, as demanded by microelectronics technological nodes will require the application of different complementary techniques such as Medium Energy Ion Scattering, Scanning Transmission Electron Microscopy, Spectroscopic Ellipsometry as well as Grazing Incidence X-ray Fluorescence Analysis (GIXRF). The development of the mentioned techniques and the understanding of their complementariness for USJ analysis will be the task of a research

activity within the running EC project ANNA (European Integrated Activity of Excellence and Networking for Nano and Micro-Electronics Analysis). Within the frame of this activity the X-ray group of the Atomic Institute develops GIXRF as a laboratory source driven tool for USJ analysis. The technique relies on the measurement of fluorescence signals at various incidence angles of the exciting X-ray beam. As the penetration of the primary X-rays becomes larger as a function if increasing incidence angles, GIXRF provides information on the total implanted dose in the substrate material. Since GIXRF is very sensitive in the first few nanometres it delivers satisfactory results for sample depths where SIMS has its drawbacks.

To successfully accomplish GIXRF analyses a tabletop measuring chamber is currently under development.

In the present work the design as well as the current status of the prototype will be presented. Hardware and software requirements to meet the demands of depth profiling with GIXRF will be discussed. Moreover first results obtained on As doped Si wafers will be presented.

F-56

MICRO X-RAY FLUORESCENCE SPECTROMETER FOR LIGHT ELEMENT ANALYSIS WITH LOW POWER TUBE EXCITATION

S. Smolek,[1] C. Streli,[1] N. Zoeger[1] P. Wobrauschek,[1] F. Meirer[1]
[1] *Vienna University of Technology, Atominstitut, Stadionallee 2, 1020 Vienna, Austria*

Micro X-ray Fluorescence (Micro-XRF) is a well established tool to determine the spatial distribution of major, minor and trace elements in a sample. It is widely used to investigate samples from different fields (biology, geology, life science, etc.). The method is non-destructive, requires little sample preparation and allows simultaneous multi-element detection.

Most available Micro-XRF spectrometers operate in air which does not allow the analysis of low-Z elements ($Z \leq 14$). To extend the analytical range down to light elements ($Z \geq 6$) a special micro-XRF spectrometer has been designed.

This system consists of an air cooled low power X-ray tube (50W) with molybdenum anode and a thin (70µm) exit window. An optional beam filter can be inserted to reduce spectral background. The beam is focused onto the sample using a polycapillary X-ray optics, offering a focal spot of about 30µm FWHM. Characteristic X-rays from the sample are detected by means of a Si(Li) detector with ultra thin window. An optical microscope attached to a high resolution CCD camera is used to control the measurement position. Sample positioning and scanning is performed using a motorised xyz sample stage.

The new spectrometer offers improved excitation and detection conditions, necessary for light element analysis. The thin window of the X-ray tube allows both, the molybdenum L-lines and K-lines to sufficiently excite the sample over a wide energy range. Detection of the low energetic characteristic radiation is possible due to the ultra thin window of the detector. To eliminate absorption of the exciting and fluorescent radiation in air the system operates under vacuum condition. Sample scanning is automated and controlled by specialized computer software developed for this spectrometer. Access to the spectrometer will be available for external users through the transnational programme of a running EC project (ANNA, www.i3-anna.org).

In this work the spectrometer design as well as first test measurements on different samples, such as artificially created elemental patterns of light elements and human bone will be presented.

F-55

GRAZING-EXIT-XRF EXPERIMENTS AT HASYLAB BEAMLINE L

F. Meirer[a], G. Pepponi[b], C. Streli[a], P. Wobrauschek[a], N. Zoeger[a]
[a] *Atominstitut, Vienna University of Technology, 1020 Wien, Austria.*
[b] *ITC-irst, via Sommarive 18, 38050 Povo (Trento) Italy*

Total reflection X-ray fluorescence analysis (TXRF) operates with the incident beam impinging below the critical angle of total reflection on the surface of a flat polished surface of reflector. The interference between incident and reflected beam causes in case of microcrystalline samples an intensity increase of the fluorescence signal by a factor (1+R) where R is the reflectivity numerically close to 1. The additional effect due to the penetration depth in the nm region is a low background. Both effects are leading to excellent detection limits in TXRF and are widely used in ultra trace element analysis. Grazing incidence XRF (GI-XRF) uses the angle dependent wavefield intensity in order to characterize the structure of layered materials and the composition gradient of materials that are inhomogeneous along the direction perpendicular to the surface. The inverse GI-XRF with the incident beam perpendicular to the reflector's surface and collecting the fluorescence under grazing angle can also be applied [1]. This mode of analysis was named grazing exit X-ray fluorescence (GE-XRF) and is theoretically based on the reciprocity theorem [2]. The interference in this case is not between primary and reflected beam but among the superposition interference of the fluorescent waves emitted from the sample and observed under the critical angle of total reflection φ_{crit}.

A GE-XRF experiment was performed at HASYLAB beamline L using the newly designed equipment from the Atominstitut Vienna X-ray group. The setup was designed with the axis of rotation of the detector exactly in the plane of the reflector. The experiments were performed with the aim to study XANES self-absorption effects, which were observed previously in GI-XRF geometry.

A series of dried residues with different total amounts of arsenic masses on quartz reflectors were investigated. Angle dependent measurements of the samples were carried out by rotating the detector around the sample in the center of the reflector. The experimental data and the theoretical curves showed good agreement. The GE setup allows spatially resolved measurements of the sample. In order to achieve measurements with higher lateral resolution a polycapillary half lens was used to produce a focal spot of 40μm in diameter. With this setup 2D-scans of the samples have been performed and compared with data from confocal microscopy. XANES measurements of the samples were performed and compared with data gained for the same samples under GI conditions.

[1] T. Noma, A. Iida, K. Sakurai, Phys. Rev. B 48 (1993) 17524.
[2] R.S. Becker, J.A. Golovchenko, J.R. Patel, Phys. Rev. Lett. 50 (1983) 153.

F-54

SAMPLE MORPHOLOGY: INFLUENCE ON TOTAL REFLECTION X-RAY FLUORESCENCE ANALYSIS

C. Horntrich[1], F. Meirer[1], C. Streli[1], P. Kregsamer[1], G. Pepponi[2], N. Zoeger[1], P. Wobrauschek[1]
[1] *Vienna University of Technology, Atominstitut, Stadionallee 2, 1020 Vienna, Austria*
[2] *ITC-irst, via Sommarive 18, 38050 Povo (Trento) Italy*

Total Reflection X-ray Fluorescence Analysis (TXRF) is a method for qualitative and quantitative analysis of trace elements. In general TXRF is known to allow for linear calibration typically using an internal standard for quantification [1,2]. Absorption effects concerning exciting and detected radiation are usually disregarded. This is justified because mostly small sample amounts are used. The thin film approximation in particular assumes a very thin sample and therefore differential absorption for photons with different energies can be ignored. Furthermore the elements in the sample are assumed to be homogeneously distributed. Hence the loss of the fluorescence signal due to absorption of the primary beam equally affects all elements and quantification by using an internal standard is justified. However, for higher total amounts of samples deviations from the linear relation between fluorescence intensity and sample amount have been observed [3].

The topic of the presented work is an investigation of the parameters influencing the absorption phenomenon. A simulation model was developed to calculate the influence of the absorption effects. Samples with different total amounts of arsenic have been prepared to determine the upper limit of sample mass where the linear relation between fluorescence intensity and sample amount is no longer guaranteed. It was found that the relation between fluorescence intensity and sample amount is linear up to ~100 ng Arsenic. The parameters necessary for the simulation (sample dimensions and volume) were determined by analyses with a confocal white light microscope. Even though the results of the simulations are not satisfying yet it could be shown that the key parameters for the absorption effect are the density of the investigated atom in the dried residues and the shape of the residue. Difficulties for the simulation appeared due to the determination of the density of the arsenic atoms in the sample. To improve the simulation model further investigations are necessary.

[1] P. Wobrauschek, X-ray Spectrometry 36 (2007) 289-300.
[2] R. Klockenkamper, Wiley-Interscience, New York, 1997.
[3] D. Hellin, J. Rip, S. Arnauts, S. De Gendt, P.W. Mertens, C. Vinckier,
Spectrochimica Acta Part B: Atomic Spectroscopy 59 (2004) 1149-1157.

F-59

DOSAGE OF SILICA IN POLYMERS BY X-RAY FLUORESCENCE

P. Ricou, S. Kodjie, X. Shen
Arkema Inc., 900 First Avenue, King of Prussia, PA 19406-0936

Silica is an additive commonly used in polymers for modifying their properties such as flow for example. There is a balance between not adding enough (lack of flow, blockage) and adding too much (surface blooming, haziness). Hence, accurately measuring the amount of silica in the polymer is of primary importance. We recently worked on different approaches for the measurement of silica using X-ray fluorescence. They are applicable over the range of silica concentrations we explored so far (up to 1.3 wt%). Different methods called for different sample preparations, which were found to affect directly the precision of the measurements. The ultimate precision achieved was around 5% relative at a 2σ level, and the presentation will illustrate the different approaches we took to develop this new method.

F-30

DEVELOPMENT OF SOIL STANDARD MATERIALS CONTAINING HAZARDOUS METALS FOR X-RAY FLUORESCENCE ANALYSIS

Yasuhiro SHIBATA, Junnosuke SUYAMA, Masaru KITANO, and Toshihiro NAKAMURA
Department of Applied Chemistry, Meiji University

Standard material of soil containing hazardous metals i.e., Cr, As, Se, Cd, Hg, and Pb was developed for the X-ray fluorescence (XRF) analysis. Homogeneous standard soil was prepared by adding appropriate amount of aqueous standard solutions to the base soil and then drying and mixed with V-type mixing machine. Base soil powders ground to under 12.5 μm of modal particle size were Tachikawa loam, brown forest soil, and weathered granite soil containing 17.9, 9.43, and 3.49 mass% of Fe_2O_3, respectively. Concentrations of Cr, As, Se, Cd, Hg, and Pb in soils were determined with metal furnace atomic absorption

spectrometry of decomposed samples. For the XRF determination analytical lines were selected CrKα, AsKα, SeKα, CdKα, HgLα and PbLβ accompany with the corrections for overlapping of SeKβ to PbLβ and PbLα to AsKα. Specimens for XRF analysis were prepared by powder briquette pressed in the 23mmφ Al ring with 300 kgf cm^{-2} and loose powder in 31mmφ of polyethylene cup covered with 6 μm polypropylene film. The durability of the standards was checked by intermittently XRF measuring, and was good endurance for 240 min irradiation of primary X-ray (50 kV, 80 mA). The calibration curves drawn with proposed standards were good linearity under 3000 mg kg-1 for Cr, As, Se, Cd, Pb, and 300 mg kg^{-1} for Hg. Calibration curves of 6 determinants in the 3 different base soils with two specimen mounting methods were remarkably differed with each other. Corrections with Compton scatter for AsKα, SeKα, CdKα, HgLα and PbLβ, and with background scatter for CrKα were effective and gave same slope of the calibration curves with different soil characters and mounting methods. The lower limits of detection were 0.5-6.4 mg kg^{-1}. The spike test for 5 determinants showed good recovery for gravel soil and pumice soil.

F-19

PREPARATION OF THE MULTI-LAYERED PLASTIC REFERENCE MATERIALS FOR CONFOCAL 3D-MICRO X-RAY FLUORESCENCE ANALYSIS

K. Nakano[1,2], K. Tsuji[1]

[1]*Department of Applied Chemistry, Graduate School of Engineering, Osaka City University, 3-3-138 Sugimoto, Sumiyoshi-ku, Osaka 558-8585; Japan*

[2] *JST-Innovation Plaza Osaka, 3-1-10 Technostage, Izumi-city, Osaka, 594-1144; Japan*

Recently, micro region analysis has been one of the significant trends in XRF study. The latest approaches are remarkable in that they enable determining the depth of elemental distribution, leading to three-dimensional analysis. In particular, confocal 3D-micro XRF analysis combined with a polycapillary X-ray lens is a promising method. We have investigated laboratory-made confocal 3D-XRF instrument with laboratory X-ray sources, and applied for the plant seed [1, 2], rice grain [3], and solid/liquid analysis [4].

Reference materials are essential tool in order to obtain the accurate and precise depth information of analyte in the thick samples. However, reference materials for 3D-micro XRF analysis were not available. The aim of the study is the preparation of the multi-layered plastic reference materials for the confocal 3D-XRF analysis. The reference materials of multi-layered film were prepared by the spin-coating method. The detailed experimental results will be presented.

[1] K. Tsuji, K. Nakano: "Development of confocal 3D XRF spectrometer with Cr-Mo dual excitation", *X-ray Spectrom.*, 36, 145-149 (2007).
[2] K. Tsuji, K. Nakano, X. Ding, “Development of Confocal Micro-XRF Instrument using Two X-ray Beam”, *Spectrochim. Acta B.*, 62, 549-553 (2007).
[3] K. Nakano and K. Tsuji: “Development of Confocal 3D micro XRF Spectrometer and Applications of the rice grain”, *Bunseki Kagaku*, 55, 501-509 (2006) (In Japanese).
[4] K. Tsuji, T. Yonehara, K. Nakano: " Application of confocal 3D micro-XRF for solid/liquid interface analysis", *Anal. Sci.*, 24, 99-103 (2008).

F-22

SAMPLE PREPARATION FOR TOTAL-REFLECTION X-RAY FLUORESCENCE ANALYSIS OF BLOOD SAMPLE

Kouichi Tsuji[1], Hiroshi Matsui[1], Masayuki Hino[2], Hideki Wanibuchi[2], Hisayuki Kohno[3], Kazushi Aranami[3], Yuuichirou Shimizu[3], Takashi Yamada[3]

[1]Department of Applied Chemistry, Graduate School of Engineering, Osaka City University, 3-3-138 Sugimoto, Sumiyoshi-ku Osaka 558-8585 Japan

[2]Graduate School of Medicine, Osaka City University, 1-4-3, Asahi-cho, Abeno-ku, Osaka-shi, Osaka 545-8585, Japan

[3]Rigaku Industrial Corporation, 14-8 Akaoji, Takatsuki, Osaka 569-1146, Japan

We studied the sample preparation for total-reflection X-ray fluorescence (TXRF) analysis of the whole blood sample of human body. Although the TXRF analysis of the blood sample has been reported[1], a simple and rapid preparation procedure for TXRF analysis of the blood sample is required. After the whole blood was diluted 8 times by Milii-Q water[2], it was dropped onto a glass substrate. By adding the water to the blood, the red blood cells were destroyed due to “hemolysis” phenomenon; therefore, the flat dried residue was obtained, leading to the improvement of limits of detection limits. Since any separation processes were not necessary, TXRF analysis could be rapidly performed. A commercially available TXRF instrument (Nanohunter, Rigaku. Co.) was used for TXRF analysis. The quantitative data of Ca, Fe, Cu and Zn in whole blood were obtained by addition of internal standard (V) and were compared by the data obtained by ICP-AES. Both data showed a good agreement. It would be merit of TXRF over ICP-AES that Br and Cl could be determined without any problems. Finally, the whole blood of the rat, which drank the polluted water with As, was measured by TXRF, after the same sample preparation.

References

(1) A. Prange, H. Boddeker : *Fresenius Z Anal. Chem.,* **335**, 914 (1989).
(2) Y. Matsuoka, K. Tsuji : *BUNSEKI KAGAKU*, **54**, 749 (2005).

F-23

LARGE AREA SILICON DRIFT DETECTORS

A. Pahlke, T. Eggert, S. Pahlke, R. Stötter, F. Wiest
KETEK GmbH, Hofer Str. 3, 81737 Munich, Germany

Silicon Drift Detectors (SDDs) are commercially available for more than 10 years. They are widely used in XRF, TXRF, electron microprobe analysis systems and synchrotron applications.

The big benefit of SDDs compared to other X-ray detectors as Si(Li)s or pindiodes is the spectroscopic performance principally being independent of the sensitive area. As there is a growing demand for larger detector areas, KETEK has developed SDDs with active areas up to 100 mm².

We will present spectroscopic measurements of SDDs with areas varying from 10 to 100 mm². Energy resolution below 130 eV for the Manganese Ka line and peak to background values of more than 10,000 will be shown for devices with active areas of 100 mm² when cooled down to -60°C. Count rate dependency of the energy resolution and the peak position is shown to be negligible up to count rates of 100,000 counts per second.

Temperature dependent measurements of the energy resolution will be shown for different detector areas. We will present improved cooling techniques for KETEK VITUS modules which allow detector temperatures down to -50°C at an ambient temperature of +20°C. Energy resolutions below 135 eV for 100 mm² SDDs and 130 eV for 30 mm² devices at -50°C are achieved.

F-17

CRYSTALLINE PHASE ANALYSIS AND ELEMENTAL ANALYSIS OF ALKALI-WASHED FLY ASH AND ACTIVATED SLUDGE ASH

Atsushi OHBUCHI, Masaru KITANO and Toshihiro NAKAMURA
Department of Applied Chemistry, Meiji University

Crystalline phase of fly ash caused from municipal solid waste was analyzed by X-ray diffractometry (XRD). Quartz (α-SiO_2), calcite ($CaCO_3$), anhydrite ($CaSO_4$), calcium chloride hydroxide (CaClOH), halite (NaCl), sylvite (KCl) and rutile (TiO_2) were identified on the diffraction patterns of raw fly ash samples.

Crystalline phase of activated sewage sludge ash was analyzed using XRD combined with chemical extractions. Crystalline phases of aluminum calcium phosphate ($Ca_9Al(PO_4)_7$), aluminum phosphate ($AlPO_4$), iron phosphate ($FePO_4$), quartz, crystobalite (SiO_2), plasioclase (Ca-$NaAlSiO_3$) and hematite (Fe_2O_3) were identified on diffraction patterns of sewage sludge ash.

X-ray fluorescence analysis (XRF) for 13 major and 5 minor elements in fly ash samples were developed using powder briquette method. The calibrating standards of major elements were prepared by extra-pure reagents containing respective determinants using hand mixing with alumina mortar. The calibration curves of 18 elements showed a good linearity within the ranges of the calibration. The samples were ground for 80 min with a centrifugal ball mill till particle size became under 10 μm of modal diameter. The quantitative results are in good agreement with those obtained by the coal fly ash standard reference material (NIST 1633b). Chlorine and Br could be analyzed though their volatile characters. The main components of fly ash were Al_2O_3, SiO_2, Cl and CaO. Several thousand ppm of Zn and Pb were included in the most of fly ashes.[1)]

The glass bead/XRF was used for the determination of 10 major and 5 minor elements in sewage sludge ash. The main components of sewage sludge ash were Al_2O_3, SiO_2, $P2O_5$ and CaO, which several thousand parts per million of Cu and Zn were included.

Reference
1) A. Ohbuchi, M. Kitano, T. Nakamura, *X-ray Spectrom.*, in press.

F-58

X-RAY FLUORESCENCE (XRF) ANALYSIS OF HANFORD LOW ACTIVITY WASTE SIMULANTS: METHOD DEVELOPMENT

D. M. Missimer, A. R. Jurgensen, R. L. Rutherford
Savannah River National Laboratory, Aiken, SC 29808

The Hanford Tank Waste Treatment and Immobilization Plant (WTP) is evaluating a X-ray Fluorescence (XRF) as a rapid turnaround technique to support the pretreated low activity waste (LAW) stream to the LAW Vitrification Plant. The LAW stream is primarily a liquid supernatant comprised of sodium hydroxide and sodium nitrate. It also contains sulfate, aluminum, potassium, and trace metals. The low activity treated waste will be concentrated along with any LAW vitrification recycle solutions to 5 to 8-M sodium. The target concentration of the treated LAW batch will be defined by the relative concentrations of sodium and sulfate. Each pretreated batch will be transferred to a temporary holding tank, Concentrate Receipt Vessel (CRV), where after analysis, it will be moved to the Melter Feed Preparation Vessel (MFPV). The glass formers will be added in

amounts determined by the treated LAW analysis. Because of the limited capacity of the CRV, a turnaround time of < 15-hr is required.

The overall objective of this study was to develop an XRF analytical method that provides rapid turnaround time (<8 hours), while providing sufficient accuracy and precision to determine variations in waste. The results of this research will be presented.

F-47

ANALYSIS OF ORES AND CONCENTRATES BY USING BENCHTOP WDXRF

Yoshiyuki Kataoka[1], Hisashi Homma[1], Yasujiro Yamada[1], Hisashi Inoue[2], Hisayuki Kohno[1]
[1]Rigaku Industrial Corporation, Takatsuki, Osaka, Japan
[2]Rigaku Americas Corporation, The Woodlands, Texas

The demands of rare metals and base metals have risen by the recent rapid growth of developing countries and the requirement of rapid and precise analysis of ores and concentrates such as for copper and zinc and iron ore has increased. In the analysis of the ores and concentrates, wavelength dispersive spectrometers, which give high spectral resolution and high light element sensitivity, are commonly used to obtain high precision analysis of target element and the analysis of light elements.

High power spectrometers have generally been used in WDXRF for the purpose of these analyses. However, compact spectrometer is requested in the analysis at mining site and satellite laboratory for easier installation requirement.

We have developed a bench-top WDXRF spectrometer. The spectrometer is equipped with a new air cooled 200W X-ray tube and the analyzable element range is from F to U. We have measured several ores and concentrates such as iron ore and zinc ore and could obtain accurate results for both heavy and light elements and the result demonstrated that this spectrometer can also be used as backup system in a main laboratory.

The spectrometer configuration and some examples of analyzed results will be presented.

C-10

THE SYNERGY OF XRD AND XRF IN A SHALE AND SLATE ANALYSIS

L. Fields*, M. Martin, Rigaku Americas Corporation, The Woodlands, TX, USA

A sample of slate and shale were each analyzed with X-ray diffraction and X-ray fluorescence techniques. Phase identification was possible from XRD and elemental analysis combined with mapping was possible with XRF.

Results are displayed in XRD as 2 plots with line markers overlaid for phases present and, in XRF, as a semi-quantitative “standard-less” elemental results table. Additionally, individual elements are mapped across the surface of both samples.

The combined analytical techniques of XRD and XRF prove synergistic, specifically in cases with high amorphous content, moisture /organics, sulfur, and low crystallite size (clays). These sample characteristics limit or hinder the XRD ability to identify specific phases without elemental confirmation from XRF.

XRF can detect trace elements (possibly hidden to XRD) and provides relative elemental abundance. By sampling multiple (500 micron diameter) points across the samples, surface, XRF’s 3-D elemental mapping creates an elemental “topographical” view of the specimen.

This information can illustrate homogenous or non-homogenous distribution. The mapping can provide insight to the composition of inclusions, for example, faster than a microprobe. Since many microscopy labs can be inundated with work, an XRF with mapping capability can relieve the burden in a cost effective manner, as it still maintains its primary purpose as a tool for bulk elemental analysis.

With both XRF and XRD, better phase identification is possible. It is also possible to assign likely geological points of origin by determining a similar set of trace elements and specific combinations of phases.
The XRF-derived elemental information can also be used by the to support, or as an indication of, possible environmental conditions and the period of elapsed time for the (diagenesis) phase transition to occur.

F-33

HANDHELD XRF FOR ARCHAEOMETALLURGICAL STUDIES: IN-SITU ALLOY AND METAL ANALYSIS OF A PRIVATE SWORD COLLECTION

J. Feuer, T. Turner, K. Russell
Innov-X Systems, Inc. Woburn, MA USA
info@innovxsys.com

Archaeometallurgy involves the compositional analysis of archaeological and other historically and/or artistically significant metal objects. Primary metals and alloys can be identified along with their relative concentrations utilizing XRF. Handheld XRF

is ideally suited for in-situ, non-destructive measurements of these valuable objects. This surface analysis can perform major, minor and trace analysis to confirm metal and alloy identification without damaging the material. Such information helps to accurately describe the bulk metal, inlay, plating and/or other coatings. The identity and/or concentration of alloys and metals helps determine the composition, origin, technology, authenticity and value of an archaeometallurgical object, and aids in optimal restoration and preservation. Trace element analysis can help in the discovery of the provenance of an object or the metals it was made of. A series of related objects can be analyzed to learn patterns of alloy and specific metal use. A private sword collection from a Salem, Massachusetts collector was characterized for metal and alloy content. The specifications of the Portable XRF used in this study, the data collection techniques, results of the compositional analysis, and a description of the collection will be discussed.

F-46

APPLICATIONS OF POLARIZED EDXRF SYSTEM FOR LIGHT MATRIX SAMPLES

Tokuhiro Nakamura[1], Takao Moriyama[1], Makoto Doi[1], Hisayuki Kohno[1], Hisashi Inoue[2]
[1]Rigaku Industrial Corporation, Osaka, Japan
[2]Rigaku Americas Corporation, The Woodlands, Texas

The polarized source configuration in EDXRF reduces system background, improving precision and light element detection limit compared to direct excitation configuration. We have developed a new polarized EDXRF (EDXL 300) which can hold large samples up to 380mm in diameter to expand the applications such toys. Elements from Na to U can be measured simultaneously, without the need for specialized sample preparation.

One of the effective applications for polarized EDXRF system is oil analysis. Fuel oil consists of the light matrix (C and H) and then the large background is observed in the direct EDXRF system because of the scattered radiation of the continuous X-rays from X-ray tube. The polarized EDXRF system reduces the background drastically by the polarized optical configuration and then a low content of sulfur and phosphorus in biodiesel can be analyzed with ultra low detection limit. The advantage of the polarized EDXRF appears especially in the applications for light matrix samples because of efficient background reduction for the analysis for both heavy and light elements.

Further results and more effective applications by the EDXRF system will be presented.

F-78

TISSUE ELEMENTAL MAPPING USING HDXRF WITH DOUBLY CURVED CRYSTALS

D. Li, Z. Chen, A.H. Koeppen, and S.C. Michael
(X-ray Optical Systems, East Greenbush and V.A. Medical Center, Albany, New York)

The bio-essential elements Fe, Cu, and Zn are thought to be major contributors to the pathogenesis of cardiovascular and neurological disorders, and perhaps other diseases. Highdefinition X-ray fluorescence (HDXRF) is a convenient method for mapping of elemental distributions in tissues collected by biopsy or autopsy. Monochromatic beams give a low signal-to-noise ratio and, therefore, higher sensitivity than other methods. The micro-focusing beam also provides mapping with high spatial resolution.

The excitation X-ray beam is constructed from a conventional laboratory X-ray tube. It is focused by doubly curved crystal (DCC) optics based on Bragg diffraction. The monochromatic focusing beam strikes a tissue sample and produces X-ray fluorescence of metals in the specimen. An energy dispersive detector (ED) is used to detect the fluorescence spectrum. The tissue sample is scanned in the x-y plane that lies perpendicularly to the focused X-ray beam, allowing observation of highly localized metal concentrations. Metal composition at each location can be determined through ED spectra.

This work demonstrates the use of DCC optics in obtaining a monochromatic focusing beam. The experimental system was constructed using a 50 W X-ray tube, DCC optics, and a silicon drift detector. A beam spot of 70 μm was obtained. X-ray fluorescence lines were detected for Fe, Zn, and Cu in human brain tissues while the sample was scanned in an x-y plane. Trace elemental tissue mappings for both normal and abnormal tissues were performed.

F-70

HEALTHY PHARMACEUTICAL DRUGS - CONTROL OF IMPURITIES IN ACTIVE PHARMACEUTICAL INGREDIENTS BY EDXRF

Kai Behrens*, Andrew Scothern*, Heiko Ress*, Alexander Seyfarth**
**Bruker AXS Inc., Madison, Wisconsin, USA
*Bruker AXS GmbH, Karlsruhe, Germany

Palladium is amongst a number of metals used as catalysts in industrial hydrogenation reactions. Hydrogenation involves the addition of hydrogen to unsaturated organic compounds and is a key component in the production of pharmaceutical products. The Palladium is usually added as a ten percent constituent of a carbon matrix. Other metal catalysts used in hydrogenation can include Platinum, Rhodium and Ruthenium.

Knowledge of the amount of catalyst used is important in controlling the reaction. The residual catalyst metal is usually present in the 1 to 20 parts per million (ppm) ranges. Too little Palladium results in an inefficient hydrogenation process whilst too much has an adverse economic impact on manufacturing costs.

Determination of the residual Palladium in the finished product can give vital information on the efficiency and economics of the hydrogenation reaction. Traditional methods of catalyst analysis have incorporated wet chemical techniques.

Clearly an updated method that yields simpler, faster and more accurate Palladium concentration would give a large advantage to the site laboratory. XRF is the obvious answer to this analytical problem.

Today elemental analysis with (ED-XRF) has become a very important tool in research and for process or quality control. Flexible to cover different analytical tasks, low in maintenance for cost-effective operation, small in size for easy relocation - these characteristics are making the S2 RANGER attractive for a wide range of applications in industry e.g. cement, oils, lubricants, chemicals, refinery, research, environmental monitoring and waste management.

F-84

EVALUATION OF X-RAY FLUORESCENCE SPECTROMETERS FOR POSSIBLE IMPLEMENTATION IN A MANFACTURING LABORATORY - METALS IN ALUMINA

Lora L. Brehm, Don W. Burns
The Dow Chemical Company, Midland, Michigan, 48667

X-ray fluorescence (XRF) spectrometry is often used in manufacturing laboratories to monitor elemental composition of materials for process and quality control. There are many types of wavelength and energy dispersive XRF spectrometers available for these types of applications including hand-held, bench-top, on-line and fully equipped floor models. This paper will describe the results of a three vendor application study that was done to assist in the selection of an XRF spectrometer that would be implemented in a manufacturing laboratory for determination of metals in alumina. The Bruker S4 Explorer, PANalytical Mini-Pal 4 and Rigaku ZSX Mini II spectrometers were evaluated in this study. The performance of the spectrometers will be compared for quality of the fit of the standard calibration, precision, accuracy and detection limit. Other factors considered important for installation in a manufacturing lab will also be discussed.

C-21

STRUCTURE ANALYSIS AND EXTINCTION COEFFICIENT OF PbSe COLLOIDAL NANOCRYSTALS

Iwan Moreels[a], David De Muynck[b], Frank Vanhaecke[b], Zeger Hens[a]
[a]Physics and Chemistry of Nanostructures, Ghent University, BE-9000 Ghent, Belgium
[b]Laboratory of Analytical Chemistry, Ghent University, BE-9000 Ghent, Belgium

Colloidal lead selenide nanocrystals (Q-PbSe) promise to be an important material for nearinfrared applications. Due to quantum confinement, their band gap can be tuned over the entire telecom wavelength range. In combination with their bright luminescence and high nonlinear refractive index, this could lead to a whole range of new applications, such as quantum dot LED.s, lasers, and all-optical photonic devices.

To gain quantitative insight into the Q-PbSe optical properties, absorbance spectroscopy was used in combination with inductively coupled plasma mass spectrometry (ICP-MS). ICP-MS yields the absolute concentration of Pb and Se, from which both the Pb:Se ratio, and the concentration of the nanocrystals can be determined. The Pb:Se ratio of the nanocrystals revealed that these colloidal nanocrystals are non-stoichiometric, showing an excess of Pb atoms for all samples studied. A detailed structural model was used to confirm that this excess is located at the nanocrystal surface.

Absorbance spectroscopy on a Q-PbSe suspension of known concentration showed that we can distinguish two regions in the absorbance spectrum. Near the band gap of the nanocrystals, strong confinement effects are observed through a blue shift of the band gap with decreasing nanocrystal size, accompanied by an increase of the extinction coefficient. However, at high energies (>2.5 eV) confinement effects are no longer observed, and the extinction coefficient matches that of bulk PbSe.

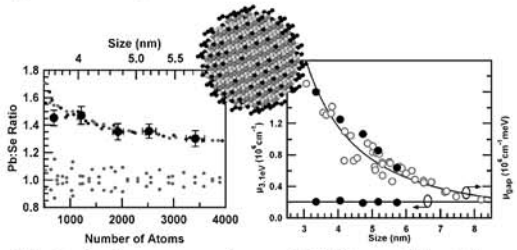

Fig. 1: Left: Experimental Pb:Se ratio (black dots), compared to a Q-PbSe model without (green dots) and with (red and blue dots) addition of surface Pb atoms. Inset: The nanocrystal model consists of a stoichiometric core of Pb (grey dots) and Se (red dots) atoms, terminated by a Pb surface shell (black dots). Right: The extinction coefficient at 400nm ($\mu_{3.1eV}$) is equal to the bulk PbSe value. At the band gap, μ_{gap} increases with decreasing Q-PbSe size, showing that smaller Q-PbSe are more efficient absorbers.

F-73

EXPANDING THE ANALYTICAL RANGE OF WDXRF - NEW XRF ANALYZER CRYSTALS

Kai Behrens*, Alexander Seyfarth**
*Bruker AXS GmbH, Karlsruhe, Germany
** Bruker AXS Inc., Madison, Wisconsin, USA

New synthetic multilayer crystals enhance the analytical range and performance of WD XRF instruments such as the S8 TIGER. The newly developed X-ray optics provide extra sensitivity, improve resolution and precision for light elements. The applicable application range of WDXRF is therefore expanded.

Industrial minerals and the cement industry require fast and very precise determination of Si and Al among others. For Al and Si traditionally the organic crystal pentaerythrite crystal is used. PET crystals are very sensitive to temperature changes due to their high thermal expansion coefficient, which results in peak shifts of 0.5 degree 2theta or more. Although conventional WDXRF instruments are stabilized better than 0.1 degree, downtime will occur when an instrument undergoes maintenance and requires time to get back to temperature. It can take up to 1 day for the PET crystal to be fully equilibrated. Failures and changes in the temperature stabilization will also dramatically affect results. Being cut from an organic material, the PET also degrades over time due to X-ray exposure. This slow decrease of intensity requires a drift correction of the system or finally replacement of the crystal. All factors add to increases in downtime and cost of ownership.

The new multilayer structure XS-CEM is a non-temperature sensitive, stable, non-degrading synthetic crystal with increased sensitivity for Al and Si. Analytical data will show how it outperforms the PET crystal for a typical cement application.

The new multilayer crystal, made out of a La-B4C structure with a typical layer thickness of 190 nm, offers slightly better resolution due to lower d-spacing, but 20% more intensity than traditional Mo-B4C based multilayers. For light element applications, the combination of the XS-B crystal and a coarse collimator is paramount for good analytical performance.

Especially for petrochemical applications the determination of low concentrations of sulphur and phosphorous is challenging. The new curved germanium(111) crystal has increased the intensity by more than 40% for P and more than 20% for S resulting in detection of 0,2 ppm in automotive fuels.

F-75

THE QUANTITATIVE LINK – THE WAY TO BETTER RESULTS

Kai Behrens*, Larry Arias**, Alexander Seyfarth**
*Bruker AXS, Karlsruhe, Germany
**Bruker AXS,Inc. Madison Wisconsin, USA

The value of analytical data is increased if results are not just collected, but also combined during the evaluation step. Typically the commercial value of industrial products, like cement, concentrates, minerals or metals is determined by the major and minor element concentrations. The trace element concentrations are becoming more important for regulatory reasons to avoid harmful effects on health or the environment during the later use of these products or having a commercial effect on the price of the goods. The major objective for industrial chemists and analysts is therefore to achieve more precise, more accurate results in less time without high investments.

In modern laboratories complimentary analytical techniques are widely used, each instrument delivers the optimum result for the selected parameters. Different sample preparation techniques are used to target the appropriate concentration ranges. Up to now often the results are simply stored in a laboratory database (LIMS) and combined by statistical calculations. A large potential of information is not yet used.

Including relevant information from method A during the evaluation of method B improves the quality of the results dramatically. Including values for “non XRF” elements or components into an XRF method will enable correction of matrix effects properly and produce more accurate results.

As an example: Major and minor constituents are analyzed using a fusion method for preparation, traces and volatiles are typically measured using the pressed pellet method for the same sample. Linking this information enables the use of accurate and precise concentration data for the major elements to enhance the matrix correction for traces. Modern XRF evaluation software can automatically link the results and use this information for automatic matrix correction.

For phase identification by XRD, element information and quantification from XRF can help to reduce the number of matches and increase the accuracy. Combining the resources and values already available, the results for XRF or XRD are improved by linking complimentary methods and techniques. The LINKIN approach is the integration of results with added benefit. Not intended to remove a LIMS, LINKIN functionality enables the transmission of better data into the LIMS, benefitting the whole operation and process.

F-88

ANALYSIS OF SAPPHIRE AND RUBY BY EDXRF

Richard E. Phillips, Thermo Scientific
Christopher M. Breeding, Ph.D, G.G., Gemological Institute of America

Doped synthetic sapphires were evaluated for their efficacy in performing Energy Dispersive X-ray Fluorescence (EDXRF) analysis for trace elements in unknown sapphire and ruby samples. Synthetic sapphires were grown and doped with Fe, Ti, Ga, Cr, and V in order to have proper matrix matched geochemical analytical standards. These lab grown samples were produced by the Czochralski (or pulled) method of corundum synthesis, which is known to produce a very uniform product. Small variations in trace element chemistry can have important implications for detecting treatment in ruby and sapphire and for determining the geographical locality from which they were mined.

The standards were carefully tested for homogeneity using a grid of several hundred Laser Ablation Inductively Coupled Plasma Mass Spectrometry (LA-ICP-MS) analyses in three dimensions. The absolute concentrations were established by Secondary Ion Mass Spectroscopy (SIMS) analysis using ion-implanted sapphire standards of well constrained composition. Initial testing results using EDXRF confirmed that the standards are feasible for this technique, however variation among internal company laboratories was quite large (50% differences) using the same instrument and standards. Optimal analysis parameters were established and implemented in order to reduce the poor reproducibility of data between the laboratories. Based upon this work, inter-laboratory reproducibility was reduced to less than 10%.

S214

MATERIALS STATE AWARENESS: DEALING WITH UNCERTAINTY IN DESIGN AND SERVICE

R. Bruce Thompson
Center for Nondestructive Evaluation, Departments of Materials Science and Aerospace Engineering, Iowa State University, Ames, Iowa 50014

In an ideal world, structural components would be designed in such a way that they would provide safe service for a specified period of time and could then be automatically removed from service with no further remaining life. There are many factors that prevent attaining this utopian goal, including uncertainties in the initial condition of the manufactured part, the stochastic nature of various failure processes, and uncertainties in the environment in which the part operates. The resulting stochastic nature of part performance, combined with the competing desires for safe operation and full utilization of potential lifetime, has led to a variety of design/service strategies which will be briefly reviewed. These all involve sensing the state of individual components in some manner, and the sensing strategies that have resulted will be discussed. The goals have evolved from the detection of the presence of discrete damage, the quantification of that damage, and the detection and characterization of microstructual and environmental precursors to that damage, including residual stress. Examples of successes, and occasional failures, of these approaches, will be given. The talk will conclude with a discussion of current research results motivated by present strategies for dealing with the stochastic nature of failure, a set of activities sometimes referred to as Materials State Awareness. Including will be a discussion of new techniques for stress measurement and strategies for using the resultant information such as unified life cycle engineering, health monitoring and prognosis.

S191

DENTAL STRESS, MECHANICAL NOT PSYCHOLOGICAL, EVEN SOME RESIDUAL STRESS

Michael D. Bagby
West Virginia University School of Dentistry, Morgantown, West Virginia

Stresses abound in the dental office. Most first think of the psychological stress brought on by the fear of “a shot” or “the drill.” Of greater interest to the materials scientist are the significant mechanical stresses our teeth and fillings must endure when we eat or grind our teeth. This paper will discuss the various sources of mechanical stress that occur in the oral cavity.

Mechanical stress results from the function of teeth (biting and grinding), polymerization shrinkage of resins and the mismatch of elastic modulus or coefficient of thermal expansion of layered materials. Residual stresses in dental materials have been studied with X-ray diffraction, relaxation and computational modeling techniques.

Several very interesting dental materials exhibit stress induced phase transformations. Yttrium stabilized zirconium oxide also called “ceramic steel” is used to produce high strength ceramic crowns. Nickel-titanium wires are commonly used in orthodontics to straightened teeth.

In addition, a theory of stress corrosion of teeth will also be presented.

S212

RESIDUAL STRESSES IN U.S. NUCLEAR POWER SYSTEMS

Aladar A. Csontos, Ph.D
Senior Materials Engineer, Office of Nuclear Regulatory Research, U.S. Nuclear Regulatory Commission, Washington, DC 20555

Environmentally assisted cracking of components in nuclear power systems is an area of continued focused research by the domestic and international nuclear power industry and regulatory bodies. Domestically, the U.S. Nuclear Regulatory Commission (NRC) is currently conducting several research programs evaluating environmentally assisted cracking in pressurized (PWR) and boiling water reactors (BWR) components. One of these programs recently indicated that residual stresses may play a key role in the growth and arrest of stress corrosion cracks (SCC) in PWR piping components containing dissimilar metal butt welds. Residual stresses in these types of components typically arise from fabrication, fit up, joining, and repair processes. This talk will present a few case studies demonstrating the role of residual stresses on SCC initiation and growth in PWR and BWR components and conclude with a discussion on SCC mitigation activities using engineered residual stresses to potentially limit SCC initiation and growth in PWR components.

S190

MORE MILES FOR TIRED IRON: THE APPLICATION OF ENGINEERED COMPRESSIVE RESIDUAL STRESSES IN AGING AIRCRAFT

Michael Shepard, Materials and Manufacturing Directorate, Air Force Research Laboratory, Wright-Patterson Air Force Base, Ohio
Michael.shepard@wpafb.af.mil, 937-255-1384

The Air Force inventory of airframes and engines is older than it has ever been. The current rate of fleet recapitalization dictates that the average age of the fleet will continue to increase for the foreseeable future. This means that a comprehensive engineering strategy must be developed to facilitate the safe and efficient sustainment of these aging systems. The increasing use of engineered residual compressive stresses may play an important role in this strategy.

In this talk an overview of the most common processes for inducing residual stresses will be provided. Some of the more prevalent distress and wear-out modes associated with aging aircraft will be discussed and typical data demonstrating the use of engineered residual stresses to combating these modes will be presented.

D-19

HIGH-PERFORMANCE SILICON STRIP DETECTOR FOR IN-HOUSE XRD SYSTEM

TAGUCHI Takeyoshi [1], TORAYA Hideo [1], KURIBAYASHI Masaru [1], Pawel GRYBOS [2], Robert SZCZYGIEL [2] and Piotr MAJ [2]

[1] Rigaku Corporation, 3-9-12 Matsubara-cho, Akishima-shi, Tokyo 196-8666, Japan

[2] AGH University of Science and Technology, Faculty of Electrical Engineering, Automatics, Computer Science and Electronics, Al. Mickiewicza 30, 30-059 Krakow, Poland

X-ray diffraction measurement can be speeded up significantly by using a position sensitive detector (PSD). This skill was proposed about 30 years ago and became commercially available around year of 2000. A PSD can be a position sensitive proportional counter (PSPC), a charge-coupled device (CCD), a photo diode array or a silicon strip detector (SSD). A SSD was initially developed as a beam tracker for high-energy physics and turned to an X-ray detector later. Its unique characteristics, such as single photon counting capability, high special resolution, good energy resolution, room temperature operation, etc., are ideal for the use with an in-house X-ray Diffraction (XRD) system and established from a few venders. However, the performance of SSD is strongly rely on its read-out electronics, especially a read-out ASIC (Application Specific Integrated Circuit). A high-performance read-out ASIC for a silicon strip detector is developed as the result of collaboration with Rigaku Corporation and AGH University of Science and Technology. The read-out ASIC is compiled to a silicon strip detector, namely "D/teX Ultra". Some performance of in-house XRD system with D/teX Ultra will be presented.

D-6

X-RAY DIFFRACTOMETRY WITH A MICROFOCUS SOURCE

Bernd Hasse[1], Carsten Michaelsen[1],
Uwe Preckwinkel[2], Holger Cordes[2], Ning Yang[2]

[1] Incoatec GmbH, Max-Planck-Strasse 2, 21502 Geesthacht, Germany

[2] Bruker AXS Inc., 5465 East Cheryl Parkway, Madison, WI 53711-5373, USA

The increasing importance of X-ray diffractometry with 2-dimensional detectors has lead to a rising demand for highly intense X-ray sources enabling the analysis of very small and weakly scattering samples in the home-lab within a reasonable time frame. Therefore, various microfocusing sealed tube X-ray sources with focal spot sizes below 100µm are now available.

Results of the new low-maintenance high-brilliance Incoatec Microfocus Source IµS are presented. The source incorporates an optimized combination of an extremely bright and very durable stationary air-cooled 30 W microfocus source and the newest type of 2-dimensional beam shaping multilayer optics, the so called Quazar optics.

We show measurements with the IµS equipped with different 2-dimensional beam shaping multilayer optics. The comparison of IµS with typical sealed tube fine focus systems shows data of outstanding quality in diffractometry applications using a 2-dimensional detector. A huge improvement in intensity and resolution by factors of about 15 was observed. Especially for the measurements of powders in transmission geometry the IµS delivers very promising results. A focusing on the detector enables better crystallite statistics and better resolution. For some applications there are even intensity gain factors in the range of 100 achievable. For small angle scattering a factor of 5 in comparison to a typical sealed tube instrument was observed when using an IµS with optics for a parallel beam.

D-34

WAVELET ANALYSIS OF X-RAY DIFFRACTION SIGNAL FROM MEASUREMENTS OF STRESS AND AUSTENITE

George Roy

Natural Resources Canada, CANMET/MTL, 568 Booth Street, Ottawa, Ontario, K1A 0G1, Canada

Real materials are subjected to deformations, which can be adequately described by a strain tensor. However, the common practice in the engineering world is to assess the materials in terms of stress. Therefore, the calculated stress, used in characterizing the structural stability of the material, must be deduced from the strain tensor, using appropriately constructed constitutive equations. There are several methods to measure the strain tensor, but the most important non-destructive one is X-ray Diffraction method (XRD). It is based on quantum mechanical assumptions, but its major analytical features can be cast in the form of mathematical transformations. If a constitutive equation, relating the strain and stress tensors, determined experimentally from crystallographic measurements, is provided, the state of stress can be calculated from the constitutive equation. Therefore, it is important to measure the strain tensor as accurately as possible. To carry out the task, the X-ray signal must be analyzed very accurately, and some of the strain components must be calculated through a level of arising ellipticity of the recorded signal. Since the signal is non-parametric and probabilistic, Wavelet Analysis (WA) is a good mathematical tool to carry it out. In the paper to be submitted, the WA approach is presented as a very good alternative to analyze the X-ray signal. It will be demonstrated how the analysis is carried out to minimize the error. It will be shown how the engineering world can benefit from the novel method of stress measurement in a variety of applied and residual stress states as well as in retained austenite determination.

D-51

NEW HIGH-PERFORMANCE DEVICE FOR PARALLEL-BEAM X-RAY DIFFRACTOMETER SCAN

H. Toraya
X-ray Research Laboratory, Rigaku Corporation, Matsubara, Akishima, Tokyo 196-8666, Japan

Diffractometers with the Bragg-Brentano para-focusing geometry have been widely used in laboratory diffraction analysis of polycrystalline bulk and thin-film materials. Recently diffractometers using a parallel-beam geometry become increasingly popular for synchrotron radiation and laboratory X-ray experiments. Both para-focusing and parallel-beam geometries have advantages and disadvantages. The para-focusing geometry can achieve high intensities and high-angular resolution, while it suffers optical aberrations arising from various causes such as of flat specimen, specimen absorption, specimen position variation, q-2q decoupling, etc. On the other hand, the parallel-beam geometry is free from specimen-position dependent aberrations. It can achieve high angular resolution and low background intensities when a perfect crystal analyzer is used on the diffracted beam side. However, the diffracted intensities are generally sacrificed, as a trade-off for high resolution.

In the present study, a high-performance diffracted-beam analyzer consisting of perfect crystals is proposed as a simple and compact device for increasing the diffracted intensities by one order of magnitude compared to that of a single crystal analyzer. It has been widely believed that an analyzer for obtaining high angular resolution cannot be placed in front of a multi-dimensional detector. In the present study, results on a new application of this new analyzer together with a one-dimensional silicon strip detector will be presented.

D-25

AN INNOVATIVE EDXRD PROBE

Charles Dozier and Noureddine Anibou
XStream Systems, Inc., Sebastian, FL

Energy Dispersive X-ray Diffraction (EDXRD) provides a number of distinct advantages for the detection and verification of materials. Unlike Angular X-ray Diffraction (AXRD), which uses a monochromatic beam, EDXRD uses a “white” X-ray beam to probe the samples. No moving parts are necessary; source, sample, and detector positions are fixed. With an energetic beam the X-rays can penetrate through relatively thick materials and diffract from crystalline sample materials within a defined diffraction region. The sample materials can be identified even when they are located within opaque, sealed containers. That is, for many cases, samples without any sample preparation can be located and examined even when hidden in other materials.

XStream Systems, Inc has developed a table top EDXRD system that fits a number of applications. The table top unit uses a confocal geometry to maximize the X-ray intensity from a relatively low-powered, air-cooled 80 kV X-ray source. The beam is collimated by a circular slit assembly before the sample. A similar slit assembly after the sample collimates the diffracted beam and defines the diffraction region. A single CdTe solid-state detector with a multichannel analyzer is used to process the diffracted signal. This collimation system allows us to interrogate a doughnut-shaped volume within the sample under test. In addition, the confocal geometry provides an effective gain of more than 200 times over that of a simple, single beam system with the same resolution.

One of the design goals for the instrument was to develop a unit that is capable of performing quick verification or detection of complex materials such as pharmaceuticals and, yet can be operated by personnel with minimal scientific knowledge. The rapid identification of unknowns is possible using advanced pattern matching techniques, such as neural networks and other pattern matching algorithms. A localized SQL database is used to store a Material Recognition Software Engine’s (MRSE) library of material detectors. The MRSE is capable of matching an unknown sample’s spectrum to a known material’s spectrum by first processing the raw data and then performing pattern matching. This engine has demonstrated that it can verify a number of drugs, each in less than 5 min, to better than a 97 percent accuracy.

The current application of the system has been directed toward the verification of pharmaceuticals in sealed containers. The theory of operation and examples of data of various drugs will be discussed in the paper. Techniques to apply the unit to analysis and other applications will also be shown.

D-66

DETECTORS FOR DEMANDING X-RAY DIFFRACTION EXPERIMENTS

Karsten Knorr, Bernd Hinrichsen, Geert Vanhoyland
Bruker AXS, Östliche Rheinbrückenstr. 49, 76187 Karlsruhe, Germany

State-of-the-art detectors are indispensable for successful X-ray diffraction experiments. They determine the quality, reliability and throughput of X-ray diffraction and scattering investigations in the laboratory as well as at synchrotron beam lines.

The most important requirement for XRD is real photon counting with lowest possible detector noise to achieve large peak-to-background ratio, high dynamic range, and high maximum count rate capability. Basically, two technologies became accepted: gas-filled proportional counters and silicon based solid state detectors. Both technologies still offer potential enhancement

concerning above mentioned properties as well as energy and spatial resolution. Not surprisingly numerous activities are focused on achieving further performance progress to allow more demanding or even new applications.

The different technologies for 0-, 1- and 2-dimensional XRD detectors will be discussed in the view of application specific capabilities on e.g. energy range and resolution, count rate limit, background and dynamic range, size and spatial resolution. The example shown below illustrates optimized discriminator settings for Fe-bearing samples measured with Cu-radiation and a 1D-detector (LynxEye) in only 30 minutes total scan time. The vastly improved peak background ratio due to suppressed fluorescence is apparent.

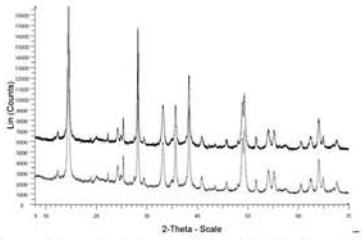

Fig: Fe-bearing bauxite XRD data (LynxEye detector, Cu radiation) with standard (top) and optimized (bottom) discriminator settings to reduce fluorescence. Data are normalized to maximum intensity.

F-71

NEW S2 PICOFOX BENCHTOP TXRF

Alexander Seyfarth*, Michael Rider*, Hagen Stosnach**, Armin Gross**
*Bruker AXS Inc. Madison, Wisconsin, USA; **Bruker AXS Microanalysis, Berlin, Germany

The S2 PICOFOX is the new portable benchtop TXRF System to quantify elemental concentrations from 0.1 ppb to % levels. TXRF previously was limited to floor standing units or large lab systems with emphasis to the semiconductor and coatings metrology.
The S2 PICOFOX was made for the analytical laboratory and field use thus enabling TXRF performance for clinical, nutritional, environmental applications for the first time.
The TXRF system offers "Zero-wait sample prep", that does not require time-consuming digestion by hazardous chemicals. In contrast to AAS/ICP instrumentation the S2 PICOFOX is suitable for almost all sample types such as liquids, suspensions, filters, particles and body fluids.
Making use of Bruker's award winning XFLASH® detector technology the system is equipped with a 30mm^2 XFLASH® detector with superb energy resolution and maintains resolution stability at count rates of over 100,000 counts.
Operating without any external gasses, water cooling, or any other media, the S2 Picofox can detect elements from Al-U and quantify them down to ppb levels. Sample amounts can be in the nano gram range with the ability to analyze solid samples directly. Customer Application studies have shown the versatility of the S2 PICOFOX in the fields of Pharma authenticity, environmental testing, food, agricultural products, nutritional supplements, biochemical and medical applications as well as mining.
Successful applications studies with clients from the mining sector enable the S2 PICOFOX to be used as well for geochemical screening, optimization of ore processing and exploration.
The S2 PICOFOX is directly supported thru our centers in The Woodlands, Texas and Madison, Wisconsin by a team of experienced application scientists and engineers.
Both manual and auto sampler models of our benchtop TXRF S2 PICOFOX can be equipped with different excitation sources (Mo and W) to optimize the analytical performance.
Unlike traditional WD or ED XRF, TXRF does not suffer from matrix effects requiring dedicated calibrations for each material. All S2 PICOFOX instruments are pre calibrated from the factory in Berlin, Germany and traceable to primary standards.

F-53

NEW DEVELOPMENT FOR THE AUTOMATION OF BORATE FUSION SAMPLE PREPARATION FOR XRF

Mr. Luc Bérubé, Corporation Scientifique Claisse

It is often overlooked that weighing is an important source of error in the borate fusion- XRF analytical process. In fact, a weighing error of less than a milligram for the sample can have a significant effect on the measured concentration of major oxides such as calcia in cement and iron oxide in ores. Moreover, accurately weighing flux and sample can account for more than 60% of the total technician time invested in fused bead preparation. The automation of weighing for borate fusion can be the solution both to improve the consistency of results and to free technician resources from repetitive tasks.

Corporation Scientifique Claisse will introduce the first step of its automation project for borate fusion, rFUSION. The rFUSION Automated Weighing System is capable of achieving the accuracy and precision required for the fusion technique 24/7/365 without human intervention. The modular approach of rFUSION allows ease of use and simplicity of maintenance. The same approach will also make automation affordable for more laboratories by allowing an upgrade path to configure the system step by step, module by module. During the presentation, we will explain the rFUSION automation approach and describe the specifications of the weighing system and their benefits.

F-81

HIGH VOLUME SCRAP MATERIAL SORTING USING XRF

E. Brown, D. Carolan, X. Chen, J. Egan, B. Hubbard-Nelson, R. Nasella, I. Rosmarin, R. Russell, D. Sackett, C. Weaver
Innov-X Systems, Inc., Woburn, MA, USA, info@innovxsys.com

High commodity prices and the increased use of recycled materials has led to a need for sorting scrap materials (metal, glass, plastic, rubber, wood, etc) at high volume and speed over a conveyor. Elemental analysis through XRF provides a powerful edge over other techniques provided the analysis can be done at the requisite speed and accuracy. We have developed an XRF system to address these general requirements, and which can extract contaminants from recycled glass or from ferrous scrap metal at conveyor speeds up to 5-6 feet/sec and volumes up to 150 tons per hour. The system uses an array of tubes and Si PIN diode detector to classify material in a modular system of digital pulse processors, and is designed to operate in the harsh environment of scrap yards. A graphical user interface provides the operator with a simple means of adjusting selection criteria and operating the conveyor and XRF system. We show the performance in terms of selection efficiency and wastage for two of these applications.

F-76

TURN-KEY SOLUTIONS WITH INTEGRATED FLEXIBILITY FROM PACKAGE TO REAL SOLUTION

Kai Behrens*, Karen Roscoe**, Alexander Seyfarth**
*Bruker AXS, Karlsruhe, Germany; **Bruker AXS Inc., Madison, WI

Today X-ray fluorescence spectrometry (XRF) has to cover all analytical tasks in modern industrial process and quality control. A single instrument has to provide full flexibility for all kinds of samples, from geological materials, like ores and minerals, to final industrial products, like steel, copper and alloys, side products, like slag, as well as environmentally relevant materials like ashes, filter dusts and sludge. Depending on the specific application, a concentration range from the ppm-level to 100% has to be analyzed with high accuracy and reproducibility.
New Bruker XRF solution packages, based on the S8 TIGER WDXRF, enable turn-key analysis of samples in different application fields, such as petrochemicals, industrial and regulatory. All packages are flexible to enable customization and interoperation with user methods and extending the capabilities of the SPECTRA^{plus} software.
A solution package consists of more than just a calibration! Samples, quality control and validation samples as well as accessories and consumables, are included. All settings and methods enhance SPECTRA^{plus} integrated analytical expertise. Commissioned on site, the turnkey solution also involves dedicated hands-on user training and access to Bruker Training Central. Bruker Training Central is your one-stop shop for maximizing the solution implementation. Training courses offered in-person, via live webcast and on-demand - on topics ranging from fundamental theory to practical applications - ensure you get the most out of the instrument.
The talk will illustrate NEW solution packages on the S8 TIGER WDXRF systems as well as how our Bruker Training Central course offerings make them 360 degree solution.

F-7

DEVELOPMENT OF A NOVEL MULTI-ELEMENT SILICON DRIFT DETECTOR ARRAY

L. Feng, V.D. Saveliev, C.R. Tull, S. Barkan, M. Takahashi, and E.V. Damron
SII NanoTechnology USA Inc., 19865 Nordhoff St., Northridge, CA 91324, USA

A novel, four-element silicon drift detector (SDD) array (the Vortex-ME4™) has been developed for X-ray fluorescence (XRF) applications requiring a large detection area, such as fast XRF imaging and X-ray absorption spectroscopy (XAS) using synchrotron radiation. The new compact SDD array spectrometer, cooled without liquid nitrogen (LN), can replace traditional, bulky, LN-cooled multi-element germanium detectors. The SDD element is fabricated on ~ 0.35 mm thick, high resistivity n-type silicon with an active area of ~ 42 mm^2, featuring extremely low capacitance (~ 0.06 pF) and excellent energy resolution (< 130 eV FWHM, at 5.9 keV and optimum peaking time). The SDDs also feature a very short signal rise time (< 100 ns) allowing for pulse processing using very short peaking times (~ 0.25 μs) to achieve very high signal throughput (up to 500 kcps output rate). The four-element SDD array, offers a total active area of ~ 170 mm^2 with a maximum output rate up to 1.5 – 2 Mcps.
Vacuum-sealed with a 12.5 μm thick beryllium window, the four SDD elements are in a square arrangement around the center and are cooled using separate Peltier coolers, with the heat removed through an innovative heat pipe heat transfer system. The SDD array spectrometer utilizes the X-ray Instrumentation Associates 4-channel digital pulse processor, (the DXP xMAP system), in conjunction with the National Instruments PXI/CompactPCI module, offering 4 MB on-board high speed memory and ~100 MB/s data transfer speed. Figure 1 shows the external and internal views of the Vortex-ME4™. Performance and application data from the new Vortex-ME4™ will be presented.

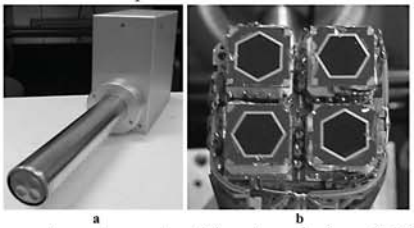

Figure 1. Vortex-ME4™ 4-element spectrometer: (a) external view; (b) internal view of the 4 SDD elements.

F-64

EXPANDING THE DETECTOR EFFICIENCY OF SILICON DRIFT DETECTORS WITH OPTIMIZED RADIATION ENTRANCE WINDOW

A. Niculae[1], H. Soltau[1], G. Lutz[1], P.Lechner[1], A. Bechteler[1], R. Eckhardt[1], K. Hermenau[1], O. Jaritschin[2], A.Liebel[2,] A. Simsek[2], G. Schaller[3], F. Schopper[3] and L. Strüder[3]

[1]PNSensor GmbH, Römerstr. 28, D-80803 München, Germany

[2]PNDetector GmbH, Emil-Nolde-Str. 10, D-81735 München, Germany

[3]MPI Halbleiterlabor, Otto-Hahn-Ring 6, D-81739 München, Germany

Silicon Drift Detectors (SDDs) with integrated FET have been fabricated by PNSensor in cooperation with the Semiconductor Laboratory of the Max-Plank-Institutes in Munich since many years. With optimum spectroscopic performance values (123 eV @ Mn-K_α), excellent light element performance down to Be (42 eV @ C-K_α) and P/B values up to 20,000 the SDD is a state of the art detector for X-rays.

The detector efficiency is an important feature in any detection system. This is especially true for applications like analysis of trace elements requiring high throughput within a given time. There are three factors determining the detector efficiency:

- detector performance (energy resolution, P/B ratio)
- quantum efficiency
- detector area and geometry

In this presentation we will analyze the quantum efficiency as a function of photon energy. The detector performance at lower energies has been greatly improved with the introduction of the optimized detector entrance window named *pnWindow.* Compared to standard entrance window, the quantum efficiency for this window type is slightly lower, which is a small price to be paid in view of an energy resolution for Boron of only 38 eV or 42 eV for Carbon. Concerning the detector performance in the higher energy range, some interesting possibilities for the improvement of the detection efficiency are presented. By combining the detector with modern scintillation materials the detection capability can be further extended into the Gamma range.

Larger areas SDDs become more and more attractive for applications requiring short measuring time. The spectroscopic performance of the 20 and 30 mm^2 SDDs will be shown. Besides a larger detection area, the detection efficiency can be enhanced by optimizing the detector geometry with respect to the probe. This is for example the case of the 4-channel SD3 detector with central hole for the exciting beam.

Owing their high count rate capability, SDDs are becoming very interesting as energy dispersive detectors for WDXRS applications. Multi-channel SDDs with special geometry adapted to the various WDS instruments (flat or curved optics geometries) are presented.

F-66

Mg-BASED MULTILAYER XRF ANALYZERS WITH TWO- AND THREE-LAYERS STRUCTURE DESIGN

Yuriy Platonov[1], Kazuaki Shimizu[2], Gary Fournier[1], Jim Rodriguez[1]

[1] Rigaku Innovative Technologies, 1900 Taylor Rd., Auburn Hills, MI 48326, USA

[2] Rigaku Industrial Corporation, 14-8, Akaoji-cho, Takatsuki-sh, Osaka 569-1146, Japan

Multilayer XRF analyzers are traditionally applied for elemental analysis from Mg to Be since their first introduction in 1980's. Wide variety of material combinations with dspacing ranging from 1.5nm to 10nm are currently in use. For analysis of a particular element one can find an optimal structure for the best available performance. But there is always demand for improvements. It can just be request for improving quality of existing analyzers, or for lowering number of analyzers in a spectrometer without narrowing number of analyzed elements and loosing much in a performance, or it can be request for an analyzer with new capabilities. For example, in analysis of TiN a Sc-based multilayer is very effective for nitrogen but it does not work for titanium. Crystals such as LiF are used to analyze titanium but they are useless in analysis of nitrogen. To find a single analyzer for TiN material is one of challenging tasks.

To satisfy this particular demand as well as some others we, in this paper propose new multilayer structures working in a wide spectral range and having a superior performance in comparison with existing analyzers. The new structures are Mg-based and may contain three layers in the period. The third layer is introduced for both improving an analyzer performance and for a flexibility to smoothly tune characteristics of an analyzer such as intensity, resolution and peak/background ratio by changing a relative thickness of the layers. Such new capability gives a tool to optimize an analyzer performance depending on application.

Different Mg-based structures were deposited and tested along with traditional multilayer analysers. Essential, up to 100%, improvement in performance was observed for new structures and it was in a good agreement with a simulation.

e-mail: yuriy.platonov@rigaku.com

C-3

MICROFOCUS LIQUID-METAL-JET X-RAY TUBES AND APPLICATIONS

O. Hemberg[1], M. Otendal[1], T. Tuohimaa[2], H. M. Hertz[2]
[1] Excillum AB, Rådjursvägen 16, SE – 182 76 Stocksund, Sweden
[2] Biomedical and X-ray Physics, Royal Institute of Technology, SE – 10691 Stockholm, Sweden

We have previously demonstrated a liquid-metal-jet anode X-ray source concept with potential for a 100-1000× increase in brightness [1]. In the present paper we report on recent progress and demonstrate long-term operation of a high-brightness microfocus source based on this concept. The tube uses a Ga/In/Sn alloy with strong line emission at 9.25 keV (comparable to conventional copper anode sources) as well as significant continuum radiation up 100 keV, depending on settings. The spot size is 5-20 μm with an electron-beam power up to 200 W and a power density of ~10 W/μm. This is >10× more than current state-of-the-art microfocus tubes. This second generation prototype incorporates a continuous recycling system for uninterrupted operation as well as reduced footprint and enhanced reliability. This source shows promise to enable many laboratory-scale X-ray applications, today limited by source brightness. Also, for novel imaging modalities, like phase-contrast imaging [2], source brightness is crucial. Furthermore the system will enable faster and/or more accurate XRF and XRD analysis due to the increased source brightness. The system is now mature enough for scientific and industrial applications and long-term performance data will be presented.

[1] O. Hemberg, M. Otendal, and H. M. Hertz, “Liquid-metal-jet anode electron-impact X-ray source”, Appl. Phys. Lett. 83, 1483 (2003)
[2] T. Tuohimaa, M. Otendal, and H. M. Hertz, “Phase-contrast X-ray imaging with a liquid-metal-jet-anode microfocus source”, Appl. Phys. Lett. 91, 074104 (2007)

D-75

POSSIBILITIES AND LIMITATIONS OF X-RAY DIFFRACTION USING HIGH ENERGY X-RAYS ON A LABORATORY SYSTEM

Hans te Nijenhuis, Milen Gateshki and Martijn Fransen
PANalytical, Almelo, The Netherlands

The recent interest in nanomaterials has increased the need to analyze structures on a local (nano) scale. However, the atomic structures of nanoparticles and nanostructured materials are not accessible by conventional methods used to study crystalline materials, because of the short ordering range in these materials. One of the most promising techniques to study nanostructures using X-ray diffraction is total scattering pair distribution function (PDF) analysis. This technique is successfully applied in a number of application areas in materials science and technology.

The PDF analysis technique makes use of high quality, high energy X-ray scattering data, usually obtained at synchrotron facilities, available in several national and international research centers around the world.

Despite the advantages and data quality that measurements at synchrotron beam lines offer to the researcher, in practice it can be difficult and time-consuming to get access to the facilities required. In order to be prepared as good as possible and to make optimal use of the valuable experiment time offered, it is highly desirable to perform selective measurements on candidate samples in the own research laboratory.

In this study, we have investigated the possibilities and limitations of the use of high-energy X-rays on a homelab system. We will answer this question and illustrate it with examples.

C-17

FORMATION OF NOVEL OXIDE NANOSTRUCTURES

Zhong Lin (ZL) Wang
School of Materials Science and Engineering, Georgia Institute of Technology, Atlanta 30332-0245
e-mail: zhong.wang@mse.gatech.edu

Quasi-one-dimensional (1D) nanostructures (nanowires, nanobelts and nanorods) are the forefront nanomateirals for nanotechnology. Oxide nanostructures have been synthesized for a wide range of semiconducting oxides [1] that are potential building blocks for constructing numerous nanodevices. Using the technique demonstrated for measuring the mechanical properties of nanotubes [2,3], the mechanical and field emission properties of the oxide nanobelts have been characterized. Field effect transistors [4], ultrasensitive nano-size gas sensors [5], nanoresonators and nanocantilevers [6] have been fabricated using nanobelts.

Among all of the oxide nanostructures we have investigated, ZnO is very unusual. The two important characteristics of the wurtzite structured ZnO are the non-central symmetry and the polar surfaces. The structure of ZnO can be described as a number of alternating planes composed of tetrahedrally coordinated O^{2}- and Zn^{2+} ions, stacked alternatively along the *c*-axis. The oppositely charged ions produce positively charged (0001)-Zn and negatively charged (000-1)-O polar surfaces, resulting in a normal dipole moment and spontaneous polarization along the *c*-axis. The polar surfaces give raise a few interesting growth features, such as the formations of nanosprings [7], nanorings [8], nanobows [9] and nanohelices [10]. These nanostructure are semiconductive and piezoelectric and have potential applications as nano-scale sensors, traducers, and actuators. This presentation will be about the synthesis, characterization and potential applications of these novel nanostructures [11].

[1] Z.W. Pan, Z.R. Dai and Z.L. Wang, *Science*, 209 (2001) 1947.
[2] P. Poncharal, Z.L. Wang, D. Ugarte and W.A. de Heer, *Science*, 283 (1999) 1513.
[3] R.P. Gao, Z.L. Wang, Z.G. Bai, W. de Heer, L. Dai and M. Gao, *Phys. Rev. Letts*., 85 (2000) 622.
[4] M. Arnold, P. Avouris, Z.L. Wang,. *Phys. Chem. B*, 107 (2002) 659.
[5] E. Comini, G. Faglia, G. Sberveglieri, Zhengwei Pan, Z. L. Wang *Applied Physics Letters*, 81 (2002) 1869.
[6] W. Hughes and Z.L. Wang, *Appl. Phys. Letts*., 82 (2003) 2886.
[7] X.Y. Kong and Z.L. Wang, *Nano Letters*, 2 (2003) 1625 + cover.
[8] X.Y. Kong, Y. Ding, R.S. Yang, Z.L. Wang, *Science*, 303 (2004) 1348.
[9] W.L. Hughes and Z.L. Wang, *J. Am. Chem. Soc*., 126 (2004) 670
[10] P.X. Gao, Y. Ding, W.J. Mai, W.L. Hughes, C.S. Lao and Z.L. Wang, *Science*, 309 (2005) 1700.
[11] Thanks the support from NSF, DARPA, NASA and Airforce.
[12] for details see: http://www.nanoscience.gatech.edu/zlwang/

C-18

PULSED LASER DEPOSITION TECHNIQUE FOR THE SYNTHESIS OF NANOSTRUCTURES

Jung-Il Hong, Melanie Kirkham, Joonho Bae, Zhong Lin Wang, and Robert L. Snyder
School of Materials Science and Engineering, Georgia Institute of Technology, Atlanta, GA

Pulsed laser deposition (PLD) technique has been extensively used to fabricate thin films of various materials. Good controllability of the deposition conditions is expected to be beneficial to the controlled growth of nanowires. Therefore, the effect of the PLD conditions on the structures of the deposited films or nanowires was investigated in this study. ZnO and Fe_3O_4 were used as target materials. The ambient pressure, substrate temperature, and laser pulse power were varied resulting in the various structures such as continuous thin film, nanowires, and nanoparticles deposited on the substrates. Small window of conditions for the direct growth of nanowires was identified. On the other hand, for the continuous film, the texture of the film was found to be controllable. It is demonstrated that these films can be used as templates for the subsequent growth of nanowires in epitaxy with the textured films.

F-60

XAFS STUDIES OF NANOSYSTEMS: HOW X-RAY, ELECTRON MICROSCOPY, AND OPTICAL TECHNIQUES EACH CONTRIBUTE TO STRUCTURAL CHARACTERIZATION

B. A. Bunker Department of Physics University of Notre Dame Notre Dame, IN 46556

X-ray Absorption Fine-structure Spectroscopy (XAFS) has been shown to be valuable in the structural characterization of nanoparticles and nanowires. The technique is particularly useful because it can be used for amorphous or liquid systems in addition to those with crystalline order. XAFS is particularly powerful when used in conjunction with other techniques such as TEM (imaging and diffraction) and optical spectroscopy. Examples of work on core-shell nanoparticles, metal nanoparticle/carbon nanotube systems, and metal-semiconductor nanoparticle interfaces will be presented. Prospects for using the technique with micro- or nano-focused X-ray beams will also be discussed.

C-12

HARD X-RAY FULL FIELD 3D IMAGING WITH sub-50 nm RESOLUTION

A. Tkachuk, M. Feser, F. Duewer, J. Gelb, G. Hsu, S. Wang, Wenbing Yun
Xradia, Inc. 5052 Commercial Circle, Concord, CA, USA 94597

One of the key strengths of hard X-ray full-field microscopy is the large penetration depth of hard X-rays into material, which allows one to image the interior of optically opaque objects. Combined with tomographic techniques, the three dimensional interior structure of the object can be reconstructed nondestructively regardless of its state of crystallinity. Projection X-ray microtomography is now routinely available using X-ray microCT scanners with spatial resolution ~1 micron, which is limited by the combination of X-ray source spot size and detector imaging resolution. Higher imaging resolution typically requires X-ray magnification using specialized X-ray lenses, such as Fresnel zone plates. This talk will primarily concentrate on operation principles and applications of compact sub-50 nm resolution full field zone plate based X-ray microscopes using both synchrotron and commercially available laboratory X-ray sources[1]. These systems employ highly efficient reflective capillary condensers[2] and high-resolution (<30 nm) objective zone plates[3] using X-rays with energy 8 keV and higher. Imaging resolution of such microscopes is independent of the X-ray source parameters and ultimately limited by the ability to manufacture zone plates with finer outermost zone widths (resolution) and high aspect ratio (efficiency). In the past several years substantial progress has been made in manufacturing zone plates with <30 nm imaging resolution and up to 1:40 aspect ratio. Modern state of the art zone plate based full field X-ray microscopes coupled to high brightness synchrotron sources allow data acquisition speeds up to 0.1 s per 2D projection image. At the same time substantial progress has been made in proliferation of sub-50 nm X-ray microscopy to the laboratory environment using commercially available X-ray sources where imaging time per 2D image approaches only a few minutes. Applications of sub-50 nm 3D hard X-ray microscopy will be presented in analysis of internal structures of various nanomaterials.

References:

[1] A. Tkachuk, F. Duewer, H. Cui, M. Feser, S. Wnag, W. Yun, Z. Kristallogr. **222** , 650-655, (2007)
[2] Xianghui Zeng, Fred Duewer, Michael Feser, Carson Huang, Alan Lyon, Andrei Tkachuk and Wenbing Yun (to be published at Applied Optics)
[3] Y. Feng, M. Feser, A. Lyon, S. Rishton, X. Zeng, S. Chen, S. Sassolini, W. Yun, J. Vac. Sci. Technol. B 25(6), (2007)

D-57

ALUMINA-SUPPORTED PALLADIUM CATALYST CRYSTALLITE SIZE DETERMINATION BY EXAFS, XRD, AND TEM

E.J. Peterson, T.R. Conant, P. Burton, A. De La Riva, J.P. Gabaldon, L.R. Houk, H. Pham, K. Lovato, J. Paiz, A.K. Datye
University of New Mexico Center for Micro-Engineered Materials, Albuquerque, NM

Catalyst crystallite size is an important parameter affecting the behavior of many catalytic systems in use today. Crystallite sizes of interest can range from tens of Angstroms to tens of nanometers. Techniques employed in the determination of crystallite sizes in this size range include EXAFS, XRD, and TEM. Each of these techniques has strengths and weaknesses. Short range order around absorbing atoms can be precisely determined by EXAFS, and inference of crystallite size can be made from the

measurement of the fraction of incompletely-coordinated surface atoms in nano-sized clusters. However the crystallite size that is inferred from this analysis is model dependent, and the technique loses sensitivity as the clusters approach sizes where bulk properties dominate. X-ray diffraction, useful over a somewhat broader crystallite size range, is also somewhat model dependent and suffers from sensitivity issues when the catalyst of interest is highly diluted by support material. Transmission electron microscopy provides unambiguous information regarding observed crystallite sizes and shapes, but typically only samples a small fraction of material. In this work we present the results of EXAFS, XRD and TEM analysis of palladium catalyst particles supported on alumina, comparing crystallite sizes obtained using the three techniques.

D-33

NATURAL NANOPARTICLE SHAPE, STRUCTURE, PROPERTIES AND REACTIVITY FROM X-RAY STUDIES

G.A. Waychunas[1], B. Gilbert[1], H. Zhang[2], C. Kim[3], Y-S. Jun[1,2], and J.F. Banfield[1,2]
[1]Lawrence Berkeley National Laboratory, Earth Sciences Division, Berkeley CA 94720
[2]University of California, Berkeley, Dept. of Earth and Planetary Sciences, Berkeley CA 94720
[3]Chapman University, Dept. of Physical Sciences, Orange CA 92866

Natural nanoparticles and synthetically-prepared analogs are being studied to understand their functionality in environmental processes, especially those connected with acid mine drainage (AMD) and other inorganic toxic contaminant sources. Additional processes involving the creation, dissolution or sequestration of nanoparticles by natural biota feature nanoparticle-organic interactions that are poorly understood, but of prime interest in predicting biogeochemical mechanisms and environmental impact of biological remediation schema.

Our efforts have been focused on ZnS, TiO_2 and Fe oxyhydroxides. ZnS nanoparticles have high sensitivity to the type of surface ligand binding, and adopt a core-shell type structure with varying core size and extent of shell distortion directly equitable to the strength of ligand bonds[4]. Exchange of surface ligands can have dramatic effects on the nanoparticle structures, as can aggregation and disaggregation. These changes are best studied by a combination of MD simulation and high energy PDF analysis, with supplemental SAXS, TEM and X-ray spectroscopic measurements.

α-FeOOH nanoparticles undergo changes in growth mode as they progress from few to 100 nm dimensions[5]. At the smallest sizes there is evidence for several structural transformations. Studies of sorption behavior indicate deviations from larger particle behavior. Aggregation/sorption processes can encapsulate toxics making them difficult to localize or remove by remediation efforts. Other Fe oxide nanoparticles may be unstable as larger single crystals and adopt nanocluster structures, e.g. ferrihydrite[6]. Crystal truncation rod diffraction work suggests deviations from stoichiometry at α- Fe_2O_3 surfaces, which could affect nanoparticle stability. Fe oxide nanoparticles nucleated on surfaces and examined via GISAXS show evidence for varying growth modes depending on size and ionic strength. Such particles can effectively activate or passivate environmental surfaces, leading to changes in reactive transport predictions.

[4]Zhang et al. Nature 424, 1025-1029 (2004)
[5]Waychunas et al. J. Nanoparticulate Res. 7, 409-433 (2005)
[6]Michel et al. Science 316, 1726-1729 (2007)

D-72

ANALYSIS OF THE CRYSTALLINE STRUCTURE AND MAGNETIC PROPERTIES OF Fe NANOPARTICLES

Todd C. Monson, Dale L. Huber, Judith M. Lavin
Sandia National Laboratory, Post Office Box 5800, Albuquerque, NM 87185–1415, USA
Valeri Petkov, Central Michigan University
Yang Ren, Advanced Photon Source

We have developed a solution based synthesis for oxide-free, surfactant coated iron nanoparticles. By controlling the parameters of the synthesis, the reaction can produce particles with a diameter anywhere between 2 and 10 nm. These particles are both synthesized and characterized under inert conditions in order to prevent any oxide formation. Through characterization of the nanoparticles using SQUID magnetometry we have shown that they have a saturation magnetization slightly below that of bulk iron and an anisotropy far greater than bulk iron. In an attempt to explain the magnetic behavior of these Fe nanoparticles we have studied them using high energy X-ray diffraction and analyzed the data using the atomic pair distribution function (PDF) technique. The diffraction data shows that our nanoparticles have short correlation lengths (on the order of 2 nm or less), a distorted bcc lattice, and a larger lattice spacing than bulk iron. These observations may begin to explain the magnetic behavior we observe in these nanoparticles. Sandia is a multiprogram laboratory operated by Sandia Corporation, a Lockheed Martin Company, for the United States Department of Energy's National Nuclear Security Administration under contract DE-AC04-94AL85000.

D-60

DETERMINATION OF CRYSTALLOGRAPHIC POLARITY OF THIN FILMS USING HIGH RESOLUTION XRD

Katsuhiko INABA
Rigaku Corporation, Tokyo Japan
inaba@rigaku.co.jp

It is well known that the crystallographic polarity for noncentrosymmetric crystals can be determined by analyzing the XRD profiles using the X-ray wavelength close the absorption edge of the constituent elements. [1] A new determination technique of the crystallographic polarity using conventional high resolution XRD (HR-XRD) system has been proposed recently.[2] By using Au X-ray source, polarity determinations for GaN-, GaAs- related materials, or ZnO related materials are possible. High resolution XRD analyses for these materials, such as X-ray Rocking Curve (XRC) measurements, Reciprocal Space Mappings (RSM), X-ray Reflectivity (XRR) measurements, are also possible by employing the channel-cut monochromating crystals in the incident/receiving optical system.

Applying this technique to the epitaxial films, crystallographic polarity of non-polar GaN epitaxial films on *r*-sapphire substrates was clearly determined, and these results will be shown together with the result of crystallinity analysis of these films, as well as the polarity determination for GaAs and ZnO crystals.

1. for example, A.N. Mariano and R.E. Hanneman, *J. Appl. Phys.*, **34** (1963) 384

2. K. Inaba and H. Amano, *Physica Status Solidi*-(b), **244** (2007) 1775-1779

D-28

LOCAL RESIDUAL STRESSES AND THERMAL FATIGUE IN CrN COATINGS ON STEEL CHARACTERIZED BY HIGH-TEMPERATURE SYNCHROTRON X-RAY DIFFRACTION

K.J. Martinschitz[a], Ch. Kirchlechner[a], , R. Daniel[b], Ch. Mitterer[b] , J. Keckes[a]
[a]Erich Schmid Institute for Materials Science, Austrian Academy of Sciences and Department of Materials Physics, University of Leoben, Leoben, Austria
[b]Department of Physical Metallurgy and Materials Testing, and Christian-Doppler Laboratory for Advanced Coatings, University of Leoben, Leoben, Austria

Hard coatings are routinely used to protect working tools from abrasion and corrosion. The friction between the coating and the work piece results in local thermal and mechanical stresses which can negatively influence the tool performance and the lifetime. In the case of
interrupted services, temperature pulses up to 1000 °C in millisecond range can cause cyclic thermo-mechanical loads in the coating/substrate composite resulting in phenomena like coating cracking, delamination or spalling.

In this contribution, residual stresses in thermally cycled CrN coatings on steel are characterized using high-temperature synchrotron X-ray diffraction. In order to simulate the thermal fatigue, CrN/steel samples were at first thermally cycled using a laser beam in the temperature range of 50-650 °C applying up to 100 000 times in home laboratory. Subsequently, the structures were analysed at the EDDI beamline of BESSY (Berlin, Germany) and G3 beamline of Hasylab (Hamburg, Germany). In both cases, the samples were characterized in-situ in a temperature range of 25-700 °C using a heating chamber DHS1100 (Anton Paar GmbH, Graz, Austria). The measurements at the EDDI beamline using high energy photons (20-100 keV) were used to evaluate residual stress gradients in the spot irradiated by laser as a function of the penetration depth. In the case of the measurements at the G3 beamline, a lateral distribution of residual stresses in and around the irradiated spot with a resolution of 24 microns was determined.

In this way, it was possible to determine 3D distribution of residual stresses in the irradiated spot as a function of temperature whereby the structures exhibited complex changes in the morphology and in the residual stress state as a result of the thermal fatigue. The laser treatment caused a relaxation of compressive stresses in the coating and a formation of high tensile stresses resulting in a plastic deformation of the steel substrate. This effect was depended on the number of applied cycles.

The presented approach allows a complex characterization of thermo-mechanical processes in coating-substrate composites and opens the possibility to understand phenomena related to the thermal fatigue of coated tools.

This work was supported by Austrian NANO Initiative within the project "StressDesign - Development of Fundamentals for Residual Stress Design in Coated Surfaces". The authors are grateful for the support from the European Union.

D-30

A NOVEL DIFFRACTION TECHNIQUE TO DETERMINE MECHANICAL MODULI OF FIBRE-TEXTURED THIN FILMS

K.J. Martinschitz and J. Keckes
Erich Schmid Institute for Materials Science, Austrian Academy of Sciences and Institute of Metal Physics, University of Leoben, Leoben, Austria

A determination of elastic constants of thin films with the thickness in the nm range represents a serious difficulty. The purpose of this contribution is to introduce a *new self-consistent diffraction technique* that allows for a rapid experimental determination of in-plane Young's modulus and Poisson's number of thin films by X-ray diffraction. The mechanical elastic constants are extrapolated from thin film X-ray elastic constants considering specific sample anisotropy. The X-ray elastic constants can be determined by a simultaneous application of $\sin^2\psi$ and X-ray diffraction substrate curvature techniques. The basic idea resides in the fact to use a monocrystalline substrate with known mechanical properties as an internal standard to determine the relationship between the measured X-ray elastic strains and the macroscopic stress. The macroscopic stress imposed on a film which is deposited on a mono-crystalline substrate can be calculated from the substrate curvature using Stoney's formula. The curvature is determined by the measurement of rocking curves on the substrate symmetrical reflections at different sample positions. This gives an opportunity to characterize the X-ray elastic strains for different *hkl* reflections and also the curvature of the substrate in one XRD system without remounting the sample. The knowledge of the macroscopic stress and the elastic strains can then be used to quantify X-ray elastic constants for different *hkl* reflections. In order to extrapolate mechanical elastic constants from X-ray elastic constants, however, it is necessary to consider the preferred orientation in the thin film. One of the main goals of this contribution is to demonstrate for which *hkl* reflection (and the value of the anisotropic factor Γ) the X-ray elastic constants are equal to their mechanical counterparts. This analysis is made by comparing calculated mechanical and X-ray elastic constants of thin films possessing various orientation distribution function $f(g)$. At the end a certain type of a selection rule will be presented.

The new approach is demonstrated on a variety of thin film systems like TiN, CrN, Al, Cu deposited on Si(100) wafers and measured using laboratory and synchrotron source (BESSY and Hasylab) at room and at high temperatures up to 600°C.

This work was supported by Austrian NANO Initiative within the project "StressDesign - Development of Fundamentals for Residual Stress Design in Coated Surfaces".

F-32

SIMULTANEOUS DETERMINATION OF MAIN, MINOR AND TRACE ELEMENTS IN FERTILIZERS BY TOTAL REFLECTION X-RAY FLUORESCENCE

R.E. Ayala-Jiménez*, C.H. Alvarado
Fisichem Incorporated, Miami, USA and Universidad de San Carlos de Guatemala

TXRF was applied to determine main, minor and trace elements in the following type of fertilizers: phosphoric rock, monoammonium phosphate, diammonium phosphate, potassium chloride, calcium carbonate, potassium sulphate, ammonium sulphate and mixtures of such raw materials. The following elements were analyzed simultaneously after dissolution of the sample in water or acid digestion and the appropriate dilution: P, S, Cl, K, Ca, Cr, Mn, Mn, Fe, Cu, Zn, As, Br, Se and Pb.

A critical step in the analysis of the fertilizers is the adequate dilution of the sample once it is dissolved in water or after acid digestion. It is demonstrated that erroneous analytical data arise when the sample dried onto the quartz reflector it is not thin. X-ray transmission calculations were made in order to estimate the amount of sample to be deposited onto the quartz sample carrier which would give a transmission of 95% or higher for the less energetic characteristic fluorescence line in each type of fertilizer.

The samples were also analyzed by ICP emission spectroscopy. In this contribution the results are presented and compared, and the advantages and disadvantages of both methods are listed and discussed. The TXRF spectrometer used was a benchtop system equipped with a planar X-ray waveguide resonator. The detection limits for the trace elements found in the samples analyzed are also presented and discussed.

* Author to whom correspondence should be addressed.

D-1

LONG-RANGE SCANS AND MANY-BEAM EFFECTS FOR HIGHRESOLUTION X-RAY DIFFRACTION FROM MULTILAYERED STRUCTURES

T.A.Ulyanenkova[1], A.I.Benediktovich[2], I.Feranchuk[2], T.Baumbach[1], A.Ulyanenkov[3]
[1]University Karlsruhe, Engesserstr.15, 76131 Karlsruhe, Germany
[2]Belarussian State University, 4 Nezavisimosty Av., 220050 Minsk, Belarus
[3]Bruker AXS GmbH, Östliche Rheinbrückenstr. 49, 76187 Karlsruhe, Germany

Thin crystalline films and multilayers are recently of wide use in modern nanoscale manufacturing in semiconductor, coating, optical and infrared industry. The broad use of these structures requires the adequate methods for characterization and quality control as well as for development of new electronic and optical devices with predictable properties.

A high dynamical range of X-ray measurements in modern instruments and synchrotron sources makes it possible to measure the diffraction peaks with a high accuracy and detailed fine structure, containing plenty of information. A special attention is paid to long angular range scans (LRS) containing multiple Bragg reflections, which deliver the comprehensive and consistent information on the investigated samples in a wide range of the sample crystallographic parameters. However, the complex scattering of X-rays within the sample in high-resolution LRS demands a precise theoretical interpretation of the measured data.

In present work, the multi-beam dynamical diffraction theory is proposed, which takes into account all the required corrections to provide a high accuracy of calculated diffraction spectra. The precision of the method is proved by comparison with experimental high-resolution X-ray diffraction scans from 22 nm $YBa_2Cu_3O_7$ layer on $SrTiO_3$ substrate, containing 16 Bragg reflections.

D-36

GRAIN GROWTH AND TEXTURE SHARPENING IN COPPER, NICKEL AND PALLADIUM THIN FILMS, INVESTIGATED BY NON-AMBIENT X-RAY DIFFRACTION MEASUREMENTS

Y. Kuru, M. Wohlschlögel, U. Welzel and E. J. Mittemeijer
Max Planck Institute for Metals Research, Heisenbergstr. 3, D-70569 Stuttgart, Germany

The microstructure evolution (texture, crystallite size, microstrain and residual stress) of Cu, Ni and Pd thin films (nominal thickness 50 nm) on Si substrates during annealing has been investigated by in-situ X-ray diffraction measurements in a temperature range between 25°C and 250°C.

The thermoelastic behaviour was investigated excluding the occurrence of thermally activated relaxation processes by in-situ stress measurements below ambient temperature. On this basis, above ambient temperature, effects of stress relaxation and emerging secondary stresses (due to grain growth and annihilation of crystal defects, giving rise to a considerable tensile stress contribution) could be identified for all three layers in the temperature regime between ambient temperature and 250°C.

The results are discussed in the light of literature data obtained for thicker films and compared to predictions of different grain-growth models for various thicknesses and temperature regimes.

It is shown that the excess volume in grain boundaries can be determined from the evaluation of the residual stress and crystallite size with temperature.

D-9

DETERMINATION OF ACTIVATION ENERGY IN TEXTURED METAL-METAL MULTILAYER FILMS VIA 2D XRD

Mark A. Rodriguez, David P. Adams, and Ralph Tissot, Sandia National Laboratories, Albuquerque, NM 87185-1411

Metal-metal multilayer thin films have found use in many electronic, optical and magnetic applications. In order to estimate the thermal stability of multilayer films, we investigated the behavior of films subjected to slow heat treatment at moderate temperatures (~100–300 ^{o}C). XRD analysis observed intensity decay for diffraction peaks associated with the constituent metal phases due to inter-diffusion of the differing metal bilayer species (e.g., Al/Pt and Ni/Ti). This slow diffusion process is important with regard to long term functionality of the film. Monitoring the peak intensities of the decaying chemical species as a function of temperature allows the derivation of the activation energy for the diffusion reaction in the metal-metal multilayer films. However, there is one caveat — the metal layers often demonstrate significant out-of-plane texture. The peak intensity decay due to reaction may also be coupled with significant increase of mosaic spread of the decaying peak intensities. Hence, there are two possible sources of intensity loss which makes quantification difficult with standard q-2q analysis. We therefore have employed an area detector methodology to monitor both peak intensity loss and mosaic spread in order to better derive the activation energy of textured films. The results of this method for the determination of activation energies in various multilayer film systems will be presented.

*Sandia is a multiprogram laboratory operated by Sandia Corporation, a Lockheed Martin Company, for the United States Department of Energy under Contract DE-AC04- 94AL85000.

DXC Wednesday p.m.
Fusion & Industrial Applications of XRF

F-34

FURTHER STUDIES OF THE BORATE FUSION METHOD OF SAMPLE PREPARATION

Maggi Loubser[a], Peet H van Rooyen[b] and Johan PR de Villiers[c].
[a]X-ray Analytical Facility, Geology Department, University of Pretoria, Pretoria, 0002, South Africa. E-mail: maggi.loubser@up.ac.za
[b]Department of Chemistry, University of Pretoria, Pretoria, 0002, South Africa. E-mail: phvr@up.ac.za
[c]Department of Materials Science and Metallurgical Engineering, University of Pretoria, Pretoria, 0002, South Africa. E-mail: jpdev@postino.up.ac.za

This paper is a summary of a study conducted to identify and elucidate the reactions occurring in the formation of a lithium borate glass, but also between the lithium borate and oxides during glass formation. Thermo Gravimetric Analysis and Differential Thermal Analysis were used to evaluate the reactions occurring during the fusion of lithium borate glasses, and at a later stage, oxide/flux mixtures. During the TGA analysis certain reactions were observed and to investigate these similar samples were prepared in a muffle furnace and analysed by X-ray Powder Diffraction and Raman Spectroscopy.

The results presented will include some elucidation of the fusion process and some methods to deal with difficult to fuse materials will be presented.

F-83

FURTHER STUDIES OF THE BORATE FUSION METHOD OF SAMPLE PREPARATION: THE APPLICATIONS

Maggi Loubser[a], Peet H van Rooyen[b] and Johan PR de Villiers[c].
[a]X-ray Analytical Facility, Geology Department, University of Pretoria, Pretoria, 0002, South Africa. E-mail: mloubser@postino.up.ac.za
[b]Chemistry Department, University of Pretoria, Pretoria, 0002, South Africa. E-mail: phvr@up.ac.za
[c]Department of Materials Science and Metallurgical Engineering, University of Pretoria, Pretoria, 0002, South Africa. E-mail: jpdev@postino.up.ac.za

In a previous paper an overview was given of a study of the reactions occurring during a lithium borate fusion by using analytical techniques like TGA/DSC, XRD and Raman Spectroscopy. In this paper the application of the abovementioned techniques to real life problems will be illustrated, proving that a thorough investigation can solve laboratory sample preparation problems.

Some of the problems addressed using this approach were metallic content in samples. XRF spectroscopy is one of the major tools used in evaluation of refractory failures, but pressed powder briquettes have analytical limitations when metal particles are present in the interface between the refractory and melt phases. Fused bead preparation of such samples has always been problematic due to reaction of metal with platinum crucibles. XRD was used to evaluate a pre-oxidation step, which was included into the preparation. This method was further developed to fuse pure metallic samples with a simple pre-oxidation step. Sample preparation for sulphide-bearing matrixes was also optimised using TGA and XRD to evaluate the pre-oxidation step. The next problem evaluated using the insight gained from investigating the temperature behaviour of fluxes, was difficult to fuse materials including rutile, zircon and chromite-bearing ores. Successful fusion recipes were compiled with much lower dilutions than used in the past.

F-74

IRON ORE ANALYSIS - A NEW APPROACH FOR NEW REQUIREMENTS

Kai Behrens*, Alexander Seyfarth**
*Bruker AXS GmbH, Karlsruhe, Germany
**Bruker AXS Inc, Madison, Wisconsin, USA

International standards, such as the Australian ISO 9516-1 method, describe the calibration and elemental analysis of iron ore using a fusion method. The approach is based on synthetic standards uses empirical matrix correction terms. The fusion method, being an excellent tool for this application, is quite complex and benefits from advances in the fusion instrumentation with respect to temperature control and agitation. By using improved matrix correction algorithms, the difficult and very sample intensive approach of empirical corrections can be avoided. Computations also allow therefore the use of variable dilutions, a real benefit for complex iron ores.

The environmental impact of harmful substances during steel making turns the analytical process into another direction. Trace elements and volatiles are not possible to be determined accurately using a fusion based preparation. A repeatable, accurate pressed pellet preparation is readily made but has traditionally not achieved the accuracy levels needed and suffered from mineralogical matrix effects.

- How can accurate trace element analysis be obtained in a matrix which is as variable as iron ores, why not correct using “jump edge” correction?
- Can international reference materials be used to provide accurate analysis?
- Can a turnkey system be delivered to customers for the analysis of iron ore?

- What are the limitations of using the pressed powder method?
- What are the implications of matrix correction for the analysis?

In the talk we will show and discuss a novel approach, which combines the traditional fusion method results with a pressed powder pellet calibration for the analysis of traces in iron ore. The questions raised before will be answered and discussed for this linked approach.

F-9

NEW DEVELOPMENT IN LITHIUM BORATE FUSION FOR FERROALLOYS

P. Daigle, Corporation Scientifique Claisse, Inc., Ste-Foy, Quebec, Canada

Ferroalloys are used to adjust the final composition of steels. They play a key role in the physical and chemical properties such as hardness, strength, resistance to oxidation, etc. Ferroalloys are expensive and a careful management of the quantities added in the steel making process can lead to important savings.

XRF spectrometry has become the main instrumentation technique for ferroalloys because it allows accurate and precise multi-elemental determination. However, ferroalloys are not suitable for direct XRF analysis and sample preparation must be performed. In the past, borate fusion was not recommended for ferroalloys because they are composed of metallic species that are insoluble in borate salts and that metallic species can cause severe damage to Pt-Au ware. A few manual fusion techniques are described in the literature but they are time consuming and the results are dependant of the operator's skills. Moreover, they involve frequent manipulations of hot materials.

Recent improvements in borate fusion techniques have overcome the danger of fusing ferroalloys and made it easier. Automated fusion techniques with dry oxidation on a fluxer allow minimizing the preparation time and the number of manipulations and weighing steps. Perfectly flat, homogenous glass disks, without mineralogy nor particle size effects are now produced which also reduce inter-element effects. Optimization of the fluxer parameters and timing sequences now allow for easy and accurate borate fusion for ferroalloys such as FeV, FeMo, FeSiMn and FeV with high precision.

F-82

APPLICATIONS OF XRF IN THE OIL INDUSTRY

R. W. Morton
ConocoPhillips, Bartlesville, OK

X-ray fluorescence (XRF) spectrometry has been used by the oil industry since the 1950s. XRF can be found supporting activities in exploration, production, research as well as intellectual properties. Traditional applications for XRF were the analysis of single element or a limited range of multiple elements. Today, XRF encompasses high precision full spectral elemental profiles along with high accuracy and high precision single element testing for government regulations. This presentation will discuss how XRF is used in the oil industry and how the technology is changing to meet the oil industry of the future.

F-50

OPTIMIZING THE BALANCE OF QUALITY AND TURNAROUND TIME FOR A PROCESS CONTROL XRF LABORATORY

Suzanne W. Bowe, Kennecott Utah Copper, Magna, UT

The Kennecott Utah Copper Smelter relies on WDXRF data for much of its process control. Because of the nature of the Smelter design and the need for optimum performance to maximize efficiency, as well as the use of some results in metals accounting calculations, the XRF work must be very accurate. However, this must be balanced against the need for rapid reporting of results to allow close to real-time process control. This presentation describes the setup of a program to maximize the value of XRF in process control from the standpoint of both quality and turnaround time.

The program is guided by initial determination of customer requirements and regular customer communication to keep program developments aligned with needs and avoid wasting resources on what will not add value. Quality starts with well thought-out preparation procedures and good calibration curves, keeping in mind that proper attention up front saves time later on. Where a quality improvement would increase turnaround time, a choice must be made, weighing the advantages and disadvantages. Attention must be given to the quirks of each sample stream (there are 16 routine sample types), and method limitations must be explained to data users. The initial quality is maintained with repeatable preparation procedures, optimized drift correction, and instrument and support equipment maintenance. Scheduling of maintenance procedures and research and assessment samples is designed to minimize interruption to the normal flow of work. Other factors that help minimize turnaround time are an efficient sample logging and data reporting system, teamwork among analysts, and management support for system improvements. New technology and new uses of existing technology are considered to increase the contribution of the lab to efficient Smelter operation. Continuous improvement is an important part of the program.

F-2

FINDING AN ELEMENT TRACER FOR USE IN THE EARLY DETECTION OF 4 ½ BEARING FAILURE IN J52P408 ENGINES BY EDXRF

Gary R. Humphrey
Pratt & Whitney Aerospace, Inc.
Walter Lastinger, J52 FST Team Lead U.S. Navy

Physical Sciences Dept Team Lead
Joint Oil Analysis Program Technical Support Center
85 Millington Road, Pensacola, Florida 32508
Tel: 850-452-3191 ext 105; ghumphrey@joaptsc.navy.mil

The J52P408 engines suffers from a catastrophic failure that involves the 4 ½ bearing assembly. The U.S. Navy.s J52 engineering group uses FilterCheck (FC) 300 instruments to perform filter debris analysis (FDA) on J52P408 engines to detect the failure of the 4 ½ bearing assembly. The failure of the 4 ½ bearing assembly is detected through the FDA process by presence of excessive amounts of M-50. However, the J52P408 engine has 5 other bearing assemblies with the same alloy compositions and all seven bearing assemblies are plated with silver (Ag).

In an attempt to ascertain when the 4 ½ bearing assembly has failed, the U.S. Navy J52 engineers contracted Pratt & Whitney Aerospace to plate 4 ½ bearing cages with various elements other than Ag and see if these elements could perform as good as or better than Ag when a bearing cage is fractured. The candidate elements are cobalt (Co), rhodium (Rh), gold (Au), platinum (Pt), palladium (Pd), Indium (In) and Ag. Napoleon Engineering Services, Inc. (NES) was subcontracted by Pratt & Whitney Aerospace to set up and run a test rig with fractured 4 ½ bearing assemblies that were plated with candidate elements. The Joint Oil Analysis Program Technical Support Center (JOAPTSC) performed FDA with a FC300 instrument on filter elements from the test rig and Spectro, Inc. performed traditional rotrode atomic emission spectroscopy (RAES) and rotrode filter spectroscopy analyses on oil samples (RFS) to detect particles of the plating material being liberated from a fractured bearing cage. Early on in the testing, it became apparent that RAES and RFS could not detect the candidate plating material. Only FDA using the FC300 instrument could detect the plating candidates/elements. This paper will outline the results of the evaluation of the candidate elements/plating materials.

F-44

ANALYSIS OF HEAVY AND LIGHT ELEMENTS BY COMPACT X-RAY FLUORESCENCE SPECTROMETER

K. Muraoka, Y. Araki, T. Utaka, and K. Taniguchi
Institute of X-ray Technologies Co. Ltd,
Dai-3 Maruzen-Bldg. 3-5-21, Kigawahigashi, Yodogawa-ku, Osaka 532-0012, Japan

The Energy Dispersive X-ray Fluorescence Analysis (EDXRF) is a very popular analytical method for screening, of whose advantage is to simultaneously inspect the multiple heavy elements in non-destructive manner.

The compact (approx. 14kg) EDXRF that performs on-site analyses of heavy and light elements for soil, plastic and metal has been developed. The specialized analyzers (for WEEE & RoHS, Soil and Toy) are developed for the detection of hazardous elements in such kind of samples. The compact X-ray tube (W target, maxima 48kV and 0.2mA) and silicon drift detector realizes for downsizing, and higher energy resolution, respectively. The digital signal processor is also applied for high counting measurement and higher energy resolution. In this work, the fundamental parameter method is approached also.

For demonstration in plastic measurement, Cr, As, Se, Br, Cd, Sb, Ba, Pb and Hg are measured simultaneously, and also light elements S and Cl are measured by this analyzer. For the quantitative analysis, not only calibration curve method but also fundamental parameter method are applied depend on some request. In the simultaneous analysis, we studied how to measure optimization of a primary filter for continuous X-ray from a W target, also to use secondary filter in order to prevent Cr-Kα intensity from almost absorption decreasing. The overlap correction of the Pb-Lη peak for Se-Kα, the Pb-Lα peak for As-Kα and the Cd-Kβ peak for Sb-Kα are performed respectively. As a result, the minimum detection limits of below 3ppm for As, Se, Br, Cd, Pb and Hg is achieved, and 15ppm for S is also achieved respectively, and 5ppm was obtained for Cd in Brass. Some actual results obtained by the EDXRF “ED-05” will be introduced later.

DXC Thursday a.m.
Cultural Heritage I

F-77

CONFOCAL X-RAY FLUORESCENCE OF PAINTINGS: DECONSTRUCTING AN ATYPICAL 17TH C. COLLABORATION FROM ANTWERP, ASSESSING A 14TH C. CATALONIAN PANEL, AND IMAGING A LOST N.C. WYETH

Jennifer Mass[1,2], Arthur Woll[3], Christina Bisulca[4], Matt Cushman[5], and Noelle Ocon[6]
[1]Winterthur Museum and Country Estate, Winterthur, DE
[2]Art ConservationDepartment, University of Delaware, Newark, DE
[3]Cornell High Energy Synchrotron Source, Cornell University, Ithaca, NY
[4]Istituto di Ricerca sulle Onde Elettromagnetiche, Florence, Italy
[5]Williamstown Art Conservation Center, Williamstown, MA
[6]North Carolina Museum of Art, Raleigh, NC

The 17th c. Flemish painting on panel, *The Armorer.s Shop,* has long been attributed to David Teniers the Younger (1610-1690). During dendrochronological examination of the painting, a portion of one oak plank in the overall structure was found to have been carved out so that a smaller plank, depicting a pile of parade armor, could be inserted into the resulting depression. This unusual construction, combined with the identification of several paintings by Jan Brueghel the Younger (1601-1678) depicting this same parade armor, raised questions about the attribution and chronology of construction of the painting. Confocal X-ray fluorescence microscopy (CXRF) revealed the composition and location of buried paint layers by combining depth scans to produce virtual cross-sections over 20 mm in length. The relationship of the paint layers at the interfaces provided evidence for the armor panel having been painted separately and prior to the rest of the composition. This data provided a chronology of construction for the painting that supports a Brueghel attribution.

A late 14th c. Catalonian painting on panel depicting St. Louis of Toulouse was examined by conventional and confocal XRF, cross-section microscopy, and Raman spectroscopy to characterize the materials used in the manufacture and restoration this work. The panel is thought to have been part of an altarpiece with extant panels at the Philadelphia Museum of Art and the Johnson Art Museum of Cornell University. Materials identified are consistent with those observed in other late medieval Catalonian paintings on panel, and with a late nineteenth-century restoration campaign.

X-radiography of N. C. Wyeth's family mural study (c. 1922-1924) revealed the presence of a second painting underneath the presentation surface. This painting has been identified as an illustration for a 1919 *Everybody.s Magazine* story entitled "The Mildest- Mannered Man", a painting previously thought to have been lost. Confocal X-ray fluorescence microscopy (CXRF) was chosen to non-destructively probe the composition of the buried paint layers.

F-13

DISCOVERY OF A HIDDEN VAN GOGH PAINTING BY MEANS OF HIGH-ENERGY XRF MAPPING

Joris Dik[1], Koen Janssens[2], Geert Van der Snickt[2], Karen Rickers[3], Luuk Van der Loeff[4]
[1] Delft University of Technology, Materials Science, Rotterdamseweg 137, 2628 AL Delft, the Netherlands
[2]University of Antwerp, Department of Chemistry, Universiteitsplein 1, 2610 Wilrijk, Belgium
[3] DESY, Hamburger Synchronstrahlungslabor, D-22607 Hamburg, Germany
[4] Kroeller-Mueller Museum, Houtkampweg 6, 6731 AW Otterlo, the Netherlands

The painter Vincent Van Gogh (1853-1890) is generally considered as one of the most important painters of the 19th-C. As a result, his short but very productive career is subject of intensive study by art historians, historians, (conservation) scientists, etc. In the past, traditional radiographies made clear that Van Gogh covered several of his paintings with a new composition. The recycling of canvases might have been prompted by his difficult financial situation. In addition, his style changed so dramatically at certain moments in time that he might have regarded preceding works of art as obsolete and thus eligible for overpainting.

An examination of the Van Gogh paintings and the corresponding radiographies of the Kröller-Müller museum (NL) confirmed the existence of these concealed compositions. However, radiographies usually allow only to discern some coarse outlines but prevent to observe further details. The visualization of such covered compositions would be of great interest to both Van Gogh specialists as the public audience.

This talk discusses the first successful attempt to re-establish a hidden portrait by means of elemental mapping with synchrotron based μ-XRF. A small canvas (ca. 30 x 20cm), representing a patch of grass (ca. 1886-'87) was transported to beam line L at the HASYLAB synchrotron facility in Hamburg. A conventional radiography of this painting reveals the outlines of a human face but no identification or correlation with the existing oeuvre of the artist was feasible. A square area of ca. 15x15 cm, corresponding with the position of the head, was scanned with a quasi monochromatic X-ray beam of 35.5 keV of 0.3x-0.3 mm^2 cross-section.

One of the (trace) element maps obtained in this manner allows to visualize the covered portrait of a peasant woman with unprecedented detail. On-going spectroscopic research is focused on the identification of the nature of the pigmented compound with which the portrait was painted. Additionally, art historians are currently involved in a stylistic comparison between Van

Gogh's existing oeuvre and the newly revealed portrait, including a re-examination the preserved correspondence of Van Gogh in an attempt to identify documentary links to this portrait.

C-2

ANCIENT WARRIORS AND THE ORIGIN OF CHINESE PURPLE

Zhi Liu
Advanced Light Source Division, Lawrence Berkeley National Laboratory, CA 94720

In March 1974 during the sinking of wells for farmland irrigation near Xi'an, China, several farmers made one of the world's most remarkable archaeological finds: the discovery of an army consisting of more than 8000 life-size terra cotta figures of warriors and horses of the First Emperor of Qin. One of the most intriguing puzzles is the purple synthetic pigments ("Chinese Purple" or "Han Purple") found on the terra cotta soldiers. Until the 19th century, most pigments were based on naturally occurring colored minerals and dyes, with three significant exceptions: Egyptian Blue ($CaCuSi_2O_{10}$), Chinese Blue ($BaCuSi_2O_{10}$)/Purple ($BaCuSi_2O_6$) and Maya Blue. The former two are alkaline-earth copper silicates, and because of this similarity it has been proposed that the Chinese pigments were derived from Egyptian Blue.

In our study, we analyzed clumps of pigment (above) from the Qin warriors and discovered that in spite of the structural similarity to Egyptian Blue, the micro-structural morphology of Chinese Purple is very different. Based on the morphology and the phase distribution in the clumps of the pigment, it appears that the process by which Chinese Purple was synthesized is very similar to that of barium-containing glasses. Combining these results with other archaeological evidence, we propose that the synthesis technology for the Chinese pigments was a by-product of high-refractive index glasses (artificial jades) produced by Taoist alchemists.

In summary, we argue that Chinese Purple was invented as a by-product of the technology originally developed for synthesizing barium-containing glasses, which, in turn, were invented for the purpose of imitating jade. The barium compounds were added to increase the refractive index of the glass, thus giving the glass a similar appearance as jade. The development of this process also benefited from two well-developed technologies in ancient China: the earlier bronze making (adding lead compounds to reduce the melting temperature) and pottery making (advanced pottery kilns) technologies.

C-1

XRF AND XRD ANALYSIS OF CONVERTED LEAD PIGMENT ON A GEORGIA O'KEEFE PASTEL DRAWING

Lynn B. Brostoff,[1] Catherine Maynor,[2] and Robert J. Speakman[1]
1 Museum Conservation Institute, Smithsonian Institution, 4210 Silver Hill Rd., Suitland, MD 20746
2 Smithsonian American Art Museum, Smithsonian Institution, 750 Ninth Street NW, Washington DC 20001

X-ray fluorescence (XRF) spectrometry and micro-X-ray diffraction (μXRD) were used to analyze the composition of pigments on a pastel drawing, *Special No. 32*, by Georgia O'Keefe. The analyses were undertaken to identify the nature of what was suspected to be discoloration in certain red- and orange-hued areas of the drawing, and to determine if the pastel's current appearance is a significant departure from the artist's original intent.

XRF instrumentation consisted of a handheld Innov-X ED-XRF with a silver anode X-ray tube, Al filter, and Si PiN diode detector. The instrument was operated at 35 kV and 13 μA and at 15 kV and 12 μA; resolution was < 0.2 keV. The spectrometer was attached to a tripod arm that extended over the object on a laboratory benchtop (that did not contribute to the elemental signature) and positioned 2–3 mm above the surface so as not to detach any of the extremely friable media. A precise distance was maintained throughout the analyses by repositioning the drawing. Four areas also were examined using a window mask, which limited the spot size to < 5 mm. XRD analyses were performed on a Rigaku D/Max Rapid diffractometer using copper Kα radiation, 50 kV acceleration voltage, 40 mA current, chi axis fixed at 45º, omega axis fixed at 0º, and phi axis spun 360º. For these analyses, two tiny particles, about 30 μm each, were mounted on glass fibers and exposed for 180 seconds using a 0.1 mm collimator.

XRF analyses show that the drawing's masterfully layered and blended red, orange and yellow pigments are associated with the elements Pb, Cr and Ca. This suggests the presence of pigments made from lead chromates, red lead oxides, and/or lead carbonates, plus a pastel filler such as whiting ($CaCO_3$). These results cannot be strictly interpreted in a quantitative manner because of non-ideal examination conditions, as described above. However, it is shown that comparison of Pb:Cr ratios detected in select areas of the drawing, as derived from standard calibration curves, allow the more stable red and orange lead chromate pigments to be differentiated from other likely lead pigments. Red lead oxide pigment is well known to be unstable to light and air, often leading to nonuniform darkening. XRD analysis of a sample removed from a blackened stripe in a red area of the drawing in fact confirms that the darkened appearance and high Pb:Cr ratio in this case is associated with the presence of red lead oxide, minium (Pb_3O_4).

F-48

RESEARCH IN THE IDENTIFICATION AND PROVENANCING OF 20TH CENTURY PHOTOGRAPHS

Dusan C. Stulik and Art Kaplan, Getty Conservation Institute
David Miller, Department of Chemistry, California State University at Northridge

Silver gelatin black and white (B&W) photographic paper was by far the most commonly used photographic printing material during the 20th century. Available in many varieties and different grades and produced by a great number of large and small manufacturers in many countries of the world, this type of paper was the medium for millions of art, technical, and documentary photographs now preserved in museums, historical collections and archives.

As a very chemically complex material object, a photograph might harbor some important material clues to support its provenancing and authentication. Scientific investigations conducted independently at the GCI have identified a number of chemical and physical markers, or signatures, of baryta-coated B&W photographic paper that could be used in provenancing, authenticating, and in some cases even dating of photographic material and photographs.

The XRF analysis of a large number of 20th century photographs and photographic paper from the GCI's and Paul Messier's reference collections has shown that photographs and photographic papers contain-in addition to silver-several other chemical elements such as barium, strontium and calcium. These elements are introduced in different stages of the photographic paper manufacturing process as part of the paper substrate (calcium), baryta layer coating (barium and strontium).

The XRF investigation has further shown that the concentration of these elements is very uniform for any given emulsion run; and this concentration depends on production technology and the purity of raw materials used in the manufacture of photographic paper. Our investigation has shown that actual concentrations of key chemical elements found in photographic paper and many individual physical parameters of photographic paper differ enough from one type of photographic paper to another and vary enough between different manufacturers to provide the rationale for the development of a scientifically based provenancing methodology for both photographic paper and photographs.

The success of determining a new provenancing methodology and its widespread application depends on both the quality of the analytical and scientific methodologies used for quantitative determination of all key chemical and physical parameters applied in the provenancing methodology and on a quality of a photographic paper database available for parameter matching.

F-51

DETERMINATION OF STRONTIUM CONCENTRATIONS IN CALCIUM-BASED GROUNDS WITH XRF & ICP-MS

Carole Namowicz, Marc Walton, and Karen Trentelman
Getty Conservation Institute
1200 Getty Center Drive, Suite 700, Los Angeles, CA 90049-1684

Non-invasive *in-situ* analysis of paintings by X-ray fluorescence (XRF) spectroscopy allows inference of the general class of ground present (*i.e.*, calcium- or lead-based), but the concentrations of individual elements are difficult to assess based on XRF data alone. For calcium-based grounds, strontium (not associated with strontium-based pigments) is frequently detected, and the determination of its concentration may prove valuable in assisting attribution studies. While the strontium concentration can be accurately measured using inductively coupled plasma mass spectrometry (ICP-MS), this technique requires the removal, and destruction, of small samples. In this paper, we describe the development of a methodology to calibrate the response of XRF to strontium in calcium-based grounds as a means to better understand the relative abundance of strontium without subjecting samples to ICP-MS.

In reviewing XRF data produced from rhenium and rhodium target XRF spectrometers, it was found that calcium-based grounds demonstrated strontium peaks with high intensities relative to the calcium peaks. This may be misinterpreted as an abnormally high concentration of strontium within the ground material. However, the same samples analyzed via ICP-MS revealed only trace amounts of strontium. To rationalize these contradictory results, a systematic study was undertaken to determine the detection sensitivities of XRF to calcium and strontium.

A series of pressed pellets designed to mimic the bulk composition of a gesso painting ground (containing approximately 0.001 - 10% strontium in a calcium sulfate matrix) were prepared and analyzed using both instrumental techniques. Preliminary results indicate that the XRF spectrometers used in this study are extremely sensitive to strontium and have indicated concentrations as low as 10ppm. These results will be compared to those obtained by ICP-MS to develop a correlation between the techniques, thereby allowing better estimates of strontium concentrations to be assessed from XRF data.

This work is the first step in a larger project that will apply trace element analysis and the determination of strontium isotopic ratios by ICP-MS to the analysis of gesso painting grounds. This may serve to support attribution studies by determining possible relationships between paintings or identifying the geologic source of the ground material

F-68

X-RAY FLUORESCENCE OF A MEDIEVAL MOSAN RELIQUARY OF SAINT AMANDUS

J. Giaccai
Division of Conservation and Technical Research, Walters Art Museum, Baltimore MD, USA

The components of a reliquary shrine of Saint Amandus are analyzed using X-ray fluorescence. The reliquary was acquired by the Walters family in 1930 from an art dealer in Paris. Stylistic examination dates the shrine to the 11th through 13th centuries, in the Mosan region of Belgium. The reliquary consists of a wooden tomb-shaped box covered with over 100 pieces of gilded copper, as well as enameled plaques, silver columns and numerous gemstones. Repoussé, engraving, and stamping were all used when decorating the copper plaques in a number of different designs. Although it is very clear that the various components of the reliquary have been moved, lost and replaced over time, it is unclear which, to determine which plaques were original, which were added in the 13th century or over the course of its liturgical lifetime, and which may have been added by the dealer in the early twentieth century.

An open-architecture XRF was used to identify the colorants and opacifiers in the enamel plaques without requiring the removal of a sample. The colorants and opacifiers can be compared to published analyses of medieval Mosan enamels. Similarly, the trace elements identified in the copper plaques were analyzed with XRF to try and separate the various components into groups that may have been manufactured together. Stylistic analysis and examination of the method of manufacture are combined with the XRF data to form a picture of how the reliquary's plaques have been moved, added to and replaced during its history.

DXC Thursday a.m.
Industrial Applications

D-37

X-RAY AND THERMAL ANALYSIS OF CEMENTS AND CONCRETE FOR EVALUATION OF CEMENT ADDITIVES AND CONCRETE ADMIXTURES

Jeffrey P. Nicolich, Derek R. Brown, Frank G. Serafin, Urszula B. Latosiewicz, Josephine H. Cheung and Paul J. Sandberg
W. R. Grace & Co. - Conn., 62 Whittemore Ave, Cambridge, MA 02140

Cement additives and concrete admixtures have been in use since the 1930s to improve the quality of building material components. Important quality enhancements include strength, set time, freeze-thaw behavior, color, workability, durability and increased grinding efficiency. The effect of additives on the properties of cement and concrete depend to a large extent on the composition of the cement. Therefore, detailed analysis of cement can help improve the additives used to optimize the performance of cement and concrete.

Rietveld analysis of X-ray powder diffraction patterns is a powerful tool in the analysis of cement samples due to its ability to give precise quantitative analysis of crystalline phases and total amorphous content despite similar chemical composition. Verifying the accuracy poses a particular challenge due to the extremely complex nature of cement mixes. Various approaches to verify the accuracy will be presented, including the use of thermal analysis and selective dissolution techniques.

Worldwide manufacture of cement accounts for about 5 % of total world CO_2 production. To mitigate the problem, cement can be replaced by secondary cementitious material (SCM), primarily fly ash and blast furnace slag, without adverse effects in the concrete. Both fly ash and blast furnace slag are industrial waste products and pose a challenge to the X-ray diffractionist as both are either poorly crystalline or amorphous. Attempts to validate the composition of cements containing secondary cementitious material will be presented.

D-2

APPLICATION OF 2-DIMENSIONAL XRD FOR THE CHARACTERIZATION OF MICROSTRUCTURE OF SELF-LEVELING COMPOUNDS (SLC)

Severin Seifert[1], Juergen Neubauer[1], Friedlinde Goetz-Neunhoeffer[1],
and Hubert Motzet[2]
(1) Mineralogy, University of Erlangen-Nuremberg,
Schlossgarten 5a, 91054 Erlangen, Germany
(2) Schoenox GmbH, Alfred-Nobel-Strasse 6, 48720 Rosendahl, Germany

The microstructure of hardened self-leveling compound (SLC) has a decisive influence on the final properties like surface strength as well as adhesion of the SLC to the substrate. Thereby, the development of the microstructure, especially the formation of ettringite, strongly depends on the properties of the used substrate for underground. By the application of a non-absorbent substrate, ettringite is evenly formed over the whole SLC from the bottom to the top. In contrast, the application on an absorbent substrate leads to a reduced content of ettringite in the top layer of the SLC. Consequently, surface strength of the SLC will also be reduced, because early strength is mainly attributed to ettringite.

For determination of the ettringite content in different areas from the bottom to the top of the SLC the 2-dimensional X-ray diffraction (GADDS) was used. The GADDS (Bruker) equipped with crossed Goebel mirrors primary X-ray optics enables the detection of the phase composition of the hydrating mortar in horizontal slices. Thus the vertical phase distribution could be analyzed in position-sensitive mode at different areas. For investigations of SLCs from the very early hydration stage up to a few hours, a custom-made *in-situ* sample holder was designed and constructed. This sample holder offers a smooth surface from the cross section of the SLC without any mechanical preparation. Additionally, it fits the requirements which allow us to work under *in-situ* conditions as well as in a manner conforming as closely as possible to the technical conditions. After preparation of the SLC the sample holder can be easily integrated into
the diffractometer. Finally, these investigations have shown that the combination of GADDS with a custom-made *in-situ* sample holder provides the possibility to characterize the time-resolved microstructures of hydraulic-setting cements.

D-4

QUANTITATIVE IN-SITU X-RAY DIFFRACTION ANALYSIS OF EARLY HYDRATION OF PORTLAND CEMENT AT DEFINED TEMPERATURES

C. Hesse[1], F. Goetz-Neunhoeffer[1], J. Neubauer[1], M. Braeu[2], P. Gaeberlein[2], M. Degenkolb[3]
[1]Mineralogy, University of Erlangen-Nuremberg, D-91054 Erlangen, Germany
[2]BASF Construction Chemicals GmbH, D-83308 Trostberg, Germany
[3]PCI GmbH, D-86159 Augsburg, Germany

X-ray diffraction (XRD) is widely used for the determination of phase composition of Portland cement powders. To understand interactions between additives and the cement phases also a time resolved quantitative phase analysis of the early hydration at defined temperatures is necessary.

Technical white cement was mixed with water and prepared in a custom-made sample holder maintaining the surrounding temperature at a constant value. The sample was covered by Kapton film which prevents water evaporation. A D5000 diffractometer (Bruker) equipped with a SolX energy dispersive detector was used. Eighty-eight diffraction patterns were recorded within 22 hours of hydration.

Each diffraction pattern was refined by the Rietveld method with the software Topas 3.0 (Bruker). In consequence of the used Kapton film, a background model must be developed for the diffuse diffraction maximum of the material. The lattice parameters, crystallite size, and microstrain were refined for the hydrate phases. The parameters for the clinker phases, calcite, and anhydrite were determined by measurements of dry cement and were fixed during refinement of the cement paste. The content of X-ray amorphous C-S-H gel in the paste linked with the formation of portlandite was calculated from the content of portlandite. The quantification shows the progress of the silicate and the aluminate reaction and the dependence of their kinetics on the temperature. The link between the formation of ettringite and the dissolution of the aluminate phase and anhydrite could be shown.

The measurements and their Rietveld refinements exhibit a very good reproducibility. Additionally, the noise of the phase content development within 22 hours is very low. The investigations have shown that quantitative *in-situ* XRD of cement hydration can be performed also with lab diffractometers.

F-1

ANALYSIS OF PLATINUM GROUP ELEMENTS (PGE) BY MEANS OF TOTAL REFLECTION X-RAY FLUORESCENCE (TXRF) SPECTROMETRY

Hagen Stosnach, Bruker AXS Microanalysis GmbH, Berlin, Germany

Platinum group elements (PGE) are of crucial importance in many industrial and medical application fields. For the cost-effective exploration and mining of PGE, an accurate and fast analysis of these elements must be ensured. That applies to industrial applications of PGE as catalysators too. Here, the concentrations of PGE must be controlled with regard to process control, recycling processes or contamination control.

A special application is the use of PGE distributions in rocks, minerals and meteorites in order to investigate and understand geological processes.

In addition, PGE are used in medicine for cancer treatment by chemotherapy. The important analytical task is the continuous control of PGE concentrations in blood, serum and the cancer drugs themselves.

For the accurate analysis of PGE common analytical techniques face a number of difficulties. Applying wavelength XRF, the sample preparation is often complicated, the number of certified reference standards is limited and the detection limits are not sufficient in many cases. Atomic spectroscopy strictly requires digestion of the sample material. Additionally, there is always the risk of long system down-times after a concentrated sample was introduced accidently.

In contrast TXRF is an ideal technique for PGE analysis due to the ability to process solid and liquid samples. Major benefits are the quantification, based only on internal standardization, and a broad analytical range, which allows the accurate analysis from low ppb up to % concentrations.

A low-power benchtop TXRF spectrometer was used for the analysis of different sample types including Pt-bearing ores, catalysts, wash-coats, blood and docimastic digestion solutions. The results clearly indicate the suitability of this technique for an accurate PGE analysis in different sample types.

D-20

PROBING THIN-LAYERED AND NANO-STRUCTURED MATERIALS – X-RAY SCATTERING TOOLS

J.F. Woitok
PANalytical B.V., Almelo, The Netherlands

Advanced thin-layered and nano-structured materials are essential for todays and future electronic, optical, mechanical and energy devices. The necessary scaling of the applied structures challenges the thin film deposition and patterning processes as well as the measurement and monitoring tools. A detailed knowledge of the material properties is important for its application and crucial for further development and improvements. Typical materials involved are semiconductors, metal alloys, dielectrics and also polymers.

X-ray techniques provide great potential not only in the research and development phase, but also offer unique options for process development and monitoring. X-ray fluorescence, X-ray diffraction and X-ray reflectivity have been successively used for elemental and structural analysis. From X-ray scattering data information is extracted to identify and quantify phases, to determine composition and strain profiles, thickness, roughness, density, grain size, residual stress and preferred orientation.

This presentation will give an overview on the experimental aspects, including recent hardware developments and evaluation processes of X-ray methods. A range of examples of technologically relevant materials will be used to demonstrate the high potential of X-ray techniques.

D-41

RESIDUAL STRESS ANALYSIS OF NON-POLAR GaN EPI-LAYERS BY GIXRD

Young-il Jang, Kyu-ho Park, Sung-ryong Cho*, Ho-ki Kwon*
Devices & Materials Lab., LG Electronics Institute of Technology, 16 Woomyeon-Dong, Seocho-Gu, Seoul 137-724, Korea
*LED Lab., LG Innoteck, 16 Woomyeon-Dong, Seocho-Gu, Seoul 137-724, Korea

There have been many achievements in optic devices industries such as LEDs and LDs. It is true that the packaging techniques and the circuit design techniques are important, but it is inevitable to see the limits of the devices without epi characteristic improvements itself. Today's commonly used LEDs and LDs are composed of multi-stacked epi layers grown on C-plane sapphire or GaN free standing substrates. Epi layers can be easily grown on those symmetric plane substrates. But in that case there are several problems inevitably go with in. For example, when using C-plane as a substrate, the devices should suffer form strong polarization effect along the active layers where the radiative recombination occurred. This phenomenon is originated from the fact that GaN is wurzite structure material. Polarization effect can make not only the device's efficiency decreased but also the wavelength shifted to red region, because the electrons and holes are separated by this polarization effect so that the recombination efficiency is drastically decreased.

In order to reduce and avoid the polarization effect on the active region, the promised method is to use asymmetric, non-polar plane as a
substrate. Already the performances of non-polar based device are revealed as outstanding by other groups. But the structural properties of these non-polar epi layers are not well understood. In point of the stress, there can be anisotropic stress state along grown axis. But the ways to measure and analysis the residual stress are not established very well. In this work, using Grazing Incidence XRD method and the modified $\sin^2$psi method, the in-plane and anisotropic mechanical properties of non-polar GaN epi layers will be discussed.

D-16

STUDY ON THE X-RAY DIFFRACTION BEHAVIOR OF A BIG CRYSTAL GRAIN IN ORIENTED 3% SILICON STEEL

Jianfeng Fang, Zhiling Tian, Jing Huo, Jinyuan Zhang, Yi Zhang
Central Iron and Steel Research Institute, Beijing, 100081, P.R. China

In this paper, X-ray diffraction behavior of a big [011] oriented grain (millimeter scale) which deviated from the sample surface by 10.6 degree in oriented 3% silicon steel was studied. The results showed that diffraction from the (011) crystal planes was very strong, if normal of the (011) planes was just on diffraction plane. However, the diffraction intensity of the grain decreased other than vanished, if the normal of the crystal planes deviated from diffraction plane through rotating the sample was around its surface normal. Nevertheless, it was found that the bigger of the deviating angle between the normal of the crystal planes and diffraction plane, the lower of the diffraction intensity from (011) crystal planes of the grain. The diffraction intensity decreased to 53.6 percent and 36.8 percent of the strongest intensity, if the sample was rotated by 10 degree and 15 degree around its surface normal from the position in which the normal of (011) crystal planes was just on the diffraction plane.

F-85

SCREENING TOYS AND CONSUMER GOODS WITH HANDHELD XRF

Stanislaw Piorek, Thermo NITON Analyzers LLC, Billerica, MA

The problem of lead contamination in our environment is not new. Most recently, it resurfaced with increased intensity when, last summer, the Consumer Product Safety Commission (CPSC) initiated a wave of recalls for toys containing excessive amount of lead. Hundreds of thousands of popular toys were found to be decorated with paint containing more than 600 mg/kg of lead, and many children's articles such as furniture, jewelry, art supplies and even baby supplies contained thousands of mg/kg lead. As it turned out, the overwhelming majority of those "leaded" toys were manufactured in China.

Understandably, this situation has caused a nationwide public outcry and harsh criticism of the toy industry as well as the CPSC for not being vigilant enough in protecting the youngest and most vulnerable group of our society.

Those events uncovered gross deficiencies in existing testing protocols, and in the analytical methods for toy testing; they also exposed the inadequacy of the pertinent U.S. regulations. At the same time, it also became evident that toy manufacturers had lost control of their production processes, especially when the actual manufacturing of toys was subcontracted to factories in China.

In order to address the immediate problem of testing the massive number of recalled toys, the industry reached for the tried and field-proven analytical method of handheld X-ray fluorescence (XRF).

In this paper, we will address the problem of the gross inadequacy of the current test protocols based on the ICP or AA methods as they apply to toys' testing, and discuss the benefits and challenges of using the XRF technique to screen toys and consumer products for lead and other toxic elements. To complete the picture, we will discuss the existing U.S. and EU regulations limiting the levels of lead in toys and, finally, outline the legislative efforts to improve them.

F-8

FORENSICS APPLICATIONS OF X-RAY FLUORESCENCE MICROSCOPE.

Sergey Mamedov, Jon Goldey, George Setola, Andrew Whitley
Horiba Jobin Yvon Inc., Edison, NJ 08820, USA

The goal of this study was to investigate the utility of X-ray Fluorescence (XRF) microscope in determination of trace elements concentration and distribution in Gun Shot Residue, Antiques, Museum objects, and Counterfeit Products. The advent of XRF microscope for laboratory use presents new applications for the forensic scientists.

This presentation will impact the forensic community and/or humanity by providing practical insight into the application of XRF Microscope in analysis of Gun Shot Residue, Fingerprints, Museum and Archeological objects, and Counterfeit products.

Micro-XRF technology is a relatively recent introduction to the field of art conservation, archeology, boarder security, trace analysis and forensic science. XRF analysis gives a rapid, non-destructive reading of the elemental composition of any material for elements starting from Na till U in the periodic table. Horiba XGT-7000 XRF analytical microscope was used in this study. This desktop unit utilizes a portable 50W X-ray source for excitation, two switchable (as small as 10 microns) monocapillary for different special resolution, and capability to work in vacuum and in ambient condition.

We will show several examples of using micro XRF for:
1) Analysis of Gun Shot Residue (GSR). In addition to the chemical images, micro transmission images will be presented. Chemical images will be compared with Fluorescence images;
2) Fingerprints chemical images;
3) Chemical images of original and counterfeit devices;
4) Mapping of museum and archeological objects.

F-28

FDA REGULATORY APPLICATIONS OF FIELD PORTABLE EDXRF

Richard Jacobs, FDA, San Francisco District Laboratory; Peter T. Palmer, San Francisco State University

FDA has accumulated valuable experience employing field portable EDXRF to regulated products. These devices are currently in use at both FDA.s Center for Food Safety and Applied Nutrition (CFSAN) and at the San Francisco District. They are a valuable asset for routine and non-routine elemental analysis investigations. In 2007, FDA's Division of Field Science sponsored a pilot study to explore the use of these analyzers in the field. Investigators from the San Francisco District were trained and certified in the use of these analyzers and used them to identify products containing abnormal levels of toxic elements. This pilot study demonstrated that investigators and non-chemists can use this equipment to quickly and accurately screen large numbers of FDA-regulated products. In the lab and for most samples, XRF will not substitute for techniques such as ICP-MS for sub-ppm level analyses. But XRF dramatically increases a lab.s ability to triage and to investigate component of samples as well as the samples

themselves. Significant advantages include minimal sample preparation, rapid and definitive identification of target elements, and semi-quantitative determinations of target elements at relatively low ppm levels.

This presentation will highlight the use of XRF for investigational and forensic-type applications of food and regulated products within the FDA, and illustrate how FDA can make better use of XRF results in the regulatory process in the future. At the present time, FDA has not established approved, validated XRF-based methods for specific target analytes and matrices. However, XRF results are used for sample triage both in the field and in the lab for identifying products that contain elevated levels of toxic elements as the basis for further investigation to trigger a regulatory action. Examples of products of interest include dietary supplements, Asian patent medicines, and some foods. Presently, we screen all dietary supplements via XRF before they enter our regular analytical process that is focused on low levels of toxic elements (which is most often based on microwave digestion followed by ICP-MS analysis). While XRF results alone have *not* been used as the *sole* means for regulatory decisions, they have provided convincing confirmatory evidence that is essential for the FDA regulatory process. In the future we plan to utilize XRF as a definitive regulatory tool where possible (e.g. dietary supplements that contain percent levels of toxic elements).

F-40

SEARCHING FOR PURE TIN ON ELECTRONIC COMPONENTS: TIN WHISKER PREVENTION

George J. Havrilla and Martin Sweet, Los Alamos National Laboratory, Los Alamos, NM 87545

Tin whiskers are a known phenomena which occurs in electronic circuitry, mechanical fasteners, and sensor assemblies causing untold problems from failed circuits to tin plasmas[1]. Tin whiskers arise from using pure tin as solder or coatings on electrical contacts. These whiskers have been discovered on both active and passive circuit components, with and without so-called boundary layers and even with mitigation coatings. The best remedy to date is insuring that there is no pure tin within the circuitry. This usually means using a tin/lead solder with a minimum composition of at least 3 weight percent of lead present. Even specifying “no pure tin” on procurement agreements does not insure that “no pure tin” will be delivered. This is especially aggravated with recent requirements for ROHS compliance. It is apparent that the burden of proof is incumbent on the user of the materials to insure that there is no pure tin on the parts and in the materials being used for critical electronic applications.

X-ray fluorescence is a rapid and direct method for elemental analysis. It is a recommended method for determining whether the parts in question are pure tin or not. However, the actual answer is quite dependent upon the excitation area where the instrument is actually looking. Recent measurements in our laboratory have identified parts which originally had been tinned by the vendor. Since this was known to the user of the electrical parts, the offending pure tin was removed and the part re-soldered with a tin/lead alloy. The cleanup was to be verified by doing spot MXRF analyses to confirm the proper tin/lead alloy was deposited onto the leads of the part. While spot analyses did indeed confirm that 60/40 tin/lead solder was used, we also identified regions of pure tin close to the insulating base of the part which were difficult to reach with the soldering iron. This pure tin identification was only achieved using elemental MXRF mapping. One can easily be fooled by single point spectra providing false security that all pure tin has been eliminated. The implication of this is whether the tin/lead coatings are done in house or by a commercial vendor, ultimately one needs to double check to insure all the tin is alloyed.

1. http://nepp.nasa.gov/WHISKER/

F-72

RoHS COMPLIANCE IN PAINTS AND RESINS

A.Seyfarth*, A. Buehler**, K. Behrens**, J. Sardisco***
*Bruker AXS Inc., Madison, Wisconsin, USA; **Bruker AXS GmbH, Karlsruhe, Germany; ***Analytical Services, The Woodlands, Texas, USA

ROHS compliance requirements impact more and more suppliers. Clients require traceable analysis for the ROHS suite of elements.

Traceable ROHS standards are available for PE and PVC as well as for Polycarbonate matrix. Bench top EDX or WDX based implementation of ROHS compliant screening for these matrices was described previously at DXC 2007. Liquid samples and especially modern solvent based paints offer a much more difficult challenge:

- How can a design of experiment (DOE) approach be implemented to screen for more than 10 000 or more different formulations?
- How to best prepare a sample with pigment, different solvents?
- What IF clients have additional elemental requirements?
- How can raw materials be screened before they are dosed into the product?
- How can we avoid a false negative?

The talk will discuss a DOE based approach to screen for ROHS and additional elements in liquid paints.

Using organometallic compounds and adequate organic matrices it is possible to create DOE based calibration space. Key to the standard preparation is knowledge of stabilizers and homogenizers to keep the compounds in solution for the various matrices. Measurement conditions are selected to cover the calibration space as well as potential interferences to minimize the risk for false negatives. With a suitable matrix correction approach, based on experience since 1999 with a universal Petro calibration, a set of calibrations is established and validated. Encountered Validation difficulties are discussed as is the approach for calibration maintenance.

F-79

CHOOSING XRF FOR RoHS APPLICATIONS

James R. Bogert
Matrix Metrologies, Inc.
Holbrook, NY 11741 USA

Although no one analytical instrument technique is capable of completely satisfying all RoHS validation requirements, X-ray Fluorescence (XRF) Spectroscopy is the most versatile, capable of analyzing all the restricted elements with no sample prep and in most cases, nondestructively.

Of the two instrumental approaches to XRF analysis, Energy Dispersive XRF (EDXRF) and Wavelength Dispersive XRF (WDXRF), EDXRF has been most widely adopted for RoHS analysis. This is due to the ability of EDXRF to inspect samples of widely varying shapes and sizes. Of the EDXRF instruments commercially available handheld XRF and bench-top micro-beam XRF systems have proven the most applicable.

Because RoHS level analysis (1000ppm Pb, 1000ppm Hg, 1000ppm Cr^{+6}, 1000 ppm Br as PBB and PBDE, and 100 ppm Cd)[1] is trace analysis from an EDXRF perspective, EDXRF detection limits are ppm levels, equipment used for RoHS inspection and validation require 2 important hardware features to enable this kind of analysis. These are a solid-state detector for peak resolution and incident X-ray beam filtration to provide the necessary peak-to-background (signal-to-noise) response. Both handheld and bench-top units may offer these features. So, how does one decide between a handheld and a bench-top unit? As is usually the case, it depends on the form of the samples and the analytical requirements and expectations. And in some cases you may want to consider both.

This paper will speak to X-ray spectrometer features and capabilities – hardware and software that should be considered when choosing EDXRF (Handheld and / or Bench-top) for RoHS applications, including:

1. Analysis area – incident spot size and beam collimation.
2. Is the analysis area vertically homogenous, ie., is it a plated material, in which, case thickness must be accounted for with thickness and composition software.
3. If it is vertically homogenous, is the sampled area infinitely thick to analyte emission, ie., Cd in plastic? Again, if not then thickness must be part of the analysis.
4. Is the sample horizontally homogeneous, ie., a populated printed circuit board? How does the analyst sample this?

XRF RoHS applications are complicated and present many gray areas that should be addressed when choosing and implementing an X-ray instrument and reporting the results.

[1] XRF provides total elemental content it does not differentiate between Cr+3 and Cr+6 or the molecular state of Br.

F-43

ANALYSIS OF ELEMENTS IN ENVIRONMENTAL SAMPLES BY MICRO-XRF

Y. Araki[1], S. Maeo[2], M, Krämer[2], T. Utaka[1, 2] and K. Taniguchi[1, 2]
[1]Institute of X-ray Technologies Co. Ltd,
Dai-3 Maruzen-Bldg. 3-5-21, Kigawahigashi, Yodogawa-ku, Osaka 532-0012, Japan
[2]Osaka Electro-Communication University
18-8, Hatsumachi, Neyagawa-shi, Osaka 572-8530, Japan

Micro-XRF is an effective tool for the qualitative and quantitative analysis of elements in environmental samples such as soil, air particulate, biological and medical samples and so on. The micro-XRF spectrometer consists of an X-ray tube with multi excitation sources, the doubly curved crystals (DCC), silicon drift detector (SDD) system, and position detection unit of micro-particle.

The micro-focus (approx.30μm) and high brightness X-ray tube is used in this system. The X-ray tube has three targets (Cr, W, Rh) on anode. The targets can be selected by moving the anode position.

Generally the capillary optics or DCC optics are used for focusing X-rays system on micro scale area. In capillary optics, X-rays can be focused but unnecessary continuous X-rays and characteristic X-rays are focused on a sample surface, too. However, in the DCC optics, the X-rays are not only focused but also monochromatized on a sample and then, the background should be reduced and should be improve lower limits of detection. For higher counting rate and higher peak to background ratio, SSDD is selected as a detector with large effective diameter.

Particles in atmosphere air and trace elements in glasses were measured and performance of this system was evaluated. The performed elemental mapping is done, also.

This study, thus, introduces the micro-XRF for environmental samples, and discusses the results obtained in our laboratory.

DXC Thursday p.m.
Cultural Heritage II

C-8

PORTABLE XRD/XRF INSTRUMENTATION FOR THE STUDY OF WORKS OF ART

G. Chiari[1], P. Sarrazin[2], M. Gailhanou[3]
1 - Getty Conservation Institute - 1200 Getty Centre Dr Suite 700 -Los Angeles, Ca 90049 (GChiari@getty.edu)
2 - inXitu, Inc., 2551 Casey Ave., Mountain View, CA 94043 (psarrazin@inxitu.com)
3 - TECSEN, UMR CNRS 6122, Université Paul Cézanne, 13397 Marseille (France)

In Cultural Heritage research, truly non-invasive analytical procedures not only require that no sample is taken from the object, but also that the object does not move from its location. The transport of the object to an instrument comes at a risk of accidental damage, which translates into high insurance fees. Therefore portable instruments that are taken to the object are highly favored to conventional laboratory instruments. The typical example is XRF with the handheld analyzers that have become one of the major tools in diagnostics.

A small Portable XRD/XRF instrument, named X-Duetto, is being jointly developed by the Getty Conservation Institute and inXitu, Inc to enable non-invasive analysis of works of art. The instrument head, configured in reflection geometry, is placed on the sample using a stand or a photographic tripod, and precisely adjusted with an X-Y-Z stage and laser alignment guides. A fine X-ray beam, produced by a small copper tube and miniature slits illuminates the object at 10° incidence. A 2D CCD detector collects the X-rays scattered in an angular range of 20 to 50° 2θ, in direct detection (nophosphor) to allow energy discrimination and enable parallel XRD and XRF measurements. A power & control unit, packaged in a separate rugged case, includes Li-ion batteries for autonomous operation in the field, a miniature computer for control of the instrument, and a wifi access point for remote operation and data download from any laptop PC. Each of the two units weights less than 10kg and can easily be transported to any remote site.

Usable XRD patterns can be obtained in as little as 5 minutes. The XRF data collected from the same spot, informs on the chemical composition of the sample and can be used for screening during phase identification with the XRD data. Several iterations of prototypes of X-Duetto have been tested on a variety of samples. The results of the most significant case studies will be presented.

F-25

XRF DETECTION OF HEAVY METAL PESTICIDES IN ARCHAEOLOGICAL AND ANTHROPOLOGICAL ARTIFACTS

Aaron N Shugar, Art Conservation Department, Buffalo State College, 1300 Elmwood Ave Rm 230, Buffalo, NY 14222

A wide range of pest control techniques have been used on museum collections. Some of these pest control techniques involve the use of heavy metals which are considered the most persistent forms of pesticide. The specific heavy metals which are of greatest concern are Arsenic (As), Mercury (Hg) and Lead (Pb) (see Goldberg (1996) and Odegaard *et al* (2005) for details concerning types of pesticides used). These elements were applied to artifacts (wood, textiles, leathers, skins, feathers etc…) in various ways including spraying in aerosol form, sprinkling with dust, painting with a solution or submerging items in liquid compounds. Contact with the contaminants may put individuals such as museum staff, visitors using the collections, and Native Communities, to which many objects are being repatriated, at risk. Investigations into contaminated collections have been carried out and reported by a number of institutions worldwide (See Sirois *et al*, in print, for more details).

Because it is difficult to gain permission from many museums to take physical samples from contaminated objects for traditional investigation, portable XRF offered a less invasive method of analysis. The use of a portable handheld X-ray Fluorescence (XRF) to investigate heavy metal contamination in museum collections began around 1998. A main concern with the handheld XRF is the lack of understanding of the reported results of analysis. Few standards exist for pesticides of this nature and for the wide range of materials found in museum collections. Without proper calibration we are unable to say what difference a reported result of 20 ug/cm^2 is to 500ug/cm^2 of Hg in an object. In addition, there is no understanding of how these pesticide treatments infiltrated the objects (i.e. the depth of penetration, homogeneity of application and surface contamination, and rate of decay and evolution during storage). All of these issues must be clarified, before a good understanding of the health risks of using a contaminated object can be calculated.

Recent research has focused the production of reference materials which match the diverse nature of materials found in museum artifacts to ensure consistent calibration. This is a large collaborative program including the Smithsonian, NIST, the Canadian Conservation Institute, the EPA, Various museums around the world as well as the main manufactures of handheld XRFs.

Goldberg, L. "A History of Pest Control Measures in the Anthropology Collections, National Museum of Natural History, Smithsonian Institution." *JAIC* 35 (1996) pp. 23- 43.

Odegaard, N. and A Sadongei. *Old Poisons, New Problems: A Museum Resource for Managing Contaminated Cultural Materials.* Walnut Creek: Alta Mira Press, 2005,

Sirois, J., Johnson, J., Shugar, A., Poulin, J. and Madden, O. (in print) "Pesticide Contamination: Working Together to Find a Common Solution" Forthcoming article from Symposium 2007: Preserving Aboriginal Heritage: Technical and Traditional Approaches. Ottawa Canada September 2007

F-52

ON THE USE OF HANDHELD XRF FOR DETERMINATION OF ARSENIC AND MERCURY IN A MUSEUM COLLECTION

Kara Cross and Peter T. Palmer, San Francisco State University

In the past, artifacts stored in public and private museums have been treated with a variety of pesticides to protect and preserve them for future generations. These substances are toxic and people working with contaminated artifacts may be at risk of exposure. This presentation will describe the determination of arsenic and mercury in a collection comprising over 2500 baskets which were acquired by the Oakland Museum between 1910 and 1940, along with a smaller collection of birds.

XRF is an ideal technology for this application due to its simplicity, speed, and nondestructive analysis capabilities. Its detection limits for arsenic and mercury are in the low ppm range and hence more than adequate for determining whether or not a basket had been treated with these pesticide agents. Rather than analyzing each and every basket in this collection, a subset of baskets obtained from different origins and/or collectors were analyzed. Two different locations on each of these baskets were analyzed using readings that were typically no longer than one minute, which was short enough to facilitate the completion of the analyses over four working days. For the bird analyses, only one sample was acquired.

This presentation will include a description of the data quality objectives, methods, and quantitation procedures. Of particular concern in this work was providing reliable and accurate detection and quantitation of arsenic and mercury in the samples. Ideally, the presence of two lines at close to their tabulated energies is desired to confirm positive identification of a given element. However, the spectral overlaps of the analytes (the K_β line for arsenic at 11.73 keV overlaps the L_β line for mercury at 11.82 keV) and some of the matrix species (i.e., lead and bromine) presented complications. For quantitation, a series of custom-made standards in a cellulose-type matrix were prepared and analyzed on the same dates as the samples. For some samples, an alternate line was chosen for quantitation to avoid spectral overlap with an interfering species. In all cases, a modified form of Compton Normalization was employed to correct for varying sample densities. The detection limits were on the order of 10 and 25 ppm for arsenic and mercury, respectively. Approximately 20% of the baskets were found to contain detectable levels of arsenic and/or mercury, with the highest concentrations found in birds and on a basket coated with vermillion pigment. This work will illustrate some of the difficulties in confirming the presence of both of these elements, especially near the detection limits, and the fairly complicated data analysis procedures required to provide accurate quantitation in a fairly diverse collection of samples.

F-49

ISSUES, TRANSITIONS AND COLLABORATIONS ASSOCIATED WITH USE OF HAND-HELD XRF IN NATURAL HISTORY MUSEUMS

Cheryl Podsiki
The Field Museum, Chicago

This presentation will provide an overview of major issues that natural history museums face as they transition their testing methods and strategies to include the use of hand-held XRF analyzers. The increased numbers of large and small institutions as well as Native American tribes that wish to use the hand-held XRF instruments are relying on their ability as a nondestructive tool to accurately analyze elements on archaeological and ethnographic objects and natural history specimens.

The analyzers have proven to be an excellent screening tool for qualitative results on inorganic and organic objects typically found in natural history collections. There is, however, a gross misconception among users that the instruments can provide quantitative results on organic materials. The ability to do so exists but until appropriate reference materials become available for use and accurate calibration curves can be determined the instruments cannot be relied on for quantification on natural history collections. The analyzers were simply never designed to be used on organic materials for the purpose of quantification using the analyzer.s current modern metal alloy or soil standards.

The confusion over the qualitative and quantitative abilities of the XRF analyzer has resulted in an array of new issues and concerns among museum staff and scientists. Included in those issues are the needs for users to understand the physics of XRF, determine the limits of detection, correctly interpret the spectrum, and accurately report the results. Most museum staff do not have this sort of training, nor are museums in a position to provide resources to support it. New testing protocols must be developed based on XRF qualitative spectrum results rather than the necessary quantitative data.

The situation offers an opportunity for museums and manufacturers of the XRF analyzers to collaborate for the benefit of all parties involved. Museums can provide ample spectra taken from the collections to establish reference materials and calibration curves. Manufacturers have the resources to provide the scientists, knowledge, and materials. Collaboration may be the key to obtaining quantification for museums and a true comprehensive software package for the manufacturers.

D-47

CULTURAL HERITAGE STUDIES WITH HIGH-ENERGY X-RAYS AT THE APS 1-ID BEAMLINE

D. R. Haeffner*, J. D. Almer, Argonne National Laboratory, Argonne, IL, USA
F. Casadio, Art Institute of Chicago, Chicago, IL, USA
D. C. Dunand, Northwestern University, Evanston, IL, USA
B. D. Newbury, ExxonMobil Development Company, Houston, TX, USA
M. L. Young, Ruhr-Universität Bochum, Germany

The 1-ID beamline at the Advanced Photon Source is one of the world's premier sources of high energy X-rays (50 – 120 keV, 0.10 – 0.25 Å). Experiments at this facility cover a wide range of scientific subjects, and several studies have been carried out in collaboration with major area museums on artifacts with importance for cultural heritage. For example, high-energy XRD, XRF, and radiography have been used to non-invasively examine antique astrolabes, ancient Chinese bronzes, and ancient bronze bracelets from the Middle East. Results from these experiments have helped to uncover information on the manufacturing technology used to make these artifacts and to determine the state of preservation for the various specimens. Advantages and disadvantages of the use of high-energy X-rays and synchrotrons for studies of cultural heritage will be discussed.

Use of the Advanced Photon Source was supported by the U. S. Department of Energy, Office of Science, Office of Basic Energy Sciences, under Contract No. DE-AC02-06CH11357

F-6

THE YIN AND YAN OF XRF ANALYSIS AS A TOOL IN THE INVESTIGATION OF CULTURAL HERITAGE WORKS

By Dr. Bruce Kaiser, Bruker AXS, Kennewick, WA

Over the past 8 years I have been privileged to support several museums and universities in the application of XRF technology in their quest to better understand the elemental make up of cultural heritage works of all types. This paper will go into the detailed XRF setup and analytical approaches that have been developed for 7 specific measurement challenges. In discussing the development of these applications not only the technique will be discussed but also the interaction physics that underlies the approaches chosen. Also, the limits and of strengths of XRF analysis in these applications will be discussed. The specific topics are the determination of trace elements in bulk materials, the determination of the location of elements in layered materials, the identification and quantification of chlorine and sulfur contamination on various substrates, the quantification of titanium in the presence of barium, general XRF quantification (when it works and when it does not), the measurement of various patinas on Cu alloys, and the quantification of elements in a paper substrates**.**

F-61

SANDRA: A PORTABLE XRF SYSTEM FOR NON DESTRUCTIVE STUDIES OF MEXICAN CULTURAL HERITAGE

J.L. Ruvalcaba Sil
Instituto de Física, Universidad Nacional Autónoma de México, Mexico

In the last years, a portable X-ray fluorescence system has been developed specially for non-destructive characterization of cultural heritage collections of Mexico. This system, called SANDRA (Sistema de Análisis No Destructivo por RAyos X), is a second prototype designed for in-situ analysis in museums and libraries. Oxford Instruments X-ray tubes of Mo, W, or Rh of 75 W, may be employed as excitation source depending on the analytical problem and the studied materials. Two detectors fabricated by AmpTek may be used: A Cadmium Zinc Telluride (CZT) and a Si-Pin as a function of the elemental range to be analyzed. The beam may be collimated from 0.25 up to 3mm, but usual X-ray beam diameter is 1 or 2 mm. Various research topics has been carried out using SANDRA and other complementary techniques: Mexican paintings from XIX century, colonial paintings (XVI-XVII century), pre-Hispanic and colonial manuscripts, pre-Hispanic metallic artifacts, and recently green stone and turquoise pre-Hispanic items, among others.

In this work, the main features of the SANDRA system are presented as well as two examples of research on Mexican cultural heritage collections. First, the main results of the study of an important colonial manuscript of traditional medicine using herbals, the *de la Cruz-Badiano* codex, written in 1552 in the school for Indians of Santa Cruz de Tlatelolco during the early colonial period after the conquest of Mexico, is presented. XRF was used for the analysis of inks and colored figures. On the other hand, the most outstanding results of a set of almost 50 pre-Hispanic artifacts of gold and silver artifacts discovered in the Tomb 7 of Monte-Alban, Oaxaca, one of the most important treasures discovered in Mexico. From XRF study, the alloys composition and some technological aspects are discussed.

This research has been supported by CONACyT-Mexico project U49839-R.

C-13

TIME-RESOLVED X-RAY FULL FIELD MICRO-IMAGING OF TRANSIENT FLUID DYNAMICS

Kamel Fezzaa
X-ray Science Division, Argonne National Laboratory, 9700 S. Cass. Ave., Argonne IL 60439

The X-ray beam afforded by third-generation synchrotrons, such as the Advanced Photon Source (APS), has unique properties: extremely high intensity, wide energy tunability extending to over 100 keV, high coherence, and flexible lattice timing structure. To take full advantage of these properties at the APS, we are developing a novel X-ray research tool, involving ultrafast phase-enhanced full-field X-ray imaging, with both micrometer-spatial and sub-nanosecond temporal resolutions. Such a novel capability will make tremendous impact on numerous fields, both scientifically and technologically.

We will present some examples of our work combining the X-rays time-structure and detectors gating possibilities. Many detection modalities are available, ranging from a single 150 ps (or 472 ns) X-ray exposure, to multiple-successive exposures, to ultra-high frame rate videos. We will present highlights from some ongoing research on hydrodynamics singularities, such as droplets pinch-off, breakup and coalescence [1, 2], and jetting and cavity collapse upon impact on liquids [3]. We also applied a variation of this technique to measure velocity field distribution of dense liquid jets near nozzle orifices [4], and cavitations in a Venturi system.

We expect this synchrotron-based time-resolved broadband X-ray edge-enhanced radiography to provide crucial validation data for computer models and increasingly contribute to the fundamental understanding of problems where high penetration depth, temporal, and spatial resolutions are needed.

1. K. Fezzaa and Y. Wang. *Phys. Rev. Lett*. **100**, 104501 (2008)
2. Y. Wang, K-S. Im, and K. Fezzaa. *Phys. Rev. Lett*. In Print.
3. Y. Wang, and K. Fezzaa. In review.
4. Y.J. Wang et al., *Nature Physics*. 10.1038/nphys840 (2008).

* The use of the Advanced Photon Source was supported by the U. S. Department of Energy, Office of Science, Office of Basic Energy Sciences, under Contract No. DE-AC02-06CH11357, and Argonne National Laboratory Director's Competitive Grant (LDRD) 2006-023-N0.

F-12

A HIGH RESOLUTION HARD X-RAY BIOIMAGING FACILITY AT SSRL

P. Pianetta, J. Andrews, S. Brennan, SLAC, Menlo Park, CA
E. Almeida, NASA Ames Research Center, Moffett Field, CA
M. van der Meulen, Cornell University, Ithaca NY
A. Tkachuk, J. Gelb, J. Rudati, M. Feser, W. Yun, Xradia, Concord, CA

The Stanford Synchrotron Radiation Laboratory (SSRL) in collaboration with Xradia Inc., the NASA Ames Research Center and Cornell University has implemented a commercial hard X-ray full field imaging microscope on the 54 pole wiggler beam line at SPEAR3. This facility will provide unprecedented analytical capabilities for a broad range of scientific areas and will emphasize research on nanoscale phenomena and structures in biology, materials science, and environmental science. The basic instrument itself is a full-field transmission microscope (TXM) based on zone plate optics using imaging in the first order of the zone plate from 5-14 keV and phase contrast at 8 keV. A resolution of 45 nm in first order has been demonstrated in both absorption and Zernike phase contrast including 3D tomographic reconstructions. High quality images were obtained using single exposure times of 0.5 seconds. Spectroscopic capabilities have been demonstrated with XANES spectra taken across the iron edge in an Antarctic meteoritic spallation fragment. The microscope will see further improvement with the addition of higher resolution zone plates and a phase contrast capability at 5 keV to improve contrast in biomaterials. A scanning microprobe capability is integral to the system thus allowing elemental mapping and fluorescence yield XANES to be performed with a spatial resolution in the micron range without introducing any changes to the optical configuration of the instrument.

We will describe the optical configuration of the beam line and show how the X-ray beam propagates though the microscope resulting in an optimized image. We will also show imaging results from mouse bones as well as a variety of materials science examples.

C-19

3-D TOMOGRAPHIC STUDIES OF ANNEALED NANOPOROUS GOLD USING TRANSMISSION X-RAY MICROSCOPE (TXM) AT ADVANCED PHOTON SOURCE

Yu-chen Karen Chen[1,2], Yong Chu[2], Jaemock Yi[2], Marie Cox[1], David C. Dunand[1] and Qun Shen[1,2]

1. Department of Materials Science and Engineering, Northwestern University, Evanston, IL 60208
2. Advanced Photon Source, Argonne National Laboratory, Argonne, IL 60439

Three dimensional tomography has become a powerful tool on studying the internal structure of various materials and hence acquiring quantitative 3-D information. X-ray imaging is ideal for tomography for it is nondestructive analysis. The study on porous materials, with complicated 3-D structure, has benefited from advanced X-ray 3-D tomography technique.

Nanoporous metals display novel physical, chemical and mechanical properties, accompanied with potential applications in such diverse areas as catalysis, heat exchange, mechanical actuation, and sensors. Especially, nanoporous gold is scientifically intriguing and significant because of the complex 3-D structure formations and evolutions, which are not fully understood. We developed nanoporous gold foam by dealloying Ag-Au alloys. Nanoporous gold was annealed on different temperature to acquire different pores scales.

By using transmission X-ray microscope 3-D tomography techniques, we have observed the internal 3-D porous cavities at a few hundred nanometers. The transmission X-ray microscope at the Argonne National Laboratory has demonstrated a 2-D resolution down to 40 nm. In addition, the synchrotron X-ray source is crucial because of its high-intensity hard X-ray beams to penetrate the whole sample object and also the high-flux to obtain imaging data within reasonable time scale. This tomography information will be critical to quantitative analysis on the structure formation. We propose to establish analysis method for imaging porous nano-materials to correlate the process, structure and properties. We also plan to design *in-situ* imaging experiments to directly follow the nanoporous structure evolution as a function of time.

Acknowledgement: Use of the Advanced Photon Source was supported by the U. S. Department of Energy, Office of Science, Office of Basic Energy Sciences, under Contract No. DE-AC02-06CH11357.

D-58

NANOSTRUCTURE ANALYSIS OF METALLIC MATERIALS BY COHERENT X-RAY DIFFRACTION MICROSCOPY

Yukio TAKAHASHI[1], Hayato FURUKAWA[1], Hideto KUBO[1], Kazuto YAMAUCHI[1], Yoshinori NISHINO[2], Tetsuya ISHIKAWA[2], and Eiichiro MATSUBARA[2]

[1]Osaka University, Yamada-oka, Suita, Osaka 565-0871, Japan
[2]RIKEN SPring-8 Center, Kouto, Sayo-cho, Sayo-gun, Hyogo 679-5148, Japan
[3]Kyoto University, Yoshida, Sakyo, Kyoto 606-8501, Japan

Coherent X-ray diffraction microscopy[1] (CXDM) is a novel technique for reconstructing a two- or three-dimensional image. After the first demonstration of CXDM by Miao *et al.*, several applications of CXDM have been reported. CXDM has a great potential as a new technique for structural studies of metallic materials because it is not only a non-destructive method but also applicable to a sample of micrometer thickness. In the present study, the validity of CXDM for this kind of observation was demonstrated using an age-hardened aluminum alloy in practical use. Also, Cu thin line samples were fabricated on Si_3N_4 membranes towards demonstration of electromigration analyses. Coherent X-ray diffraction patterns of the metallic materials were measured at BL29XUL in SPring-8. As the result, the internal structure and the shape of the aluminum alloy particles were three-dimensionally visualized[2]. Characteristic diffraction patterns resulting from both the shape of the Cu thin lines and the defects formed by the application of the current were observed[3].

1) J. Miao, P. Charalambous, J. Kirz, and D. Sayer, Nature 400, 342 (1999).
2)Y. Takahashi, Y. Nishino, T. Ishikawa, and E. Matsubara, Applied Physics Letters 90, 184105 (2007).
3)Y. Takahashi, H. Furukawa, H. Kubo, K. Yamauchi, Y. Nishino, T. Ishikawa, and E. Matsubara, Surface and Interface Analysis (in press)

C-9

REALTIME XRF AND XRD IMAGING – THE INSTRUMENTATION AND THE APPLICATIONS

Kenji Sakurai
National Institute for Materials Science
1-2-1, Sengen, Tsukuba, Ibaraki 305-0047 Japan

The present talk describes novel powerful imaging for X-ray fluorescence (XRF) and X-ray diffraction (XRD). So far, the scanning-type imaging has been widely used in those techniques. Though recent progress in high-spatial-resolution imaging using synchrotrons is significant, there have been a clear limit; because of the step-scan, the imaging requires a long measuring time. In many scientific applications, X-ray imaging that are much more rapid, e.g., capable of high-speed resolution rather than high-spatial resolution, have been demanded. It is possible to do X-ray imaging without performing any scans. Here, the method uses quite a wide beam, which illuminates the whole sample surface in a low-angle-incidence arrangement (0.5~3 deg). The detector used is a CCD camera working at 30 fr./sec, equipped with a collimator inside, and the distance between the sample surface and the detector is set extremely close, in order to enhance both spatial resolution and efficiency. Note that the imaging is done with one shot. In the case of XRF imaging, distinguishing elements are required and, therefore, most of the experiments were performed with monochromatic or quasi-monochromatic X-rays. The
procedure for XRD imaging uses a combination of exposure and incident X-ray energy scan (or just tuning). Since the present experiment employs a fixed small-angle incidence and also a fixed diffraction angle of around 90 deg, the diffraction plane here is inclined at about 45 deg from the surface of the specimen. By scanning the energy of the incident X-rays, one obtains a diffraction peak, which corresponds to the lattice spacing. Further instrumental details and many applications will be presented.

References
[1] K.Sakurai, *Spectrochimica Acta* B54, 1497-1503 (1999)
[2] K.Sakurai and H.Eba, *Anal. Chem*. 75, 355-359 (2003)
[3] K.Sakurai and M.Mizusawa, *Nanotechnology,* **15,** S428-431 (2004)
[4] H.Eba and K.Sakurai, *Chemistry Letters* **34,** 872-873 (2005)

F-39

A TOP-DOWN APPROACH USING X-RAY IMAGING TECHNIQUES: INSTRUMENTAL DEVELOPMENTS AND APPLICATIONS IN LIFE SCIENCE

Björn De Samber[1], R. Evens[2], T. Schoonjans[1], G. Silversmit[1], B. Vekemans[1], K. De Schamphelaere[2], C. Janssen[2], B. Masschaele[3], L. Van Hoorebeke[3], S. Bohic[4], K. Rickers[5], G. Falkenberg[5] and L. Vincze[1]
[1] X-ray Microspectroscopy and Imaging (XMI), Department of Analytical Chemistry, University of Ghent (UGent), Krijgslaan 281 (S12), 9000 Gent, Belgium
[2]Laboratory of Environmental Toxicology and Aquatic Toxicology, UGent, Belgium
[3]Centre for X-ray Tomography (UGCT), UGent, Belgium
[4]European Synchrotron Radiation Facility (ESRF), Grenoble, France
[5]Hamburger Synchrotronstrahlungslabor at DESY/PETRA III, Hamburg, Germany

Synchrotron radiation X-ray fluorescence micro- and nanobeam techniques at second- and third generation SR sources offer the potential of non-destructive multi-element analysis down to trace concentration levels with unrivalled spatial resolution among X-ray based analytical techniques. At these sources, relative detection limits at the sub-ppm (fg/ng) level can be achieved. With respect to absolute detection limits (DL), sub-micron sized X-ray beams can offer DLs below 1 ag for the most efficiently excited transition elements, with a potential lateral resolution level better than 100 nm.

These characteristics of micro/nanobeam SR-XRF allow spatially resolved multi-element determination of major, minor and trace constituents in microscopic sub areas and volumes within biological specimens in an essentially non-destructive/non-invasive manner. However, the complexity of performing such an experiment is often quite considerable, involving dedicated sample preparation, transportation towards and experimenting at the synchrotron facility, installing an appropriate experimental set-up and performing a thorough data analysis on large amounts of spectral data.

The ecotoxicological research on *Daphnia magna*, a frequently used model organism for investigating the mechanisms of toxicity of metals, has often been difficult because many analytical techniques are not able to investigate trace metal distributions in a spatially resolved manner at a (sub)microscopic resolution. As illustrated by this presentation, SR-XRF microanalysis allows to fill this gap and moreover, due to the variety in sizes of X-ray beams available, this research can be performed from the organism level towards the tissue and cellular level, representing a top-down approach.

Reference:
Three-dimensional elemental imaging by means of synchrotron radiation micro-XRF: developments and applications in environmental chemistry, Anal. Bioanal. Chem. (2008) 390:267-271

F-38

APPLICATIONS OF CONFOCAL MICRO X-RAY FLUORESCENCE 3-DIMENSIONAL ELEMENTAL IMAGING

George J. Havrilla and Brian Patterson
Los Alamos National Laboratory, Los Alamos, NM 87545

Confocal micro X-ray fluorescence (CMXRF) offers a new paradigm in materials characterization. CMXRF utilizes monolithic polycapillary optics on both the excitation and detection paths to create an overlap region of the two focal spots. This confocal volume allows XRF elemental information to be obtained nondestructively by moving the confocal volume in 3 dimensions. Although a powerful analytical concept it is still not fully understood within the analytical community.

This paper will explore the use of CMXRF in collecting 3 dimensional information for a variety of samples including a resistor, layered paint sample, an ICF target, and a variety of uranium particles. In each application, the utility of CMXRF is highlighted by providing unique nondestructive 3-dimensional information about the samples. In the case of the resistor, distributions of lead and tin are important for mitigation of tin whisker formation. The layered paint sample offers a new perspective for potential art conservation applications. Simple depth profiles are only single point while a CMXRF scan can show the texture of the applied paint as well. The ICF target is an ideal sample of light material with transition element dopants as well as contaminants. The key feature in this case is obtaining elemental information nondestructively. Finally a 3D map of an array of uranium particles offers insights into 3D spatially resolved detection of particles. Particle sizes ranging from 10 to 100 micrometers are captured in a volume 1 x 1 x 0.4 mm.

Scanning parameters as well as insights into the 3D elemental structures of these samples will be presented.

C-22

COMBINED MICRO-XRF/XRPD TOMOGRAPHY FOR THE CHARACTERIZATION OF FeCrAlY-FOAM-BASED CATALYSTS

K. Janssens[a], W. De Nolf[a], F. Basile[b], P. Benito[b], S. Bugani[b], G. Fornasari[b], L. Morselli[b], E. Scavetta[c], D. Tonelli[c] and A. Vaccari[c]
(a) *Department of Chemistry, University of Antwerp, Wilrijk, Belgium*
(b) *Department of Industrial Chemistry and Materials, University of Bologna,Bologna, Italy*
(c) *Department of Physical and Inorganic Chemistry, University of Bologna,Bologna, Italy*

Steam reforming (SR) of hydrocarbons (i.e. natural gas, biomasses, alcohols) is the most commonly used method to produce hydrogen (H_2) on an industrial scale. Since this is an endothermic reaction, temperatures of about 1173-1273 K have to be maintained. These hard conditions have a destructive effect on the reactor tube material and shorten its life time. Catalytic partial oxidation (CPO) can be used instead of SR for small-scale H_2 production. This slightly exothermic reaction has to be performed at ultra-high space velocity to prevent total oxidation. Metallic foams such as FeCrAlY are promising catalyst supports for both SR (because of its thermal stability and conductivity) and for CPO (because of its high porosity).

The catalyst can be deposited on this support in two ways: (a) wash-coating of calcined foam with bohemite in HNO_3, followed by impregnation with a hydrotalcite-type (HT) of catalyst precursor (b) direct electrochemical deposition (ECD) of the HT precursor, a method used for the preparation of modified electrodes.

A combination of X-ray Fluorescence and X-ray Powder Diffraction on a micro scale has been employed to visualise in a completely non-invasive manner the layered structure of the catalyst after impregnation and its distribution on the foam-walls in both methods. XRF and XRD tomograms show virtual two-dimensional cross-sections of foam-pillars in which the elemental and crystal phase composition of the catalyst layers are visualized. In order to obtain these maps, Pawley fitting of thousands of two-dimensional diffraction patterns collected with an area detector was performed. During this procedure, the relative intensities of diffraction lines belonging to one crystallographic phase are kept constant and the remaining phase scaling factors allow to visualize the distribution of that phase after tomographic reconstruction with an MLEM algorithm. XRF spectra that are recorded simultaneously with the XRD data by means of two SDDdetectors are fitted to an analytical model in order to extract the net intensities of the element specific X-ray lines; these net data are used to construct element specific tomograms.

In all cases, it could be observed that an Al_2O_3 layer was formed between foam and catalyst, as intended in order to ensure catalyst phase dispersion and protection of the metallic foam under industrial conditions from corrosion, oxidation effects, etc. The formation of the active catalyst phase [$Ni(Mg)(Al)_2O_4$, Ni(Mg)O] from the HT precursor could be demonstrated. By means of the ECD method, thinner layers of the catalyst could be deposited than by means of the conventional wash-coating approach.

DXC Thursday p.m.
High Temperature In-situ Analysis

D-35

IN-SITU CHARACTERISATION OF NOVEL FUEL CELL MATERIALS

S.J. Skinner
Department of Material, Imperial College London, Prince Consort Road, London, SW7 2BP, UK.

As alternative energy technologies such as solid oxide fuel cells near commercialisation, there is a requirement to develop next generation materials to enhance performance, both in terms of electrochemical performance and component durability. A vital part of this development is understanding the phase evolution of these novel materials as a function of temperature and atmosphere, as each component is exposed to demanding environments during processing and operation.

Recently materials with complex crystal structures and/or oxygen interstitial content have been proposed as potential fuel cell materials [1]. Of these, we have been involved with the *in-situ* characterisation of several solid solution series under variable atmospheres, using both laboratory X-ray diffraction and neutron diffraction techniques. The materials of interest in this work are from the $Ln_2Ni_{1-x}Co_xO_{4+\delta}$ and $Ce_{1-x}La_xNb_{1-y}V_yO_{4+\delta}$ solid solution series, both of which contain oxygen excess materials, and $La_2Mo_2O_9$ a novel fast oxide ion conductor.

In this presentation the structural evolution of these materials will be discussed as will the complimentarity of both X-ray and neutron diffraction techniques, as well as some of the challenges in defining the suitability of materials for fuel cell applications.
[1] A.Lashtabeg and S.J. Skinner, J. Mater. Chem., 2006 **16** 3161

D-11

IN-SITU XRD ANALYSIS OF THE GROWTH OF ZnO NANOWIRES

Melanie Kirkham, Zhong Lin Wang, Robert L. Snyder
School of Materials Science and Engineering, Georgia Institute of Technology

Quasi-one-dimensional (1D) nanostructures of ZnO, with large aspect ratios and dimensions on the order of nanometers, have many potential applications such as photonics materials, gas sensors and nanogenerators. The synthesis of ZnO nanowires from zinc at moderately low temperatures (around 500°C) has been reported and attributed to a self-catalysis mechanism, in which molten zinc droplets serve both as a source of zinc and as a catalyst to promote the reaction with O_2. The purpose of this study is to gain a greater understanding of the selfcatalysis synthesis mechanism by collecting and analyzing in-situ X-ray diffraction data during the growth of ZnO nanowires. Data were collected at a range of temperatures from 350°C to 550°C, and the dependence of growth rate on temperature was investigated. Various morphologies were observed, including branched and unbranched nanowires, and the morphology was affected by synthesis parameters such as the heating rate and growth temperature. Increased understanding of the synthesis process should allow higher yields and better control of the nanowire morphology and properties.

D-17

KINETICS OF PARTICLE GROWTH FOR SUPPORTED Pt AND Pt/Pd DETERMINED USING HTXRD

A.R. Drews and R.J. Kudla
Ford Research and Advanced Engineering, Dearborn, Michigan 48121

We have used High Temperature X-ray Diffraction (HTXRD) to study the growth kinetics of platinum and platinum/palladium alloy particles supported on alumina in a wet, oxidizing atmosphere. Diffraction data were collected during isothermal aging exposures over time scales from 150 to 1.4×10^5 seconds and at temperatures from 773K to 1173K. The average precious metal particle size was determined from the diffraction peak widths, and the amount of crystalline material contributing to the peak was determined from the normalized peak area. Growth of crystalline particles was found to closely follow a power-law in time over the duration of the measurements, with the rate constant following an Arrhenius model for activation. The amount of crystalline material reached a maximum level determined by the aging temperature. Addition of palladium did not appear to limit the kinetics of crystallization, but did strongly suppress the maximum amount of crystalline material. Rescaling the exposure time using the measured Arrhenius behavior allows us to compare different time-temperature experiments and predict particle growth.

D-54

IN-SITU HEATING STUDIES ON THE INTERNAL STRESSES OF MULTILAYER ENVIRONMENTAL BARRIER COATINGS

Bryan J. Harder, Katherine T. Faber; Northwestern University, Evanston IL
Jon Almer; Advanced Photon Source, Argonne, IL
Kang N Lee; Rolls-Royce Corporation, Indianapolis, IN

Silicon-based ceramics such as SiC and Si_3N_4 are promising materials for use in gas turbine engines due to high melting temperatures and excellent thermomechanical stability. Unfortunately the SiO_2 layer on surface of these materials reacts with water to form $SiO(OH)_2$ that volatizes in the high pressure and gas flow of combustion environments. Environmental barrier coatings (EBCs) were developed to protect the underlying component from recession. However, mismatch of the coefficient of thermal expansion (CTE) in these coating systems results in stresses that can cause cracking or spallation, which exposes the

substrate to the combustion atmosphere and drastically reduces component lifetime. State-of-the-art coatings for SiC/SiC composites consist of a $Ba_{1-x}Sr_xAl_2Si_2O_8$ (BSAS) topcoat, a mullite or mullite + $SrAl_2Si_2O_8$ (SAS) interlayer, and a silicon bond coat. When heated above 1200°C, the as-deposited BSAS undergoes a crystallographic transformation accompanied by a change in volume and CTE reduction. Internal stresses in these candidate systems were investigated using microfocused highenergy X-rays in a transmission diffraction geometry. Strains were measured *in situ* during cooling from 900°C in samples with a metastable hexacelsian or a stable celsian BSAS topcoat, and converted to stresses using X-ray elastic constants, where available. Changes in the CTE of the BSAS layer influenced the sign and the magnitude of the stresses in the other coating layers. In addition to stress measurements, the CTE of the EBC materials were measured. The coating CTE values and elastic properties were used to model the evolution of coating stresses versus temperature, which were compared to the measured X-ray internal stresses.

D-48

NOVEL PROCESSING OF NICKEL CONTAINING CORDIERITE GLASS-CERAMICS FOR MICROPOROUS GAS SEPARATION MEMBRANES

Michelene E. Miller, Scott T. Misture
Alfred University

The production of microporous membranes using the well-established glass-ceramic process combines the advantages of both amorphous silica and zeolites. In this process, traditional glass forming methods are employed, and the pore structure is controlled by the crystalline phases. The process involves the exposure of a glassceramic to a reducing atmosphere to produce a microporous membrane with evenly dispersed nickel metal colloids. Stoichiometric Ni-doped cordierite glasses having the composition (2-x)MgO xNiO $2Al_2O_3$ $5SiO_2$ are synthesized, where $0 \leq x \leq 1$. The glasses crystallize to form varying amounts of spinel, cordierite and β-quartz phases depending on the heat treatment temperature and time. Subsequent exposure of the glass-ceramic to a reducing atmosphere results in a hydrogen reduction reaction with nickel. Divalent nickel (Ni^{2+}) is reduced to the metallic state (Ni^0), while the Al- O-Si framework remains intact. Selective reduction of transition metal ions from crystalline aluminosilicate phases presents a novel route to produce nanoporous materials.

Spinel and spinelloids are investigated for this method because of the large range of transition metal ions that can be incorporated into the structure. The spinel solid solution series $Mg_{1-x}Ni_xAl_2O4$, where $0 \leq x \leq 1$ is studied for this method using *in-situ* high temperature diffraction with full atmosphere control. Rietveld analyses for phase quantification and cell refinements are presented. The $Ni_xMg_{1-x}Al_2O_4$ spinel framework remains intact following the complete reduction of nickel for compositions where $x \leq 0.50$. For $Ni_xMg_{1-x}Al_2O_4$ spinel containing $x \geq 0.75$, decomposition of the spinel framework is marked by the formation of $NiAl_{32}O_{49}$. The weight percent of nickel formed during the reduction reaction directly relates to the formation of nickel vacancies in $Ni_xMg_{1-x}Al_2O_4$ spinel.

D-44

STUDY OF COMBUSTION SYNTHESES BY TIME-RESOLVED X-RAY DIFFRACTION: COMPARISON OF SYNTHESIS MECHANISMS FOR DIFFERENT COMBUSTION MODES

C. Curfs, J.P. Wright, G.B.M. Vaughan, ESRF, France
H. Boutefnouchet, Badji Mokhtar University, Algeria

Combustion synthesis is a cheap, quick and easy technique to fabricate a large range of materials, including ceramics and composites. It is based on the exothermic properties of the chemical reaction to synthesize a whole sample. Two combustion modes exist depending whether the synthesis occurs in the form of a wave traveling through the sample (Self-propagating High-Temperature Synthesis SHS) or if it occurs simultaneously in the whole sample (Thermal Explosive Synthesis TES).

In this study, both combustion modes have been used to synthesize an equiatomic mixture of Aluminium, Nickel, Titanium and Carbon powders in order to obtain NiAl/TiC composites.

The reactions have been followed in-situ by time-resolved diffraction using synchrotron X-rays within time scales of the order of several hundreds of milliseconds. The combustion by self-propagating mode (SHS) has been performed in air, triggered by a tungsten wire heated by the Joule effect, to ignite the reaction. The combustion by thermal explosion mode (TES) was carried out in an induction furnace, specifically made for in-situ diffraction. In both combustion modes, experiments were performed in transmission in order to probe the crystallographic changes occurring in the bulk materials.

Scanning Electron Micrographs and X-ray diffraction patterns of the samples after synthesis have shown that the same final products were obtained when the mixture was synthesised under both combustion modes: a composite made of small and round TiC particles (~1 micron) embedded into a matrix of larger NiAl grains (5 microns). However, the time-resolved diffraction studies have shown that, even with the same reactants and final products, the two combustion modes follow two different routes.

D-55

NANOSCALE PHOTOCATALYSTS DERIVED FROM LAYERED PHASES FORMATION AND CHARACTERIZATION

Eric J. Nichols, Scott T. Misture
Alfred University

Layered Aurivillius phases have in the past been shown to be photochemically active for hydrogen production, water purification, and similar applications. These phases consist of perovskite-like blocks sandwiched between $[Bi_2O_2]^{2+}$ layers, which can be selectively removed via an acid leaching procedure. This allows for the formation of high surface area photocatalysts with grain sizes in the nanometer range. Cationic substitutions on the perovskite A sites allow for the manipulation of the band gap of these materials and potential red-shifting of the band gap into the visible light region. Systematic manipulation of the local environments surrounding the TiO_6 and NbO_6 octahedra will be discussed in regards to photocatalytic & band gap engineering.

$K_4Nb_6O_{17}$, another type of layered structure, has been previously demonstrated to be a viable UV-sensitive photocatalyst for use in water splitting applications. For this study, $K_4Nb_6O_{17}$ has been synthesized via solid state reaction of the stoichiometric mixture of the precursor materials Nb_2O_5 and K_2CO_3. The proton exchanged form ($K_XH_{(4-x)}Nb_6O_{17}$) of the material was subsequently produced and reacted with TBAOH to form chemically-exfoliated sheets. Following titration with HCl, the scrolled form of $K_XH_{(4-x)}Nb_6O_{17}$ was created and analyzed using *in-situ* X-ray diffraction to show the conversion to nanotubes on heating.

F-67

HIGH-DEFINITION X-RAY FLUORESCENCE: PRINCIPLES AND APPLICATIONS

W.M. Gibson, D. Li, H. Huang, and Z. Chen
X-ray Optical Systems, Inc., 15 Tech Valley Drive, East Greenbush, NY

Monochromatic Micro beam X-ray fluorescence (MμEDXRF) has proven to be remarkably powerful in measurement of trace element concentrations and distributions in a large variety of important medical, environmental and industrial applications. When used with state-of-the-art doubly curved crystal (DCC) X-ray optics, this technique enables high-sensitivity, compact, low-power, safe, reliable, and rugged analyzers for *in-situ*, on-line, measurements in industrial process, clinical, and field settings. This new Optic Enabled MμEDXRF technique is known as High-Definition X-ray Fluorescence (**HD XRF™**). Principles and selected applications of HD XRF are described in this paper.

F-5

MCLLS APPROACH TO EDXRF ANALYSIS ON XOS DEVICES

Robin P. Gardner[1]*, Fusheng Li*, Zewu Chen**, and Matthew Cusack**
* Center for Engineering Applications of Radioisotopes (**CEAR**) Nuclear Engineering Department, PO Box 7909, North Carolina State University Raleigh, NC 27695, [1]e-mail: gardner@ncsu.edu
** X-ray Optical Systems, Inc., Albany, New York

The Monte Carlo – Library Least-Squares (MCLLS) approach has been developed and implemented to model the complete spectral response of energy-dispersive X-ray fluorescence (EDXRF) spectrometers and perform an inverse elemental analysis by an iterative linear Library Least-Squares method for sample composition when an initial guess is provided. The approach contains three advanced technologies developed by CEAR researchers since 1970: a comprehensive and accurate Monte Carlo forward simulation code – **CEARXRF5**, Differential Operators for elemental libraries, and Detector Response Functions. From benchmark experiments with standard reference materials (stainless steels from NIST and aluminum alloys from Alcoa), this approach has been demonstrated to be very accurate. It is also very fast when Monte Carlo pre-calculations can be made for anticipated classes of samples. An integrated visualization system (Graphical User Interface) has been designed for analysts to easily use this approach.

The approach has been implemented on trace elemental analysis instruments from X-ray Optical Systems, Inc. (XOS) developed for medical and industrial applications. XOS uses their doubly curved crystal (DCC) beam optics to provide a mono-energetic source and focus it to a very small spot. This instrument technology is called high definition XRF, or HD XRF. HD XRF also uses a digital pulse processor on the detection side, which is not required for MCLLS. Since the counting rates are generally high in real-time applications and there exist pulse pile up problems in the measurement spectra, the authors have also developed an exact method to correct for any spectral distortion due to pulse pile up. The authors have also developed an accurate detector response function for XOS specific devices. Benchmark experiments on standardized materials using the XOS systems are presented and illustrate that the entire sample spectra from samples can be generated and used. The CEAR and XOS teams compared the MCLLS results to the fundamental parameters (FP) approach as well. Some of those results are discussed here.

F-18

PRECONCENTRATION OF THE ENVIRONMENTAL WATER BY AGAR FOR XRF ANALYSIS

K. Nakano[1, 2)], K. Okubo[1)], K. Tsuji[1)]
1) Department of Applied Chemistry, Graduate School of Engineering, Osaka City University, 3-3-138 Sugimoto, Sumiyoshi-ku, Osaka 558-8585; Japan
2) JST-Innovation Plaza Osaka, 3-1-10 Technostage, Izumi-city, Osaka, 594-1144; Japan

For the analysis of the trace amount of elements in the environmental water sample by X-ray fluorescence (XRF) spectrometry, it is generally necessary to preconcentrate the analytes through the sample pretreatments, such as evaporation, solvent extraction, ion exchange, and precipitation by the chelating agent. Evaporation technique is conventionally used in combination with the filter paper method, but its sample volume on the filter paper is limited lower than 100 μL.

We have developed a convenient and effective XRF analysis procedure for trace amount of K, Ca, V, Mn, Fe, Ni, Cu, Zn, Cd, and Pb in environmental water with a preconcentration using the natural polymer (agar) by following procedure. A 10 mL volume of the aqueous sample and 0.07 g of the dried agar powder were mixed in a glass crucible. The mixed solution was heated for 10 min on hot plate and was poured into a hollow Teflon cup (inner diameter: 36 mmφ) stretched the polyimide film (7.5 μm thick) on the bottom of the cup. After 20 min the solidifying solution was dried at 100°C for 3h, and those in form of thin polymer was obtained. The preconcentrated thin agar films containing trace metals were shown good reproducibility, and SB (signal - noise) ratios of the XRF intensity of the analytes were improved drastically. The linear calibration curves of K, Ca, V, Mn, Fe, Ni, Cu, Zn, Cd, and Pb showed a good linearity within the calibration ranges. The lower limits of detection (LLD) were 1.4 μg/mL for K, 0.26 μg/mL for Ca, 0.088 μg/mL for V, 0.029 μg/mL for Mn, 0.11 μg/mL for Fe, 0.016 μg/mL for Ni, 0.030 μg/mL for Cu, 0.017 μg/mL for Zn, 0.20 μg/mL for Cd, and 0.066 μg/mL for Pb, respectively. The proposed preconcentration method was applied to the several environmental water samples for the determination.

F-31

HEAVY METAL ANALYSIS OF WATER SAMPLES DOWN TO SUB-ppb LEVEL BY USING X-RAY FLUORESCENCE ANALYSIS COMBINED WITH THE CONCENTRATION TECHNIQUES

Shinjiro Hayakawa, Masamichi Iwaki, Yuka Nishimoto, Kazuma Yamane and Takeshi Hirokawaa
Department of Applied Chemistry, Graduate School of Engineering
Hiroshima University, Hiroshima 739-8527, Japan

Detection limit of X-ray fluorescence analysis has been greatly improved by using two types of concentration techniques. Both methods concentrate trace elements in the water samples onto a small piece of filter paper. One method utilizes a special sample holder that is made of a small filter paper (ca. 1mm^2) attached onto a thin poly-ethylene (PE) sheet. A water droplet on the sample holder is concentrated onto the filter section because of the hydrophobic nature of PE. A water droplet of 1 mL can be processed within a day under ambient condition. The other method utilizes a small section of ion exchange cellulose paper (Whatman P-81). A suction filtration attachment made of Delrin has been developed, and cations in a water sample up to 9 mL can be concentrated onto the filter paper. A water sample of 1 mL can be processed in 3 minute.

The performance of these two methods are investigated with an X-ray fluorescence instrument composed of a sealed Mo tube, a graphite monochromator, beam collimator and a Si detector. The beam size on the sample is approximately 3 mm in diameter, and the X-ray tube is operated with 40 kV and 35 mA. The detection limit of the XRF instrument is less than 1 ng (Cu) in absolute amount. The detection limit for water samples is around 1 ppb level with the special holder, and the detection limit less than 1 ppb can be achieved with the ion exchange method. The sensitivity with the ion exchange method is strongly affected with the pH and the co-existing anions, and the quantification should be made with the standard addition method.

The principles of the developed methods, the feasibilities and their application especially for Pb analysis in the tap water and processed water will be presented.

F-35

AUTOMATED PICOLITER SOLUTION DEPOSITION FOR TXRF ANALYSIS OF SEMICONDUCTOR SAMPLES

Chris Sparks[1], Ursula Fittschen[2], and George Havrilla[2]
1. Process Characterization Laboratory, ATDF, Austin, TX 78741
2. Chemistry Division, Los Alamos National Laboratory, Los Alamos, NM 87545

In the semiconductor industry, there are steps in the manufacturing process where trace metal contamination on the silicon wafer needs to be controlled down into the 10^{09} atoms/cm^2 range thus requiring a technique with detection limits at the 10^{08} atoms/cm^2 level. One analytical method for achieving these low limits is vapor phase decomposition (VPD) as a sample preparation procedure to concentrate the contamination from the entire wafer into one discreet sample which is then analyzed as a solution by inductively coupled plasma mass spectrometry (ICP-MS) or as a dried residue by total reflection Xray fluorescence (TXRF). This study follows in the path of earlier successful studies where nanoliter quantities of solution were deposited on silicon wafers to simulate the dried VPD residue[1,2]. With the advancement in inkjet deposition technologies it is possible to deposit picoliter quantities of solution on a wafer. An HP Thermal Inkjet Pico-fluidic System (TIPS) is used to deposit picoliter volumes of solution onto silicon wafers. The array deposits provide a capability of depositing closely spaced (100 micrometers or less), typically 10-20 micrometer droplets in a multi-droplet array. This deposition approach increases reproducibility of the deposition, insures thin film formation of the dried residue and offers the potential of increased accuracy for TXRF measurements of semiconductor samples. By matching the size of the array to the analytical X-ray spot, there is an increase in signal to noise and reduction in error.

The authors thank Hewlett Packard Company for the loan of the TIPS device and their collaboration in developing this technology for analytical applications. TIPS is a prototype laboratory device used internally at HP and with selected research partners.

1. C. M. Sparks et.al. Spectrochimica Acta B 61, 2006, 1091-1097
2. U. E. A. Fittschen, et al. Anal. Chem., in press, 2008.

F-37

PICOLITER DEPOSITION FOR MXRF CALIBRATION AND QUANTIFICATION USING PROTOTYPE THERMAL INKJET TECHNOLOGY

Ursula E.A. Fittschen, George J. Havrilla
Los Alamos National Laboratory, Los Alamos NM, USA

Modified ink jet printers have been used for various purposes, where reliable jetting of small volumes is needed[1]. Just recently this technology has been adapted for analytical chemistry using a modified HP DeskJet printer[2]. In this study an HP picoliter pipette prototype was used called the Thermal Inkjet Pico-Fluidic System (TIPS). Its design allows for easy exchange of solutions for deposition. The device comes with either single volume tips or multiple volume tips. The volume can be software selected in discrete steps between 2 and 220 pL. There are no apparent memory effects from the reservoir tip, yet it can easily be exchanged if this is a concern. In this work different characteristics of the spotted drops and dried residues were examined

including volume, diameter of dried droplets and the mass of delivered metal ions. The aim is to show to the extent this device can be used for calibration and quantification purposes in MXRF.

Aqueous single element and multi-elemental standard solutions were used. The droplets were jetted on polypropylene film. An x,y,z stage was used to adjust the distance from substrate to the TIPS and to generate patterns. Two different tip designs were tested, a single volume tip of 220 pL with 16 nozzles and a multiple volume tip with 35 pL, 10 pL, 5 pL and 1 pL with 4 each nozzles.

The actual volume of the droplets was determined by weighing multiple jetted droplets. The diameter of the dried residues was determined with a light microscope and the delivered elemental amounts were determined using MXRF.

The results show that the delivered volumes vary from the nominal given values, for example 31±0.5 pL were found instead of 35 pL and 199±16 pL instead of 220 pL. The diameter of the dried residues covered a size range from 13±0.6µm to 58±4.9µm using a 10 g/L Ni solution with varying droplet volume. The results from the MXRF analysis show a linear correlation between the count rate and most of the measured volumes with a relative standard deviation between 6 and 12%. The actual mass measured directly by the MXRF is in the 50 pg range for single droplet of 5.3 pL. Preliminary detection limit calculations are 706 fg (10^{-15}g) for a dried spot size of 19 micrometers and a 100 live second acquisition time using an EDAX Eagle III with a polycapillary optic and excitation spot size of nominally 50 micrometers. A dried spot which would be closer to the excitation spot size would be expected to result in a higher signal-to-noise and therefore potentially lower detection limit.

Additional work is being done to explore different solution depositions along with direct deposition onto a variety of substrates to create direct calibration spots on specimens for quantitative analyses.

The authors thank Hewlett Packard Company for the loan of the TIPS device and their collaboration in developing this technology for analytical applications. TIPS is a prototype laboratory device used internally at HP and with selected research partners.

[1] De Gans, B.-J. et al. Adv. Mater. (2004), 16, 203-213.
[2] Fittschen, U. E. A. et al. Anal. Chem., in press, 2008.

F-63

SYNCHROTRON XRF ANALYSES OF ELEMENT DISTRIBUTION IN FOSSILIZED SAUROPOD DINOSAUR BONES

A.R.Pyzalla[1], M. Dumont[1], N.Zoeger[2], C.Streli[2], P.Wobrauschek[2], G.Falkenberg[3], P.M.Sander[4]
[1]Max-Planck-Institut für Eisenforschung GmbH, Max-Planck-Straße 1, D-40237 Düsseldorf, Germany
[2]Atomic Institute of the Austrian Universities, Stadionallee 2, A-1020 Wien, Austria
[3]Hamburger Synchrotronstrahlungslabor HASYLAB am Deutschen Elektronen-Synchrotron, DESY, Notkestrasse 85, D-22603 Hamburg, Germany
[4]University of Bonn, Institute of Palaeontology, Nusseallee, D-53115 Bonn, Germany

Sauropod dinosaurs were typically one magnitude larger than any other living or extinct terrestrial animal. This sheer size of the sauropod leads to scale effects in their biology and physiology that still are only inadequately understood. The only remnants of the sauropods are their fossilized bones. These fossilized bones have sustained burial for some hundred million years and thus may have experienced significant diagenetic changes. These diagenetic changes often are not affecting bone preservation on the histological level, but, lead to significant alterations of the bone microstructure.

We investigated the influence of diagenesis on the microstructure of fossilized sauropod bones using bone cross-sections of Brachiosaurus brancai and Barosaurus africanus long bones (femuri and humeri) that were excavated in the Tendaguru beds in Tanzania. The change in chemical composition due to interactions between bone and sediments was characterized by synchrotron X-ray fluorescence analyses. The high spatial resolution achievable using this microanalysis technique provided us with two-dimensional images of the distribution of U, Sr, Pb, Fe, Cu, Mn, V, Cr, Co in the fluorapatite of the fossilized bone and in the calcite filling the bone cavities (e.g. Lacunae, Havers systems). The results reveal distinct differences in the spatial distribution of theses elements. U and Sr are mainly present in the fluorapatite and show a similar distribution in all samples investigated. Fe, Cr and V distributions show maxima in the same locations near the fluorapatite-calcite interfaces. The inhomogeneities of the element distribution observed in the dinosaur bone thus give some indications about the interdiffusion between the bone and its environment.

DXC Friday a.m.
Microbeam X-ray Analysis II

C-11

USING FOCUSED HARD X-RAYS FOR INVESTIGATIONS RELATED TO NUCLEAR WASTE DISPOSAL

M.A. Denecke
Institut für Nukleare Entsorgung, Forschungszentrum Karlsruhe, Postfach 3640, D-76021 Karlsruhe, Germany

Micro-focused synchrotron radiation techniques to investigate determinant processes in actinide element transport in geological media are becoming an increasingly used tool in nuclear waste disposal research. There are a number of reasons for this but primarily they are driven by the need to characterize radionuclide speciation localized in components of heterogeneous natural systems. The advantage of using X-rays is that *in situ* investigations are possible, due to elimination of a vacuum requirement, no need for invasive sample preparation, and the high penetration capability of X-rays. The ultimate goal of such studies is to advance development of reliable predictive models for radionuclide transport processes at varying spatial and temporal scales, with a reliable estimate of uncertainty. This information is necessary for designing safe nuclear disposal concepts by assessing potential hazards associated with any radioactive contamination release.

The first two examples deal with characterizing what are referred to as natural analogs, in this case clayey sediments rich in uranium [1,2,3], using μ-XRF, μ-XAFS, and μ- XRD. Natural analogs are considered to mimic repository geochemical and geological conditions on a geological time scale and knowledge gained from their study can be used to span the long time scales in a top down approach for predicting repository radiological safety. The last example pertains to actinide transport in column tracer studies [4], which are important for identifying processes determinant in the fate of radionuclides in the environment (e.g., sorption, precipitation, solid solution formation reactions), as well as for disposal site specific characterization.

[1] M.A. Denecke, W. De Nolf, K. Janssens, B. Brendebach, A. Rothkirch, G. Falkenberg, U. Noseck, Spectrochim. Acta B (in print).
[2]. M.A. Denecke, A. Somogyi, K. Janssens, R. Simon, K. Dardenne, U. Noseck, Microscopy Microanal. **13**(3), 165-172 (2007).
[3] M.A. Denecke, K. Janssens, K. Proost, J. Rothe, U. Noseck, Environ. Sci. Technol. **39**(7), 2049-2058 (2005).
[4] M.A. Denecke, B. Brendebach, W. De Nolf, G. Falkenberg, K. Janssens, R. Simon, Spectrochim. Acta B (in review).

D-40

NANODIFFRACTION FROM PERFECT/WEAKLY-DEFORMED SINGLE CRYSTALS

Hanfei Yan,[1] Ozgur Kalenci,[2] Conal Murray,[3] Cevet Noyan[2] and Jorg Maser[4]
[1]National Synchrotron Light Source II, Brookhaven National Laboratory, Upton, NY 11973
[2]Department of Applied Physics and Mathematics, Columbia University, New York, NY 10027
[3]IBM TJ Watson Research Center, 1101 Kitchawan Road, Yorktown Heights, NY 10598
[4]Center for Nanoscale Materials, Argonne National Laboratory, Argonne, IL 60439

During the last decade advances in X-ray sources, optics, and detectors have enabled diffraction strain mapping in crystalline samples with micron/sub-micron resolution. Recent progress in mirrors, zone plates, and refractive lenses has pushed the frontier for hard X-ray focusing into the 25-50 nm range, and true nanometer sized beams (<10 nm) are envisioned in the near future by using novel optics, such as multilayer Laue lenses [1], advancing diffraction strain mapping techniques into the nanodiffraction regime. In addition to possessing a large divergence, a nanobeam typically has a high degree of spatial coherence, which requires a full wave theory, no ray tracing, to be used to study the propagation of the X-rays and the resulting diffraction pattern. We will present a theoretical description of wave propagation from a spatially coherent, divergent beam diffracted from a perfect or weakly deformed single crystal, and discuss the physical meaning of a nanodiffraction pattern. Experimental results of nanodiffraction images will also be presented.

[1] H. C. Kang, J. Maser, G. B. Stephenson, C. Liu, R. Conley, A. T. Macrander, and S. Vogt, Physical Review Letters 96, 127401 (2006)

D-27

BIFOCAL MINIATURE TOROIDAL X-RAY MIRRORS

Sterling Cornaby[1,2], Detlef Smilgies[2], and Donald Bilderback[1,2]
[1]Cornell High Energy Synchrotron Source (CHESS)
[2]Department of Applied and Engineering Physics, Cornell University

We have fabricated a bifocal miniature torodial mirror that horizontally and vertically focuses to two different locations. The mirror produces a 100 μm horizontal by 25 vertical μm focus 50 mm from the tip of the optics, and a 35 μm horizontal by 100 vertical μm focus 150 mm from the tip of the optics. This mirror was made to provide a smaller foot print of beam for GIWAXS, while at the same time focusing the beam in the horizontal direction on the detector. At CHESS we traditionally use glass single-bounce monocapillary optics in a wide range of X-ray experiments to get a fine 5 to 20 μm X-ray spot. This miniature toroidal mirror was made by designing and fabricating an X-ray focusing capillary, in which the sagittal and meridional focusing is decoupled, and only a quadrant of the accepted annulus is used for focusing.

F-20

APPLICATIONS OF POLYCAPILLARY OPTICS TO MICRO AND TWO DIMENSIONAL XRF ANALYSIS

Kouichi Tsuji[1], Akinori Matsuda[1], Kazuhiko Nakano[1,2], Shintaro Komatani[3], Sumito Ohzawa[3], Hiroshi Uchihara[3]
1) Department of Applied Chemistry, Graduate School of Engineering, Osaka City University, Sugimoto 3-3-138, Sumiyoshi-ku Osaka 558-8585 Japan
2) JST Innovation Plaza OSAKA, 3-1-10 Technostage, Izumi-city, Osaka, Japan
3) Horiba Ltd. Minami-ku, Kyoto 601-8510, Japan

The analysis of small regions of a sample has become one of the significant trends in X-ray fluorescence spectrometry (XRF) studies. XRF has been applied to micrometer-scale analysis (micro-XRF) by using various focusing X-ray optics in the laboratory. We have studied applications of micro-XRF with polycapillary X-ray lens [1-3]. The micro X-ray beam less than 0.01 mm, however, were hard to achieve by using the polycapillary X-ray lens, because this is limited by the "halo effect" [4]. In this study, we investigated that a new optics system for micro-XRF instrument combined capillary optics, such as the polycapillary X-ray lens and the X-ray guide tube or the single capillary. The polycapillary X-ray lens was attached to an X-ray tube (Mo tube). A spot size of 0.07 mm was obtained at the output focal distance. This micro X-ray beam was collimated by using the X-ray guide tube or the single capillary, and the beam size was be decreased to about 0.02 mm with reasonable intensity. Another application of the polycapillary optics will also be presented.

References

[1] Emoto T, Sato Y, Konishi Y, Ding X, Tsuji K. *Spectrochim. Acta, Part B*, **59** (2004) 1291-1294.
[2] K. Tsuji, T. Emoto, Y. Matsuoka, Y. Miyatake, T. Nagamura, and X. Ding. *Powder Diffraction,* **20**, (2005) 137-140.
[3] K. Tsuji, K. Nakano, *X-ray Spectrom.*, **36** (2007) 145-149.
[4] N. Gao, I. Y. Ponomarev, *X-ray spectrum.* **32** (2003) 186-194

C-7

LATEST DEVELOPMENTS OF ADVANCED X-RAY OPTICS AND THEIR APPLICATIONS IN X-RAY MICROANALYSIS

N. Gao, Z. Chen, I. Ponomarev, Y. He, and W. Gibson
X-ray Optical Systems, Inc., East Greenbush, New York, USA

Both polycapillary X-ray optics and doubly curved crystal (DC) optics have undergone significant development in the past years, and the technologies have been widely used in X-ray analytical instruments and a variety of research applications. This paper will review the applications of those optics in microanalysis and repor some of the latest optic development work that aims at enhancing optic performance and extending the capability of the technologies.

A polycapillary X-ray optic is a broad-band optic that collects a large solid angle of X-rays from a divergent X-ray source and converts then to either a parallel beam or a focused beam. The optic consists of up to millions of small channels that are precisely curved to a designed profile to efficiently transmit X-rays by multiple external total reflections off the inner surface of each individual capillary channel. A doubly curved crystal (DCC) optic, on the other hand, is a diffractive X-ray optic that collects X-rays from a divergent X-ray source and redirects a narrow band of them by diffraction. By bending a crystal in two dimensions one can achieve point-to-point focusing from a microfocus X-ray source and therefore obtain a focused, monochromatic beam. The two optic technologies have their own characteristics and advantages. But they are also complementary technologies, so one can choose one or another or combined for specific applications. Experimental results of the state-of-the-art performance of the optics will be presented and reviewed in this paper. Application examples will be given to demonstrate the benefits of using each type of the optic or combining the two types of optics in meeting specific application requirements.

F-24

STUDY OF MICROHETEROGENEITY USING μXRF, INAA, AND CHEMOMETRIC METHODS

John L. Molloy, John R. Sieber and Rolf Zeisler
National Institute of Standards and Technology, Gaithersburg, MD

Micro X-ray Fluorescence (μXRF) has been used to nondestructively investigate elemental heterogeneity by constructing two-dimensional maps of elemental concentrations in reference materials. Chemometric methods of analysis, such as principal component analysis (PCA), show promise in describing complex data patterns obtain using μXRF to study various samples. PCA can identify if "nugget" effects exist within a material, a case where an element is enriched in small, isolated areas of the sample. Each element must be treated according to its level of heterogeneity within the sample as determined by comparison of mapping data to a PCA model. The model is built based on the variation of analyte signal at a single location within the sample. Examples of this analysis methodology are shown for several different reference materials to demonstrate how PCA treatment can be used to identify which elements exhibit nugget effects within the ng and μg mass range. Additionally, a method of calculating the minimum recommended mass for solid samples is suggested. PCA methods are iteratively used on X-ray maps from which adjacent data points have been averaged, simulating an increasing X-ray spot size. This is repeated until the mass sampled in a map is indistinguishable from data taken at a single location.

While the above analysis is straightforward and relatively fast, it is difficult to confirm the results obtained using other available techniques. Instrumental Neutron Activation Analysis (INAA) is a potentially useful technique for this purpose. It is able to

measure small samples of material in the range of 1 mg to 100 mg, thus bridging the gap between current, bulk analysis methods and μXRF as well as other solid sampling microanalysis methods such as graphite furnace and laser ablation techniques. INAA gives complimentary information to μXRF because the more penetrating radiation is able to thoroughly probe thicker samples containing many heavy elements. However, analyses investigating microheterogeneity using μXRF typically do not agree with results obtained using INAA because of the former's limited penetration depth within the sample. It is possible to compare the microheterogeneity observed in a sample using μXRF by placing a high Z element behind a sample. The resulting signal obtained from that high Z element shows attenuation at locations which correlate with nuggets present within a sample. This can reveal if nuggets observed in traditional μXRF maps have been revealed completely or if only a small portion of a larger nugget has been exposed to routine analysis. In this way, a picture of the entire sample can be obtained and combined with mapping data taken simultaneously to give a complete analysis of the microheterogeneity present within the sample.

D-5

ANALYSIS OF SHEAR STRESS DISTRIBUTION IN Al (Cu) INTERCONNECTS INDUCED BY ELECTROMIGRATION BASED ON SCHMIDT'S LAW AND STUDIED BY SYNCHROTRON POLYCHROMATIC X-RAY MICRODIFFRACTION

K. Chen, K.N. Tu, UCLA, Los Angeles, CA
N. Tamura, B.C. Valek, Lawrence Berkeley National Laboratory, Berkeley, CA

We report here an in-depth synchrotron radiation based polychromatic X-ray microdiffraction study of plasticity in individual grains of An Al (Cu) interconnect during the early stage of electromigration. It has been well known that distortional strain/stress tensor can be obtained with high accuracy by analyzing the deviation of the Laue peak positions from their ideal positions scattered by an unstrained crystal. However, for the case of electromigration study, the Laue peaks are greatly streaked due to the arrangement of the geometrically necessary dislocations, so that it is very difficult to determine precisely the peak positions. Therefore, the strain/stress cannot be accurately measured by the conventional method. Furthermore, since the X-ray beam has a certain spot size, rather than an ideal spot, there is strain gradient, as well orientation gradient, within the irradiated volume of the sample. As a result, we developed a new method to estimate the shear stress loaded in an individual grain based on Schmidt's law by two steps, including the analysis of the activated slip system in a given grain by simulation method and followed by Schmidt factor calculation. By this means, we obtained the shear stress distribution within the sample induced by electromigration.

F-42

QUANTITATIVE ANALYSIS OF NANO-PARTICLE BY XRF

T. Utaka[1,2], S.Maeo[2], Y.Araki[1], N.Kawada[1,2], K.Muraoka[1], T.Itoh[1], M.Kurakado[2], and K. Taniguchi[1,2]
[1]Institute of X-ray Technologies Co. Ltd.
(Dai-3 Maruzen-Bldg. 3-5-21, Kigawahigashi, Yodogwa-ku, Osaka 532-0012, Japan)
[2]Osaka Electro-Communication University
(18-8 Hatsucho, Neyagawa, Osaka 572-8530, Japan)

Recently, μ-area analysis by the XRF technique has gained popularity. The synchrotron radiation source is responsible for the increase in the popularity of μ-XRF analysis. However, most people find it difficult to gain access to the synchrotron radiation facility. On the other hand, the laboratory μ-XRF spectrometers with the capillary lens optics had been developed [1]. The capillary lens can focused X-rays but it cannot monochromatize. Then the background of measurement spectra is higher than using monochromatic X-rays as excitation source.

In this study, a sub μ-XRF spectrometer for the quantitative analysis of nano-particle has been developed for use in laboratories. To enable the use of this system, it is necessary to satisfy the following two conditions: (1) the excitation source must be optional for efficient excitation of the sample and (2) the X-rays must be focused on the sample. An X-ray tube with multi excitation sources has also been developed [2]. In the tube, there are three metals as target, namely, Cr, W, and Rh, on the anode, and each target can be excited sequentially without changing focal spot position. An Einzel lens is applied to the X-ray tube as the electron gun. The operating power of the tube is set to 50 watts (50 kV, 1 mA), and it is cooled by forced. The diameter of the focal spot is 10 μm. As the optics for focusing of X-rays, Johansson type Doubly Curved Crystal (DCC) which is Si(111) and Si(110) crystal have been made according to the monochromatic condition of Cr-Kα, W-Lβ, Rh-Lα and Rh-Kα respectively. A DCC has Johansson focusing geometry along horizontal direction and Von Hamos geometry along vertical direction. Then the effective area of diffraction is almost all surface of crystal. In addition, the focusing efficiency is quite good as compared with Johann geometry. Therefore, the focus size becomes smaller and intensity gain becomes higher. Silicon drift detector (SDD) and superconducting tunnel junctions (STJs) are selected and developed as X-ray detector.

A system composed of an X-ray tube and DCC optics and detectors is used to perform the small particle analysis. In this report, some estimation results of the sub μ-XRF system and capabilities of the system are discussed.

[1] D. A. Carpenter, X-ray Spectrom., 18 (1989) 253-257.
[2] S. Maeo, T. Utaka, T. Kubota, K. Taniguchi, Adv. X-ray Chem. Anal., Japan, 38 (2007) 165 – 174.

DXC Friday a.m.
Small Angle Scattering

C-20

STRUCTURE AND KINETICS OF SELF-ASSEMBLED NANOCYRSTAL SYSTEMS PROBED BY SMALL ANGLE X-RAY SCATTERING TECHNIQUES

Xiao-Min Lin*, Center for Nanoscale Materials, Argonne National Laboratory
Jin Wang, Advanced Photon Sources, Argonne National Laboratory

Development of colloidal nanopartice synthesis has created a variety of highly monodispersed colloidal nanoparticle systems. These nanocrystals can act as building blocks to form supercrystals or be dispersed into different matrix to form composite materials. Because the typical length scales between nanoparticles in systems are on the order of a few or a few tens of nanometers, small angle X-ray scattering (SAXS) or grazing incidence small angle X-ray scattering (GISAXS) provide ideal techniques to study these self-assembled structures. Coupled with real space optical and electron microscopy and other X-ray techniques such as photon correlation spectroscopy and X-ray standing wave, X-ray scattering techniques can be used to study self assembly kinetics, structural transition and particle diffusion kinetics. In this talk, I will introduce some basic small angle X-ray scattering techniques and illustrate their applications in studying nanocrystal systems by two specific examples: one is self-assembly of nanocrystals during colloidal droplet evaporation another is nanoparticle diffusion in polymer thin film matrix.

D-49

FLEXIBILITY AND HIGH THROUGHPUT: SUPPORTING SAXS USERS AT A JOINT INDUSTRIAL ACADEMIC BEAMLINE

Steven Weigand[1], Ben Stillwell[1], William E. Guise[2], John P.G. Quintana[3], Denis T. Keane[1]
1) Northwestern University — DND-CAT at APS/ANL, Argonne, Illinois 60439
2) E. I. duPont de Nemours & Co., Wilmington, DE
3) Argonne National Laboratory, Argonne, IL

From its inception, DuPont-Northwestern-Dow Collaborative Access Team (DND-CAT) at the Advanced Photon Source has had to adapt to the changing needs of industry as well as a diverse academic user base. This has resulted in a sector with support for a broad range of techniques and sample environments.

Among the techniques supported at DND-CAT are small and wide angle scattering, reflectivity, spectroscopy, tomography, and powder diffraction. The D station on the insertion device line at DND-CAT (5ID-D) is a general purpose hutch that is primarily used for small angle X-ray scattering (SAXS). Approximately 10^{12} photons/sec can be delivered to a .04mm^2 spot using multiple sets of slits with pinhole camera geometry. Scattering can be measured down to $2\theta = 0.014°$ on a 10m long camera with 1.5Å to 0.7Å radiation.

Many of 5ID-D users are polymer scientists, thus standard techniques supported include SAXS and WAXS image collection simultaneous with thermal, extension/compression, shear, or calorimetric data. Often times an individual user will come with arrays of several sample types requiring different environments and/or camera configurations to fully analyze.

The focus of my talk will be on how the joint goals of flexibility and high throughput are balanced at 5ID-D for small and wide angle X-ray scattering, and discussing several case studies where these features have been critical for the success of an experiment.

D-65

A NEW HIGH-THROUGHPUT SAXS SCREENING TOOL

P. Kotnik, H. Schnablegger, Anton Paar GmbH, A-8054 Graz, Austria
G. Langenbucher, Anton Paar USA, Ashland, VA

Small Angle X-ray Scattering (SAXS) is an established technique for nano-structure analysis in various application fields. However, the technique has not been widely used for combinatorial or, more generally, automated measurements till now. Technical limitations have prevented maintaining the desired resolution of the measurement while achieving the high through-put requirement.

A combination of several technological concepts has lead to the design of a SWAXS system for high-resolution and high-throughput measurements.

The technical aspects include requirements to simultaneously characterize materials in the small and wide angle range for documentation of nano-structure and phase behavior, a short exposure time to reduce radiation damage and other stability effects, and a control software which can coordinate the system components, acquire data, and convert the two-dimensional scattering image into the desired result.

All these requirements were met in the SAXSess system. The technical aspects and selected results are discussed.

D-69

ULTRA-SMALL-ANGLE X-RAY SCATTERING (USAXS) IMAGING, CONTRAST MECHANISM AND APPLICATIONS

Fan Zhang, Gabrielle G. Long, Advanced Photon Source, Argonne National Laboratory, Argonne, IL, 60439
Lyle E. Levine, Metallurgy Division, National Institute of Standards and Technology, Gaithersburg, MD 20899
Jan Ilavsky, Pete R. Jemian, Advanced Photon Source, Argonne National Laboratory, Argonne, IL, 60439

Ultra-Small-Angle X-ray Scattering (USAXS) imaging has been proven useful in studies of metallurgical, biological and polymeric materials. This is a size sensitive imaging technique to directly probe the morphology and three-dimensional arrangements of the small-angle scattering objects, where images acquired at different scattering vectors can reveal different microstructural features within the same sample volume. In this study, we offer a general treatment of X-ray imaging contrast for USAXS imaging. It makes use of phase propagation and dynamic diffraction theory to account for the intensity distribution in the detector plane. Simulated results from a model system of micron-sized spherical SiO_2 particles embedded in a polypropylene matrix show good agreement with experimental measurements. Simulations with an alternative geometrical ray-tracing method also account for the features in the USAXS images, and offer a complementary view of the small-angle X-ray scattering contrast mechanism. We will also present a few examples to show the capability of USAXS imaging to identify local scattering length density inhomogeneity and orientational anisotropy.

D-53

ADDRESSING CHALLENGES IN MATERIALS ENGINEERING AND BIOTECHNOLOGY THROUGH COMBINED SAXS AND SANS MEASUREMENTS

A.J. Allen, NIST, Gaithersburg, MD

There have been important advances in the small-angle X-ray and small-angle neutron scattering (SAXS and SANS) methods in recent years. Measurements using these techniques now contribute significantly towards addressing the complex challenges associated with a wide range of materials of technological importance. Many examples of current interest exist that demonstrate how SAXS and SANS can extract statistically representative microstructure information (e.g., void or particle volume fraction size distributions, internal surface areas, pore or particle ensemble morphologies) that complements the information obtained from diffraction methods, X-ray microtomography, or electron microscopy.

By combining SAXS and SANS methods, deeper insights can be gained into the processing–microstructure–property relationships that frequently govern technological performance. For example: although Portland cement concrete is the world's most widely used manufactured material, basic questions persist regarding its internal structure and water content, and their effect on concrete behavior. By combining SAXS and SANS data, it has been possible, for the first time without recourse to drying methods, to measure the composition and solid density of the principal binding reaction product of cement hydration, calcium–silicate–hydrate (C–S–H) gel which is, itself, one of the most complex of all gels.

In a range of industries including biotechnology and medicine, solution-mediated reaction routes are increasingly exploited for the formation of non-agglomerated and mono-dispersed nanoparticle systems. To gain insights into such processes, SAXS and SANS can provide representative and quantitative microstructure characterization, for example, of a nucleating solid phase from solution. In this context, SAXS can accommodate fast time resolution and small sample volume; SANS can exploit the strong neutron contrast isotope effect to establish the distribution of hydrated phases in and around such nanoparticles.

These and other examples will be presented and discussed to demonstrate the impact of combined X-ray an neutron scattering methods.

References:
A.J. Allen, J.J. Thomas and H.M. Jennings; "Composition and Density of Nanoscale Calcium– Silicate–Hydrate in Cement," Nature Mater., **6**, 311-316 (2007).

A.J. Allen; "Characterization of Ceramics by X-ray and Neutron Small-Angle Scattering," J. Am. Ceram. Soc., **88**, 1367-1381 (2005).

D-56

CHARACTERIZATION OF NANOMATERIALS FOR LASER FUSION TARGETS

T. van Buuren[1], T. Willey[1], S. Kucheyev[1], C. Saw[1], T. Baumann[1], J. Ilavsky[2], A. Nikroo[3], A. Hamza[1]
1) Lawrence Livermore National Laboratory, Livermore, CA
2) Advanced Photon Source, Argonne National Laboratory, Argonne, IL, USA
3) General Atomics Co., San Diego, USA

The National Ignition Facility (NIF) at Lawrence Livermore National Laboratory is a one-of-a-kind scientific facility, able to create the temperatures, pressures, and densities conducive to nuclear fusion. All of these experiments have one common requirement: a miniscule (~2mm) target, precisely centered in the drive laser target chamber. To be successful NIF targets must be machined to meet precise requirements, including specifications for elemental composition, geometry, density, and surface

smoothness. The focus of our group has been the design and development of innovative new materials and structures for use in these targets, such as high strength nanocrystalline metal alloys, graded density materials and various nanoporous structures.

We have applied the ultra small angle X-ray scattering (USAXS) technique to understand how processing conditions affect the density and void structure of spherical beryllium (Be) capsules and low density high Z foams. These measurements provide feedback in order to optimize the fabrication of fusion targets. For example, it is desirable to produce homogeneous, isotropic, dense, and mechanically strong Be coatings. However, density measurements of the Be capsules produced show that they are only 96% of full density. TEM measurements confirm that small voids exist; however, the number density of these voids can not explain the decreased density of this material. Scattering allows us to determine the shape and volume of the voids and evaluate new preparation techniques for void mitigation.

Another goal is to quantify the microstructure of highly porous materials and to determine how processing of the porous material relates to the structure and ultimately to the mechanical behavior. We are able to quantify structural changes with a combination of USAXS and high-resolution X-ray imaging**.** Finite element modeling, based on the structures determined experimentally is used to study the effects of mechanical loading on the cell structures and to map out relationships between processing, density, and strength.

This work is supported by the US-DOE, under contract DE-AC52-07NA27344, LLNL. APS is supported by the U.S. DOE, BES, Office of Science under contract No. W-31-109-ENG-38.

D-18

QUANTITATIVE MEASUREMENT OF NANOPARTICLE HALO FORMATION AROUND COLLOIDAL MICROSPHERES IN BINARY MIXTURES USING SMALL-ANGLE X-RAY SCATTERING

Jan Ilavsky, Fan Zhang, Gabrielle G. Long, Pete R. Jemian, X-ray Science Division, Advanced Photon Source, Argonne National Laboratory, Argonne, IL; Valeria T. Milam, School of Materials Science and Engineering, Georgia Institute of Technology, Atlanta,
GA; Jennifer A. Lewis, Frederick Seitz Materials Research Laboratory, Materials Science and Engineering Department, University of Illinois at Urbana-Champaign, Urbana, IL.

A new colloidal stabilization mechanism, known as nanoparticle “haloing”, has been predicted theoretically and inferred experimentally in microsphere-nanoparticle mixtures that possess high charge and size asymmetry. The term “halo” implies the existence of a non-zero separation distance between the highly charged nanoparticles and the negligibly charged microspheres that they surround. For the first time, we quantify this interparticle separation distance, which we found is similar to the Debye screening length of the solution. We also quantify the average number of nanoparticles associated with each microsphere and the spatial arrangement of the nanoparticles in the halo. Our observations based on ultra-small-angle X-ray scattering measurements reveal the magnitude of the haloing effect, and show that the nanoparticles are not strongly adsorbed to the surface of the microspheres.

F-11

GENERATING RELIABLE QUALITATIVE AND QUANTITATIVE XRF RESULTS TO SUPPORT FDA LAB AND FIELD INVESTIGATIONS

Peter T. Palmer, Peter E. Baker, and Kara Cross, San Francisco State University
Richard Jacobs, FDA, San Francisco District Laboratory

Although FDA has yet to employ XRF at its many regional and district laboratories, these devices are currently in use at both FDA.s Center for Food Safety and Applied Nutrition (CFSAN) and the San Francisco District Laboratory. This work has shown that XRF fills an important niche and that field portable XRF analyzers are an exceedingly valuable tool for routine and non-routine elemental analysis investigations. For FDA lab-based applications, XRF will not replace techniques such as ICP-MS for sub-ppm level analyses but offers significant advantages including rapid identification and quantitation of toxic elements *when used correctly*.

Our experience with XRF analyzers has illustrated several shortcomings in the vendor supplied algorithms for detecting and quantifying various elements for certain applications. Obviously, visual inspection of spectrum is *essential* to confirm the presence or absence of a particular element, with positive detection of an element indicated through observation of two or more of fluorescence lines at their tabulated line energies. When these analyzers are used by non-experts who rely solely on the results displayed on the analyzer, the algorithms can generate false positives and negatives. An example of a false positive is illustrated in the analysis of baby food containers in which a high level of lead was indicated. A more detailed evaluation of the spectrum showed that this misidentification was due to the presence of a sum peak originating from high levels of iron in the sample. An example of a false negative is illustrated in the analysis of tableware in which the presence of uranium was not indicated. Evaluation of the spectrum clearly indicated the presence of two uranium
lines that were attributed to the presence of a dye in the glaze. These erroneous results point out the need for more “guarded” use of these analyzers, especially by nonexperts, as well as more powerful “expert system” type algorithms that perform more thorough evaluation of spectra prior to displaying elemental composition information.

With respect to quantitation, surprisingly good accuracies can sometimes be obtained using vendor calibrated instruments and Compton Normalization. Applications requiring more accurate quantitative results require sample homogenization and calibration of instrument response through the use of authentic standards in the matrix of interest. If sufficient sample is available, the standard addition method can be used for more accurate quantitation. This presentation will focus on the more practical aspects of XRF for detecting and quantifying toxic elements, with examples provided from several FDA and related applications.

F-62

XRF BY SIMULTANEOUS USE OF K- AND L-LINES OF AN ELEMENT

M. Mantler[1], B. Beckhoff[2]
[1]Technische Universität Wien, Wiedner Hauptstr. 8-10, 1040 Vienna, Austria
[2]Physikalisch-Technische Bundesanstalt, Abbestr. 2-12, 10587 Berlin, Germany

In various applications K- and L-lines of the same element are simultaneously excited and occasionally also employed methodically, for example to distinguish elemental contents in different sample depths or layers. However, this simultaneous excitation leads also to more complex indirect excitation effects due to the electron cascades most probably initiated by K←L2,3 after K-ionization and is strongly influenced by Coster- Kronig/Auger transitions. This is equally true for M-lines.

This effect can be well isolated by synchrotron measurements, where a distinct jump of L-intensities is observed when the monochromatic primary photon energy exceeds the K-edge, multiplying the intensity by a factor of 5 and more. When conventional techniques with X-ray tubes are applied a fraction of tube photons with lower energies will typically excite only L-lines while those with higher energies are capable of exciting both, K- and L-lines including L-excitation via primary K-ionization; this leads to a steady change of the L-intensities as a function of tube voltage rather than a sharp jump.

This paper shows results from synchrotron experiments in comparison with computational models and translates these findings to applications with continuous excitation. The extensive employment of fundamental parameters including less commonly found values for Coster-Kronig/Auger transitions invites also a discussion of available tables.

F-80

BENEFITS OF IMPROVED RESOLUTION FOR EDXRF

R. Redus, T. Pantazis, J. Pantazis, A. Huber, Amptek, Inc., Bedford, MA
B. Cross, CrossRoads Scientific, El Granada, CA

The accuracy and precision of energy dispersive X-ray fluorescence (EDXRF) clearly get better with improvements in detector energy resolution, count rates, and sensitivity. However, there is always a tradeoff between the highest energy resolution and the highest count rates, there are practical difficulties in achieving the very best energy resolution, and there are many system level issues beyond energy resolution alone. Energy resolution is commonly used to differentiate systems but it is not entirely clear how much one benefits from improved energy resolution, in terms of the accuracy and precision of the analytical results in a realistic system. In the results reported here, EDXRF analysis has been carried out on a set of reference alloys. Several different detectors were used, including Si-PIN, silicon drift diodes (SDD), and CdTe detectors. Their operating parameters were adjusted to give a range of energy resolutions. At 5.9 keV, the resolution ranged from 134 eV FWHM for the SDD, to 300 eV for 25 mm2 Si-PIN at elevated temperature, to 600 eV for the CdTe. The source was a 40 kVp Ag anode X-ray tube used in a backscatter geometry and the spectra were analyzed using the XRF-FP software. The accuracy and precision of the analysis results versus detector resolution and count rate will be presented.

F-41

Lα/Lβ INTENSITY RATIO DEPENDS ON THE SPECTROMETER RESOLUTION

Jun Kawai, Ryosuke Shioi, Nobuharu Sasaki, Kenji Okada, Goro Kinugawa, Shinsuke Kunimura, Takashi Yamamoto
Department of Materials Science and Engineering, Kyoto University

Figure 1 shows XRF spectra of the Pb metal by a WDX spectrometer with the change of the Soller slits. The Lα/Lβ intensity ratio changes as the change of the Soller slits resolution. Figure 2 shows the L series line position as a function of atomic number. It is found that the ordinary Pb Lβ is the mixture of $L\beta_1$+$L\beta_2$ but they are separated for Bi (neighbor element). Thus the Lα/Lβ intensity ratio changes as the atomic number changes. Figure 3 compares the Pb spectra measured (i) by a high resolution double-crystal XRF spectrometer, and (ii) by a typical ED-XRF. The quantum mechanics predicts $L\alpha_2$:$L\alpha_1$:$L\beta_1$ = 1:9:5, which is observable by a high resolution spectrometer, but the EDX spectra does not show this ratio. The Lα/Lβ intensity ratio depends on (1) atomic number, (2) chemical state, (3) concentration, (4) X-ray tube voltage, (5) target, (6) filter, (7) spectrometer resolution, (8) counting rate, (9) powder grain size, (10) surface roughness, and (11) self-absorption.

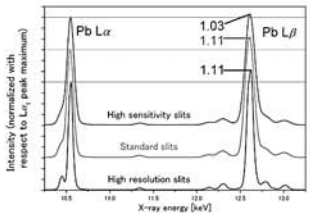

Fig.1 WDX spectrometer resolution dependent intensity ratio.

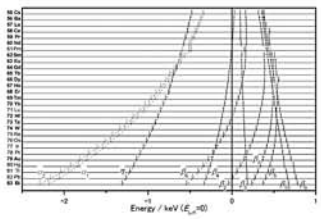

Fig. 2 Atomic number dependent L line series energy

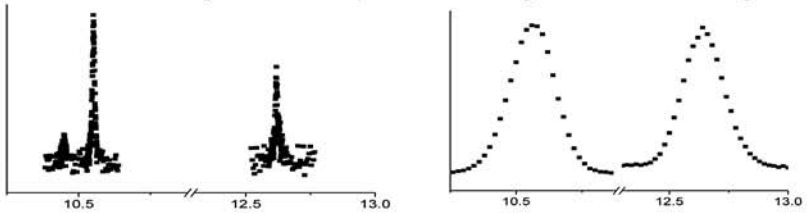

Fig.3 (Left) Double-crystal spectrometer measured Pb Lα and Lβ, where Lα2:Lα1:Lβ1 = 1:9:5, (Right) ED-XRF, where Lα:Lβ=1:1.

F-4

ELEMENTAL ANALYSIS OF POLYOLEFINS BY X-RAY FLUORESCENCE USING CHARACTERIZED POLYMER STANDARDS

D.W. Burns, T.L. Lewis, T. Bradley, Dow Chemical, Freeport, TX
T. Hasan, W. Rigot, Dow Chemical, Midland, MI
F. Franklin, Dow Chemical, Houston, TX

The analysis of catalyst residues and additives in polyolefins is an important measurement for evaluating catalyst efficiency, process control, product development and specifications. X-ray fluorescence (XRF) can be powerful tool for these analyses. The blending of polyolefins with various additives and subsequent elemental characterization has provided standards for quantitative XRF data. Fifteen polypropylene standards were blended with triple extrusion containing the following elements: Na, Mg, Al, Si, P, S, Cl, Ca, Ti and Zn. The standards were characterized and/or validated using inductively coupled plasma (ICP) atomic emission spectrometry, neutron activation analysis (NAA), and XRF fundamental parameters (FP) analysis. For standards with additives containing P and S, gravimetric data were used for the certified values, but verified using XRF-FP. The characterized standards were evaluated for linearity and precision. Because Zn interferes with Na, the standards were blended to allow a

correction factor to be applied during the XRF calibration. An overview of the characterization process and use of these standards for XRF analysis will be discussed.

F-15

IMPROVING TRACE ELEMENT DETECTION IN EDXRF BY REDUCING PILEUP ARTIFACTS

W. T. Elam, Bruce Scruggs, Michael Solazzi, and Joseph Nicolosi
EDAX, Inc., a business unit of AMETEK Materials Analysis Division, Mahwah, NJ 70430

Pileup artifacts appear in energy-dispersive X-ray spectra at high count rates when Xrays arrive at the detector with time separations less than the resolving time of the pulse processor. These artifacts often appear as extra peaks in the spectrum and can mask (or be mistaken for) weak peaks of trace elements. In X-ray fluorescence (XRF) the background is very small compared to charged-particle excitation techniques. This makes it ideal for trace element quantification but also makes it particularly susceptible to pileup artifacts.

Recent improvements in high-speed digital discrimination have improved rejection of near-simultaneous events leading to pile-up at very high count rates. This new capability also improves the predictability of pileup rejection, which is essential for accurate modeling and reliable removal of the inevitable events that get past the pileup inspection. We have successfully reduced pileup artifacts by a combination of hardware changes and software correction. We will report the results for a variety of spectra to demonstrate their effectiveness.

To evaluate the effect of pileup artifacts on trace element determination, we will show spectra from trace amounts of Zr in a Ni alloy with and without the new pileup rejection methods.

F-26

PRECONCENTRATION, QUANTITATION, AND SPECIATION OF SUB-PPM LEVELS OF ARSENIC (III) AND (V) IN WATER VIA HAND-HELD XRF

Peter E. Baker, Rene Johnson, Peter T. Palmer, San Francisco State University
Richard R. Jacobs, San Francisco District Laboratory, FDA

ED-XRF instruments have greatly reduced the time and effort to screen environmental samples for various toxic metals down to ppm levels. However, XRF has not been widely used to detect toxic elements in water, due to the fact that the limits of detection (LOD) for most toxic elements are around 10 ppm or higher, and the regulatory limit for many toxic elements are in the low ppb range. The introduction of the X-ray tube-based field portable ED-XRF has greatly facilitated on-site semi-quantitative analysis, thus eliminating the need to collect and transport all samples back to the laboratory for quantitative analysis (including the ones that don't contain excessive levels). Using a field portable ED-XRF for on-site determination of toxic elements in water samples would be of great utility for many applications, from import screening of bottled water, environmental samples, and food security.

Certainly, colorimetric-based test kits represent an alternative technique for on-site arsenic determination. However, these kits are often prone to false positives. They also generate arsine gas in the detection process, which poses a health hazard to the analyst. Total reflection X-ray fluorescence (TXRF) is able to detect trace levels of toxic elements in water without pre-concentration. However, these instruments are not readily portable, cannot analyze a sample in bulk, and require evaporation of water samples prior to analysis.

This presentation will describe a procedure for on-site detection arsenic (As) in drinking water down to 10 ppb with the use of resins and a field-portable ED-XRF. The procedure involves the speciation and pre-concentration of As (III) and (V), the most toxic forms of arsenic found in drinking water, followed by analysis via a handheld XRF. Speciation takes advantage of the different charge states of As using an anion exchange resin to first isolate and concentrate As (III). The sample is then pre-concentrated and analyzed under a different set of conditions to determine As (V). Analysis of the resin is then performed, resulting in semi-quantitative analysis of both As (III) and (V). We will discuss the effect of resin mass, sample volume, and flow rate and how each affects the sensitivity and detection limit. The presentation will include a case study analysis and profiling of a California Superfund site known to be highly contaminated with As. It will also include a discussion of the practical applications of the method, as well as the simultaneous detection of several other toxic elements such as lead, mercury and selenium using a mixed-bed resin.

S5

STRESS GRADIENTS IN $Ti_xCr_{1-x}N$ COATINGS

A.Ulyanenkov[1], V.V.Uglov[2], T.A.Ulyanenkova[3], A.Lazar[4], H.Guérault[1],
V.M.Anishchik[2], S.V.Zlotski[2], T.Baumbach[3]
[1]Bruker AXS GmbH, Östliche Rheinbrückenstr. 49, 76187 Karlsruhe, Germany
[2]Belarussian State University, 4 Nezavisimosty Av., 220050 Minsk, Belarus
[3]University Karlsruhe, Engesserstr.15, 76131 Karlsruhe, Germany
[4]Institute of Solid State Physics, 17 Brovki Str., 220072 Minsk, Belarus

Thin hard $Ti_xCr_{1-x}N$ coatings fabricated by the cathodic arc vapour deposition are now widely used as corrosion and wear resistance protective coatings. Ternary transition metal nitride coatings provide a wide range of structures that enable control of mechanical and electronic properties. Moreover, ternary compound coatings often exhibit fine-grained and distorted structures resulting in high hardness. The coatings have been produced by condensation from a plasma phase in a vacuum with ion bombardment of sample surfaces while combining Ti and Cr plasma flows of variable density in a residual nitrogen atmosphere.

The residual stress gradient within the coating has been studied using wide angle X-ray diffraction measurements and modified $\sin^2\psi$ method. Multiple Bragg reflections are analyzed to evaluate stress tensor components. The variable incidence angle of X-rays allowed to control a penetration depth and to perform a depth-selective scanning of the crystalline structure of the coatings. Supplementary, specular X-ray reflectivity technique has been utilized to probe a concentration profile of layers.

S6

RESIDUAL STRESS ANALYSIS WITH MULTIPLE HKL RINGS COLLECTED BY AREA DETECTORS

Bob B. He
Bruker AXS Inc., Madison, Wisconsin, USA

Measurement of residual stresses in thin films or textured materials by X-ray diffraction is always a challenge task. The limited diffraction volume in thin films or the directions with low pole density in sharply textured materials results in a weak diffraction signals. The sharp stress gradient, anisotropic grain shape and inhomogeneous phase and microstructure distribution also add difficulties in stress analysis with the conventional X-ray diffraction method. The nonlinear $\varepsilon\psi\phi - \sin^2\psi$ behavior commonly associated with thin films and textured materials produces poor results. This paper introduces a method using diffraction rings from multiple (hkl) crystalline planes collected with area detectors to analyze residual stresses.

The stress measurement with an area detector is based on a direct relationship between the stress tensor and the diffraction cone distortion. The fundamental equation for stress measurement is developed with the matrix transformation defined for the two-dimensional diffraction. The diffraction vectors cover more directions at each measurement and the diffraction vectors do not have to be distributed along a longitudinal direction as the conventional $\sin^2\psi$ method. Since the diffraction frames collected with area detectors typically contains more than one diffraction ring, the stress analysis can be calculated from diffraction rings from multiple (hkl) crystalline planes. First, this will increase the available data points for stress calculation and so to improve the sampling statistics. Secondly, due to the different orientation distributions from different (hkl) planes, the weak diffraction signal from one plane at certain diffraction vector direction is most likely to be compensated by a strong diffraction signal from another plane at a nearby diffraction vector direction. By using multiple diffraction rings, it is also possible to reduce the number of sample tilt angles without reduce the angular coverage. An example is given by stress measurement on a 1 μm textured Cu film on a proprietary substrate using 1.4Å synchrotron beam and CCD detector. The stress calculations with single (331) or (420) peak and combined analysis with both peaks are compared.

S9

ASSESSING THE QUALITY OF X-RAY OPTIC SURFACES OF Si CRYSTALS CUT BY DIAMOND-WIRE AND ROTATING BLADE SAWING TECHNIQUES

Michael Wieczorek[a], Xianrong Huang[a], Jozef Maj[a], Ray Conley[a], Jun Qian[a], Albert Macrander[a], Cynthia Christensen[b], John Hodsden[b], and Ruben Khachatryan[a]
[a] X-ray Science Division, Argonne National Laboratory, Argonne, IL 60439
[b] Diamondwire Technology, Colorado Springs, CO 80916

The next generation of X-ray diffraction optics will benefit from crystal surfaces with very high quality (extremely flat and strain-free), but knowledge on how to achieve such surfaces and how surface imperfections affect the diffraction properties is sparse in the literature. As a first step to initialize a systematic study on this topic, we evaluate in this paper the surface quality of two Si (111) wafers cut by a diamond-wire saw and a rotating blade saw, respectively. We concentrate on revealing lattice strains induced by the two cutting methods and on strain evolution during three rounds of chemical etching (without polishing). The measurements may provide basic guidelines for fabrication of high-quality monochromators, and they provide some important clues as to how surface roughness affects rocking curve widths and other diffraction properties.

S17

INVESTIGATIONS OF LATTICE SPACING ON IN718 VIA NEUTRON LARMOR DIFFRACTION

J. Repper[1], M. Hofmann[1], C. Krempaszky[2], T. Keller[3], W. Petry[1], E. Werner[4]
[1]Forschungsneutronenquelle Heinz Maier-Leibnitz (FRM II), TU München, D-85747 Garching, Germany
[2]Christian-Doppler-Laboratory of Material Mechanics of High Performance Alloys, TU München, D-85748 Garching, Germany
[3]Max-Planck-Institute for Solid State Research, D-70569 Stuttgart, Germany
[4]Institute for materials science and mechanics of materials, TU München, D-85747 Garching, Germany

The residual stress analysis via conventional diffraction methods is based on the comparison of the lattice spacing d of a stressed component with the lattice spacing d_0 from a macroscopically stress free reference sample. In neutron Larmor diffraction the lattice spacing d is encoded in the spin precision of a polarized monochromatic neutron beam scattered at the sample. In contrast to conventional neutron diffraction methods Larmor diffraction is independent of the divergence of the initial beam, the spread of the wavelength and the scattering angle 2θ [1]. Based on this, the Larmor technique is relatively insensitive to alignment errors of the sample, which cause large shifts in measured 2θ–values in conventional diffractometer techniques. Hence, the method enables the measurement of reference values d_0 with a very high accuracy (in the order of 10^{-5} Å) hitherto not possible using classical diffractometers [2]. In addition Larmor diffraction provides the unique possibility to resolve the fluctuation of the lattice spacing resulting from a variation of the stress state within the sample over the whole gauge volume [3]. Therefore, this method allows to determine particularly in the case of complex, high performance superalloys micro stress levels and their fluctuations over the sample geometry and to study their influence on macroscopic stress analysis.

In this contribution first results are presented, which were achieved with the new neutron Larmor diffraction method carried out at the spin echo triple axis spectrometer TRISP on the industrial employed Ni based multiphase superalloy Inconel 718.

[1] M.T. Rekveldt, T. Keller, W.H.Kraan, *Europhys. Lett*, 54, 342-346 (2001).
[2] C. Pfleiderer, P. Böni, T. Keller, U.K. Rößler, A. Rosch, *Science*, 316, 1871-1874 (2007).
[3] M.T. Rekveldt, W.H.Kraan, *J. Neutron Research*, 8, 53-70 (1999).

S23

INFLUENCE OF ALLOY COMPOSITION ON RESIDUAL STRESS IN HEAT TREATED ALUMINIUM ALLOYS

Jeremy S. Robinson
Department of Materials Science and Technology, Materials Surface Science Institute
University of Limerick, Ireland
Edward C. Oliver
ENGIN-X Instrument Scientist, ISIS Facility
Rutherford Appleton Laboratory, United Kingdom

The residual stress distribution has been measured in samples prepared from seven different aluminium alloys after heat treatment. Through thickness residual stresses were measured using neutron diffraction on the ENGIN_X instrument at ISIS, UK. For comparison purposes, surface residual stress measurements were also made using X-ray diffraction. The seven alloys were chosen to encompass a wide range of strengths. The low to medium strengths alloys were 6082 and 2618A, medium to high strength 2014, 7175 and 7010 while the very high strength alloy was two variants of 7449. Samples were prepared from forgings or rolled plate. To assess the as quenched strength, tensile properties were determined from samples tested immediately after quenching. The as quenched tensile properties are related to the residual stress magnitudes with the objective of being able to predict the maximum residual stress as a function of as quenched alloy strength.

S43

OPTIMIZING STEEL WELDING PROCEDURES BY USING NEUTRON AND X-RAY DIFFRACTION

Vladimir Luzin – Bragg Institute, ANSTO, Australia (vladimir.luzin@ansto.gov.au)
Benjamin Gross – WTIA, Australia (b.gross@wtia.com.au)
Philip Bendeich – IME, ANSTO, Australia (Philip.Bendeich@ansto.gov.au)
Thomas Gnäupel-Herold – NCNR, NIST, USA (tg-h@nist.gov)

The carbon manganese steel is widely used as structural material (e.g. alumina production industry) and has a tendency to suffer from caustic stress corrosion cracking (CSCC) adjacent to welds. The susceptibility to CSCC is a function of the residual stress produced as a result of welding and the heat affected zone (HAZ) microstructure. Traditionally the industry uses post weld heat treatment (PWHT) to reduce the residual stresses arising from welding but this is a costly exercise for some of the large plant involved.

A research project has been established to develop a welding procedure that provides the lowest possible as-welded residual stress to potentially avoid having to carry out PWHT. The welding variables being addressed are weld-metal yield strength, weld heat input and pre-heat/inter-pass temperature. An experimental matrix has been established to explore these three variables by means of X-ray and neutron diffraction on the specifically designed test samples in order to incorporate a level of shrinkage constraint similar to that experienced when welding full sized structures. With the help of the diffraction techniques the role of the welding parameters on resultant stress was established, e.g. pre-heat and heat input can have as much effect on residual stress as weld metal (electrode) strength.

The project is being carried out by the Welding Technology Institute of Australia (WTIA), ANSTO, the University of Wollongong and the Australian Alumina Industry through the Industry Cooperative Innovation Program.

S50

NEW DEVELOPMENTS AT MATERIALS SCIENCE DIFFRACTOMETER STRESS-SPEC AT FRM II

J. Kornmeier[1], M. Hofmann[2], U. Garbe[3], C. Randau[4], J. Repper[2], A. Ostermann[2], W. Tekouo[5], G.A. Seidl[2], R.C. Wimpory[1], R. Schneider[1], H.G. Brokmeier[3,4]

[1]Hahn-Meitner-Institut (HMI), Glienicker Straße 100, D-14109 Berlin Wannsee, Germany
[2]Forschungsneutronenquelle Heinz Maier-Leibniz (FRM II), TU München, D-85747 Garching, Germany
[3]GKSS-Forschungszentrum Geesthacht GmbH, Max-Planck-Straße 1, D-21502 Geesthacht, Germany
[4]TU Clausthal, Adolph-Roemer-Straße 2A, D-38678 Clausthal-Zellerfeld, Germany
[5]Institut für Werkzeugmaschinen und Betriebswissenschaften (*iwb*), TU München, D-85748 Garching, Germany

The Materials Science Diffractometer STRESS-SPEC at the German neutron source FRM II is designed to meet the demands of non-destructive residual stress and texture determination by diffraction methods.

With slit based optics used at STRESS-SPEC accurate residual stress determinations can be carried out even with small gauge volumes down to 1x1x1 mm³ [1]. For measurements deep inside big components (e.g. ship crankshafts, engines…), however, the spatial resolution is often limited by the instrumental set up. The slits, for example, have to be positioned relatively far away from the measurement position resulting in a blurred definition of the gauge volume due to divergence of the neutron beam. In addition the maximum of neutron flux is found at the slit exit.

The replacement of the primary slit system with a parabolic focussing guide enables both a better definition of the gauge volume and a maximum of neutron flux at the measurement position as the focal point of the guide is several centimetres away from the end of the tube [2]. First experimental results for a prototype parabolic guide measured at STRESS-SPEC are in good agreement with simulations and will be presented in this contribution as well as the simulations of an optimised parabolic guide for STRESS-SPEC.

Furthermore, we will show the enhancement of the capabilities by STRESS-SPEC in sample positioning using a robotic system. This system will be added to the conventional goniometers (Eulerian cradles) on STRESS-SPEC and is optimised for sample weights up to 50kg, speed, translation range and positioning accuracy for 3-D residual stress determination and texture analysis respectively.

References

[1] M. Hofmann, R. Schneider, G.A. Seidl, J. Rebelo-Kornmeier, R.C. Wimpory, U. Garbe and H.-G. Brokmeier, Physica B, 385–386 (2006) 1035–1037
[2] T. Hils, P. Boeni, J. Stahn, Physica B, 350 (2004) 166-168

S54

TEXTURE EVOLUTION DURING SEVERE PLASTIC DEFORMATION AND RESIDUAL STRESSES AT LOW AND HIGH TEMPERATURE OF A COPPER MATRIX REINFORCED BY NIOBIUM NANOTUBES

J.B. Dubois*, V. Vidal, L. Thilly, P.O. Renault
PHYMAT, University of Poitiers, 86962 Futuroscope, France
S. Van Petegem, U. Stuhr, H. Van Swygenhoven
Paul Scherrer Institute, CH-5232 Villigen-PSI, Switzerland.
F. Lecouturier
Laboratoire National des Champs Magnétiques Pulsés, UPS-INSA-CNRS, 31400 Toulouse, France

The development of reinforced conductors, with high electrical conductivity and high strength, is essential to provide non-destructive high pulsed magnetic fields over 80 Teslas: a compromise is obtained with Cu-based continuous nanofilamentary wires (2 GPa ultimate tensile strength and 0.6 =ohm.cm electrical resistivity at 77K). The fabrication process of these nanocomposite wires is based on severe plastic deformation (SPD) applied by accumulative drawing and bundling, leading to a multi-scale copper matrix containing up to $N=85^4$ ($52.2\ 10^6$) continuous and parallel niobium nanotubes.

Electron microscopy as well as laboratory X-ray diffraction experiments have been carried out on samples taken throughout the fabrication process to study the formation of microstructure, i.e. grain size and grain type distribution in Cu and Nb phases, as well as texture evolution. Nb nanotubes exhibit a rather homogeneous microstructure with strong <110> axial texture and grains in the 100nm range. However, a complex microstructure was pointed out in the Cu matrix with different size and type of grains in the different Cu channels. The large Cu channels exhibit a microstructure similar to ultra fine grain Cu produced by other SPD techniques, with a majority of grains in the 200-400 nm range and grains remaining in the µm range, while the finest Cu channels (inter-tube and inner-tube Cu) are composed of only one or two grains between Cu/Nb interfaces. The formation of texture in Cu is analyzed with respect to the SPD steps and the occurrence of heat treatments and reveals two different states: the "deformation" texture (major <111> fiber texture) and the "recrystallization" texture (major <200> fiber texture). The texture of the final product is therefore the result of the interplay between these texture states and the grain size distribution.

In addition, neutron diffraction experiments have been performed on full wires at several temperatures (from 77K to 1073K) to measure the residual stresses in each phase of the nanocomposites. The observed complex residual stress state is related to the Cu-Nb codeformation mechanisms and to the microstructure evolution imposed by the severe plastic deformation process.

S60

MICROMECHANICAL MODELLING OF ELASTIC THIN FILMS AND COMPARISON WITH IN SITU TENSILE TEST WITH XRD MEASUREMENT

G. Geandier[a,b], O. Castelnau[a] , L. Thilly[b] , E. Le Bourhis[b], P.-O. Renault[b], Ph. Goudeau[b]
[(a)] *LPMTM – CNRS, Paris XIII, 99 Avenue Jean-Baptiste CLEMENT F-93430 VILLETANEUSE*
[(b)] *PhyMat – UMR 6630- SP2MI, BP 30179 - 86 962 FUTUROSCOPE CHASSENEUIL cedex*

Our aim is to determine the elastic modulus softening for poly-crystalline materials with nanometric grain size. The use of metallic multilayers materials deposited as thin films permit to control the deposition process, the grain size and the sample microstructure. We used X-rays diffraction experiments coupled with in situ tensile test to determine the Bragg peaks displacements for several {hkl} planes, crystalline orientations and for the different films constituents. A micro-mechanical model was developed for results interpretations. There are two levels of heterogeneities in the material. Macroscopic applied stress is distributed between the layers as a function of their effective modulus, the stiffer layers supporting higher stresses. Then, inside the layers, stress is not homogeneously distributed because of the elastic anisotropy at the grain scale, and as for the layers, stress is located at the "stiffer grains". The micro-mechanical model presented here is developed to take into account the structure of each layer on the displacement of the peaks obtained by X-ray diffraction [1]. More precisely, we calculate the inter-granular interactions inside each layer with an homogenization method in mean field. For bulk poly-crystals, the self consistent model (SC) is generally adopted and gives results in good agreement with experimental determinations and with other calculations methods in full field [2]. This model gives the exact effective behavior for some random microstructures. In a first time, we adopt the same formalism for poly-crystals in thin layer as considered here, with encouraging results from Faurie and al [3]. Then we propose to use some results from literature in order to estimate the effective behavior of a multilayer material. When the layers show a homogeneous elastic behavior, if the interfaces are perfect (plane and parallel), the exact results can be expressed easily. This model with two scale changes, from grain to layer and from layers to multilayers, permit to take into account of the microstructure (texture, crystallography, ...) of each layer in the estimation of the stress and elastic strain distributions at the layer and grain scales.

The results is compared to experimental data collected during a campaign at the ALS (Berkeley National Lab.) with in situ tensile test in the elastic domain. Comparison between experimental data and model is very good, showing the model aptitude to reflect the stresses localisation in the different films constituents. The global agreement associated with the proposed model (allowing very fast numerical resolution) opens the opportunities to use this model in an inverse way to estimate the elastic modulus softening for materials with low dimensions.

[1] Castelnau O., G. Geandier, P.O. Renault, P. Goudeau, E. Le Bourhis, Thin Film Solids, 516, 320 (2007).
[2] Lebensohn R.A., O. Castelnau, R. Brenner, P. Gilormini, Int. J. Solids Struct. **42**, p.5441-5459, 2005.
[3] D. Faurie, O. Castelnau, P.O. Renault, G. Patriarche, R. Brenner, E. Le Bourhis, P. Goudeau, Surface and Coatings Technology, (2006), 4300-4304.

S67

STUDIES of STRONTIUM TITANATE THIN FILMS by X-RAY METHOD

H. Ji[1]*, X.Y. Zhou[2], Y.R.Li[1], Y. Wang[2]
[1] State Key Laboratory of Electronic Thin Films and Integrated Devices, University of Electronic Science and Technology of China, Chengdu 610054, P.R.China
[2] Department of Applied Physics and Material Research Centre, The Hong Kong Polytechnic University, Hong Kong, P.R.China

$SrTiO_3$ (STO) films have attracted much attention in recent years, because of their potential applications for various microelectronic devices**.** In this paper, a STO thin film grown on Si substrate with Sr buffer layer, was fabricated by laser molecular beam epitaxy (L-MBE), we studied the structural characterization of this thin film, including the crystalline quality, preferred orientation, texture, lattice strain, etc. Several techniques such as 2θ/ω scan, ω scans, φ scans and pole figure were used to measure the microstructure and crystallization behavior in the STO thin film. X-ray diffraction (XRD) revealed high crystallinity with FWHM of 0.3º in the STO (002) rocking curve. XRD study of the in-plane orientation clarified a cube-on-cube epitaxy in which STO [100] was rotated by 45º with respect to Si [100]. The significant utility of the X-ray reflectivity (XRR) in contrast to XRD as an important structural probe was first used to study the STO/Sr/Si heterostructure. The quantitative information on density, interface roughness and surface roughness was extracted. In addition, in order to gain a better understanding of the origins of the STO film stress, a homoepitaxial STO thin film was fabricated by plused laser deposition (PLD), a high resolution X-ray diffraction (HRXRD) measurement was performed by a ω/2θ scan mode using multiple-order-reflection monochromator. HRXRD study focuses on the microscopic lattice distortion of the homoepitaxial STO thin film, The a and c lattice constants for the STO thin film without any buffer layer were found to be 0.3861nm and 0.3915 nm. Therefore, the strain was also maintained in this film due to the presence of intrinsic stress. The aim of this paper is to investigate the effects of stress in biaxial textured or epitaxial STO thin film. The strategies for lattice constant measurement of epitaxial films were carefully described here.

Keyword: strontium titanate ($SrTiO_3$), Sr buffer layer, epitaxial film, X-ray reflectivity (XRR), and high resolution X-ray diffraction (HRXRD) *Corresponding author: Hong. Ji
E-mail address: jihong@uestc.edu,cn

S68

SALSA: RESIDUAL STRESS DETERMINATION USING NEUTRONS

D. J. Hughes, T. Pirling, J-C Collet-Fenetrier and S. Rowe.
Institut Laue Langevin, 6 rue Jules Horowitz, 38042 Grenoble, FRANCE

In the two years since it became available to users SALSA has matured into a worldclass neutron diffractometer for the evaluation of residual stress. Making use of the high neutron flux available at the Institut Laue Langevin (ILL) reactor in Grenoble, allows rapid measurement of local macrostrain at significant neutron beam penetrations. The availability of flexible collimator or slit optics allows gauge volumes to be defined which are appropriate for both bulk and near-surface studies.

In this paper we present the current technical status of the SALSA instrument and discuss futures aims and perspectives for strain measurement using neutrons at the ILL. We present the performance of the instrument against current standards and present examples of application to stress problems. In particular we discuss how concurrent developments using high-energy X-rays at the neighbouring European Synchrotron Radiation Facility (ESRF) are leading users to utilise both neutrons and X-rays to fully understand residual stress in industrial components.

S72

DETAILED PROFILING OF RESIDUAL STRESS IN A COLD EXPANDED HOLE

D. J. Hughes
Institut Laue Langevin, 6 rue Jules Horowitz, 38042 Grenoble, FRANCE

The technique of split-sleeve cold hole expansion is now adopted in many industries world-wide. The process effectively draws an oversized mandrel through a hole in order to plastically deform the bore of a hole. It was developed to impart a beneficial compressive residual stress state around the bore and thus to improve fatigue performance and lifetime. Various techniques are available to investigate the postexpanded stress state although diffraction techniques using highly penetrating radiation are particularly applicable (X-rays, neutrons).

A number of studies have shown the well accepted profile of near-bore compressive hoop stress balanced by a low tensile component away from the hole. Most of these studies have used relatively coarse measurement steps and have simply considered the 1D profile of stress at midlength of the hole (mid-thickness).

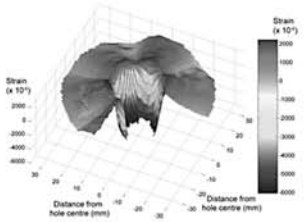

This paper presents a series of measurements of 3D residual strain and stress around split-sleeve cold expanded holes. Measurements were made using high energy synchrotron X-rays at the European Synchrotron Radiation facility (ESRF). Two expanded hole specimens were studied of bore diameters 6mm and 12mm both with nominal 4% expansion. The variation of residual stress is shown both in-plane and through-thickness. The influence of the raised 'pip' in the bore resulting from the split-sleeve is presented.

S73

PLASTIC STRAIN MAPPING BY PEAK BROADENING ANALYSIS IN TITANIUM

F. Hofmann, S. Y. Zhang, T. S. Jun, A. M. Korsunsky
Department of Engineering Science, University of Oxford, Parks Road, Oxford, OX1 3PJ
Corresponding author: alexander.korsunsky@eng.ox.ac.uk

X ray diffraction measurements in bulk engineering component traditionally concentrate on the evaluation of lattice spacing variation by application of Bragg law. By comparison with strain free specimen reference, elastic strains are computed and hence local stress is inferred. This methodology primarily concentrates on the diffraction peak centre position, neglecting the wealth of information about the local material state contained in the shape of the measure diffraction peaks.

It has been shown that diffraction peak width is closely linked to local dislocation density, which in turn gives hints to the plastic strain a particular material volume has experienced. Thus by correlating peak width and corresponding plastic strain in a given material, it should be possible to determine plastic strain distribution and magnitude in a specimen for which a map of diffraction patterns has been collected.

To test this hypothesis a plate specimen with two circular notches was loaded in tension to achieve a known plastic strain distribution localised around the notches. Mapping of the central region with X-ray in energy dispersive mode was carried out on beamline 16.3 at SRS in Daresbury, England. The measured residual elastic strains show good agreement with a finite element model of the geometry. Single peak widths for the entire gauge area were computed, combined in a number of ways and then plotted in the gauge area. These maps show good agreement in terms of the extent of significantly broadened peaks with the numerically predicted zone of most prominent plastic deformation, confirming that peak broadening does indeed give important clues to the spatial distribution of plastic deformation.

S76

CYCLIC VARIATION OF RESIDUAL STRESS INDUCED BY MACHINING

J.C. Outeiro [1,2*], J.C. Pina[2], J. Kornmeier[3], M. Hofmann[4]
[1]Faculty of Engineering, Portuguese Catholic University, Rio de Mouro, Lisbon, Portugal
[2]CEMDRX, Department of Physics, FCTUC, University of Coimbra, Coimbra, Portugal
[3]Hahn-Meitner-Institut (HMI), Glienicker Straße 100, Berlin Wannsee, Germany
[4]Forschungsneutronenquelle Heinz Maier-Leibniz (FRM II), TU München, Garching, Germany

In metal cutting, due to the cyclic nature of the chip formation process the forces, temperatures and stresses are not constant, but they vary over each cycle, so as the residual stresses over the machined surface. This cyclic variation of the residual stress has never been measured and, therefore, imposes new experimental challenges. The objective of this work is to search for eventual periodic variation of the residual stresses along the cutting path.

Residual stresses were analyzed in machined specimens along the cutting path using neutron diffraction, at the STRESS-SPEC instrument at FRM II facilities. They were measured in the machined surface layer (1 mm depth) in hoop, axial and radial directions. Two work materials were analyzed: a plain carbon steel, AISI 1045, and an austenitic stainless steel, AISI 316L.

The results show a cyclic variation of the residual stresses, which seems to be evident for the case of the AISI 316L steel. This cyclic stress variation can be easily detected when considering the frequency of the chip formation process, which depends on the work material and cutting conditions. This cyclic residual stress variation could also be caused by the tool vibration during the cutting process. In order to separate these two effects (cyclic nature of chip formation and tool vibration), the frequencies of the chip formation and tool vibration must be identified and isolated.

Keywords: Metal cutting; Machining; Residual stresses; Neutron diffraction.

* Corresponding author. Tel.: +351 214269790; Fax: +351 214269800. E-mail address: jcouteiro@fe.lisboa.ucp.pt (JC Outeiro)

S92

RESIDUAL STRESSES ANALYSIS IN THICK HVOF INCONEL 718 COATINGS FOR FUTURE REPAIR APPLICATIONS

Christophe Lyphout[1, a], Adrian Manescu[2, b], Thilo Pirling[3, c]
[1]University West, Departement of Technology, Gustava Melins Gata 6, S-46132
Trollhättan, Sweden
[2]Università Politecnica delle Marche, Dipartimento SASC, Via Brecce Bianche 1,
60131 Ancona, Italy
[3]Institut Laue-Langevin, 6, rue Jules Horowitz, F-38042 Grenoble, France
[a]christophe.lyphout@hv.se, [b]a.manescu@alisf1.univpm.it, [c]pirling@ill.eu

Residual stresses in HVOF sprayed Inconel 718 thick coatings on Inconel 718 substrates were determined by neutron diffraction, using the strain imager for engineering applications, SALSA, at the ILL in Grenoble.

Cylindrically shaped specimens having different coating and substrate thicknesses were analyzed. For each specimen through thickness scans were performed, with finer steps close to the interface between coating and substrate, measuring in two orthogonal directions and assuming radial symmetry. A special analysis method was developed in order to eliminate peak shifts due to aberration effects near the surface and interface. The specific difficulty was that diffraction peaks of coating and substrate overlap.

The obtained residual stresses and their dependence on the coating thicknesses are essential information for the future development of thick coatings that will enable expansion of the application area of thermal sprayed products into new repair and aeronautical maintenance applications.

S93

MICRO AREA X-RAY RESIDUAL STRESS MEASUREMENT USING MULTILAYER MIRROR OPTICS

Katsunari Sasaki[1 2], Yukio Hirose[1] Ryoichi Monzen[1] Akira Hosokawa[1] and Toshihiko Sasaki[1]
[1] Division of Innovative Technology and Science, Graduate School of Natural Science & Technology, Kanazawa University, Kanazawa 920-1192, Japan
[2] Rigaku Corporation, Akishima 196-8666, Japan

The multilayer optics, depositing alternating layers of light-element and heavy-element-containing materials onto an appropriately curved substrate, is well known as a strong X-ray optics which produces very high characteristic X-ray flux mainly in the protein crystallography. Recently the use of this optics for material property study such as residual stress and pole figure are started but still there are few applications.

Measuring residual stress requires uniformity of grain direction distribution and narrowing the X-ray irradiation area results both X-ray flux and accuracy problem. To fix these problem both X-ray flux and sample oscillation using high accuracy goniometer is required.

We will introduce the qualitative analysis and residual stress applications using high accuracy goniometer with CrKα multilayer optics and discuss about the problems such as irradiated area and X-ray intensity using Imaging Plate cylindrical two-dimensional detector system.

S95

GENETIC ALGORITHMS USED FOR OPTIMISATION OF ELASTIC PROPERTIES

J. Tarasiuk[1], K. Wierzbanowski[1] and A. Lodini[2]
[1] WFiIS, AGH University of Science and Technology, al. Mickiewicza 30, 30-059 Kraków,Poland
[2] LACM, Université de Reims Champagne Ardenne, 9, bd. de la Paix, 51100 Reims, France

The method of genetic algorithms (GA) is a modern computer technique based on some ideas taken from the evolution theory [1,2]. GA is especially useful for a study of problems being not completely determined. They are, e.g., problems having a few but not very different solutions or problems without a strict (exact) solution. The last situation may occur if it is enough to find a good solution but not necessarily the best one. In GA approach it is not necessary to know a priori a general scheme of problem solution; however, it is important to have a procedure estimating the quality of a solution. This procedure is used to eliminate some solutions and to accept another. In last years the GA method was applied with success in different areas of science, e.g., in: sociology, construction engineering, artificial intelligence and many others. The present authors have already used it in the field of texture analysis [3].

The present work reports the application of GA for optimisation of elastic constants of a polycrystalline material. This is obtained by finding a respective crystallographic texture which leads to a given property. The same approach can be used to optimise other material properties (e.g., diffraction elastic constants, plastic flow parameters, electric and magnetic characteristics, etc.).

1. J.H. Holland, Adaptation in natural and artificial systems, The University of Michigan Press, USA (1975)
2. D.E. Goldberg, Genetic Algorithms in Search, Optimisation and Machine Learning, The University of Alabama, USA (1989)
3. J. Tarasiuk and K. Wierzbanowski, Application of genetic algorithms in texture analysis and optimization, Materials and Manufacturing Processes (M. Dekker Editions), **18**, 463- 473 (2003)

S97

CORRECTIONS IN X-RAY GRAZING INCIDENCE TECHNIQUE USED FOR STRESS MEASUREMENT

S. Wroński[1], K. Wierzbanowski[1], A. Baczmański[1] and A. Lodini[2]
[1] WFiIS, AGH University of Science and Technology, al. Mickiewicza 30, 30-059 Kraków,Poland,
[2] LACM, Université de Reims Champagne Ardenne, 9, bd. de la Paix, 51100 Reims, France

X-ray grazing incidence technique can be used to study samples with important stress gradients. Using this method, it is possible to perform a non-destructive analysis of the heterogeneous stress field for different (and well defined) volumes below the surface of the sample. Moreover, the stress can be measured at very small depths, of the order of a few μm. Asymmetric geometry is used in this technique. The penetration depth of radiation is almost constant in a wide 2θ range for a given incidence angle α. It can be easily changed by an appropriate selection of α angle (or also by using a different type of radiation). This enables the investigation of stress variation with depth below the sample surface.

There are, however, some factors which have to be corrected in this technique. The most important is the refraction of X-ray wave (with refraction coefficient smaller than one): it changes the wave length and direction of the beam inside a sample. These two effects cause some shift of a pick position and they have to be taken into account in data treatment. For small incidence angles ($\alpha 1 \leq 0°$) the corrections are significant and can modify the measured stress even of 70 MPa. The refraction correction decreases, however, with increasing the incidence angle. Other corrections (absorption, atomic factor, Lorentz-polarization factor) are less important for the final results.

The studied corrections were tested on three reference ferrite powder samples with different FWHM and on a sample of AISI316L stainless steel.

S98

RELAXATION OF RESIDUAL STRESSES IN THIN FILMS INVESTIGATED USING SYNCHROTRON RADIATUION

Tatsuya MATSUE[1], Takao HANABUSA[2], Kazuya KUSAKA[2], Osami SAKATA[3]
[1]Niihama National College of Technology
[2]Faculty of Engineering, Tokushima University
[3]Japan Synchrotron Radiation Research Institute/SPring-8

The structure and residual stresses of TiN thin films deposited by arc ion plating (AIP) on a steel substrate were investigated using a synchrotron radiation system that emits ultra-intense X-rays. In a previous study, the crystal structures of TiN films

deposited by AIP were found to be strongly influenced by the bias voltage. However, when film thickness were approximately 200-nm, TiN films deposited by bias voltage of –100V and 0V had a preferred orientation of {110}. In this present study, the two-tilt method was used to evaluate the residual stresses in TiN films by measuring lattice strains in two directions determined by the crystal orientation. The TiN films deposited by bias voltage of –100V had the compressive residual stress of -8.0GPa. These residual stresses decreased on increasing the annealing temperature, and it became residual stresses of –3.5GPa in the annealing temperature at 800°. On the other hand, TiN films deposited by bias voltage of 0V TiN films had the compressive residual stress of –6.5GPa. These residual stresses decreased on increasing the annealing temperature, and it became residual stresses of -5.2GPa in the annealing temperature at 800°. Residual stresses of bias voltage of –100V/0V double layers film in the {110} oriented layer had the compressive residual stress of –8.5GPa. These residual stresses decreased on increasing the annealing temperature, and it became residual stresses of -5.8GPa in the annealing temperature at 800°.

S101

RESIDUAL STRESS EVALUATION OF RAILWAY RAILS

Shunichi TAKAHASHI[1], Toshihiko SASAKI[2], Fusayoshi AOKI[3] and Yukio HIROSE[2]
[1]Graduate student of Department of Natural Science and Technology, Kanazawa University, Kakuma-machi, Kanazawa, Isikawa 920-1192 Japan
[2]Department of Materials Science and Engineering, Kanazawa University, Kakuma-machi, Kanazawa, Isikawa 920-1192 Japan
[3]East Japan Railway Company, Nisshin-cho, Saitama-shi, Saitama

Rolling contact fatigue is one of the fatigue damages of the railway rails. A lot of researches have been made about the rolling contact fatigue based on the fracture mechanics. Rolling contact fatigue occurs by repeated contact stress at the railhead by running wheels. Contact stress generally forms compressive stress. Tensile stress helps to progress the fatigue failure and it decreases rapidly under the contact surface, so a lot of cracks usually stop at the depth of several millimeter. However, it finally breaks when the crack propagation in the rail changes the direction because the crack receives the cyclic bending stress of the rail and the influence of the tensile residual stress. In order to obtain the crack growth rate, the measurement of the residual stress distribution is needed. But, in Japan, the example of measuring the residual stress distribution of railway rails is a few.

In this research, it has aimed at the assistance of the inspection period and the cycle decision of the rail maintenance. For these purposes, the residual stress distribution in the railway rails was measured by using the X ray diffraction method and the strain gauge method, etc.

S105

APPROACHES TO THE PROBLEM OF THE INVERSE LAPLACE TRANSFORM IN RESIDUAL STRESS ANALYSIS BY COMPARISON OF EXPERIMENTAL RESULTS OF $\sigma(\tau)$ AND $\sigma(z)$

Thorsten Manns[1], Ingwer A. Denks[2], Ch. Genzel[2] and Berthold Scholtes[1]
[1] Institute of Materials Engineering, University of Kassel, Mönchebergstr. 3, 34125 Kassel, Germany, e-Mail: manns@uni-kassel.de
[2] Hahn-Meitner-Institute Berlin, Department of Structural Research, Glienicker Str. 100, 14109 Berlin, Germany, e-Mail: denks@hmi.de

Surface treated 100Cr6 steel samples were analysed concerning their residual stresses. The aim of the project is the development of measurement and evaluation strategies for determining stress gradients by energy and angle dispersive X-ray diffraction. The main problem of conventional Laplace methods is that they only determine real stress values $\sigma(z)$ if no gradient of the residual stresses within the X-ray penetration depth τ occurs. Otherwise the measured Laplace profiles $\sigma(\tau)$ have to be recalculated by inverse Laplace transform (ILT) to obtain the residual stresses in real space being those from practical relevance for engineering applications.

Strain distributions of deep ground and shot peened 100Cr6 samples were measured by energy dispersive Laplace methods up to X-ray energies of approximately 80 keV. The used setup allows the analysis of several lattice planes in one measurement and realizes penetration depths of more than 100 μm. The surface near regions were additionally analysed by monochromatic synchrotron radiation, equivalent to Cukα and Mokα wavelengths, at the {110} and the {431/510} lattice plane respectively to affirm the energy dispersive values since this method may lead to scattering results here. The in depth stress distributions were calculated via Universal plot method and afterwards transformed by ILT applying different exponentially damped fit functions. Comparisons of these distributions with stress profiles obtained by successive layer removal, using minimal increments of 1 μm, show a good agreement for the ground as well as for the shot peened samples, provided the fit function in Laplace space is able to represent the $\sigma(\tau)$ data satisfactorily.

We gratefully acknowledge the financial support of this project by the German Research Foundation (DFG).

S108

MULTIAXIAL STRESS ANALYSIS WITH AREA DETECTOR TYPE DIFFRACTION METHOD

Toshihiko SASAKI[1], Shunichi TAKAHASHI[1], Katsunari SASAKI[1, 2] Yuichi KOBAYASHI[3] and Yukio HIROSE[1]

[1] Division of Innovative Technology and Science, Graduate School of Natural Science & Technology, Kanazawa University, Kanazawa, 920-1192 Japan

[2] Rigaku Corporation, Akishima 196-8666, Japan

[3] Hitachi, Ltd., Automotive Systems Kawasaki, 210-0011 Japan

One of the authors has proposed an area detector type X-ray multiaxial stress measurement method in 1995. It is found that the method is useful when diffraction data is precise enough, but it sometimes presents erroneous result due to scattering of diffraction data. The stress, σy, has an inclination to be influenced to scattering of data comparing with other stress components.

In order to improve the precision of stresses, a new measurement method, which is called the second method, was proposed in this paper. The effect on the accuracy of the stress calculation was investigated by a simulation study and an experiment comparing with the first method. As a result, it was found that the second method is useful even when the strain data involve error at the fifth decimal place.

The number of diffraction rings which is needed to the stress calculation in the second method is four, while that in the first method is two. Considering the use of the method at outdoors such as railway rails in service, the third method was also developed in this paper. The method uses the incident angle of 45 deg along both x and y axes as well as the normal incident angle. The number of diffraction ring can be decreased to be three. The incident angle of 45 deg is the optimum for the strain sensitivity. The third method was also compared with other two method and was found to be useful for the practical use.

S110

RESIDUAL STRESS EVALUATION OF THE SURFACE OF RAILWAY RAILS WITH SYNCHROTRON RADIATION

Toshihiko SASAKI[1], Yohei MIYAZAWA[2], Shunichi TAKAHASHI[3] , Ryohei MATSUYAMA[2] and Yukio HIROSE[1]

[1]Graduate School of Natural Science and Technology, Kanazawa University, Japan

[2]Graduate Student of Education, Kanazawa University, Japan

[3]Graduate Student of Natural Science and Technology, Kanazawa University, Japan

In the field of railway technology, there are problems of rolling contact fatigue (RCF). It is necessary to elucidate the mechanism of the initiation and the growth of the RCF cracks in order to prevent accidents caused by them. Hirakawa recently reported the residual stress influencing the growth of the RCF crack based on the fracture mechanics.

In this study, the authors clarify the residual stress state in the surface of the rail head by the X-ray stress measurement for the purpose of contributing to the RCF problem mentioned above. Considering the practical use, the authors adopted an Image Plate and the cosα method. The method is expected to obtain higher precision in comparison with the standard method because of the use of information of whole X-ray diffraction ring.

However, the penetration depth of X-ray of each diffraction beam at the diffraction ring differs from each other due to the position (the central angle of the diffraction ring α). The stresses obtained from the cosα method are averaged over the penetration depth of X-ray. The depth decreases when the incident angle of X-ray is larger. The range of the change of the depth of X-ray along the diffraction ring depends on the wave length of X-ray. Synchrotron radiation is useful to achieve optimum condition for this study. The authors conducted the stress evaluation in rails in the depth direction using Synchrotron radiation at The Photon Factory (PF) of KEK. As a result, the stress distributions of the surface layer in rails were obtained in both depth and width directions.

S111

NON-DESTRUCTIVE HARDNESS TESTING OF STEEL MATERIALS USING X-RAY DIFFRACTION

Shigeki TAKAGO[1], Katsuyuki FUNAKI[1] Haruyuki YASUI[1], Kaname FUJII[1], Toshihiko SASAKI[2] and Yukio HIROSE[2]

[1] Division of Metal and Machinery, Industrial Research Institute of Ishikawa, Kanazawa, 920-8203 Japan

[2] Division of Innovative Technology and Science, Graduate School of Natural Science & Technology, Kanazawa University, Kanazawa, 920-1192 Japan

Inspection of machine product is very important for the quality control in metal working industry. Hardness test is useful for estimation of material strength. Many producers hope that, establish of the evaluation technique by non -destructive test. In the case of X-ray diffraction technique, the full width at half maximum (FWHM) correlate with the hardness of steels. However, the parameter of the FWHM is dependent the any factor of material.

In this study, fundamental X-ray measurement conditions for high carbon chromium bearing steels were considered. Moreover, influence of the mechanical working effected layer on X-ray parameters was discussed.

It was found that X-ray diffraction technique enable us estimate a hardness of steel materials with equal properties, surface treatment and chemical compositions. The parameter the FWHM change with wavelength of characteristic X-ray target.

S112

EFFECT OF THE BOTTOM-HOLE FILLET RADIUS ON THE RESIDUAL STRESS ANALYSIS BY THE HOLE DRILLING METHOD

M. Scafidi[a], E. Valentini[b], B. Zuccarello[a]
scafidi@dima.unipa.it, emilio.valentini@sintechnology.com, zuccarello@dima.unipa.it
[a]Dipartimento di Meccanica, Università degli Studi di Palermo – ITALIA
[b]SINT Technology S.r.l. – Calenzano, Fi – ITALIA

In the residual stresses analysis by the hole drilling method, the evaluation of the residual stresses is performed by using influence functions determined numerically by considering a perfect cylindrical hole. Unfortunately, due to various experimental influence parameters the hole shape is different from the considered one in the numerical simulations. One of the most important deviations is constituted by the the bottom-hole fillet radius.

In this work the effects of the bottom-hole fillet radius in the relaxed strains measured on surface in presence of a uniform residual stress distribution, have been analysed by systematic numerical simulations carried out by a BEM code. Consequently, a closed form expression that allows the user the evaluation of strain deviation $sd_{\%}$ has been found by a least square procedure:

$$sd_{\%} = 100\frac{\varepsilon_\rho - \varepsilon_0}{\varepsilon_0} = \sum_{i=1}^{3}\sum_{j=0}^{5}\left[\left(c_{0ij} + c_{1ij}d + c_{2ij}d^2\right)\left(\rho\right)^i h^j \log h\right], \qquad (1)$$

In eq.(1) ε_ρ and ε_0 are respectively the strains relaxed in presence and in absence of the fillet radius, $h=z/R$ is the ratio between the hole-depth z and the rosette average radius R, $\rho=r/D_0$ is the ratio between the bottom-hole fillet radius r and the hole diameter D_0, $d=D_0/D$ the ratio between the hole diameter D_0 and the average diameter D of the rosette. The c_{sij} coefficients (s=0÷2; i=1÷3; j=0÷5) are the parameters provided by the least square method; these coefficients depend on the rosette geometry and on the Poisson ratio.

The micrographic analysis of the section of holes drilled by several procedures, has shown that the bottom-hole fillet radius can reach $\rho = 0.30$ for EDM, whereas the use of an inverted cone tungsten carbide end-mill can lead a bottom-hole fillet radius with $\rho=0.10$. Especially for small hole-depth, as confirmed also by several experimental tests, these ρ values lead to $sd_{\%}$ greater than 20% and, consequently, wrong nonuniformity test results and wrong residual stresses are evaluated by the ASTM E837 Standard Test procedure.

In the present work a simple procedure to evaluate the effect of the bottom-hole fillet radius as well as the relative stress uncertainty due to the fillet radius estimation, is proposed.

S115

WELDING RESIDUAL STRESS OF AUSTENITIC STAINLESS STEEL AND ITS MEASUREMENT BY HOLE-DRILLING METHOD

Li Rongfeng
Senior Engineer (Professor) in R&D Center of WISCO, Wuhan, China, 28 YieJing Rd, Qingshan District, Wuhan 430080, P.R.China, Email: wglrf@wisco.com.cn, Fax: 86-27-86487717

Urgent requirement of residual stresses information in stainless steel structures which is the basis of technical policy or treatment is driven by a large amount of stress corrosion cracking failure. It has been found that simple and available hole-drilling method is suitable for residual stress measurement of stainless steel if the match between rosette of strain gage with hole diameter and preparation of surface to be measured are selected appropriately. It is supposed that the match between strain gage type BE120-3BA with Φ2.3×3.0mm drilled hole could be used for residual stresses measurement of austenitic stainless steels. Wet-grinding in water adopted to stainless steels surface preparation for strain gage bonding is appropriate. Moreover, its feasibility measuring higher residual stress in stainless steel is better than in carbon steels.

It has been shown through experiments that welding residual stress in stainless steel is higher than yield stress of base metal. The peak of longitudinal residual stress in SMAW butt-welded joint consisted of SUS 321 base metal and E347-16 weld accesses to value 540MPa.

Key words: welding residual stress, hole-drilling method, austenitic stainless steel

S123

X-RAY IN-SITU RESIDUAL STRESS MEASUREMENT OF FIBER REINFORCED PLASTIC COMPOSITE

Yoshitaka Watanabe[1], Masayuki Nishida[2]
[1]Advanced Course of Mechanical System engineering, Kobe, Hyogo, Japan
[2]Department of Mechanical engineering, Kobe City College of Technology, Kobe, Hyogo, Japan

Recently, the importance of fiber reinforced composite materials (FRP) are increasing with the explosion of applications due to development of new materials in industrial fields. The stress estimation of FRP is expected and needs to establish the reliable measurement method under there background. In this study, the residual stresses in FRP samples were examined by X-ray stress measurement technique. These FRP samples were manufactured from high density polyethylene (HDPE) matrix and tungsten reinforced fibers. There are few report of residual stress investigation in macromolecule materials by using the X-ray stress measurement with typical reflection method. The two kinds of reason exist in these situations, one is the diffraction peaks from macromolecule appear on 2θ low angle region. The accuracy of strain measurement is reduced in such case. Another is the problem of ψ angle width in $\sin^2\psi$ method. If diffraction peak appear in 2θ low angle, ψ offset angle is restricted seriously. To solve these problems, transmission method was employed for residual stress measurement of HDPE composite as the new trial in this study. In actual experiment, the small tensile testing machine was mounted on the X-ray diffractometer. After following preparation of tensile system, alternation of peak positions were measured under the several applied stresses. From these results, 2θ-$\sin^2\psi$ diagram expressed the good linearity on regression line of the measurement data, and gradients of regression line correspond to applied stress levels. Furthermore, the in-situ thermal stress measurement was performed at several temperatures. the small furnace mounted on the diffractometer was used, and temperature was change from R.T. to 60°C. Thermal residual stresses in HDPE matrix changed to compressive state with temperature rising. The other hand, in the case of decreasing temperature stage, thermal residual stresses shifted to tensile residual stress states.

S128

HRXRD STRAIN ANALYSIS ON DRIE ETCHED SILICON

A. Neels[1], A. Dommann[2], A. Schifferle[3], O. Papes[3], E. Mazza[3]
[1] IMT-UniNE / CSEM, Jaquet-Droz 1, 2002 Neuchâtel, Switzerland
[2] CSEM, Jaquet-Droz 1, 2002 Neuchâtel, Switzerland
[3] ETHZ, IMES, Tannenstrasse 3, 8092 Zürich, Switzerland

Microsystem engineering involves design, manufacturing, and packaging of microelectromechanical systems (MEMS). Applications of microsystems in aerospace, automotive, watch industry or sensors create a strong demand in quality control and failure analysis [1].

Monocrystalline material, and especially single crystal silicon (SCSi), is preferentially used due to its potential resistance against aging. However, quantified results on this assertion are rarely published. The reasons are manifold, and among others are related to surface roughness and defects, as for instance introduced by the ion bombardment in dry reactive ion etching (DRIE). In single crystals, such perturbances of the perfect lattice are recognized to favor failure. This makes it necessary to treat structural and material influences as inseparable parts of the problem.

Mechanical tests may be used to assess the resistance of SCSi structures to loading [2]. However, for the understanding of failure it is essential to obtain further going information about the stressed material on the atomic scale. This makes it necessary to conduct detailed investigations, which may include the comparison of experimental methods as well as numerical simulations. Experimental measurements of local deformations and an analysis of defects may be approached by High Resolution Diffraction Methods (HRXRD) and the simulation of deformations by the well-established Finite Element Method (FEM).

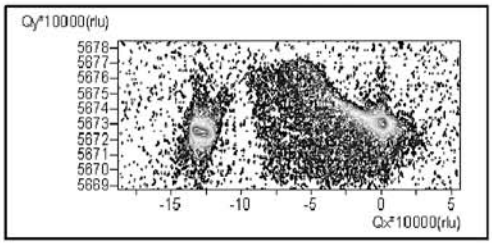

A methodic approach in the above sense will be demonstrated on the example of a loaded DRIE etched SCSi device. The strain field in the critical regions of the structure was investigated by HRXRD and compared with the results of a FEM analysis. The X-ray rocking curve method and Reciprocal Space Mapping (RSM, Fig. 1) were used to determine the strain in the crystal as well as the defect concentration.

References:

[1] A. Dommann, G. Kotrotsios and A. Neels, MEMS Reliability and Testing, *MST News*, (2007).
[2] E. Mazza and J. Dual, Mechanical behavior of a µm-sized single crystal silicon structure with sharp notches. *J. Mechanics and Physics of Solids* 47 (1999) 1795-1821.

S129

STRAINET: STRESS AND TEXTURE ANALYSIS STANDARDISING INTERFACES

R.C. Wimpory[1], R. Schneider[1], A.G. Youtsos[2], O. Kirstein[3], M. Hofmann[4], C. Ohms[5], H.G. Brokmeier[6, 7]
[1]Hahn-Meitner-Institut (HMI), Glienicker Straße 100, D-14109 Berlin Wannsee, Germany
[2]NCSR Demokritos, Institute of Nuclear Technology . Radiation Protection, 153 10 - Agia Paraskevi, Athens P.O. 60228, Greece
[3]Bragg Institute, ANSTO, Australia
[4]Forschungsneutronenquelle Heinz Maier-Leibniz (FRM II), TU München, D-85747 Garching, Germany
[5]European Commission, Joint Research Centre, Institute for Energy, Westerduinweg 3, 1755 LE Petten, The Netherlands
[6]T. Univ. Clausthal, Adolph-Roemer-Straße 2A, D-38678 Clausthal-Zellerfeld, Germany
[7]GKSS-Forschungszentrum Geesthacht GmbH, Max-Planck-Straße 1, 21502 Geesthacht, Germany

In October 2007, the `STRAINET going global: STRESS and TEXTURE ANALSIS STANDARDISING INTERFACES' took place. Over 50 experts, not only from the world of neutron scattering but also engineering and computing, expressed the overriding opinion: that of Harmonization. This is the aim of STRAINET, the harmonization of stress and texture measurement at neutron sources to the international level.

The first step is the standardization of data file formats. This is a crucial foundation stone as it has an influence of other important aspects such as, data storage and archiving, instrument control software and data analysis software etc. The format must have, on one hand, a standard structure whilst, on the other hand, have the flexibility to incorporate new and different concepts and parameters as instrument development continues. It was agreed that the NEXUS data file format [1] offers these possibilities. The foundation of such a data file format is effectively also a database that characterizes each instrument which in turn offers a myriad of possibilities. By developing an intelligent interface one can use the NEXUS format/database to: simulate instruments more easily, implement automatic alignment/calibration/collision-avoiding algorithms, suppress artifacts, visually recreate and playback an experiment, allow easy implementation of a measurement standard protocol and create a springboard into the inevitable world of artificial intelligence. Presented here is the status so far before the next STRAINET meeting, due in December 2008 in Sydney Australia.

Reference

[1] Könnecke, M, .The state of the NeXus data format., Physica B **385.386** (2006) 1343.1345

S135

NEUTRON DIFFRACTION STRESS ANALYSIS OF NEAR SURFACE STRESS GRADIENTS OF SURFACE TREATED STEEL SAMPLES

Jens Gibmeier[1*], Joana Kornmeier[2] and Michael Hofmann[3]
[1]Hahn-Meitner-Institute, c/o Bessy II, Albert-Einstein-Strasse 15, D-12489 Berlin
[2]Hahn-Meitner-Institute, Glienicker Strasse 100, D-14109 Berlin
[3]FRM-II, TU München, Lichtenbergstr. 1, D-85747 Garching
* corresponding author

In order to tap the full optimisation potential for technical parts the residual stress distribution in the near surface region is of major interest for engineering work. The knowledge of the stress distribution is a necessary prerequisite for exactly tailored near surface layers of highly loaded technical components.

The most important and most frequently applied tools for residual stress analysis are the diffraction methods. Surface layers affected by mechanical surface treatments like e.g. shot peening typically ranges up to depths of some tenth of a millimetre. For non-destructive stress analysis of surface treated steel samples the application of laboratory X-rays or high energy synchrotron radiation in reflection mode covers the region from some micrometers up to a depth of about 150-200 μm. To access the depth region > 200 μm an incremental layer removal technique in combination with reapplication of X-ray stress analysis for the new surfaces can be applied. However, this procedure is destructive, laborious and furthermore it has to be checked, whether corrections have to be applied. Using neutron radiation generally penetration depths up to several millimetres can be achieved. The most widely used set-up for neutron diffraction stress analysis is the 90° scattering technique. Stresses at the surface can be analysed using a strain scanning technique and a gauge volume, which is possibly partially immersed in the sample. Here corrections have to be applied using stress free reference samples. In addition the local resolution is generally poor.

In the present project an alternative approach has been pursued to overcome these shortcomings. The stress depth distribution of shot peened steel samples (SAE 4140) was determined by means of neutron diffraction according to the well known $\sin^2\psi$-method, being a standard technique in X-ray stress analysis. The experiments were carried out at the STRESS-SPEC-instrument at the research reactor FRM II, Munich. For data evaluation the universal-plot method was applied, which directly assign stress measures for each sample orientation to the mean penetration depth τ. By that the stress depth gradient can be determined up to large distances from the sample surface non-destructively. The results determined that way are in good agreement with stress depth distributions determined in a round robin test for identical samples by means of X-ray diffraction in combination with incremental layer removal.

S137

EVIDENCE AND ANALYSIS OF THERMAL STATIC STRAIN AGING IN THE DEFORMED SURFACE ZONE OF FINISH-MACHINED HARDENED STEEL

Jürgen Gegner, Lorenz Schlier and Wolfgang Nierlich
SKF GmbH, Dept. of Material Physics, Ernst-Sachs-Strasse 5, 97424 Schweinfurt, Germany

After heat treating of formed workpieces, finish machining of the hardened steel, e.g. by turning, milling, cutting, grinding and honing, polishing or lapping, represents the last manufacturing step in the standard production cycle of machine elements. By this final shaping, functional surfaces of adjusted roughness and optimized profile for good wear resistance and fatigue strength are fabricated. Crack-inhibiting compressive residual stresses built up by efficiently cooled mechanical material removal in the plastically deformed edge zone further improve the lifetime, e.g., of Hertzian loaded parts like rolling bearings, camshafts or cogwheels. The practically most important finishing operation of grinding is applied to ensure best surface quality and dimensional accuracy of complexly shaped components. Metal removal involves high plastic deformation work. Glide and intersection processes raise the dislocation density and produce lower energy substructures, such as multipoles. In hardened steel, where grinding generates residual stresses of up to about .500 MPa on the surface, the X-ray diffraction (XRD) line broadening thus simultaneously decreases slightly in the plastically strained edge zone. These considerations suggest that subsequent heating is suitable to stabilize the mechanically formed energetically favorable dislocation configuration by the development of interstitial carbon Cottrell atmospheres, which should enhance the fatigue resistance.

The temperature and time dependence of post-machining thermal treatment (PMTT) is investigated on the example of ground and honed through hardened SAE 52100 rolling bearing steel. The associated microstructural stabilization is expressed in a large XRD line width decrease on the surface. The measured kinetics of isothermal PMTT can be modeled by ratecontrolling carbide dissolution that represents the source of carbon for dislocational segregation. The corresponding reduction in line width follows an Arrhenius-type time-temperature relationship. The superimposed decrease due to thermal recovery occurs much slower so that both effects are separable. Static strain aging is also verified by the formation of a slight white etching surface layer. Temper carbides in the outermost material are cut or deformed by the grinding process. The tendency of these damaged nanosized particles to dissolve and release carbon is high since the surface energy increases with curvature. Reheating below the martensite tempering or bainite transformation temperature prevents hardness loss by post-tempering. The narrow edge zone of about 10 µm thickness, which is mechanically affected by grinding and subsequently thermally refined by reheating, represents the highest loaded region of the steel, for instance, in case of dense raceway indentations or under boundary lubrication and mixed friction. Such surface-critical service conditions occur, e.g., in the majority of bearing, cogwheel or camshaft applications. Accelerated rig tests of finished balls under poor lubrication provide an increase of the lifetime by a factor of about two due to PMTT. This result indicates practical potential of the simple low-cost reheating treatment for certain operation conditions in the surface failure mode of rolling contact fatigue.

S139

IN-SITU INVESTIGATION OF GRAIN ROTATIONS DURING TENSILE STRAINING OF STEEL WIRES

M. Moscicki, H. Pinto, A. Borbély and A.R. Pyzalla
Max-Planck Institut für Eisenforschung GmbH, Max-Planck Strasse 1, 40237 Düsseldorf, Germany

Understanding deformation behavior of polycrystals and its modeling are matter of great technological interest. So far, several models have been proposed to describe the plastic deformation behavior of polycrystals, however, all of them rely on assumptions and simplifications regarding the grain-to-grain interactions. In order to study these interactions the orientation change of single grains during plastic deformation was followed by X-ray diffraction. As specimens steel wires (grade numbers 1.4310 (X10CrNi18-8) and 1.4841 (X15CrNiSi25-20)) of 300 µm in diameter and of about 60 µm average grain size were used. The indexing method of grain orientation is similar to the method introduced with the three dimensional X-ray diffraction (3DXRD) procedure [1], but the new software accounts for the position of the grains in the sample, too. Experimentally determined grain rotations are compared with results of crystal plasticity simulations based on the simple Taylor and more complex self-consistent models. The new indexing software has the possibility to be further developed for the evaluation of the components of the residual strain tensor, which might be a better measure of grain interactions. A preliminary study on how to evaluate these strain components shows in case of a model system that extremely good experimental conditions are necessary for their accurate determination.

1. E. M. Lauridsen, S. Schmidt, R. M. Suter and H. F. Poulsen, *J.Appl. Cryst* (2001) 34, 744-750.

S143

RESIDUAL STRESS FIELDS OF AERONAUTICAL MATERIALS CAUSED BY MECHANICAL SURFACE TREATMENTS

Yu-kui GAO, Xue-ren WU
Beijing Institute of Aeronautical Materials, P.O.Box 81-5, Beijing 100095, China

The residual stress fields of aeronautical materials (300M, AerMet 100 steels, 7050-T7451, 7475-T7351 aluminum alloys, TC4, TC21 titanium alloys) induced by mechanical surface treatments (hot peening, cold expansion, laser shock peening, ultrasonic impact peening) were investigated by XRD method. The six parameters of these surface strengthening residual stress fields were proposed, these parameters are surface residual stress (σ_{srs}), maximum compressive residual stress (σ_{mcrs}), maximum tensile

residual stress (σ_{mtrs}), the distance from surface to where maximum compressive residual stress is (Z_{mcrs}) , the distance from surface to where maximum tensile residual stress is (Z_{mtrs}) , and the depth of residual compressive stress filed (Z_0). The relationships between these parameters and materials properties were discussed and the effect of residual stress by mechanical surface treatments on fatigue crack initiation and propagation behaviors was also investigated. The experimental results show that the fatigue life of surface strengthened specimens can be predicted by the resultant stress three dimensions intensity factor of external and residual stresses.

Key words: residual stresses, shot peening, cold expansion, laser shock peening, ultrasonic impact peening.

S145

SURFACE RESIDUAL STRESSES IN DRY TURNING OF 0,45% C STEEL

Tadeusz Leppert
University of Technology and Life Sciences, Bydgoszcz, Poland
Ru Lin Peng
Linkoping University, Linkoping, Sweden

The residual stresses in a subsurface layer determine many exploitation characteristics of machined parts/components. Depending on the kind and value, their influence can be negative or positive. Tensile residual stresses usually exert highly detrimental impact on several functional aspects such as strength, fatigue life, corrosion, wear resistance, etc., whereas comprehensive residual stresses are considered to have a beneficial effect on these features. The residual stresses found in many mechanical parts are mainly generated in the final steps of machining processes and are highly dependent on the used machining conditions. The main reasons of residual stresses generation in machining operations are mechanical and temperature impacts which change the subsurface physical and chemical properties. Increasingly popular in industry and environmentally desirable elimination of cutting fluids from machining processes substantially changes machining conditions, influencing relationship among factors causing residual stresses. Therefore, considering the significance of residual stresses for reliability and longevity of a part, a lot of attention is paid to the residual stress problem in terms of machining zone cooling and lubrication application together with the process parameters selection. Unfortunately the mechanism of residual stresses generation is still not completely recognized, particularly the influence of lack of cutting fluids in machining processes. The main purpose of the presented investigations was to identify a relationship between residual stress in a surface layer and the mode of cooling cutting zone. On the basis of empirical results the influence of dry turning and turning with the application of emulsion on residual stresses in steel C45 was identified in a broad range of cutting parameters. The effect of cooling cutting zone, cutting speed, feed and depth of cut on residuals stresses was determined. By X-ray diffraction the surface residual stresses were analysed in circumferential and axial directions. The results show that the modes of cooling and cutting parameters exert a substantial influence on the magnitude of residual stresses. The elimination of cutting fluid from turning process increases the magnitude of residual stresses in surface layer. The residual stress components values in the cutting direction and in the feed direction to a great extend depend on the cutting parameters. The results of presented investigation can make up the guidelines for cutting parameters selection taking into account the residual stresses constituted in the cutting process.

S147

USABILITY OF A STANDARD SAMPLE OF SINTER GLASS DISC

Vjera Novosel-Radović, Nikol Radović*, Franjo Šafar, Katica Dužić
Sisak Tube Mill Ltd, 44000 Sisak, Croatia
*Faculty of Geodesy University of Zagreb, 10000 Zagreb, Croatia, nradovic@geof.hr

Sinter samples were prepared for the determination of SiO_2, CaO, and Fe mass concentrations by X-ray emission spectrometry using the melting technique. The same technique was used for preparation of standard samples. The relative intensities of the analytical lines SiK_α, CaK_α, and FeK_α measured in those samples during use differed from the initially recorded values. Model samples were taken from a BCS - 378 sinter sample. The samples were ground and homogenized with the $Li_2B_4O_7$ - Li_2CO_3 - La_2O_3 - $NaNO_3$ (100 : 10 : 5 : 2.5) melting mixture prepared earlier, in a Spex mixer mill. They were then fused in a flat - bottomed graphite crucible of own manufacture, at 1000 °C for 25 minutes, and left to slowly cool down. Before measurement the glass disc surface was lightly polished. The usability of glass disc was determined by t - test. Samples of glass disc were stored in a desiccator. Relative intensities of the SiK_α, CaK_α, and FeK_α analytical lines were measured in a Philips semi - automatic sequential X - ray spectrometer (chromium anode, 20 mA/ 45KV) after periods of 1, 10, 30, 60, 90, 180, 360, 720, 1080, and 1444 days of storage.

The measured values of relative intensities of the SiK_α, CaK_α, and FeK_α analytical lines were compared to the initial values. The largest differences were noticed at the end of 1444 days. The measured relative intensities of the SiK_α analytical line decreased by 35 per cent, of the CaK_α Line by 25 per cent, and of the FeK_α line by eight per cent.

Examination by electron scanning microscopy showed the occurrence of crystallites on the glass disc surface as a result of extended storage in the dessicator and/ or of damage by radiation taking place in the course of measurement. The phenomenon first became noticeable as early as after 180 days of storage.

S149

ANALYSIS OF SHEAR STRESS DISTRIBUTION IN AL (Cu) INTERCONNECTS INDUCED BY ELECTROMIGRATION BASED ON SCHMIDT'S LAW AND STUDIED BY SYNCHROTRON POLYCHROMATIC X-RAY MICRODIFFRACTION

K. Chen, K.N. Tu, UCLA, CA
N. Tamura, B.C. Valek, ALS—Lawrence Berkeley National Laboratory, Berkeley, CA

We report here an in-depth synchrotron radiation based polychromatic X-ray microdiffraction study of plasticity in individual grains of an Al (Cu) interconnect line during the early stage of electromigration. It has been well known that distortional strain/stress tensor can be obtained with high accuracy by analyzing the deviation of the Laue peak positions from their ideal positions scattered by an unstrained crystal. However, for the case of electromigration study, the Laue peaks are greatly streaked due to the arrangement of the geometrically necessary dislocations, so that it is very difficult to determine precisely the peak positions. Therefore, the strain/stress cannot be accurately measured by the conventional method. Furthermore, since the X-ray beam has a certain spot size, rather than an ideal spot, there is strain gradient, as well orientation gradient, within the irradiated volume of the sample. As a result, we developed a new method to estimate the shear stress loaded in an individual grain based on Schmidt's law by two steps, including the analysis of the activated slip system in a given grain by simulation method and followed by Schmidt factor calculation. By this means, we obtained the shear stress distribution within the sample induced by electromigration.

S150

MEASURING RESIDUAL STRESSES IN STAINLESS STEEL USING XRD - RECENT EXPERIENCES WITHIN A VAMAS INTER-COMPARISON EXCERSISE

A.T. Fry, J.D. Lord
National Physical Laboratory, Hampton Road, Teddington, Middlesex, TW11 0LW, UK

Residual stresses impact on a wide variety of industrial sectors including the automotive, power generation, industrial plant, construction, aerospace, railway and transport industries, and a range of materials manufacturers and processing companies. The X-ray diffraction (XRD) technique is one of the most popular methods for measuring residual stress, used routinely in quality control, materials characterisation for validating models and design.

The VAMAS TWA20 Project 3 activity on the "Measurement of Residual Stresses by X-ray Diffraction" examined various aspects of the XRD test procedure in support of developing an international standard in this area. The purpose of this project was to examine and reduce some of the sources of scatter and uncertainty in the measurement of residual stress by X-ray diffraction on metallic materials, via an international round robin exercise. One of the major issues the round robin highlighted was the problems associated with measuring residual stresses in austenitic stainless steel. The following paper reviews the results of the exercise and details additional work looking the developing best practice for measuring residual stresses in austenitic stainless steel.

S159

RESIDUAL STRESSES IN BRUSH-PLATED GOLD COATING

H. Lille[1], J. Kõo[1], A. Ryabchikov[1], R. Laaneots[2]
[1]Estonian University of Life Sciences, Chair of Structural Mechanics and Engineering, Tartu, Estonia
[2]Tallinn University of Technology, Institute of Mechatronics, Tallinn, Estonia

Electroplated gold coatings have attracted much attention because of their desirable properties such as resistance to oxidation, low electrical resistance, overall chemical inertness and low processing temperature. One of the methods of electrodeposition is brush-plating (selective plating, contact plating, swab plating), which is known as a slow method applied primarily in cases where the areas to be coated are small and somewhat unique [1]. In general, this method only requires a power pack, and a number of different solutions and brush tools to perform the brush-plating process.

To determine residual stresses in brush-plated coatings, a conventional deformation method was used where an unclosed ring strip serves as the substrate [2].This kind of substrate makes possible the automatic deposition of the coating. The substrate is fixed to a mandrel, which makes free slipping of the edges as well as momentless deformation of the coated substrate possible. The slit increment of the substrate is measured as successive layers of the coating are deposited and the ring is free from the mandrel. The calculation formula is extended Stoney's formula which takes into consideration the real shape of the substrate, and the difference between the elasticity moduli and the coefficient of thermal expansion of the coating and the substrate materials.

In this study residual stresses were determined depending on current density in gold coating deposited from a commercial SIFCO Dalic Solution (Gold (Hard Alloy), Code SPS 5370) on brass substrate. The sensitivity of the method is studied and the uncertainties of computed mean values of the residual stresses are presented.

Residual stresses in coatings represent significant tensile stresses and their maximum values are higher than the values of stresses in coatings obtained in a bath solution.

Keywords: brush-plating, ring strip substrate, coating, slit increment, residual stress

References
1. M. Rubinstein. Electrochemical Metallizing. Van Norstrand Reinhold Company Inc., New York, 1987.
2. H. Lille, J. Kõo, A. Ryabchikov. Materials Science, Lithuania, 2002, **4,** pp. 417-420

S165

PHASE COMPOSITION AND INTERNAL STRESS DEVELOPMENT DURING THE OXIDATION OF IRON ALUMINIDES

Pedro Brito[1], Haroldo Pinto[1], Michael Spiegel[2], M. Klaus[3], Ch. Genzel[3], Anke Pyzalla[1]
[1]Max-Planck-Institut für Eisenforschung GmbH, Düsseldorf, Germany
[2]Salzgitter Mannesmann Forschung GmbH, Düsseldorf, Germany
[3]Hahn-Meitner Institut Berlin (c/o BESSY), Germany

Iron aluminides are considered potential candidates for high temperature applications because of their low cost, elevated strength to weight ratio and excellent oxidation resistance, which relies upon the formation of a continuous and stable α-Al_2O_3 scale. However, it is known that metastable alumina polymorphs, detrimental to the overall oxidation resistance of the alloy, may also be formed at low temperatures. Oxidation resistance is also affected by internal growth stresses developed during the oxidation process, and the resulting residual stresses that appear after cooling. These residual stresses represent one of the main factors inducing oxide layer spalling, which is the main reason for failure of protective oxide layers.

The aim of the present work is to investigate the relation between oxide phase composition during early stages of oxidation and the internal growth stresses developed within the layer. To this end, Fe-15at.%Al and Fe-26at.%Al polycrystals and single crystals were oxidized at low temperature (700°C) to favour the formation of metastable alumina polymorphs. The chemical composition of the layers was determined using X-ray photoelectron spectroscopy and the microstructure of the oxide scales was studied using TEM and X-ray diffraction with grazing incidence geometry. In-situ stress analysis was performed using the Energy Dispersive (ED) method with synchrotron X-rays. Texture in the scales after 5 h oxidation was also studied using the ED method.

The results reveal oxide scales with a thickness of approximately 100 nm, consisting of an external α-Fe_2O_3 layer and an internal α-Al_2O_3 layer. Minor quantities of θ-Al_2O_3 were also detected in the first minutes of oxidation. After 5 h of oxidation, there appears to be no impact of substrate orientation on scale texture. In-situ stress analysis showed that α-Al_2O_3 develops compressive internal stresses, whereas the α-Fe_2O_3 sub-scale is subject to tensile residual stresses after cooling to room temperature.

S171

MICROSCOPIC LOAD-SHARING IN A DUPLEX STAINLESS STEEL AND THE INFLUENCE OF PHASE PROPERTIES

R. Lin Peng[1], G.C. Chai[2], A. Ellerman[3], S. Johansson[1] and T. Manns[3]
[1]Linköping University, Sweden
[2]Sandvik Materials Technology, Sweden
[3]University of Kassel, Germany

Duplex stainless steels (DSSs) constitute an important stainless steel group which has found increasing use in recent years in engineering structures exposed to aggressive environment. The typical properties of DSSs, which combine high strength and good resistance to corrosion, are derived from a microstructure consisting of comparable amount of austenite and ferrite. In general, the ferrite is considered to be the strong phase that provides the high strength to a duplex stainless steel. Nevertheless, the macroscopic behavior of the steel under external loading also depends on the mechanical properties of the austenite and interactions between the two phases. Because of their different elastic and plastic properties, the applied stress is unavoidably distributed unevenly between the two phases. As the microscopic load-sharing has a direct influence on the mechanical properties of the steels, understanding the interactions between the applied load and microstructure and the influence of structural factors is important for the application of duplex stainless steels in engineering structures.

In the current work, we focus on studying the influence of the relative phase properties of austenite and ferrite on the microscopic load-sharing for superduplex stainless steel SAF 2507. Hot rolled bars with 43 vol.% ferrite and 57 vol.% austenite were received in solution treated and water quenched condition. To vary the property ratio of austenite to ferrite, the bars were further processed by 8% stretching or aging at 470°C for 4 hours, respectively. After the processing, while in the deformed steel the austenite has higher strength than the ferrite, the ferrite is much harder than the austenite in the aged steel. Flat specimens were then milled from the bars and polished for use in X-diffraction experiments under in-situ tensile loading. Using the $\sin^2\psi$-method as well as the ferrite- 211 and austenite-220 reflections, the evolution of phase-specific stresses with applied load was studied for three loading-unloading cycles, with the applied peak stress larger than the yielding point of the steels. In the paper, the observed different microscopic behaviors between the deformed and annealed steels are presented and analyzed with regards to the relative phase properties and initial residual stresses.

S178

THE BASIC RELATIONSHIP BETWEEN RESIDUAL STRESS PROFILE PATTERNS AND FATIGUE LIFE OF PRECISION MACHINED SURFACES IN ROLLING CONTACT

Y.B. Guo∗, A.W. Warren
Dept. of Mechanical Engineering, the University of Alabama, Tuscaloosa, AL 35487, USA
∗Corresponding author: Tel.: +1 205 348 2615; fax: +1 205 348 6419; E-mail address: yguo@eng.ua.edu (Y.B. Guo).

The patterns of residual stress (RS) profiles and their effects on rolling contact fatigue life for precision turned and ground surfaces with a white layer (WL) are very controversial. The key findings of this study are: (a) The basic RS profiles by a sharp tool can be fundamentally changed by a turned WL but not a ground WL; (b) The hook shaped RS profile of a turned surface may have about 40% more fatigue life than a ground one; (c) The white layer may reduce fatigue life as much as 7-8 times despite the deep compressive RS in the subsurface.

Keywords: Residual stress, fatigue, surface, machining

S179

FINITE ELEMENT MODELING OF RESIDUAL STRESS PROFILE PATTERNS IN HARD TURNING

Y.B. Guo∗
Dept. of Mechanical Engineering, the University of Alabama, Tuscaloosa, AL 35487, USA
∗Corresponding author: Tel.: +1 205 348 2615; fax: +1 205 348 6419; E-mail address: yguo@eng.ua.edu (Y.B. Guo).

Hard turning produces the unique “hook” shaped residual stress (RS) profile characterized by surface compressive RS and subsurface maximum compressive RS. However, the formation mechanism of the unique RS profile is not yet known. In this study, a novel hybrid finite element modeling approach based on thermal-mechanical coupling and internal state variable plasticity model has been developed to predict the unique RS profile patterns by hard turning. The most important controlling factor for the unique characteristics of residual stress profiles has been identified. The predicted characteristics of residual stress profiles favorably agree with the measured ones. In addition, friction coefficient only affects the magnitude of surface residual stress but not the basic shape of residual stress profiles.

Keywords: Residual stress, modeling, machining, finite element

S182

LAYER GROWING/REMOVING METHOD FOR DETERMINATION OF RESIDUAL STRESSES IN ORTHOTROPIC NON-HOMOGENEOUS CYLINDERS

J. Kõo, J. Valgur, Estonian University of Life Sciences, Tartu, Estonia

In [1] an algorithm of the layer growing/removing method is presented for the determination of residual stresses in the case of the isotropic non-homogeneous cylinder with a central hole. In the present paper the method is extended to the orthotropic non-homogeneous cylinder. It is assumed that elastic parameters depend on the radius only. Layer growing/removing may occur either on the cylinder’s external or internal surface. One proceeds from a generalized algorithm [2] by employing differential approach. The suggested algorithm presents interest above all in studying residual stresses in composite cylinders and growth stresses in trees.

According to the general algorithm the mechanical effect of formation of an elementary boundary layer is reduced to radial boundary load and axial edge load. These loads are expressed through the circumferential initial stress and axial initial stress of the surface layer, assuming that initial stress changes only in the radial direction. Residual stresses are found by the summation of the initial stresses of the cylindrical elementary layer and additional stresses arising as a result of adding further elementary layers.

In order to determine additional stresses, the centrally symmetric problem of theory of elasticity is solved for the long orthotropic cylinder with a central hole and elementary surface and edge loads. As a result, the following will be obtained: (1) relations between elementary additional stresses and initial stress; (2) relations between elementary strains on the stationary boundary and initial stresses. Relations (1) allow calculating additional stresses from initial stresses by integration. Initial stresses are determined e.g. by X-ray diffraction measurements on the cylinder’s moving boundary, or by strain measurements on the free stationary boundary, where circumferential and axial strains are measured and, proceeding from this, initial stress is calculated using relations (2).

It is shown that under certain conditions the layer growing and layer removing methods can be covered by one algorithm.

A computer program based on the present algorithm is introduced, and an example of application is presented.

References

1. J. Kõo. J. Valgur. *Layer Growing/Removing Method for the Determination of Residual Stresses in In-homogeneous Cylinders.* In Proc. of ICRS-5 (Ed-s T. Ericsson, M. Odén and A. Andersson), Linköping (Sweden), 1997, Vol. 2, 732-737.

2. J. Kõo. *Layer-Growing and Layer-Removing methods for Residual stress Analysis: General Algorithm.*In Proc. of ECRS-4 (Ed-s S. Denis, J.-L. Lebrun, et al.), Cluny en Bourgogne (France), 1996, Vol.1, 223-232.

S183

MICROSTRUCTURE AND RESIDUAL STRESSES OF HIGH-STRENGTH STEEL TO ALUMINIUM ALLOY FRICTION STIR WELDS

R.S. Coelho[1], A. Kostka[1], H. Pinto[1], J. dos Santos[2] and A. Pyzalla[1]
[1]Max-Planck-Institut für Eisenforschung GmbH, 40237 Düsseldorf, Germany
[2]GKSS Forschungszentrum Geesthacht GmbH, 21502 Geesthacht, Germany

The increasing use of light weight constructions requires the development of reliable and cost efficient joining methods. Based on the plastic deformation in the solid state and without associated melting, friction stir welding (FSW) has become an important process for joining dissimilar alloys. In automotive and other transportation industry particular interest arises in hybrid systems containing both steel and aluminium alloys.

In the present work, FSW was applied to produce a dissimilar butt-joint between HC260LA high-strength steel and AA6181-T4 aluminium alloy. The complex material flow and the different thermo-mechanical material properties result in a very complex microstructure. The results show a well defined interface aluminium-steel, where fine intermetallic bands are formed. The dynamic recrystallization process, which occurs during welding, results in the formation of nanosized grains in the steel side, while in the aluminium side the grains are only slightly smaller than in the base material.

Unlike similar FSW joints, the residual stress analyses reveal in the present case an asymmetric stress profile when going from the aluminium to the steel side. The stress values are in general low and the mechanical properties of the butt-joints, consequently, appear to be not influenced by the residual stress state.

S184

THE NEW ENGINEERING NEUTRON DIFFRACTION INSTRUMENT AT HFIR AND ITS APPLICATION TO STUDIES OF THE BEHAVIOR OF STRUCTURAL MATERIALS

C.R. Hubbard, W.B. Bailey, K. An and J. Schmidlin
Materials Science and Technology Division, Oak Ridge National Laboratory, Oak Ridge, Tennessee 37831-6064

The High Flux Isotope Reactor, HFIR, at Oak Ridge National Laboratory is the highest flux reactor-based source of neutrons for materials research in the United States. Thermal and cold neutrons produced by the HFIR are used for research in physics, chemistry, materials science, engineering and biology. One of the new scattering instruments at HFIR is the 2nd generation Neutron Residual Stress Facility, NRSF2, for high spatial resolution mapping of residual stresses throughout the thickness of components and for measurement of material behavior during in situ and/or real-time processes.

NRSF2 components include: a two Si wafer, doubly bent focusing monochromators; a large capacity XYZ sample positioning system with two different Z-stages; incident and diffracted beam collimators with slits that define the gage volume ranging from 0.3 mm to 20 mm; seven position sensitive detectors which increase data count rates; and LabView data collection and data analysis programs. Sample environment systems include a 5000 lb load frame for in situ tensile/compression experiments, a 2-circle Huber sample orienter, several furnaces and a unique induction heater insert for use with a 5T superconducting magnet. Tests show an increase of nearly 100 fold faster data collection over the older instrument. Selected research highlights will be presented that show the breadth of external user projects recently conducted at NRSF2.

S193

SIMULATION OF THE EFFECT OF SHEAR STRESSES ON THE MEASURED STRESSES INSIDE 50 MM ID PIPES

M. Belassel[1], J. Pineault[1] and M. Brauss[2]
[1]Proto Manufacturing Ltd., 2175 Solar Crescent, Oldcastle, Ontario, Canada.
[2]Proto Manufacturing Inc., 1980 E.Michigan Avenue, Ypsilanti, MI, USA, e-mail: proto@protoxrd.com

Stress corrosion cracking (SCC) and thermal fatigue of pipes can be accelerated by the presence of tensile residual stresses. The presence of such residual stresses can not be easily determined non-destructively. The proposed instrument uses a forward beam in a single inclination mode, i.e. single exposure technique (SET). The simulation conducted deals with the effect of shear stresses when using SET on the measured axial stresses inside a 50 mm inner diameter. These stresses are assumed to be present in the material generated during manufacturing. The accuracy of SET was evaluated to be satisfactory.

S195

VULCAN – THE DIFFRACTOMETER AT THE SNS FOR ENGINEERING MECHANICS

K. An[1], X.-L. Wang[1], T.M. Holden[2], A.D. Stoica[1], P.K. Liaw[3], H. Choo[3] and C.R. Hubbard[4]
[1]Neutron Scattering Science Division, Oak Ridge National Laboratory, Oak Ridge, TN
[2]Northern Stress Technology, Deep River, ON, Canada
[3]Dept. of Mat. Sci. and Eng., The University of Tennessee, Knoxville, TN
[4]Mat. Sci. and Tech. Div., Oak Ridge National Laboratory, Oak Ridge, TN

The VULCAN diffractometer at the SNS is scheduled for commissioning in 2008. This instrument is designed for materials science and engineering studies. With VULCAN users can not only conduct mapping of residual stresses, chemistry,

microstructure and texture but also measure dynamically mechanical deformation response, material chemical properties change and microstructure evolution under dynamic loading (e.g. fatigue) or severe material processing (e.g. welding).

The optics design features a focusing neutron guide system, wide-angular detector coverage, and a small-angle area detector. By employing an interchangeable neutron guide-collimator system, the instrument can be optimally configured for individual experiments. In the high-resolution mode, the instrument resolution is 0.2%, with an incident beam flux of 2.5×10^7 n/cm^2/s. In the high-intensity mode, the incident beam flux reaches 1.5×10^8 n/cm^2/s while the resolution remains better than 0.6%. With such a high flux, the count rate in detector is estimated to reach a few thousand counts per pulse. With special sample environments, such as the vacuum furnace and unique multi-axial tension-torsion load frame, etc., VULCAN extends the neutron study into wider areas of material science and engineering mechanics.

VDRIVE, a user-friendly Data Reduction & Interactive Visualization softwarE, is being developed for VULCAN. VDRIVE aids users to observe and interpret scientific/engineering data instantly and to assure the best use of neutrons, which is especially critical for kinetic behavior measurements. VDRIVE automatically reduces, analyzes and visualizes time-of-flight (TOF) neutron data in various interactive outputs. The real-time data analysis reduces the hassle of dealing with massive TOF data and the visualization gives users a sense of vivid projection of the scientific/engineering results

The construction of VULCAN is supported by the Canada Foundation for Innovation. In addition, the US National Science Foundation [Major Research Instrumentation (MRI) Program: DMR-0421219, with Dr. C. L. Bouldin as the Program Director] funded the sample environment suite for VULCAN, which includes load-frames, furnaces, and electro-chemical cells. The US Department of Energy, Office of Energy Efficiency and Renewable Energy, provides additional funding for completing the instrument.

S202

THERMAL MODELING AND EXPERIMENTATION FOR RESIDUAL STRESS PREDICTION IN BRAZE-WELDED BERYLLIUM VIA A SURROGATE CuZn10 ALLOY

Peter Backlund, Jason Lee, Sanjiv Shah, Carolyn Seepersad, Jack Howell and Eric Taleff
University of Texas at Austin
Michael B. Prime
Los Alamos National Laboratory, ESA-WR

Thermal stresses arise during welding processes and often lead to significant residual stresses in welded structures. These residual stresses can adversely affect part performance by accelerating stress corrosion cracking, hydrogen-induced cracking and fatigue cracking. For this reason, it is useful to predict residual stresses through simulations of the welding process. A method is being developed for predicting residual stresses created during braze welding of Beryllium. As part of the method, Gas Metal Arc Welding (GMAW) experiments are being conducted using a CuZn10 (90% Cu with 10% Zn, by weight) alloy, which serves as a surrogate that closely matches the thermal properties for Beryllium. Controlled welding takes place on a custom-designed welding test station that is equipped to collect temperature data from welding specimens via thermocouple measurements and an infrared camera. Temperature data are compared with computational (Finite Volume) and analytical results. Temperature history data collected at specific locations are combined with model predictions to estimate the full temperature field history surrounding the weld zone. These results serve as inputs into models of structural behavior for the prediction of residual stress fields produced by the braze-welding operation.

S204

THE ENGINEERING MATERIALS DIFFRACTOMETER "TAKUMI" AT J-PARC

Stefanus Harjo*, Atsushi Moriai[1], Kentaro Suzuya, Kazuya Aizawa, Takeshi Nakatani,
Masatoshi Arai, Yo Tomota[2], Koichi Akita[3], Kaori Shirakihara[4], Yukio Morii[1]
J-PARC Center, JAEA, [1]QUBS, JAEA, [2]Ibaraki University, [3]Musashi Institute of Technology, [4]Suzuka College of Technology

The Engineering Materials Diffractometer TAKUMI designed to solve many problems in materials science and engineering including investigations of stresses and crystallographic structures within engineering components is now being developed at JPARC. The design of TAKUMI is carried out for: 1) evaluation of strains or stresses and crystallographic investigation of small regions inside engineering components, 2) evaluation of microstructural evolutions during deformations and /or thermal processes, 3) in situ measurements of engineering materials during manufacturing and/or during service, and 4) crystallographic texture analysis. The best resolution of this instrument is 0.15%, which will give good accuracies on the strain values. The incident fluxes simulated using a Monte Carlo simulation for 0.8-4.31 Å wavelength bandwidth are 4.8×10^7 n/cm^2/s for high intensity mode, and 2.2×10^7 n/cm^2/s for high resolution mode. The construction is now in the final step, and the commissioning will be started very soon.

S210

RESIDUAL STRESSES AND FAILURE IN A WELDED COBALT-MOLYBDENUM HCP ALLOY

Peter Huson, Everett Criss and Bimal Kad
University of California, San Diego
Michael B. Prime
Los Alamos National Laboratory, ESA-WR

The effect of residual stresses in the failure of a cobalt-molybdenum welded material has been investigated numerically and experimentally. The proposed simulation method incorporates a sequentially coupled thermal-stress finite element model utilizing the "element birth and death" technique to simulate effects of multi-pass welding procedures. The FE models are evaluated through various residual stress measurement techniques, including the crack compliance method, the contour method and neutron diffraction. Of particular interest is the behavior of a heat treated 90-10 wt% Cobalt- Molybdenum alloy, which has been designed to experimentally surrogate residual stress distributions and failure mechanisms in beryllium welded structures. Surrogate selection has been validated through X-ray diffraction, scanning electron microscopy and thermalmechanical material characterization.

S217

SIMULATION OF TIME-OF-FLIGHT NEUTRON DIFFRACTION USING A NEW SAMPLE KERNEL

S. Y. Lee and E. Ustundag
Department of Materials Science and Engineering, Iowa State University, Ames, IA 50011

L. Li and I. C. Noyan
Department of Applied Physics and Applied Mathematics, Materials Science Program, Columbia University, New York, NY 10027

B. Clausen
Lujan Center, Los Alamos National Laboratory, Los Alamos, NM 87545

Interpretation of neutron diffraction data is essentially an *inverse problem analysis* that attempts to gain insight into materials from their diffraction patterns. These patterns, however, result from a complex convolution of instrument and specimen contributions. A proper interpretation of diffraction data, therefore, necessitates a systematic comparison of experimental results with sophisticated simulations of the entire diffractometer that includes a sample kernel. In other words, the success of the inverse analysis is largely dictated by the sophistication of the *forward* simulation of the experiment.

As a first step towards an accurate simulation of an engineering neutron diffraction experiment, the widely used Monte Carlo code *McStas* was employed in the simulation of the SMARTS diffractometer at Lujan Center. A new sample kernel was developed that simulates polycrystal deformation via a self-consistent solid mechanics model (the *EPSC* code from Los Alamos). This way, the effects of lattice strain and grain orientation distributions on peak position and profile could be incorporated into the instrument simulation. The simulation also employed the Python-based framework developed in the DANSE project (http://danse.us).

S219

NEUTRON DIFFRACTION STUDY OF STRESS DISTRIBUTION IN STEEL SHEET AROUND ACTIVE NiTi INSERTS

V. Davydov[1], B. Malard[2], M. Vrána[1], P. Lukáš[1], J. Pilch[2] and P. Šittner[2]
[1]Nuclear Physics Institute, 250 68 Rež, Czech Republic.
[2]Institute of Physics, Na Slovance 2, 182 21 Praha, Czech Republic

The quality and life time of stone processing tools is significantly affected by generation and accumulation of internal stresses during their operation. The rim of the cutting disc is exposed to a relatively high level of external working stresses of about 300 MPa and increased temperature (~70° C) which results in generating of non-homogeneous stress fields in the disc. To overcome this problem, the concept of active inserts made from shape memory alloys has been adopted. In the studied case, the small pre-strained elliptical NiTi elements were placed into elliptical holes cut in the cutting disc in locations of expected maximum stress concentration. To study the stress interaction of the NiTi inserts with cutting disc in detail, the method of neutron diffraction mapping if internal stresses was applied. The diffraction experiments were focused mainly to scanning of residual stresses around inserts and to describe the evolution of these stress-fields with increased temperature.

S220

EFFECTS OF OVERLOADS AND UNDERLOADS IN COLD-WORKED HOLES IN FATIGUE

Robert Reuter, AFRL/RBSM, Jim Harter, AFRL/RBSM, Daniel Hill, CaStLE

The cold-working process is a commonly used fatigue life improvement technique for improving the lives of cracked airframes; however, little investigation has been performed to show the effects of gross overloads and underloads in a stress spectrum which have the potential to distort a fatigue life prediction. In this study, several material systems including Al-2024, Al-7075, and the steel alloy 4043 were studied under varying nominal stress levels and varying overload ratios. Furthermore, optical crack measurements along with digital image correlation were used quantify to the behavior of the propagating cracks. Finite element analysis was also employed to determine the ability of ABAQUS and FRANC3D to accurately measure the residual stress field. It was found that both the compressive overloads and underloads increased the life of the cold-worked specimen relative to a constant amplitude counterpart. Difficulties and successes of performing the finite element analysis and developing the laboratory procedure are also presented.

S222

RESIDUAL STRESS DISTRIBUTION IN SINTERS OF DISTALOYAE AND DISTALOYHP

Stanislaw J.Skrzypek[1], Anders Bergmark[2], Marcin Goly[1]
[1]Faculty of Metals Engineering and Industrial Computer Science AGH-University of Science and Technology, Kraków Poland
[2]Höganäs AB, Research and Development SE-263 83 Sweden

Purpose of this paper is to elaborate X.ray diffraction methodology for to characterize two PM steels: DistaloyAE and DistaloyHP from Höganäs AB, Sweden. The beneficial feature of diffraction methods is the non-destructive character and large amount of structural information contained in the diffraction pattern.

Design/methodology/approach. The qualitative and quantity phase analysis, classical $sin^2\psi$ and modified $g\text{-}sin^2\psi$ [1] methods were used to residual stresses measurement (σ_I). The profile diffraction line analysis (PDLA) was used to quantify the lattice distortion $<\varepsilon>$ and to evaluate the average crystalline size All methods were elaborated for both i.e. classical Bragg-Brentano (BB) and grazing incidence angle X-ray diffraction (GID) geometry. In the case of last one, the mentioned above properties can be scanned versus depth under surface in non-destructive way.

The results obtained for the sintered samples indicate that diffusion grain-growth takes place during sintering. The gradients of elements concentration versus grain cross-section and the irregular space distribution of austenite make this alloy an composite with gradient-like microstructure. This gradient-like structure is confirmed here by residual macroscopic stresses measurement, quantitative X-ray diffraction phase analysis, micro-stresses and texture factor.

The ability of X-ray diffraction methods based on GID geometry to scan structural properties layer by layer is promising to this type of composite-like materials. The results from GID geometry measurements confirm non-uniformity of structural, phase composition and some properties as well. The method can be used to characterize structural properties of thin surface layer versus thickness in non-destructive way.

Practical implications. The results have put emphasis on the importance of the surface state of PM steel. The detailed information about distribution of alloying elements as revealed by the residual stresses and amount of retained austenite form a solid base for further development of PM steel for high loaded applications.

[1] S.J.Skrzypek, A. Baczmañski: Progress in X-ray Diffraction of Residual Macro-stresses Determination Related to Surface Layer Gradients and Anisotropy, ***Advances in X-ray Analysis***, 44, (2001), 134-145

S223

INTERFACE RESIDUAL STRESSES IN DENTAL ZIRCONIA USING LAUE MICRO-DIFFRACTION

Hrishikesh A. Bale[1], Jay C. Hanan[1], Nobumichi Tamura[2], Martin Kunz[2], Paulo Coelho[3], Van Thompson[3]
[1]Oklahoma State University, Stillwater, OK; [2]Advanced Light Source, Berkeley, CA; [3]New York University, New York, NY.

Due to their aesthetic value and high compressive strength, dentists have recently employed ceramics for restoration materials. This change is in contrast to the previous five decades when dental restorations were principally composed of high noble alloys such as gold-platinum, gold-palladium, and silver-palladium. Typical structural ceramics in modern dentistry include alumina and zirconia in coordination with metals as metalceramic crowns, or veneered with porcelain. Among the ceramic materials, zirconia provides high toughness and crack resistant characteristics due to its intrinsic behavior of stress induced crystallographic transformation. The phase transformation from tetragonal to monoclinic produces local volume expansion favoring crack closure resulting in additional strength.

Residual stresses develop in processing due to factors including grain anisotropy and thermal coefficient mismatch. These residual stresses also influence the phase transformation. Quantitative determination of residual stresses in zirconia is challenging. Along with stress induced phase changes, grain-grain stresses are significant; and for application to dental materials, local variations from edges and surfaces are important. It is at these surfaces where bonding to the veneer takes place. In the present study, polychromatic X-ray (Laue) micro-diffraction provided grain orientation and residual stresses on a clinically relevant zirconia model ceramic disk. The ceramic disks were fabricated at a dental research laboratory maintaining thermal history, layer thickness, and finishing parameters found in typical clinical restorations. A 0.5 mm by 0.012 mm region at a 500 nm scale was observed.

Due to the symmetry in the tetragonal phase, 8 to 10 high intensity reflections were seen as compared to the monoclinic phase, in which, around 20 to 30 lower intensity peaks were observed. The deviatoric strains developed within zirconia were determined by indexing and fitting the peaks from the tetragonal phase of zirconia. A representative powder was used as a strain free reference. The analysis reveals a normal distribution of the residual stresses, with a mean compressive residual stress. A small fraction of localized compressive and tensile stresses reached 1 GPa, more than twice the mean stress. The above results on neat zirconia are compared to interface residual stresses caused by the thermal coefficient mismatch on a similar area veneered with porcelain.

S140

IN-SITU SYNCHROTRON X-RAY TOMOGRAPHY STUDIES OF CREEP VOID EVOLUTION IN BRASS ALLOYS AND STEELS

A. Pyzalla[1], K. Dzieciol[1], A. Isaac[1], F.Sket[1], A. Borbély[1], G. Sauthoff[1], T. Buslaps[2], M. Di Michiel[2]
[1]Max-Planck-Institute for Iron Research, Max-Planck-Str.1, 40237 Düsseldorf, Germany
[2]European Synchrotron Radiation Facility, ESRF, BP220, Grenoble, France

Synchrotron X-ray tomography allows in a unique way the non-destructive, three-dimensional study of creep damage evolution in bulk materials. The results of the experiments reveal the development of the number and the size of creep voids and damage with increasing creep time. For the first time the evolution of individual creep pores during creep time can be investigated and void coalescence can be monitored. Void sizes, shapes, orientations and coalescence are quantified. It can further be shown that in-situ tomography combined with a constant temperature gradient along the gauge length of the sample allows for the determination of the activation energy of creep of only one single specimen.

S37

STUDY OF COMPUTERIZED TOMOGRAPHY AND STRAIN MAPPING IN THE VICINITY OF CRACK TIP IN STEEL MATERIAL USING SYNCHROTRON WHITE X-RAY

Jun-ichi SHIBANO*, Kentaro KAJIWARA**, Kouji KIRIYAMA***, Takahisa SHOBU***, Kenji SUZUKI****, Takayuki ARAI*,
Setsuo MIURA* and Michiaki KOBAYASHI*
* Dept. of Mech. Eng., Kitami Inst. of Tech., Kouen-cho, Kitami, 090-8507 Japan.
** JASRI, Kouto Sayo-cho, Sayo-gun, Hyogo, 679-5148 Japan.
*** JAEA, Kouto Sayo-cho, Sayo-gun, Hyogo, 679-5148 Japan.
**** Dept. of Tech. and Living Sci., Niigata Univ., 8050, Igarashi-2-no-cho, Niigata, 950-2181 Japan.

A computerized tomography and a strain mapping in the vicinity of a crack tip in steel were investigated using a high energy white X-ray obtained from BL28B2 beam line at SPring-8 in Japan. Low-alloy and high-tensile steel (JIS G3128 SHY685) was used as a specimen prepared in the cylindrical geometry. A fatigue crack was introduced into the specimen by a cyclic loading. The computerized tomography of the crack in the specimen was carried out by using the X-ray CCD camera that can detect the X-ray transmitted through the specimen. To measure the strain, the synchrotron white X-ray beam, which had a height of 100μm and a width of 100μm, was incident on the specimen with the Bragg angle θ of 5 degrees using the energy dispersive X-ray diffraction technique. The internal strain in the vicinity of the crack tip was mapped out by scanning the irradiated X-ray position around it.

As the results, the computerized tomography of the crack in the specimen under the loading of crack opening was practicable by using the synchrotron white X-ray [Fig.1]. The contour map of the internal strain near the crack tip of the steel of 5mm diameter could be obtained using the white X-ray with energy ranging from 50keV to 150keV [Fig.2]. It was confirmed that the synchrotron white X-ray is useful for the computerized tomography of the internal crack and the strain mapping near it.

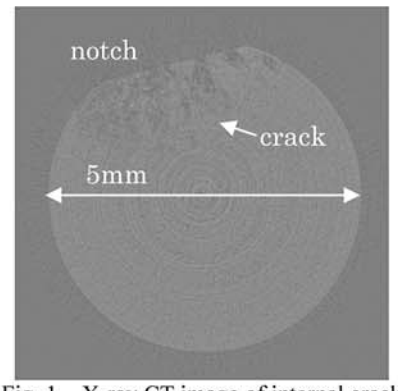

Fig. 1 X-ray CT image of internal crack

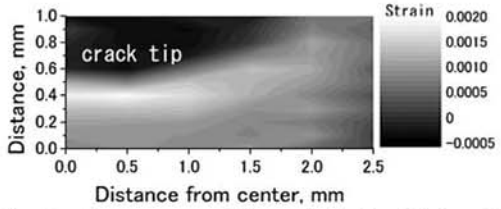

Fig. 2 Contour map of the strain in the vicinity of the internal crack tip

S109

SIMULTANEOUS MEASUREMENT OF IMAGING AND STRAIN OF FATIGUE CRACK IN STEEL BARS USING HIGH ENERGY SYNCHROTRON RADIATION

Takahisa SHOBU, Japan Atomic Energy Agency
Keisuke TANAKA, Meijo University

Fracture mechanics have been successfully applied for damage tolerant design of engineering structures against fatigue and stress corrosion cracking. The stress intensity factor is a key parameter to predict the progress of cracking behavior, and is computed from the shape of cracks and the loading stress distribution. When cracks are propagating within bulk samples, nondestructive methods are required to determine the three-dimensional shape of cracks. In the present study, using monochromatic high energy X-rays from the synchrotron radiation source, SPring-8. we have developed a system to perform the simultaneous measurement of imaging of cracks and strain scanning around cracks within bulk samples. We applied the system to a part-through fatigue crack in a round bar made of carbon steel.

The measurement was carried at a beam line BL22XU at SPring-8 using monochromatic X-rays of 68.2 keV. The specimen was a round bar made of carbon steel (JIS-S45C). The diameter of the specimen was 4 mm. A fatigue crack was generated from a drill hole with 0.1 mm in diameter and 0.05 mm in depth under completely reversed cyclic tension compression with the amplitude 240 MPa. Two specimens were prepared. The total length of a crack on the surface was 1 and 3 mm.

Computer tomography (CT) of the specimen was performed under the application of the maximum stress. The three-dimensional shape of a thumb-nail was successfully obtained using CT. Scanning of strain along the loading axis around cracks was conducted under the zero and maximum applied stresses. High tensile strain ahead of the crack was measured at the maximum stress, while the strain on the crack face was low because of crack opening.

S39

CHARACTERIZATION OF A NEW BONE RECONSTRUCTED AT THE INTERFACES WITH IMPLANTS

A. Benmarouane[1], T. Buslaps[2], T. Hansen[3] ,V. Honkimaki[2] and A. Lodini[1]
[1]UFR Sciences Exactes et Naturelles, LACM, B.P 1039, 51687 Reims Cedex 2, France
[2]ESRF, 6 Rue Jules Horowitz, BP 220, 38043 Grenoble Cedex 9, France
[3]ILL, 6 Rue Jules Horowitz, B.P. 156, 38042 Grenoble Cedex 9, France

Nanotechnology in material science and engineering has been developed with great success in the last decade. In orthopaedic surgery Titanium (Ti-Al-4V) implants are currently coated with nano-hydroxyaptite (n-HAp), Ca_{10} $(PO_4)_6$ $(OH)_2$, in order to obtain a stable and functional direct connection between the bone and the implant. Bone is a composite material associating a mineral phase in the form of HAp-crystals and an organic matrix constituted by collagen. The c-axes of HAp and the collagen fibres are preferentially oriented in the direction of the stresses that the bones need to withstand. At the implant-bone interface the new bone reconstituted after implantation must have the same orientation as the natural bone in order to accept the implant. Therefore we studied the mechanical properties of the new bone crystals reconstituted at the interface applying non destructive X-ray diffraction. The required high spatial resolution was achieved utilizing high-energy synchrotron radiation on ID15 at ESRF.

In this study a sheep received two different types of implants coated with n-HAp and with HAp. After 60 days the implants have been extracted together with the bones. The specimen have been prepared in the Pius Branzeu Centre of Laparoscopic Surgery and Microsurgery (Romania).

The results of the new bone crystals at the interface obtained by the synchrotron radiation study are particularly interesting and reveal a great advantage of the n-HAp coated implant interface.

References:

A. Benmarouane, T. Hansen and A. Lodini, Physica B, 350, (2004)p. E611-E614.
A. Benmarouane, T. Hansen P. Millet and A. Lodini (2005) Solid State Phenomena105:407.
H. -R. Wenk., Y. Xie, L. Lutterotti, et al (2001) J. Appl. Cryst,34:442.
J.Mr.S. Skaklea and R.M. Aspdenb, J. App. Cryst. Vol. 35 (2002), p. 506
S. Matthies, H.-R. Wenk and G. W. Vinel: J. Appl. Cryst.Vol 21 (1988), p. 285
H.-R. Wenk., Y. Xie, L. Lutterotti, L. Ratschbacher, J. Richardson, J. Appl. Cryst. Vol.34 (2001), p. 442

S14

MEASURING STRAIN IN AMORPHOUS SOLIDS BY HIGH-ENERGY X-RAY SCATTERING

Todd C. Hufnagel
Department of Materials Science and Engineering
Johns Hopkins University
Baltimore, MD 21218-2681 USA

While strain measurement by X-ray and neutron scattering is well established for crystalline solids, relatively less attention has been paid to the possibility of strain measurement in amorphous solids. Recently, several groups have shown that elastic strains

in metallic glasses can be reliably measured using high energy X-ray scattering, either directly from the scattering data in reciprocal space or from the pair correlation functions in real space.

In this talk, we review strain measurements in metallic glasses and other amorphous solids, with an emphasis on the physical basis for these measurements. We discuss the effect of anisotropic atomic arrangements (inherent to any solid with a deviatoric component of strain) on the process of Fourier transformation of reciprocal space data to obtain pair correlation functions in real space. For the special case of uniaxial tensile or compressive strains in the elastic regime we show that the effect of anisotropy is sufficiently small that it can be neglected. We also examine the effects of anelastic atomic rearrangements and homogeneous plastic deformation ("bond-orientation anisotropy") on elastic strain measurements. Finally, we conclude with a discussion of the prospects for future applications of these techniques in metallic glasses and amorphous solids more generally.

S28

ELASTIC-PLASTIC DEFORMATION OF A POLYCRYSTALLINE TITANIUM ALLOY STUDIED IN SITU BY ENERGY-DISPERSIVE SYNCHROTRON X-RAY DIFFRACTION

Shu Yan Zhang, Xu Song, Alexander M. Korsunsky
Dept of Engineering Science, Uni. of Oxford, Parks Road, Oxford OX1 3PJ, UK

Elastic lattice strain in polycrystalline assemblies evolves as a function of applied load due to elastic and plastic deformation mechanisms. The detailed nature of this deformation is complex and depends on the local arrangement of grains, their morphology and orientation, etc. To obtain mesoscopic (intermediate) scale description of polycrystal deformation, one approach that can be adopted is to measure the average lattice strain response of grain groups sharing common orientation by diffraction as the sample is subjected to increasing uniaxial load [1]. This reveals the anisotropy of the response of individual reflections (orientation grain groups), and enables the determination of the inhomogeneous fields of elastic and eventually plastic strain, if the measurements are combined with suitable interpretation and modeling approaches. Regions of localized macroscopic plasticity may be identified, and the prediction of fatigue crack initiation may also be addressed using energy dissipation at the micro-scale [2].

In the present study in situ loading and synchrotron X-ray diffraction experiments on Ti-6Al-4V alloy were performed. Multiple diffraction peaks were obtained from the experiments and both single peak fitting and Pawley pattern refinement were used for interpretation. The calculation of stress-strain response of *hkl* lattice planes based on the *a* and *c* lattice parameters obtained from Pawley pattern refinement was in good agreement with the results obtained by single peak fitting. The orientation dependence of polycrystal lattice stiffness and strain is discussed and a modified profile function for pattern refinement is proposed to provide an improved description of anisotropic behavior. Diffraction peak broadening was considered and the correlation between peak width and plastic strain was found (Fig 1). The intergranular strain responses for differently oriented crystallites obtained from the diffraction experiments were compared to the crystal plasticity finite element model predictions and used for validation of the model.

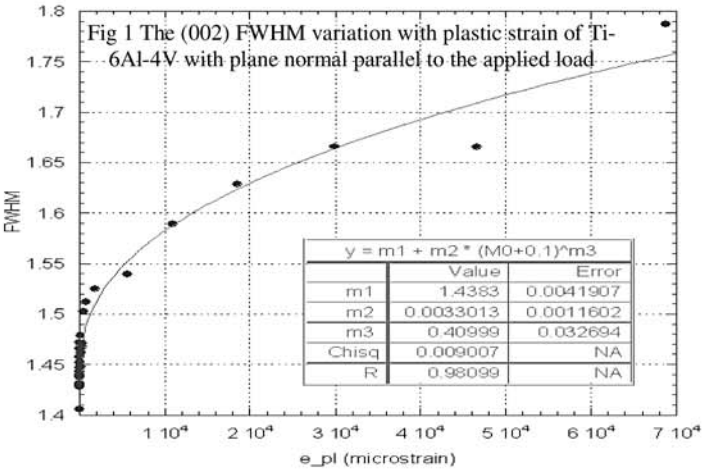

Fig 1 The (002) FWHM variation with plastic strain of Ti-6Al-4V with plane normal parallel to the applied load

[1] D. Dye, H.J. Stone, R.C. Reed, Intergranular and interphase microstresses, Current Opinion in Solid State and Materials Science 5 (2001) 31 –37

[2] X. Song, S Y Zhang, D Dini and A M. Korsunsky, Inter-granular residual stresses in polycrystalline aggregates: finite element modelling and diffraction post-processing, Proceedings of MECA SENS IV (2007)

S80

RESIDUAL STRESS DETERMINATION IN SURFACE TREATED ALUMINA SAMPLES APPLYING BEAM LIMITING MASKS

Thorsten Manns[1], André Rothkirch[2] and Berthold Scholtes[1]
[1] Institute of Materials Engineering, University of Kassel, Mönchebergstr. 3, 34125 Kassel, Germany, manns@uni-kassel.de
[2] HASYLAB at DESY, Notkestr. 85, 22603 Hamburg, Germany, andre.rothkirch@desy.de

Determining residual stresses by diffraction techniques is a widely used method. Conventional Laplace methods thereby determine mean stress values within the X-ray penetration depth τ. In case of small variations of the residual stresses over τ, the discrepancies between real space stresses $\sigma(z)$ and the measured ones $\sigma(\tau)$ are negligible. This assumption usually does not hold

when determining stress in depth distributions of surface treated alumina samples where steep stress gradients can often be observed.

The use of highly absorbing beam limiting masks can be a suitable way to overcome these problems as long as in the irradiated volume, defined by the mask design, no significant change of the residual stress state occurs. The idea for such masks was theoretically described by Predecki in 1993. The practical implementation discussed in this paper led to the conceptual design of one mask for each measurement depth and tilt angle ψ. During the assembly of the masks, accurate aligned slit structures were written by UV lithography on a polyimide film bonded on a silicon wafer. The absorbing layer was deposited by a subsequent gold galvanic process. Image series taken with a position sensitive CCD-camera, equipped with a multi channel plate for 2-dimensional beam collimation, demonstrate that the procedure is able to detect interferences from gauge volumes beneath the sample surface for defined slit geometries. These images clearly show the slit structure of the masks by crystallites which fulfil Bragg condition. Due to the highly absorbing masks the amount of detectable photons is poor and thus long exposure times are necessary to receive suitable data. For increasing measurement depths (altering masks) a decrease of intensity can be detected which leads to the assumption that the diffracted photos derive from deeper regions in the material.

We are grateful to the German Research Foundation (DFG) for the financial support of this project.

S30

THE BAUSCHINGER EFFECT IN NANOFILAMENTARY CU/NB WIRES EVIDENCED BY IN-SITU TENSILE TESTS UNDER SYNCHROTRON RADIATION

L. Thilly*, P.O. Renault, V. Vidal
PHYMAT, University of Poitiers, 86962 Futuroscope, France
S. Van Petegem, H. Van Swygenhoven
Paul Scherrer Institute, CH-5232 Villigen-PSI, Switzerland.
F. Lecouturier
Laboratoire National des Champs Magnétiques Pulsés, UPS-INSA-CNRS, 31400 Toulouse, France

Nanocomposite wires are processed by severe plastic deformation (Accumulative Drawing and Bundling) to obtain a multiscale Cu matrix embedding Nb nanotubes. They exhibit high strength that results from size effects in the Cu nanochannels and in the Nb nanotubes (Scripta Mat 57 (2007) 245).

The macroscopic stress-strain curve during tensile loading-unloading cycling exhibits an increasing hysteresis, evidencing the presence of internal stresses (Bauschinger effect). By performing such load-unload experiments in-situ under synchrotron radiation at the Swiss Light Source, it is possible to follow continuously the diffraction peak positions and peak widths of the large and the fine Cu channels as well as the Nb nanotubes, revealing the details of the load sharing and deformation mechanisms responsible for the Bauschinger effect.

During tensile loading, the large Cu channels provide most of the plastic strain and dislocation storage can be evidenced. The fine Cu channels and Nb nanotubes however mainly store elastic energy. Upon tensile unloading, this energy is partly released via reverse yielding in compression of the large Cu channels: in other words, the large Cu channels are subjected to a built-in true Bauschinger test (inversion of load direction). The observed large plastic strain gradient, added to the sink character of the Cu-Nb interfaces, induce the continuous build-up of internal stresses during co-deformation.

These results evidence unambiguously the reverse yielding of the soft phase in composite material with strong yield stress mismatch and bring further understanding to the complex residual stress state of nanocomposite materials obtained by severe plastic deformation processes where repeated loading-unloading cycles are applied (APL 90 (2007) 241907).

S66

RESIDUAL STRESSES IN FRICTION STIR WELDING: NUMERICAL SIMULATION AND EXPERIMENTAL VERIFICATION

G. Buffa[1*], L. Fratini[1], S. Pasta[2]
[1] Dipartimento di Tecnologia Meccanica, Produzione e Ingegneria Gestionale, Università di Palermo, Italy;
[2] Dipartimento di Meccanica, Università di Palermo, Italy

It is well known that Friction Stir Welding (FSW), presented and patented by TWI in 1991, is nowadays a very effective welding technology even with the so called difficult to be welded or even unweldable materials, such as aluminum alloys, since no melting is reached. In the most recent years several researches have been developed on FSW with the aim to fully highlight and optimize its process mechanics, material flow, metallurgical aspects, and both static and dynamic resistance. High residual stresses can be thus considered the last main obstacle inhibiting the full application of the FSW process by the manufacturing industries, due to the detrimental bending and distortion of the welding plate. As a matter of fact, although FSW does not show many of the metallurgical problems generally observed in fusion welding, such as liquation and solidification cracking, it still undergoes from similar levels of residual stresses, resulting from the weld thermal field. In the present paper the effects of the thermal and mechanical actions, occurring in FSW processes of AA7075-T6 aluminum alloy, on the residual stresses found in the welded joint in the three main directions are investigated. In particular both numerical simulations and experiments have been developed in order to highlight the occurring metallurgical phenomena and the induced residual stresses in the FS welded blanks. The FSW has been simulated using a continuous rigid-viscoplastic FEM model with FEA software DEFORM-3D^{TM}, previously developed by some of the authors to simulate the FSW process with a single block approach. Then, the temperature histories of each node of the FE model, were extracted and transferred to a further FE model of the joint considering an elasto-plastic behaviour of the AA7075-T6 material. The used model was developed with Abaqus/Standard using the Coupled Temperature-Displacement analysis option. As far as the experiments are regarded, the method of cut-compliance was used to determine the depth profile of residual stresses as well as the stress intensity factor (SIF); this provides extremely accurate measurements of longitudinal and transversal residual stresses occurring in FSW joint. Furthermore, the method enables the residual stresses in front of the crack-tip to be determined, which in crack retardation play a role as important as the closure effects. The performed analysis permitted to fully highlight the residual stress distribution in the longitudinal, transverse and along thickness directions.

Keywords: Friction Stir Welding, residual stress, FEM.

S53

INFLUENCE OF THE WELDING SEQUENCE ON RESIDUAL STRESSES IN LASER WELDED T-JOINTS OF ALUMINIUM ALLOYS

P. Staron, F.S. Bayraktar, W. Machold, S. Riekehr, M. Koçak, A. Schreyer
Institute of Materials Research, GKSS Research Centre, 21502 Geesthacht, Germany

Replacing riveted by laser beam welded (LBW) joints of aluminium alloys is a current topic in the aircraft industry due to weight and cost savings. Such LBW joints have already been realized for skin-stringer joints in several aircraft types. However, extension of this technique to short-distance T-joints of so-called clips to the skin is still needed. The start (run-in) and end (run-out) locations of short skin-clip welds are critical locations with respect to crack initiation and growth due to high stress concentration. Recent measurements indicated that longitudinal tensile stresses are lower at the run-in locations than at the run-out locations. Therefore, in the present study, the LBW joint of 2 mm thick AA6013-T6 clips to 4.5 mm thick AA6156-T6 base plates – resembling a skin-clip joint of an airframe – using a 3.3 kW Nd:YAG Laser source are investigated. Particularly, the effect of different welding sequences on the residual stress state was studied. One welding sequence was made straight from one end of the clip to the other, a second with two starting points in the centre, and a third with starting points at the clip ends. Experimental determination of residual stresses was done using neutron and high-energy X-ray diffraction. In addition, welding temperature field measurements were made to verify the predictions of a finite element simulation of the welding process, which is used for predictions of the residual stress distribution. The results show that the stress distribution around the weld depends strongly on the welding sequence. Two run-ins in the middle produce low tensile longitudinal stresses and compressive transverse stresses in the middle of the clip. On the other hand, two run-ins at both ends of the clip produce low tensile longitudinal stresses and compressive transverse stresses at the clip ends.

S55

THE INFLUENCE OF ANNEALING ON RESIDUAL STRESSES AT WELD STOP/START POSITIONS

S K Bate - Serco Technical & Assurance Services
I Symington - Serco Technical & Assurance Services
P Hurrell - Rolls-Royce
J A Francis - University of Manchester
M Turski - University of Manchester

The measurement and finite element modelling of a single pass bead on plate specimen indicate peak stresses which occur at or close to the weld stop/start positions. These welds may be considered analogous to finite length weld repairs which are commonly used as a means of repairing defects found in operating plant. These peak stresses may have a detrimental affect on the creep/fatigue and stress corrosion initiation assessments for non-stress relieved stainless steel welds.

Weld simulations of multi-pass welds have shown that the consideration of annealing affects due to subsequent overlaying material reduces the predicted residual stresses. Note the term annealing used here is defined as the temperature at which the material melts and the finite element code, ABAQUS, assumes that the material loses its hardening memory, i.e. the effect of prior work hardening is removed by setting the plastic strain to zero. Thus for multi-pass welds the peak stresses observed at stop/start positions in underlying material may be relieved by subsequent weld passes.

In order to investigate this behaviour, welded mock-up specimens have been manufactured and residual stress measurements and finite element analyses have been carried out. Type 304 stainless steel plates containing 5-pass and 8-pass groove welds were produced. The fifth weld pass in each specimen contains a ramped weld stop/start and an abrupt weld stop/start, which is then overlaid in the 8 pass weld specimen.

This paper describes the manufacture of the specimens, which includes a record of the temperatures measured in the specimen during welding; the residual stress measurements which have been carried out using neutron diffraction (more are planned using a variety of techniques) and the 3D finite element simulations using the code SYSWELD. The results of the measurements and predictions are compared and the influence of weld overlays on weld stop/start positions is discussed.

S56

FINITE ELEMENT ANALYSIS AND NEUTRON DIFFRACTION EVALUATION OF RESIDUAL STRESS IN STELLITE COATING BY PTA PROCESS

A. Nady[1], A. Benmarouane[1], H. Bonnefoy[1], V. KloseK[2], M. H. Mathon[2], A. Lodini[1]
[1]UFR Sciences Exactes et Naturelles, LACM, B.P 1039, 51687 Reims Cedex 2, France
[2]Laboratoire Léon Brillouin, CEA Saclay, 91191 Gif sur Yvette, France

A grade 6 cobalt-based superalloy was coated on steel substrate by the Plasma Transferred Arc (PTA) method. The macrostructure and microstructure of the interface and of the co-based superalloy layers are studied. The superalloy grains are deformed during the cladding process.

At the interface, the superalloy grains elongate and tend to follow the geometry of the interface. Observation with a scanning microscope reveals zones of localised Affected Zone Thermal at the interface.

A numerical analysis has been carried out to simulate the PTA process deposition with physical conditions and mechanical properties using the Abaqus code. A simplified model based on energy conservation and wall functions is used to predict the process, solid shield and shroud on the temperature and the residual stress of the PTA technology at the surface of coating layer and the interface.

The results reveal that the residual stress obtained by the numerical simulation are in very good agreement with experimental results performed by the neutron diffraction.

References:

Turquier, F., Hairy, P., Fitzpatrick, M.E., Edwards, L., Ceretti, M., Lodini, A., 1997. Stress Measurement in a Tool Steel Structure Coated With Plasma Sprayed Zirconia, Mat-Tec 97 Analysis of Residual Stress from Materials to Biomaterials. IITT-International.

Elsing, R., Knotek, O., Balting, U., 1990a. Calculation of residual thermal stress in plasma sprayed coatings: the effect of substrate temperature. Surf. Coat. Techn. 43/44, 426–435.

Gawne, D.T., Zhang, T., Liu, B., 2002. Computational analysis of the influence of a substrate, solid shield and gas shroud on the flow field of a plasma jet. Surface and Coatings Technology 153, 138–147.

S185

USING FINITE ELEMENT ANALYSIS AND SYNCHROTRON X-RAY DIFFRACTION TO UNDERSTAND STRESS DISTRIBUTIONS IN DEFORMING POLYCRYSTALS

M.P. Miller[1], J.-S. Park[1], T.-S. Han[2] and P.R. Dawson[1]
[1]Sibley School of Mechanical and Aerospace Engineering
Cornell University, Ithaca, New York
[2]Civil and Environmental Engineering
Yonsei University, Seoul, Korea

High energy X-ray sources combined with new sophisticated data reduction methodologies are enabling the measurement of complex deformation processes within metallic polycrystals. These experimental results, when coupled with multiscale modeling formulations, have the potential to build understanding of important micromechanical processes such as fatigue crack initiation, recrystallization and phase transformations. This talk describes such a hybrid approach created to understand deformation partitioning in sintered copper. The experiments employ synchrotron X-ray diffraction combined with in-situ mechanical loading to measure lattice Strain Pole Figures (SPFs) for an aggregate of crystals. Our group has developed a method, based on quantitative texture analysis, for inverting the SPFs for the lattice strain distribution function and crystal stress distribution within the aggregate. The simulation environment consists of a restricted slip polycrystal plasticity formulation with each crystal in the aggregate discretized using finite elements. Trends in the distribution of stress over orientation space measured in the experiment and calculated using the model are compared directly using spherical harmonic expansions of each stress component. Even though the macroscopic stress state is uniaxial, multiaxial stress states arise at many orientations within the aggregate with both magnitude and direction of stress varying significantly.

S87

MODELING THE RELAXATION DUE TO TWINNING IN AN *HCP* ZIRCONIUM ALLOY

M.R. Daymond, R.Y. Zhang, F. Xu, R.A. Holt.
Dept. of Mechanical and Materials Engineering, Queen's University, Kingston, ON.

Twinning can play an important part in the deformation of many metals, particularly those with lower crystal symmetries, for example zirconium, titanium, magnesium and their alloys. The twin is a region within a parent grain which has undergone a shear strain in response to stress characteristic of the particular twin system. This shear results in a crystallographic reorientation with respect to the parent crystal. As a consequence of this reorientation the physical properties of the twinned region (e.g. elastic constants) also have a different orientation from those of the parent grain. Further, this crystallographic re-orientation allows the accommodation of the deformation imposed on the parent grain by the stress, and hence results in a reduction in the stress in the parent grain.

Self-consistent models have been used extensively to simulate the elasto-plastic and visco-plastic deformation of anisotropic polycrystal materials, both for the prediction of deformation textures and to understand the contribution of various microscopic deformation modes to the macroscopic response. A new twinning model has recently been implemented within an Elasto-Plastic Self Consistent framework by Clausen and Tomé [1]. The model accounts for both crystallographic re-orientation and stress relaxation, and has provided improved agreement with experimental studies on the deformation of an extruded magnesium alloy [1]. Here, we compare the predictions of this new model against our extensive deformation neutron diffraction data set collected *in-situ* during deformation of Zircaloy-2 [2], a material which also undergoes twinning.

In addition, we have been carrying out a parametric finite element modeling study [3, 4] to investigate the possible stress states under which it is energetically favourable for twinning to occur, and the corresponding stress states after twinning both in parent grain and newly formed twin. The FE predictions are compared with the results obtained by fitting the EPSC model to the neutron diffraction data.

[1] Clausen, B., Tomé, C.N., Brown, D.W. & Agnew S.R., *in press* Acta Mater.
[2] Xu, F., Holt R.A., Daymond M.R., Rogge R.B. & Oliver E.C., *in press* Mat Sci Eng. A, doi:10.1016/j.msea.2007.11.018 (2007).
[3] Zhang, R.Y., Daymond, M.R. & Holt, R.A., Mat. Sci. Eng. A.; 473, p139-146 (2008).
[4] Zhang, R.Y., Daymond, M.R. & Holt, R.A., *to be submitted* Mat. Sci. Eng. A.

S116

MODELING AND MEASUREMENT OF RESIDUAL MACRO AND LATTICE STRAINS DURING FOUR-POINT BENDING OF ZIRCALOY-2

Feng Xu [1], R.A. Holt [1], M.R. Daymond [1] and R.B. Rogge [2]
[1] Department of Mechanical and Materials Engineering, Queen's University, Canada
[2] National Research Council, Chalk River Laboratories, Chalk River, Canada

Zircaloy-2 is an hcp zirconium alloy. It is used to make calandria tubes, which are a structural part of a CANDU nuclear reactor core. We are carrying out a combined modeling and experimental study of the development of internal strains of textured Zircaloy-2 during bending. The bending process is complex due to the highly anisotropic deformation of textured Zircaloy-2.

Understanding the residual strains left by the bending process will make direct and significant contributions to the understanding of the material's real-life deformation and design of next-generation components.

Beams were machined in three different directions relative to a parent plate and deformed ex-situ. The residual macroscopic strain field on the beam surfaces were recorded with an image correlation technique. The residual microscopic lattice strains distributed on the cross-section plane in three directions were measured by neutron diffraction.

Residual strains were modeled at two different length scales. Macroscopic strains were determined using finite element modeling (ABAQUS) and lattice strains were determined with polycrystal plasticity modeling, using an elasto-plastic self-consistent (EPSC) model. Material parameters obtained from uni-axial loading were used as the input to the finite element model. Subsequently, the averaged stresses and strains over a group of elements, representative of the diffraction measurement gauge volume, were used as the boundary constraints for the EPSC models, in order to calculate the residual lattice strains as a function of position in the beams. The modeling results are compared with experimental data at both length scales.

Keywords: Bending, Residual strain, Neutron Diffraction, Finite element model, EPSC, Zircaloy-2

S216 INVERSE ANALYSIS OF ENGINEERING NEUTRON DIFFRACTION DATA

Seung-Yub Lee[1], Baris Denizer[1], Youngshin Kim[1], Halil Ceylan[2], Ersan Üstündag[1]

[1] Iowa State University, Materials Science and Engineering, Ames, IA, U.S.A.

[2] Iowa State University, Civil, Construction and Environmental Engineering, Ames, IA, U.S.A.

Integration of engineering neutron diffraction (ND) data analysis and solid mechanics modeling offers a powerful approach to deduce *in-situ* constitutive behavior of materials. The basic approach is to perform an *inverse analysis* of ND data so that experimental strains fit predictions of the model by optimizing the model parameters that define the constitutive law. This presentation will outline recent results from the use of finite element analysis (FEA) in the interpretation of ND data from metallic glass composites. Various optimization algorithms (including least-square and artificial neural network analyses) were employed. The latter also allowed the study of the relative influence of various model parameters and yielded suggestions on optimum experiment design.

S79

INDUSTRIAL CHALLENGES FOR RESIDUAL STRESS XRD APPLICATIONS

Alfried Haase, Rainer Stabenow and Achim Schafmeister
GE Inspection Technologies
SEIFERT Analytical X-ray, Bogenstrasse 41, D-22926 Ahrensburg, GERMANY

In the automotive and aerospace industries, the highest standards of quality and safety must be demanded of supplied products to ensure the highest quality of final products. XRD measurements allow manufacturers and designers of new components to exploit the full potential of material properties and meet the requirements of quality control, in terms of product reliability, weight, performance, cost-effectiveness and operational lifetime.

Non-destructive testing of large and heavy components of complex geometry by X-ray diffraction is shown in various set-ups. A novel robotic X-ray analyzer .Charon XRD. was developed at MTU Aero Engines in a joint partnership project.

The understanding of stress especially in micromechanics becomes more and more significant. A microdiffraction system with precise mechanics and excellent spatial resolution, in the micron range, will be discussed.

For optimum throughput, a high level of automation of the sample measuring point or grid selection with data evaluation is required. Special X-ray optics and a new ultra-fast 1Ddetector allow high-speed data acquisition with high accuracy.

S16

X-RAY STRESS MEASUREMENT OF NICKEL-BASE SINGLE CRYSTAL SUPERALLOY USING TWO-DIMENSIONAL DETECTOR

Keisuke TANAKA, Meijo University
Shutarou MACHIYA, Daido Institute of Technology
Yoshiaki AKINIWA, Nagoya University

The stress in a single crystal of nickel-base superalloy with 72% volume fraction of γ'-phase was measured by the X-ray method. The specimen whose surface normal was parallel to [001] direction was oscillated around ϕ-axis during recording of the X-ray diffraction pattern with a two-dimensional position sensitive proportional counter (PSPC). The stress was determined from the measured strain using the multiple regression method and the two-tilt method.

The uniaxial stress was applied along [100] direction and the stresses were measured with the X-ray methods. The stress along [100] direction, σ_{11}, measured with the X-ray method increased proportionally to the applied uniaxial stress, and the measured stress was about 5 % smaller than the applied stress. The other stress components, σ_{22} and σ_{12} , did not change with the applied stress. With respect to the machined surface, the residual stress was a compression of about 700 MPa on the surface and abruptly decreased to zero at about 15μm beneath the surface. The increase in the full-width at half maximum was observed within the depth of about 15μm from the machined surface.

S40

ANALYSIS OF RESIDUAL STRESS IN POLYCRYSTALLINE COATINGS – FROM SCIENTIFIC TECHNIQUE TO INDUSTRIAL METHOD

Arnold C. Vermeulen
PANalytical, Lelyweg 1, 7602 EA Almelo, The Netherlands

The presence of residual stresses in polycrystalline specimens is an important issue in both science and industry. X-ray diffraction is the most versatile tool for analyzing stresses, but to obtain reliable results the technique has to be applied with great care. Normalization is essential to promote stress measurements from science to industry. The current standardization literature covers the procedures for the classical stress analysis based on single-{*hkl*} measurements on homogeneous 'bulk' specimens.

However, in materials research there is a need for a reliable and robust method to analyze residual stresses in less ideal specimens like thin films, coatings and surface layers. The classical residual stress measurement technique is not sufficient for such specimens. Hence another approach is required that may involve techniques like the use of multiple {*hkl*} reflections, grazing incidence beam, combined tilts and/or low diffraction angles. These techniques are already applied in dedicated scientific research, but more knowledge about the possibilities and limitations is required for a wider application in materials research in science and industry.

In this paper we will discuss the set-up of the measurements and the analysis of residual stress in polycrystalline coatings.

With respect to the X-ray diffraction measurements the influence of alignment errors will be discussed. In principle all alignment errors are relevant when using focusing optics. However for the parallel beam geometry certain errors become irrelevant.

For multiple {*hkl*} stress measurements an accurate calibration of the zero 2theta angle is important. Especially for grazing incidence measurements and despite the use of parallel beam optics the zero beam shift error introduces a systematic error in the final stress result. Direct measurement of the zero beam will not give sufficient accuracy, so that additional measurements on a stress-free reference specimen are advised.

With respect to data analysis of multiple {*hkl*} reflections a proper indexing of the measured peaks is essential. Since the peaks are shifted due to the presence of residual stresses indexing is not straightforward. Even in the case of cubic phases wrong indices can be assigned. Hence a modified indexing algorithm is required.

S41

APPLICATION OF X-RAY DIFFRACTION STRESS ANALYSIS AT CONSTANT PENETRATION DEPTH FOR THE DETERMINATION OF BOTH REAL-SPACE RESIDUAL-STRESS AND LATTICE-PARAMETER GRADIENTS

M. Wohlschlögel, U. Welzel* and E.J. Mittemeijer
Max Planck Institute for Metals Research, Heisenbergstr. 3, D-70569 Stuttgart, Germany
* contact author; u.welzel@mf.mpg.de

A γ'-Fe_4N_{1-x} layer on a α-Fe substrate (thickness 6 μm) has been produced by gas nitriding in a quartz-tube furnace. As a consequence of the specimen-preparation process a nitrogen concentration-depth profile is built up in the layer, thus causing a combined lattice parameter- and residual stress-depth gradient. The analysis of such combined gradients by X-ray diffraction is complicated by the fact that the asymmetry of the measured diffraction line is a function of the orientation of the diffraction vector with respect to the specimen surface normal. In the current study the unraveling of the residual stress and the strain-free lattice-parameter depth profiles has been realized by X-ray diffraction stress analysis at constant penetration depths employing the combined ω/χ mode. In order to cover a large range of penetration depth different photon energies have been employed using a laboratory diffractometer and a synchrotron beamline. The $\sin^2\psi$ method was adopted to calculate the residual stress gradient and the strain-free lattice parameter gradient was determined by measurement along the strain-free direction. Realspace profiles for residual stress and strain-free lattice parameter were obtained by fitting calculated to measured Laplace-space (penetration-depth) profiles. The systematic change of diffraction line asymmetry with measurement direction has been accounted for using the centroid of the measured diffraction line as diffraction-line position. The results for the concentration-depth profile (as follows from the strain-free lattice parameter depth profile) and the stress-depth profile are discussed with reference to literature data.

S96

RESIDUAL STRESS MEASUREMENTS BY X-RAY DIFFRACTION: CRITICAL EVALUATION OF ERROR SOURCES

Rogério Machado[1], Alexei Kuznetsov[1], Carlos Alberto Achete[1,2] and Thomas Hirsch[3],
[1]Divisão de Metrologia de Materiais (DIMAT), Inmetro, CEP 25250-020, Xerém, Duque de Caxias, RJ, Brazil
[2]Programa de Engenharia Metalúrgica e de Materiais (PEMM), Universidade Federal do Rio de Janeiro, Cx. Postal 68505, CEP 21945-970, Rio de Janeiro, RJ, Brazil
[3]Institut fuer Werkstofftechnik, Bremen, Germany

X-ray diffraction measurements of residual stresses in crystalline samples require a precise determination of *d*-spacings of a particular set of crystallographic planes as a function of orientation of this set with respect to the sample surface. Differences in experimental settings, like the state of sample surface, instrumental and sample alignment, as well as different approaches to the data processing may affect the obtained values of residual stresses. Therefore, characterization of the influence of these factors on the result of residual stress measurements is essential for reproducible and reliable evaluation of residual stresses in materials by the X-ray diffraction method. With the objective of studying the influence of different factors on the result of residual stress measurements with modern computer controlled diffractometers a set of carbon steel samples SAI 1070 was prepared. Sand blasted surfaces ensure similar values of surface residual stresses and residual stress depth profiles. The surface residual stresses states were measured in different diffractometers at IWT (Germany) and Inmetro (Brazil) using Ψ geometry. The results of measurements are compared for different conditions of diffraction measurements and instrumental alignment, and included the variation of 2Θ step size, 2Θ range, counting time, number of Ψ tilts, sample positioning, a sample area probed by X-ray beam, centre of diffractometer with respect to X-ray beam path. Different approaches to the data processing including the evaluations of different background subtraction methods and evaluation of influence of instrumental function on the position of measured Bragg reflections are presented.

S124

RESIDUAL STRESS ESTIMATION OF TI CASTING ALLOY BY X-RAY SINGLE CRYSTAL MEASUREMENT METHOD

Ayumi Shiro[1], Takao Hanabusa[2], Masayuki Nishida[3] and Tian Jing[4]
[1]Graduate Student, The University of Tokushima, Tokushima, Japan
[2]The University of Tokushima, Tokushima, Japan
[3]Kobe City College of Technology, Kobe, Hyogo, Japan
[4]Harbin Institute of Technology, Harbin, China

Recently, titanium casting technology attracts attention in the industrial fields. These casting metals are including a various residual stresses due to the heat shrinkage and inclusion particles, et al. In order to apply the casting technology, the accurate estimation of residual stresses is desired in many cases. In this study, it aims at the nondestructive stress evaluation of titanium casting material by the X-ray stress measurement technique. Moreover, the measuring sample is the cylindrically-shaped of Ti-6Al-4V alloy manufactured by vacuum casting method in Harbin Institute of Technology. As the first trial in this study, the sin^2 psi method for the usual X-ray stress measurement was investigated to measure the residual stresses. However, it was unsuitable for measurement of titanium casting material because of including coarse grains. Therefore, another X-ray method for single crystal system was employed to coarse crystal grains, in order to investigate the possibilities of residual stress estimating. Four-axes sample table which can set the both of tilt angle psi and rotate one kai on the sample surface was prepared for experimental measurement. The stereographic diagrams and the theory of elasticity were used to measure the single crystal stresses on the sample surface. From measurement results, it is possible to apply X-ray stress measurement method for single crystal system to the residual stresses in this sample. The coarse crystal grains can be taken as single crystals. Furthermore, results of residual stress distribution in center and edge position are tensile stress. The other hand, residual stresses in middle position between center and edge is compression stress state.

S168

ASTM STANDARDS FOR RESIDUAL STRESS MEASUREMENT

Clayton O. Ruud
Chair of the ASTM Residual Stress Measurement Subcommittee
and Professor Emeritus, College of Engineering, The Pennsylvania State University.

The origination of, and rationale for the American Society for Testing Materials (ASTM) will be reviewed including the initial rationale concerning failures in railroad equipment. Presently there are approximately 130 ASTM standard-writing technical committees with more than 32,000 volunteer members from about 100 countries. The Residual Stress Measurement Subcommittee is one of the 130 technical committees.

The jurisdiction of the Residual Stress Measurement subcommittee will be described as well as the system for designation of the standards. This will be followed by a discussion of specific residual stress measurement standards, and the process for review and renewal of these standards. Finally the procedure for developing new standards will be explained and new standards in development will be described.

S208

EXPERIMENTAL INVESTIGATION OF RESIDUAL STRESS IN LASER SHOCK PEENED FRICTION STIR WELD JOINTS

Omar Hatamleh[1], Adrian T. DeWald[2], and Michael R. Hill[2]
[1]NASA – Johnson Space Center, Houston, TX, USA
[2]Hill Engineering, LLC, 5022 Bailey Loop, McClellan, CA, USA

Friction stir welding (FSW) is currently being used to join materials from plastics to highstrength steels in industries including automotive, aircraft, and shipbuilding. The FSW technique employs a non-consumable cylindrical pin that rotates at high speeds, which is plunged into butting edges of the work pieces to be joined. This process transforms the metal into a plastic state at a temperature below the melting temperature of the material, and then mechanically stirs the material together under pressure to form a welded joint. Although the thermal input during FSW is relatively low compared with conventional welding techniques, residual stresses still develop during the FSW process. The magnitude and distribution of these residual stresses can be detrimental to performance and can be a significant contributor to the durability of the FSW joints and surrounding material.

This paper investigates the residual stress generated by friction stir welding on 2195 and 7075 aluminum alloy samples. Residual stress measurement data was obtained using the contour method. This paper also investigates the ability of mechanical surface treatments (e.g., shot peening and laser shock peening) to mitigate the tensile residual stresses in these FSW joints.

S78

THERMAL STABILITY OF MECHANICAL SURFACE TREATMENT INDUCED RESIDUAL STRESS IN AUSTENITIC STAINLESS STEEL BY NEUTRON AND SYNCHROTRON DIFFRACTION

A.D Evans[1], M. Turski[2], S. Clitheroe[2], J. Kelleher[2] and P.J. Withers[2]
[1]European Synchrotron Research Facility (ESRF), 6 rue Jules Horowitz, Grenoble, 38043, France
[2] School of Materials, University of Manchester, Manchester, UK

The fatigue and stress corrosion cracking behaviour of engineering materials have been shown to be significantly improved through the application of optimized mechanical surface treatments. These processes tend to generate significant compressive residual stresses in the near surface layers of material following localized plastic deformation of the surface of the treated material. In the case of mechanical surface treatments such as laser shock peening and ultrasonic impact treatment (UIT) among others, the compressive residual stress layer can extend to a depth in the order of millimeters beneath the surface, with balancing tensile stresses extending deeper still. These typical depths are of an order of magnitude greater than conventional shot peening. The presented study is a part of a wider ranging project to understand the stress corrosion cracking benefits gained by mechanical surface treatment of welded stainless steel structures operating at elevated temperatures. The presented results characterize the magnitudes and depth of compressive residual stresses generated in 304 austenitic stainless steel plates using monochromatic neutron diffraction using oscillating radial collimator optics to suppress spurious strains. The samples were treated with both high and low intensity variations of shot peening (SP), laser shock peening (LSP) and ultrasonic impact treatment (UIT). Ex-situ measurements followed in order to characterize the thermal relaxation the as-treated residual stresses exposed to typical operating temperatures (350°C) and higher operating temperature (550°C). Subsequent monochromatic synchrotron diffraction measurements on thin slices electro-discharge machined from the samples were performed to characterize the reduction of plastic work following thermal relaxation by correlating the peak widths of the surface treated slices to samples strained to known levels of plastic strain. These measurements aimed to assess empirically the influence of plastic deformation on the extent of thermal relaxation observed. By combining these complementary diffraction techniques, the thermal stability residual stresses can be characterized and an estimation of plastic work levels and their stability can be assessed.

S74

SMALL CREEP DEFORMATIONS AND RESIDUAL STRESS RELAXATION IN WELDED AND SHOT PEENED ALMGSICU-ALUMINUM ALLOYS

Stefan Daichendt and Thomas Hirsch
Stiftung Institut fuer Werkstofftechnik, Badgasteiner Str. 3, 28359 Bremen, Germany

Precipitation hardened aluminum alloys are found in various applications of components for the aircraft, automotive and railway industry. Effective joining techniques are tungsten inert gas- and laser beam welding. These joining techniques result in microstructural changes and hardness losses in the different welding zones as well as in the generation of complex residual stress states depending on the initial heat treatment state of these alloys. These inferior properties of the welding zones are often compensated by shot peening processes. Service loads near the endurance limit reduce the peening induced residual stresses not completely. However there is some lack of information about residual stress relaxation after service loads at higher temperatures as the temperature for starting creep deformation is around 100°C. This paper reports results of residual stress stability after mechanical relaxation tests and thermal relaxation from a laser beam welded and shot peened wrought Aluminum alloy 6056. After shot peening typical distributions of residual stresses and strain hardening are observed for the base material whereas the weld material show some reduced residual stress levels. The relaxation tests for temperatures 100°C<T<150°C prove the

existence of high threshold stresses. The level of these threshold stresses can be estimated to be in the range of Orowan stresses of the metastable precipitates. This is additionally proved by experimental data analysis. With the knowledge of back stresses the experimental results of relaxation tests could be well fitted with the Feltham equation. After the stress relaxation tests the shot peening induced residual stresses decrease to a large extend in the welding zones and remain almost stable in the base material. Pure thermal relaxation reduces residual stresses for temperatures >100°C and similar differences between welding zones and base material occur. Calculations of residual stress relaxation based on the stress relaxation tests underestimate the relaxation behavior due to the different nature of load stresses and residual stresses. This has to be taken into account during the service of surface treated components.

S99

NEAR SURFACE STRESS GRADIENTS ANALYSIS BY GIXRD ON LASER SHOCKED 6056 ALUMINIUM ALLOY SAMPLES

H.B. Song[1], P. Peyre[2], V. Ji[1,3], C.H. Jiang[4]
[1]LIM UMR CNRS 8006, ENSAM, 151 bd. de l'hôpital, 75013 Paris; France
[2]LALP UPR CNRS 1578, Arcueil 94114, France
[3]ICMMO/LEMHE UMR CNRS 8182, Université Paris-Sud 11, 91405 Orsay, France
[4]School of Mat. Sci. & Engin., Shanghai Jiaotong University, Shanghai, P.R. China

Laser shock peening (LSP) can introduce a compressive stress profile for improving the materials' surface mechanic properties. 6065 Aluminium alloy is widely used in the aeronautic components. The surface performances of the components are related directly to the surface activity and surface corrosion properties which are influenced by the near-surface stress gradient. So, the determination of residual stress dues to LSP near the surface layer of 6065 alloy is very important for the surface strengthen and for surface activity. Pseudo-grazing incidence X-ray diffraction (GIXRD) is a non-destructive method and can be used to evaluate the residual stress gradient below the surface at very shallow depths of a few micrometers according to the different materials. The experiments were carried by two GIXRD methods: multi-reflection method using the various crystallographic {hkl} family planes and $\sin^2\psi^*$method using the various corrected angles ψ^*, ϕ^*, Ω^* with only one crystallographic family. The purpose of this study is to quantify the stress gradient of 6056 aluminium alloy from surface up to 10 micrometer by these two GIXRD methods, then to compare the results for the determination of their limits.

Keywords: Residual stress; GIXRD; 6065 aluminium alloy ; Laser shock peening; multi-reflection; $\sin^2\psi^*$ method

S188

RESIDUAL STRESS MEASUREMENTS USING SYNCHROTRON X-RAY ON NICKEL-BASED SUPERALLOY AT CRYOGENIC TEMPERATURES

Koichi Akita[1], Yoshinori Ono[2], Takahisa Shobu[3], Daisuke Miyashita[1], Tetsumi Yuri[2], Toshio Ogata[2] and Shin-ichi Ohya[1]
[1]Musashi Institute of Technology, Setagaya, Tokyo, Japan
[2]National Institute for Materials Science, Tsukuba, Ibaraki, Japan
[3]Japan Atomic Energy Agency, Sayo-gun, Hyogo, Japan

High-cycle fatigue properties of Ni- and Ti-alloys at cryogenic temperatures have recently been investigated with the goal of improving the reliability of launch vehicles. Some unique fatigue behaviors have been reported especially for shot-peened samples of the alloys. In this study, residual stress distributions beneath the surface of a shot-peened Ni-based superalloy INCONEL718 were measured at cryogenic temperatures from 5K to room temperature using monochromatic high energy synchrotron X-rays in SPring-8. The effects of the temperature dependence of the residual stress on the fatigue behaviors were discussed.

The compressive residual stress was introduced into the surface to a depth about 120 μm by shot-peening. The changes in residual stress distributions with temperature were observed within about 50 μm depth from the surface. The maximum residual stress just beneath the surface increased with decreasing temperature. The residual stress distribution deeper than 50 μm was not changed in spite of the temperature changes.

The changes in the fatigue crack initiation sites from the surface at room temperature to inside at cryogenic temperatures can be explained by the results obtained in this study; namely, the temperature dependence of the residual stress just beneath the surface.

S64

EFFECT OF RESIDUAL STRESSES ON FATIGUE STRENGTH OF SEVERE SURFACE DEFORMED STEELS BY SHOT PEENING

Yoshiaki Akiniwa and Hidehiko Kimura
Department of Mechanical Science & Engineering, Nagoya University, Nagoya 464-8603, Japan

The compressive stress distribution below the specimen surface of severe surface deformed steels by shot peening was investigated by using laboratory X-ray and high-energy X-rays from a synchrotron radiation source, SPring-8 (Super Photon ring-8 GeV) in the Japan Synchrotron Radiation Research Institute. Medium carbon steel plates were heat treated in two different conditions. The Vickers hardness after heat treatment is 408 and 617 HV. The specimens were shot-peened with fine cast iron

particles of the size of 50 μm. The coverage was 5000%. The compressive residual stress on the specimen surface measured by laboratory X-ray is -684 and -1240 MPa, respectively. For the synchrotron radiation, by using the monochromatic X-ray beam with several energy levels, the stress values at the arbitrary depth were measured by the constant penetration depth method. The real stress distribution was estimated by using the optimization technique. The peened specimens were fatigue by four point bending. The improvement of fatigue strength of the soft steel was not so large because of large surface roughness. On the other hand, for the hard steel, the surface roughness was smaller and the fatigue strength was higher than that of non-peened steel.

S117

USING XRD ELASTIC AND PLASTIC STRAIN DATA TO EVALUATE THE EFFECTIVENESS OF DIFFERENT COLD-WORKING TECHNIQUES IN AEROSPACE MATERIALS

Beth S. Matlock, Technology for Energy Corp., Knoxville, TN, USA
Daniel J. Snoha and Scott M. Grendahl, US Army Research Laboratory, Aberdeen Proving Ground, MD, USA

Studying stresses in aerospace materials is important for aircraft sustainment and for developing new materials and designs for next generation air and spacecraft. Due to natural vibrations and mechanical mechanisms, fatigue failures are a primary concern in aerospace structures. For this reason, residual compressive stresses are generally desired. The effectiveness of compressive stresses in protecting an aerospace structure depends on not only the magnitude of the stresses but also on the depth or range to which they extend.

X-ray diffraction (XRD) is a direct method for measuring the elastic strains (residual stresses) in crystalline materials. Additionally, the diffraction peak width is a measure of the plastic strain in a part. The elastic and plastic strains can be used to better assess the true condition of a sample compared to just using residual stress data. This paper deals with two studies on aerospace materials. In the first case, compressive stresses were introduced into samples by shot peening. Several shot peening conditions were evaluated. Residual stresses were measured and profiled. Fatigue tests were also performed to determine optimum life relative to the peening conditions and correlated to the residual stresses. The peak widths were compared to the stress profiles and showed that coupling elastic and plastic strain information from the surface could indicate which samples had the deeper layer of compressive stresses.

The second study involved cold-worked holes in aluminum alloys. The split-mandrel technique was used to impart compressive residual stresses at and around holes simulating rivet holes in aircraft structures. Some holes were not cold worked. The residual stresses and diffraction peak widths were then used to determine if the samples had been cold worked and to rank the samples according to the amount of cold working.

These two studies show the importance of using elastic and plastic strain data to evaluate the true condition of materials used in the aerospace industry. It also shows the possibility of using the plastic strain information from the surface to predict subsurface behavior.

S151

NUMERICAL AND EXPERIMENTAL INVESTIGATION ON SHOT-PEENING INDUCED DEFORMATION. APPLICATION TO SHEET METAL FORMING.

F. Cochennec[1*], E. Rouhaud[1], L. Roucoules[1], B. Flan[2]
[1]University of technology of Troyes, Charles Delaunay Institute – FRE 2848, Laboratory of Mechanical Systems and Concurrent Engineering. 12, rue Marie Curie BP2060 10010 TROYES Cedex FRANCE.
[2]Sisson Lehmann – Wheelabrator group. 24, rue Camille Didier BP39 08000 Charleville-Mezieres Cedex FRANCE.

The peen forming process is commonly used in the aeronautical industry to form large wing skin panels. This process presents many advantages in terms of cost, production time, and beneficial induced residual stresses. Setting the accurate process parameters to form a given pattern requires however a certain experience and sometimes many trials and errors. Different numerical models have been proposed in the last twenty years to support the manufacturing engineering activity. These models mostly rely on artificial equivalent loads that are fitted to experimental measurements. The authors propose to model the shot peening induced deformations by elastically equilibrating the real plastic strain gradient present in the whole structure. A complete numerical and experimental protocol is proposed to determine the plastic strain gradient assuming the knowledge of some experimental data. A proposed approach consists in determining the plastic strain field by inverse calculation based on experimentally obtained residual stresses fields. This approach is applied to two different shot-peening cases: the shot peening treatment of an Almen strip and the partial treatment of an aluminium alloy sheet. A second approach is based on the inverse calculation of shot peening induced plastic strain with the assumption of a specific form for the plastic strain gradient and knowing the global deformation of the treated sheet. A comparison between the proposed approaches applied to partially treated sheets is presented along with experimental data.

S70

ADVANCES IN NEAR SURFACE RESIDUAL STRESS GRADIENT ANALYSIS OF POLYCRYSTALLINE MATERIALS BY MEANS OF ENERGY DISPERSIVE DIFFRACTION

I.A. Denks
Hahn-Meitner-Institut Berlin, Glienicker Straße 100, 14109 Berlin, Germany

Residual stress analysis by energy dispersive (ED) diffraction using a white beam of up to 100 keV allows the determination of near surface residual stress distributions within the first tens to hundreds of micrometers [1]. However, the methods currently applied - LAPLACE- and real-space-methods – only deliver limited information.

Applying LAPLACE-methods the integral information from the surface region is detected and the in-plane stress distribution $\sigma(\tau)$ obtained represents the stresses relative to the mathematical abstract LAPLACE-space. The calculation of the real space distributions $\sigma(z)$ from the $\sigma(\tau)$-profiles is complicated since it requires the application of the inverse Laplace transform (ILT) on scattering experimental data.

The alternative method is to determine the out-of-plane depth distributions $\varepsilon(z)$ by applying the strain-scanning method and calculating the in plane residual stresses $\sigma(z)$ by means of the transversal contraction requiring the precise knowledge of the lattice parameter d_0. Apart from the presumptions made, the main problem rises from the fact that the gauge volumes are usually large in respect to the depth region of interest requiring complex correction terms and deconvolution procedures.

Considering the problems, a real space "stress-scanning" method has been developed allowing the direct determination of stress distributions $\sigma(z)$ by means of ED diffraction. The high spatial resolution within the micrometer range is realized by detecting the diffraction signal in different orientations ψ from the identical flat gauge volume being aligned parallel to the sample surface.

Both the stress-scanning method and the LAPLACE-method were applied to samples with complex stress states using ED diffraction. The experimentally obtained stress distributions $\sigma(z)$ and $\sigma(\tau)$ of the same depth region give access to the problems involved with the currently applied procedure of the ILT. The results obtained on a multilayer system containing several layers of identical composition demonstrate the uniqueness of the stress-scanning method allowing the direct access to buried layers.

[1] Ch. Genzel, I. A. Denks, J. Gibmeier, M. Klaus, G. Wagener, Nucl. Instr. Meth. A578 (2007), 23.

S148

FATIGUE DAMAGE EVALUATION OF RAILWAY CARBODY STRUCTURE USING HIGH ENERGY SYNCHROTRON RADIATION

Keisuke Matsumoto, Railway Technical Research Institute, Hikari-cho 2-8-38, Kokubunji-shi, Tokyo, 185-8540, Japan
Takahisa Shobu, Japan Atomic Energy Agency, Kouto, Sayo-gun, Hyogo, 679-5148, Japan
Masataka Yamamoto, Tsuyoshi Yagi, Railway Technical Research Institute

The railway carbody structure for commuter and suburban services in Japan is often made of austenitic stainless steel, which is used in the form of thin metal sheets manufactured by cold rolling. Laser welding at lapped joints is used in the construction of such carbodies, but it is difficult to observe the strain distribution around these weld zones, which represent the critical area of the body structure.s fatigue strength. The objective of this study is to ascertain the strain and stress distribution in the stainless steel around the weld zone of the carbody structure. To enable observation of this distribution, a strain scanning method using high-energy synchrotron radiation in SPring-8 was applied to the strain measurement of austenitic stainless steel. The transmission and reflection method was applied in order to observe the internal weld zone. Using this method, we can measure the strain distribution from the surface to the inside of the weld zone. A lapped joint specimen, prepared by welding 2mm- thick plates using the laser welding method, was used for measurement. Austenitic stainless steel generally poses problems in the measurement of strain due to its coarse grain and crystal texture. The gage volume in this measurement had a width of 2 mm and a height of 0.15 mm. The measurement provides the strain distribution of both residual strain and strain under loading, and the results obtained successfully show the distribution of strain in the weld zone. The differing tendency between the distribution of residual strain and that of strain under loading is clarified. In addition, the specimen after fatigue test was measured. The results of specimens before and after fatigue test were compared. The full width at half maximum (FWHM) value shows a difference between the tendency of the measured value of the weld zone and that of the base material.

S61

THE NEW HIGH ENERGY MATERIALS SIENCE BEAMLINE (HEMS) at PETRA III

N. Schell, F. Beckmann, H.-U. Ruhnau, R. Kiehn, and A. Schreyer
GKSS-Research Center Geesthacht GmbH, Max-Planck-Str. 1, 21502 Geesthacht, Germany

The future **H**igh **E**nergy **M**aterials **S**cience Beamline **HEMS** at the new German high brilliance synchrotron radiation storage ring PETRA III will have a main energy around 100 keV, be fully tunable between 50 to 200 keV, and be optimized for sub-micrometer focusing with Compound Refractive Lenses and Kirkpatrick-Baez Multilayer mirrors. Design, construction,

operation and main funding is the responsibility of the Research Center Geesthacht, GKSS. Approximately 70 p.c. of the beamtime will be dedicated to Materials Research, the rest reserved for general physics experiments covered by DESY, Hamburg.

The materials science activities will be threefold:
• Fundamental research will encompass metallurgy, physics and chemistry which are more and more merging. First experiments are planned for the investigation of the relation between macroscopic and micro-structural properties of polycrystalline materials, graingrain- interactions, recrystallisation processes, and the development of new and smart materials or processes. For this purpose a dedicated 3D-microstructure-mapper will be designed.
• Applied research for manufacturing process optimization will benefit from the high flux in combination with ultra-fast detector systems allowing complex and highly dynamic *in-situ* studies of microstructural transformations, e.g. during welding processes (an *in-situ* friction stir welding device for measurements with synchrotron radiation has been designed at GKSS). The beamline infrastructure will allow accommodation of large user provided equipment.
• Experiments targeting the industrial user community will be based on well established techniques with standardised evaluation, allowing full service measurements. Environments for strain mapping on large structural components up to 1 t will be provided as well as automated investigations of large numbers of samples, e.g. for tomography and texture determination.

The current design for the beamline consists of a nearly five meter in-vacuum undulator source optimized for high energies, a general optics hutch, an in-house test facility and three independent experimental hutches working alternately, plus additional set-up and storage space for long-term experiments. HEMS should be operational in late spring 2009 as one of the first beamlines running at PETRA III.

S134

IN-SITU STUDY OF THE CYCLIC DEFORMATION BEHAVIOUR OF THE MAGNESIUM BASE WROUGHT ALLOY AZ31 BY MEANS OF HIGH ENERGY SYNCHROTRON DIFFRACTION

Jens Gibmeier[1], Martin Götting[2] and Berthold Scholtes[2]
[1]Hahn-Meitner-Institute, c/o Bessy II, Albert-Einstein-Strasse 15, D-12489 Berlin
[2]University of Kassel, Inst. of Mat. Eng., Mönchebergstr. 3, D-34125 Kassel
* corresponding author

With regard to the processing of structural lightweight components there exists an increasing demand for the application of Mg-base wrought alloys, which are basically highly textured due to the cold forming process. By this means the flexibility for the design of the components is higher and apart of that the strength of the material state can be partially tailored to the operational demands.

However, magnesium has a poor deformability at room temperature due to the fact that only a limited number of glide planes are activated. Furthermore twinning can occur for loading the hexagonal magnesium unit cells in compression parallel to the basal planes or in tension normal to the basal planes. After twinning has occurred it has been shown that the twins can recover during cyclic loading when reversing the loading direction.

Although the focus of recent research activities on light metals is on the investigation of the texture evolution and the mechanical behaviour of Mg-base alloys during processing and in service, there still exist a lack of understanding of the mechanical-technological characteristics of magnesium wrought alloys, e.g. the knowledge about the deformability or the cyclic deformation behaviour with respect to the initial crystallo-graphic texture of the material state.

In the present research project the deformation behaviour during cyclic loading of the highly textured hot rolled magnesium wrought alloy AZ31 has been investigated in-situ using energy dispersive diffraction for high energy synchrotron radiation in transmission mode on bars subjected to purely elastic as well as elasto-plastic 4-point-bending. Loading or residual stress distributions were determined for one load cycle including loading, load release and load reversion. The experiments were carried out at the EDDI-Beamline at Bessy II, Berlin using a white beam up to energies of 150 KeV.

The results obtained for the multitude of reflexions being recorded simultaneously in one single diffraction spectrum clearly indicate the highly elastic isotropic behaviour of the textured alloy. For elasto-plastically bended bars a strong plastic anisotropy was observed leading to a distinct shift of the neutral fibre of the bars. Reverse loading causes a shift of the neutral fibre almost symmetrically in the opposite direction of the bar which can be attributed to the reversibility of the twinning. Twinning and the untwinning process can clearly be observed on basis of the diffraction results by local changes of the texture caused by the elasto-plastic loading.

S205

EVALUATION OF SUBSTRUCTURE PARAMETERS BY PEAK PROFILE ANALYSIS OF HIGH-RESOLUTION NEUTRON DIFFRACTION SPECTRA

P. Lukáš[1], P. Strunz[1], V. Davydov[1] and R. Kužel[2]
[1]Nuclear Physics Institute, 250 68 Řež, Czech Republic
[2]Charles University, Faculty of Mathematics and Physics, Ke Karlovu 5, 121 16 Prague, Czech Republic

The peak profile shape analysis has been preferentially used in evaluation of X-ray and synchrotron powder diffraction spectra. However, neutron diffraction facilities of new generation frequently offer the instrumental resolution high enough to study efficiently the effects of broadening of neutron diffraction profiles. Moreover, high penetration ability of neutrons enables us to use a large variety of sophisticated sample environments at neutron diffraction instruments, such as deformation machines, furnaces, cryostats, high-pressure cells, etc. These features make the high-resolution neutron diffraction instruments an unique experimental tool especially for in situ studies.

The present paper describes the procedure for a detailed evaluation of Bragg peak shape based on the method of transformed model fitting (TMF) which has been recently developed particularly for treatment of neutron diffraction profiles. Microstructure modeling is performed in the reciprocal space and the convolution of the model with the instrumental resolution curve is fitted to the profiles recorded in the diffraction experiment. The practical application of the TMF procedure will be demonstrated at the study of evolution of microstructural parameters of the ferritic steel *in situ* upon tensile straining. In this case, the Wilkens dislocation model and a lognormal crystallite size distribution were implemented into the model of the line broadening.

S192

TECHNIQUES FOR NEUTRON STRESS DETERMINATION WITH HIGH SPATIAL RESOLUTION

Thomas Gnäupel-Herold
University of Maryland, College Park MD 20742, USA
NIST Center for Neuron Research, Gaithersburg MD 20899-6102

Many sub-surface strain measurement problems require spatial resolutions of the order of 10^{-1} mm to be meaningful. The use of neutron diffraction can be both time effective and otherwise advantageous compared to synchrotron radiation if measurement directions and beam shapes are chosen such that scattered intensity is maximized. The first point refers to preferred orientation which boosts the diffracted intensity in certain directions; the second point refers to the shaping of the incident beam for maximizing the illuminated volume in the material even for curved specimens. Guidelines and limitations such high spatial resolution measurements are discussed.

S127

NEUTRON DIFFRACTION STRESS MEASUREMENT - REMARKS ON CALIBRATION AND ALIGNMENT

C. Ohms
European Commission, Joint Research Centre, Westerduinweg 3, 1755 LE Petten, The Netherlands

The topics of this presentation are generally well known and understood. However, this leads to situations where appropriate attention is sometimes lacking in residual stress measurement.

The work presented here is based on long established principles, but shads some new light on calibration and alignment procedures in certain areas.

Monochromatic neutron diffraction instruments for stress analysis are generally calibrated for their wavelength and detector angular response by measuring several diffraction peaks of a well characterized powder material. While there is no argument that calibration is necessary to measure lattice spacing reliably, the question has to be asked, how well an instrument needs to be calibrated to measure strain. In strain measurement, the dominant factor is the relative peak shift between a measurement from a material under stress and from the corresponding unstressed material. A peak shift can be very well measured without calibrating the instrument. A brief and simple analysis should indicate how important calibration is when making this consideration. Subsequently, an example is given from a real measurement campaign at the JRC, where a small calibration related error has been detected long after completion of the measurements and the data analysis.

In addition to the above main considerations on calibration, some comments are made on the use of

$$\varepsilon \approx -\cot\theta\Delta\theta\ .$$

In the context of this presentation, specimen alignment will be looked at. No consideration is given to the alignment of the instrument. For aligning a specimen with respect to the sampling volume there are basically several possibilities. Neutron intensity scanning is the option looked at here. Under the assumptions of idealized sampling volume shapes and homogeneous materials response there are some cases, which have analytical solutions to fit the neutron intensity data against. Some of the

known cases are reiterated, with comparison to real measurement data. One additional solution is looked at - tentatively called sideways intensity scanning. Finally, some old examples from VAMAS TWA 20 and RESTAND are shown to demonstrate the importance of knowing where the specimen is with respect to the neutron beams.

S172

ACCURATE SPECIMEN MOUNTING AND ALIGNMENT FOR NEUTRON STRAIN MAPPING AT ORNL

C.R. Hubbard[1], W.B. Bailey[1], J. James[2], and J. Schmidlin[1]
[1]Materials Science and Technology Division, Oak Ridge National Laboratory, Oak Ridge, Tennessee 37831-6064
[2]Materials Engineering, Open University, Milton Keynes, UK

The High Flux Isotope Reactor (HFIR) and the Spallation Neutron Source (SNS) at Oak Ridge National Laboratory are two of the highest flux sources of neutrons for neutron scattering in the world. Engineering and materials science diffractometers are to part of the instrument suite at each facility. The new instrument at HFIR is the recently commissioned and operating 2nd generation Neutron Residual Stress mapping Facility, NRSF2, which excels at high resolution strain mapping and in situ, real time measurements within the bulk of samples. At SNS the world-class Engineering and Materials Science Diffractometer VULCAN is nearing completion and will receive neutrons later this year. The two facilities are accessible to users from other institutions through corresponding User Programs. To take advantage of the exceptional performance and to improve accuracy, specimen mounting, alignment and experiment planning tools are being assembled and developed for use at both facilities.

The specimen set up/mounting is based on modular, T-slotted profiles of high strength aluminum that can be rapidly assembled. The T-slotted profiles are 25 mm in cross section and conform to 50 mm M-6 hole pattern on the XYZ sample positioner system. The specimen alignment tools include laser trackers and a laser ScanArm-coordinate measuring system. These tools help define the origin of the sample and its relationship to fiducial points on the sample or the sample mount. The measurements provide the as-received sample geometry, which can be compared to engineering drawings or be used to "reverse engineer" and develop as-is drawings of the specimen. One output of the ScanArm measurements and data processing is the deviation from the ideal geometry that is determined to approximately +/- 50μm. This actual 3-D surface geometry is then entered into SScanSS, a software tool written at Open University for neutron strain mapping experiment planning and optimization. SScanSS is a virtual instrument simulation tool for sequential robotic motion positioners that assists the user to define of the desired measurement locations, consider beam path length, and assure the measurement plan is free of collision. When the sample is mounted on the diffractometer's sample positioning system (SPS), the fiducial locations are remeasured and SScanSS creates the command file for driving the SPS. This improves accuracy in positioning the sample and relating the measurement location back to engineering drawings of the sample. Such knowledge is proving valuable to groups validating finite element analysis models with neutron strain/stress mapping results.

S154

IMPROVED SENSITIVITY FROM MULTIPLE IMAGES IN RESIDUAL STRESS MEASUREMENT BY ESPI HOLE-DRILLING

Gary S. Schajer, University of British Columbia, Vancouver, BC, CA
Michael Steinzig, Los Alamos National Laboratory, Los Alamos, NM, USA

The hole drilling method for residual stress measurement is a common technique, typically utilizing a strain gage to quantify the in-plane strains that are released as a result of drilling a hole. Electronic speckle pattern interferometry has also been used to measure deformation around the hole, and gains some out-of-plane component of deformation. Results can be calculated based on a single set of images, with a sensitivity vector defined by the bisector of the incoming laser light and the reflected light that is imaged. In this paper, we will investigate the sensitivity improvements that result from incorporating more than one sensitivity vector, by using two imaging cameras.

S104

A NEW PROCEDURE FOR THE EVALUATION OF RESIDUAL STRESSES BY THE HOLE DRILLING METHOD BASED ON NEWTON-RAPHSON TECHNIQUE

G. Petrucci[a], M. Scafidi[b]
Dipartimento di Meccanica, Università degli Studi di Palermo, Viale delle Scienze – 90128 Palermo – ITALIA
e-mail: [a]petrucci@dima.unipa.it, [b]scafidi@dima.unipa.it.

In the hole drilling method, the non-uniform residual stresses can be determined from the measured relaxed strains using several techniques, the most used of which are the power series method and the integral method. The relationship between relaxed strains and stresses is

$$\varepsilon(z) = \int_0^z F(Z,z)\ \sigma(Z)\ dZ; \quad Z \le z; \tag{1}$$

being z the depth of the hole, Z the distance from the surface along the hole axis, $\sigma(Z)$ a combination of the unknown residual stresses, $F(Z,z)$ is the influence function determined by numerical analysis, $\varepsilon(z)$ the relaxed strains measured at the surface. In the method proposed in this paper $\sigma(Z)$ is approximated by a $\sigma'(Z)$ function given by a set of n polynomials $\sigma\, j(Z)$ of iM degree, each one representing $\sigma(Z)$ in a limited field
$z_{j-1}<Z<z_j$, being $j=1\div n$:

$$\sigma_j(Z) = \sum_{i=0}^{i_M} a_{ij} Z^i, \quad z_{j-1} \le Z \le z_j, \quad j = 1 \div n \tag{2}$$

In this case eq. (1) becomes

$$\varepsilon'(z) = \sum_{k=1}^{n} \sum_{i=0}^{i_M} a_{ik} \int_{z_{k-1}}^{z_k} F(Z,z)\ Z^i\ dZ \tag{3}$$

The a_{ij} coefficients in eq.(3) are the only unknowns of the problem described by eq.(1) and their determination is effected by successive approximations by the *Newton- Raphson* method, minimizing a least square difference between the $\varepsilon(z)$ values and the $\varepsilon'(z)$ function.

It is interesting to note that using n=1, the proposed method reduces to the power series method, while considering i_M=0, the proposed method becomes a sort of *optimized* integral method. The application of the method is very simple and allows to obtain more precise results than the most used existing techniques.

S181

THE APPLICATION OF DIGITAL IMAGE CORRELATION TECHNIQUES FOR MEASURING RESIDUAL STRESS BY INCREMENTAL HOLE DRILLING

J.D. Lord and P. Whitehead *
National Physical Laboratory, Hampton Road, Teddington, Middlesex, TW11 0LW, UK
* Stresscraft Ltd, St. Winefride`s Chapel, Pick Street, Shepshed, Loughborough, Leicestershire, LE12 9BB, UK

The measurement of residual stress using the incremental hole drilling is well established, but the main limitations with the conventional strain gauge approach are the requirements for surface preparation and the need for accurate alignment and drilling, together with the restricted range of hole geometries commensurate with the specific gauge designs, and the limited range of strain data averaged over the footprint of the strain gauge grid. Recent developments to extend the method have seen the application of full field optical techniques such as ESPI and holographic interferometry for measuring the strain fields around the hole, but these methods are sensitive to vibration and this limits their practical use to controlled laboratory environments.

There are significant potential benefits therefore of using a more robust technique based on digital image correlation (DIC), and work is presented in this study on the development of the method for measuring surface displacements and strain fields during hole drilling. Some of the practical issues associated with the technique development, including the optimization of applied patterns, the development of the optical system and integration with current hole drilling equipment are discussed, together with results on a range of materials and components with different stress profiles. Validation data comparing results from conventional strain gauge data and FE models is also presented.

S3

COMBINATION OF DIFFERENT MEASUREMENT TECHNIQUES FOR THE DETERMINATION OF RESIDUAL STRESS DISTRIBUTIONS IN WELDMENTS WITH MECHANICAL SURFACE TREATMENTS

Thomas Nitschke-Pagel, Klaus Dilger
Institute of Joining and Welding, University of Braunschweig

The evaluation of residual stresses resulting from welding or post weld treatment processes with regard to their influence on the mechanical properties of welded joints depends on the amount of reliable knowledge about the residual stress field in the surrounding of potential failure initiation sizes in a welded joints. Critical locations are usually the transition zones from the weld seam to the adjacent base material e.g. the weld toes. In typical weldments this weld toe is characterized by a sharp notch geometry which complicates residual stress measurements with common measurement methods. In steel weldments residual stress measurements with help of X-ray diffraction is usually a state of the art method as long as the measurements are limited on the surface. The determination of subsurface depth profiles is rather difficult because a certain constant removal by electrochemical polishing is usually impossible. On the other hand alternative techniques like the hole drilling method are also not applicable at the weld toe because the calculation algorithms which are used to calculate the residual stresses require a plane surface for the application of the strain gage rosettes and this is usually not assured at the weld toe.

Residual stress measurements on MAG-welded high strength steels have been performed with different measurement techniques to determine the entire residual stress depth distribution in the weld toe zone. The surface residual stresses were measured with help of X-ray diffraction and with synchrotron radiation. The depth distributions have been measured with help of neutron diffraction and the results of the diffraction measurements have been compared with results obtained with the incremental hole drilling technique.

It can be shown that the combined application of X-ray diffraction, hole drilling method, neutron diffraction and energy dispersive diffraction of synchrotron radiation enables the determination and characterization of the entire residual stress field in locally post weld treated joints. Therefore such investigations offer very useful possibilities to evaluate the benefit of post-weld improvement techniques with help of the local fatigue strength concept.

S126

RESIDUAL STRESS MEASUREMENTS ON THIN FILMS WITH A FOCUSED ION BEAM EQUIPMENT

N.Sabaté[1], D.Vogel[2], K.J. Kang[3], A.Gollhardt[2], I.Gràcia[1], C.Cané[1] and B.Michel[2]
[1]Centre Nacional de Microelectrònica (CNM-CSIC), Campus UAB sn, E-08193 Bellaterra-Barcelona, Spain
[2]Micro Materials Center Berlin, Fraunhofer Institute for Reliability and Microintegration (IZM), Gustav- Meyer Allee 25, D-13355 Berlin, Germany
[3]Department of Mechanical Systems Engineering, Chonnam National University, Kwangju, 500-757, Korea

The rapid development of the MEMS industry demands new concepts and approaches of reliability topics. Because residual stress is one of the main sources of failure, its prediction and measurement are crucial to assess reliability of any structure during its lifetime. Thus, in the past years a great deal of research effort has been directed towards residual stress determination. Methods like the curvature measurements at wafer level or the bulge based tests have become common ways to obtain stresses in thin films whereas other approaches have focused on the onpurpose fabrication of micro-machined test structures. However, none of these techniques offers the possibility of very localized measurement. Novel methods of local stress measurement, like X-ray, micro/nano Raman or EBSD based tools, are very expensive or suffer from limitations with respect to materials they can be applied to. For that reason the authors made effort to set-up the traditional hole drilling and slot milling techniques at a new micro or even nano scale dimension. The downscaling of the stress-release measurement methods is based on the combined milling-imaging capabilities provided by a Focused Ion Beam (FIB) equipment. Thus, the ion beam replaces the traditional milling instruments, whereas Scanning Electron Microscope (SEM) imaging combined with Digital Image Correlation (DIC) techniques allows monitoring of the displacements originated by stress release.

The authors show from basic experiments how the mentioned approaches can be used to determine residual stress values from membrane or thin film structures. Analytical solutions as well as Finite Element Analyses (FEA) of the respective mechanical stress release problems are utilized to calculate stresses from deformations. Basic capabilities and limitations of the method are studied taking account of performance of recent FIB equipment and Digital Image Correlation (DIC) software. This method is verified in comparison to independent measurements with other methods. Some emphasis is placed on stress extraction from thin film objects, especially from multilayer structures. As far as residual stress measurements of the discussed type are extremely sensitive to underlying stress hypotheses and stress extraction algorithms, both issues are discussed in some detail. In order to understand the effect of imperfect feature milling on stress release, especially with regard to size reduction, FEA is applied.

Examples of stress measurements on MEMS structures, coatings and micro-wires are presented. Finally, an outlook is given on issues, which require further investigations and development of the measurement method in future.

S125

MICROSCALE RESIDUAL STRESS MEASUREMENT IN STEEL USING FOCUSED ION BEAM SLOTTING AND DIGITAL IMAGE CORRELATION

N. Daynes[1], G. Horne[1], P.J. Heard[2], D.Z.L. Hodgson[1], A. Shterenlikht[1]
1. Department of Mechanical Engineering, University of Bristol, Queen's Building, University Walk, Bristol, BS8 1TR, UK
2. Interface Analysis Centre, University of Bristol, Oldbury House, 121 St. Michael's Hill, Bristol, BS2 8BS, UK

This paper describes experimental procedure for measuring residual stress on subgrain scale in metals using focused ion beam (FIB) milling and digital image correlation (DIC). In contrast to most previously published research in this area the authors applied the method to steel samples and used FIB for imaging as well as for milling.

In this work residual stress was simulated by uniaxial compressive applied stress. To this end a 20x5x3mm mild steel sample was compressed uniaxially below the elastic limit to 400MPa using a simple clamp loaded by M8 bolt. The loading strain was monitored with a strain gauge.

The sample was polished and positioned under the focused ion beam (FIB). The FIB principle is similar to the more conventional SEM with the exception that heavy gallium ions are used instead of electrons to bombard the metal surface. The FIB was used in this work both as a micro-milling and as imaging tool. The sample was positioned normal to the incipient ion beam. Initial surface preparation involved uniform exposure to the beam (socalled etching) to remove the oxide layer. A very useful side effect of etching is that it reveals
identifiable surface features. After etching an image of the initial surface was taken with FIB. Then FIB milling was done normal to the sample surface which produced a 12x1x3.5 micron (length x width x depth) slot in the first experiment and a 20x1.5x6.5 micron slot in the second experiment. Finally the second image of the sample surface, capturing surface relaxation due to slotting, was registered with FIB. After that the slot profile was measured with a second cut across the slot.

The surface relaxation was measured with a 2D digital image correlation (DIC) method using FIB images. The raw output of the DIC method were displacement fields due to stress release after slotting. The maximum displacements on the slot flanks were only 20 nm.

The experimentally measured displacements were compared with those calculated with 3D finite element (FE) model of the test. A good qualitative and quantitative agreement was observed. Some disagreement between the FE model and the experimental results are attributed to the oversimplified FE model which used isotropic elastic material behaviour.

The paper will discuss ways of achieving optimal image quality with FIB imaging, creation and preservation of artificial surface patterns with FIB, effects of grain orientation on slot depth and measured displacement.

Keywords: focused ion beam (FIB), digital image correlation (DIC), slotting, steel, microscale, residual stress

S35

CHARACTERIZATION OF LONGITUDINAL RESIDUAL STRESSES IN FRICTION STIR WELDS USING THE CUT-COMPLIANCE TECHNIQUE

A.P. Reynolds, C. Canaday, University of South Carolina, Columbia, SC

Friction stir welding (FSW) was originally promoted by the inventors as being a very low to no residual stress welding technique. While under some conditions, joints made by FSW exhibit low residual stresses, this is not always the case. For example, it has been observed that fatigue crack growth behavior in friction stir welds is strongly influenced by residual stress. Friction stir welds, like other welds, are microstructurally heterogeneous, meaning that unstressed lattice spacing is not a constant across the weld. This situation complicates the use of diffraction techniques for stress determination. Mechanical methods of stress determination are not influenced by lattice parameter variation and may therefore be quite robust. In this presentation, we will present results of cut compliance residual stress determination in friction stir welds made in (1) aluminum alloy (thick plate and thin plate), (2) titanium alloy and (3) steel. Cut compliance residual stress results will be correlated with fatigue crack growth behavior and compared to residual stress determined by (1) the ACR (adjusted compliance ratio) method, (2) neutron diffraction, and (3) the contour method. Other examples will illustrate the use of cut compliance to determine the through thickness variation of the longitudinal residual stress in a thick aluminum plate FSW and verification of residual stress relief by mechanical stretching. In general, we have observed that cut compliance is a simple and accurate technique for determination of the average (averaged through thickness) longitudinal residual stress in a wide range of friction stir welds.

S69

RESIDUAL STRESS MEASUREMENTS IN STEEL BEAMS USING THE INCREMENTAL SLITTING TECHNIQUE

D.Z.L. Hodgson[1], D.J. Smith[1], A. Shterenlikht[1], M.B. Prime[2]
[1]Department of Mechanical Engineering, University of Bristol, Queen's Building, University Walk, Bristol BS8 1TR, UK
[2]Engineering Sciences and Applications Division, Los Alamos National Lab, Los Alamos, NM 87545

This paper examines the application of the incremental slitting technique for residual stress measurement to plastically deformed four-point bent beams and autogenously edge welded steel beams. Prior to application a series of finite element studies were carried out using Legendre polynomial stress fields to develop the necessary strain release matrix. This was conducted using the SIGINI user sub-routine for the ABAQUS FE code in conjunction with a least squares fit.

This study investigated the effects of the number of polynomials used to define the strain release matrix, the effect of elasto-plastic material properties on the method and the ability of the method to predict linear stress fields. Due to the over-determined nature of the least-squares approach appropriate selection of polynomial series order was necessary to develop the best prediction. When elasto-plastic material properties were used in the FE models very poor strain release matrices were created which lead to incorrect predictions. The effect of these properties in experimental situations also led to errors but this was limited to shallow depths and to gauges situated near the slit.

The specimens used for the plastic four-point bending were manufactured from ferritic steel with dimensions of width 10mm, depth 25mm and length 250mm. This allowed for the use of a plane stress analytical model. These experiments were conducted to allow a better understanding of the incremental slitting procedure and its experimental application. The measured stresses were found to be in reasonable agreement with the FE predictions.

A set of autogenously welded ferritic beams of width 10mm, depth 50mm and length 200mm were also measured. These beams were edge welded to create a through depth residual stress field. Residual stress measurements for two different weld torch speeds were obtained.

We show that a suitably chosen set of polynomials and gauge locations produce residual stress measurements with an uncertainty of about 7MPa. The paper discusses the influence of the number of terms in the polynomial expansion series and the measurement locations.

S22

DIFFRACTION ANALYSIS OF STRESS GRADIENTS IN TIN THIN FILMS: AN EXPLANATION FOR THE OCCURRENCE OF WHISKER FORMATION?

M. Sobiech[1,2], U. Welzel[1*], E.J. Mittemeijer[1], W. Hügel[2] and A. Seekamp[2]
[1]Max Planck Institute for Metals Research, Heisenbergstr. 3, D-70569 Stuttgart, Germany
[2]Robert Bosch GmbH, Dieselstraße 6, D-72770 Reutlingen, Germany
*contact author; u.welzel@mf.mpg.de

Sn thin films (layer thicknesses of some microns) on Cu substrates have been prepared by electrodeposition. Upon subsequent storage at ambient temperatures, Cu diffuses into the Sn thin film and the formation of an intermetallic compound η'-Cu_6Sn_5 takes place at the Cu/Sn-interface, and in particular also along the Sn grain boundaries intersecting the Sn/Cu interface. The η'-Cu_6Sn_5 formation is accompanied by a volume expansion and as a consequence, compressive residual stresses can be generated in the Sn thin films. During storage at ambient temperatures whiskers form on the Sn surface. Filamentary Sn-whisker growth can cause short circuits in microelectronic devises and therefore Sn-whiskers became a serious issue in high-reliability applications.

The microstructural development, phase formation and residual stress evolution during ageing at ambient temperatures have been investigated employing scanning electron and focused ion beam microscopy, electron backscatter diffraction, X-ray photoelectron spectroscopy and, in particular, X-ray diffraction. Residual stress gradients at different ageing times have been determined by means of laboratory X-ray diffraction measurements at controlled penetration/information depths. The driving force for spontaneous Sn-whisker formation will be related to the measured stress-depth gradients.

S15

MICRO STRESS ACCUMULATION IN MULTIPHASE SUPERALLOYS

J. Repper[1], M. Hofmann[1], C. Krempaszky[2], W. Petry[1], E. Werner[3]
[1]Forschungsneutronenquelle Heinz Maier-Leibnitz (FRM II), TU München, D-85747 Garching
[2]Christian-Doppler-Laboratory of Material Mechanics of High Performance Alloys, TU München, D-85748 Garching, Germany
[3]Institute for materials science and mechanics of materials, TU München, D-85747 Garching, Germany

The thermal and mechanical properties of high performance alloys are strongly affected by changes in the microstructure due to thermo-mechanical treatments during the production processes. In addition to changes in the microstructure this often goes along with the accumulation of macroscopic (type I) and microscopic (type II) residual stresses. While the effects leading to the evolution of macroscopic stresses are well understood, the exact microscopic mechanisms responsible for the accumulation of microscopic stresses are known only to a lesser extent. However, to understand mechanical behaviour of components made from complex materials like superalloys (e.g. Inconel 718) micro stresses can not be neglected. Micro stresses can be distinguished into two groups: Intergranular micro stresses originate from the elastic and plastic anisotropy of differently oriented grains, whereas interphase micro stresses result from the different micro-mechanical behaviour of different phases.

One method of choice to study the accumulation of micro stresses in dependence of the microstructural properties of matrix and precipitates (grain size, grain shape, volume fraction, type of precipitates, coherency…) are in-situ loading experiments using synchrotron and neutron diffraction. In this contribution we will present the results of a comprehensive diffraction study on Inconel 718 samples possessing different microstructures.

S27

RESIDUAL STRESSES AND LOAD PARTITIONING IN NOVEL METAL/CERAMIC COMPOSITES EXHIBITING LAMELLAR MICROSTRUCTURES

Siddhartha Roy, Alexander Wanner, Universität Karlsruhe (TH), Institut für Werkstoffkunde I, Kaiserstr. 12, D-76131 Karlsruhe, Germany
Jens Gibmeier, Hahn Meitner Institute Berlin, Structural Research Division, Albert-Einstein-Straße 15, D-12489 Berlin, Germany

The aim of our study is to analyze the mechanics of a new class of metal/ceramic composites on a mesoscopic length scale. These composites are produced by meltinfiltration of porous ceramic preforms produced by freeze-casting and sintering. This production route has a high application potential since it offers a cost-effective way to obtain composites with ceramic content in the range 30-70 vol%. The as-produced material exhibits a hierarchical domain structure with each domain composed of alternating layers of metallic and ceramic lamellae.
We have analyzed the residual stresses present in all phases present in composites produced by infiltrating alumina preforms with a autectic aluminium-silicon alloy. Integral as well as spatially resolved measurements were carried out on both singledomain and poly-domain samples at the high-energy, energy-dispersive diffraction (EDDI) beamline at the synchrotron radiation source BESSY (Berlin, Germany). Results show that considerable and strongly fluctuating residual stresses are introduced by the production process, which can be rationalized based on a mechanical model taking into account the thermal expansion mismatch of alloy and preform. First results from in situ compression tests shedding light on the internal load transfer from the soft and compliant alloy to the hard and stiff ceramic are also presented.

S31

SIZE EFFECT IN THE PLASTICITY OF MULTISCALE NANOFILAMENTARY Cu/Nb COMPOSITE WIRES DURING IN-SITU TENSILE TESTS UNDER NEUTRON BEAM

V. Vidal, L. Thilly*, P.O. Renault
PHYMAT, University of Poitiers, 86962 Futuroscope, France
U. Stuhr, S. Van Petegem, H. Van Swygenhoven
Paul Scherrer Institute, CH-5232 Villigen-PSI, Switzerland.
F. Lecouturier
Laboratoire National des Champs Magnétiques Pulsés, UPS-INSA-CNRS, 31400 Toulouse, France

Nanocomposite wires composed of a multiscale Cu matrix embedding Nb nanofilaments exhibit a high strength that results from a size effect in the finest Cu channels (single dislocation regime) and whisker-like behavior of the Nb nanofilaments (PMA 82 (2002) 925). In-situ tensile tests under neutron beam were performed at POLDI, PSI on nanocomposite wires composed of Nb nanofilaments with a diameter of 267nm and spacing of 45nm. The evolution of elastic strains and peak profiles versus applied stress evidenced the codeformation behavior with different elastic-plastic regimes: size effect is confirmed in the finest channels while the Nb nanowhiskers remain elastic up to the macroscopic failure, with a strong load transfer from the Cu matrix onto the Nb filaments. The measured yield stress in the finest Cu channels is in agreement with calculations based on a single dislocation regime (APL 88 (2006) 191906).

Furthermore the temperature dependence of the residual stress in the as-drawn wires was studied. We find that at room temperature the Nb filaments are in axial tension whereas the Cu channels are in axial compression. Since Cu and Nb exhibit very different thermal expansion coefficients this residual stress signature changed drastically at 77K and is expected to have an important influence on the mechanical properties of the wires.

S213

CHARACTERIZATION OF STRAINED SILICON ON INSULATOR (sSOI) SUBSTRATES USING HIGH-RESOLUTION X-RAY DIFFRACTION

Matthew Wormington[1*], Tamzin Lafford[2], Paul Ryan[2]
[1]Bede Scientific Inc., 14 Inverness Drive East, Suite H-100, Centennial, CO 80112, USA
[2]Bede plc, Belmont Business Park, Durham, DH1 1TW, UK
*Corresponding author email address: matthew.wormington@bede.com

For the past 40 years, tremendous progress has been made by the silicon semiconductor industry in its relentless pursuit of Moore's law. This progress has largely been achieved through lithographic scaling of the traditional CMOS transistor. In recent years, however, the industry has been forced to introduce new materials and processes to maintain the requisite improvements in transistor performance.

Strain engineering to improve the carrier mobility in advanced transistors was introduced at the 90 nm technology node and is now becoming widespread as the industry moves from the 65 nm to the 45 nm nodes. To date, local strain engineering approaches have been used. SiGe embedded in the source/drain regions of the transistor gives impressive mobility enhancements in PMOS devices by introducing compressive uniaxial strain into the channel region. SiN stressor layers deposited over the transistor can be made with compressive or tensile strains and have been used to enhance the mobility in both PMOS and NMOS devices.

As the industry moves forward, a number of companies and consortia are investigating global strain approaches using engineered substrates, such as strained silicon on insulator (sSOI). These substrates comprise a thin, strained layer of silicon bonded to an insulating oxide layer atop a silicon carrier wafer. The manufacturing process is quite complex. A very thin (~10 nm) Si layer is grown strained to a relaxed SiGe buffer layer grown on a donor Si wafer. The Si layer is bonded to an oxide layer atop a carrier wafer and then the SiGe is removed. The process must produce a layer that is free of defects and retains its strain both as delivered and during subsequent device processing.

X-ray diffraction is a well-known technique for measuring the strain in crystalline materials from small shifts in the position of their Bragg diffraction peaks. High resolution X-ray diffraction (HRXRD), employing crystal optics to condition the beam in both angle and divergence, is used to characterize single crystal substrates and epilayers. The conventional, out-of-plane, HRXRD technique has been used previously to characterize silicon on insulator (SOI) and strained SOI wafers. We will first show data from such measurements and describe what information is available together with the drawbacks of the technique for automated, fast measurement. We will then describe the in-plane HRXRD technique that we developed to address these issues. The technique uses the angular separation from two in-plane reflections to directly determine the strain and twist of the thin, strained Si layer with respect to the carrier wafer. Results from four bonded substrates (two SOI wafers and two sSOI wafers) will be presented to illustrate the technique.

S161

HIGH PRESSURE DEFORMATION STUDY OF ZIRCONIUM

S.C. Vogel*, D.W. Brown*, N. Nishiyama**, H. Reiche*, T.A. Sisneros*, H. M. Volz*, Y. Wang**, J. Zhang* and Y. Zhao*
*Los Alamos National Laboratory, Los Alamos, NM 87545, USA
**APS, Argonne, IL 60439, USA

In situ deformation studies of polycrystalline materials using diffraction are an established method to understand elastic and plastic deformation of materials. Parameters studied by diffraction are typically lattice strains and texture evolution, which in combination with the macroscopic flow curve allow improvements of predictive model. In situ uni-axial deformation at ambient conditions has been established over 10 years and in the last 5 years uni-axial deformation at temperatures above and below ambient have become routine. However, only few devices exist which allow deformation at high pressure and only a few investigations using these devices are reported in the literature. Here, we report results on a study of the uni-axial deformation of zirconium alloy (Zircaloy-2) at 2 and 5 GPa and ω-zirconium at the BM13 beamline at the Advanced Photon Source. The deformation-DIA apparatus generates a confining hydrostatic pressure using a cubic anvil setup. Two differential rams allow to increase (compressive) or decrease (tensile) the uni-axial loading in the vertical direction, resulting in plastic deformation at high pressures. The stress is measured from the lattice response while the macroscopic strain is measured using the beam line in radiography mode. In diffraction mode, diffraction of a monochromatic beam (λ=0.1901 Å) is detected using CCD detector. Deviations from Debye rings allow derivation of the lattice strains resulting from the uni-axial deformation. Intensity variations along the ring allow quantitative texture analysis. Both quantities are compared with our previous studies at ambient conditions for the same material. Our results indicate an increase in the twinning activity for the Zircaloy at elevated pressures whereas the ω- zirconium appears to deform by slip rather than twinning.

S59

IN-SITU X-RAY DIFFRACTION STUDY OF NANOCRYSTALLINE METALS

S. Brandstetter, S.Van Petegem*, J. Zimmermann, B. Schmitt, H. Van Swygenhoven
Paul Scherrer Institut, CH-5232 Villigen PSI, Switzerland

It is well known that the strength of metals increases with decreasing grain size, a behaviour that is well described by the phenomenological Hall-Petch relation down to grain sizes of 100 nm and even lower. Deformation mechanisms in coarse grained metals are based on a dislocation mechanism where dislocations are created during deformation with their propagation and multiplication being an essential mechanism for the resulting ductility and strength. Molecular dynamics simulations suggest that in nanocrystalline materials slip is generated at the grain boundaries (GB); dislocations nucleated at GBs propagate through the grains and are absorbed at the opposing GB, leaving no dislocation debris in the grain interiors (Acta Mat 54(2006)1975.

In order to understand the elastic and plastic deformation properties of nanocrystalline metals we have developed an in situ synchrotron X-ray-diffraction technique which allows the simultaneous measurement of many diffraction peaks continuously during mechanical testing, providing a direct link between the evolving microstructure and the macroscopic mechanical data (Rev. Sci. Instr. 77 (2006) 013902).

In this talk we will present new in-situ results obtained for nanocrystalline NiFe with a mean grain size of 20nm and compare them with results obtained from former in-situ experiments on electrodeposited Ni with mean grain sizes of 30nm.

For Ni we showed that during plastic deformation peak broadening is reversible upon unloading; hence, the deformation process does not build up a residual dislocation network (Science 304 (2004) 273). Furthermore it is shown that when the samples are deformed at 180K peak broadening is not fully reversible anymore. However, by then warming the sample to 300 K, peak broadening recovers to a great extent and all subsequent plastic deformation load/unload cycles are characterized again by a reversible peak broadening. The temperature-dependent residual peak broadening provides explicit evidence of a thermal component in the nanocrystalline deformation mechanism (Appl. Phys. Lett. 87 9(2005) 231910). By performing multiple load/unload cycles it is shown that different strain-hardening mechanisms in the micro- and macroplastic regimes are evident, and that the generally used 0.2% yield criteria does not correspond to the onset of macroscopic plasticity in all materials (Adv.. Mater. 18 (2006) 1545). The findings are discussed in light of recent results obtained from calculated X-ray diffraction spectra from computer generated atomic configurations (Acta Mat 56(2008) 165).

S77

NEUTRON DIFFRACTION STUDY OF INTERGRANULAR STRESS DEVELOPMENT IN AUSTENITIC STAINLESS STEEL WELD METAL

S. Sharma[1], M. Turski[2], R. Haigh[1], L. Edwards[1], M. E. Fitzpatrick[1]
[1]Materials Engineering, The Open University, Walton Hall, Milton Keynes MK7 6AA, UK
[2]Materials Performance Centre, A11 The Mill, Sackville St Campus, University of Manchester, Manchester M60 1QD, UK

Austenitic stainless steel is widely used in the nuclear power industry for its excellent resistance to corrosion and its good mechanical performance at high temperature. Many austenitic components are welded, and the properties of the weld metal will have a significant role in determining the overall structural integrity of welded plant. Weld metal can be highly anisotropic due to directional solidification and grain orientation. For structural integrity calculations it is very important to input the appropriate

elastic stiffness modulus for weld metal: the elastic modulus can vary considerably between different types of welds material, and even between different directions within the same weld.

We have investigated different austenitic stainless steel samples extracted from welds produced with different techniques and with different welding conditions. The materials investigated were 316 stainless steel using MMA welding, and 304 stainless steel using TIG welding.

In-situ deformation of the samples was performed on the ENGIN-X neutron diffractometer at the ISIS pulsed neutron source, UK. The samples were deformed in tension and compression, and the response of several diffraction peaks was monitored during deformation. A Rietveld analysis of the data was also performed to observe the overall lattice strain response to the applied load. The specimens were compressed up to 2% elastic strain.

There are large differences observed in the elastic response of the samples depending on the direction of applied loading. The macroscopic elastic modulus of the samples varies between 120 GPa and 220 GPa. The internal lattice plane responses vary, as expected, from a high stiffness response of the {111} planes (up to 280 GPa) to a low stiffness response of the {200} planes. There is good correlation between the observed crystallographic texture, the response of the individual planes, and the macroscopic elastic response. The elastic modulus of the weld metal is found to be highly directiondependent, and is influenced by the grain alignment within the weld.

The TIG weld material is shown to have a lower anisotropy in mechanical properties than the MMA weld, as a result of a less strong texture.

S201

A STUDY OF RESIDUAL STRESSES IN VACUUM PLASMA SPRAYED TUNGSTEN COATINGS

Tea-Sung Jun[1], Shu Yan Zhang[1], G. Thomas[2], P.S. Grant[2], A M Korsunsky[1]
[1]Dept of Engineering Science, University of Oxford, Parks Rd, Oxford, OX1 3PJ
[2]Dept of Materials, University of Oxford, Parks Rd, Oxford, OX1 3PH

Thick tungsten coatings are potential plasma facing materials in fusion reactors but the coefficient of thermal expansion (CTE) mismatch between W and Cu or steel substrates leads to large thermally induced stresses and premature failure. While inter-layers can be used to grade and distribute stresses away from a discrete planar tungsten-steel interface, in the present study an alternative approach was used based on patterning of the interface with repeating mm-scale 3D features or "sculptures". Up to 2mm thick W coatings were manufactured directly on water-cooled patterned substrates using vacuum plasma spraying (VPS), without any inter-layers. Synchrotron-based white beam, high energy X-ray diffraction measurements [1] of lattice parameters was used to obtain maps of residual strains and stresses in the VPS tungsten. Residual elastic lattice strains were deduced from energy-dispersive diffraction profiles collected by two detectors mounted in the horizontal and vertical diffraction planes, providing information about lattice strains in two nearly perpendicular directions lying in the plane of the coating. On the basis of these data, maps of residual stresses in the VPS coatings were constructed. The findings are discussed in the context of the geometry of the substrate-coating interface and any inelastic processes operating to relieve and manage successfully the thermal expansion mismatch induced stresses.

[1] A. M. Korsunsky, S. P. Collins, R. A. Owen, M. R. Daymond, S. Achtioui and K. E. James (2002) "Fast residual stress mapping using energy-dispersive synchrotron X-ray diffraction on station 16.3 at the SRS", J. Synchrotron Rad. **9**, 77-81.

S142

RESIDUAL STRESS PROFILES IN ALUMINA-ZIRCONIA CERAMIC COMPOSITES FABRICATED BY TAPE CASTING

J. Ruiz-Hervias[1], A. Steuwer[2], J. Gurauskis[3], T. Buslaps[4] and C. Baudin[3]
[1]Dpto. Ciencia Materiales, UPM, Profesor Aranguren, s/n, E-28040 Madrid, Spain
[2]FaME38, ILL-ESRF, 6 J. Horowitz, 38042 Grenoble, France
[3]Instituto de Ceramica y Vidrio (CSIC), Kelsen 5, E-28049 Madrid, Spain
[4]ESRF, 6 J. Horowitz, 38042 Grenoble, France

Multilayer ceramics were initially developed as laminated structures for the packaging of microelectronics. However, improved mechanical performance made them interesting materials for structural applications. One of the most promising systems is alumina-zirconia. Different laminate designs and methods to obtain multilayer ceramics with controlled layer thicknesses have been developed.

Ceramic composites are fabricated by stacking together different tapes previously fabricated by tape casting. It has been found that even if tapes with the same composition are used to fabricate the ceramic structure, the composite has better mechanical properties than the monolithic piece. In general, authors suggest that this behavior might be due to the development of some degree of texture in the microstructure, due to preferential orientation of the grains in the tapes, and/or anisotropic residual stresses originated by the pressing procedure followed to stack together the different tapes. Nevertheless, no conclusive data have been provided.

In the present work, alumina-zirconia ceramic laminates are studied. Two different compositions within Al_2O_3/YTZP (tetragonal ZrO_2 stabilized with 3 mol% Y_2O_3) system were investigated, containing 5 and 40 vol.% YTZP respectively. The processing route involved tape casting of individual tapes, stacking with gluing agent and pressing under low pressure to form the ceramic structure. Different stacking sequences were employed, including alternating layers of 5 and 40 vol.% YTZP. In addition, monolithic samples of the same composition were also fabricated for comparison. Through-thickness residual strain profiles were measured by synchrotron radiation in both phases (alumina and zirconia) along two directions: in-plane and normal. Measurements were performed in beamline ID15A (ESRF, Grenoble, France).

Previous measurements with neutron diffraction gave average strains through several ceramic tapes. However, in this case, the gauge volume (0.5x0.05 mm) and the step size employed (0.05 mm) are very small, thus allowing several measurements in each individual tape (approximately 0.5 mm thickness). This will provide additional data on the development of residual stresses in the ceramic composites, by probing the interaction between neighboring tapes.

S121

NEUTRON DIFFRACTION STUDIES ON STRAIN EVALUATION OF REBAR IN REINFORCED CONCRETE

Hiroshi SUZUKI, Japan Atomic Energy Agency
Manabu KANEMATSU, Tokyo University of Science
Koichi KUSUNOKI, Yokohama National University

It is typical method to measure the strains on a rebar in a reinforced concrete using strain gauges glued on the rebar. The waterproof treatment and wiring of the strain gauges, however, should affect the accuracy of the strain evaluation of the rebar in the reinforced concrete. Therefore, the neutron diffraction technique, which is nondestructive and noncontact technique, might be useful for measuring the strains of the rebar in the concrete accurately. It has been believed that the neutron studies on the concrete are quite difficult due to neutron absorption by the water in hydrated cement paste and the evaporative water in pore spaces. Sufficient dry curing, however, enables the strain measurement of the rebar even in the concrete using neutron diffraction. In this study, we applied the neutron diffraction technique to two kinds of the strain evaluation on the rebar in the reinforced concrete.

At first, the strain behavior on the rebar covered with the concrete blocks, the sizes of 50x50x150 mm^3 and 70x70x150 mm^3, was measured under uni-axial tensile condition. Measured strains in each stress condition well agreed with the stress-strain relation of rebar only. In addition, the stresses on the rebar in the reinforced concrete were measured. The compressive residual stress was generated in the rebar due to drying shrinkage. The share stresses in the rebar were 60% to 80% of the applied stresses, and the stress distribution near the cracks in the concrete were much scattered.

Secondly, the bond strength and the bond region between the rebar and the concrete were evaluated under the pulsating tension using neutron diffraction technique. Stress distributions on the rebar measured using neutron diffraction were different pattern from those measured using strain gauges. In particular, bond region evaluated using neutron diffraction was larger than that evaluated using strain gauges.

S26

RESIDUAL STRESSES OF EB-PVD THERMAL BARRIER COATINGS EXPOSED AT HIGH TEMERATURE

Kenji SUZUKI, Niigata University
Takahisa SHOBU, Japan Atomic Energy Agency
Keisuke TANAKA, Meijo University

The substrate material was nickel-based superalloy (In738LC), CoNiCrAlY was pressureless plasma-sprayed on the substrate as the bond coating. As the top coating, zirconia with 4 mol percents yittria was made by a electron beam-physical vapor deposition (EB-PVD) under rotating the substrate. The thickness of the bond coating was about 0.18mm, and the thickness of the top coating was about 0.12mm. The rotation speeds in the EB-PVD process were 5rpm, 10rpm and 20rpm. The specimens were exposed at 1273K for 200h in an atmosphere.

The in-plane residual stress was measured by a conventional X-ray method, and the outof- plane residual strain was measured by a strain scanning method with hard synchrotron X-rays. For the specimens with 5rpm and 10rpm, the in-plane compressive residual stresses were released by the high temperature exposure. For the specimen with 20rpm, the in-plane residual stress did not change by the high temperature exposure, because it was very small before exposing. The in-plane residual stress near the interface was a large compression. For the specimens with 5rpm and 10rpm, the out-of-plane stresses were small from the coating surface but became a compression near the interface. Both in-plane and out-of-plane residual stresses of the specimen with 20rpm were very small. From a viewpoint of reduction of the residual stress, the rotation speed of 20rpm was the excellent condition.

The EB-PVD TBC was made of columnar structure which consisted of a core and a peripheral part. The peripheral part had feather-like structure. According to the observation with a scanning electron microscope, the feather-like structure cohered and shrank after the high temperature exposure. The volume reduction of the columnar structure caused the release of the in-plane residual stresses.

S156

NEUTRON DIFFRACTION MEASUREMENTS ON A LARGE SIZE ROLLER BEARING RING

R.H. Vegter, SKF Engineering & Research Centre, Nieuwegein, The Netherlands
T. Pirling, Institut Laue-Langevin, Grenoble, France
M. Peel, European Synchrotron Radiation Facility, Grenoble, France

In common with many engineering applications the introduction of compressive surface stresses plays an important role in the performance of roller bearings. Since the introduced stress profiles depend on the treatment method and the necessary balancing tensile stresses may have unexpected consequences, it is necessary to quantify the stresses throughout the bearing. This can be difficult in large bearings as the requirements of spatial resolution to resolve the high gradients near the surface and high penetration to measure in the bulk are usually mutually exclusive. As a result it is necessary to combine multiple, complementary methods to solve the problem.

In this paper we present an investigation into the residual stresses in a large bearing ring of 700 mm diameter. The bulk stresses were determined using neutron diffraction at the SALSA beam line at the Institute Laue-Langevin (ILL), Grenoble, France. Two different set-ups were used, conventional slits and oscillating collimators. Thereby information was gathered from the whole cross-section of the large ring. The surface stresses were measured using laboratory X-rays combined with successive layer removal. X-ray diffraction was used to measure the residual stresses as well as the strain free lattice constant. Since the material has a hardness gradient, the strain free lattice constant was needed at a large number of positions in the bulk of the material.

S175

THE EFFECTS OF CASTING PARAMETERS AND HEAT TREATMENT ON RESIDUAL STRESSES AND MICROSTRUCTURE VARIATIONS OF AN Al-Si ALLOY

Mohsen Sadrossadat, Sten Johansson
Linköping University, Linköping , Sweden

Different casting parameters and heat treatment can change the microstructure and residual stresses of castings. The microstructure of Al-Si cast alloys are influenced by morphology of silicon particles (shape, size and distribution), aluminum grain size and dendrite parameters. Dimensional changes resulting from casting residual stresses can particularly affect the quality of near net shape castings. Suitable stress relieving treatment can decrease the extent of residual stresses of the cast parts.

In this research, the influence of casting process parameters such as modification, superheat temperature, mould hardness and mould design on residual stresses and microstructure of an Al-Si-Mn alloy have been investigated. Experiments were conducted with two different superheat (70 and 100 C), mould hardness (50 and 85), modification (unmodified and sr-modified) and two different casting designs. The microstructural changes associated with these parameters have been studied by optical microscopy, scanning electron microscopy and image analysis. The type and extent of residual stresses of all samples were determined using cutting method.

The results show that all of the mentioned casting parameters have clearly effects on residual stresses. The residual stresses decrease as the superheating temperature and mould hardness decrease. Modified structures show different amount of residual stresses. Residual stresses are dependent on casting design. The suitable stress relieving treatment for such a material was determined.

S90

RESIDUAL STRESS DISTRIBUTION BELOW SUBSURFACE CARBURIZED LAYER IN CARBON STEEL GEAR BY NEUTRON DIFFRACTION

Yoshihisa Sakaida [a], Motonori Kawauchi [a] and Michiya Manzanka [b]
[a] Dept. of Mech. Engineering, Shizuoka University, 3-5-1 Johoku, Hamamatsu, Japan.
[b] Motorcycle Headquarters, Yamaha Motor Co., Ltd., 1280 Nakajo, Hamamatsu, Japan

Residual strain and stress distributions below subsurface carburized layer in motorcycle transmission gear were nondestructively measured by neutron diffraction in order to understand deformation behavior of gear after carburizing and quenching. The material used in this study was chromium-molybdenum steel. The transmission gear was quenched and tempered after carburizing. Using cut gear, the carburized case depth was first determined by microscope and measuring hardness distribution. Second, diffraction angles below subsurface carburized layer were measured by scanning neutron beam of 2 millimeters-square along axial direction near the internal spline. The diffractions from Fe-110 and 211 planes were used, and axial, radial and hoop residual strains were obtained from the lattice spacing change. Reference coupon cubic specimens with a width of 2 millimeters were cut from the same carburized gear, and then lattice spacing was measured as stress-free one. Axial, radial and hoop residual stresses were calculated on the assumption that axial, radial and hoop residual strains were principal strains. As the results, each residual strain distribution near the internal spline along the axial direction was found to be not uniform in carburized gear. Large tensile residual strain parallel to the axial direction was generated in the shift fork groove. And tensile residual strains parallel to the axial and hoop directions were also generated in the gear wheel. Furthermore, the maximum tensile residual stress was

observed parallel to axial direction at the shift fork groove. By measuring residual stress distributions below subsurface carburized layer, the inside base layer of transmission gear was found to be locally deformed, and then the shape of gear was locally changed after carburizing and quenching.

S131

DEVELOPMENT OF INDUCTION SURFACE HARDENING PROCESS FOR SMALL DIAMETER CARBON STEEL

Daisuke SUZUKI, Koji YATSUSHIRO, Seiji SHIMIZU [a], Yoshio SUGITA [b], Motoki SAITO [c], Katsuhiko KUBOTA [d]
[a]Yamanashi Industrial Technology Center, Kofu, Yamanashi 400-0055, Japan
[b]YS Electronics, Kofu, Yamanashi 400-0043, Japan
[c]ASAKAWA HEAT TREATMENT, Nakakoma-Gun, Yamanashi 409-3853, Japan
[d]Marushin Heat Treatment, Kai , Yamanashi 400-0116, Japan

In case of Induction Hardening, the highly frequency generator brings shallow hardened layer. And hardening for smaller diameter specimen is enabled. In this study, we developed an induction surface hardening process with a super high frequency generator of 2MHz that almost had not been used general conventional process. The purpose of this study is to reduce distortion and to provide compressive residua stress for small diameter carbon steel in induction surface hardening.

Specimens (6mm in diameter) were hardened under various conditions of generator voltage and specimen transfer speed. Hardened specimens were evaluated by measuring residual stress distribution, cross-section observation and hardness distribution.

As a result, the depth of hardened layer was 0.4mm and hardness near the surface was 600HV brought about the best hardening condition. In addition, the maximum compressive residual stress of this specimen had nearly -500MPa at the surface in the longitudinal direction, and it decreased slightly from surface to center. However, in the hoop direction, compressive residual stress was -50 ~ -150MPa. This anisotropy was due to large thermal stress compared with the present induction hardening.

Furthermore, the best result in 3mm diameter specimen was the 0.09mm depth of hardened layer and the hardness near the surface was 600HV.

S209 NEUTRON DIFFRACTION MEASUREMENTS OF RESIDUAL STRESS IN WELDS FABRICATED FROM HIGHLY ANISOTROPIC MATERIALS

T.M. Holden[1], D.W. Brown[2], B. Clausen[2] and D.G. Carr[3]
[1]Northern Stress Technologies, Deep River, Ontario, Canada K0J 1P0
[2]Los Alamos Neutron Science Center, Los Alamos National Laboratory, Los Alamos, New Mexico 87545, USA
[3]Australian Nuclear Science and Technology Organisation, Lucas Heights, NSW, Australia

Neutron diffraction measurements have been made of the stresses in welds fabricated from Zircaloy, beryllium, titanium and uranium over the past couple of decades. These materials display easy and hard slip directions, and therefore are plastically anisotropic, elastic anisotropy and, in three of the above cases, coefficients of expansion which vary with the crystallographic direction. The plastic anisotropy often leads, through the manufacturing route, to strong texture in the parts to be joined but melting and consequent solidification then generate texture gradients through the weld. Melting may also cause gradients of lattice parameter of a chemical nature. The anisotropy of thermal expansion upon cooling always leads to thermal intergranular stresses upon which the weld stresses are superposed. The experiments must avoid the artifacts associated with texture or chemistry gradients and must take account of the intergranular effects. Examples of stress analysis, with various degrees of assurance, are presented which are drawn from neutron diffraction experiments on the above materials. The stresses associated with welding are usually found to be conventional in form even though the materials are anisotropic.

S122
RESIDUAL STRESS MEASUREMENT OF COARSE CRYSTAL GRAIN IN TITANIUM CASTING ALLOY BY NEUTRON DIFFRACTION

Masayuki Nishida[1], Ayumi Shiro[2], Tian Jing[3], M. Refai Muslih[4] and Takao Hanabusa[5]
[1]Kobe City College of Technology, Kobe, Hyogo, Japan
[2]Harbin institute of Technology, Harbin, China
[3]Neutron Scattering Lab., BATAN, PUSPIPTEK, Indonesia
[4]Tokushima University, Tokushima, Japan

Neutron stress measurement can detect strain and stress information in deep region because of large penetration ability of neutron beams. The present paper describes procedure and results in the residual stress measurement of titanium casting alloy by neutron diffraction. In this study, the three axial method using Hooke's equation was employed for neutron stress measurement. This method was applied to the two type samples of titanium casting alloy. One is a simple cylindrical shape. Another has relatively complicated shape of one which is nearly practical mechanical parts. Form the results of this study, both of two samples have large crystal grain which was grown up during casting manufacture process. Furthermore, the peak profile used to the stress measurement appears in very weak because of the HCP crystal system of titanium character. These conditions usually make difficult to measure the accuracy values of residual stresses. Therefore, it had to spend a long time to measure the satisfied data from titanium sample, and oscillating operation was emploied in this measurement. Regarding to the results of stress measurement, Residual stresses in the cylindrical sample change from the compressive state in the outer part to the tensile state in the inner part gradually. The other hand, residual stresses in the mechanical parts sample case had all compressive residual stresses in center position. It is seemed that these different between cylindrical sample and another one is effected from cooling history of manufacturing processes.

S107
INTERNAL STRESS GENERATION IN PURE TITANIUM DURING CYCLIC LOADING

Edward C. Oliver
ISIS Neutron Scattering Facility, STFC Rutherford Appleton Laboratory, Harwell Science and Innovation Campus, Didcot, OX11 0QX, United Kingdom
Mark R. Daymond
Department of Mechanical and Materials Engineering, Queen's University, Kingston, Ontario, K7L 3N6, Canada

The cyclic loading responses of hexagonal alloys are commonly characterized by tensile/compressive yield asymmetry, underpinned by mechanical anisotropy at the granular level coupled with crystallographic texture. This anisotropy can lead to the generation of large intergranular microstresses and differing intergranular stress responses during tensile and compressive straining. This paper presents a neutron diffraction study to examine the case of forward followed by reverse loading in IMI-125 commercially pure titanium plate for comparison to recent results for other hexagonal metals. The plate exhibited moderately strong texture with basal poles oriented primarily along the transverse direction with respect to rolling. Neutron diffraction spectra were recorded during uniaxial loading tests performed in tension-compression and compression-tension along the plate transverse direction, and in tensioncompression along the rolling direction. During straining along the transverse direction, large axial grain family lattice strains develop in the compressive part of the cycle, but are relieved during subsequent tensile loading. This behaviour is explained on the basis of the operation of a small degree of mechanical twinning. There is some evidence that twin formation is reversible. The results are discussed with comparison to the results of cyclic loading studies in magnesium alloys where mechanical twinning is the dominant deformation mode.

S176

APPLICABILITY OF THE SIN^2(Ψ) TILT METHOD IN NEUTRON STRAIN MAPPING

C.R. Hubbard, Oak Ridge National Laboratory, Oak Ridge, TN
R.A. LeMaster and J.V. Kolwyck – University of Tennessee at Martin, Martin, TN

The carburization of many steel parts, such as gears, presents a complexity for neutron strain mapping as the conventional method requires that the lattice spacing in the strainfree condition (d_0) be known at each location within the sample. However, residual stresses at the surface of carburized steel components are often measured using X-ray diffraction methods that utilize the $\sin^2(\psi)$ method. This method assumes that the stress normal to the surface is zero, and when this condition exists the need for d_0 is eliminated. With the depth of penetration of X-rays being limited to a few microns, the plane stress condition is frequently met. With X-rays, depth profiling can be accomplished using electro polishing to remove layers and repeating the X-ray stress measurements. Yet, due to the time required for electro polishing and the need for correction to the derived stresses due to the layer removal, the effective depth of stress mapping by X-rays is limited.

The low attenuation and consequential deeper penetration of neutrons is widely used for non-destructive measurement of stress within the bulk of components. Typically, the neutron stress measurement depth extends from tenths of a millimeter to several centimeters. In the neutron diffraction method the changes in d-spacing between stressed and unstressed states leads to the determination of strains and consequently the stresses as a function of location. Determination of d_0 as a function of depth, however, is required when chemical gradients exist. However, obtaining d_0 at each location when chemical gradients exist can be a significant challenge for the neutron diffraction method.

This paper presents the effort to assess the potential of applying the $\sin^2(\psi)$ method to neutron strain mapping in order to measure d_0 as a function of depth when the plane stress condition exists. Measurements of the d-spacing as a function of tilt angle and depth were made using the second generation Neutron Residual Stress Mapping Facility (NRSF2) at HFIR. Corrections for settings where the gage volume was partially buried in the sample were made based on measurements from an iron powder sample packed into a flat surface sample holder. Assuming the plane stress condition is valid and applying corrections for partial burial of the gage volume then one can calculate the in-plane stresses and the d_0 at each depth. Efforts to apply a neutron diffraction based $\sin^2(\psi)$ method to measuring the total stress in an un ground carburized spur gear will be presented.

The HTML User Program is sponsored by the U.S. Department of Energy, Office of Energy Efficiency and Renewable Energy, FreedomCAR and Vehicle Technologies Program. ORNL is managed by UT-Battelle, LLC for the U.S. Department of Energy under contract DE-AC05-00OR22725.

S42

GRAIN STATISTICS IN NEUTRON STRESS EXPERIMENT

Vladimir Luzin – Bragg Institute, ANSTO, Australia (Vladimir.Luzin@ansto.gov.au)

Every experimental scientist who has dealt with stress or/and texture measurements using neutron or X-ray radiation on coarse grained materials is familiar with the problem of "grain-size" or "grain statistics" caused by insufficient number of grains in the gauge volume. In a texture diffraction experiment, this leads to variations in the diffraction peak intensity and spots appearing pole figures. In diffraction stress measurements it can lead to large fluctuations in the apparent d-spacing values - even in stress free samples.

The impact of the grain statistics on the result of strain measurements is two-fold. Firstly, local stain variations are observed on the scale of grain size instead of the average value which is attributed to larger scale or sampling. Elastic anisotropy and particular orientations of individual grains, their local neighbourhoods and other micromechanical details all play role in this case.

Another aspect of grain statistics, which is less appreciated but can even be more important, is purely instrumental effects and it is directly related to the methodology of strain measurements. It arises from the fact that the experimentally measured strain on individual grains depends on the specific spatial arrangement of these grains within gauge volume. Particularly, the result of strain measurement on an individual grain is not the "true" strain but it depends on exact location of this grain within gauge volume. In that regard it is akin to another instrument related phenomenon, the "partial illumination" effect.

Theoretical and practical aspects of grain statistics effects are considered and treated numerically. Some experimental results are presented to illustrate our conclusions.

S11

ASSESSMENT OF MACHINING INDUCED NEAR-SURFACE DAMAGE ON THE BASIS OF X-RAY ELASTIC CONSTANTS

Wulf Pfeiffer, Bernhard Blug, Verena Fuhr, Eduard Reisacher
Fraunhofer Institute For Mechanics Of Materials (IWM)
Wöhlerstr. 11, 79108 Freiburg, Germnany

It is well known that voids, pores and cracks affect the elastic properties of materials. These discontinuities do not carry internal or external stresses and thus reduce the macroscopic Young's modulus. This has been proven for porous materials as well as for materials with high crack densities, e.g. thermal barrier coatings. Also for machining induced cracks in brittle materials, particularly mono-crystalline silicon, this has been proven through nano-indentation experiments and laser-acoustic methods.

This paper focuses on the barely investigated influence of mechanical machining procedures on the X-ray constants of elasticity (XEC) of silicon nitride ceramics. The XEC are used to determine (residual) stresses from lattice strains and thus are vitally for a quantative correct assessment of stress states. In addition, from the comparison of XECs of materials in perfect and damaged conditions, respectively, the amount of damage may be quantified. X-ray measurements of loading stresses are predestined for the assessment of machined near surface regions due to the high surface sensitivity of the method.

The results of our investigations yield an unreckoned high sensibility of the near surface XEC on different machining conditions. Differences in the XECs up to 100% could be determined for common grinding and polishing procedures. From the XEC a quantitative measure for crack sizes and densities could be evaluated using finiteelement modelling of cracked surfaces. Additionally performed nano-indentation experiments validate the ranking concerning the machining damage. In conclusion, the experimental determination of near-surface XEC of differently machined ceramics is regarded to be vitally for a quantitatively correct determination of macroscopic stresses and an efficient method to assess the near-surface integrity.

S29

A METHOD FOR DETERMINATION OF 2nd RANK STRAIN TENSOR FROM NANOCRYSTALLINE DIFFRACTION DATA AND ITS APPLICATION TO MICROMECHANICAL DEFORMATION

Apurva Mehta, Matt Bibee, SLAC/Stanford, Menlo Park, CA, USA
David Bronfenbrenner, UC Berkeley, Berkeley, CA, USA

When a material is subjected to an external load, the resultant mechanical deformation is a complex three-dimensional response function best captured by a second rank strain tensor. Further the resultant deformation comprises of several micromechanical modes. Traditionally these modes are classified as reversible (elastic) or irreversible (plastic), but in fact there are several more subclasses of micromechanical deformation and to understand the mechanical response of an advance material (such as superelastic NiTinol) it is often necessary to better understand the partitioning of the global (macromechanical) deformation into its constituent micromechanical modes.

The 3D local mechanical response of a component under external load can be visualized as an ellipsoidal distortion of a spherical surface centered at that point. The local strain in any direction is then measured as deviation from sphericity. Traditional strain measurements, which depend on measuring the deformation of an externally applied 1 or 2D gage, can only sample a limited portion of the strain ellipsoid. In addition, the spatial resolution of these measurements is several mm and it is impossible to distinguish between the different modes of deformation.

A technique of obtaining the deviatoric portion of the 2^{nd} rank strain tensor from white beam laue diffraction is well established when the crystallite size of the material is comparable or larger than the beam size. But because of extreme difficulty in obtaining a nanometer beam size with sufficient flux this technique fails for nanocrystalline materials. In here, we will show a multiwavelength focused beam X-ray powder diffraction technique using an area detector that overcomes all of the shortcomings of traditional strain determination in nanomaterials and yields the full (deviatoric + hydrostatic) 2^{nd} rank strain tensor.

In the second part of this talk we will apply this technique to obtain insight on several interesting issues in micromechanics, including the role of the first order phase transition in superelastic NiTi and remnant crystallographic elastic anisotropy in nanocrystalline metals.

S48

X-RAY DIFFRACTION AT CONSTANT PENETRATION DEPTH: A VIABLE APPROACH FOR CHARACTERIZING STEEP RESIDUAL STRESS GRADIENTS

T. Erbacher, E.ON Kernkraft, Hannover, Germany
A. Wanner, O. Vöhringer, Universität Karlsruhe, Karlsruhe, Germany
T. Beck, Forschungszentrum Jülich, Jülich, Germany

The experimental analysis of near-surface residual stresses by X-ray diffraction methods is based on measuring the spacings of lattice planes while the inclination ψ with respect to the surface plane is changed stepwise. A characteristic feature of conventional techniques is that the penetration depth of the X-rays is altered as inclination is varied. By simultaneously varying three different goniometer angles in a particular fashion, both the penetration depth and the measuring direction can be held constant while ψ is varied. Thus the normal and shear stresses can be derived from the $\sin^2\psi$ plots by means of standard evaluation procedures developed for gradient-free stress states. The depth profile of residual stress is then obtained via Laplace transformation of the results from several stress measurements carried out at different penetration depths.

The feasibility of this experimental approach for characterizing the strongly graded, non-equiaxed stress state existing at a machined surface is demonstrated. The results from constant-penetration-depth measurements on the ground surface of an engineering ceramic are compared with those from conventional $\sin^2\psi$ measurements.

S65

APPLICATION OF ENERGY-DISPERSIVE DIFFRACTION TO THE ANALYSIS OF HIGHLY INHOMOGENEOUS RESIDUAL STRESS FIELDS IN THIN FILM STRUCTURES

M. Klaus[1], W. Reimers[1], Ch. Genzel[2]
[1]Technische Universität Berlin, Ernst-Reuter-Platz 1, 10587 Berlin, Germany
[2]Hahn-Meitner-Institut Berlin, Glienicker Straße 100, 14109 Berlin, Germany

X-ray stress analysis (XSA) in polycrystalline thin films is usually performed by means of angle-dispersive (AD) diffraction methods with rather low-energy monochromatic X-rays between about 5 and 10 keV. AD thin film strain depth-profiling, however, is a time consuming and demanding procedure, which yields the in-plane residual stress distribution within the film but, as a consequence of the strong X-ray absorption, not in the near interface substrate zone.

Energy-dispersive (ED) diffraction in reflection geometry using high energy synchrotron radiation, on the other hand, has been applied so far only to stress gradient analysis in the near surface zone of mechanically treated bulk materials [1, 2], or as shown recently, in the interfacial substrate zone of coated WC inserts [3]. However, only little work has been done so far to use the information stored in the ED diffraction spectra for analyzing the film inherent stresses [4]. The main reasons therefor are the up to now rather small application of this method, the limited availability of suitable ED (synchrotron) sources and, perhaps, the unfounded idea that high energy diffraction and thin film stress analysis do not match up in an appropriate way.

In the presentation it will be shown that the ED diffraction method is even suitable for evaluating simultaneously steep stress gradients in thin films as well as the stress distribution in the interfacial substrate region beneath. The results which were obtained at the materials science beamline EDDI at BESSY [5] are in excellent agreement with conventional AD-XSA measurements performed in the lab, thus demonstrating that the ED method has the potential to become a powerful tool for fast and reliable thin film stress gradient analysis.

[1] H. Ruppersberg, I. Detemple, Mat. Sci. Eng. A161 (1993), 41.
[2] Ch. Genzel, C. Stock, W. Reimers, Mat. Sci. Eng. A372 (2004), 28.
[3] M. Klaus, Ch. Genzel, H. Holzschuh, Thin Solid Films, submitted.
[4] U. Zschenderlein, B. Kämpfe, B. Schultrich, G. Fritsche, Solid State Phenomena 130 (2007), 39.
[5] Ch. Genzel, I. A. Denks, J. Gibmeier, M. Klaus, G. Wagener, Nucl. Instr. Meth. A578 (2007), 23.

S158

DIFFRACTION STRESS MEASUREMENT ON COARSE GRAINED MATERIALS

Takao Hanabusa[1], Masayuki Nishida[2], Kazuya Kusaka[1]
[1]The University of Tokushima, Tokushima, Japan
[2]Kobe City Collage of Technology, Kobe, Japan

The present paper deals with the measurement of residual stresses in cast materials and/or a heat affected zone in welding part. The crystal grains in these parts grow in size due to the thermal history suffered in a sequence of process. In the case of stress measurement by X-ray or neutron diffraction, lattice strains in a group of crystals are measured by diffraction. In the $\sin^2\psi$ method of X-ray stress measurement, the diffraction intensity must be observed in any orientation in a plane containing the surface normal and the direction in which the stress will be evaluated. Neutron stress measurement normally necessitates three principal strains. These conditions are satisfied when a grain size is small enough with comparing to the X-ray or neutron irradiation volume.

In cases of cast materials and/or a heat-affected zone in a welding part, the grain size will be too large not to obtain diffraction intensities in an arbitrary orientation. An oscillation method intending to get diffraction in an objective orientation is a successful method in the case where the grain size is not so large. However, a more growth in size of crystals gives difficulties in observing diffraction intensities even by the oscillation method. The method proposed in this paper uses a rocking curve measurement. The strains measured in the orientations where the diffraction is observed in the rocking curve are applied to estimate principal strains. These strains are followed by the evaluation of stress components. The generalized method is explained and the experimental results on a coarse grained aluminum cast specimen are described.

S218

FROM SURFACE PROFILE TO RESIDUAL STRESS USING THE CONTOUR METHOD

Yuan-Shen Xiong, Joe Kelleher, Philipp Frankel, Philip Withers
Materials Science Centre, University of Manchester, Grosvenor St., Manchester M1 7HS, UK

The contour method has proven to be an elegant residual stress measurement technique, providing 2D stress data for a range of components. However, one of the factors limiting the accuracy of these measurements has been the inability to sufficiently describe the measured surface of the cut component. This problem has been most apparent in samples where sharp, localised, features have been present. The bivariate spline algorithms used previously have often suffered from either under-fitting of sharp features or over-fitting remotely to these features as they relied on a single knot spacing throughout the surface. Often a manual selection has also been required on the best knot spacing for a particular measurement, limiting the reproducibility of the technique.

This work describes the use of a modified bivariate spline algorithm to estimate displacement of surface contours and demonstrates its advantages for measuring residual stresses using the contour method. The raw data is mapped onto a variable grid, where the local densities and locations of vertices are determined by analyzing the distribution of the surface contour measurements. A grid fitting algorithm is included to minimise the edge effect commonly seen when the surface contour is extrapolated near the perimeter of the sample and fourier power spectrum analysis allows the optimal number of spline knots to be set by identifying and removing noise from surface measurements.

The effectiveness of the algorithm is demonstrated by comparing its results to those achieved with a uniform knot spacing. The new algorithm performs particularly well when both broad and narrow features are present in the same sample, describing the surface contour reliably while suppress the measurement noise. The use of efficient data analysis methods, such as FFT also allows to the technique to operate with much less CPU time than other fitting algorithms that rely on smoothing optimisation.

S113

MAPPING MULTIPLE RESIDUAL STRESS COMPONENTS USING THE CONTOUR METHOD AND SUPERPOSITION

P. Pagliaro, B. Zuccarello, University of Palermo, Palermo, Italy
M.B. Prime, B. Clausen, M.L. Lovato, M.L. Steinzig, H. Swenson, Los Alamos National Laboratory, Los Alamos, NM
J.S. Robinson, University of Limerick, Limerick, Ireland
G.S. Schajer, University of British Columbia, BC, Canada

The standard contour method determines the residual stress component normal to the plane of measurement. This talk presents extensions to the contour method to allow determination of multiple stress components. Two extensions are presented, both using additional stress measurements and then superposition to determine the original residual stresses. The first extension involves making additional cuts to determine stresses on multiple cut planes, using only the contour method. The second extension involves measuring in-plane stresses on the surface exposed by the original cut, using X-ray diffraction and hole drilling in this case. Experiments were preformed on indented disks of both 316L stainless steel and 2024-T351 aluminum. Results are compared with a finite element prediction and with stresses independently measured using neutron diffraction to show that the new theories are valid. Additional issues discussed will include the necessity to include a calibrated cyclic hardening model in the finite element simulation, difficulties in measuring surface stresses, and the repeatability of contour measurements on identical specimens.

S4

VALIDATION OF A NEW DEEP HOLE DRILLING (DHD) TECHNIQUE FOR MEASURING NEAR YIELD RESIDUAL STRESSES

A.H. Mahmoudi*, C.E. Truman, D.J. Smith and M.J. Pavier
Department of Mechanical Engineering, University of Bristol, Queen's Building, University Walk, Bristol BS8 1TR, UK
* Corresponding author (A.H.Mahmoudi@Bristol.ac.uk)

An accurate measurement of residual stresses is essential to determine their effect on the structural integrity of engineering components. Semi-destructive and destructive measurement techniques, involving cutting and removal of material, are the only methods that can be used to measure the stresses deep within large section components. Recently it has been shown that such mechanical measurement techniques can fail to measure the stresses correctly when the stresses are of high magnitude because plastic redistribution may occur when cutting is carried out. In previous work the authors developed a new deep hole drilling (DHD) technique that appears to have solved this problem.

In the present investigation the new DHD technique is validated using a variety of different residual stress fields. Shrink fit specimens have been used to generate axisymmetric and non-axisymmetric stress fields. Low yield stress aluminium alloys have been used to examine the performance of the technique when plasticity occurs. The results of the simulation were compared with experimental measurements and a very good correlation was observed.

S51

INFLUENCE OF COLD COMPRESSION ON THE RESIDUAL STRESSES IN 7449 FORGINGS

Jeremy S. Robinson
Department of Materials Science and Technology, Materials Surface Science Institute, University of Limerick, Ireland
Sayeed Hossain, Christopher E. Truman
Department of Mechanical Engineering, University of Bristol, UK
Edward C. Oliver
ISIS Facility, Rutherford Appleton Laboratory, Didcot, UK
Darren J. Hughes
Institut Laue Langevin, 6 rue Jules Horowitz, 38042 Grenoble, FRANCE
Matthew E. Fox, Materials Science Centre, University of Manchester, Manchester, UK

The aluminium alloy 7449 has very high compression strength and finds application, for example, as an aerospace upper wing skin alloy. Heat treatment includes cold water quenching from 470±5°C. Rapid cooling from this solution treatment temperature leads to the development of thermal gradients, which in turn result in thermal stress driven plasticity. The plastic deformation is inhomogeneously distributed which ultimately results in residual stresses when the thermal gradients have dissipated. The through-thickness residual stress distributions within three large rectilinear 7449 forgings have been determined using neutron diffraction. Two neutron diffraction instruments were used, ENGIN-X at ISIS, UK and SALSA at ILL, France. Two of the forgings had been stress relieved by cold compression and had significantly lower residual stress than the as-quenched forging. The neutron diffraction results are compared to measurements made by the new incremental deep hole drilling technique.

S84

DETERMINATION OF THE RESIDUAL STRESS FIELDS AROUND SCRATCHES IN Al ALLOYS

M.K. Khan[1], M.E. Fitzpatrick[1], L. Edwards[1], S.V. Hainsworth[2]
[1]Department of Materials Engineering, The Open University, Milton Keynes, MK7 6AA, UK
[2]Department of Engineering, University of Leicester, Leicester, LE1 7RH, UK

The use of high-strength and low-weight aluminium alloy parts is widespread in aerospace structural applications. Aluminium alloy parts help to reduce overall weight and, thus, to reduced energy consumption. During service and maintenance, small defects like scratches can occur, which can act as initiation sites for fatigue damage. The local residual stress field around the scratch will be a key factor in determining how much it influences fatigue life. The overall aim of the present study is to study residual stresses around scratches in aerospace Al materials.

Scratches of different depths and root radius were produced, in Al2024-T351 with and without a clad pure-Al layer, with repeated sliding of an automated sharp tool. During the scratching process there will be local hardening of the material owing to the passage of the tool, and residual stress generation. Synchrotron X-ray diffraction has been used to determine the residual strains around the tip of the scratches. Measurements were made in 2024 aluminium, and also in fine-grained 5091 aluminium to improve the spatial resolution with which the strain data could be obtained. The results show high (~100 MPa) tensile stress at the tip of the scribed notch, and that the stresses generated are dependent upon the tool used to make the scribe mark. There is a correlation between the stress at the notch time and the observed fatigue lives. Nanoindentation can be used to determine hardness and residual stresses local to the scratch tip from careful analysis of the nanoindentation load displacement curve. Additionally, the effect of residual stresses on the nanoindentation data can be modelled using Finite Element Analysis.

Here we present results from nanoindentation experiments and Finite Element modelling using ABAQUS. Stresses were introduced in material as an initial condition before indentation. The results of the simulation agree well with the observed trends in the nanoindentation response around the notch. The results from nanoindentation and FE modelling are finally compared to the results from the Synchroton X-ray diffraction and show a good correlation.

S71

RESIDUAL STRESSES IN A MACHINED AND SHRINK FITTED ASSEMBLIES

Bin Su, Foroogh Hossainzadeh, David Smith and Chris Truman
Department of Mechanical Engineering, University of Bristol, Queen's Building, University Walk, Bristol BS8 1TR, UK

A shrink-fit is a semi-permanent assembly system, widely used in industry, which is designed to resist the relative movement or transmit torque between two components. This done by creating high radial pressures at the interface of the constituent parts. Examples include fitting of gears to shafts to transmit torque and shrink fitted hard wearing sleeves to shafts for steel rolling mills. This paper presents measured and predicted residual stresses from a variety of shrink fitted assemblies, including aluminium alloys, stainless steel and cast irons. In a number of cases the sleeves shrink fitted to the shaft were subjected to prior machining or prior quenching to introduce initial residual stresses in the sleeve.

Residual stresses were measured using a combination of deep-hole drilling (DHD) and incremental centre hole drilling (ICHD) techniques. The ICHD method provided near surface residual stress measurements to depths up to about 1mm. The DHD method measured through thickness residual stresses along radial lines through the outer sleeve and into the shaft up to depths of 400mm. Results are shown for a variety of assemblies and reveal residual stress that are significantly different from both simple analysis and finite element studies. For example, prior machining introduced near surface compressive residual stresses, that is then expected to be counteracted by the near surface tensile shrink fit residual stresses. However, measurements reveal that this is not the case.

S45

PROCEDURES FOR NONDESTRUCTIVE RS-MEASUREMENTS OF INNER SURFACES OF BALL BEARING COMPONENTS

Jérémy Epp and Thomas Hirsch
Stiftung Institut fuer Werkstofftechnik, Badgasteiner Str. 3, 28359 Bremen, Germany

Thin walled ball bearing rings are sensitive to geometry and shape distortions caused by the sum of manufacturing processes. In the past only one single or a few X-ray diffraction measurements on the outer circumference were considered as representative for the complete part. Local differences at surfaces or across different cross sections as well as residual stress states on the inner surface often have been neglected due to insufficient measurement time, geometrical constraints and therefore high costs. In an ongoing research program, residual stress states in ball bearing rings have been identified as pronounced distortion potentials. A rough estimate for the determination of residual stress states after all steps of a manufacturing process of rings with diameters >100mm will easily lead to a hundred of measurements. These components in the sequence of manufacturing operations are not allowed to be cut for residual stress measurements. Therefore, more than one method has to be applied for the measurement of

outer and inner circumference. As state of the art residual stresses are determined by X-ray diffraction techniques. The use of micromagnetic methods is promising due to easier accessibility on inner surfaces and to the measurement time required. However any analysis by micromagnetic methods has to be calibrated by X-ray diffraction measurements. In this paper a procedure for nondestructive RS measurements on inner surfaces of cylindrical and tapered ball bearing is presented. As one example for the any manufacturing process the analysis of machining induced residual stresses has been investigated. 36 measurements in axial and tangential direction on the outer and inner surface of these rings with X-ray diffraction and micromagnetic methods form the database. The effect of different machining parameters was demonstrated. A combination of X-ray diffraction and micromagnetic measurement methods seem to be an interesting solution for a reliable characterization of components with an important gain of time compared to the use of X-ray diffraction analysis only.

S106

COMPLEMENTARITY OF EXPERIMENTAL AND NUMERICAL METHODS FOR DETERMINING RESIDUAL STRESS STATES

George Roy
Natural Resources Canada, CANMET/MTL, 568 Booth Street, Ottawa, Ontario, K1A 0G1, Canada

Residual stress states in engineering structures are determined usually by measuring components of stress tensors with depth below the material surface. There are destructive and nondestructive methods to measure strain tensor components and converting them into stress tensor components by a variety of techniques derived from constitutive (material) equations. In this study, four methods for determining the strain tensor components are presented: X-ray Diffraction (XRD), Magnetic Barkhausen Noise (MBN), Hole Drilling (HD), and Cut-and-Section (CS) methods; first two are nondestructive, and the third and fourth are semi-destructive and destructive, respectively. However, in many cases, the structures available for residual stress measurements are only parts of much more complex engineering structures. To determine the stress tensor in the complex structures, it is necessary to apply numerical methods in which the experimentally determined stress components are used as initial or boundary conditions in an iterative process to estimate the original stress state. An application of the experimental methods to measure residual stress states in one laboratory specimen, hydrogen-charged milled magnesium, and two industrial components, weld area of a gas pipeline and an L-shaped supporting column and will be presented. A complementarity of the experimental and two numerical methods, Finite Element Method and Boundary Element Method, to determine stress will be demonstrated.

S120

DETECTION OF SURFACE RESIDUAL STRESSES IN MATERIALS BY PHOTOACOUSTIC IMAGES OF MICROINDENTED AREAS

A.L.Glazov, K.L.Muratikov
Physical-Technical Institute of RAS, St.Petersburg, Russia.

The influence of the surface residual stresses on the photoacoustic images of indented ceramics and metals has been demonstrated. However, some details of the residual stress influence on the photoacoustic signal are not clear up to now. Therefore, in this work we have tried to clear up the situation by detailed theoretical and experimental investigations of the photoacoustic effect in indented ceramics and metals.

In a theoretical part of this work the theoretical non-linear model of the photoacoustic effect in stressed is presented. This theory expresses the influence of stresses on the photoacoustic signal by the dependence of elastic modulii and thermoelastic parameter of a material on stress. The developed theory has been used for analysis of experimental results and deformations produced by a.c. pump laser light due to the thermoelastic effect near the vertical crack tips in ceramics.

Experimental part of this work is based on a complex approach proposed by us recently which provides an opportunity to control thermal, thermoelastic and elastic parameters independently. This approach allows us to find out experimentally the mechanism of the residual stresses influence on the photoacoustic effect in various materials. It is demonstrated, for example, that in silicon nitride ceramic and composite Al_2O_3-SiC-Tic ceramic the dependence of the photoacoustic signal on the stress is related with the influence of residual stresses on its thermoelastic parameter.

In this work an experimental photoacoustic and photothermal investigation of the residual stresses has been made mostly on Vickers indented samples. Various images obtained on the indented ceramic and metal samples demonstrate the influence of the residual stresses and cracks on the photoacoustic and photothermal signals. It is shown that joint photoacoustic and laser thermal wave measurements can be used for a complex characterization and imaging of stresses fields near Vickers indentations. Based on the obtained experimental data on samples with the residual stresses and developed theory non-linear elastic and thermoelastic parameters of materials have been estimated. It is shown that they are in a good correspondence with the parameters obtained by different methods.

S57

RESIDUAL STRESSES ANALYSIS IN BRUSH-PLATED GALVANIC COATINGS DEPOSITED FROM NICKEL SULFATE ELECTROLYTE

H. Lille, J. Kõo, A. Ryabchikov
Estonian University of Life Sciences, Chair of Structural Mechanics and Engineering, Tartu, Estonia

Sometimes there arises the need to deposit a galvanic coating with a reasonable thickness in limited or selected surface areas of worn or mismachined large-sized parts. For this purpose, brush-plating (electrochemical metallizing) method has been employed [1]. Presence of residual stresses is typical for all coatings.

Residual stresses are investigated in hard coatings deposited from nickel sulfate electrolyte. To determine residual stresses, a conventional deformation method was used, where a coating is manually deposited on a strip substrate with slipping edges, which deforms without bending during deposition. The change in the axial strain of the free surface during the depositing process is measured by a self-temperature compensated strain gauge. The dependence of strain on coating thickness is used as experimental information. As the derivative of the strain parameter (whose values fluctuate to a great extent) in the calculation equations is presented in accordance with coating thickness, the experimental results were previously approximated by an analytical expression assuming that the dependence of residual stress on coating thickness is linear-fractional [2].

Residual stresses are also determined by the X- ray diffraction technique, based on the $\sin^2\psi$ method. Using the X- ray diffraction technique, residual stresses can be measured on the superficial layer of the coating at room temperature. For comparing the results obtained by the two methods, residual stresses determined by the deformation method at final coating thickness should be corrected taking into account thermal stresses. Uncertainties in measurement of residual stresses are evaluated.

The values of residual stresses determined in the surface layer, obtained by the mechanical and X-ray diffraction techniques, are comparable within a maximum limit of measurement uncertainty.

Keywords: strip substrate, coating, axial strain, X-ray diffraction, residual stress

References

1. M. Rubinstein. Electrochemical Metallizing. Van Norstrand Reinhold Company Inc., New York, 1987.
2. H. Lille, J. Kõo & T. Pihl. Proc. of the 3rd Int. Conf. DAAAM Nat. Est., Tallinn Technical University, Tallinn, Estonia, 2002, pp.185-188.

S82

RESIDUAL STRESSES IN COLD-DRAWN RODS: EFFECT OF AN ALTERNATIVE TREATMENT

J. Ruiz-Hervias[1], M. Hofmann[2], J. Rebelo-Kornmeier[2], V. Luzin[3], and M. Elices[1]
[1]Dpto. Ciencia Materiales, UPM, Profesor Aranguren, s/n, E-28040 Madrid, Spain
[2]FRM-II, TU München, Lichtenbergstr. 1, D-85747 Garching, Germany
[3]Bragg Institute, ANSTO, MENAI NSW 2234, Australia

Cold-drawn steel wires and rods are widely used in industry, i.e. for tyre (very thin wires) and concrete reinforcement (wires and rods). The fabrication process (cold-drawing) consists of pulling the wire through a conical die to reduce its diameter. Several steps are usually employed to achieve a large section reduction. The material deformation during the process is quite inhomogenous. Consequently, residual stresses are generated in the wires.

Wire manufacturers are aware of the problem and try to alleviate residual stresses by means of in-line post-drawing thermomechanical treatments. These treatments involve stretching the wire to a certain deformation at a moderate temperature. Other alternatives have been proposed, for example to subject the wires to a final drawing step with a very small section reduction (termed "skin pass"). However, its effectiveness in terms of residual stress reduction has not been assessed yet.

In this work, samples of single phase (ferrite) and two-phase (pearlite) steel rods were studied. Both were subjected to one drawing pass and some samples were given a second drawing pass with only a 1% section reduction ("skin pass"). Through-thickness residual strain profiles were measured by neutron diffraction in the ferrite phase along the three principal directions of the rods, namely radial, hoop and axial. Measurements were performed in the strain scanner StressSpec (FRM-II, Garching, Germany). The reference lattice spacing was measured in "comb-like" specimens fabricated by EDM.

The experimental data are very good, with narrow diffraction peaks and very low background. A significant residual stress development was found in the samples subjected to one drawing step, with compressive residual stresses at the rod center and tensile ones at the surface (especially the hoop and axial components). Stress balance is approximately fulfilled in the single phase (ferrite) rods. However, in the two-phase (pearlite) rods, the residual stress profiles are clearly unbalanced because the stresses in the second phase (cementite) could not be accounted for. The "skin pass" step produces a considerable reduction of the residual stresses, which makes it an interesting alternative to existing post-drawing treatments.

S100

NEUTRON DIFFRACTION STUDY OF INTERGRANULAR STRESS DEVELOPMENT IN ZR-2.5%NB

O. Zanellato[1], M.E. Fitzpatrick[1], M.R. Daymond[2], L. Edwards[1]
[1]The Open University, Keynes, UK
[2]Queen's University, Kingston, Canada

The harsh environment in the core of a nuclear reactor imposes high constraints for the choice of materials for structural components: materials need high corrosion resistance, good mechanical properties at high temperatures and must sustain their properties under high irradiation. Zr-2.5%Nb is a zirconium-based alloy which fulfils these criteria and has a low neutron cross section. Therefore it is used for the manufacture of pressure tubes in CANDU reactors, for example.
It is now well understood that Zr crystals, because of their hexagonal close packed structure at room temperature, present a strong plastic anisotropy [1]. In polycrystals, this anisotropy is responsible for the heterogeneity of grain-to-grain behaviour and the generation of high intergranular misfits after deformation. Moreover, the strong texture usually found in processed materials brings the anisotropy to a macroscopic level. It is therefore important to understand the mechanisms of deformation. The use of neutron diffraction during in-situ mechanical deformation has proven to be a real asset for such studies and much work has been performed on various alloy systems [2]. However some gaps remain in our understanding of how to link, model and predict the behaviours at the macro and micro scales. The influence of some parameters such as initial texture, grain size/shape and the initial intergranular stress state is also not very well identified.
This paper presents the results of a set of in-situ thermo-mechanical processes on coupons cut from a Zr2.5%Nb pressure tube. The experiment was performed in-situ at ENGIN-X, the engineering neutron diffractometer at ISIS, UK. A first set of samples were compressed at room temperature along the three processing directions and up to 10% deformation. Another two samples were briefly annealed in-situ up to 560°C and 620°C respectively and then compressed at room temperature.
During compression in the as received state, the macroscopic as well as the microscopic anisotropy were evidenced. As expected from the texture, the hoop direction was stronger than the other directions. The neutron diffraction results show that the 0002 reflections generally bear most of the load in the alpha hcp phase. In the rolling direction no such reflections are present and during compression along this direction the second phase undergoes very high strains. In the Poisson.s directions the intergranular strains are particularly high (up to 5000 microstrain). During annealing substantial changes in the diffraction spectra are evidence of the Beta phase decomposition. By comparing the initial and the post heat treatment d-spacings, it was found that some strain relief occurred.

[1] E. Tenckhoff, *Deformation Mechanisms, Texture and Anisotropy in Zirconium and Zircaloy,* ASTM, Philadelphia, 1988, p. 77.
[2] J. W. L. Pang, T. M. Holden, P. A. Turner, T. E. Mason, *Intergranular stresses in Zircaloy-2 with rod texture,* Acta Materialia 47 (1999), pp.373-383.

S102

RESIDUAL STRESSES IN METAL MATRIX COMPOSITES FOR HEAT SINK APPLICATIONS DURING THERMAL CYCLING

M. Schöbel[1], H.P. Degischer[1], T. Buslaps[2], M. di Michiel[2], T. Poeste[3], R. Schneider[3], S. Kleiner[4], J. Hemptenmacher[5], A. Herrmann[6]
TU Vienna[1], ESRF Grenoble[2], HMI Berlin[3], EMPA Thun[4], DLR Köln[5], IPP Garching[6]

Metal matrix composites with superior thermal properties are designed for heat sinks under extreme conditions like in power electronic devices or in prototype fusion reactor systems to avoid delamination between the heat generating part and the heat sink and to maintain high thermal flux. Materials with a low thermal expansion coefficient combined with a high thermal conductivity are needed. Particles as well as fibers with high thermal conductivity and low thermal expansion are embedded into high conducting metals. The thermal expansion mismatch between the reinforcements and the matrix metal causes high residual stresses already from cooling during processing. Debonding at the internal interfaces and plastic deformation of the matrix are expected. The long term stability of MMC is tested by in situ investigation of the residual stress levels during thermal cycling and the effects of different reinforcement structures and interface designs. Synchrotron and complementary neutron diffraction experiments are performed during thermal cycling to investigate thermal fatigue damage. In situ high resolution micro tomography reveals the debonding mechanisms in the μm scale. The void volume fraction changes with temperature and increases with the number of cycles. Void shrinkage is observed in interpenetrated composites during heating, whereas void growth is observed in diamond particle reinforced metals. SiC-monofilament fibers in Cu break during heating. Residual stresses decrease as soon as damage advances. Synchrotron radiation provides the means of stress measurements and tomography simultaneously during thermal cycling.

S141

RESIDUAL STRESSES AND IN-SITU MEASUREMENT OF PHASE TRANSFORMATION IN LOW TRANSFORMATION TEMPERATURE (LTT) WELDING MATERIALS

Thomas Kannengiesser[1], Arne Kromm[1], Michael Rethmeier[1] and Jens Gibmeier[2]
[1]Federal Institute for Materials Research and Testing (BAM), Unter den Eichen 87, 12205 Berlin, Germany
[2]Hahn-Meitner-Institute (HMI), c/o Bessy, Albert-Einstein-Straße 15, 12489 Berlin, Germany
e-mail: Thomas.Kannengiesser@bam.de

For the safety and cost efficiency of welded high-strength steel structures, precise knowledge of the level and distribution of welding- and cooling-specific stresses and residual stresses is essential, since they exert a decisive influence on strength, crack resistance, and finally on the bearable service load. This paper presents innovative filler materials, of which the phase transformation temperature was deliberately adjusted via the chemical composition. The transformation behaviour of these martensitic Low Transformation Temperature (LTT-) filler materials shows direct effects on the local residual stresses in the weld and the HAZ. This can purposefully be exploited to counteract the thermally induced shrinkage of the material and to produce significant compressive residual stresses in the weld. Also the stress build-up in surrounding structure is influenced.

Comparative welding experiments were carried out on 690 MPa base material using various LTT-filler materials. High energy radiation has been used for residual stress measurement and analysis of phase formation during heating and cooling cycles. Even the use of high energy synchrotron radiation makes it possible to detect the residual stress condition fast without destruction of material. Thereby, residual stress depth gradients can be determined simultaneously without removing material. In steel, gradients up to 150 μm can be resolved in such a way. Furthermore, the application of high energy radiation permits determination of residual stresses of any available residual austenite contents. Similarly, formation of phases and respective transformation temperatures can be analysed during thermal cycles to allow a correlation between phase formations and evolving phase specific stress distribution in the weld.

Investigations were carried out to determine the phase transformation behaviour of different LTT-filler materials. Transformation temperatures were identified using Single Sensor Differential Thermal Analyses (SS-DTA). Additionally Synchrotron radiation was used to measure the transformation kinetics of all involved crystalline phases during heating and cooling of a simulated weld thermal cycle. The investigations have demonstrated that targeted microstructure transformation favouring weld metal residual stresses can be observed when appropriate filler material alloy concepts are applied with specifically lowered M_s/M_f-temperatures.

S197

WHY SHOULD WE GIVE UP THE $\sin^2\psi$ AND ALL SIMILAR METHODS?

Balder Ortner, University Leoben, A-8700 Leoben, Austria

The equation

$$\varepsilon(r, hkl) = \Sigma F_{ij}(r, hkl)\sigma_{ij} \qquad (1)$$

which has been developed nearly 30 years ago by Dölle and Hauk, together with the well known least squares fit, now about 200 years old, provides us with a perfect tool for accurate data treatment in diffraction stress measurement. Eq. (1) is to be used if all six components of the stress tensor are unknown.

Eqs. (2) and (3) are derived from Eq. (1):

$$a(r, hkl) = a_0 + F_{11} a_0 \sigma_{11} + F_{22} a_0 \sigma_{22} + F_{12} a_0 \sigma_{12} \quad (2)$$

$$a(r, hkl) = a_0 + (F_{11} + F_{22}) a_0 \sigma \quad (3)$$

Eq. (2) and (3) are well suited for all cases where the unstressed lattice constant is not exactly known but if it is known that $\sigma_{33} = \sigma_{13} = \sigma_{23} = 0$, i.e. that there is a stress free surface. Eq. (2) is used when all in-plane components (σ_{11} , σ_{22} , σ_{12}) of the stress tensor are to be determined, whereas Eq. (3) is to be used if there exists a further extra condition, namely $\sigma_{11} = \sigma_{22}$ and $\sigma_{12} = 0$.

With Eq.(2) a system of simultaneous linear equations can be established which, together with the least squares fit should be used instead of the $\sin^2\psi$ method. But not only the $\sin^2\psi$ method could be replaced by a more sophisticated method, all other methods which have been developed following the principles of the $\sin^2\psi$ method can as well be replaced using one of the abovementioned equations.

It is shown that such a replacement of the $\sin^2\psi$, the Dölle-Hauk, the g, the f and other methods would be quite beneficial for different reasons. One of these benefits is a significant gain in accuracy.

All the advantages of using the proper equaion Eq. (1) (2) or (3) will be discussed briefly, the main part of the lecture will be to show the gain in accuracy.

[1] H. Dölle, J. Appl. Cryst. 12 (1979) 489—501

S164

LOAD PARTITIONING IN A DUPLEX STAINLESS STEEL WITH SURFACE STRENGTH GRADIENT AND RESIDUAL STRESSES

R. Lin Peng[1], J. Gibmeier[2], G.C. Chai[3], S. Johansson[1]
[1]Linköping University, Sweden
[2]Hahn-Meitner-Institut Berlin GmbH, Germany
[3]Sandvik Materials Technology, Sweden

Many manufacturing processes impose, intentionally or unintentionally, changes to the surface layer of engineering components, such that a strength gradient is induced and residual stresses are created. It is well known that such changes play an important role for the mechanical behavior of the components. In particular, it is well established that fatigue properties can be enhanced by a hardened surface layer with compressive residual stresses but reduced by a surface layer in tension. However, due to experimental difficulties, little work has been carried out to study the actual stress distribution across the load-carrying cross-section under external loading and to analyze the influence of load type, strength gradient and residual stresses on the induced load partitioning. Component failure is closely related to the local stress distribution and therefore such investigations on inhomogeneous load-sharing will not only help understand the true mechanisms for the development of material damage under the action of mechanical load but also provide valuable input for simulation and operation of engineering structures.

The purpose of the current work is to study the load-partitioning for superduplex stainless steel SAF 2507 with surface strength gradient and residual stresses by means of in-situ synchrotron energy dispersive diffraction. The steel used in the study was a 6.4 mm thick plate processed by hot rolling, having a microstructure of austenite and ferrite. The plate was solution treated, followed by surface mechanical treatment that introduced strain hardening and compressive stresses to a surface layer of about 0.2 mm. The in-situ experiment was carried out for two loading-unloading cycles with a larger peak plastic strain for the second cycle. Diffraction experiments in reflection geometry were employed to obtain stress information in the austenite and ferrite for the very surface layer (about 0.03 mm). Additional measurements in transmission mode were performed on the austenite and ferrite at 0.75 mm depth, the behaviour of which can be considered representative for the bulk of the specimen. The results reveal different behaviors for the surface layer and the bulk, which has generated macroscopic load transfer between the two regions during loading. In addition, hkl-plane dependent microstresses that play an important role for the load-sharing at microstructural level are observed in both regions. In the paper, the macroscopic loadsharing and interactions between the applied load and different structural features will be discussed.

S189

ASSESSMENT OF LOAD DISTRIBUTION IN DP 600 DUAL PHASE STEEL BY MEANS OF IN-SITU NEUTRON DIFFRACTION

M. Seefeldt, S. Dillien
K.U. Leuven, Kasteelpark Arenberg 44, bus 2450, B-3001 Heverlee (Leuven), Belgium

The load distribution in as-received and in cold rolled commercial DP600 dual phase steel sheet during in-situ uniaxial tensile tests was characterized by means of neutron diffraction. The material had a carbon content of 0.07 wt%, a martensite volume fraction of about 15% and initial ferrite and martensite grain sizes of about 10 and 3 μm, respectively. The as-received sheet had a thickness of 2.6 mm. Cold rolling was done down to 50 % thickness reduction. For the ferritic phase, the lattice plane spacings were measured for seven reflections in the three principal directions. The martensitic phase could not be probed due to its very low tetragonality and its rather low volume fraction. The tensile tests were done up to about 5 % deformation and in rolling

direction; so that the lattice plane spacings in rolling direction could be measured in a horizontal or "Young" setup and the ones in transverse and normal direction in a vertical or "Poisson" configuration. All measurements were done at the POLDI TOF-diffractometer with multiple pulse overlap at PSI, Switzerland.

For the as-received material, the curves of the lattice plane spacings as a function of the applied macroscopic stress gave evidence of a rather early onset of plastic deformation of the martensite at a phase stress of about 1 GPa, and of a surprisingly high work-hardening capacity of this phase. The load distribution among the two phases hardly changed throughout the fully plastic regime, indicating that the work-hardening behaviour of the martensite must be pretty close to the one of the ferrite. Moreover, in the elasto-plastic transition zone where the ferrite already deforms plastically, but the martensite still elastically, the differently oriented ferrite grains varied strongly in the evolution of the carried load fraction.

For the as-received material, all peaks remained perfectly symmetric and could be fitted with Gauss curves only throughout the whole tensile test. In the fully plastic regime, the peak FWHM evolved linearly with the square of the externally applied stress. Both observations together might indicate that little dislocation patterning took place in the ferrite phase during the test. For the cold-rolled material, on the contrary, a significant peak asymmetry evolved during straining, indicating dislocation patterning in the ferrite phase and/or the deformation-induced separation of the ferrite and martensite peaks.

S81

DEVELOPMENT OF MICROSTRESSES OF THE HOT EXTRUDED MAGNESIUM ALLOY AZ31 UNDER CYCLIC TESTING CONDITIONS

M. Huppmann, W. Reimers
Technische Universität Berlin, Ernst-Reuter-Platz 1, 10587 Berlin, Germany

Intensive work has been done during the last years in order to achieve a better understanding of the microstructural development of extruded or rolled magnesium alloys under external load [1-3].It could be shown that extruded profiles of magnesium exhibit a significant asymmetry of the mechanical properties which is known as Strength Differential Effect (SDE) and which is due to the low activation energy of the twinning system {1012}<1011> under compression [4].

In order to investigate the (hkl) dependent load partitioning under cyclic loading conditions in-situ stress measurements were performed at the beamline 7T-MPW at BESSY II. The measurements were carried out for the first load reversal with strain amplitude of 5% starting in the compressive regime and then continued in the tensile regime.

First results show that there is a strong hkl-dependence of the plastic deformation. It was observed that the {1010}-lattice planes take larger elastic strains than the {1011}- and the {1012}-lattice planes. This effect was especially significant in the tensile regime. Additionally the amount of the activated twin system {1012}<1011> under compressive load was determined by intensity measurements of the (1010)- and (0002)- reflections.

These findings are discussed in view of the underlying plastic deformation mechanisms and especially the role of twinning and de-twinning.

[1] S.R. Agnew, C.N. Tome, D.W. Brown, T.M. Holden, S.C. Vogel, Scr. Mater. 48 (2003), 1003-1008
[2] S.R. Agnew, C.N. Tome, D.W. Brown, T.M. Holden, S.C. Vogel, Mat. Sci. Eng. 9 (2005), 1-12
[3] S.-B. Yi, C.H.J. Davies, H.-G. Brokmeier et. al., Acta Mater. 54 (2006), 549-562
[4] M. H. Yoo, J. R. Morris, K.M. Ho, S. R. Agnew, Metall. Mater. Trans. A, 33A (2002), 813-822

S62

COMBINED IN SITU NEUTRON DIFFRACTION AND ACOUSTIC EMISSION INVESTIGATION OF THE DEFORMATION MECHANISMS IN MAGNESIUM ALLOYS

O. Muránsky [1], D.G. Carr [1], M.R. Barnett [2], E.C. Oliver [3]
[1] Australian Nuclear Science and Technology Organisation, PMB 1, Menai 2234, NSW, Australia; [2] School of Engineering, Deakin University, Pigdons Rd., Geelong 3217, Australia; [3]ISIS Facility, CCLRC Rutherford Appleton Laboratory, Chilton, Didcot OX11 0QK, UK

Increasing application of hcp magnesium alloys, mainly in the automotive industry requires detailed knowledge and understanding of deformation processes in these alloys. In order to obtain information on deformation processes in various magnesium alloys, we have combined *in situ* neutron diffraction (ND) and *in situ* acoustic emission (AE) in one experiment. Since both these techniques focus on different "signals", their combination may provide unique and comprehensive information on different slip and twinning deformation modes which are active at different stage of deformation.

For instance, previous *in situ* ND studies [1] have shown that newly formed twin grains are formed with a back stress which initially relieves internal stress in them relative to their parent grains but then develop internal stress more rapidly than the parent grains. However, it is not clear from ND work alone whether the twin volume fraction increases through twin nucleation or through twin growing. This is because ND is sensitive to the *overall twin population*, with no sense of either twin nucleation or twin growing. On the other hand, AE is not very accurate at measuring the overall twin population but it is sensitive to *twin nucleation* [3]. The combination of *in situ* ND with AE techniques thus provides a more complete set of information that helps to elucidate NDmeasured lattice plane strains in various grain orientations.

WITHDRAWN

In the current work we will demonstrate the usefulness of the combination of *in situ* neutron diffraction with simultaneous AE analysis.

[1] D.W. Brown, S.R. Agnew, M.A.M. Bourke, T.M. Holden, S.C. Vogel, C.N. Tomé, Mater. Sci. Eng. A 399 (2005) 1-12.
[2] S.R. Agnew, D.W. Brown, C.N. Tomé, Acta Mat. 54 (2006) 4841-4852.
[3] X.Y. Lou, M. Li, R.K. Boger, S.R. Agnew, R.H. Wagoner, Int J Plasticity 23 (2007) 44-86.

S198

EXPERIMENTAL DETERMINATION OF RESIDUAL STRESSES AROUND HYDRIDE BLISTERS IN ZrNb PRESSURE TUBES

J.R. Santisteban[1], A. Steuwer[2], G. Domizzi[3], M. Peel[4]
[1]Centro Atomico Bariloche, Bariloche, Argentina
[2]Fame38 at ESRF-ILL, Grenoble, France
[3]Centro Atomico Constituyentes, San Martin, Argentina
[4]ESRF, Grenoble, France

In CANDU nuclear power reactors, pressure tubes of cold-worked Zr-2.5Nb material are used in the reactor core at temperatures of ~300^{o}C. Appearance of hydride blisters due to unexpected contact of the tube with other reactor components are a possible mechanism for failure. The morphology of the precipitated hydrides and the propagation of cracks along the tube depend strongly on the stress field within the blister, and on the tube material around it.

We have measured strain and stress fields around a hydride blister grown on a section of a pressure tube of a CANDU nuclear reactor using synchrotron X-ray diffraction.

The blister was produced by the creation of a small cold spot (~200^{o}C) on the surface of a section of a pressure tube previously charged with a homogeneous hydrogen concentration of 300 ppm in weight. The tube sections were kept at bulk temperatures between 300^{o}C and 365^{o}C, over periods ranging from 430 hours to 3300 hours.

The experiments were performed on the wiggler beam line ID15 at the European Synchrotron Radiation Facility (ESRF), using polychromatic beam of high-energy X-rays between 60 keV and 300 keV. In these experiments the scattering angle fixed and the diffracted beam is discriminated on the basis of the photon energy.

For a specimen grown at 338^{o}C over 1000 hours we have determined the full stress tensor for a line passing through the centre of the blister and crossing the thickness of the tube, with a spatial resolution of ~100 μm. In the ZrNb matrix , the maximum macroscopic stress was (80±40)MPa at a distance ~0.4 mm away from the blister/matrix interface. 2D maps of the residual strain distribution around the blister along the radial, hoop and axial directions of the pressure tube have also been measured.

The present results are compared with finite elements simulations of the problem found in the literature.

S63

X-RAY STUDIES OF STRAINED SILICON ON INSULATOR

M. Bibee, A. Mehta, S. Brennan, P. Pianetta
Stanford Synchrotron Radiation Laboratory**,** Menlo Park, CA 94025

Strained Si on insulator (sSOI) is a promising substrate for future generations of CMOS technology. In sSOI, a thin surface layer of biaxially strained Si allows improved transistor performance through increased carrier mobility. An embedded SiO_2 layer provides insulation for overlying devices, allowing increased device operating speeds and decreased electrical power loss. Furthermore, sSOI is easily incorporated into standard semiconductor device fabrication processes.

Using epitaxy and wafer bonding technology, strained Si on insulator (sSOI) wafers can be reliably fabricated with large diameters (up to 12 inches). However, standard silicon device fabrication processes involve several moderate to high temperature (400-900°C) annealing sequences, which create opportunities for the strain in the thin (< 1 μm) Si layer to relax through formation of threading dislocations and other defects. These defects tend to lower the carrier mobility through scattering processes. Thus, an understanding of the mechanisms for the early stages of strain relaxation (specifically during heating) and the resultant dislocation nucleation is of great importance to widespread applicability of sSOI technology for fast devices. We present a study of the strain and defect pattern in sSOI wafers using synchrotron X-ray techniques. X-ray reflectivity measurements allowed characterization of the sSOI wafer structure, revealing several layers with a very high degree of flatness. High resolution X-ray diffraction (XRD) was used map the average strain and measure misalignment (due to wafer bonding) of the strained Si layer. The strained Si layer exhibited compressive strain normal to the sample surface and tensile strain inplane and was found to be aligned within a fraction of a degree to the crystal lattice of the bulk wafer substrate. XRD also provides information about defect patterns through its sensitivity to domain size and strain gradients. These properties were measured as a function of annealing time and temperature in order to track the evolution of defects during strain relaxation. Correlating these findings with nanoscopic and electrochemical tools promises to improve our understanding of strain relaxation and defect formation in sSOI.

S2

RESIDUAL STRESS RELAXATION IN WELDED JOINTS UNDER STATIC AND CYCLIC LOADING

Majid Farajian-Sohi, Thomas Nitschke-Pagel, Klaus Dilger
Institute of Joining and Welding, University of Braunschweig

Weld fatigue strength is currently the bottleneck in designing high performance and lightweight welded structures using advanced materials. Increased material utilization has necessitated increased consideration of the fatigue problem. In order to achieve a fatigue resistant welded structure, it is necessary to manage and control welding process related factors which reduce the fatigue strength of the welded structure and may lead to premature fatigue failures. These factors are sometimes present as welding defects and sometimes as inevitable and unwanted geometrical and metallurgical changes of the materials involved in the welding process. Beside material properties, loading condition, environmental aspects, geometrical features e.g. toe radius and angle, weld defects, it is well known that the influence of welding residual stresses should be taken in to consideration. The extent of the influence of the residual stresses on fatigue life is a matter of debate. Some researchers neglect the influence of the residual stresses in a case of a high quality weld and some respects the significance of the residual stresses on the fatigue strength. The uncertainty of residual stress effects on fatigue is based on the lack of knowledge in the behaviour of residual stress field. So far little information is available on the relaxation and redistribution of welding residual stress field under different types of loading e.g. thermal, static, cyclic and impact and also on the influence of the relaxation and redistribution on fatigue crack growth rate and propagation.

In this work welding residual stress behaviour in welded S235 and S355 steel specimens under static and cyclic loading were studied and the correlation between the relaxation and redistribution of the stress field and materials mechanical properties were studied. As it is known the assembly of welded components introduces residual stresses due to welding sequences and imperfect fit up which could be as detrimental as those induced by welding. In order to study these residual stresses, welding specimen were constrained in the middle of a 2 meter long I-beam during welding and kept constrained during four-point bend loading and the residual stress relaxation in these specimens were investigated.

S203

NEUTRON DIFFRACTION MEASUREMENT OF RESIDUAL STRESSES IN FRICTION STIR PROCESSED NANOCOMPOSITE SURFACE LAYER*

Hanbing Xu[1], Ke An[2], Jun Qu[1], Camden R. Hubbard[1], Zhili Feng[1], Xun-Li Wang[2]
[1]Materials Science and Technology Division, Oak Ridge National Laboratory
[2]Neutron Scattering Sciences Division, Oak Ridge National Laboratory

Friction stir processing (FSP) was successfully used to stir and mix nano-sized Al_2O_3 particles into a pure aluminum surface to form a nanocomposite layer up to 3 mm thick, which has demonstrated significantly improved surface hardness, yield strength, and wear-resistance without sacrificing the substrate ductility and conductivity. The Al_2O_3 particles were uniformly distributed in the aluminum matrix up to 15% volume fraction. Neutron diffraction analysis was conducted at HFIR to determine the residual stress distribution in the nanocomposite surface layer. For comparison, the residual stress of a pure aluminum surface that was processed identically but has no particle involved was also measured. Results showed that the residual strains of the Al matrix in the nanocomposite layer are tensile up to 1000με. The residual strains of the Al matrix in the aluminum without particles are small which are below 400με**.** The details of the results will be further discussed in the paper

* Research sponsored by the Laboratory Directed Research and Development Program of Oak Ridge National Laboratory, managed by UT-Battelle, LLC, for the U.S. Department of Energy under Contract No. DE-AC05-00OR22725

S152

RESIDUAL STRESS ANALYSIS OF ALUMINIUM WELDS WITH HIGH ENERGY SYNCHROTRON RADIATION AT THE HARWI II BEAMLINE

Torben Fischer, René V. Martins[1], Andreas Schreyer
GKSS Research Centre, Max-Planck-Str. 1, 21502 Geesthacht, Germany
[1]Joint Research Centre, Westerduinweg 3, 1755 LE Petten, The Netherlands

In civil aircraft production advanced welding techniques are used to reduce weight and production costs. The way towards a rivet-free aircraft is supported by laser beam welding (LBW) and the development of new weldable, high-strength aluminium alloys. In this study residual stresses in laser beam welded butt joints of aerospace grade aluminium alloy AA6056-T6 were characterized using high energy synchrotron radiation. Because of its improved corrosion resistance und good weldability alloy AA6056-T6 (AlMgSi) will substitute standard AA2024 alloy (AlCu) for the manufacturing of forthcoming aircraft fuselage skins. Al-sheets with a thickness of 3.2 mm and 6 mm were welded by a CO_2 laser beam. The metallographic analysis of the samples shows grains with a diameter up to 0.3 mm. This large grain size makes the measurements with high spatial resolution more difficult due to the poor grain statistics. The strain scanning was performed at the new high energy synchrotron beamline HARWI II of the GKSS research centre at HASYLAB in Hamburg, Germany. The use of high energetic photons from 80 keV – 120 keV enables diffraction experiments in a transmission geometry, which provides the information about the macroscopic stresses. A large sample-detector-distance ensures a high angular resolution for the peak position determination. The distance between the measuring points was 0.2 mm in the welding area and up to 2 mm in the base material. This yielded a very detailed profile of the residual stress for the longitudinal as well as the transversal component. Additionally, the influences of the gauge volume size and grain statistics on the strain measurements were systematically investigated. The results show that, with the given beam parameters, there exists an optimum gauge volume size for the peak position determination. For the t-joint configuration two dimensional stress maps were calculated from the data. For the near future an in-situ FSW experiment is planed to investigate the metallophysical processes during the welding.

S119

RESIDUAL STRESS MAPPING IN A PIPE WELD REPAIR USING HIGH ENERGY X-RAY DIFFRACTION

P.J. Bouchard[1], M. Turski[2] and L. Edwards[3]
(1) British Energy Generation Ltd., Barnett Way, Barnwood, Gloucester GL4 3RS, UK
(2) School of Materials, The University of Manchester, Grosvenor Street, Manchester, M1 7HS, UK
(3) Institute of Materials Engineering, Australian Nuclear Science and Technology Organisation, Menai, Sydney, NSW 2234, Austrialia

Weld repairs are introduced into pressure vessels and pipework, either as a result of remedial work to remove and make good initial fabrication defects, or as a consequence of reparation work to eliminate service-induced defects or degradation. Post weld heat treatment of stainless steel welds to relieve residual stress is generally not required by engineering construction codes and standards because of detrimental metallurgical effects. Thus in practice, weld repairs in stainless steel components are frequently returned to service duty in the as-welded state. Such weld repairs can severely compromise the life and structural integrity of industrial plant owing to strong three dimensional residual stress features that can be very different from those in original fabrication welds. Characterising complex residual stress fields in repaired pipework is a challenging undertaking whether by numerical modelling or experimental measurement.

This paper describes the first application of high energy X-ray diffraction (HEXRD) to measure residual strains in the vicinity of a short 'boat-shaped' repair in an Esshete 1250 austenitic stainless steel pipe butt weld. The test pipe was 600 mm long, and 35 mm thick, with a 180 mm outer diameter. Measurements were made at the European Synchrotron Radiation Facility on beam-line ID15A using energies in the range 0 - 300 keV. Both hoop and axial components of residual strain were measured simultaneously at more than 200 points, allowing maps of measured axial and hoop strains to be obtained on radial-hoop planes in the vicinity of the weld repair. The results give a unique insight into the distributions of strain and stress along the (circumferential) welding direction of a short length weld repair. In the HAZ the axial stress and strain maps show a classic global form; that is tension over the repair sector balanced by compression beyond the ends of the repair. The results suggest greatest stress levels concentrated beneath the repair capping pass, with a gradient in the concentration of weld cap residual stress that increases in the direction of welding.

S163

THE RELAXATION OF RESIDUAL WELDING STRESSES UPON PROGRESSIVE SECTIONING OF WELDS

J. Altenkirch[1,2], A. Steuwer[3], M.J. Peel[4], PJ Withers[1]
[1]Manchester Materials Science Centre, Grosvenor Street, Manchester M17HS, UK
[2]ILL, 6 rue J Horowitz, 38042 Grenoble, France
[3]ESS Scandinavia Secretariat, Stora Algatan 4, 22350 Lund, Sweden
[4]ESRF, 6 rue J Horowitz, 38042 Grenoble, France

Residual stress measurements are often undertaken in reference samples which are sectioned from large components, yet it remains unclear to what extend the residual welding stresses are representative of those stresses present in the entire welded engineering component. This is particularly the case for neutron or synchrotron X-ray diffraction based residual stress measurements, as the samples have to be transported to the institutions, and fulfil the dimensional constraints of the individual beam lines. We present a systematic study using different materials and welding methods to produce butt welds that afterwards have been progressively sectioned and at each length the residual welding stresses were determined.

Significant relaxation of the residual stresses was observed when the weld length is reduced to a multiple of the width of the weld path, which in turn determines the width of the tensile zone of the residual welding stresses. We found that the stress relaxation behaviour can be described with a simple mathematical equation, based on the characteristic length scales of the weld, which is presented in this work.

S94

STUDY ON THE EFFECT OF WELDING RESIDUAL STRESSES ON CRACK-TIP CONSTRAINT

X. B. Ren [a], Z. L. Zhang [a*] and B. Nyhus [b]
[a] Department of Structure Engineering, Norwegian University of science and Technology (NTNU),N- 7491 Trondheim, Norway
[b] SINTEF Material and Chemistry, N-7465Trondheim, Norway
* Corresponding author: zhiliang.zhang@ntnu.no

Welding residual stresses are unavoidable and play a crucial role in integrity assessment procedure. Proper treatment of the welding residual stresses in integrity assessment becomes increasingly important when high strength steels are widely used in the offshore industry. This study focuses on the effect of residual stresses on crack-tip constraint. Modified boundary layer models with remote displacement field controlled by a *K-field* and *T-stress* were used. A two-dimensional residual stress field was introduced into the model by the eigenstrain method. The results show that residual stresses can increase the crack tip constraint. However, the residual stress induced crack tip constraint decreases with the increase of external loading. It has also been found that the effect of residual stresses is coupled with the T stress and becomes less significant when the *T* stress is positive.

Key words: Residual stresses; Crack-tip constraint; Failure assessment

S155

INVESTIGATION OF RESIDUAL STRESS DISTRIBUTION IN FERRITIC STEEL WELD MEASURED BY NEUTRON AND SYNCHROTRON DIFFRACTION

Paradowska, A.M.[1], Price, J.W.H. [2], Finlayson, T.R.[3], Lienert U.[4], Blevins, R.[5], Ibrahim, R. [2]
[1] ISIS Facility, Science and Technology Facility Council, Rutherford Appleton Laboratory, OX11 0QX, United Kingdom, a.paradowska@rl.ac.uk
[2] Mechanical Engineering Department, Monash University, VIC 3800, Australia.
[3] School of Physics, The University of Melbourne, VIC 3010, Australia.
[4] Advanced Photon Source, Argonne National Laboratory, 9700 South Cass Ave. Argonne, IL 60439, USA.
[5] Institute of Materials and Engineering Science, ANSTO, Lucas Heights, NSW 2234, Australia.

Over the last decade, there has been a growing interest in a better understanding of welding residual stresses in engineering components. Residual stresses have a significant effect on corrosion, fracture resistance, creep and corrosion/fatigue performance and a full understanding of these stresses is desirable. Therefore, experimental measurements are essential to establish a quantitative understanding of the sign, magnitude and distribution of the residual stresses around the repair, within acceptable limits.

In this research high energy synchrotron (70 keV) radiation (at the Advanced Photon Source, Chicago, USA) and thermal neutrons (at the HIFAR Research Reactor, Lucas Heights, Australia) have been employed to investigate and compare the residual stress characteristics in fully restrained, steel, butt weld. The focus of the measurements is on the values of the sub-surface and through-thickness strain/stress variation in the middle of the weld. The advantages and limitations of the techniques have been addressed, in relation to the gauge volume, stress-free, reference sample and positioning. The measurements of residual stress around the weld achieved in this work significantly improve the resolution at which residual stress in welded components has been measured.

S47

MEASUREMENT OF RESIDUAL STRESSES IN LASER WELDED EDDS AND IFS PLATES USING XRD

C. Sunil Kishore, Sri Venkateswara College of Engineering, Anna University, Tamilnadu, India

S186

X-RAY MICRODIFFRACTION TECHNIQUES FOR MEASURING LOCAL MICROSTRUCTURE AND STRAIN DISTRIBUTIONS

J.D. Budai[1], B.C. Larson[1], G.E. Ice[1], W. Liu[2], J.Z. Tischler[1], T.Z. Ward[1] and D.D. Sarma[3]
[1]Oak Ridge National Laboratory, Oak Ridge, TN 37831
[2]Argonne National Laboratory, Argonne, IL 60439
[3]Indian Institute of Science, Bangalore, India

The physical properties of materials are generally determined by local structural and chemical inhomogeneities such as grain morphologies, precipitates or residual stress distributions. Spatially-resolved, nondestructive, quantitative measurements of such inhomogeneities can now be obtained using microdiffraction and microfluorescence techniques at high-brightness synchrotron facilities. At the XOR-UNI beamline at the Advanced Photon Source (APS), we have developed a polychromatic scanning microbeam capability with submicron spatial resolution in three-dimensions (3D). This structural probe provides real-space maps of the local crystal structure, orientation and strain tensor, and hence provides a new tool for understanding the role of mesoscale defects in determining materials behavior.

In this approach, broad-spectrum (~8-22 keV) undulator radiation is focused using a pair of achromatic Kirkpatrick-Baez (K-B) reflecting mirrors. Beam diameters of ~500 nm FWHM are now typical, and 90 nm focus has been demonstrated. The small beam size provides spatial resolution in two dimensions. Resolution in the third dimension (along the incident X-ray beam path) is accomplished by a scanning-wire differential aperture technique which uniquely determines the depth dependence for scattered X-rays [1]. Computer analysis of depth-resolved, white-beam Laue diffraction patterns yields the crystal structure, orientation and deviatoric strain tensor for each ~micronsized local volume element in the sample. In addition, monochromator scans can be employed to determine the absolute strain tensor. Thus, a four-dimensional scan (x-y sample positions, wire, and energy) provides a full, quantitative 3D map of the microstructure inside a bulk sample. This microdiffraction technique has been applied in studies on a variety of 1D, 2D and 3D materials systems and processes, including nanostructures, thin films, grain growth and deformation microstructures. We will illustrate local strain mapping in epitaxial films and in directionally-solidified, phaseseparated eutectic manganite systems.
[1] B.C. Larson *et al*, Nature **415**, 887 (2002).

Support by DOE Office of Science, Division of Materials Sciences and Engineering under contract with ORNL, managed by UT-Battelle; XOR-UNI and APS supported by DOE-BES.

S52

SMALLER IS STRONGER: IN-SITU LAUE DIFFRACTION

R. Maaß, J. Zimmermann, S.Van Petegem, H. Van Swygenhoven*
Paul Scherrer Institut, CH-5232 Villigen PSI, Switzerland

Plasticity in single crystal micron sized pillars has gained considerable interest since the development of the micro compression technique and the observation of a “smaller is stronger” effect with decreasing pillar diameter. Plastic deformation is often observed as individual slip events that are reflected in discrete strain bursts. Large scattering among the data is reported, where pillars of similar orientation are deforming according to different slip systems, sometimes shearing-off or barrelling. To address the scattering among the data, to understand the mechanism behind the increase in strength in terms of existing or new theories, one needs information on the microstructural details of the sample before, during and after deformation.

An in-situ micro compression device has been developed at the Swiss Light Source (SLS) allowing the continuous measurement of time-resolved white beam Laue diffraction patterns during compression of micron-sized pillars, capturing the initial microstructure and the changes in microstructure during deformation. Former measurements have for instance demonstrated the presence of initial strain gradients and their role on the deformation mechanisms activated during compression (PRL, 99(2007)145505) or evidenced classical type-II hardening in spite of higher yield stresses (APL 92(2008) 71905. On the other hand, Laue analysis also evidenced for some pillars the presence of microstructural characteristics (such as a low angle grain boundary) precluding them from the realm of single crystal plasticity and thus allowing for a reduction of the scatter among measurements, since these pillars no longer belong to the domain of the statistically unknown (APL 91(2007)131909).

Here we provide an overview of former results and present a new series of in-situ Laue diffraction experiments performed on Cu, Ni, Au and Al pillars with diameters between 1 to 10 micron, made in different laboratories using different FIB procedures. The results emphasize (1) microstructural defects that do not belong to the single crystal domain, (2) evolution of the microstructure during compression evidencing the complex boundary conditions of a micro-compression technique, and (3) the increase in strength when the pillar diameter gets smaller. The results will be discussed in terms of existing and new developing dislocation based theories addressing “smaller is stronger”.

S132

SPATIALLY RESOLVED STRAIN MEASUREMENTS ON MICRO MOULDS

Andreas Kienzler, Brando Okolo, Volker Schulze, Alexander Wanner, Detlef Löhe
Institut für Werkstoffkunde I, Universität Karlsruhe (TH), Kaiserstrasse 12, D-76131 Karlsruhe, Germany

Advanced production technologies for micro components, such as micro powder injection molding, require the fabrication of precise and reliable micro molds. Such molds are frequently fabricated from polycrystalline alloys by micro milling. The residual stresses introduced by the fabrication process may affect the dimensional stability and the lifetime of the molds under the cyclic thermal and mechanical loads imposed during service. The quantification of the residual stresses in such micro molds is essential for reliability considerations. It is, however, a challenging task to analyze these stresses experimentally on the relevant micrometer length scale.

The present study is conducted within the scope of the Deutsche Forschungsgemeinschaft (DFG) Collaborative Research Centre 499, "Development, production and quality assurance of molded micro components made out of metallic and ceramic materials". Steel micro moulds produced by micro milling of previously ground surfaces were investigated in the as-ground, as-milled and post treated (by micro peening) states, using the synchrotron X-ray diffraction set-up MAXIM available at the G3 beamline of HASYLAB - DESY Hamburg Germany. The MAXIM set-up has a spatial resolution of 13 µm which ensures that the strains laterally distributed over the micro mold specimen are measured in great detail. Our results show that micro milling significantly alters the surface-near residual stress state. Peening of the as-milled surface using a variety of shot materials (such as silicon carbide, corundum and glass) in the size range of 10 - 20 µm, leads to compressive residual stresses in the order of about 850 MPa. The trace marks created by the milling tool vanish due to the peening and residual stresses are homogenously distributed over the impacted surface.

S146

DETERMINATION OF STRESS AND TEXTURE GRADIENT IN CdTe THICK FILMS USING A HIGH ENERGY WHITE MICROBEAM

Patrice GERGAUD[a], Vincent CONSONNI[a], Guy FEUILLET[a], Thomas BUSLAPS[b]
[a] CEA-LETI, MINATEC, 17 rue des Martyrs 38054 Grenoble cedex 9, France
[b] European Synchrotron Radiation Facility, 6 rue Jules Horowitz, BP 220, 38043 Grenoble, France

Polycrystalline CdTe is being developed for its use as photoconductor in optoelectronic applications where large dimensions are required such as X-ray detectors in the medical field. This material is grown by close space sublimation (CSS): a CdTe solid source is evaporated and then the vapours are condensed on a graphite substrate located at a very close distance. In order to ensure an efficient collection of the charge carriers towards the electrodes, the control of the structural quality of the material such as its texture, its crystalline morphology (grain structure, diameter, and their distribution, nature of point and extended defects [1]…) and its stress state during the growth is of primary importance, in particular its variation along the thickness of the layer. Previous experimental studies such as X-ray diffraction (XRD) measurements and electron backscattered diffraction (EBSD) maps have shown that, as growth proceeds, the material is gradually textured along the <111> crystallographic orientation. It has been also observed that the crystalline morphology and the related texture depend on the different growth stages at work during growth such as nucleation of isolated islands, coalescence, and thickening: indeed, although isolated islands are randomly oriented, when island coalescence occurs, the film tends to be preferentially oriented along particular crystallographic directions. The different structural changes as growth proceeds are thus likely to generate distinct stress states along the thickness of the material [2].

The study of these stresses and their distribution in thickness as a function of the evolution of the structural properties such as local texture and local grain morphology would give some new insight into the elastic and plastic energy dissipation processes during the different growth stages: furthermore, it would enable us to provide a more accurate modelling of these phenomena.

For this purpose, we used high energy synchrotron diffraction following the method introduced by Reimers et al [3]. We used a white beam on ID15A at ESRF and by energy dispersive measurements, we measured the stress and texture gradient in thick (from a few tens to a few hundreds of µm) CdTe films. Due to the high intensity and the high parallelism of the high energy synchrotron radiation the sample gauge volume has been reduced to approximately 5 µm x 0,1 mm x 3 mm and we followed by step of 5 µm, the texture and stress of the film across the thickness.

In this paper, we will describe the experiments, the first results and we shall detail the absorption corrections needed to evaluate quantitatively and accurately the texture and stress in such films. A model is then proposed to explain the observed texture and stress evolution with film thickness.

[1] V. Consonni, G. Feuillet, and S. Renet, J. Appl. Phys. 99, 053502 (2006)
[2] V. Consonni, G. Feuillet, and P. Gergaud, Accepted in J. Appl. Phys. (2008)
[3] W. Reimers, M. Broda, G. Brusch, D. Dantz, K.-D. Liss, A. Pyzalla, T. Schmackers and T. Tschentscher, Journal of Nondestructive Evaluation, Vol. 17, No. 3, 1998

S88

NANOSCALE DIFFRACTION MICROSCOPY AT THE CNM/APS HARD X-RAY NANOPROBE BEAMLINE

M. Holt, J. Maser, R. Winarski, V. Rose, G.B. Stephenson, Argonne National Laboratory, Argonne, IL

The near-term commissioning of the Hard X-ray Nanoprobe Beamline at sector 26 of the Advanced Photon Source as part of the Center for Nanoscale Materials will provide a dedicated facility for hard X-ray diffraction microscopy at a landmark 30nm spatial resolution. Integrating a high-brightness synchrotron X-ray beamline with an advanced optomechanical experimental platform at an energy range of 3-30keV will make possible nanoscale diffraction studies of functional nanomaterials with a high degree of precision at a previously unavailable resolution. The unique capabilities of hard X-ray microscopy techniques such as large penetration depths, high sensitivity to elemental composition, crystallographic phase, and strain when applied at this length scale offer unique opportunities for many fields of science. As well, coherent diffraction techniques make possible the study of static and dynamic disorder and phase-sensitive imaging at a spatial resolution in principle beyond that of the probe itself. The challenges and scientific impact of extending scanning probe X-ray diffraction microscopy techniques to the nanoscale will be discussed.

S167

IN-SITU STUDY OF ELECTROMIGRATION INDUCED STRAIN / STRESS EVOLUTION AND DISTRIBUTION IN Sn - Cu LEAD-FREE SOLDER JOINTS USING SYNCHROTRON WHITE BEAM X-RAY MICRODIFFRACTION

K. Chen*, Lawrence Berkeley National Lab, Berkeley, CA, USA and UCLA, Los Angeles, CA
N. Tamura, Lawrence Berkeley National Lab, Berkeley, CA
F.Y. OuYang, K.N. Tu, UCLA, Los Angeles, CA

It is well known that electromigration would induce stress gradient built up in a solder joint due to the atomic transport from cathode end to the anode end, and the stress gradient will affect the atomic diffusion as a feed back according to Blech – Herring model, however, there is no literature report on the stress distribution induced by electromigration in the solder joints so far. Here we report a direct measurement of the stress evolution and distribution in a eutectic Sn - Cu lead-free solder ball as a function of electric current stressing time at enhanced temperature by using synchrotron radiation based polychromatic X-ray microdiffraction at the early stage of electromigration test. At this stage, no significant electric resistance change was observed, while the whole solder ball was under compressive strain, and the strain level is below the elastic limit. The stress, therefore, was also calculated based on the strain and elastic constant. The stress distribution in the solder ball is explained based on the current crowding theory of electromigration.

S25

THE REVERSE OF TRIAXIAL STRAIN FIELDS IN A MULTIFERROIC $BiFeO_3$ THIN FILM AS STUDIED USING SCANNING X-RAY MICRODIFFRACTION

Chung W. Bark, Kyung C. Cho, Yang M. Koo, Sangwoo Ryu, and Hyun M. Jang
Department of Materials Science and Engineering, and Graduated institute of Ferrous Technology, Pohang University of Science and Technology (POSTECH), Pohang 790-784, Republic of Korea
Nobumichi Tamura
Advanced Light Source (ALS), Lawrence Berkeley National Laboratory, Berkeley, California 94720, USA

The dramatically enhanced polarizations and saturation magnetizations observed in the epitaxially constrained $BiFeO_3$ (BFO) thin films with their pronounced grain-orientation dependence have attracted much attention and are attributed largely to the constrained in-plane strain. Thus, it is highly desirable to directly obtain information on the two-dimensional (2D) distribution of the in-plane strain and its correlation with the grain orientation of each corresponding micro-region. Here we report a 2D quantitative mapping of the grain orientation and the local triaxial strain-field in a 250nm-thick multiferroic BFO film using a synchrotron X-ray microdiffraction technique. This direct scanning measurement demonstrates that the deviatoric component of the in-plane strain tensor is between $5x10^{-3}$ and $6x10^{-3}$ and that the local triaxial strain is fairly well correlated with the grain orientation in that particular region at room temperature. We have performed a 2D quantitative mapping of the grain orientation and the local triaxial strain-field in a $BiFeO_3$ thin film at room temperature, 373K, 673K by using a synchrotron X-ray microdiffraction technique. This direct scanning measurement demonstrates that the deviatoric component of the in-plane strain tensor is reversed with temperature raising, and that the local triaxial strain is fairly well correlated with the grain orientation in that particular region.

REFERENCES

[1] J. Wang, J. B. Neaton, H. Zheng, V. Nagarajan, S. B. Ogale, B. Liu, D. Viehland, V. Vaithyanathan, D. G. Schlom, U. V. Waghmare, N. A. Spaldin, K. M. Rabe, M. Wuttig, and R.Ramesh, Science **299**, 1719 (2003).
[2] Robert C. Rogan, N. Tamura, G. A. Swift, E. ÜSTÜNGAG, Nature Mat. **2**, 379 (2003).
[3] J. S. Chung and G. E. Ice, J. Appl. Phys. **86**, 5249 (1999).
[4] C. W. Bark, S. Ryu, Y. M. Koo, H. M. Jang, and H. S. Youn, Appl. Phys. Lett. **90**, 022902 (2007).

D-58

NANOSTRUCTURE ANALYSIS OF METALLIC MATERIALS BY COHERENT X-RAY DIFFRACTION MICROSCOPY

Yukio TAKAHASHI[1], Hayato FURUKAWA[1], Hideto KUBO[1], Kazuto YAMAUCHI[1],
Yoshinori NISHINO[2], Tetsuya ISHIKAWA[2], and Eiichiro MATSUBARA[2]
[1]Osaka University, Yamada-oka, Suita, Osaka 565-0871, Japan
[2]RIKEN SPring-8 Center, Kouto, Sayo-cho, Sayo-gun, Hyogo 679-5148, Japan
[3]Kyoto University, Yoshida, Sakyo, Kyoto 606-8501, Japan

Coherent X-ray diffraction microscopy[1] (CXDM) is a novel technique for reconstructing a two- or three-dimensional image. After the first demonstration of CXDM by Miao *et al*., several applications of CXDM have been reported. CXDM has a great potential as a new technique for structural studies of metallic materials because it is not only a non-destructive method but also applicable to a sample of micrometer thickness. In the present study, the validity of CXDM for this kind of observation was demonstrated using an age-hardened aluminum alloy in practical use. Also, Cu thin line samples were fabricated on Si_3N_4 membranes towards demonstration of electromigration analyses. Coherent X-ray diffraction patterns of the metallic materials were measured at BL29XUL in SPring-8. As the result, the internal structure and the shape of the aluminum alloy particle were three-dimensionally visualized[2]. Characteristic diffraction patterns resulting from both the shape of the Cu thin lines and the defects formed by the application of the current were observed[3].

1) J. Miao, P. Charalambous, J. Kirz, and D. Sayer, Nature 400, 342 (1999).
2)Y. Takahashi, Y. Nishino, T. Ishikawa, and E. Matsubara, Applied Physics Letters 90, 184105 (2007).
3)Y. Takahashi, H. Furukawa, H. Kubo, K. Yamauchi, Y. Nishino, T. Ishikawa, and E. Matsubara, Surface and Interface Analysis (in press)

S86

RESIDUAL STRESS AND DEFORMATION SIMULATION OF NITRIDED DISC

Laurent Barrallier[1], Patrick Vardon[2], Dominique Deloison[3]
[1]MecaSurf Laboratory, Arts et Metiers ParisTech, Aix en Provence, France
[2]Eurocopter, Marignane, France
[3]EADS Innovation Works, Suresnes, France

Nitriding is a thermochemical treatment that can be used to increase fatigue life of high loaded mechanical steel parts. The combination of hardening effect and residual stress generation allows to explain the performance treatment. Precipitation phenomena can be linked to the stress and hardening generation.

In order to optimize the design of part, modeling of nitriding have been developped using a finite-element approach. The local geometry of workpiece and its influence on the nitrogen diffusion have been taken into account. Volume variation due to the precipitation has been calculated using thermodynamical calculation coupled with diffusion simulation of nitrogen and carbon. Finally, this approach has allowed to determine residual stress field using a micromechanic approach embedded within the finite element model. The deformation generated during nitriding have also been determined.

The modeling has been applied to a simple disc geometry where only one side has been nitrided. The simulation has been compared to the experiments by measurement of disc deflexion and stress analysis using X-rays diffraction and material removal method in order to derive stress in iron phase and macroscopic stress respectively.

S91

PHASE TRANSFORMATION INVOLVING RESIDUAL STRESSES DURING GASEOUS NITRIDING OF STEEL

S.Jegou[1, 2], R.Kubler[1], L.Barrallier[1], F.Roch[2]
[1]Laboratoire MecaSurf, Arts & Metiers ParisTech, Aix-en-Provence, France
[2]Aubert & Duval, ERAMET Group

Nitriding is a thermochemical surface treatment involving the di_usion of nitrogen and generating a hardening e_ect combined to compressive residual stresses. This process is often used to improve fatigue life, tribological and anti-corrosion properties of iron-based alloys.
Hardening mechanisms are mainly associated to the precipitation of complex nano MN precipitates (M=Cr,V, Mo...). Residual stresses are explained by the volume variation accompanying precipita- tion during the treatment. In both cases, relationships with the nitrogen concentration are strongly dependant of alloying elements' concentration as well as nitriding time and temperature. In case of iron-based alloys, two kinds of precipitation mechanisms occur due to the presence of carbon. First, nitrogen interacts with alloying elements initially present in solid solution in the martensite. It results in the precipitation of nano semi-coherent MN nitrides. Secondly, due to a better affinity of alloying elements with nitrogen than with carbon, carbides from earlier annealing steps are transformed into incoherent nitrides. Consequently, the released carbon diffuses either towards the surface or backward the core, driving cementite M_3C precipitation at grain boundaries. Moreover cementite is stress-driven as it precipitates oriented by the plane stress state parallel to the nitriding surface. Therefore, in parallel to the metallurgical and microstructural changes caused by nitrogen diffusion, the resulting carbon diffusion also generates secondary phases and microstructure gradients. The purpose of this study is to study the importance of carbon in case of residual stresses understanding.
This work deals with the study of residual stresses in relation with phase transformations during nitriding. Materials investigated in this work are an industrial steel 32CrMoV13 and a ternary alloy (Fe-0,37wt.%C-3wt.%Cr) manufactured by Aubert & Duval (heated, quenched then annealed). They were nitrided during 48h at 520°C and 100h at 550°C respectively. A characterization of the cementite along side of a nitrided surface is presented using image analysis coupled with optical and SEM observations. The in-depth cementite quantification profiles are then compared to the in-depth stress pro_les of ferrite. Residual stresses in the ferritic matrix are analyzed using X-ray diffraction. Phase identification are also carried out using X-ray di_ractometer at some pertinent depths chosen according to nitrogen and carbon concentration profiles.
In order to understand the link between phase transformations and the development of residual stresses, experimental characterization are compared to a simulation of nitriding. It is based on thermochemical simulation using Thermo-Calc software and a self-consistent micromechanical model considering elastic precipitates exhibiting a volume variation embedded in an infinite ferritic matrix. The volume variation for a given depth is calculated based on the volume fraction and chemical composition of each identified phase. The mechanical behavior of the ferritic matrix is taken as elastoplastic.
Experiments and simulations suggest that residual stresses development is partially attributed to a carbon redistribution. Carbon diffusion is responsible for an additional volume variation to the one associated with nitrogen diffusion. Finally, it can explain the typical growth of nitrides when getting away from the surface.

S20

PREDICTION OF RESIDUAL STRESS DISTRIBUTION IN PLASMA NITRIDED TOOL STEEL

B. Podgornik[1], V. Leskovšek[2] , D. Nolan[3], J. Vižintin[1]
[1] University of Ljubljana, Centre for Tribology and Technical Diagnostics, Ljubljana, Slovenia
[2] Institute for Metals and Technologies, Ljubljana, Slovenia
[3] University of Wollongong, Faculty of Engineering, NSW, Australia

Residual stresses may be present in engineering components as an unintended consequence of manufacturing processes, but they may also be introduced deliberately during surface engineering procedures. Plasma nitriding and nitrocarburizing are such processes of particular importance for tool steel components used in tool, die and machine applications. These processes afford significant advantages, such as greatly improved wear and corrosion resistance, as well as fatigue strength resulting from the generation of near-surface compressive residual stresses.

A precise knowledge of the level and distribution of residual stress that exist in such engineering components is necessary for product development and quality control purposes, as well as for the accurate prediction of a component's fatigue resistance. If located at the same depth as the Hertzian stress concentrations, compressive residual stress can greatly improve the fatigue properties of loaded surfaces. Therefore, reliable methods for residual stress determination are required, with residual stress measurement techniques having their limitations.

The aim of this investigation is to correlate the residual stress distribution in plasma nitrided and nitrocarburized tool steel with the microhardness depth profile, in order to determine whether a relatively simple microhardness-related parameter could be used to predict the depth of the maximum compressive residual stress, and to thereby enable optimization of the nitriding parameters for specific contact conditions.

Keywords: Plasma nitriding, Nitrocarburizing, Residual stress, Microhardness, Modelling

S170

ON SURFACE TEXTURE AND INTEGRITY IN MACHINED SURFACES

A.K. Balaji*, A.R. Paranjpe, and C. Rakurty
Sustainable Manufacturing Laboratory, Department of Mechanical Engineering, The University of Utah, Salt Lake City, Utah 84112, *Corresponding author - Email: balaji@eng.utah.edu

Fundamental understanding and modeling of surface texture and residual stresses induced in materials by the machining process is of great importance as it plays a significant role in the fatigue life and service life of these machined components. The goal of the presented research is to evaluate means by which *surface integrity and residual stresses are engineered at the manufacturing process planning stage* by careful selection of appropriate machining tools and conditions. Typically, manufacturing process planners chose conditions that will enhance other factors such as material removal rate and increased tool-life. However, we find that such selected conditions lead to a sub-optimal level of surface integrity. This leads to the need for additional expensive or time consuming post-processing techniques such as laser shock processing (LSP) and low plasticity burnishing (LPB) to correct the flaws in the sub-surface induced by poor selection of machining conditions. Our research throws new insight on means of engineering desired residual stress profiles by optimized selection of tooling and operating conditions based on experimental measurements and fundamental modeling of the machining process. The specific goal of this presented work is to investigate the effects of cutting tool geometry, tool-coatings, and lubrication conditions on the surface integrity, surface texture, and machining performance of two different machined materials: Aluminum alloy 7075-T6 and AISI 1045 carbon steel.

Machining experiments are conducted on these specimens using different cutting tools (diamond-based tools and carbide tools with thin-film wear resistant coatings). Different lubrication conditions (dry, minimal quantity lubrication (MQL) and flood) were also tested. MQL application involved the use of minimal amounts of cutting fluid to the cutting zone at a flow rate of 30 ml/hr and flood lubrication involved cutting fluid application at a high flow rate of 9 l/min. The measured responses were machining forces, residual stresses and surface texture. The surface texture was evaluated using an optical interferometry based surface characterization system. The residual stresses were characterized using a suite of different measurement techniques. The machining process was also modeled using two computational techniques: an explicit finite-element method (FEM) and the material point method (MPM). The resulting residual stress in the machined materials are predicted and compared with experimental measurements. It was observed that small changes in machining conditions (tool geometry, tool surface features, tool coatings, application of varying levels of lubricant or coolant) result in varying levels of surface texture and integrity.

S32

MEASUREMENT OF THE RESIDUAL STRESS FIELD IN AN ALUMINIUM ALLOY 2014A COMPONENT OF COMPLEX GEOMETRY

S. Hossain[1], M. Fardi[1], U. Stuhr[2], D.J. Smith[1], C.E. Truman[1]*
[1] Department of Mechanical Engineering, University of Bristol, Queen.s Building, University Walk, Bristol BS8 1TR, UK
[2] Laboratory for Neutron Scattering, ETH Zürich and Paul Scherrer Institute, CH-5232 Villigen, Switzerland
*Corresponding author: Dr Christopher E Truman, Email: C.E.Truman@bristol.ac.uk

Accurate prediction of residual stress fields plays an important role in the structural integrity assessment of engineering components. With the advent of modern computers, solving complex non-linear finite element analyses has become a routine

practice. The output of the results from such analyses however still remains dependent on accurate definition of material characteristics and process parameters. In order to achieve a reliable solution, the predictions therefore need to be verified with hard measurements. In safety-critical components it is vital to validate the initial finite element prediction with meticulous measurement before progressing into the subsequent steps within the structural integrity assessments.

In this paper, results are presented from a series of measurements using the neutron diffraction technique to measure the residual stress present in a complex geometry manufactured from an aluminium alloy 2014A followed by cold water quenching. The quenching process imparts good mechanical characteristics on the sample. The sample in the present study includes a pump casing with an aerospace application. The measured residual stress distribution along a selected number of lines through the thickness of the pump casing is compared with an earlier non-linear finite element simulation. The finite element prediction requires a good description of material physical and mechanical properties such as the heat transfer coefficient, temperature dependent and strain rate dependent yield stress, temperature dependent elastic constants, etc in order to accurately predict the residual stress field. An initial comparison illustrates a good correlation between the measurement and the prediction along a selected number of paths through the thickness of the pump casing sample. On a closer assessment, however, it is seen that more refinement of the finite element study is required, before a better correlation with the measurement along the remaining measured paths through the thickness of the sample, and hence an experimental verification of the finite element result, may be achieved.

S75

IN-SITU STRAIN MEASUREMENTS IN COMPOSITE CASTINGS USING NEUTRON DIFFRACTION

U. Wasmuth[1], M. Hofmann[2], L. Meier[1], H. Hoffmann[1]
[1]Lehrstuhl für Umformtechnik und Gießereiwesen, Technische Universität München, Garching, Germany
[2]Forschungsneutronenquelle Heinz Maier-Leibnitz, Technische Universität München, Garching, Germany

Due to different thermal expansion of the casting material and the material of the mould residual stresses occur during solidification of composite castings. These residual stresses can reduce fatigue strength and lead to distortions of the part. They can be minimised by constructive measures. Casting simulation is a suitable method to predict residual stresses and distortions and thus to optimise design of parts. To improve the accuracy of stress simulation composite castings were investigated experimentally using conventional strain gauge methods and neutron diffraction. The use of neutron diffraction enabled to obtain non-destructively, stress distributions within the bulk of the specimen. In-situ neutron diffraction strain experiments during solidification of the composite castings made it further possible to measure thermal and mechanical strains up to solidus temperature of the casting material. The results are used to verify and optimise the residual stress simulation. In the end this enables an optimised construction of composite castings.

S130

FINITE ELEMENT SIMULATION OF RESIDUAL STRESS PROFILES IN PEEN FORMING PROCESS

H.Y. Miao [1], C. Perron [1], M. Lévesque [2]
1. Aerospace Manufacturing Technology Center, National Research Council Canada, 5154 av. Decelles, Montréal, Québec, H3T 2B2, Canada
2. École Polytechnique de Montréal, Québec, H3C 3A7,Canada

Shot peeing process can induce the distortion of a thin component, which is called peen forming and is widely used for shaping aircraft wing skin. In peen forming process, a component is rigidly constrained during shot peening. As peening take place, gradual plastification of the component surface layers produces induced stress profiles. These induced stresses are not self-equilibrated and tend to stretch and bend the component. Therefore, after release of the boundary conditions, the component deform to designed shape. The advantages of peen forming are it is a dieless forming process, and it causes compressive residual stresses both at the top surface and at the bottom surface of the component, which can greatly improve the fatigue life of the component. In practical peen forming stress, shot peening intensity, shot peening coverage, impact angle and pre-bending moments are the most important parameters to control forming results (deformed shape and residuals stress profiles). Due to the insufficient investigation of these control parameters, the design of peen forming for a specific shape has been based on experimental trial and error. The objective of this paper is to simulate the real shot peening and peen forming process and relate the forming results with shot peening parameters. A newly developed 3D finite element model with multiple random shots together with an Implicit-Explicit sequence solution has been developed to simulate conventional peen forming and stress peen forming process.

KEY WORDS
Finite element method, Induced stress, Residual stress Conventional peen forming, Stress peen forming,

S138

STUDY ON THE RESIDUAL STRESS AND THE DISTORTION OF THE LARGE GEARS OR AXLES DURING THE HEAT TREATMENT

Y. Wang[1], Y. Ling[2], R. Kastelein, Z. A. Xu
SIRRIS, Zwijnaarde, Belgium
[1]yunning.wang@sirris.be; [2]Yong.Ling@sirris.be

The obstacles to the computer simulation of the heat treatment process include not only the complex heat transfer in the quenchant, the variable microstructures and their mechanical properties with the temperature etc., but also some outer factors in the practice of the industry, such as, the non-uniform heating or cooling conditions, the effect of the gravity (especially for the large components), etc.. In this work, we develop some numerical models to simulate the residual stress and the distortion during the heat treatment process. The influences of the gravity, non-uniform quenching conditions on the distortions of the large gear or axes are discussed and the results are compared with the experimental measurements.

S180

IN SITU PROBING OF CRACK GROWTH RETARDATION DURING CYCLIC LOADING

S.Y. Lee[1], H. Choo[1, 2], K. An[3], P.K. Liaw[1] and C.R. Hubbard[2]
[1]Department of Materials Science and Engineering, The University of Tennessee, Knoxville, TN 37996, USA
[2]Materials Science and Technology Division, Oak Ridge National Laboratory, Oak Ridge, TN 37831, USA
[3]Spallation Neutron Source, Oak Ridge National Laboratory, Oak Ridge, TN 37831 USA

During a constant-amplitude fatigue-crack-growth experiment, a single tensile overload was applied and a large retardation period was observed, resulting in a temporary decrease in the crack growth rate. In order to explain the crack growth retardation, several mechanisms have been proposed but the precise micromechanical mechanisms that account for these phenomena are still not fully understood. In this investigation, in-situ electric potential and neutron diffraction measurements were performed to probe the mechanism of overload effects. Electric potential technique enables us to measure the exact crack length at each cycle during fatigue crack growth. Using this method, the crack opening load was determined at various stages including retardation period during fatigue crack growth. In addition, spatially-resolved neutron strain scanning was performed to measure the evolution of internal strains around a crack tip during in-situ loading. The crack opening level was investigated at different stages through retardation period from the plot of load versus lattice strain. From both techniques, the relationship between crack tip driving force and crack growth rate is revealed.

Keywords: Overload; Crack growth retardation; Electric potential; Neutron diffraction

S153

IMPACT OF ZIRCONIUM HYDRIDE PRECIPITATES ON FRACTURE OF A ZIRCONIUM ALLOY

M. Kerr, M.R. Daymond, and R.A. Holt - Department of Mechanical and Materials Engineering, Queen's University
J.D. Almer - Advanced Photon Source, Argonne National Laboratory

Zirconium alloys are of major importance to the nuclear industry, with primary application as a structural material for the in-reactor environment. The formation of brittle hydrides in zirconium alloys results in a degradation of the mechanical properties of the component in which they form. Thus, the rate and characteristics of formation and the subsequent impact of these hydrides are critical factors in the determination of zirconium component service life. This is a three part study of hydrides in zirconium using high energy synchrotron X-ray diffraction. Part I characterized the mechanical response of zirconium hydride, *in situ* in a Zircaloy-2 matrix. This study provided quantitative data on the elastic response of the hydride, as well as load transfer and fracture of the hydride phase; confirmed with finite element and composite mechanics models. Part II studied the near crack tip behavior of unhydrided Zircaloy-2. Strain field evolution as a function of applied load as well as the initiation of crack tip twinning were characterized with 2D mapping techniques. Two material orientations relative to the parent texture were investigated in a fatigue precracked condition with the results compared to finite element models. Part III then build on the results of the mapping study to characterize the effects of hydrides in the vicinity of the crack tip. The aim is to quantify the influence of crack tip hydrides on the local strain field around the crack tip, and to characterize the internal strains in the crack tip hydrides themselves.

S18

ON THE IMPROVEMENT OF THE FATIGUE BEHAVIOUR OF AUSTENITIC STAINLESS STEEL DUE TO SURFACE RESIDUAL STRESSES PRODUCED BY LOW TEMPERATURE CARBURIZING

Giangiacomo Minak
Mechanical Engineering Dept., Alma mater Studiorum – Università di Bologna, Viale Risorgimento 2, 40136 Bologna, Italia

The attempts made in recent years to engineer the surface of austenitic stainless steels to improve their hardness and tribological properties, without deteriorating their corrosion resistance, had as a secondary effect the modification of the fatigue properties of those materials. In fact, austenitic stainless steels have a low hardness and consequently poor wear resistance.

A possibility to improve these properties is given by low temperature carburizing, that involves diffusion of large quantities of C atoms into the material at a diffusion temperature below 450 °C (to prevent the formation of undesired chromium carbides). Due to the low temperature, the treatment requires a long diffusion time of about 100 h to achieve a carburised layer of few tens of μm.

Several researchers observed a marked improvement in fatigue life due to these treatments [1-5]. In [1, 2] the authors measure residual stress at the surface by X-ray diffraction and find peaks of -1500 MPa. Using the same method in [3, 4] the maximum value of measured residual stresses exceeds -2000 MPa.

The fatigue fracture nucleation sites are preferably located in plain specimens at the interface between the treated and not treated zones, while in notched specimens or specimens with surface defects fracture starts from the surface.

Aim of the work is to set up a phenomenological model of the fatigue behaviour of these materials in order to predict the improvement of their fatigue life due to the presence of such high residual stresses.

[1] K. Tokaji, K. Kohyama, M. Akita, Int J Fatigue, 26 (2004) 543.
[2] M. Akita, K. Tokaji, Surf Coat Technol, 200 (2006) 6073.
[3] G.M. Michal, F. Ernst, H. Kahn, Y. Cao, F. Oba, N. Agarwal, A.H. Heuer, Acta Materialia, 54 (2006) 1597–1606
[4] N. Agarwal, H. Kahn, A. Avishai, G. Michal, F. Ernst, A.H. Heuer, Acta Materialia, 55 (2007) 5572–5580
[5] L. Ceschini, G. Minak , Surf Coat Technol, 202 (2008) 1778–1784

S136

OPERATIONAL RESIDUAL STRESS FORMATION IN VIBRATION-LOADED ROLLING CONTACT

Jürgen Gegner and Wolfgang Nierlich
SKF GmbH, Dept. of Material Physics, Ernst-Sachs-Strasse 5, 97424 Schweinfurt, Germany

In many engineering applications like paper making and printing press equipment, wind turbines, fans or tractors, rolling bearings are operated under external vibrations, e.g., from adjacent machines. This additional loading is usually discounted in failure analyses. However, mechanical vibrations may cause critical mixed friction running conditions that lead to near-surface fatigue eventually. Secondary electron microscopy (SEM) and failure metallography respectively show partial to complete smoothing of the machining marks and dark etching regions in the outermost edge zone, which are formed by microstructural changes due to material aging. The resulting depth profiles of residual stress and {211} martensite XRD line width are also illustrated by typical concrete examples from the field. The applied evaluation of X-ray diffraction material response analysis (XRD-MRA) is outlined. Despite indentation-free raceway, compressive residual stresses are formed up to a certain distance from the surface but far above the depth of maximum v. Mises equivalent stress of the Hertzian macro contact. These findings suggest the initially postulated failure mechanism of vibration-induced mixed friction. Two distinct types of residual stress depth profiles are observed. The analysis of the influence of friction in rolling-sliding contact provides an interpretation. Superposition of the additional tangential forces to the radial loads raises the equivalent stress and shifts its peak towards the raceway surface. The occurrence of residual stress depth profiles revealing either a secondary minimum or monotonous increase in the edge zone thus points to friction coefficients of 0.2 to 0.3. Even for non-ideal lubrication conditions, however, overall values of about 0.05 are typical of rolling bearings. The proposed model of localized friction coefficients explains the discrepancy. This assumption is supported by the thixotropy effect on the lubricant that loses viscosity due to shear loading caused by the vibrations. By satisfying the occurring average according to a mixing rule, high friction coefficients act temporarily in small regions of the contact.

Tests are carried out to experimentally simulate the effect of external mechanical vibrations on bearing performance. A specifically designed and suitably equipped rig is used. The lipless outer ring of a type N cylindrical roller bearing is axially displaced with a typical frequency of 100 Hz. Its raceway suffers maximum vibrational loading via the roller contact. This component thus becomes the test specimen although the Hertzian pressure is higher on the rotating inner ring. XRD-MRA shows that controlled sliding friction introduced by axial vibrations changes the residual stress state in the edge zone without raceway indentations and leads to material fatigue, there. Imaging and analytical SEM reveals smoothed honing marks, surface cracking along tribochemically dissolved MnS inclusion lines and gray staining, i.e. flatly expanded micropitting. Infrared spectroscopy on used aliphatic oil from the test provides evidence of oxidation and incipient resinification by polycondensation. The vibration-induced tribochemical processes thus lead to an acidification of the aging lubricant. The use of contaminated aged grease strongly increases the effect culminating in abrasive wear, plastic deformation and corrosion. The temperature in the lubricating gap depends on the type of lubricant and rises linearly with contact area-related friction power loss.

S34

ACCOUNTING FOR RESIDUAL STRESS IN INTEGRITY ASSESSMENT OF 3-D STRUCTURE

R. J. Bucci, M. A. James
Alcoa Technical Center
D. L. Ball
Lockheed Martin Aeronautics Co.

The quest for lighter and more affordable airframes has accelerated demand for thicker/wider/shaped alloy products (plate, extrusions, forgings, castings) and manufacturing technologies (e.g., high-speed machining, weld-joining) to grow applications of unitized structure. Capturing the full benefit of these technologies requires that residual stress effects be accounted for in both material characterization and final part design. In the case of thick or shaped metallic products, residual stresses from thermo-mechanical processing can introduce bias and large scatter effects into couponbased durability and damage tolerance property determinations, which in turn confounds the ensuing transfer to final design.

The presentation will describe efforts of Alcoa and others directed to developing improved fatigue crack growth rate data analysis methods and modeling tools that may be used to account for residual stress effects in testing and analysis. Two fundamental principles will be discussed at this seminar: advancements in fracture toughness and fatigue crack growth rate testing and analysis; and the way forward to account for the residual stress effect(s) in analysis and design of fatigue and fracture critical structures. Case study examples are presented to validate the recommended approach, and the presentation concludes with a vision for virtual design support to large monolithic part applications.

S206

MEASUREMENTS OF RESIDUAL STRESS FIELDS IN FRACTURE COUPONS AND RELATION TO OBSERVED FRACTURE PROPERTIES

Michael R. Hill[1]*, John E. VanDalen[2]
[1]Mechanical and Aeronautical Engineering, University of California, One Shields Avenue, Davis, CA 95616 USA
* Corresponding author: mrhill@ucdavis.edu, (530) 754-6178
[2]Hill Engineering, LLC, 5022 Bailey Loop, McClellan, CA 95652 USA

This paper describes tests carried out to measure residual stress fields in fracture test coupons and to relate those residual stress fields to observed fracture properties. A set of nominally identical fracture toughness test coupons were prepared from a single rolled plate of 7075 T6 aluminum alloy. Following fabrication, residual stresses were induced in coupon subsets using laser shock peening. Each coupon subset had a unique laser peening treatment design, such that following fatigue pre-cracking, the stress intensity factor due to residual stress varied from positive to neutral to negative over the coupon subsets created. The contour method was used to measure residual stress on the crack plane, and provided a twodimensional map of the laser shock induced residual stress field. Slitting was used to measure throughthickness average residual stress on the crack plane as well as the residual stress intensity factor as a function of crack length. Application of the contour and slitting methods to identically prepared samples allowed for a useful comparison of the residual stress fields provided by the two methods. Measured residual stress fields enabled a forecast of expected coupon behavior under monotonic loading (which would produce a crack-growth resistance curve) and under constant amplitude cyclic loading (which would produce crack growth rate data). Subsequent fracture toughness and fatigue crack growth tests provided data that are in good agreement with the expected coupon behaviors.

S89

FATIGUE CRACK GROWTH IN PLASTICALLY BENT BEAMS

K.W. Jones, M.L. Dunn, University of Colorado, Boulder, CO

The fatigue life of a crack growing through a residual stress field is commonly predicted using the original residual stress from the uncracked body, the principle of superposition, and linear elastic fracture mechanics. These fatigue predictions may contain errors due to inaccurate knowledge of the original residual stress, relaxation of residual stress due to cyclic loading, inelastic material behavior, contacting of the crack faces, ignoring the contribution of compressive loading to crack tip damage, or changes in material properties due to plastic straining during the introduction of residual stress. This paper presents modeling and experiments on plastically bent aluminum 2024-T351 beams under constant ΔK controlled four point bending fatigue. The errors mentioned above were either minimized in this experiment or accounted for in the prediction. Baseline material fatigue crack growth data was generated using middle tension specimens at R ratios ranging from -1 to 0.6. Beam residual stress was characterized theoretically, through measurement of the stress strain curve during bending, as well as experimentally by the slitting method and sectioning methods. Fatigue crack growth rates are presented along with their correlation with predictions.

S199

RESIDUAL STRESS EFFECTS ON FATIGUE LIFE OF WELDED STRUCTURES USING LEFM

Z. Barsoum[1*] and I. Barsoum[2]
[1]Royal Institute of Technology (KTH), Dep. of Aeronautical and Vehicle Engineering, 100 44 Stockholm, Sweden, zuheir@kth.se
[2]Royal Institute of Technology (KTH), Dep. of Solid Mechanics, 100 44 Stockholm, Sweden, imad@kth.se
*Corresponding author

In this paper a welding simulation procedure is developed using the FE-software ANSYS in order to predict residual stresses. The procedure was verified with temperature and residual stress measurements found in the literature on multi-pass butt welded plates and T-fillet welds. The predictions show qualitative good agreement with experiments. The welding simulation procedure was then employed on a welded ship engine frame box at MAN B&W. A subroutine for LEFM analysis was developed in 2D in order to predict the crack path of propagating fatigue cracks. The objective was to investigate fatigue test results from special designed test bars from the frame box where all test failed from the non-penetrated weld root. A subroutine was developed in order to incorporate the predicted residual stresses and their relaxation during crack propagation by isoparametric stress mapping between meshes without and with cracks, respectively. The LEFM fatigue life predictions shows good agreement with the fatigue test result when the residual stresses are taken into account in the crack growth analysis.

Keywords: Welding simulation, FEM, residual stresses, fatigue crack growth, linear elastic fracture mechanics.

S7

PREDICTION OF DISTORTION OF AIRFRAME COMPONENTS MADE FROM ALUMINUM PLATES

Sebastian Nervi*
ESRD Inc., Saint Louis, MO 63146
Barna A. Szabó**
Washington University in Saint Louis, Saint Louis, MO 63130
Keith A. Young***
The Boeing Company, Saint Louis, MO 63166

A mathematical model formulated for the prediction of distortion of airframe components manufactured from 7050-T7451 aluminum plates, caused by residual stresses introduced by the manufacturing process of the plate, was tested in validation experiments. The results indicate that distortion in thin gage parts is caused primarily by machining- induced residual stresses. The residual stresses introduced by the plate manufacturing process that includes hot rolling, quenching stretching and aging operations have a minor effect on distortion, consistent with the predictions based on the mathematical model described herein.

*Research Scientist, Research and Development Group, 111 West Port Plaza, Suite 825, St. Louis, Missouri 63146.
**Senior Professor, Department of Mechanical, Aerospace and Structural Engineering, one Brookings Drive, Campus Box 1185, St. Louis, Missouri 63130.
***Research Engineer, Boeing's Advanced Manufacturing R&D Group in Saint Louis, Saint Louis, Missouri 63166.

S200

DISTORTION PREDICTION IN MACHINED AEROSPACE COMPONENTS

Troy D. Marusich, Ph.D., P.E.
Chief Technical Officer
Third Wave Systems, Inc., Minneapolis, MN 55439, troym@thirdwavesys.com, (952)-832-5515

Machined monolithic components provide the foundation for modern aircraft structures requiring high performance designs in terms of weight, strength and fatigue properties. Part distortion and warpage arising from bulk material and machining-induced stresses frustrates manufacturing and assembly processes and necessitates expensive trial-and-error methods, shot peening and heat treating to minimize distortion. Strict weight requirements are exacerbated by thicker component section designs as a distortion control mechanism.

We present a physics-based model which takes into account the pre-machined bulk stress state and machining-induced stresses for monolithic parts. Sources of stresses include heat treatment, quenching, forging and machining operations. A customized solid model representation of the initial workpiece geometry is developed. Bulk stresses are mapped onto the solid model. CNC toolpath programs, along with corresponding tooling geometry, are read and analyzed. Bulk stresses are removed from the component as material is machined away, while machining-induced stresses are applied to the final surfaces. The final workpiece geometry is meshed automatically with finite elements and equilibrium solutions calculated. Minimum distortion configurations and strategies are analyzed. Distortion prediction, measurement and validation are presented for a number of monolithic, thin-walled components.

S133

RESIDUAL STRESSES AND SURFACE WORKHARDENING INDUCED BY MICRO CUTTING PROCESSES

Hermann Autenrieth, Brando Okolo, Volker Schulze, Alexander Wanner, Detlef Löhe
Institute for Materials Science and Engineering I, University of Karlsruhe (TH), Kaiserstrasse 12, 76131 Karlsruhe, Germany

Machining processes such as cutting constitute a critical finishing stage in production. Numerous studies reported in the literature show that the thermoplastic deformation induced by the cutting process can ultimately determine the operational behavior of a component. A number of factors have been identified as capable of markedly influencing this thermoplastic deformation. These factors include the cutting edge geometry, the depth of cut, and the hardness of the workpiece. A primary consequence of the cutting process is the development of residual stresses in the worked surface. Compressive residual stresses are beneficial for the fatigue life of mechanically loaded components while tensile residual stresses may lead to unanticipated failure. Therefore it is important to gain further knowledge of how these factors influence the state of the materials.

The present study focuses on how the depth of cut and cutting edge radius influence the residual stress state and work hardened state in normalized AISI 1045 steel which was machined by an orthogonal micro cutting process. X-ray diffraction has been used to determine the residual stress state in the micro cut surfaces applying the $\sin^2\psi$ method. Hardness profiles elucidating the depth distribution of work hardening in the subsurface regime were obtained using micro indentation. Special attention has been given to the ploughing effect determined by the ratio of the cutting edge radius to the depth of cut. The results provide a basis on which an optimization of the cutting process can be managed.

S177

CHARACTERISTICS OF RESIDUAL STRESS PROFILES IN HARD TURNED VERSUS GROUND SURFACES WITH AND WITHOUT A WHITE LAYER

A.W. Warren, Y.B. Guo*
Dept. of Mechanical Engineering, the University of Alabama, Tuscaloosa, AL 35487
*Corresponding author. Tel.: +1 205 348 2615; fax: +1 205 348 6419; E-mail address: yguo@eng.ua.edu (Y.B. Guo).

Hard turning and grinding are competitive processes in many cases for manufacturing various mechanical products. Product performance is highly dependent on the process induced residual stresses. However, there exist some inconsistencies regarding the true residual stress profiles generated by hard turning and grinding with and without the presence of a white layer. This study aims to clarify the pressing issues via an extensive residual stress measurement for five surface types: hard turned fresh (HTF), hard turned with a white layer (HTWL), ground fresh (GF), ground with a white layer (GWL), and as heat treated. The X-ray diffraction data revealed distinct differences in the residual stress profiles for the five surface types. Specifically, the results have shown that (i) HTF surfaces generate a "hook" shaped residual stress profile characterized by surface compressive residual stress and maximum compressive residual stress in the subsurface, while GF surfaces only generate maximum compressive residual stress at the surface; (ii) HTWL surfaces generate a high tensile stress in the white layer, but has highly compressive residual stress in the deeper subsurface than the HTF surface; (iii) GWL surfaces only shift the residual stress to more tensile but does not affect the basic shape of the profile; (iv) Tensile residual stress in the HTWL surface is higher than that for the GWL one. However, the residual stress for the ground white layer does not become compressive and remains tensile in the subsurface; (v) Elliptical curve fitting is necessary for measuring residual stress for the HTWL surface due to the presence of shear stress induced severe ψ splitting; (vi) Residual stresses by grinding show more scattering than those by hard turning; and (vii) Machining is the deterministic factor for the resulting residual stress magnitudes and profiles compared with the minor influence of initial residual stress by heat treatment.

Keywords: residual stress, hard turning, grinding, white layer

S10

RESIDUAL STRESS DETERMINATION IN AZ31 FRICTION STIR WELDS USING X-RAY AND NEUTRON DIFFRACTION

Loreleï COMMIN, Jean-Eric MASSE, Laurent BARRALLIER
Laboratoire MÉCASURF, ARTS ET METIERS PARISTECH, 2 cours des arts et métiers, 13617 Aix en Provence, France

The challenges of weight reduction in aerospace industry have drawn considerable interest in magnesium alloys technologies. Assessing the efficiency of new joining techniques, as Friction Stir Welding is then required. During Friction Stir Welding, the welding tool motion induces frictional heating and severe plastic deformation. Then, in addition to the microstructure and texture evolutions generally observed, significant residual stresses can result from this process.

The Friction Stir Welds have been processed using 2 mm thick hot rolled plates of AZ31 Magnesium alloy. Residual stress analysis was carried out on a Friction Stir Weld processed using optimum welding parameters. Laboratory X-rays diffraction and Neutrons diffraction were performed. Indeed, the use of Neutrons diffraction was especially interesting because it avoids matter removal required with X-rays technique. Moreover, with Friction Stir Welding, the complex thermo-mechanical input induces complex stress gradients. Then, the high penetration capability of the Neutrons diffraction technique was thus essential to allow the determination of stress gradients in a non-destructive way. Hahn Meitner Institüt (HMI, Berlin, Germany) E3 instrument and Institut Laüe Langevin (ILL, Grenoble France) SALSA instrument were used. $Sin^2\psi$ method was used to determine residual stresses obtained with X-rays diffraction and HMI Neutrons diffraction, whereas the triaxial method was used to determine residual stresses obtained with ILL Neutrons diffraction.

The aim of this study is to investigate the residual stress distribution in Magnesium Friction Stir Welds and to compare the results obtained using several techniques.

S196

EFFECT OF PRESSURE ON THE RESIDUAL STRESS DEVELOPMENT IN THE LINEAR FRICTION WELDED Ti-6246

S. Zabeen[1], M.M. Attallah[1], M. Preuss[1] and Simon Bray[2]
1. School of Materials, University of Manchester, Manchester M1 7HS, United Kingdom
2. Rolls-Royce plc., Derby, DE24 8BJ, United Kingdom

Linear Friction Welding (LFW) is an innovative solid state joining technique capable of providing high performance weld of difficult-to-weld materials. Nonetheless, the rapid cooling rates and the massive thermo-mechanical deformation associated with LFW generate a significant amount of residual stresses. This study investigates the influence of the LFW forging pressure on the residual stress development in β-forged Ti-6246 welds. Residual strain was measured using high-energy synchrotron X-ray diffraction at the European Synchrotron Radiation Facility (ESRF) and from that residual stresses were calculated. Ti-6246 is a two-phase alloy, which contains substantial proportion of the β-phase. This necessitates the determination of the residual strains associated with both phases separately. Maximum amount of residual stress was found in the thermo-mechanically affected zone, which tends to decrease with the increase in weld pressure. The advantages and limitations of using high energy synchrotron X-ray diffraction are also discussed with a particular focus on measurements at the very weld line where the β-phase volume fraction and microstructure have changed dramatically.
Keywords: Linear Friction Welding (LFW), Ti-6246, Residual stress

S194

RESIDUAL STRESS IN FRICTION STIR WELDED ALUMINUM ALLOYS

J.A. Pineault*, M. Belassel*, H.J.K. Lemmen**, M.E. Brauss***
*Proto Manufacturing Ltd., Oldcastle, Ontario, N0R 1L0, Canada
**Delft University of Technology, Delft, P.O. Box 5058, 2600 GB, the Netherlands
***Proto Manufacturing Inc., Ypsilanti, MI, 48198 U.S.A.

Recent advancements in friction stir welding (FSW) technology have enabled its use in numerous joining applications and it has recently been approved by the Federal Aviation Administration (FAA) for applications in aerospace structures. FSW features many advantages including the potential for a reduction in production costs, lead-times, and a decrease in structural weight while maintaining a high strength, high quality joint. The residual stress fields in several FS welds using three different aluminium alloys, AA2024-T3, AA7075-T6 and AA6013-T4, in the as-welded condition were measured using X-ray diffraction (XRD) techniques. Selected welds were also characterized in the as-machined condition as might be found in a typical aircraft structure. The residual stress profiles in all three welded alloys exhibited high tensile stress fields in the weld with a width comparable to the tool size. In areas adjacent to the weld, the residual stress levels were reduced to either zero or low magnitude compressive levels. It was observed that both AA2024-T3 and AA7075-T6 had comparable residual stress profiles, whereas AA6013-T4 was found to have relatively lower magnitude residual stresses. The findings described in the following paper indicate that an awareness of the residual stresses present in FS welds is necessary to ensure successful implementation of FSW in failure critical structures.

Achete, C.A. 148
Adams, D.P. 81
Afanas'ev, M.S. 57
Aizawa, K. 135
Akiniwa, Y. 147, 151
Akita K., ... 135, 151
Allen, A.J. 112
Almeida, E. 98
Almer, J. 50, 97, 102, 194
Altenkirch, J. 186
Alvarado, C.H. 80
An, K. 134, 184, 194
Andrews, J. 98
Anibou, N. 71
Anishchik, V.M. 117
Aoki, F. 124
Arai, M. 135
Arai, T. 139
Araki, Y. 84, 94, 110
Aranami, K. 61
Aranda, M.A.G. 46
Arias, L. 66
Asahi, T. 47
Attallah, M. 199
Autenrieth, H. 197
Ayala-Jiménez, R.E. 57, 80
Backlund P., ... 135
Baczmanski, A. 123
Bae, J. 77
Bagby, M. 68
Bai, F. 54
Bailey, W.B. 134, 156
Baker, P. 114
Baker, P.E. 116
Balaji, A.K. 192
Bale, H.A. 138
Ball, D.L. 195
Banfield, J.F. 78
Bark, C.W. 189
Barkan, S. 73
Barnes, C.L. 54
Barouda, E. 46
Barrallier, L. 191, 199, 196
Barsoum, I. 196
Barsoum, Z. 196
Basile, F. 101
Bate, S.K. 144
Baudin, C. 165
Baumann, T. 112
Baumbach, T. 80, 117
Bayraktar, F.S. 143
Bechteler, A. 74
Beck, T. 172
Beckhoff, B. 114
Beckmann, F. 153
Behrens, K. 64, 66, 73, 82, 93
Belassel, M. 134, 199
Bendeich, P. 118
Benediktovich, A.I. 80
Benito, P. 101
Benmarouane, A. 140, 144
Bergmark, A. 137
Bérubé, L. 72
Betancur, A.T. 52
Bibee, M. 171, 183
Bilderback, D. 108
Bingölbali, A. 56
Bisulca, C. 85
Blanton, T.N. 54
Blevins, R. 186
Blug, B. 171
Bogert, J.R. 94
Bohic, S. 100
Bonnefoy, H. 144
Borbély, A. 129, 139
Bouchard, P.J. 185
Boutefnouchet, H. 103
Bowe, S.W. 83
Bradai, D. 51
Bradley, T. 115
Braeu, M. 89
Brandstetter, S. 163
Brauss, M. 134, 199
Bray, S. 199
Breeding, C.M. 67
Brehm, L.L. 65
Brennan, S. 98, 183
Brito, P. 132
Brokmeier, H.G. 119, 128
Bronfenbrenner, D. 171
Brostoff, L.B. 86
Brown, D.R. 89
Brown, D.W. 163, 169
Brown, E. 73
Bucci, R.J. 195
Budai, J.D. 187
Buehler, A. 93
Buffa, G. 143
Bugani, S. 101
Bunker, B.A. 77
Burns, D.W. 65, 115
Burton, P. 77
Buslaps, T. 139, 140, 165, 180, 188
Cabeza, A. 46
Caliebe, W.A. 48
Canaday, C. 160
Cané, C. 159
Carolan, D. 73
Carr, D.G. 169
Casadio, F. 97
Castelnau, O. 120
Ceylan, H. 146
Chai, G.C. 132, 181
Chan, S.-W. 48
Chandra, D. 53, 54
Chellappa, R.S. 53
Chen, C.-C.A. 51
Chen, K. 110, 131, 189
Chen, M.-K. 51
Chen, X. 73
Chen, Y.-c. 99
Chen, Z. 64, 105, 109
Cheung, J.H. 89
Chiari, G. 95
Chien, W.-M. 53, 54
Cho, K.C. 189
Cho, S.-r. 91
Choi, S.-M. 53
Choo, H. 134, 194
Christensen, C. 117
Chu, Y. 99
Chupas, P.J. 48

Clark, S. 53
Clausen, B. 136, 169, 174
Clitheroe, S. 150
Cochennec, F. 152
Coelho, P. 138
Coelho, R.S. 134
Cogdill, R.P. 55
Collet-Fenetrier, J-C. 121
Colodrero, R.M.P. 46
Commin, L.
Conant, T.R. 77
Conley, R. 117
Consonni, V. 188
Cordes, H. 70
Covington, A.M. 53
Cox, M. 99
Criss, E. 136
Cross, B. 115
Cross, K. 96, 114
Csontos, A.A. 68
Curfs, C. 103
Cusack, M. 105
Cushman, M. 85
Daichendt, S. 150
Daigle, P. 83
Damron, E.V. 73
Daniel, R. 49, 79
Datye, A.K. 77
Davydov, V. 137, 155
Dawson, P.R. 145
Daymond, M.R. 145, 169, 179, 194
Daynes, N. 159
De La Riva, A. 77
De Nolf, W. 101
De Samber, B. 100
De Schamphelaere, K. 100
de Villiers, J.P.R. 82
Degen, T. 48
Degenkolb, M. 89
Degischer, H.P. 180
Deloison, D. 191
Demadis, K.D. 46
Denecke, M.A. 108
Denizer, B. 146
Denks, I.A. 124, 153
DeWald, A.T. 150
Di Michiel, M. 139, 180
Dik, J. 85
Dilger, K. 158, 184
Dillien, S. 181
Domizzi, G. 183
Dommann, A. 127
dos Santos, J. 134
Doyle, S. 48
Dozier, C.M. 71
Drahokoupil, J. 50
Drews, A.R. 102
Dubois, J.B. 119
Duewer, F. 77
Dumont, M. 107
Dunand, D.C. 97, 99
Dunn, M.L. 196
Durstock, M.F. 53
Dužic´, K. 130
Dzieciol, K. 139
Eckhardt, R. 74
Edwards, L. 163, 176, 179, 185
Egan, J. 73
Eggert, T. 62
Egorov, E.V. 57
Egorov, V.K. 57
Elam, W.T. 116
Elices, M. 179
Ellerman, A. 132
Emmons, E.D. 53
Epp, J. 176
Erbacher, T. 172
Evans, A.D. 150
Evens, R. 100
Faber, K.T. 102
Falkenberg, G. 100
Fallas, J.C. 53
Fang, J.F. 91
Fardi, M. 192
Farjian-Sohi, M. 184
Feng, L. 73
Feng, Z. 184
Feranchuk, I. 80
Feser, M. 77, 98
Feuer, J. 63
Feuillet, G. 188
Fezzaa, K. 98
Fields, L. 63
Finlayson, T.R. 186
Fischer, T. 185
Fittschen, U. 106
Fitzpatrick, M.E. 163, 176, 179
Flan, B. 152
Fornasari, G. 101
Förter-Barth, U. 48
Fournier, G. 74
Fox, M.E. 175
Francis, J.A. 144
Frankel, P. 174
Franklin, F. 115
Fransen, M. 76
Fratini, L. 143
Fry, A.T. 131
Fu, W.-E. 51
Fuhr, V. 171
Fujii, K. 125
Funaki, K. 125
Furukawa, H. 190
Gabaldon, J.P. 77
Gaeberlein, P. 89
Gailhanou, M. 95
Ganev, N. 50
Gao, N. 109
Gao, Y.K. 129
Garbe, U. 119
Gardner, R.P. 105
Gateshki, M. 76
Geandier, G. 120
Gegner, J. 129, 195
Gelb, J. 77, 98
Genzel, Ch. 124, 132, 172
Gergaud, P. 188
Giaccai, J. 88
Gibmeier, J. 128, 154, 161, 180, 181
Gibson, W.M. 105, 109
Gilbert, B. 78
Glazov, A.L. 177

Gnäupel-Herold, T. 118, 155
Goetz-Neunhoeffer, F. 89
Goldey, S.J. 92
Gollhardt, A. 159
Goly, M. 137
Götting, M. 154
Goudeau, Ph. 120
Gràcia, I. 159
Grant, P. 165
Grendahl, S.M. 152
Gross, A. 72
Gross, B. 118
Grybos, P. 70
Guérault, H. 117
Guise, W.E. 111
Guo, Y.B. 133, 198
Gupta, V. 54
Gurauskis, J. 165
Haase, A. 147
Hadj Larbi, F. 51
Haeffner, D.R. 97
Haigh, R. 163
Hainsworth, S.V. 176
Hair, C. 55
Hamza, A. 112
Han, T.-S. 145
Han, X. 53
Hanabusa, T. 123, 149, 169, 173
Hanan, J.C. 138
Hansen, T. 140
Hanson, J.C. 48
Harder, B.J. 102
Harjo, S. 135
Harter, J. 137
Hasan, T. 115
Hasse, B. 46, 70
Hatamleh, O. 150
Havrilla, G.J. 93, 106
Hayakawa, S. 106
He, B.B. 117
He, Y. 109
Heard, P.J. 159
Hemberg, O. 75
Hemptenmacher, J. 180
Hens, Z. 65
Hermenau, K. 74
Herrmann, A. 180
Herrmann, M. 48
Herrnegger, P. 52
Hertlein, F. 46
Hertz, H.M. 75
Hesse, C. 89
Hill, D. 137
Hill, M.R. 150, 196
Hino, M. 61
Hinrichsen, B. 71
Hirokawa, T. 106
Hirose, Y. 122, 124, 125
Hirsch, T. 148, 150, 176
Hodgson, D.Z.L. 159, 160
Hofmann, F. 121
Hofmann, M. 118, 119, 122, 128, 161, 179
Holden, T.M. 134, 169
Holland, M. 54
Holt, M. 189
Holt, R.A. 145, 194
Homma, H. 63
Hong, J.-I. 77
Honkimaki, V. 140
Horne, G. 159
Horntrich, C. 60
Hosokawa, A. 122
Hossain, S. 175, 192
Hossainzadeh, F. 176
Houk, L.R. 77
Howell, J. 135
Hsu, G. 77
Huang, H. 105
Huang, X. 117
Hubbard, C.R. 134, 156, 170, 184, 194
Hubbard-Nelson, B. 73
Huber, A. 115
Huber, D.L. 78
Hufnagel, T.C. 140
Hügel, W. 161
Hughes, D.J. 121, 175
Humphrey, G.R. 84
Huo, J. 91
Huppmann, M. 182
Hurrell, P. 144
Huson, P. 136
Ibrahim, R. 186
Ice, G.E. 187
Ilavsky, J. 112, 113
Inaba, K. 79
Ingerle, D. 58
Inoue, H. 63
Isaac, A. 139
Ishikawa, T. 190
Itoh, T. 110
Iwaki, M. 106
Iwasaki, Y. 47
Jacobs, R. 114
Jacobs, R.M. 92
Jacobs, R.R. 116
James, J. 156
James, M.A. 195
Jang, H.M. 189
Jang, Y.-i. 91
Janssen, C. 100
Janssens, K. 85, 101
Jaritschin, O. 74
Jegou, S. 191
Jemian, P.R. 112, 113
Ji, H. 120
Ji, V. 151
Jiang, C.H. 151
Jing, T. 149, 169
Johansson, S. 132, 167, 181
Johnson, R. 116
Jones, K.W. 196
Juez-Lorenzo, M. 48
Jun, T.S. 121, 165
Jun, Y.-S. 78
Jurgensen, A.R. 62
Kad, B. 136
Kagami, E. 54
Kahen, K.B. 54
Kaiser, B.J. 97
Kajiwara, K. 139
Kalenci, O. 108
Kamisetti, V.K. 53

Kanematsu, M. 166
Kang, K.J. 159
Kannengiesser, T. 180
Kaplan, A. 87
Kastelein, R. 193
Kataoka, Y. 63
Kawada, N. 110
Kawai, J. 115
Kawauchi, M. 167
Keane, D.T. 53, 111
Keckes, J. 49, 50, 79, 80
Kelleher, J. 150, 174
Keller, T. 118
Kempa, P.B. 48
Kendall, D.S. 49
Kerr, M. 194
Khachatryan, R. 117
Khan, M.K. 176
Khereddine, A. 51
Kiehn, R. 153
Kienzler, A. 188
Kim, C. 78
Kim, H-S. 53
Kim, Y. 146
Kimura, H. 151
Kinugawa, G. 115
Kirchlechner, Ch. 49, 79
Kiriyama, K. 139
Kirkham, M. 77, 102
Kirstein, O. 128
Kishi, A. 47
Kitano, M. 47, 60, 62
Klaus, M. 132, 172
Kleiner, S. 180
KloseK, V. 144
Knorr, K. 71
Kobayashi, M. 139
Kobayashi, S. 47
Kobayashi, Y. 125
Koçak, M. 143
Kodjie, S. 60
Koeppen, A.H. 64
Kohno, H. 61, 63
Kolwyck, J.V. 170
Komatani, S. 109
Konya, T. 47
Kõo, J. 131, 133, 178
Koo, Y.M. 189
Kornmeier, J. 119, 122, 128
Korsunsky, A. 121, 141, 165
Kostka, A. 134
Kotnik, P. 53, 111
Krämer, M. 94
Kregsamer, P. 60
Krempaszky, C. 118,161
Kriechbaum, M. 52
Kröber, H. 48
Kromm, A. 180
Kroth, S. 46
Kubler, R. 191
Kubo, H. 190
Kubo, T. 47
Kubota, K. 168
Kucheyev, S. 112
Kudla, R.J. 102
Kunimura, S. 115
Kunz, M. 53, 138
Kurakado, M. 110
Kuribayashi, M. 70
Kuru, Y. 81
Kusaka, K. 123, 173
Kusunoki, K. 166
Kužel, R. 155
Kuznetsov, A. 148
Kwon, H.-k. 91
Laaneots, R. 131
Lafford, T. 162
Laggner, P. 52
Lamb, J.H. 54
Langenbucher, G. 53, 111
Larson, B.C. 187
Latosiewicz, U.B. 89
Lavin, J.M. 78
Lazar, A. 117
Le Bourhis, E. 120
Lechner, P. 74
Lecouturier, F. 119, 142, 162
Lee, J. 135
Lee, K.N. 102
Lee, P.L. 48
Lee, S.-Y. 136, 146, 196
LeMaster, R.A. 170
Lemmen, H.J.K. 199
Lengeler, B. 58
León-Reina, L. 46
Leppert, T. 130
Leskovšek, V. 192
Leuven, K.U. 181
Lévesque, M. 193
Levine, L.E. 112
Lewis, J.A. 113
Lewis, T.L. 115
Li, D. 64, 105
Li, F. 105
Li, L. 136
Li, Y.R. 120
Liaw, P.K. 134, 194
Liebel, A. 74
Lienert, U. 186
Lille, H. 131, 178
Lin Peng, R. 132, 181
Lin, X.-M. 111
Ling, Y. 193
Liu, J. 51
Liu, W. 187
Liu, Z. 86
Lodini, A. 123, 140, 144
Löhe, D. 188, 197
Long, G.G. 112, 113
Lord, J.D. 131, 157
Loubser, M. 82
Lovato, K. 77
Lovato, M.L. 174
Lui, A. 48
Lukás, P. 137, 155
Lun, S. 48
Lutz, G. 74
Luzin, V. 118, 171, 179
Lyphout, C. 122
Maaß, R. 187
MacDonald, C.A. 56
Machado, R. 148

Machiya, S. 147
Machold, W. 143
Macrander, A. 117
Maeo, S. 94, 110
Mahmoudi, A.H. 174
Maj, J. 117
Maj, P. 70
Malard, B. 137
Mamedov, ... 92
Manescu, A. 122
Manns, T. 124, 132, 141
Mantler, M. 114
Manzanka, M. 167
Margiolaki, I. 48
Marín, J.V.R. 52
Martin, M. 63
Martinez, R.A. 49
Martins, R. 185
Martinschitz, K.J. 49, 50, 79, 80
Marusich, T.D. 197
Maser, J. 108, 189
Mass, J. 85
Masschaele, B. 100
Masse, J.-E. 199
Mathon, M.H. 144
Matlock, B.S. 152
Matsubara, E. 190
Matsuda, A. 109
Matsudaira, T. 47
Matsue, T. 123
Matsui, H. 61
Matsuo, R. 47
Matsuyama, R. 125
Maynor, C. 86
Mazza, E. 127
Mehta, A. 171, 183
Meirer, F. 58
Meirer, F. 59, 60
Miao, H.Y. 193
Michael, S.C. 64
Michaelsen, C. 46, 70
Michel, B. 159
Milam, V.T. 113
Miller, D. 87
Miller, M.E. 103
Miller, M.P. 145
Minak, G. 194
Missimer, D.M. 62
Misture, S.T. 103, 104
Mittemeijer, E. 81, 148, 161
Mitterer, Ch. 49, 79
Miura, S. 139
Miyashita, D. 151
Miyazawa, Y. 125
Mizusawa, M. 57
Molloy, J.L. 109
Monson, T.C. 78
Monzen, R. 122
Moore, M.D. 55
Moreels, I. 65
Moriai, A. 135
Morii, Y. 135
Morselli, L. 101
Morton, R.W. 83
Moscicki, M. 129
Motzet, H. 89
Muraoka, K. 84, 110
Muratikov, K.L. 177
Murray, C. 108
Muslih, M.R. 169
Muynck, D. De 65
Nady, A. 144
Nagao, K. 47
Nakamura, T. 47, 60, 62
Nakano, K. 61, 105, 109
Nakatani, T. 135
Nakayama, K. 47
Namowicz, C. 87
Nasella, R. 73
Neels, A. 127
Nervi, S. 197
Neubauer, J. 89
Newbury, B.D. 97
Nichols, E.J. 104
Nicolich, J.P. 89
Nicolosi, J. 116
Niculae, A. 74
Nierlich, W. 129, 195
Nikroo, A. 112
Nishida, M. 127, 149, 169, 173
Nishimoto, Y. 106
Nishino, Y. 190
Nishiyama, N. 163
Nitschke-Pagel, T. 158, 184
Nolan, D. 192
Novosel–Radovic´, V. 130
Noyan, I.C. 108, 136
Nyhus, B. 186
Ocon, N. 85
Oehr, A. 46
Ogata, T. 151
Ohbuchi, A. 62
Ohms, C. 128, 155
Ohya, S.-i. 151
Ohzawa, S. 109
Okada, K. 115
Okolo, B. 188, 197
Okubo, K. 105
Oliver, E.C. 118, 169, 175
Ono, Y. 151
Ortner, B. 180
Ostermann, A. 119
Otendal, M. 75
Outeiro, J. 122
OuYang, F.Y. 189
Pagliaro, P. 174
Pahlke, A. 62
Pahlke, S. 62
Paiz, J. 77
Pala, Z. 50
Palmer, P.T. 92, 96, 114, 116
Pantazis, J. 115
Pantazis, T. 115
Papes, O. 127
Paradowska, A.M. 186
Paranjpe, A.R. 192
Park, J.-S. 145
Park, K.-h. 91
Pasta, S. 143
Pate, B.D. 53
Patterson, B.M. 101
Pavier, M.J. 174

Peel, M. 167, 183, 186
Peng, R.L. 130
Pepponi, G. 58, 59, 60
Perron, C. 193
Peterson, E.J. 77
Petkov, V. 78
Petrucci, G. 157
Petry, W. 118, 161
Peyre, P. 151
Pfeiffer, W. 171
Pham, H. 77
Phillips, R.E. 67
Pianetta, P. 98, 183
Pilch, J. 137
Pina, J. 122
Pineault, J. 134, 199
Pinto, H. 129, 132, 134
Piorek, S. 92
Pirling, T. 121, 167
Platonov, Y. 74
Podgornik, B. 192
Podsiki, C. 96
Poeste, T. 180
Ponomarev, I. 109
Preckwinkel, U. 70
Preuss, M. 199
Price, J.H.W. 186
Prime, M. 135, 136, 160, 174
Pyzalla, A.R. 107, 129, 132, 134, 139
Qian, J. 117
Qu, J. 184
Quintana, J.P.G. 111
Radovic´, N. 130
Rakurty C. 192
Randau, C. 119
Rebelo-Kornmeier, J. 179
Redus, R. 115
Reiche, H. 163
Reimers, W. 172, 182
Reisacher, E. 171
Ren, X.B. 186
Ren, Y. 78
Renault, P.O. 119, 120, 142, 162
Repper, J. 118, 119, 161
Ress, H. 64
Rethmeier, M. 180
Reuter, R. 137
Reynolds, A.P. 160
Rickers, K. 85, 100
Ricou, P. 60
Rider, M. 72
Riekehr, S. 143
Rigot, W. 115
Robinson, J.S. 118, 174, 175
Roch, F. 191
Rodriguez, J. 74
Rodriguez, M.A. 81
Rogge, R.B. 145
Rongfeng, L. 126
Roscoe, K. 73
Rose, V. 189
Rosmarin, I. 73
Rothkirch, A. 141
Roucoules, L. 152
Rouhaud, E. 152
Rowe, S. 121
Roy, G. 70, 177
Roy, S. 161
Rudati, J. 98
Ruhnau, H.-U. 153
Ruiz-Hervias, J. 165, 179
Russell, K. 63
Russell, R. 73
Rutherford, R.L. 62
Ruud, C.O. 149
Ruvalcaba Sil, J.L. 97
Ryabchikov, A. 131, 178
Ryan, P. 162
Ryu, S. 189
S. Cornaby, ... 108
Sabaté, N. 159
Sackett, D. 73
Sadrossadat, M. 167
Šafar, F. 130
Saito, M. 168
Sakaida, Y. 167
Sakata, O. 123
Sakurai, K. 57, 100
Sanada, T. 46
Sandberg, P.J. 89
Sander, M. 107
Santisteban, J.R. 183
Sardisco, J. 93
Sarma, D.D. 187
Sarrazin, P. 95
Sasaki, K. 122, 125
Sasaki, M. 47
Sasaki, N. 115
Sasaki, T. 122, 124, 125
Sato, S. 46
Saveliev, V.D. 73
Saw, C. 112
Scafidi, M. 126, 157
Scavetta, E. 101
Schafmeister, A. 147
Schajer, G.S. 157, 174
Schaller, G. 74
Schell, N. 153
Schifferle, A. 127
Schlier, L. 129
Schmidlin, J. 134, 156
Schmitt, B. 163
Schnablegger, H. 53, 111
Schneider, R. 119, 128, 180
Schöbel, M. 180
Scholtes, B. 124, 141, 154
Schoonjans, T. 100
Schopper, F. 74
Schreyer, A. 143, 153, 185
Schroer, Ch. 58
Schulze, V. 188, 197
Scothern, A. 64
Scruggs, B. 116
Seefeldt, M. 181
Seekamp, A. 161
Seepersad, C. 135
Seidl, G.A. 119
Seifert, S. 89
Serafin, F.G. 89
Setola, G. 92
Seyfarth, A. 64, 66, 72, 73, 82, 93
Shah, S. 135

Sharma, S. 163
Shen, Q. 99
Shen, X. 60
Shepard, M. 69
Shibano, J. 139
Shibata, Y. 60
Shimizu, K. 74
Shimizu, S. 168
Shimizu, Y. 61
Shinoda, K. 46
Shioi, R. 115
Shirakihara, K. 135
Shiro, A. 149, 169
Shobu, T. 139, 140, 151, 166
Short, S.M. 55
Shterenlikht, A. 159, 160
Shugar, A.N. 95
Sieber, J.R. 109
Silversmit, G. 100
Simsek, A. 74
Sisneros, T.A. 163
Šittner, P. 137
Sket, F. 139
Skinner, S.J. 102
Skrzypek, S.J. 137
Smilgies, D. 108
Smith, D. 176
Smith, D.J. 160, 174, 192
Smolek, S. 59
Snoha, D.J. 152
Snyder, R.L. 77, 102
Sobiech, M. 161
Solazzi, M. 116
Soltau, H. 74
Song, H.B. 151
Song, X. 141
Sparks, C.M. 106
Speakman, R.J. 86
Spiegel, M. 132
Stabenow, R. 147
Staron, P. 143
Steinzig, M. 157
Steinzig, M.L. 174
Stenzel, Ch. 58
Stephenson, G.B. 189
Steuwer, A. 165, 183, 186
Stillwell, B. 111
Stock, S. 50
Stoetter, R. 62
Stoica, A.D. 134
Stosnach, H. 72, 90
Streli, C. 58, 59, 60, 107
Strüder, L. 74
Strunz, P. 155
Stuhr, U. 119, 162, 192
Stulik, D.C. 87
Su, B. 176
Suathoff, G. 139
Sugita, Y. 168
Suyama, J. 60
Suzuki, D. 168
Suzuki, H. 166
Suzuki, K. 139, 166
Suzuki, S. 46
Suzuya, K. 135
Sweet, M. 93
Swenson, H. 174
Symington, I. 144
Szabó, B.A. 197
Szczygiel, R. 70
Taguchi, T. 70
Takago, S. 125
Takahashi, M. 73
Takahashi, S. 124, 125
Takahashi, Y. 46, 190
Takase, A. 54
Taleff, E. 135
Tamura, N. 110, 131, 138, 189
Tanaka, K. 140, 147, 166
Taniguchi, K. 84, 94, 110
Tarasiuk, J. 123
te Nijenhuis, H. 76
Tekouo, W. 119
Terada, Y. 57
Thilly, L. 119, 120, 142, 162
Thomas, G. 165
Thompson, R.B. 68
Thompson, V. 138
Tian, Zh.L. 91
Tischler, J.Z. 187
Tissot, R.G. 81
Tkachuk, A. 77, 98
Tomota, Y. 135
Tonelli, D. 101
Toraya, H. 70, 71
Trentelman, K. 87
Truman, C. 176
Truman, C.E. 174, 175, 192
Tsuji, K. 105, 109, 61
Tu, K.N. 110, 131, 189
Tull, C.R. 73
Tuohimaa, T. 75
Turner, T. 63
Turski, M. 144, 150, 163, 185
Uchihara, H. 109
Uglov, V.V. 117
Ulyanenkov, A. 80, 117
Ulyanenkova, T.A. 80, 117
Üstündag, E. 136, 146
Utaka, T. 84, 94, 110
Vaccari, A. 101
Vaia, R.A. 53
Valek, B.C. 110, 131
Valentini, E. 126
Valgur, J. 133
van Buuren, T. 112
Van der Loeff, L. 85
van der Meulen, M. 98
Van der Snickt, G. 85
Van Hoorebeke, L. 100
Van Petegem, S. 119, 142, 162, 163, 187
van Rooyen, P.H. 82
Van Swygenhoven, H. 119, 142, 162, 163, 187
VanDalen, J.E. 196
Vanhaecke, F. 65
Vanhoyland, G. 71
Vardon, P. 191
Vaughan, G.B.M. 103
Vegter, R.H. 167
Vekemans, B. 100
Vermeulen, A.C. 147
Vianden, R. 58

Vidal, V. 119
Vidal, V. 142, 162
Vincze, L. 100
Vižintin, J. 192
Vogel, D. 159
Vogel, S.C. 163
Vöhringer, O. 172
Volz, H.M. 163
Vrána, M. 137
Wagatsuma, K. 46
Walton, M. 87
Wang, J. 111
Wang, S. 77
Wang, X.-L. 134, 184
Wang, Y. 120, 163, 193
Wang, Z.L. 76, 77, 102
Wanibuchi, H. 61
Wanner, A. 161, 172, 188, 197
Ward, T.Z. 187
Wargacki, S.P. 53
Warren, A.W. 133, 198
Watanabe, Y. 127
Waychunas, G.A. 78
Weaver, C. 73
Weigand, S. 111
Welzel, U. 81, 148, 161
Werner, E. 118, 161
Whitehead, P. 157
Whitley, A. 92
Wieczorek, M. 117
Wierzbanowski, K. 123
Wiest, F. 62
Wildfong, P.L.D. 55
Willey, T. 112
Wimpory, R. 199
Wimpory, R.C. 128
Winarski, R. 189
Withers, P. 174
Withers, P.J. 150, 186
Wobrauschek, P. 58, 59, 60, 107
Wohlschlögel, M. 81, 148
Woitok, J.F. 90
Woll, A. 85
Worley, C.G. 58
Wormington, M. 162
Wright, J. 103
Wright, J.P. 48
Wronski, S. 123
Wu, X.-R. 129
Xiong, Y.S. 174
Xu, F. 145
Xu, H. 184
Xu, X. 51
Xu, Z.A. 193
Yamada, T. 61
Yamada, Y. 63
Yamamoto, T. 115
Yamane, K. 106
Yamauchi, K. 190
Yan, H. 108
Yang, N. 70
Yasui, H. 125
Yatsushiro, K. 168
Yi, J. 99
Young, K.A. 197
Young, M.L. 97
Youtsos, A.G. 128
Yun, W. 77, 98
Yuri, T. 151
Zabeen, S. 199
Zanellato, O. 179
Zeisler, R. 109
Zhang, F. 48, 112, 113
Zhang, H. 78
Zhang, J. 163
Zhang, J.Y. 91
Zhang, R.Y. 145
Zhang, S.Y. 121, 141, 165
Zhang, Y. 51, 91
Zhang, Z.L. 186
Zhao, Y. 163
Zhou, X.Y. 120
Zimmermann, J. 163, 187
Zlotski, S.V. 117
Zoeger, N. 58, 59, 60, 107
Zuccarello, B. 126, 174

Hotel Layout

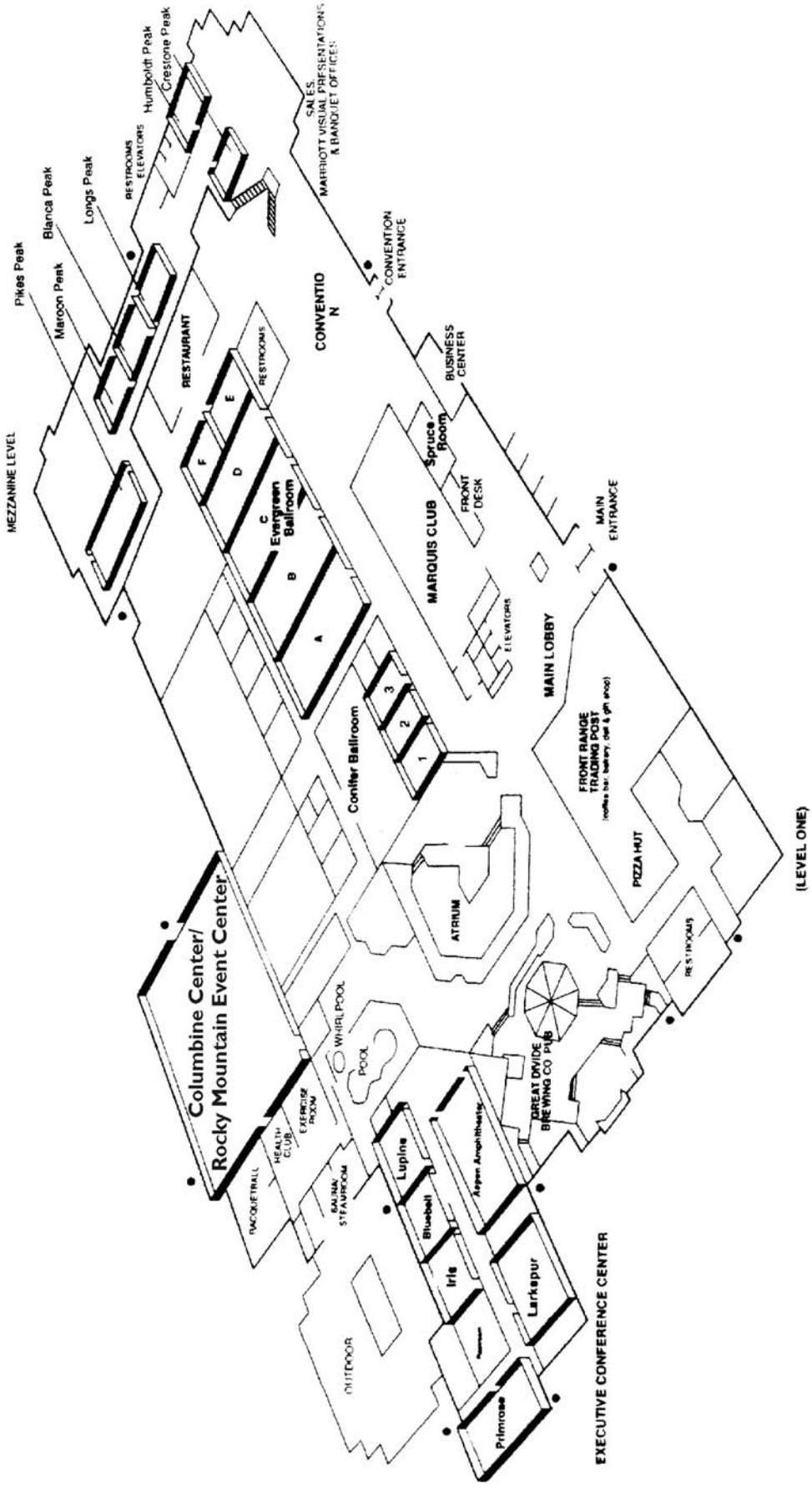

The 8th International Conference on Residual Stresses *Program-at-a-Glance*

Tuesday 9:00 a.m. – 5:00 p.m. ICRS Workshop on Stress Analysis (Noyan/Prime) Evergreen "D"				
Wednesday 8:30 a.m. – 12:30 p.m. Plenary Session: Stress and Society (Noyan/Prime/Üstündag) Evergreen Ballroom				
Special Sessions				
Day and Time	Meeting Room			
	Pikes Peak	Longs Peak	Blanca Peak	Maroon Peak
Wednesday p.m.	1:30 – 5:00 Diffraction Techniques: Synchrotrons – Macrobeam and High Energy I (Almer/Daymond)	1:30 – 5:00 Modeling I (Tome/Beyerlein)	1:30 – 4:40 Diffraction Techniques: Laboratory Applications (Goldsmith/Watkins)	2:00 – 5:00 Industrial Applications: Engineered Stresses (Bunch/Hill)
Thursday a.m.	8:30 – 9:40 Diffraction Techniques: Synchrotrons – Macrobeam and High Energy II (Almer/Daymond) 10:30 – 12:00 Diffraction Techniques: Neutron I (Brown/Wang)	8:30 – 10:00 Relaxation Techniques: Hole Drilling (Robinson) 10:30 – 12:00 Relaxation Techniques: Slitting (Prime)	8:30 – 12:00 Materials Engineering I (Murray/Gnaupel-Herold)	8:50 – 10:20 Industrial Applications: Layers and Composites (Hill) 10:40 – 12:00 Industrial Applications: Thermal Processing (Bunch)
Thursday p.m.	1:30 – 3:00 Diffraction Techniques: Neutron II (Brown/Wang) 3:20 – 5:30 Diffraction Techniques: General Methods (Üstündag)	1:30 – 3:00 Relaxation Techniques: Deep Hole and Contour (Hill) 3:30 – 5:30 Other Measurement Techniques (Robinson)	1:40 – 4:50 Materials Engineering II (Murray/Gnaupel-Herold)	1:40 – 3:00 Industrial Applications: Miscellaneous (Bunch) 3:30 – 5:10 Industrial Applications: Welding (Hill)
Friday a.m.	8:30 – 11:50 Diffraction Techniques: Synchrotrons – Microbeam (Ice/Tamura)	8:40 – 11:50 Modeling II (Tome/Beyerlein)	8:30 – 11:30 Fatigue & Fracture (Smith)	8:30 – 10:00 Industrial Applications: Distortion and Machining (Bunch) 10:30 – 11:30 Industrial Applications: Friction Stir Welding (Bunch)

Social Events:

Sun. Eve.: 6:00 – 8:00 p.m.	Welcoming Reception sponsored by Thermo Scientific and ICDD. Evergreen Ballroom.
Mon. Eve.: 6:00 – 8:00 p.m.	Wine & Cheese Reception sponsored by PANalytical; XRD Poster Session I (Blanton/Kaduk); Evergreen Ballroom.
Tues. Eve.: 6:00 – 8:00 p.m.	Wine & Cheese Reception sponsored by Chemplex Industries, Inc. and GE Inspection Technologies; XRF Poster Session (Palmer/Kawai); Evergreen Ballroom.
Wed. Eve.: 5:00 – 7:00 p.m.	Vendor-sponsored Wine & Cheese Reception; Exhibit Hall "Rocky Mountain Event Center".
Thurs. Eve.: 6:00 – 9:00 p.m.	ICRS-8 Conference Dinner and Poster Session; Evergreen Ballroom.

Denver X-ray Conference *Program-at-a-Glance*

Day & Time	XRD & XRF	XRD	XRF
Sun. Eve.: 6:00 – 8:00 p.m. Welcoming Reception sponsored by Thermo Scientific and ICDD. Evergreen Ballroom			
Mon. am: Workshops 9:00 – 12:00		Texture Analysis with Area Detectors (He/Blanton) "A" Introduction to Rietveld (Kaduk) "B"	Quantitative Analysis I (Mantler) "C" Basic XRF (Elam/Havrilla) "D"
Mon. pm: Workshops 2:00 – 5:00		Non-ambient XRD (Misture) "A" Combined Use of X-rays & Neutrons (Huq) "B"	Quantitative Analysis II (Mantler) "C" Energy Dispersive XRF (Scruggs) "D"
Mon. Eve.: 6:00-8:00 p.m. Wine & Cheese Reception sponsored by PANalytical; XRD Poster Session (Blanton/Kaduk). Evergreen Ballroom			
Tue. am: Workshops 9:00 – 12:00	Cultural Heritage I (Trentelman) "A"	Stress Analysis I (Noyan/Prime) "D"	Specimen Preparation I (Anzelmo) "C" Trace Analysis (Wobrauschek) "B"
Tue. pm: Workshops 2:00 – 5:00	Cultural Heritage II (Trentelman) "A" Nanomaterials and their Applications (Snyder/Petkov) "E&F"	Stress Analysis II (Noyan/Prime) "D" High-throughput X-rays (Toby) "B"	Specimen Preparation II (Anzelmo) "C"
Tue. Eve.: 6:00 – 8:00 Wine & Cheese Reception sponsored by Chemplex Industries, Inc. and GE Inspection Technologies; XRF Poster Session (Palmer/Kawai). Evergreen Ballroom			
Wed. am: 8:30 – 12:30 Plenary Session: Stress and Society (Noyan/Prime/Üstündag) Evergreen Ballroom			
Wed. pm: Sessions	1:30 – 5:15 New Developments in XRD & XRF Instrumentation (Buhrke) "A" 1:30 – 5:10 Analysis of Nanomaterials (Petkov/Snyder) "B"	2:00 – 5:00 Thin Films (Blanton/Huang) "C"	1:30 – 4:50 Fusion & Industrial Applications of XRF (Anzelmo) "D"
Wed. Eve.: 5:00 – 7:00 Vendor sponsored Wine & Cheese Reception. Exhibit Hall "Rocky Mountain Event Center"			
Thurs. am: Sessions	9:00 – 12:00 Cultural Heritage I (Trentelman) "A" 9:00 – 12:00 Industrial Applications (Payzant/Snyder) "B"		9:00 – 12:00 Regulatory Applications (Elam) "C"
Thurs. pm: Sessions	2:00 – 5:00 Cultural Heritage II (Trentelman) "A" 1:30 – 2:50 X-ray Microimaging (Shen) "B" 3:30 – 5:00 Microbeam X-ray Analysis I (Tsuji/Havrilla) "B"	2:00 – 4:50 High Temperature In-situ Analysis (Misture) "C"	2:00 – 4:50 Trace Analysis (Zaitz) "D"
Fri. am: Sessions	8:30 – 11:50 Microbeam X-ray Analysis II (Tsuji/Havrilla) "A"	8:30 – 11:50 Small Angle Scattering (Ilavsky) "B"	8:30 – 11:20 Quantitative Analysis (Elam) "C"

All sessions, workshops and poster sessions/socials will be held in the Evergreen Ballroom: sections "A", "B", "C", "D" or "E&F", except for Wednesday evening's social event, which will be held in the Exhibit Hall "Rocky Mountain Event Center"